NASA Contractor Report 182217

NASA Powered Lift Facility Internally Generated Noise and Its Transmission to the Acoustic Far Field

(NASA-CR-182217) NASA POWERED LIFT FACILITY INTERNALLY GENERATED NOISE AND ITS TRANSMISSION TO THE ACOUSTIC FAR FIELD Final Report (Sverdrup Technology) 219 p CSCL 14B

N89-16882

Unclas

G3/09 0190065

Ronald G. Huff

Sverdrup Technology, Inc.
NASA Lewis Research Center Group
Cleveland, Ohio

November 1988

Prepared for
Lewis Research Center
Under Contract NAS3-25266

National Aeronautics and
Space Administration

NASA POWERED LIFT FACILITY INTERNALLY GENERATED NOISE AND ITS TRANSMISSION TO THE ACOUSTIC FAR FIELD

Ronald G. Huff

Ronald G. Huff and Associates
Engineering Consultants
6137 Sherwood Dr.
North Olmsted, Ohio 44070

E-4464

ABSTRACT

Noise tests of NASA Lewis Research Center's Powered Lift Facility were performed to determine the frequency content of the internally generated noise that reaches the far field. The sources of the internally generated noise are the burner, elbows, valves, and flow turbulence. Tests over a range of nozzle pressure ratios from 1.2 to 3.5 using coherence analysis revealed that low frequency noise below 1200 Hz is transmitted through the nozzle. Broad banded peaks at 240 and 640 Hz were found in the transmitted noise. This (640 Hz peak) explains the apparent low frequency aircraft core engine noise peak frequency of 500 Hz observed during core engine noise studies. Aeroacoustic excitation effects are possible in this frequency range. The internal noise creates a noise floor that limits the amount of jet noise suppression that can be measured on the PLF and similar facilities.

INTRODUCTION

Aeroacoustic excitation has been shown to increase jet mixing rates and to increase lift and decrease drag of airfoils at high angle of attack (ref. 1). This is the result of changes in the coherent (large scale) structure, random turbulence (fine scale) structure and gross mixing characteristics in shear layers due to acoustic excitation. The source of acoustic waves used in these jet experiments was placed upstream of the jet nozzle exit thus transmitting acoustic waves through the nozzle to the jet shear layer. In the NASA Lewis Powered Lift Facility (PLF) tests are performed on nozzles, ejectors and devices that are expected to turn the flow in a desired direction for thrust vectoring. Failure to account for the flow modifications due to the acoustic waves, may lead to misinterpretation of aerodynamic results. The sources of acoustic excitation in PLF are the burner, elbows, valves and turbulence generated by the flow through the pipe.

Aircraft jet engines have noise sources that are similar to those in the PLF. Noise predictions (ref. 2), for core engine noise in turbine type aircraft engines indicate that maximum noise levels occur around a frequency range of 400 to 600 Hz. The reason for the peak occurring at a frequency of approximately 500 Hz was the subject of extensive research during the 1970's

---

*Subcontractor to Sverdrup Technology, Inc., NASA Lewis Research Center Group, Cleveland, Ohio 44135 (Subcontract Nos. 2717-01-80 and 2717-85, R.M. Nallasamy, Contract Monitor).

and early 1980's. A major source of core engine noise was thought to be the combustor. Combustors generate noise by the turbulence generated by the flow passing through turbulence generators and flow passages (cold flow), and by the interaction of the flame front with upstream generated turbulence in the combustor reference 3. Overall sound pressure levels in excess of 170 dB have been measured in core engine combustors. In addition, under certain conditions, reflections from the turbine and compressor inside the combustor can generate tones having high amplitude (ref. 4) that could be transmitted through the engine nozzle. These noise sources exist in the PLF burner and will need to be considered.

Valve noise has been recognized as a major internal noise source. Overall sound pressure levels in excess of 160 dB have been recorded downstream of butterfly valves used to control flow in air flow piping systems (ref. 5).

The problem created by unwanted noise in the PLF is illustrated by the results reported in reference 6. Interaction of screech tones in a jet-ejector configuration with the shear layer increased the pumping of the ejector and hence its thrust. If the tones are triggered by upstream generated noise, the results of similar tests in PLF may lead to errors in the desired measurements.

To evaluate PLF acoustically and determine the extent of the PLF noise reaching the acoustic far field, noise measurements were made simultaneously with internal dynamic pressure transducers and far field microphones. Extensive use has been made of coherence analysis to determine the spectral characteristics of the sound transmitted through the nozzle. This is the sound that could affect the test configurations downstream of the nozzle and possibly modify test results.

Another important result of these tests is the evaluation of the affect of internally generated noise on the measurements made on jet noise suppressors that may be tested on the PLF. Since the internal noise creates a noise floor that limits the suppression measured on the PLF it is important to at least qualitatively evaluate the internal noise floor.

The results of these tests may be used as a guide to aid future PLF users in qualitatively evaluating possible effects of PLF internal noise on their experiments. It was also necessary to determine the internal noise so the PLF may be improved as required.

Due to the lack of necessary far field microphones, the acoustic power could not be determined. These tests were not intended to be a complete acoustic evaluation of the noise generated by PLF. They were conducted to qualitatively evaluate the rig internal noise transmitted to the far field. The following report is the result of these tests.

APPARATUS

The Powered Lift Facility (PLF) is shown pictorially in figure 1. An overview is presented in figure 1(a). Figure 1(b) shows the test stand with 12 in. standard nozzle installed. The test stand has thrust measurement capability. Figure 1(c) shows pictorial details of the nozzle installation.

Air is provided by the NASA Lewis central air handling facility through an underground piping system to a point shown at the upper right corner of the schematic shown in figure 2. A positive shutoff gate valve is located just above the ground and is used to isolate the rig from the central supply system when the rig is not in operation. When PLF is operating this gate valve is completely open and is not expected to generate significant noise levels. Following the gate valve, the flow passes through two 90° elbows and then through a venturi used to measure the mass flow rate through the facility. Very little noise should be generated by the venturi provided flow separation is not present. Downstream of the venturi, the flow encounters the first flow control valve. This butterfly valve is probably the first major source of noise in the system. Downstream of this valve, a tee allows the flow to be split between two pipes. The smaller pipe leads to an in line J57 combustor can, used to heat the air supplied to the test hardware. Downstream of the tee, a 90° elbow is installed in the smaller pipe allowing the pipe to be run parallel to the large pipe. Butterfly valves are installed in both the large and small pipes to allow the flow through each of the pipes to be independently controlled. These butterfly valves are expected to be major noise generators. The burner is also a major noise generator when flow passes through it with or without the burner flame turned on. Downstream of the burner, the bypass flow passes through a 90° elbow and rejoins the flow in the larger pipe. The merged flow passes through two 90° elbows and then to a tee located at the test stand. At the tee, the flow is split as shown in figure 2. Each half passes through two 90° elbows and then through bellows to another tee where the flow enters the floating portion of the test stand through a single pipe. The bellows were installed to isolate the test hardware from the piping leading to the floating portion of the test rig to accommodate the thrust measurement. A flow straightener is installed in the straight pipe downstream of the tee and also at the entrance to the nozzle section. No acoustic mufflers or noise suppression devices were installed in the piping to suppress the internally generated noise during these tests.

INSTRUMENTATION

Aerodynamic

Aerodyamic instrumentation provided for measurement of the air mass flow rate using a venturi installed in the main supply pipe upstream of the burner bypass pipe tee. Air total temperature and pressure were measured upstream of the nozzle. Wind direction and speed were also measured. Barometric pressure was recorded. All aerodynamic measurements were recorded using a central data processing system.

Acoustic

The acoustic instrumentation consisted of two separate systems: far field acoustic measurements using microphones and internal pipe fluctuating pressures using high sensitivity pressure transducers.

Far field. - Half-inch high stability precision pressure (random incidence) response condenser microphones having a frequency response from 4.5 Hz to 20 kHz (±- 2 dB) were used to measure far field noise. A 75-ft-radius microphone circle with center at a point on the ground directly under the nozzle exit was used. The microphones were taped to a 2-ft-square plywood board laid on the ground and were pointed at the nozzle exit. They were placed on the board centerline and at a point near the boards edge such that the largest distance on the board, 18 in., was between the microphone and the nozzle. The microphones were arranged around the microphone circle at 30° (microphone 1), 45° (microphone 2), 60° (microphone 3), and 90° (microphone 4) off the jet axis (fig. 3(a)). The microphone output passed through amplifiers and then to an FM tape recorder where it was recorded for off line data analysis. The gains from each microphone were recorded manually for use during data reduction. Each microphone was calibrated before and after the run using a 250 Hz, 124 dB sound pressure level Piston phone.

Internal transducers. - The pressure transducers used to measure the fluctuating wall static pressures in the pipe, were set up to read the differential pressure between the transducer face mounted flush at the inside surface of the pipe and a static pressure tap placed in the pipe near the transducer face. A long length of tubing was connected between the transducer reference side and the static tap thus damping the dynamic pressure component coming from the tap. The transducers were installed in pairs spaced 2 in. apart along the pipe axial direction (fig. 3(b)). Pairs of transducers were installed at three axial locations in the pipe: the first in the vertical pipe leading to the test rig (transducers 5 and 6), the second just downstream of the flange in the straight pipe upstream of the nozzle (transducers 7 and 8) and the third pair just upstream of the nozzle (transducers 9 and 10) (fig. 3(c)). The output from the pressure transducer was passed through a signal conditioner and then to a linear amplifier. To eliminate electrical noise in the signal a 10 kHz low pass filter was used at the amplifier. Therefore, all of the transducer data is limited to frequencies at or below 10 kHz. As with the microphones, the output from the transducer amplifiers were recorded on FM tape for off line data reduction.

DATA REDUCTION

Aerodynamic

The aerodynamic data was recorded using the central data processing facility located at NASA Lewis for post run computer processing. A computer located at this facility later reduced the data to engineering units and produced the required output. Mass flow rates were calculated as was the nozzle pressure ratio. Table I list the reading numbers, nozzle pressure ratios, total temperature (TAMB) and pressure (PTS), mass flow rate (W), ambient temperature (TAMB) and pressure (PAMB), and the wind direction and speed.

Acoustic

The acoustic data was recorded on FM tape for post run analysis.

Third octave and overall sound pressure level. - Spectral analysis was performed on a Rockland third octave analyzer and transmitted to the central data processing facility for computer processing. The third octave and overall sound pressure level data were processed and tabulated using an existing acoustic data reduction program. The overall sound pressure level data are tabulated in table II along with the reading numbers and nominal nozzle pressure ratios.

Narrow-band and coherence function. - Narrow-band analysis were made using a Bruel and Kjaer dual channel signal analyzer, type 2032. The analyzer provided narrow-band (autocorrelation) analysis, coherence functions and phase information.

The coherence function provides a measure of the similarity between two signals. If only two signals are present and the coherence function equals unity (1.0), the signals are exactly the same. If the coherence function is zero, the two signals do not have similar time traces and are said to be uncorrelated. For coherence function values between 0 and 1, the similarity of the two signals is not as clearly defined. This is especially true when a second, strong, uncorrelated noise source is present in one of the signals. In general the data taken during these tests, that is, coherence functions between the internal pressure transducers and the far field microphones, are contaminated by the noise made by the jet mixing with the ambient air. This noise is generated outside of the pipe and is not present in the measurements made inside the pipe but is picked up by the far field microphone. When investigating the amount of internal noise reaching the far field using the coherence function between the internal pressure transducers and the far field microphones, the jet noise is a second decorrelating noise source that causes the coherence function to be less then unity. This will be discussed further in the results and discussion section of this report.

For completeness, the data as reduced from the tape recordings are shown in the appendices. Complete third octave spectral data is given in appendix A. Coherence function and phase angle plots are shown in appendix B. Appendix C contains representative cross correlations for internal to far field microphones (part I) and internal to internal pressure transducers (part II). Sample Coherent Output Power spectra and Coherence Function are shown in appendix D. Sample narrow-band Spectra are given in appendix E. For purposes of comparison, the coherence function between transducers 10 (part I) and 9 (part II) to the far field microphones are presented in appendix F. The data used to produce the figures used in the remainder of this report are taken from the appendices.

RESULTS AND DISCUSSION

As discussed in the introduction, the PLF generates noise internally at the flow control valves, the burner, at points of flow separation and along the pipe due to flow generated turbulence. To determine how much of this noise gets to the experimental test hardware downstream of the nozzles, it is necessary to determine what part passes through the nozzle and reaches the acoustic far field. Through the use of the coherence function, one can infer the spectral characteristics that two signals have in common, provided the two signals are not contaminated by other uncorrelated noise sources.

Internal to Far Field Noise

The coherence function between the internal transducer located just upstream of the nozzle (transducer 10) and the far field microphone located at

90° off the jet axis (microphone 4) is shown in figure 4 over a range of nozzle pressure ratios from 1.2 to 3.5. At pressure ratio 1.2 (fig. 4(a)), the value of coherence exceeds 0.6 at a frequency of 238 Hz. Significant coherence exist over the range of frequencies from 0 to 1000 Hz. A secondary peak coherence occurs between 400 and 600 Hz. The jet noise peak frequency based on a Strouhal number of 0.2 is 117 Hz. Since the peak coherent frequencies are well above the jet frequency, it is concluded that noise generated by the jet is not passing upstream through the nozzle thus causing an erroneous coherence between the internal and far field signals. As the nozzle pressure ratio is increased to 1.4 (fig. 4(b)), the coherence decreases at the 238 Hz frequency to 0.5 and the secondary peak also decreases. The peak jet noise frequency is 139 Hz, again well below the peak coherence frequencies. As the pressure ratio increases to near choking (1.8) the coherence decreases (fig. 4(c)), and the 238 Hz peak no longer exist. The peak coherence does, however, exist in the 400 to 800 Hz frequency range. Peak jet noise frequency is approximately 225 Hz. The peak coherence occurs at 690 Hz. Again the conclusion is that the jet noise is not a factor in the coherence function.

The coherence for pressure ratios above choking (figs. 4(d) to (f)), exhibit similar coherence functions but with lower values over the range of frequencies from 400 to 1000 Hz. A peak coherence value of between 0.15 and 0.25 is exhibited in this frequency range. At a pressure ratio of 3.5 the jet noise peaks at 330 Hz, again well below the coherence peak of 600 Hz. As has been discussed, the most probable cause of the decrease in the value of the coherence function is the decorrelating effect of the uncorrelated jet noise signal reaching the far field microphone. This is a problem that was anticipated and should not be a major concern nor detract from the results. The conclusion drawn from figure 4 is that the internal noise, measured by the internal transducer, is reaching the far field microphone throughout the range of nozzle pressure ratios tested. This conclusion applies over a range of frequencies from 0 to 1000 Hz. The frequency for peak noise transmission is in the range of 400 to 800 Hz.

This conclusion explains the early prediction of aircraft core engine noise peak frequency of 400 Hz (ref. 2). It is reasonable to expect the noise generated by the compressor, combustor and turbine to be transmitted through the core engine nozzle and subjected to the same nozzle transfer function as exists in the PLF.

Internal Noise

It is well known, that noise is attenuated as it passes through an elbow. The extent of the attenuation is a function of frequency. For random input to hard wall ducts 1 ft high, one might expect maximum attenuations on the order of 8 dB at a frequency of 600 Hz. Below 200 Hz, no transmission loss is expected and above 2000 Hz the loss is on the order of 3 dB. The one-third octave spectra for transducer number 5 located in the vertical pipe and number 10 located just upstream of the nozzle, figure 3(c) is shown in figure 5(a) as a function of nozzle pressure ratio. Over the range of pressure ratios tested, the transmission loss is relatively constant and is on the order of 40 dB. Part of this loss may be attributed to the elbows between the transducers. Four elbows or tees exist, plus two 45° turns, in the section just upstream of the nozzle. In addition, a flow straightener consisting of a honeycomb section is installed at the tee just upstream of the nozzle. If the equivalent of five elbows are assumed the 8 dB per elbow yields the 40 dB measured value. However the large loss below 200 and that above 2000 Hz cannot be accounted for by elbow transmission loss. It is possible that another process is occurring. The flow after the vertical pipe section leading to the horizontal piping is split and then rejoined at a tee just upstream of the nozzle. Noise coming from upstream is also split and rejoined at the tee. It may be possible that the acoustic waves interfere at the tee and that their amplitude is therefore reduced.

For comparison purposes, figure 5(b) shows transducer numbers 9 and 5 spectra. Transducer number 9 is 2 in. upstream of transducer number 10. At the lower pressure ratios, both transducers 9 and 10 have similar sound pressure level differences (figs. 5(a) and (b)). An anomaly exists in the data that at this time has not been explained. Figure 5(c) shows the spectra for each internal transducer at a pressure ratio of 3.5. Transducer number 10 has a much lower sound pressure level than transducer number 9 even though they are separated by only 2 in. Analysis of the duct acoustics is complicated by reflections from the tees, elbows and nozzle that can cause standing waves in the pipe. The noise also has an unknown distribution as it enters the pipe and that further complicates analysis. Given the limited number of transducers in the pipe further analysis is not likely to provide a reason for this anomaly.

Disregarding the above anomaly, the conclusion drawn from the discussion of figure 5(a) and (b), is that transmission losses on the order of 40 dB can be produced by the elbow and flow splitting arrangement employed in the PLF. It should be pointed out that any flow separation at the elbow could create noise.

Far Field Directivity

The coherence functions for the internal transducer (number 10) to each of the far field microphones are shown in figure 6. For a nozzle pressure ratio of 1.2 (fig. 6(a)), the internal noise radiated from the nozzle appears not to be highly directional. This is consistent with the usual assumption that internally generated noise acts like a monopole source and therefore is radiated equally in all directions. However, as is evident by comparing the coherence function at the 90° to the 60° microphone location, the coherence begins to fall off slightly at the 90° location.

Comparison of figures 6(a) to (b) shows that for all microphone angles, the coherence function decreases with increasing jet velocity (pressure ratio), a result already discussed herein. Since a decrease in the coherence function is expected when jet noise is present, it should be expected that the internal to far field coherence function should be less at the angular positions where the jet noise is the greatest. Jet noise peaks at angles from 30 to 60° off the jet axis and is a function of the jet temperature, probably due to the increased jet velocity with temperature. Cold jets have peak noise closer to the jet axis than hot jets. Examination of figure 6(b) shows a minimal coherence at a frequency of 690 Hz for the 30° microphone location. The coherence is greater in figure 6(c) at the 60 and 90° locations. The same trend exists in figures 6(d) and (e). Finally, at the highest jet velocity, figure 6(f), the maximum coherence exists at the 90° location with the lower angles having much lower values by comparison. This result is expected since lower jet noise exists at the 90° location, thus minimizing the decorrelating effect of jet noise on the internal to far field correlation. This result has extreme implications when the PLF or any jet noise test rig used for jet noise suppressor testing has internal noise present. In fact, the sideline jet noise suppressor results would be wrong causing erroneous results to be reported.

The conclusion based on this discussion is due to the directivity of jet noise, the internal noise is most likely to appear as a noise floor at the sideline measuring point, provided the jet noise has been suppressed. It is imperative that the internal noise be reduced below the acceptable sideline level for jet noise suppressor testing to avoid erroneous test results.

Internal Coherence

The internal fluctuating pressure measured by the transducer, is the resultant sum of the acoustic and turbulent pressures. Turbulence decays with distance and changes its character so that it decorrelates with relative small downstream distances. The coherence function between the upstream transducer, number 5 (upstream vertical pipe section) and the nozzle transducer, number 10 is presented in figure 7(a). The transducers are separated by large distances. Therefore the turbulence is not correlated at either of the transducers though it does exist in each of the pressure measurements. The coherence function therefore is a measure of the acoustic pressure that is transmitted along the pipe. The coherence at a pressure ratio of 1.2 and 3.5 is high at frequencies lower than 440 Hz. This is consistent with the fact that low frequencies tend to be transmitted, while higher frequencies tend to be attenuated by the elbows. The coherence has lower values above 440 Hz but exist up to frequencies on the order of 1200 Hz. The lower magnitude is probably due to elbow and geometry transmission loss.

The coherence function between the nozzle (transducer number 10) and a point 28 in. upstream of the nozzle (transducer number 7), figure 7(b), is a measure of the acoustic signal at the nozzle. The magnitude is larger than the previous comparison, figure 7(a), because little, if any, acoustic transmission loss exists in the pipe section between the transducers. The fact that the coherence function has significant magnitude over the frequency range 0 to 1600 Hz indicates that the acoustic signal is present in the pipe just upstream of the nozzle. The difference between the shape of the coherence function at the nozzle figure 7(b) and the shape of the coherence function between the nozzle and the far field microphones at low pressure ratios figure 4(a), is an indication of the nozzle transmission loss.

The conclusion, drawn from a comparison of figures 4(a) and 7(b), is that the nozzle transmits acoustic waves over the range of frequencies from 0 and 1000 Hz with a maximum between 40 and 300 Hz and secondary maximums between 400 and 800 Hz.

PLF OASPL Directivity

The directivity of the noise generated by the PLF is shown in figure 8. The overall sound pressure level (OASPL) in the acoustic far field is plotted as a function of microphone angular location from the upstream inlet axis (that is 180° minus the microphone angular location measured from the jet axis). At subsonic (fig. 8(a)), and transonic nozzle pressure ratios, the directivity is generally uniform. Jet noise directivity is not typically uniform. This indicates that internal noise is dominating the directivity. For nozzle pressure ratios at and above 2.5 (fig. 8(b)), Mach numbers greater than 1.22, the OASPL peaks at between 120° and 135°. This is the directivity expected for jet noise and indicates the jet noise is dominating the far field measurements above pressure ratios of 2.5. This appears consistent with the coherence function results discussion of figures 4 and 6. The conclusion drawn from this discussion, is that internal noise probably dominates the far field OASPL up to a nozzle pressure ratio of 2.5.

Narrow-band Spectra

Representative narrow-band spectral data are shown in figure 9. Comparison of the coherence function at a pressure ratio of 1.2 (fig. 6(a)), to the narrow-band spectra (fig. 9(a)), shows the narrow-band spectra maximums in the same frequency range as the coherence function maximums, that is around frequencies of 240 and 640 Hz. The conclusion is that narrow-band spectra of the internally generated noise transmitted to the acoustic far field is shown in figure 9(a).

Small, supersonic jets often generate tones as a result of an acoustic feedback from the jet mixing layer to the shear layer at the nozzle exit. These tones tend to dominate the OASPL. Large nozzles such as the one used on the PLF generally do not exhibit such tones. The PLF nozzle tested, however, did generate a strong tone at 362 Hz and its harmonics as shown in figure 9(b).

The conclusion drawn from this discussion is that the internal noise transmitted to the acoustic far field is broad-banded around a frequency of 640 Hz. As the nozzle pressure ratio is increased, the jet experiences the acoustic feed back that causes a large amplitude tone to be generated at 362 Hz and multiples thereof.

Overall Sound Pressure Level

Due to the limited number of microphones used for these tests it was not possible to determine the total acoustic power generated by the facility. A comparison of the PLF noise to prediction was not attempted. However, for informational purposes, a plot of the OASPL as a function of nozzle pressure ratio is shown in figure 10. Figure 10(a) shows the far field microphone data. Above a pressure ratio of 2.5 the OASPL increases approximately 40 dB for all microphone locations. The tones account for a significant portion of the 40 dB increase.

Figure 10(b) shows the OASPL results from the internal transducer measurements. The upstream transducers (numbers 5 and 6) are not highly dependent on pressure ratio. The transducers, located in the pipe immediately upstream of the nozzle, show an increase in level around a pressure ratio of 2.5 with the exception of transducer number 10. Transducer number 10 OASPL decreases at a pressure ratio of 2.3. No explanation for transducer number ten's behavior is presently available. Comparison of the coherence function between transducer number 9 and the far field microphones and transducer number 10 to the far field microphones were made in appendix F to validate the use of transducer 10 in this report. The coherence functions were the same for both transducer 9 and 10. The conclusion then was that the use of transducer number 10 data was justified.

Internal Noise Spectra In The Far Field

The coherence function between the internal pressure transducer at the nozzle and the far field microphones indicates a range of frequencies where the internal noise reaches the far field. The decorrelating effect of the jet noise tends to mask some of the internal noise in the far field so that the value of the coherence function cannot be considered completely definitive. As shown in figure 4 broad-banded coherence exists at 240 and 700 Hz. The far field one-third octave spectra shown in figure 11(a) (square symbols) have peaks at 250 and between 630 and 4000 Hz, corresponding to band numbers 24 and 28-36. The peak at 125 Hz (band number 21) corresponds to the jet noise peak for a Strouhal number of 0.2 and nozzle diameter of 1 ft. The conclusion is that the third octave far field spectra is dominated by the internal noise at a pressure ratio of 1.2 at the 90° sideline location. As the pressure ratio is increased through 1.8, the coherence occurring in the 630 to 1000 range remains (fig. 4). The peak third octave spectra begins in this range and extends to 4000 Hz (fig. 11(a)).

Between a pressure ratio of 1.8 and 2.0, (at choking) the magnitude of the spectra drops 20 dB but its peak remains in the internal noise frequency range (630 to 4000 Hz). This drop could be the result of choking on the nozzle acoustic transfer function. As the pressure ratio is increased above 2 (fig. 11(b)), the broad-banded peak stays in the internal noise frequency range (1600 Hz) except where aeroacoustic feedback creates tones (bands numbers 26 and 29, 400 and 800 Hz filter bands respectively, see fig. 9(b) for narrow band data).

At 60° (figs. 11(c) and (d)), similar results are found. However, at 45° (fig. 11(e)), and at pressure ratios above 1.8 (fig. 11(f)), the peak sound pressure level (SPL) occurs at 315 Hz. Based on a Strouhal number of 0.2 the jet noise peaks at 330 Hz. The conclusion is that at a pressure ratio above 1.8 and microphone angles of 45° the jet noise begins to dominate. At 30° (fig. 11(g)), and pressure ratios of 1.2 and 1.4 the internal noise dominates but above 1.4 fig. 11(h)), the jet noise dominates at the 315 Hz frequency. The conclusion is that up to a nozzle pressure ratio of 1.4 the internal noise dominates the far field SPL at microphone angles from 30° through 90°. At the 60° and 90° microphone locations, the SPL are completely dominated by internal noise. At the 30° and 45° microphone locations and above nozzle pressure ratios of 1.4 the SPL are dominated by jet noise. These conclusions are consistent with the coherence analysis of figure 6.

CONCLUDING REMARKS

It has been shown, through the use of coherence functions, that the internal noise generated in the PLF that reaches the acoustic far field has a frequency less than 1200 Hz and exhibits broad banded peaks at 240 and 600 Hz. Spectral analysis has shown that internal noise that reaches the far field exceeds the 1200 Hz and may be transmitted up to and possibly exceeding 5000 Hz. Reference 1 states that jet shear layers can be excited at Strouhal number of 0.5 and shows graphic evidence of the result of such excitation. For the PLF the excitation frequency based on the Strouhal number of 0.5 would be on the order of 500 Hz. This frequency is close to the measured internal noise frequency and should cause alarm when planning jet type experiments for the PLF.

For experiments evolving wings operating at high angles of attack, reference 1 shows that the flow attachment can be modified when the flow is excited at Strouhal number of 4. For a wing chord of 5 ft, the excitation frequency would be approximately 800 Hz or less. Again this frequency falls within the measured frequency range for the PLF. Thus, it appears that a real need exists to evaluate the effect of PLF internally generated noise on any prospective test hardware, and that steps be taken to decrease the internal noise to an acceptable level.

Another aeroacoustic effect in reference 6, is the increases of thrust due to the screech tones generated by primary nozzles in ejectors. These tones can excite the jet mixing thus increasing the ejector thrust. Since tones exist in the PLF nozzle, thrust modification could result.

Finally, as has been pointed out in this report, internal noise generated in the PLF creates a noise floor for the facility. This noise floor will prevent the testing of jet noise suppressors since when the jet noise is suppressed the internal noise floor is measured instead of the true jet noise suppression. In fact this was the case in a previous jet noise facility located in the same area as PLF some years ago. If noise of any kind is to be measured at the PLF, the internal noise must be reduced to an acceptable level.

CONCLUSIONS

1. Broad banded noise is generated in the system by air flowing through the valves, burner and associated piping.

2. Below a frequency of 5000 Hz noise is transmitted via the piping and through the nozzle to the acoustic far field over the range nozzle pressures (1.2 to 3.5) tested.

3. Coherence from the internal to far field microphones was greatest at low nozzle pressure ratios. This indicates that the coherence measurements were affected by the jet noise source acting as a second noise source observed by the far field microphones, thus causing a decreased coherence as the jet noise increased.

4. Pipe elbows and facility geometry reduce the fluctuating pressure levels by as much as 40 dB over frequency range from 50 to 10 kHz.

5. The value of the coherence function from internal to far field microphones increased with angle from the jet axis; a result that is consistent with a decrease of jet noise with angular displacement.

6. The internally generated noise below a frequency of 1600 Hz may affect the test results of any shear layer such as jets, boundary layers, flow over airfoils, and ejector mixing regions.

7. The internally generated noise creates a system noise floor that will prevent proper jet noise suppressor evaluation tests from being performed in this facility.

PLF RECOMMENDATIONS

1. Low and medium (100 through 10 000 Hz) frequency mufflers should be installed in the straight pipe section as close as possible to the nozzle.

2. The muffler must be broad banded and reduce noise in the 50 to 1600 Hz band width. Multiple mufflers in series may be required to obtain the required insertion loss.

3. The existing valves should be replaced with quiet valves that produce high frequency noise that is more easily absorbed by mufflers and lined elbows.

4. To absorb the valve generated noise, mufflers should be placed in the line just down stream of the low noise valves. This will minimize the amplification of the valve noise by the combustor.

5. One must be aware that low frequency noise is generated by combustors. Therefore when heated air is required, the low frequency mufflers will be a necessary part of the piping downstream of the combustor.

REFERENCES

1. Stone, J.R.; and McKinzie, D.J., Jr.: Acoustic Excitation - A Promising New Means of Controlling Shear Layers. NASA TM-83772, 1984.

2. Huff, R.G.; Clark, B.J.; and Dorsch, R.G.: Interim Prediction Method For Low Frequency Core Engine Noise. NASA TM X-71627, 1974.

3. Huff, R.G.: A Theoretical Prediction of the Acoustic Pressure Generated by Turbulence-Flame Front Interactions. J. Vibration, Acoustics, Stress, and Reliability in Design, vol. 108, no. 3, July 1986, pp. 315-321.

4. Huff, R.G.: The Effect of Acoustic Wave Reflections on Combustor Noise Measurements. J. Propulsion Power, vol. 2, no. 1, Jan-Feb. 1986, pp. 18-24.

5. Huff, R.G.: Noise Generated by Flow Through Large Butterfly Valves. NASA TM-88911, 1987.

6. Quinn, B.: Interactions Between Screech Tones and Ejector Performance. J. Aircraft, vol. 14, no. 5, May 1977, pp. 467-473.

APPENDIX A

ONE-THIRD OCTAVE SPECTRAL

DATA PLOTS

APPENDIX A

PART I

FAR FIELD MICROPHONE DATA

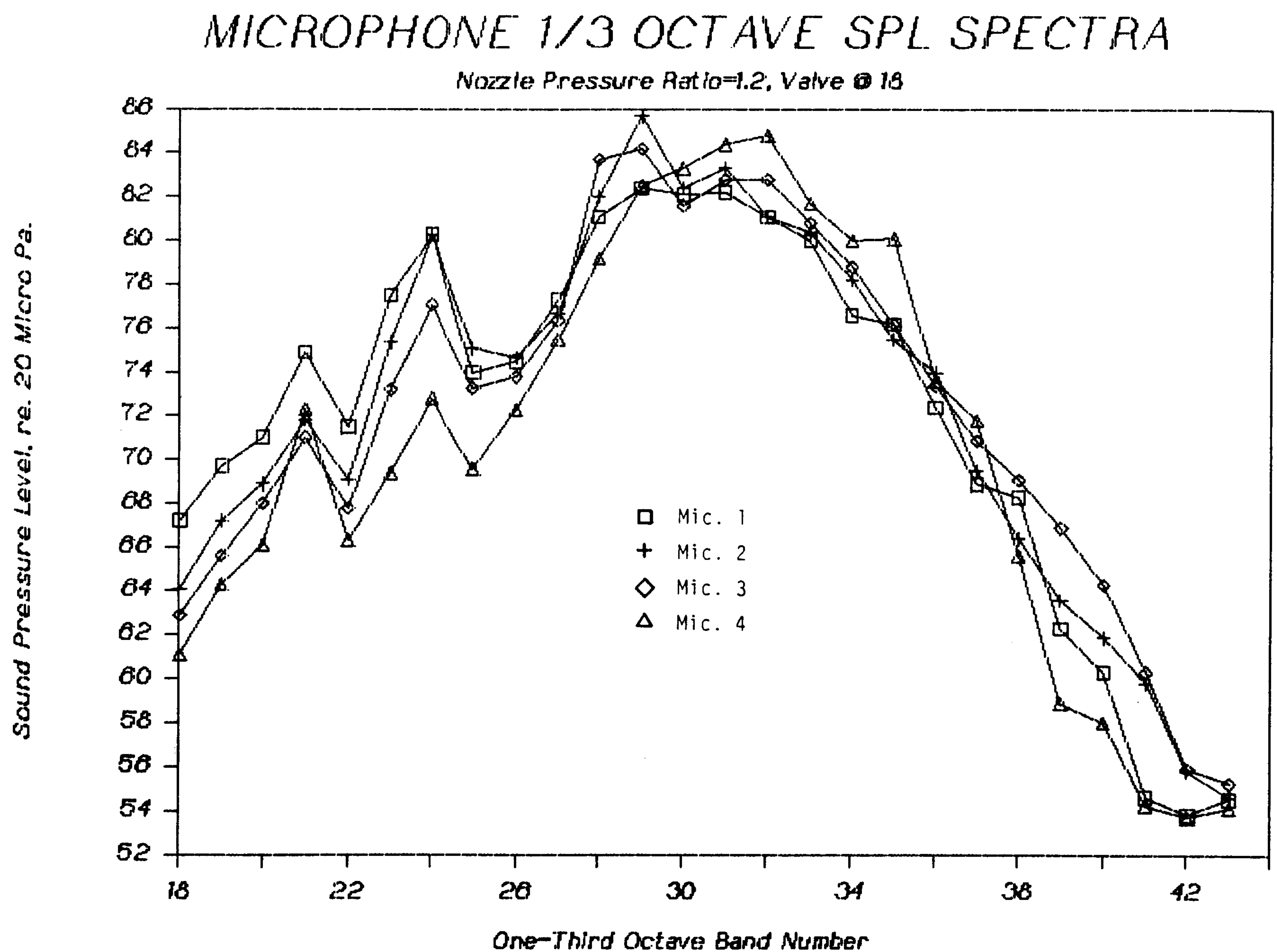
MICROPHONE 1/3 OCTAVE SPL SPECTRA
Nozzle Pressure Ratio=1.2, Valve @ 18
Sound Pressure Level, re. 20 Micro Pa.
86
84
82
80
78
76
74
72
70
68
66
64
62
60
58
56
54
52
18
22
26
30
34
38
42
One-Third Octave Band Number
Mic. 1
Mic. 2
Mic. 3
Mic. 4

ORIGINAL PAGE IS
OF POOR QUALITY

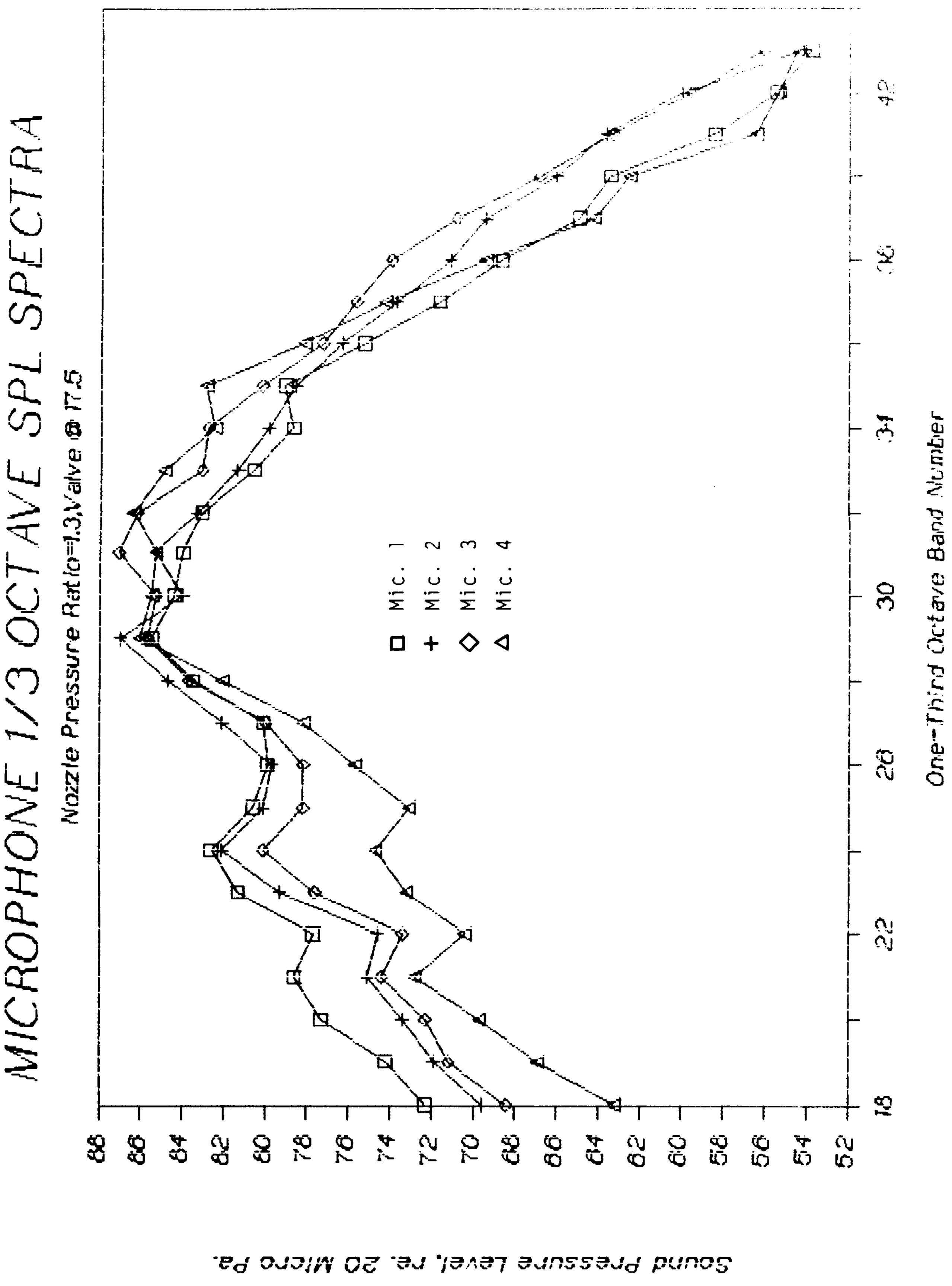

ORIGINAL PAGE IS OF POOR QUALITY

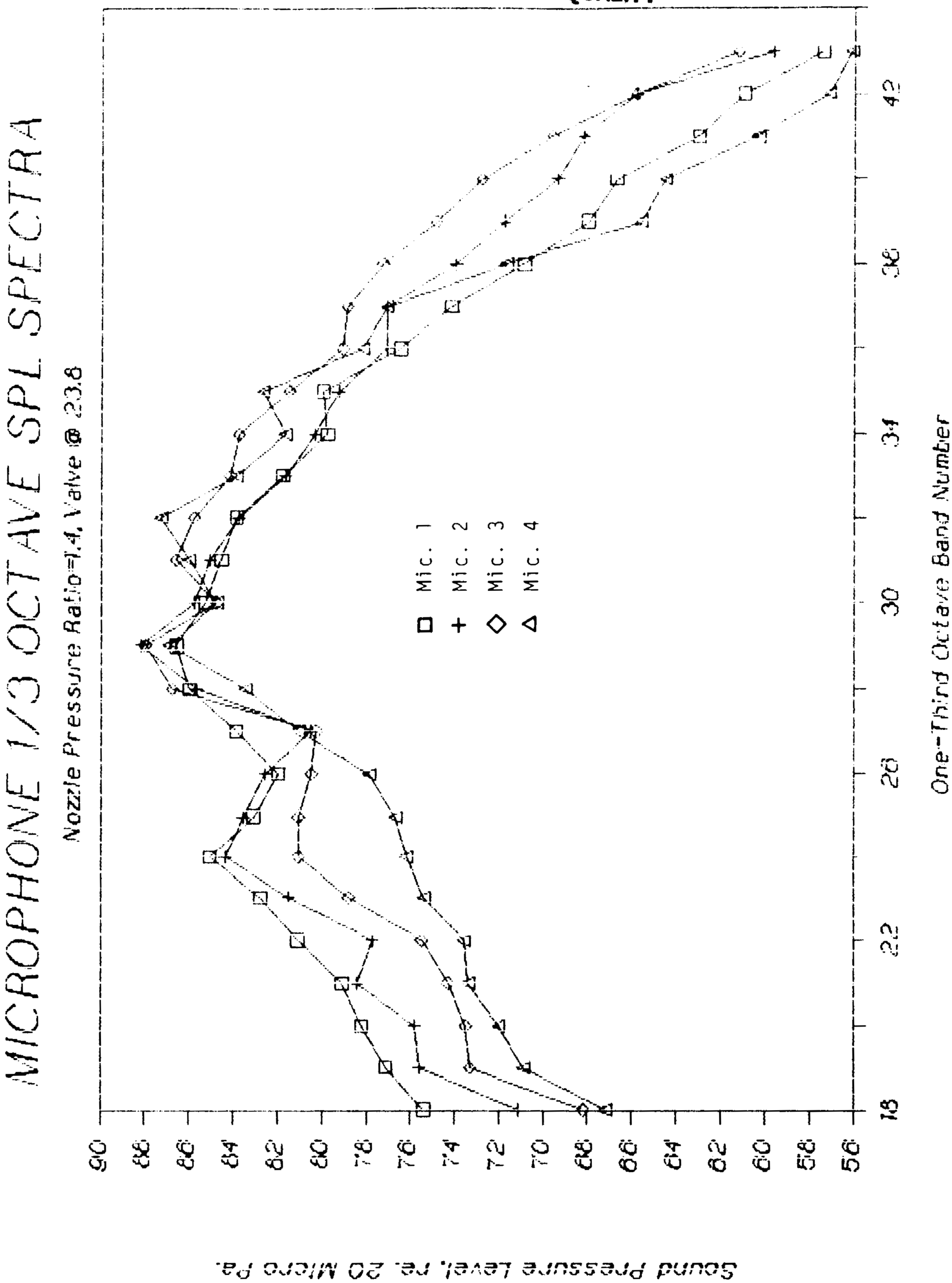

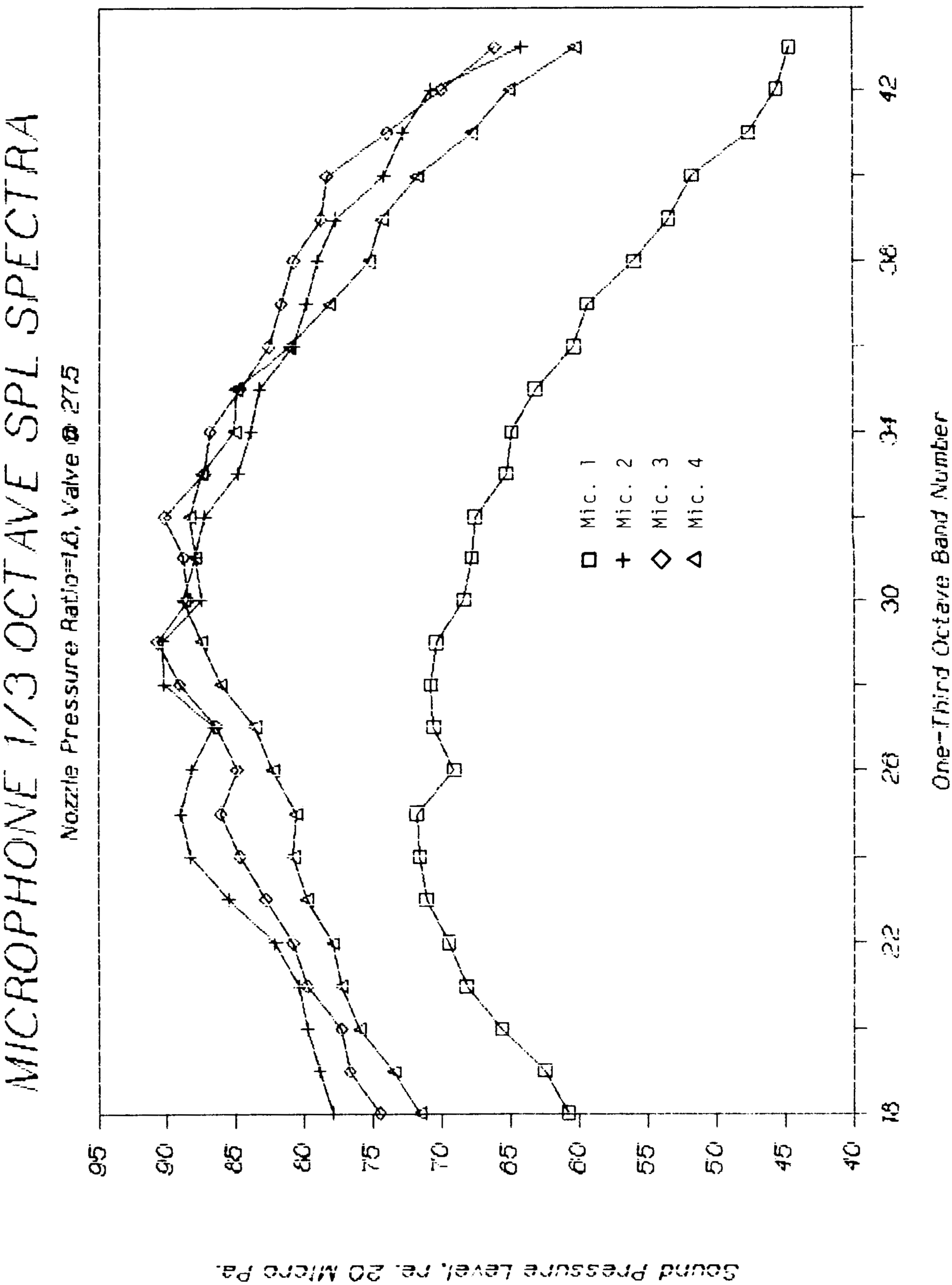

ORIGINAL PAGE IS OF POOR QUALITY

ORIGINAL PAGE IS OF POOR QUALITY

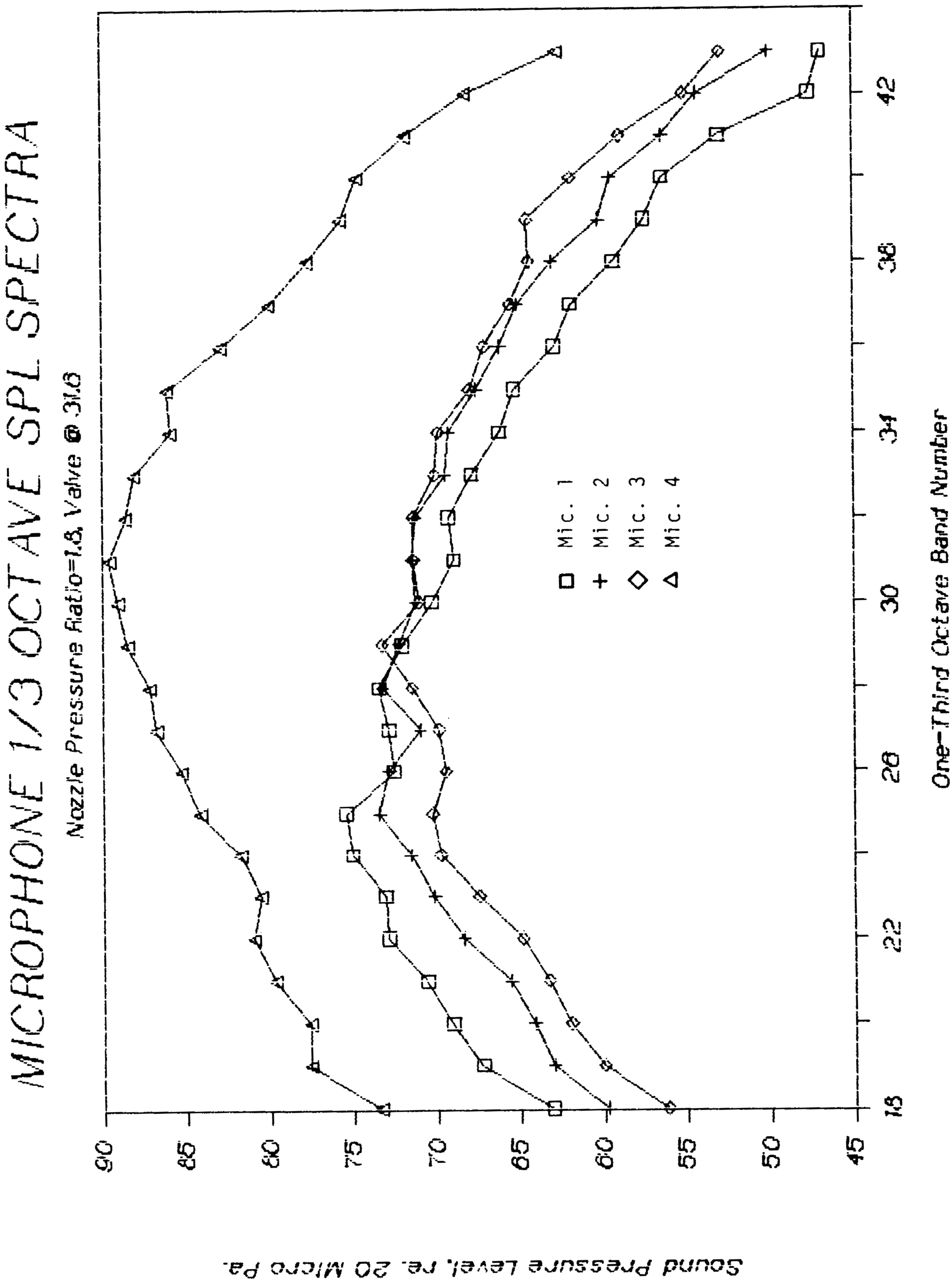

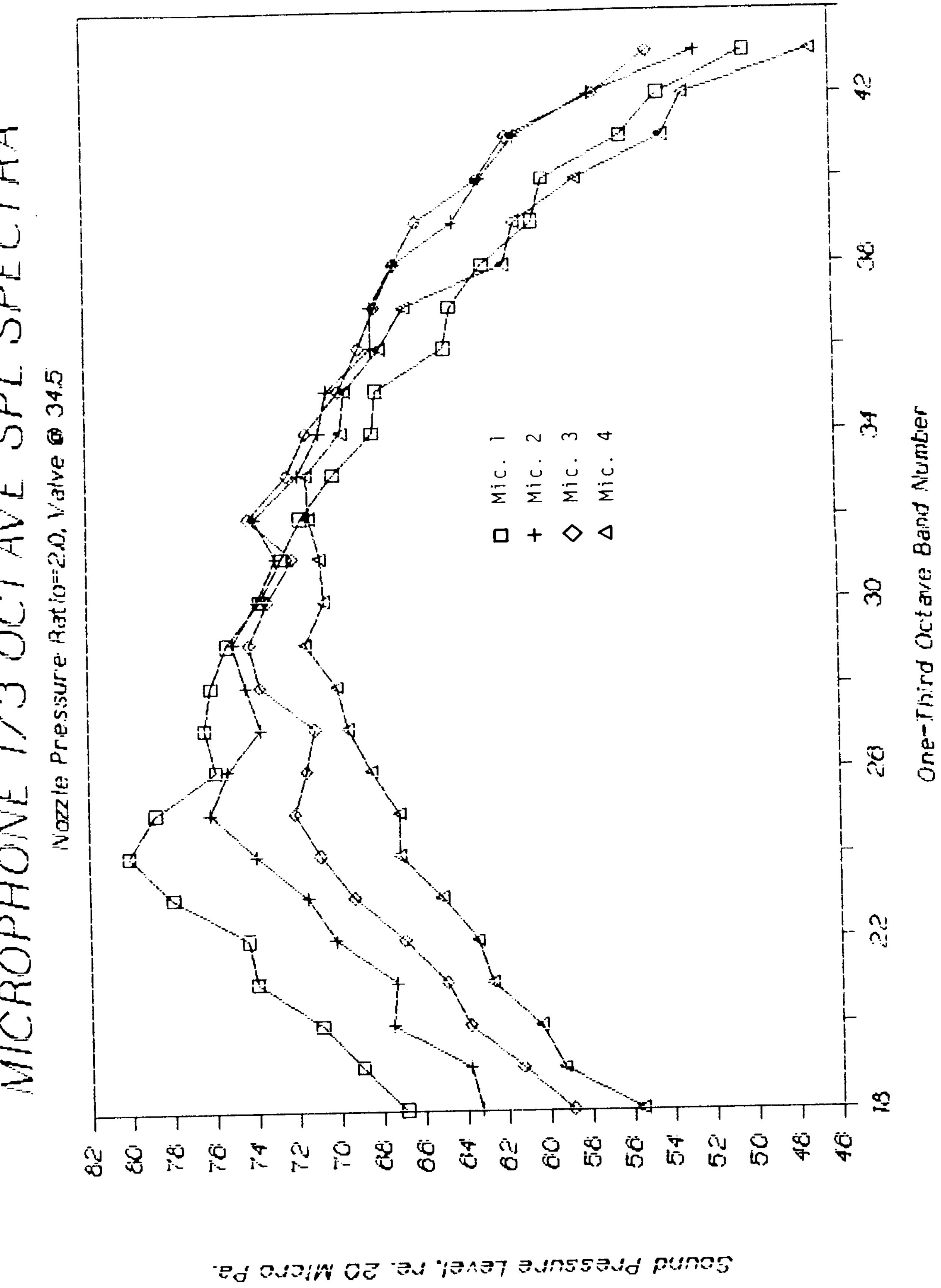

ORIGINAL PAGE IS
OF POOR QUALITY

**ORIGINAL PAGE IS
OF POOR QUALITY**

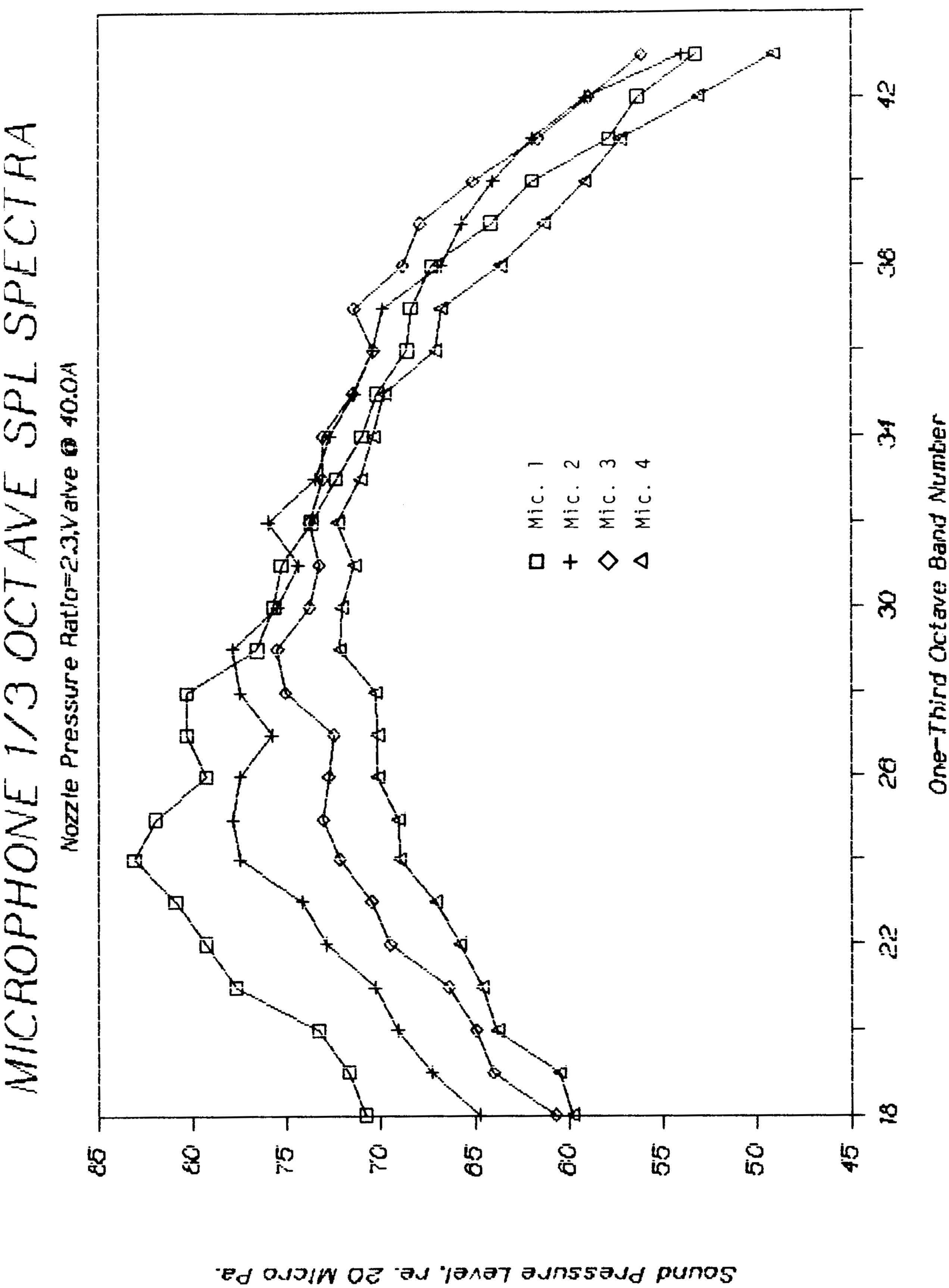

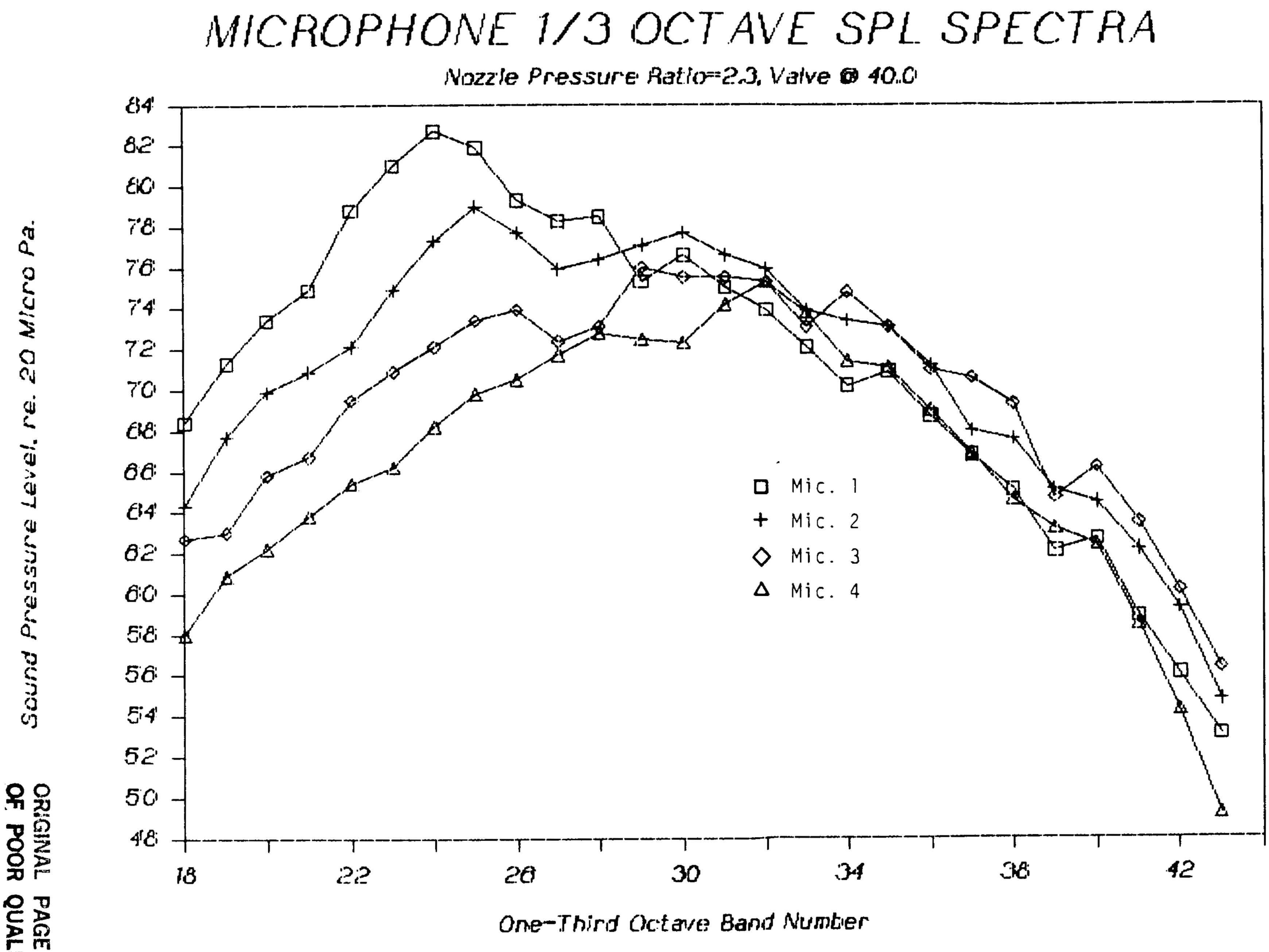

ORIGINAL PAGE IS
OF POOR QUALITY

ORIGINAL PAGE IS OF POOR QUALITY

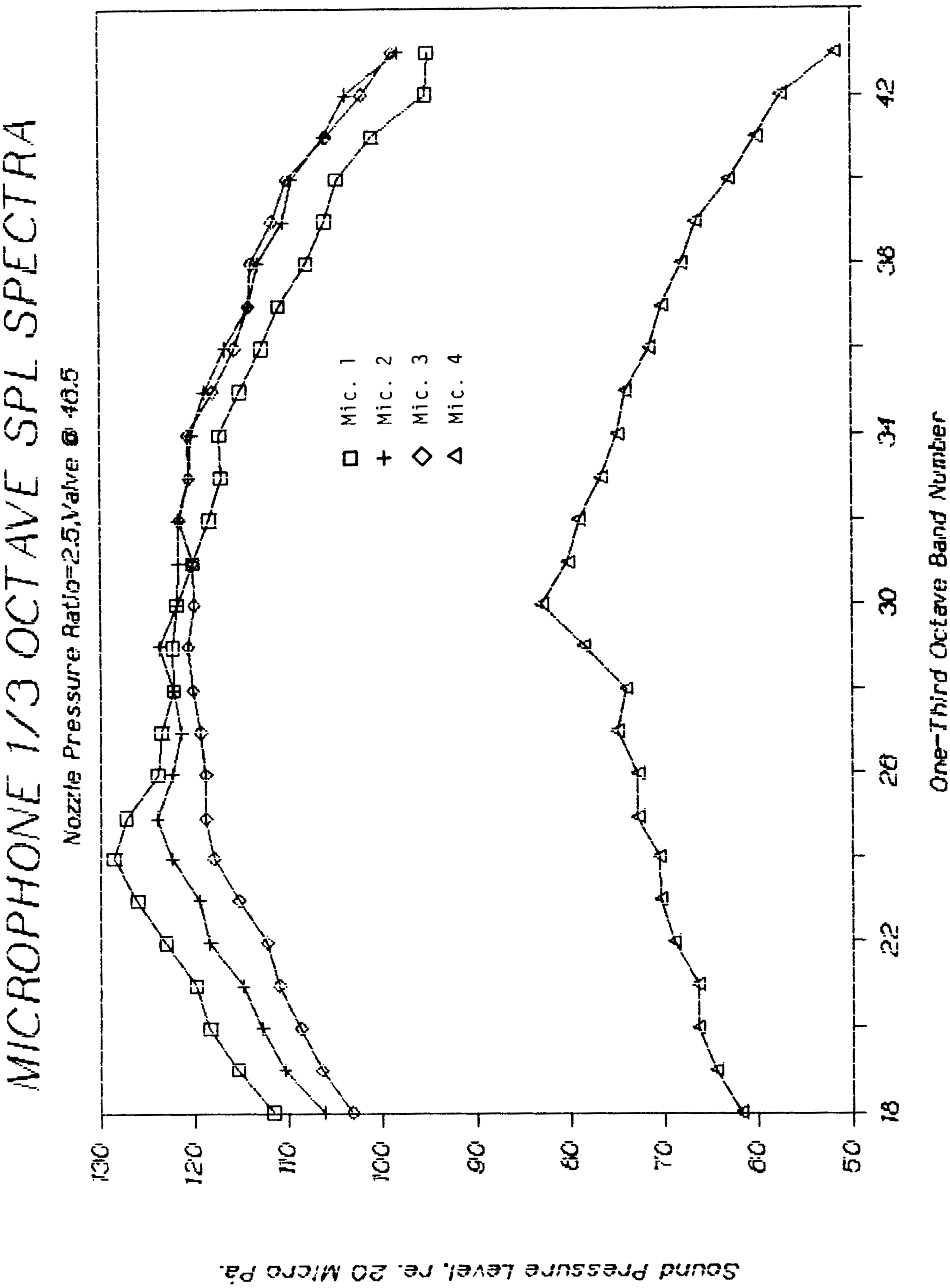

MICROPHONE 1/3 OCTAVE SPL SPECTRA

Nozzle Pressure Ratio=3.0,Valve @ 70.8

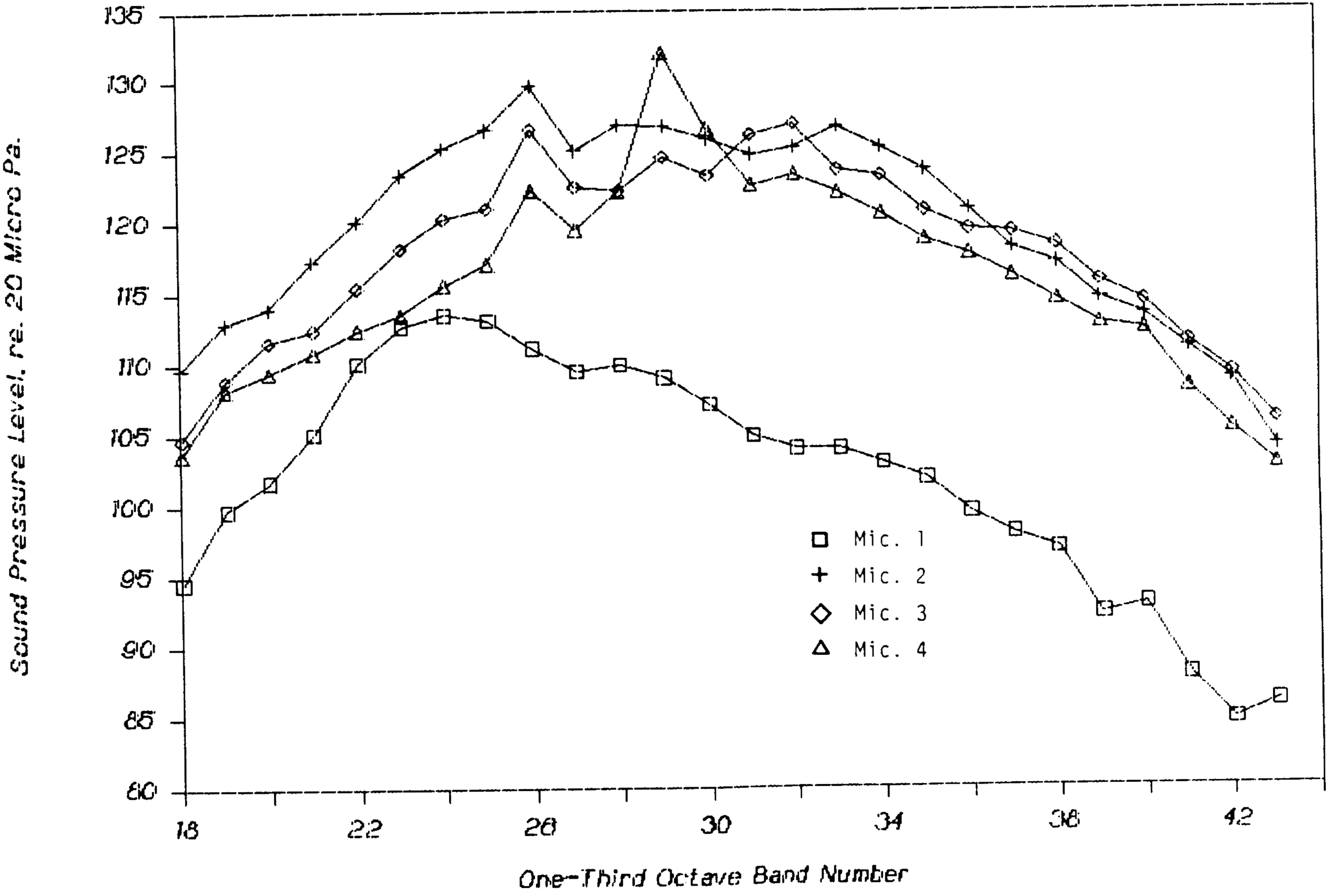

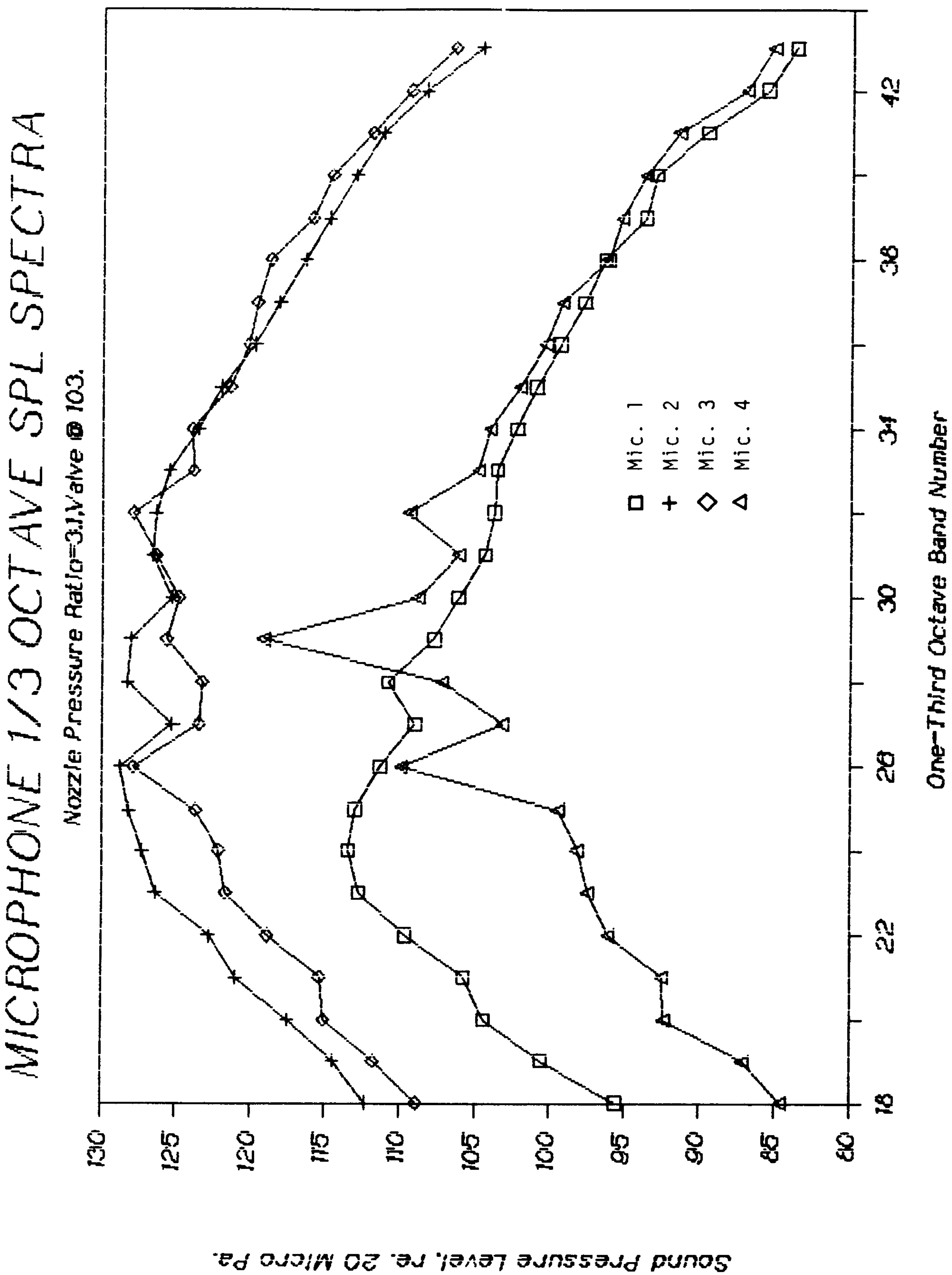
MICROPHONE 1/3 OCTAVE SPL SPECTRA
Nozzle Pressure Ratio=3.1,Valve @ 103.
Mic. 1
Mic. 2
Mic. 3
Mic. 4
One-Third Octave Band Number
18
22
26
30
34
38
42
Sound Pressure Level, re. 20 Micro Pa.
130
125
120
115
110
105
100
95
90
85
80

MICROPHONE 1/3 OCTAVE SPL SPECTRA

Nozzle Pressure Ratio=3.5,Valve @ 83.1

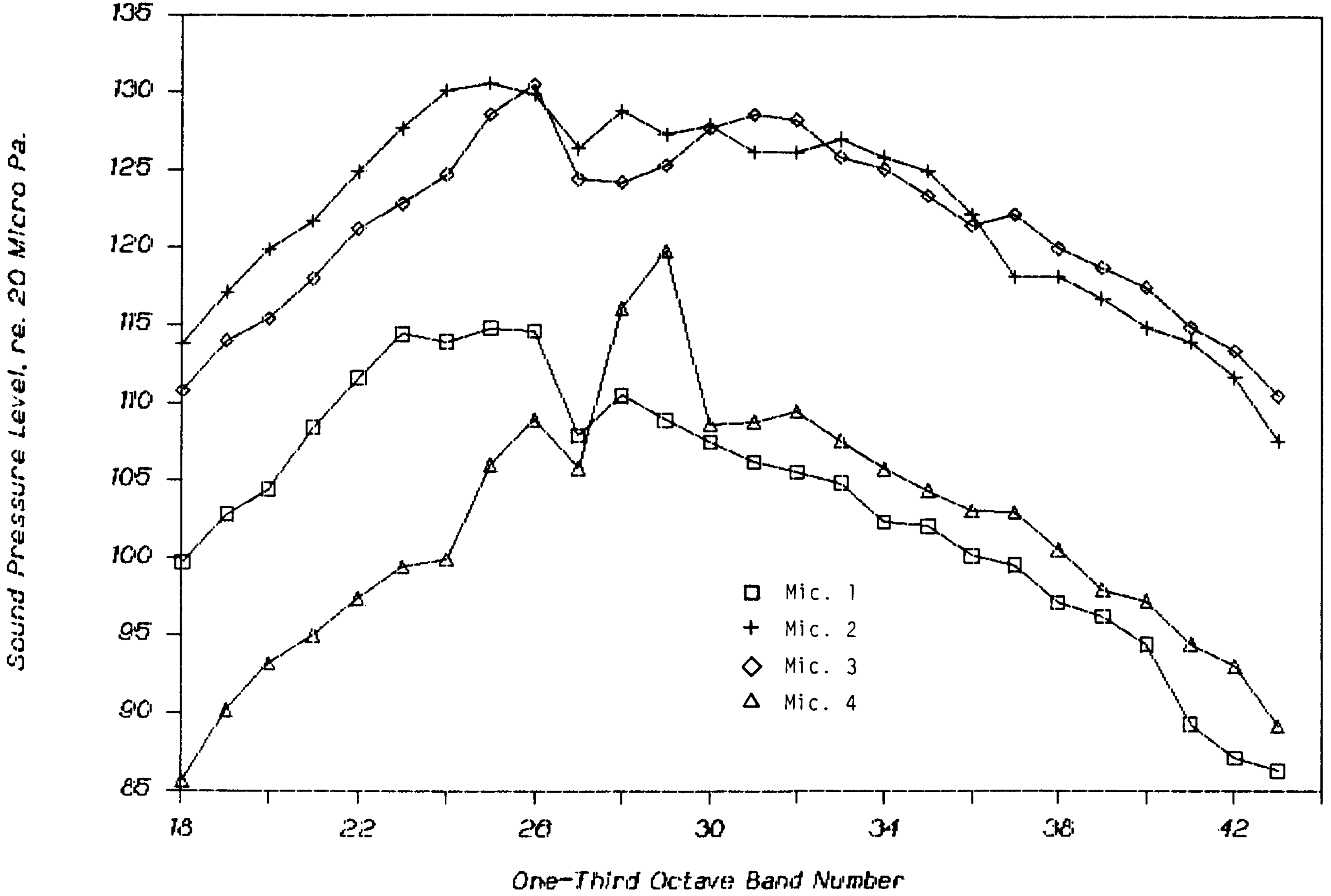

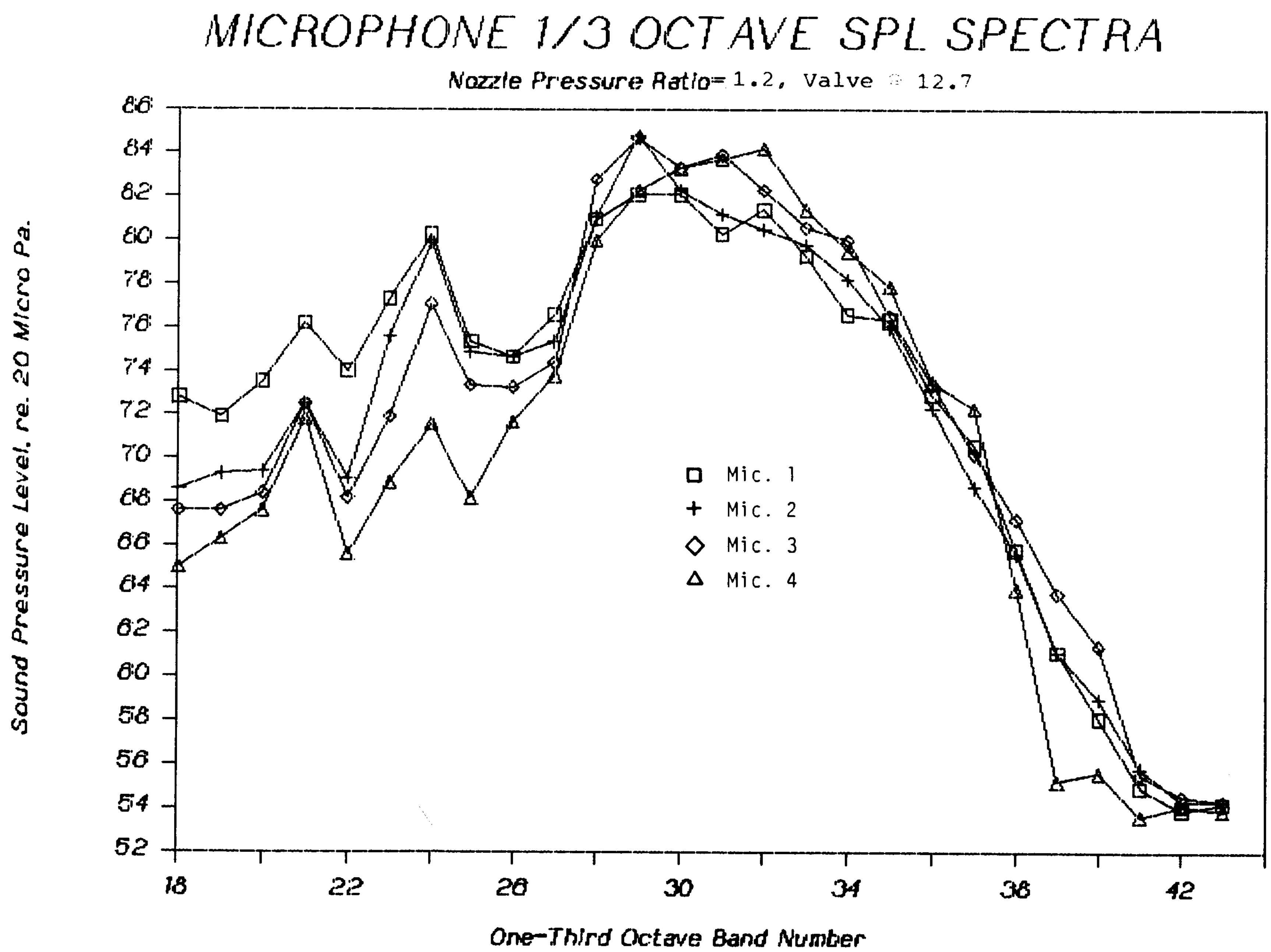

MICROPHONE 1/3 OCTAVE SPL SPECTRA
Nozzle Pressure Ratio= 1.2, Valve @ 12.7
Mic. 1
Mic. 2
Mic. 3
Mic. 4
Sound Pressure Level, re. 20 Micro Pa.
One-Third Octave Band Number

MICROPHONE 1/3 OCTAVE SPL SPECTRA

Nozzle Pressure Ratio=1.8,Valve @23.7A

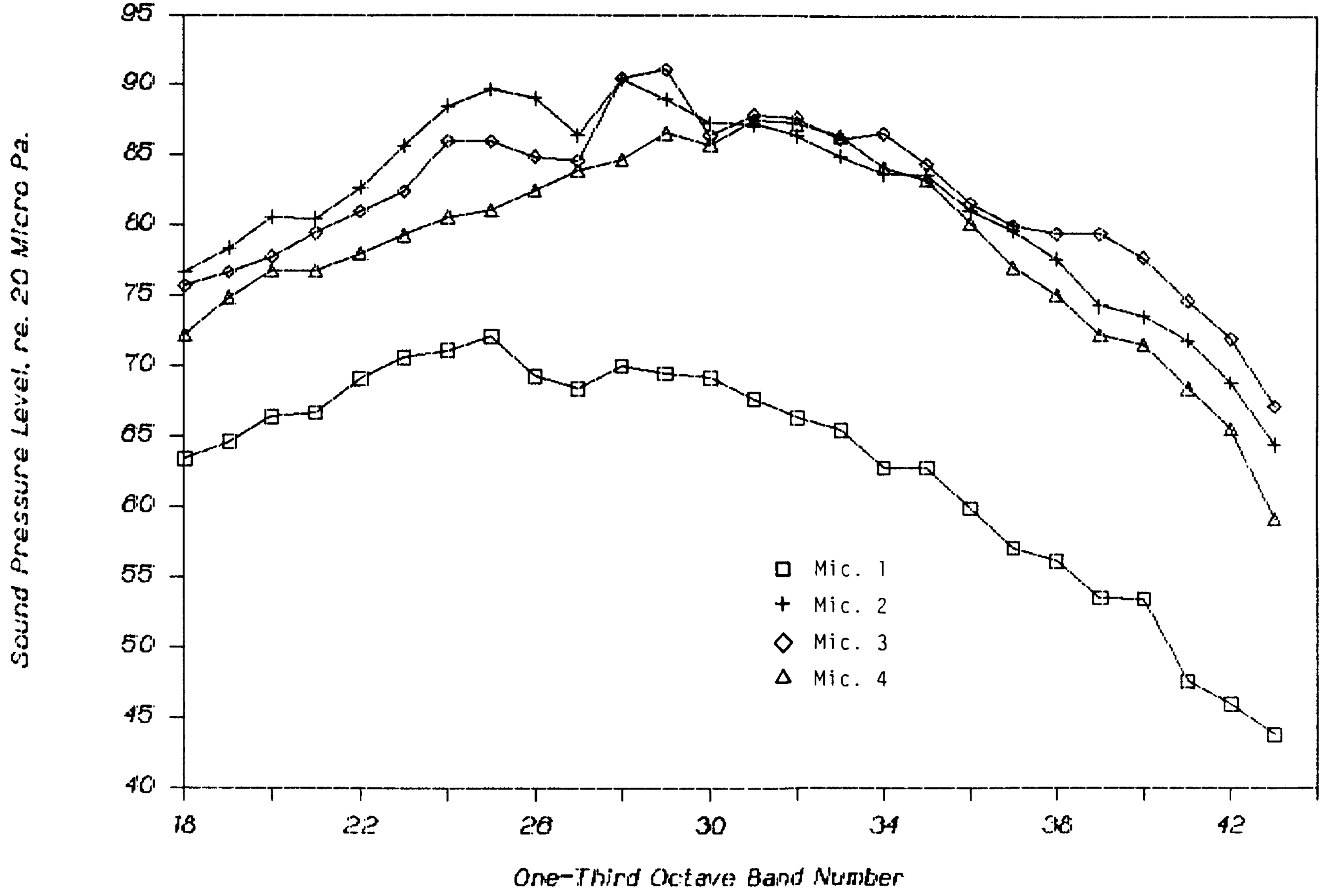

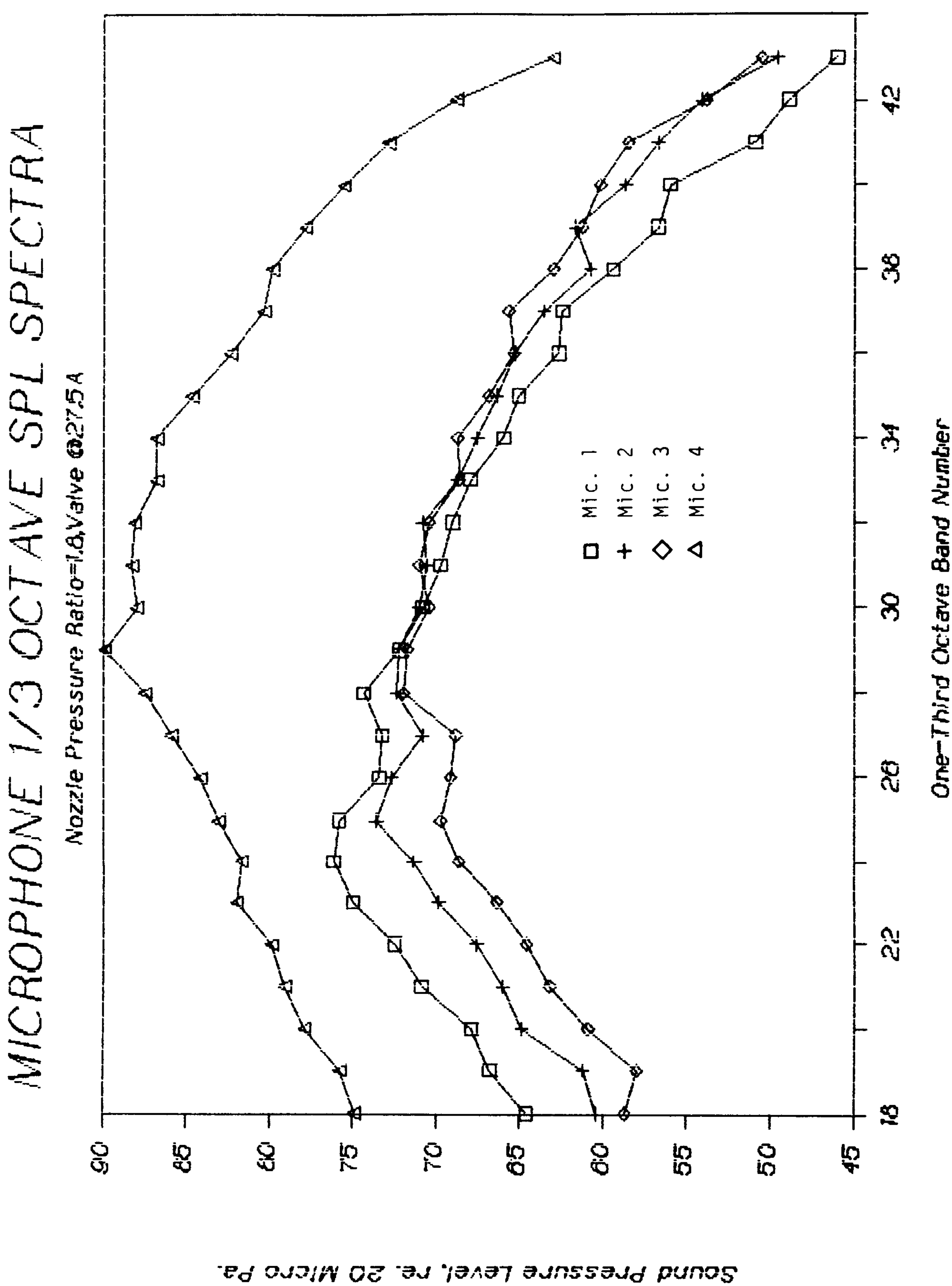
MICROPHONE 1/3 OCTAVE SPL SPECTRA
Nozzle Pressure Ratio=1.8,Valve @27.5A
Mic. 1
Mic. 2
Mic. 3
Mic. 4
One-Third Octave Band Number
Sound Pressure Level, re. 20 Micro Pa.
18
22
26
30
34
38
42
90
85
80
75
70
65
60
55
50
45

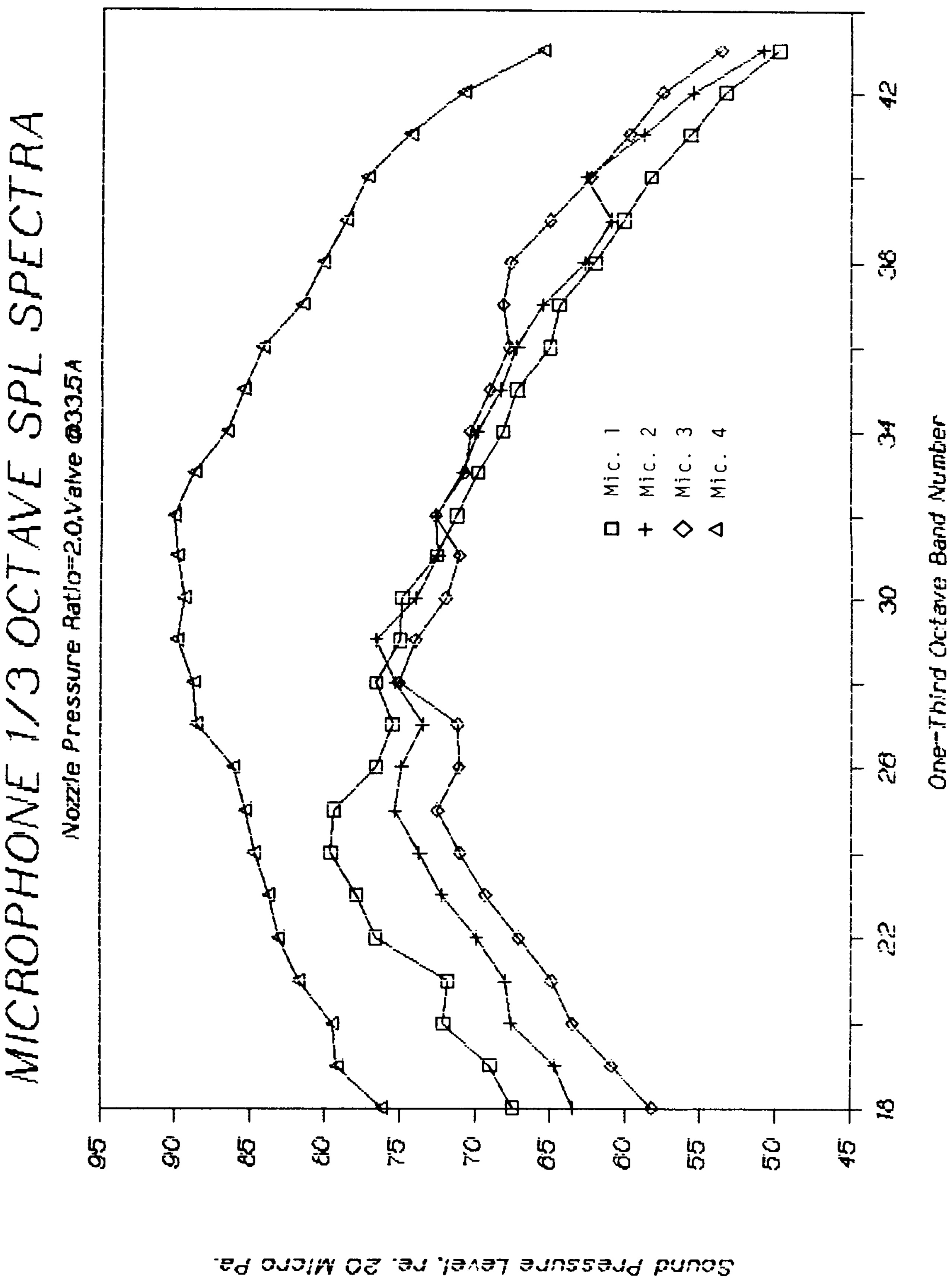
MICROPHONE 1/3 OCTAVE SPL SPECTRA
Nozzle Pressure Ratio=2.0,Valve @33.5A
Mic. 1
Mic. 2
Mic. 3
Mic. 4
Sound Pressure Level, re. 20 Micro Pa.
95
90
85
80
75
70
65
60
55
50
45
One-Third Octave Band Number
18
22
26
30
34
38
42

APPENDIX A

PART II

INTERNAL PRESSURE TRANSDUCER DATA

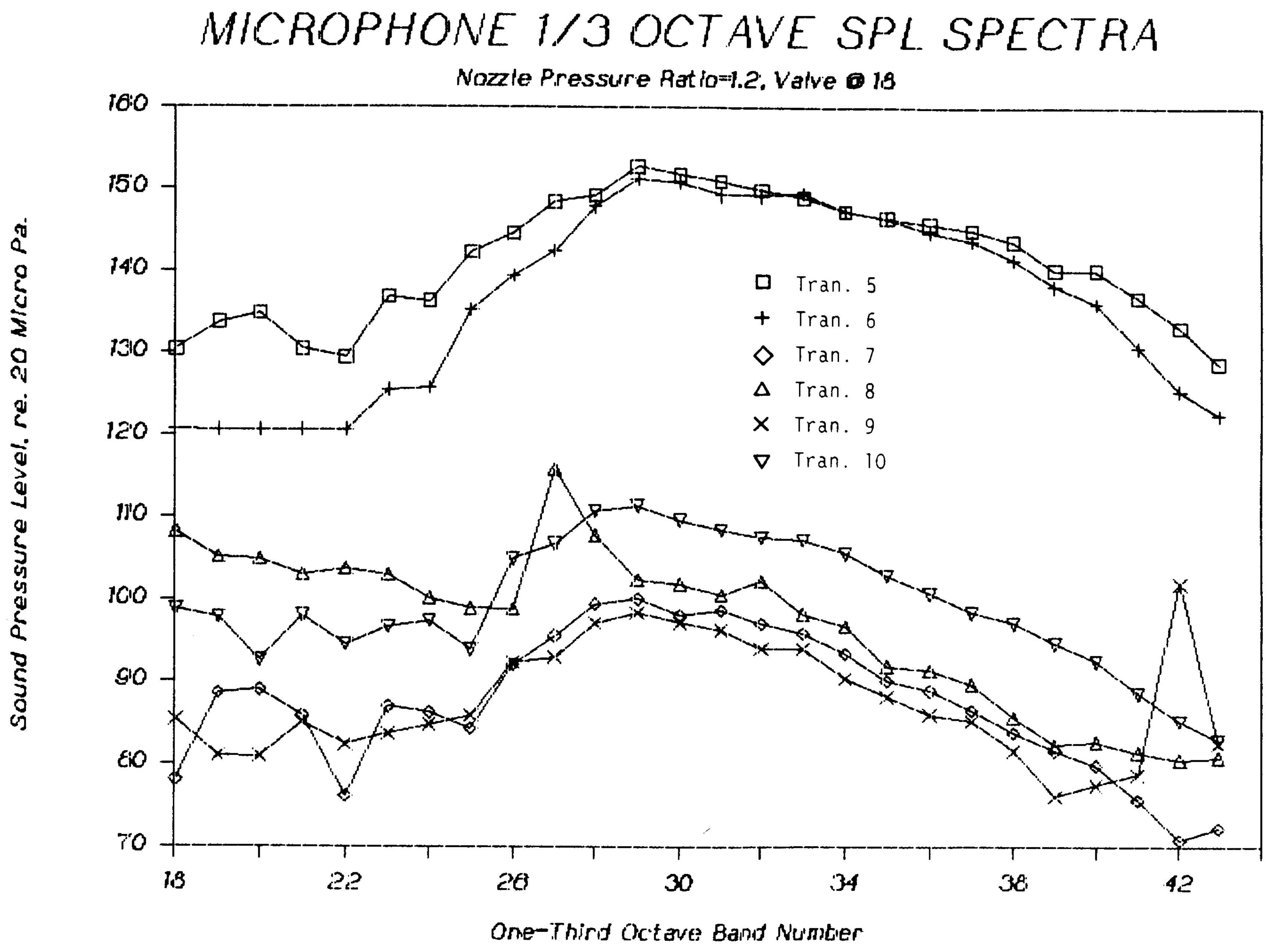
MICROPHONE 1/3 OCTAVE SPL SPECTRA
Nozzle Pressure Ratio=1.2, Valve @ 18
Tran. 5
Tran. 6
Tran. 7
Tran. 8
Tran. 9
Tran. 10
Sound Pressure Level, re. 20 Micro Pa.
One-Third Octave Band Number
160
150
140
130
120
110
100
90
80
70
18
22
26
30
34
38
42

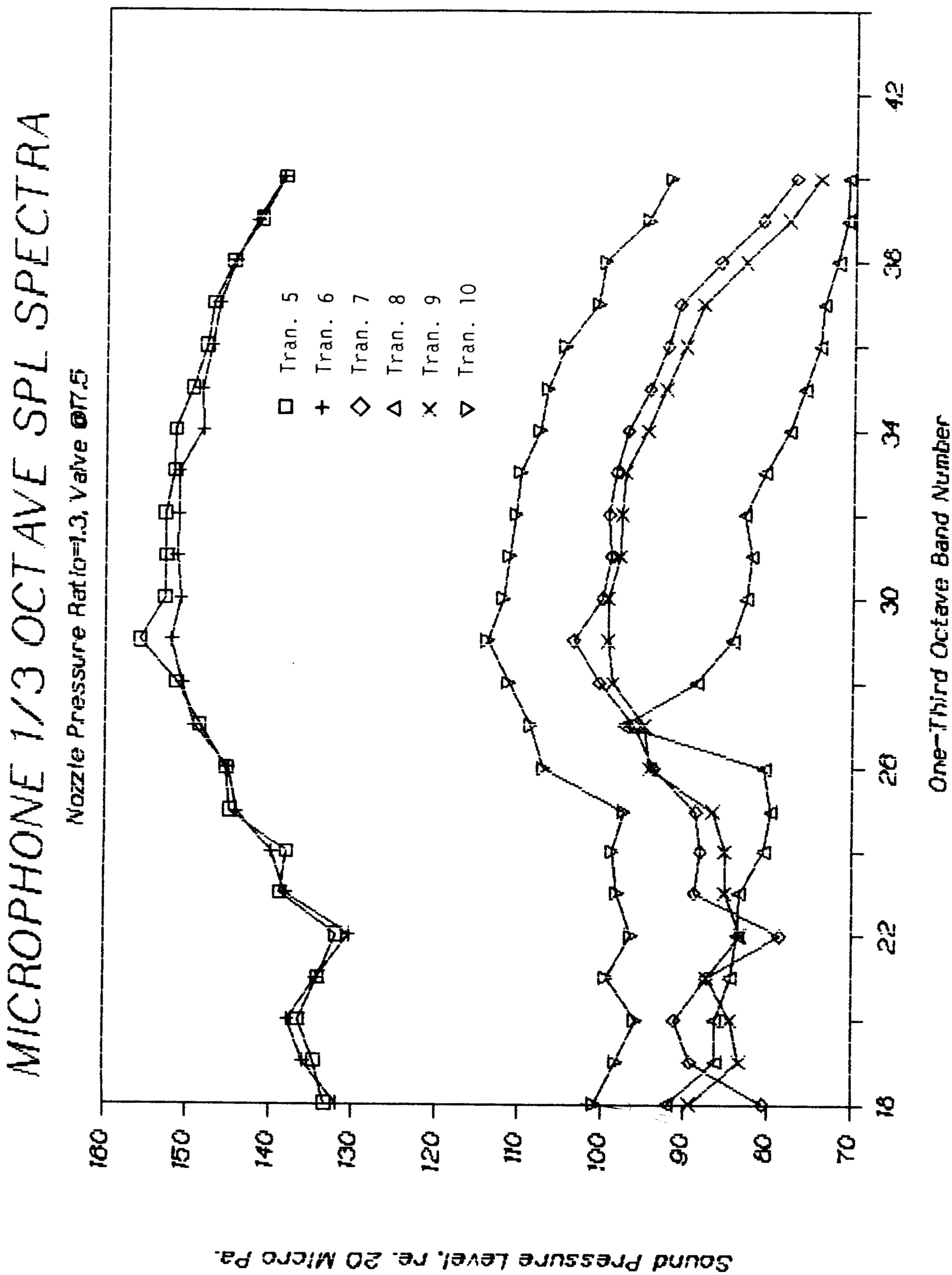
MICROPHONE 1/3 OCTAVE SPL SPECTRA
Nozzle Pressure Ratio=1.3, Valve @17.5
Tran. 5
Tran. 6
Tran. 7
Tran. 8
Tran. 9
Tran. 10
Sound Pressure Level, re. 20 Micro Pa.
One-Third Octave Band Number
160
150
140
130
120
110
100
90
80
70
18
22
26
30
34
38
42

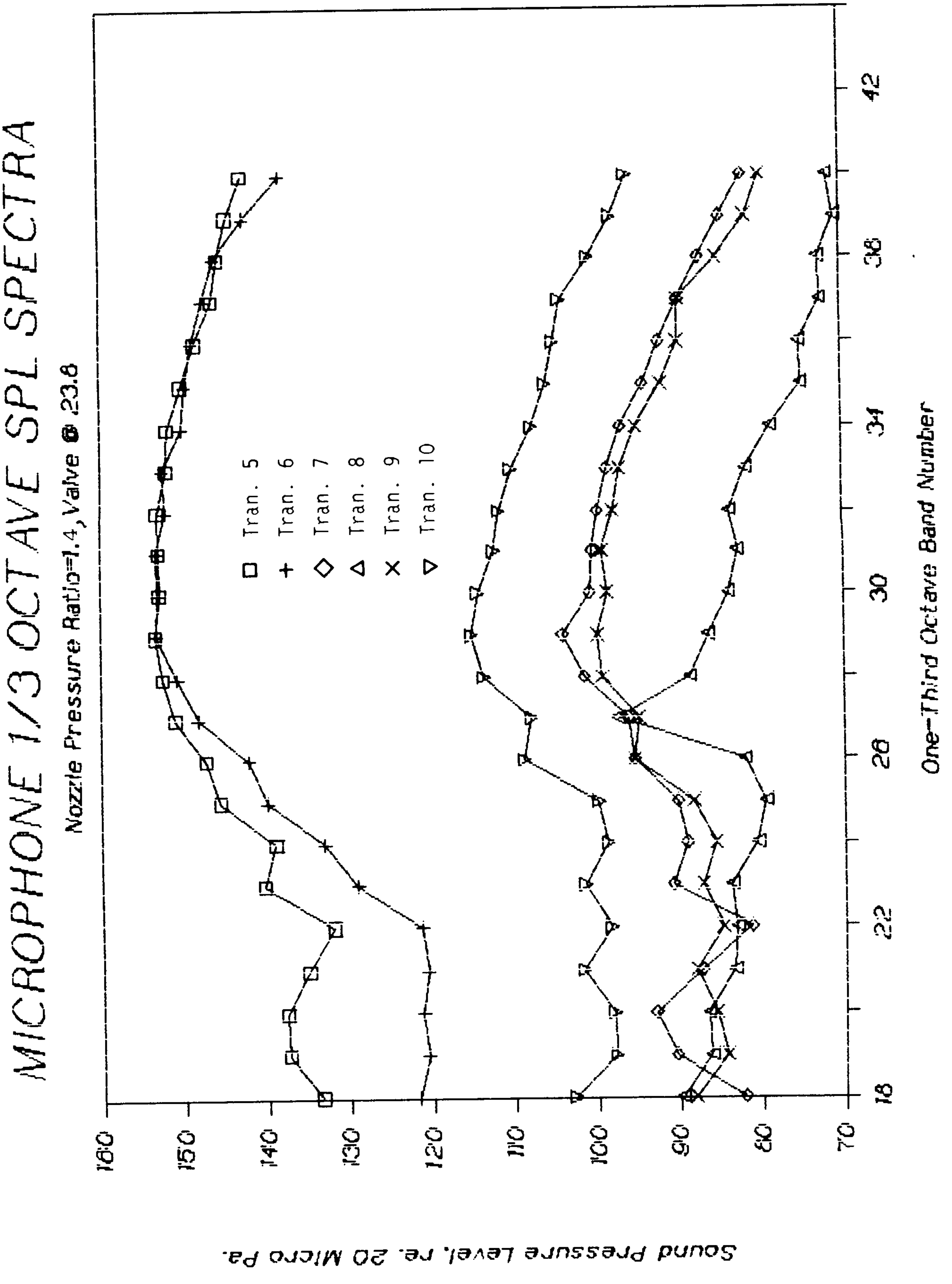

MICROPHONE 1/3 OCTAVE SPL SPECTRA
Nozzle Pressure Ratio=1.4, Valve @ 23.8
Tran. 5
Tran. 6
Tran. 7
Tran. 8
Tran. 9
Tran. 10
Sound Pressure Level, re. 20 Micro Pa.
One-Third Octave Band Number
160
150
140
130
120
110
100
90
80
70
18
22
26
30
34
38
42

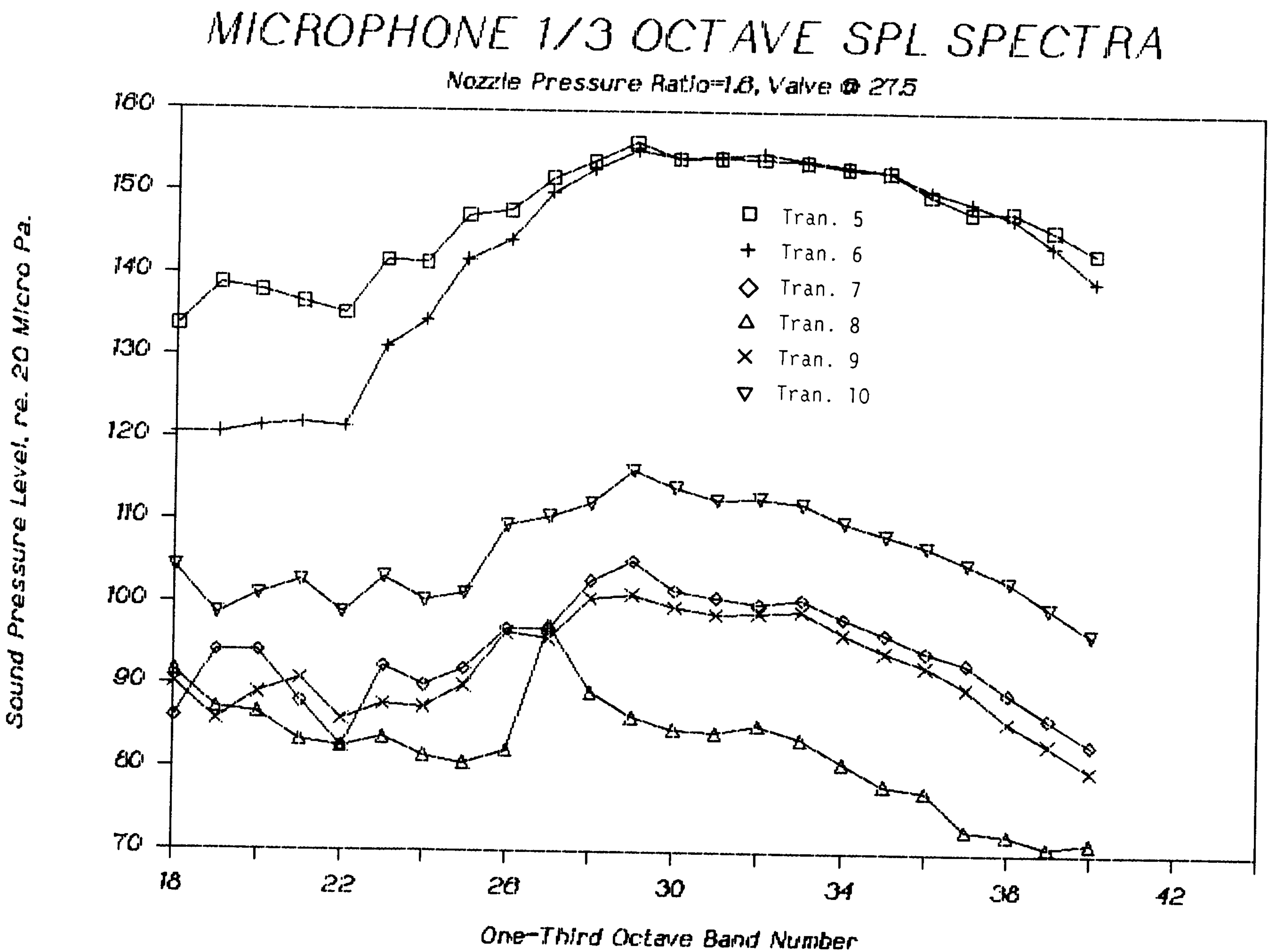
MICROPHONE 1/3 OCTAVE SPL SPECTRA
Nozzle Pressure Ratio=1.8, Valve @ 27.5
Tran. 5
Tran. 6
Tran. 7
Tran. 8
Tran. 9
Tran. 10
160
150
140
130
120
110
100
90
80
70
18
22
26
30
34
38
42
Sound Pressure Level, re. 20 Micro Pa.
One-Third Octave Band Number

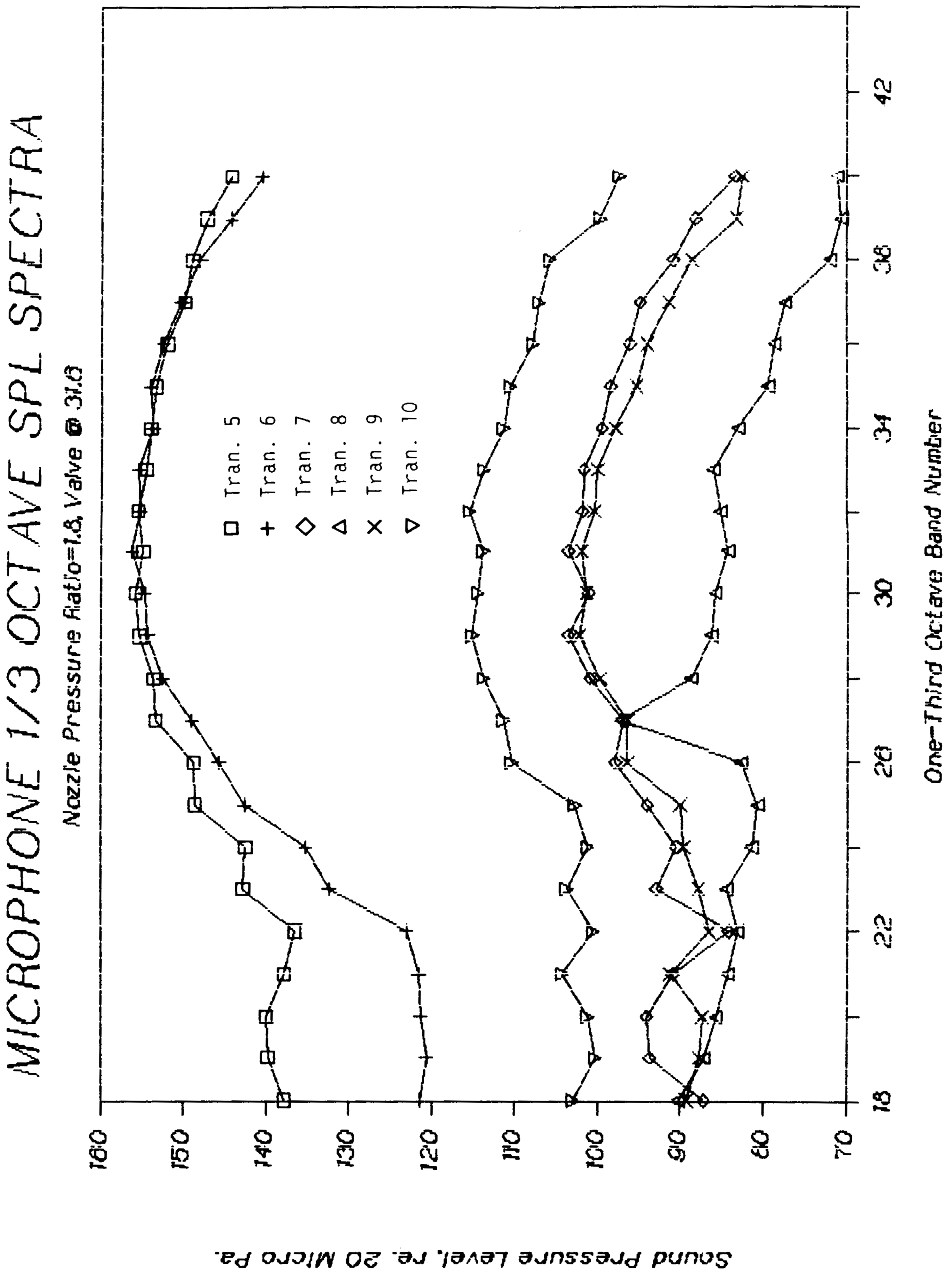
MICROPHONE 1/3 OCTAVE SPL SPECTRA
Nozzle Pressure Ratio=1.8, Valve @ 31.8
Tran. 5
Tran. 6
Tran. 7
Tran. 8
Tran. 9
Tran. 10
One-Third Octave Band Number
Sound Pressure Level, re. 20 Micro Pa.
18
22
26
30
34
38
42
70
80
90
100
110
120
130
140
150
160

MICROPHONE 1/3 OCTAVE SPL SPECTRA

Nozzle Pressure Ratio=2.3, Valve @ 40.0

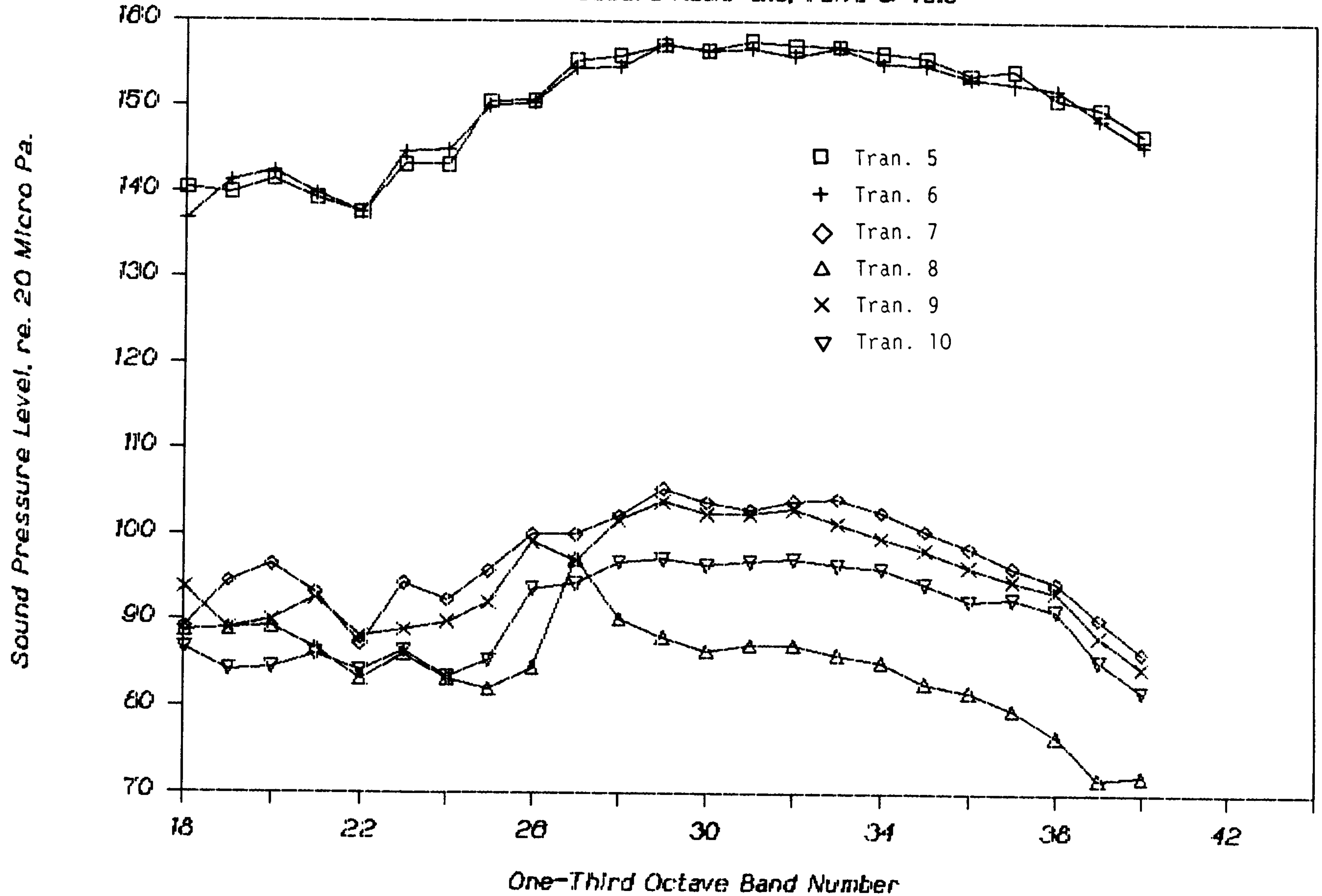

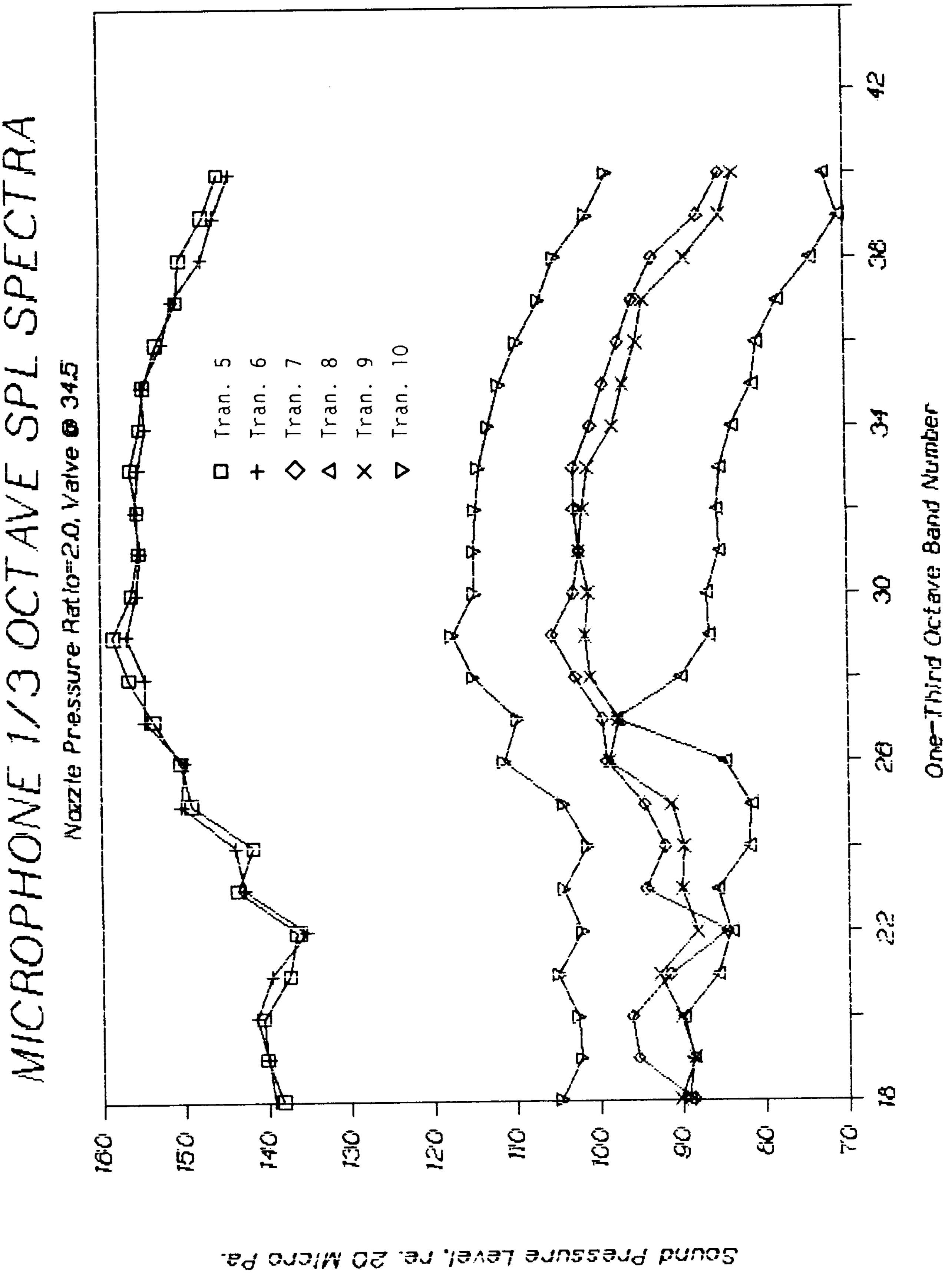
MICROPHONE 1/3 OCTAVE SPL SPECTRA
Nozzle Pressure Ratio=2.0, Valve @ 34.5
Tran. 5
Tran. 6
Tran. 7
Tran. 8
Tran. 9
Tran. 10
One-Third Octave Band Number
18
22
26
30
34
38
42
Sound Pressure Level, re. 20 Micro Pa.
70
80
90
100
110
120
130
140
150
160

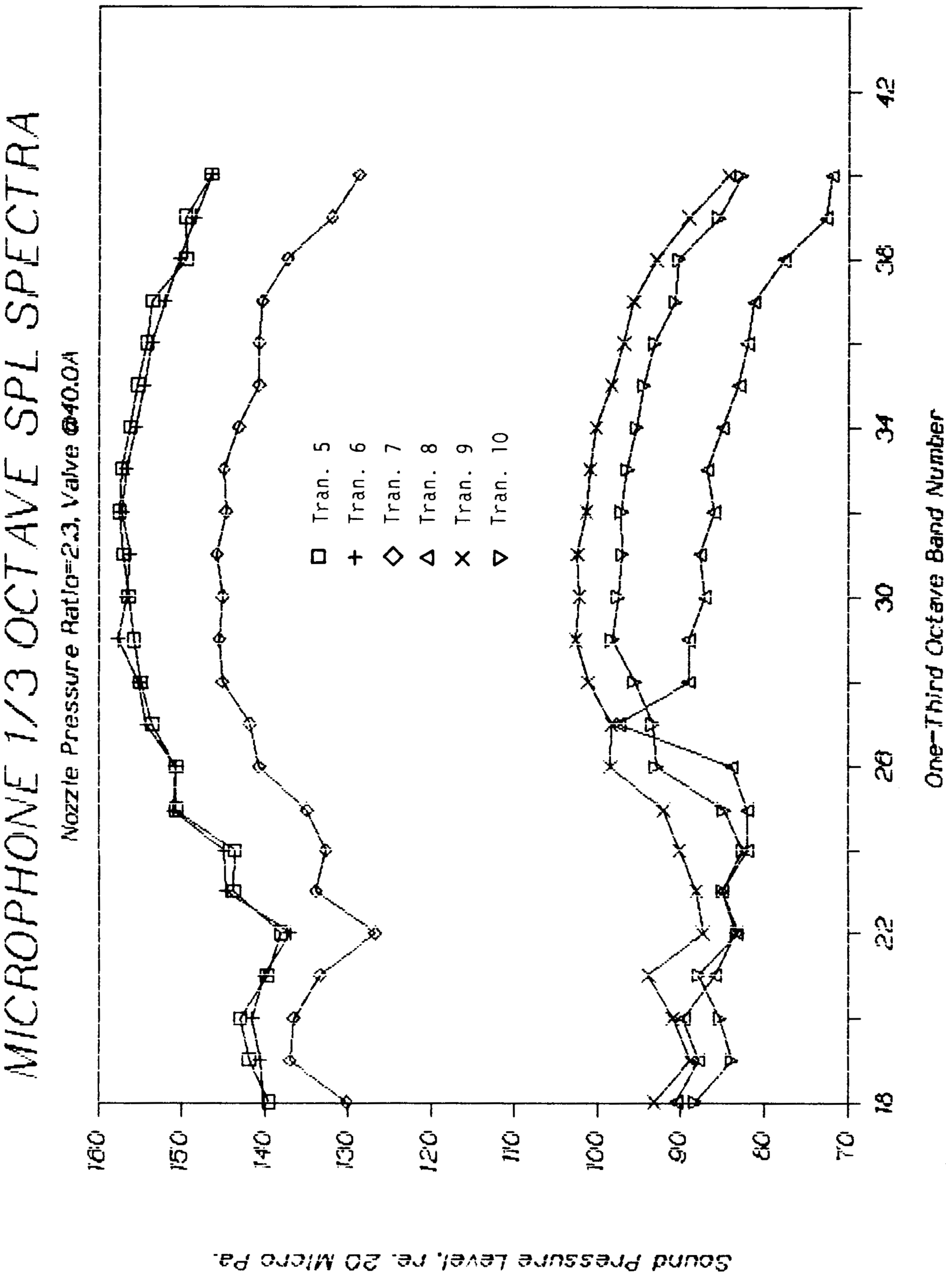
MICROPHONE 1/3 OCTAVE SPL SPECTRA
Nozzle Pressure Ratio=2.3, Valve @40.0A
Tran. 5
Tran. 6
Tran. 7
Tran. 8
Tran. 9
Tran. 10
One-Third Octave Band Number
Sound Pressure Level, re. 20 Micro Pa.
18
22
26
30
34
38
42
70
80
90
100
110
120
130
140
150
160

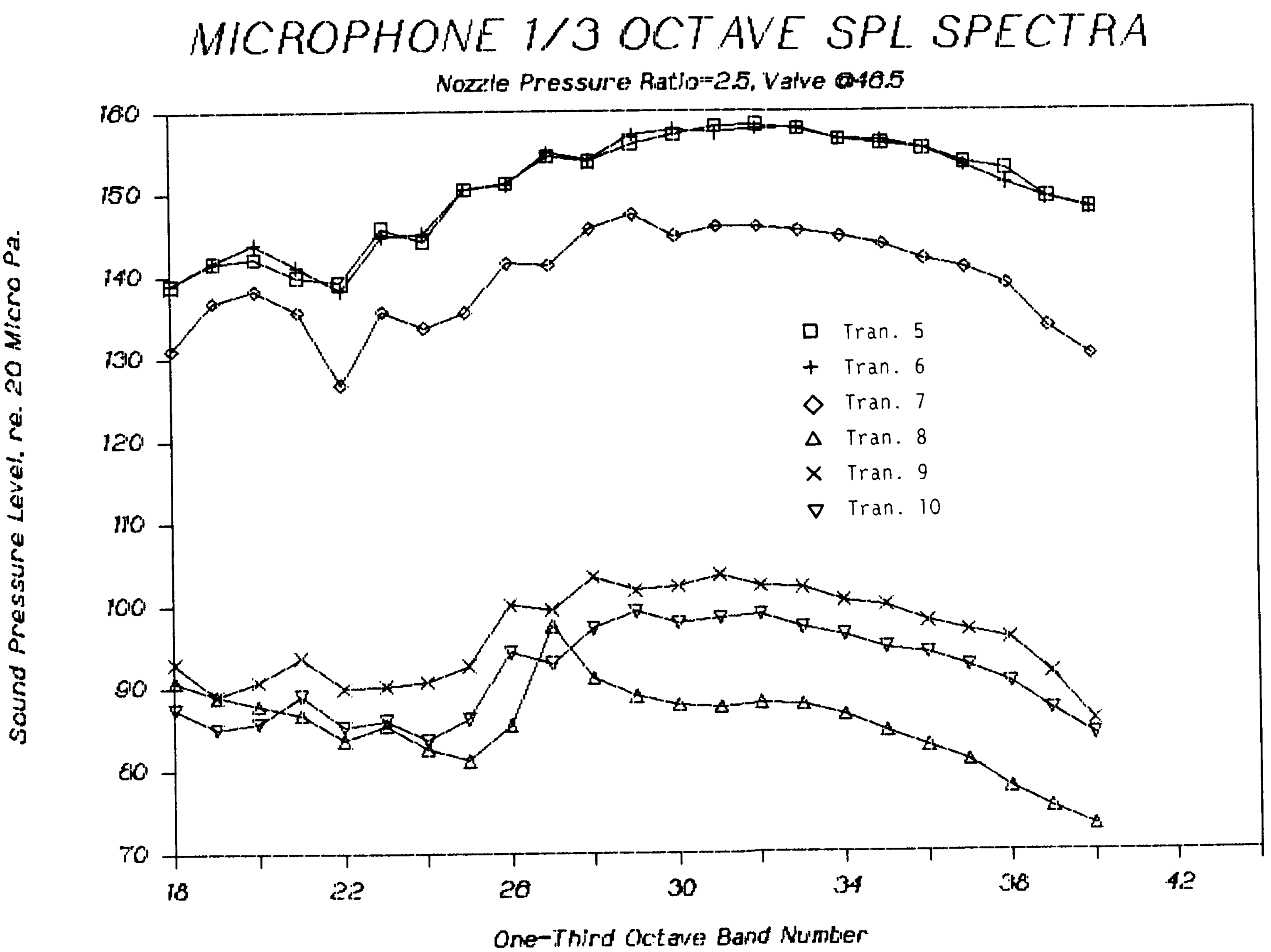
MICROPHONE 1/3 OCTAVE SPL SPECTRA
Nozzle Pressure Ratio=2.5, Valve @46.5
Sound Pressure Level, re. 20 Micro Pa.
160
150
140
130
120
110
100
90
80
70
18
22
26
30
34
38
42
One-Third Octave Band Number
Tran. 5
Tran. 6
Tran. 7
Tran. 8
Tran. 9
Tran. 10

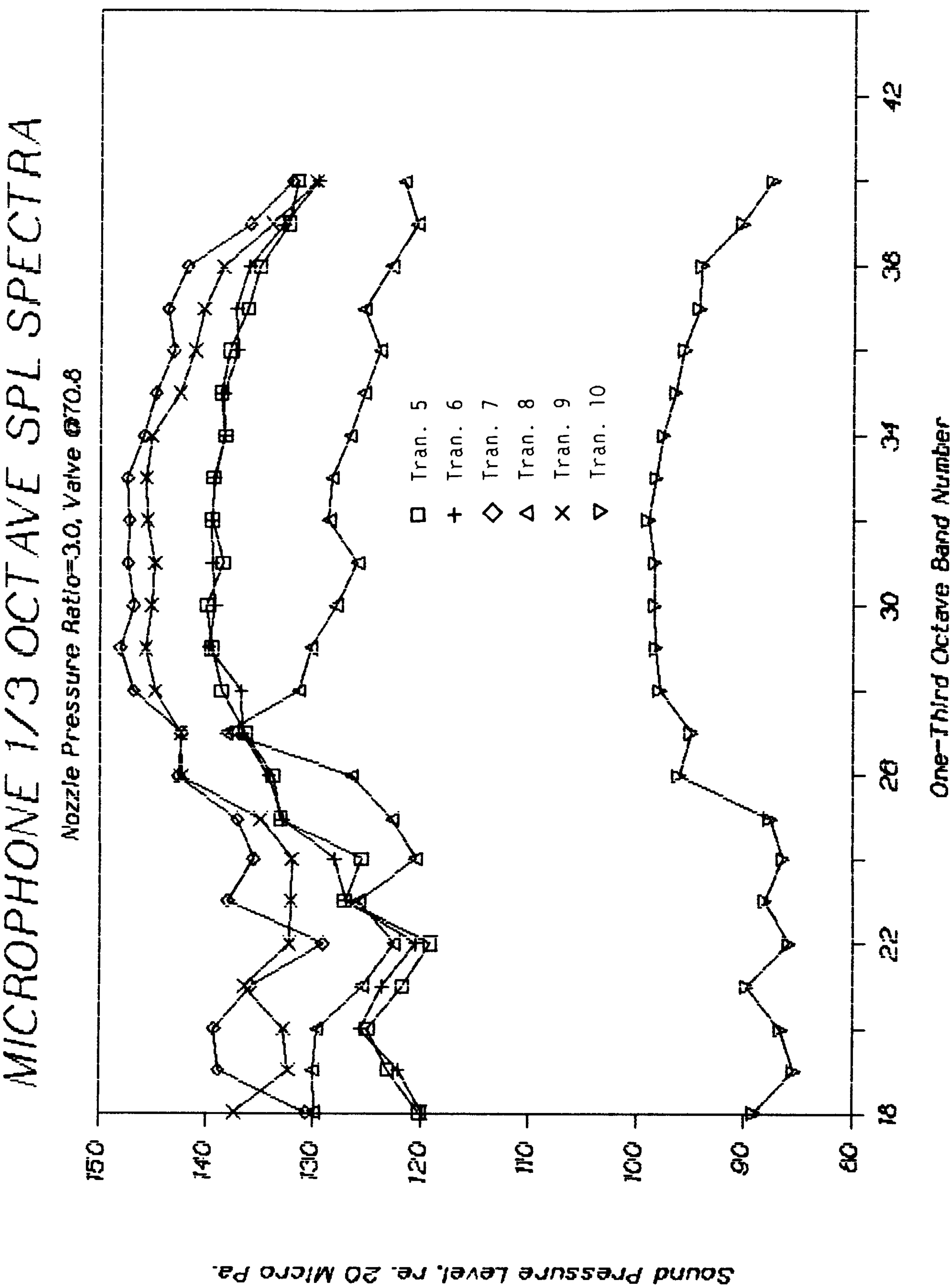

MICROPHONE 1/3 OCTAVE SPL SPECTRA
Nozzle Pressure Ratio=3.0, Valve @70.8
Tran. 5
Tran. 6
Tran. 7
Tran. 8
Tran. 9
Tran. 10
150
140
130
120
110
100
90
80
18
22
26
30
34
38
42
One-Third Octave Band Number
Sound Pressure Level, re. 20 Micro Pa.

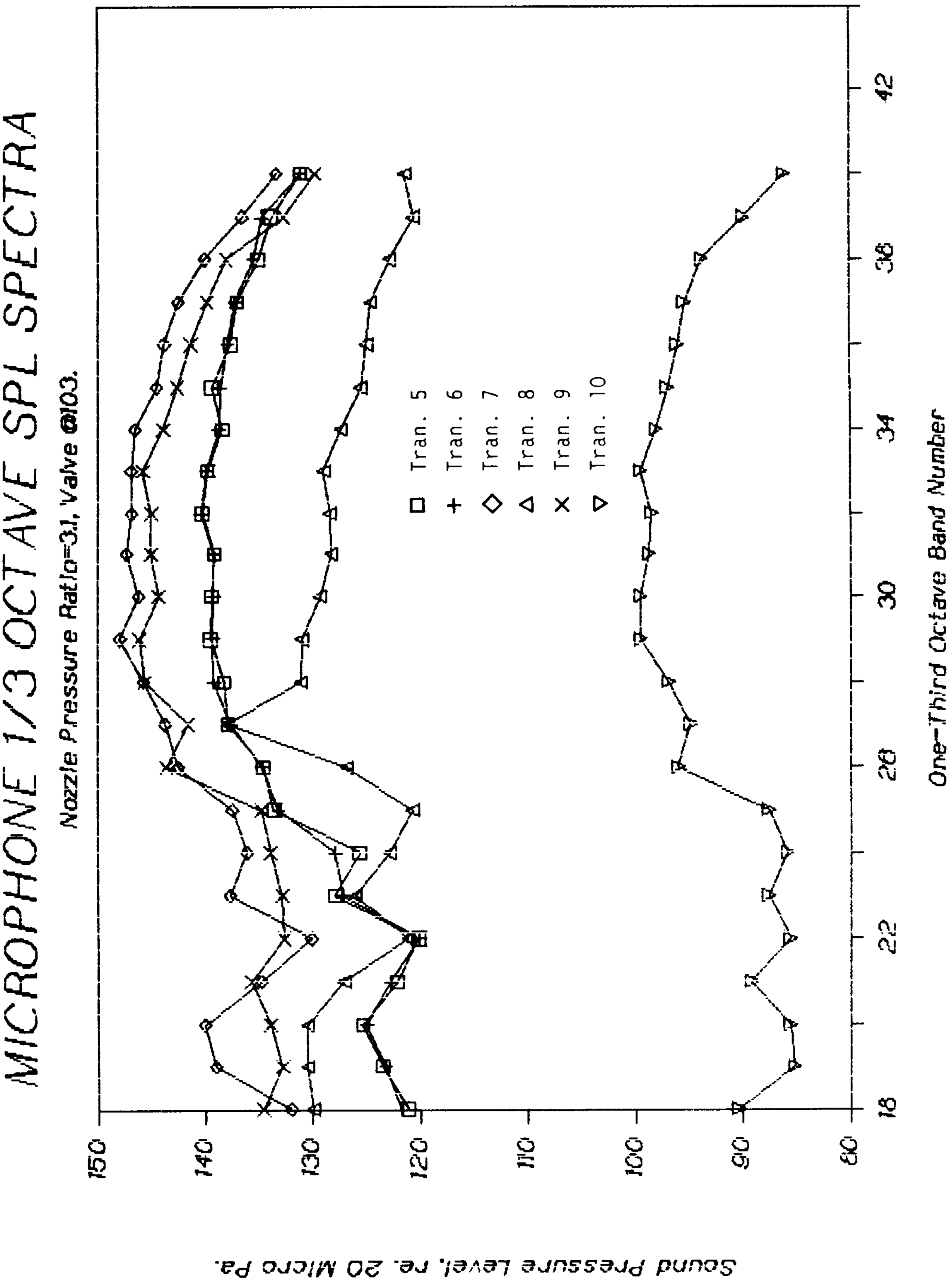
MICROPHONE 1/3 OCTAVE SPL SPECTRA
Nozzle Pressure Ratio=3.1, Valve @103.
Sound Pressure Level, re. 20 Micro Pa.
One-Third Octave Band Number
Tran. 5
Tran. 6
Tran. 7
Tran. 8
Tran. 9
Tran. 10
150
140
130
120
110
100
90
80
18
22
26
30
34
38
42

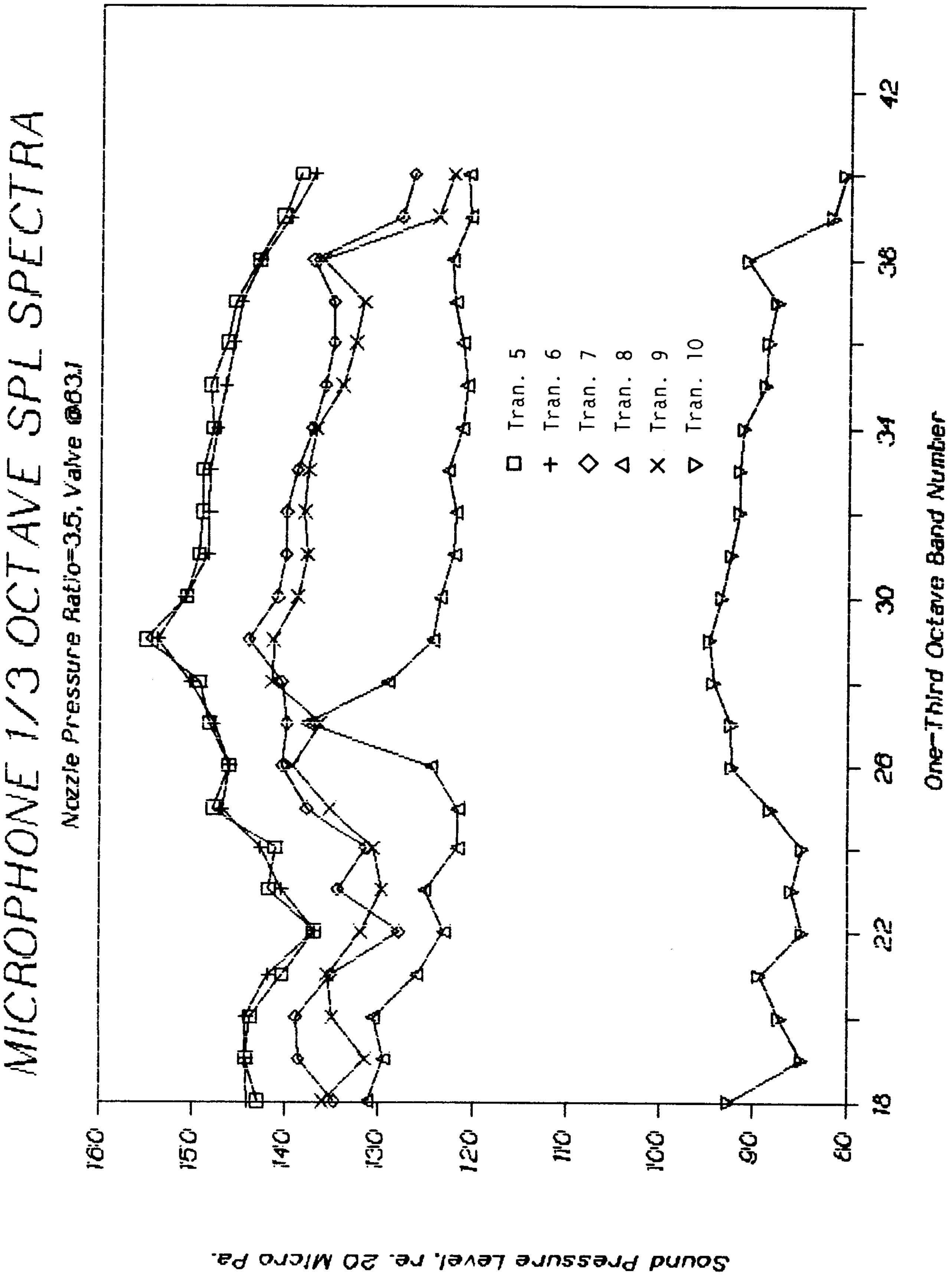
MICROPHONE 1/3 OCTAVE SPL SPECTRA
Nozzle Pressure Ratio=3.5, Valve @83.1
Tran. 5
Tran. 6
Tran. 7
Tran. 8
Tran. 9
Tran. 10
160
150
140
130
120
110
100
90
80
18
22
26
30
34
38
42
One-Third Octave Band Number
Sound Pressure Level, re. 20 Micro Pa.

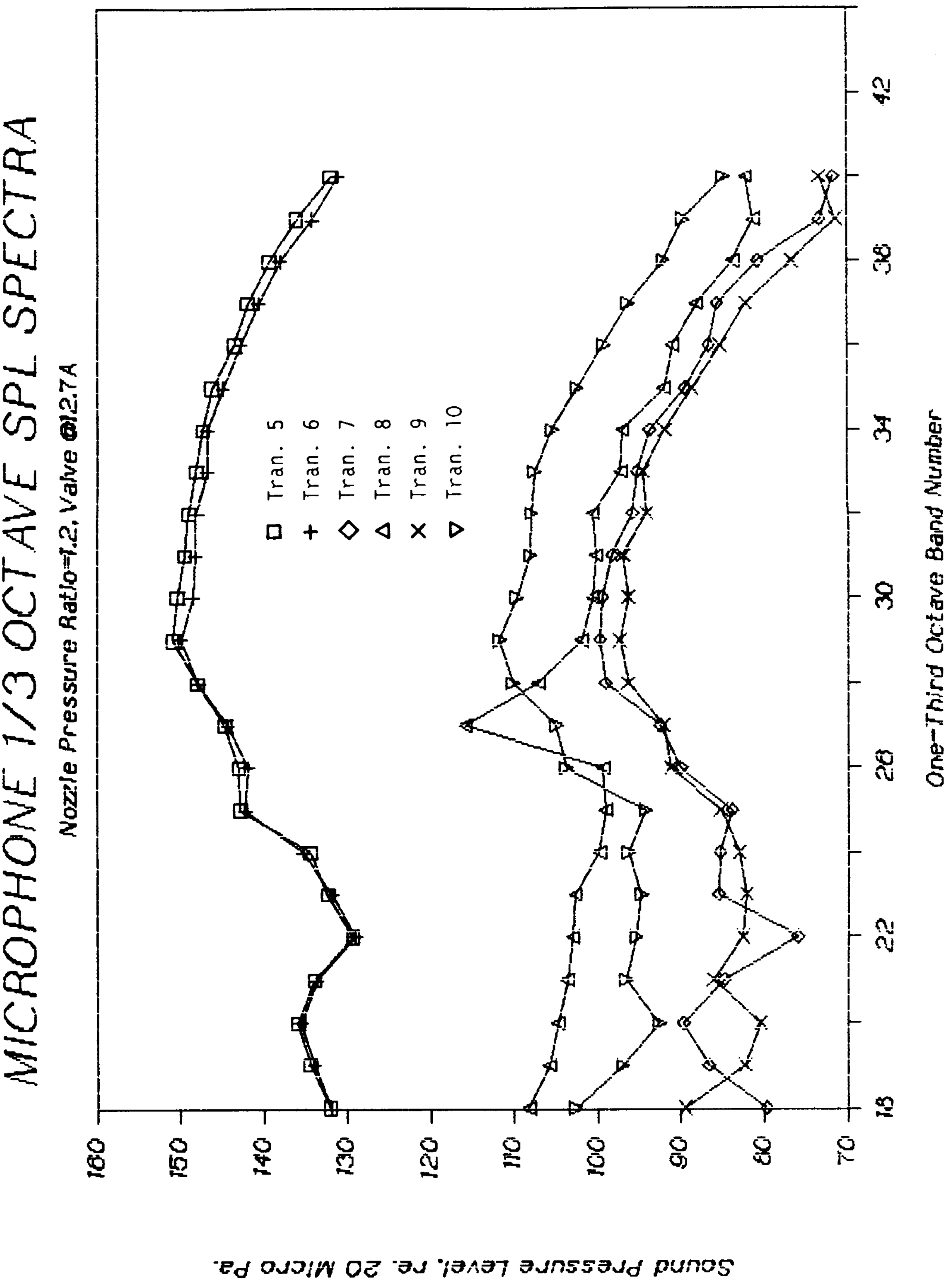
MICROPHONE 1/3 OCTAVE SPL SPECTRA
Nozzle Pressure Ratio=1.2, Valve @12.7A
Tran. 5
Tran. 6
Tran. 7
Tran. 8
Tran. 9
Tran. 10
One-Third Octave Band Number
Sound Pressure Level, re. 20 Micro Pa.
18
22
26
30
34
38
42
70
80
90
100
110
120
130
140
150
160

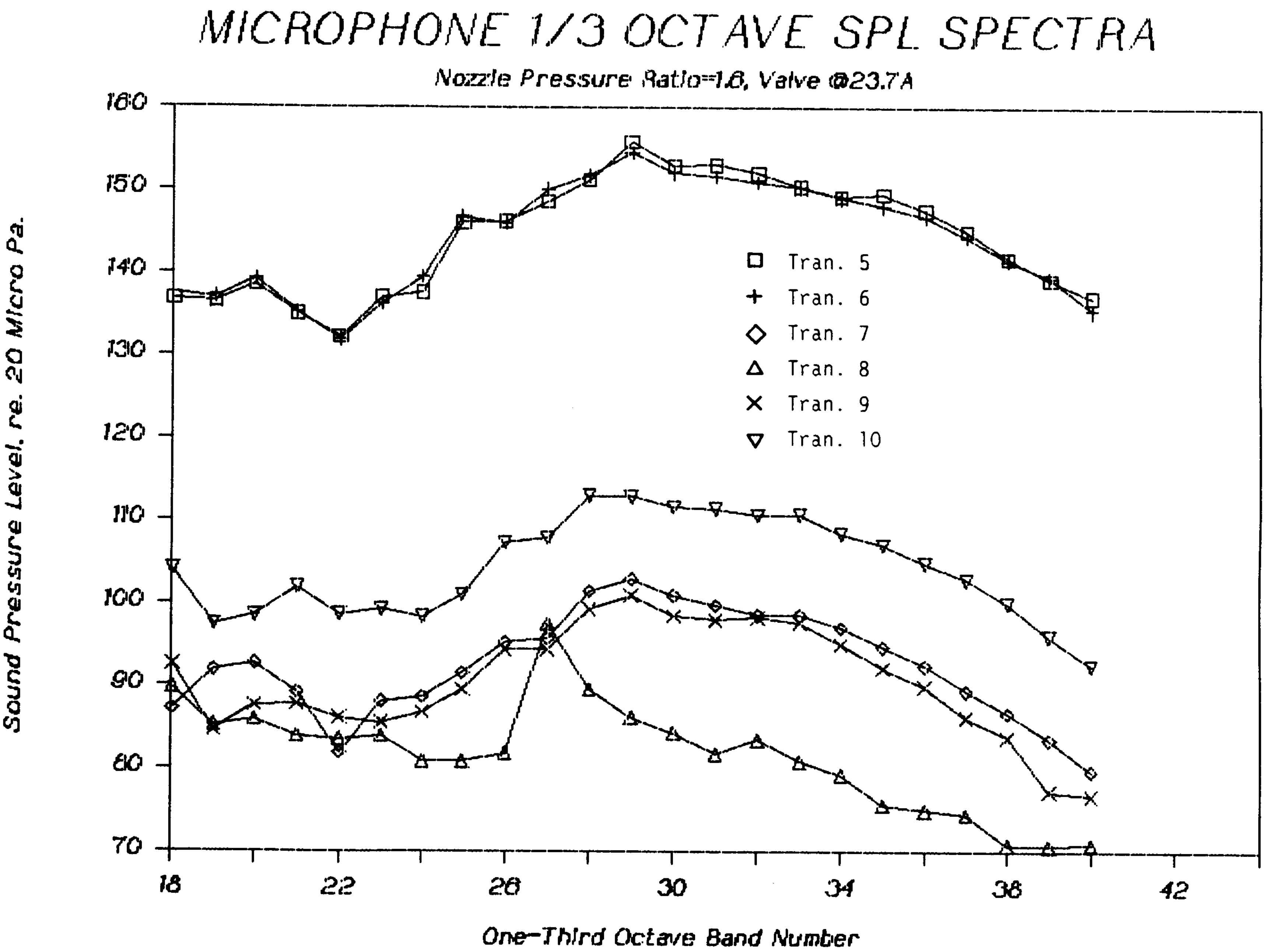
MICROPHONE 1/3 OCTAVE SPL SPECTRA
Nozzle Pressure Ratio=1.6, Valve @23.7A
Sound Pressure Level, re. 20 Micro Pa.
160
150
140
130
120
110
100
90
80
70
18
22
26
30
34
38
42
One-Third Octave Band Number
Tran. 5
Tran. 6
Tran. 7
Tran. 8
Tran. 9
Tran. 10

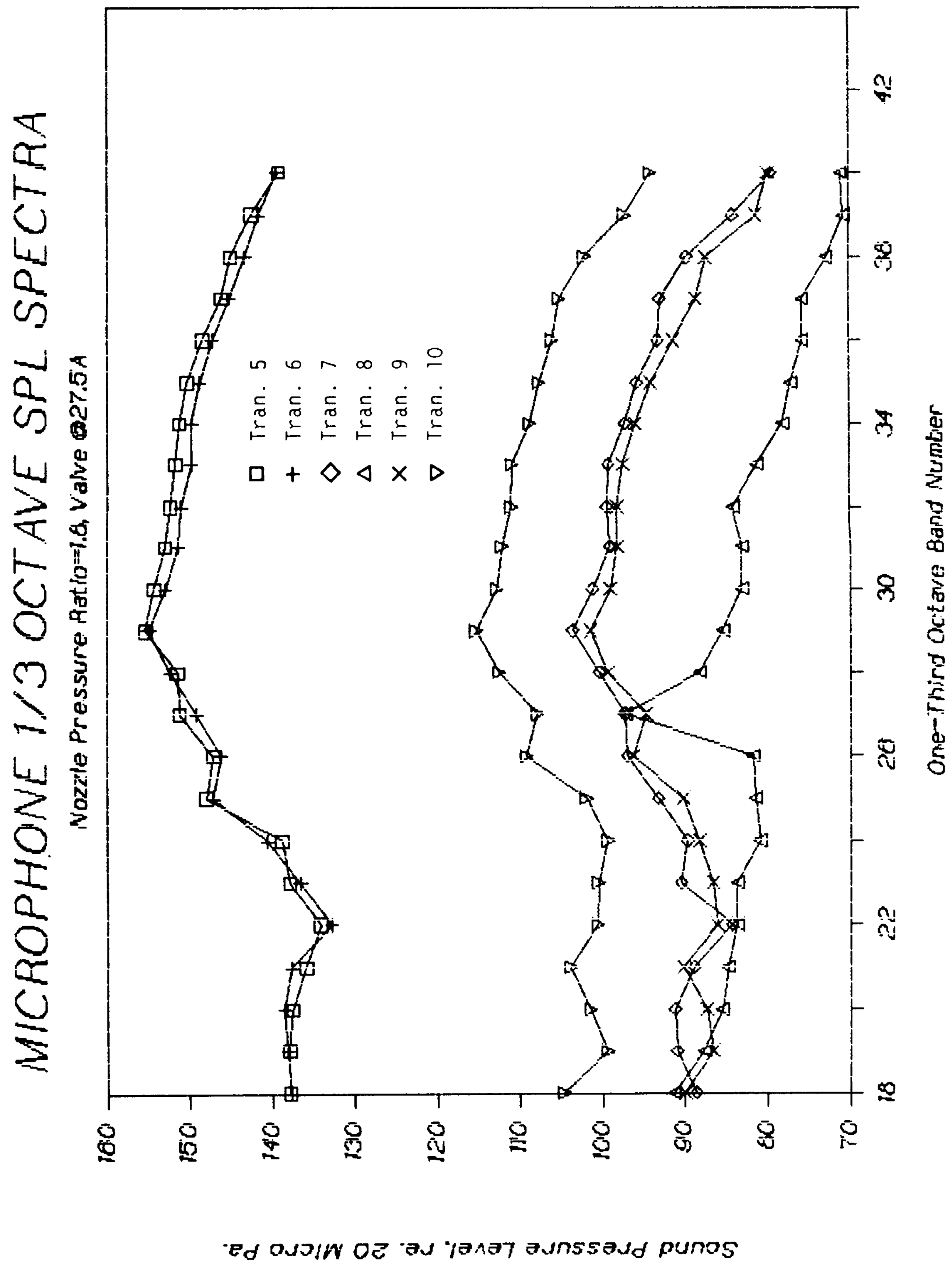
MICROPHONE 1/3 OCTAVE SPL SPECTRA
Nozzle Pressure Ratio=1.6, Valve @27.5A
Tran. 5
Tran. 6
Tran. 7
Tran. 8
Tran. 9
Tran. 10
One-Third Octave Band Number
Sound Pressure Level, re. 20 Micro Pa.
18
22
26
30
34
38
42
70
80
90
100
110
120
130
140
150
160

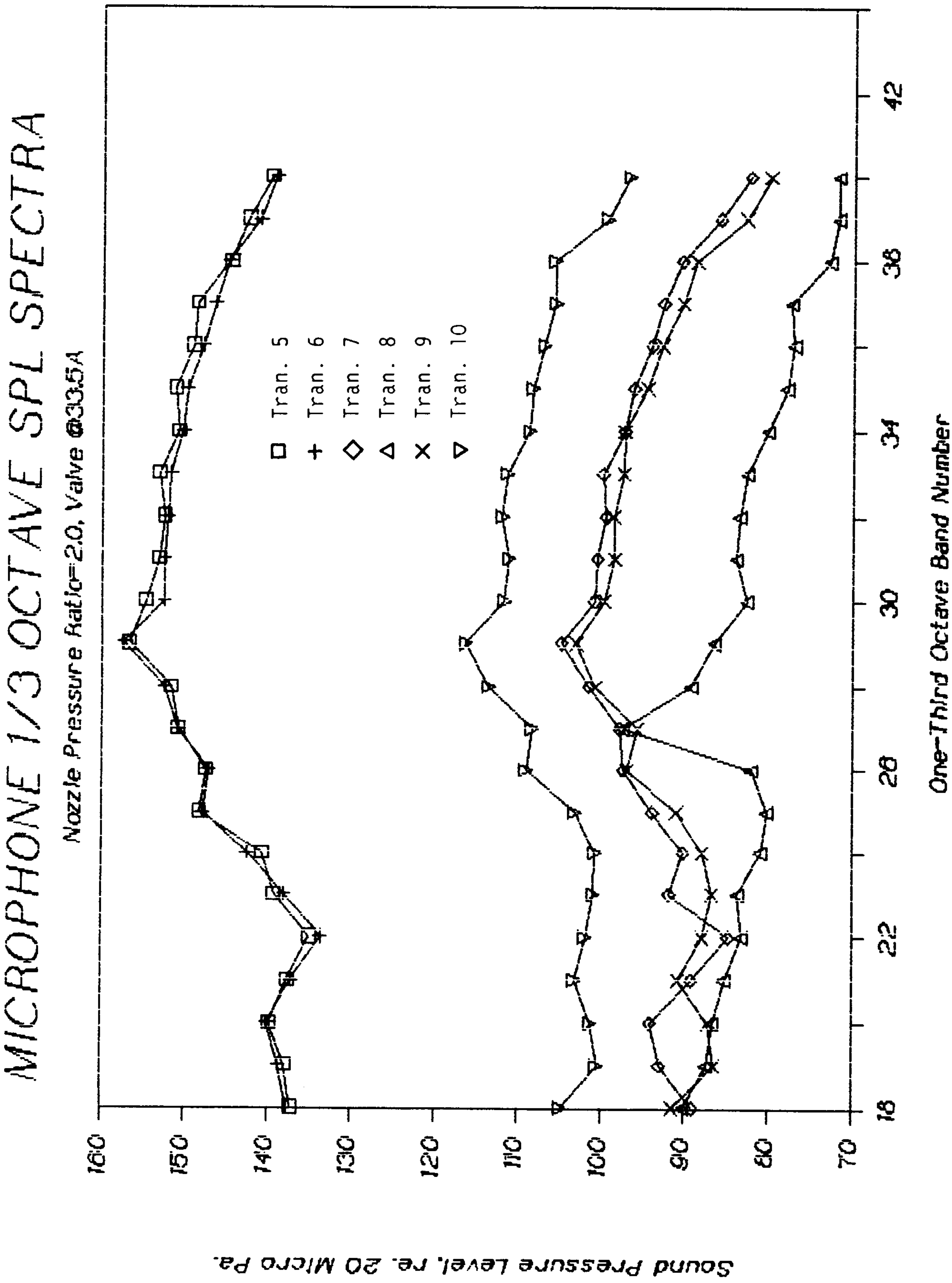
MICROPHONE 1/3 OCTAVE SPL SPECTRA
Nozzle Pressure Ratio=2.0, Valve @33.5A
Tran. 5
Tran. 6
Tran. 7
Tran. 8
Tran. 9
Tran. 10
One-Third Octave Band Number
Sound Pressure Level, re. 20 Micro Pa.
160
150
140
130
120
110
100
90
80
70
18
22
26
30
34
38
42

APPENDIX B

COHERENCE FUNCTION AND PHASE

APPENDIX B

PART I

INTERNAL PRESSURE TRANSDUCERS TO FAR FIELD MICROPHONES

Type 2032

Page No.
22

Sign.:

Meas.
Object:

PLF PR1.2

ChA = 110

ChB = M1

Kdg176

Comments:

200 Hz Max

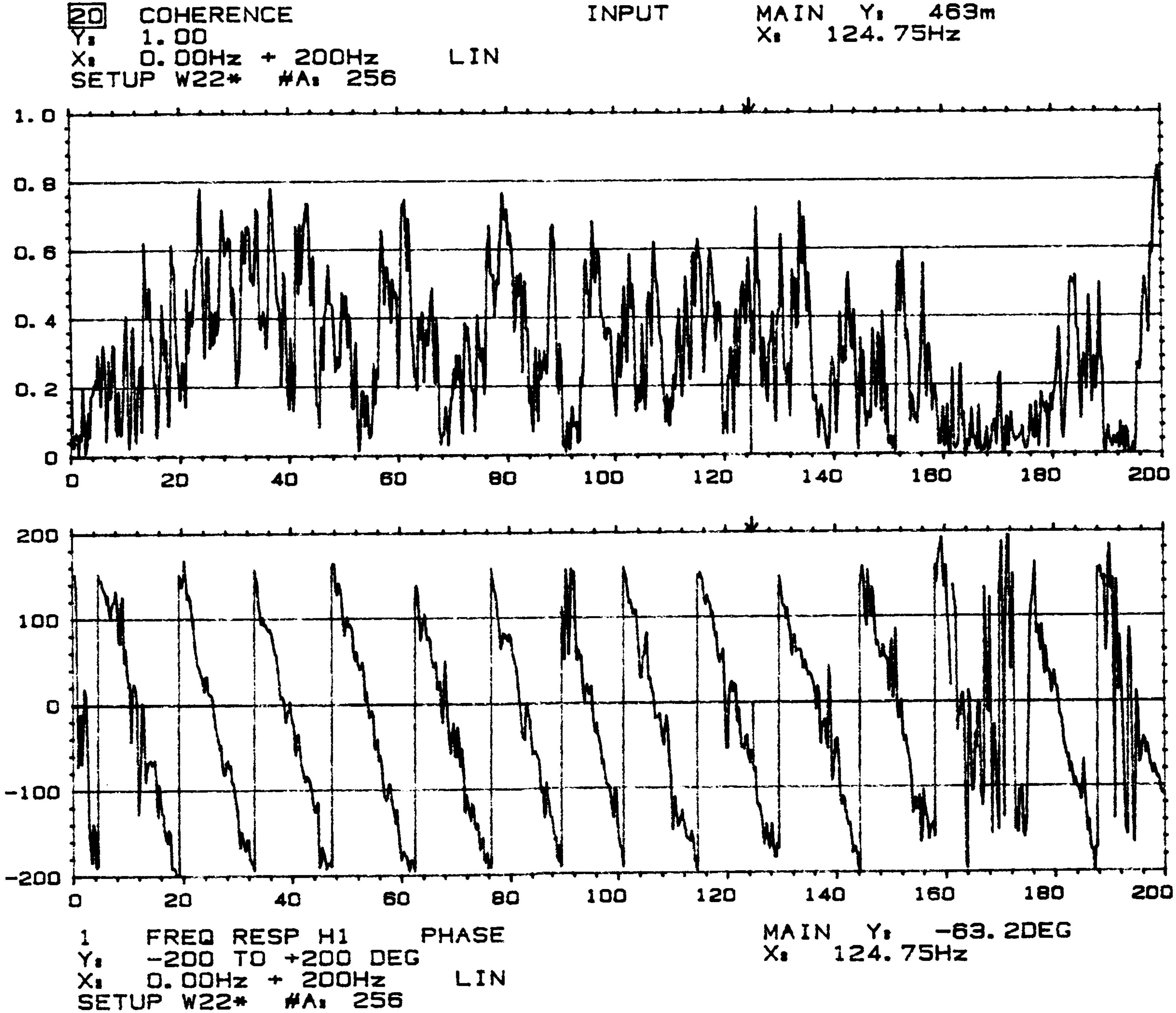

Type 2032

Page No.
20

Sign.:

Meas.
Object:
PLF PR1.2
ChA = T10
ChB = M1

Rdg 176

Comments:

400 Hz Max

20 COHERENCE
Y: 1.00
X: 0.0Hz + 400Hz LIN
SETUP W22* #A: 256

INPUT

MAIN Y: 919m
X: 249.5Hz

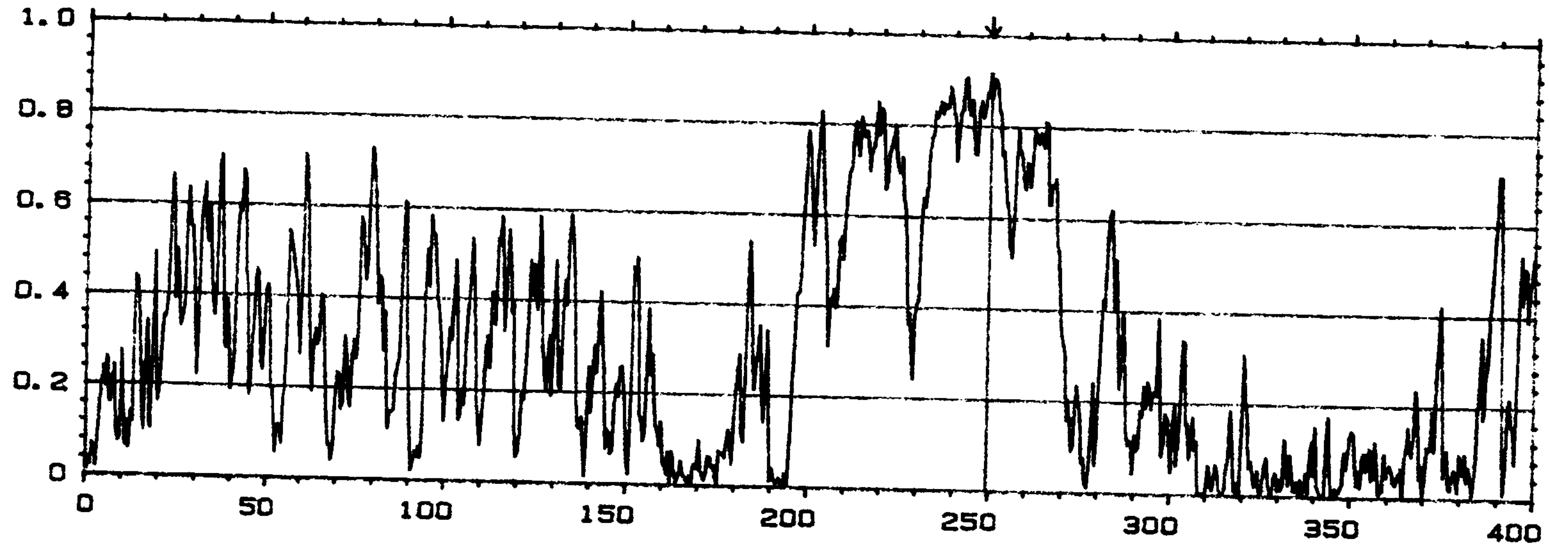

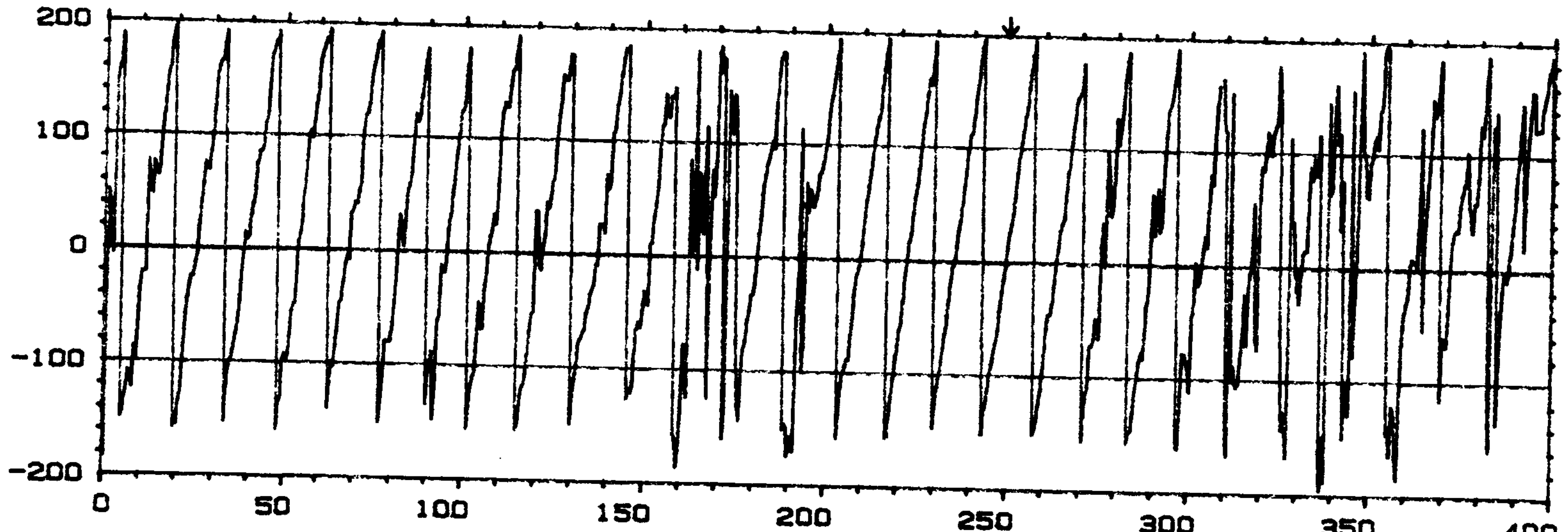

1 FREQ RESP H1 PHASE
Y: -200 TO +200 DEG
X: 0.0Hz + 400Hz LIN
SETUP W22* #A: 256

MAIN Y: -2.4DEG
X: 249.5Hz

Type 2032

Page No.
8

Sign.:

Meas.
Object:

PLF PR 1.2
ChA=T10
ChB=M1

Pipe exit 30°

Rdg 176

Comments:

300 Hz Max

W20 COHERENCE INPUT MAIN Y: 854m
Y: 1.00 X: 250Hz
X: 0Hz + 800Hz LIN
SETUP W22 #A: 256

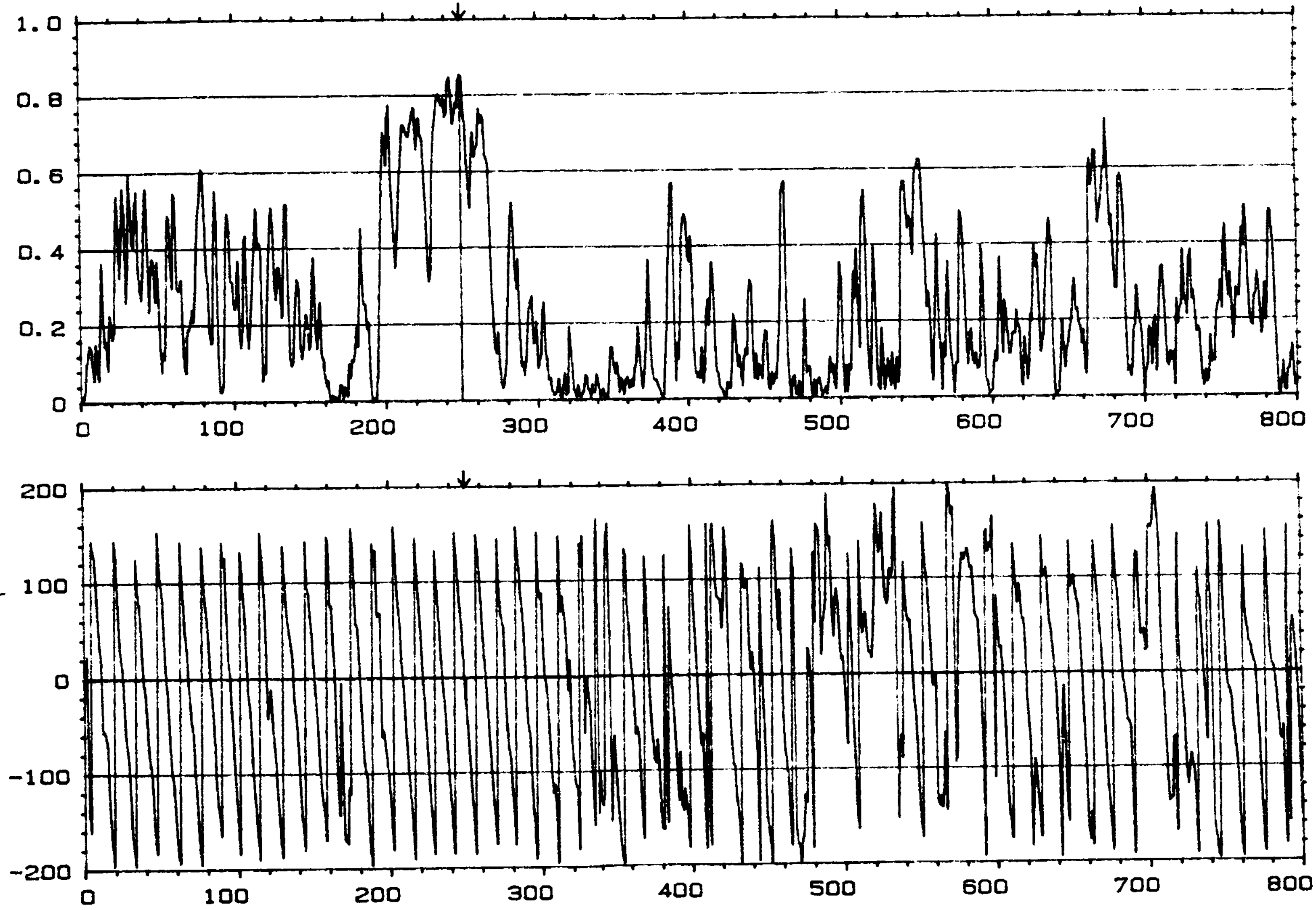

W1 FREQ RESP H1 PHASE MAIN Y: -23.9DEG
Y: -200 TO +200 DEG X: 250Hz
X: 0Hz + 800Hz LIN
SETUP W22 #A: 256

Type 2032

Page No.
30

Sign.:

Meas.
Object:

PLF PR 1.2
ChA = 7 10
ChB = M 1

Edg 176

Comments:

1.6 kHz MAX

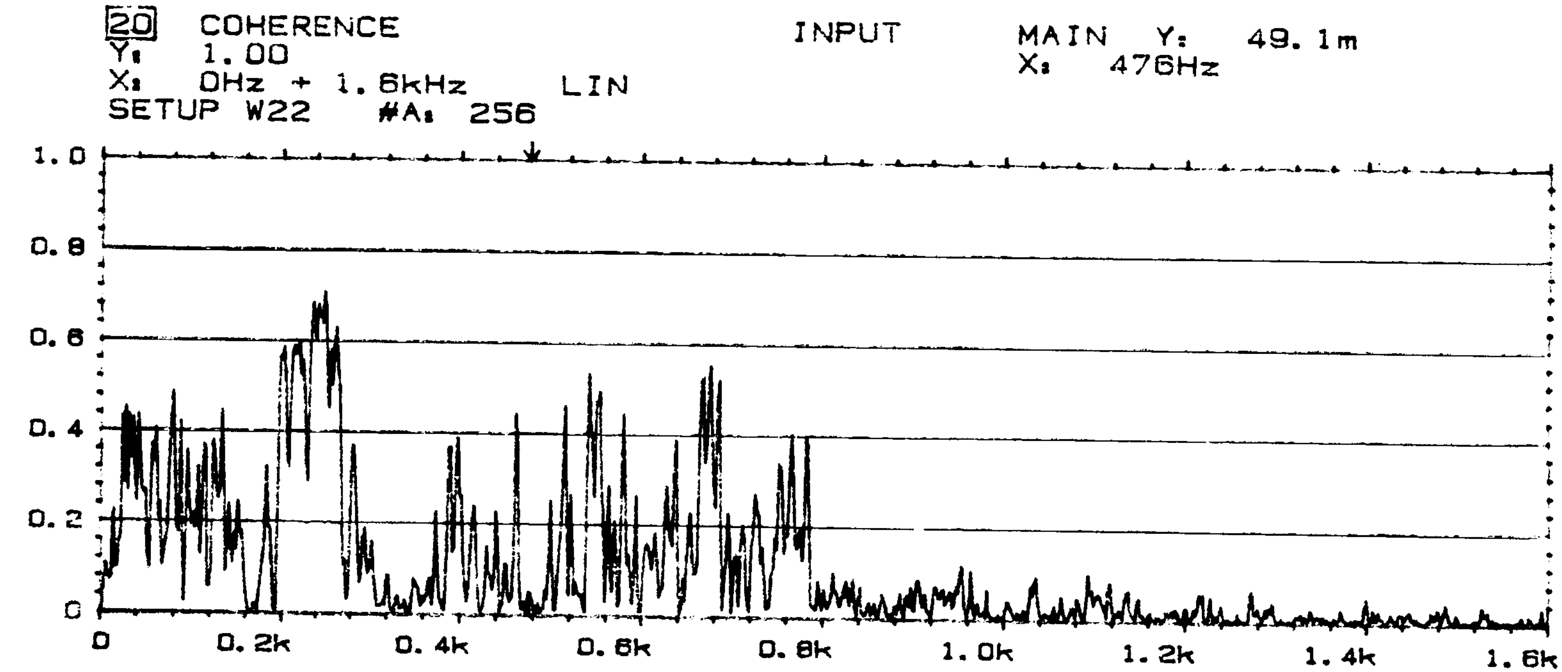

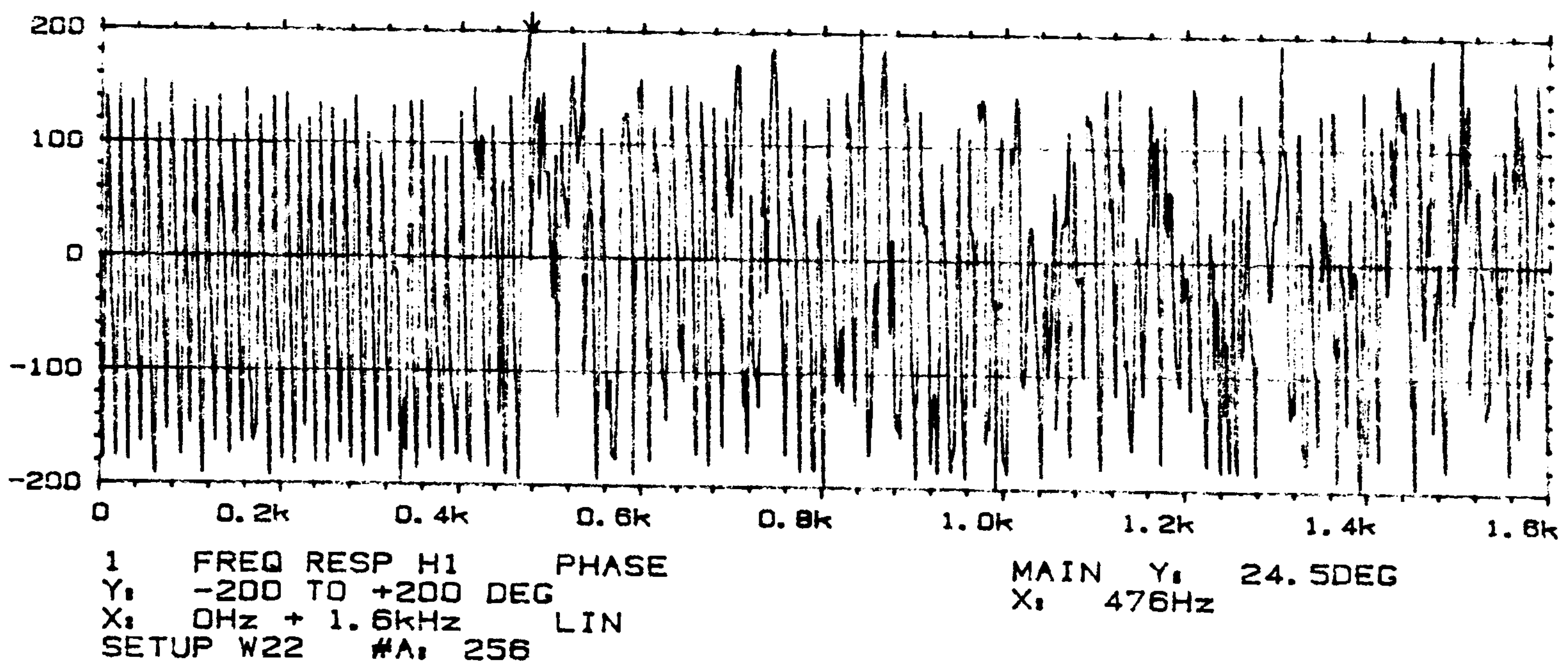

Type 2032

Page No.
18

Sign.:

Meas.
Object:

PLF PF 1.2
ChA: T10
ChB: M1

Eq 176

Comments:

γ^2 decreased
from 800Hz
Analysis Range
3.2k Hz Max

20 COHERENCE INPUT MAIN Y: 6.26m
Y: 1.00 X: 1000Hz
X: 0Hz + 3.2kHz LIN
SETUP W22 #A: 256

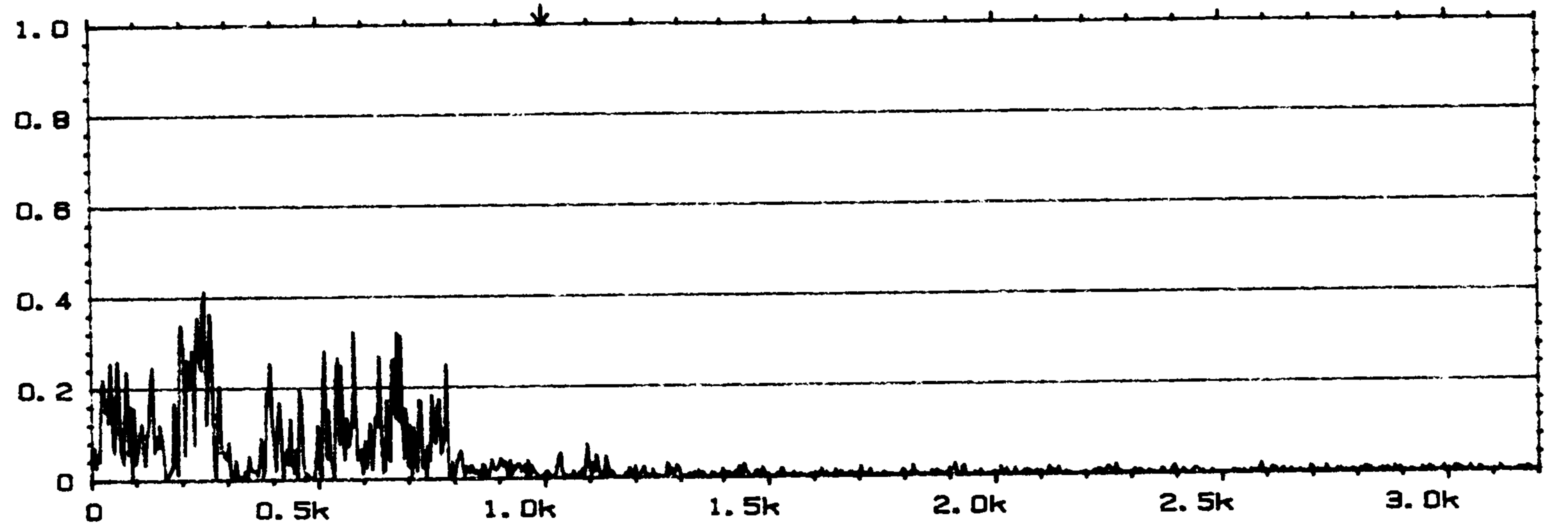

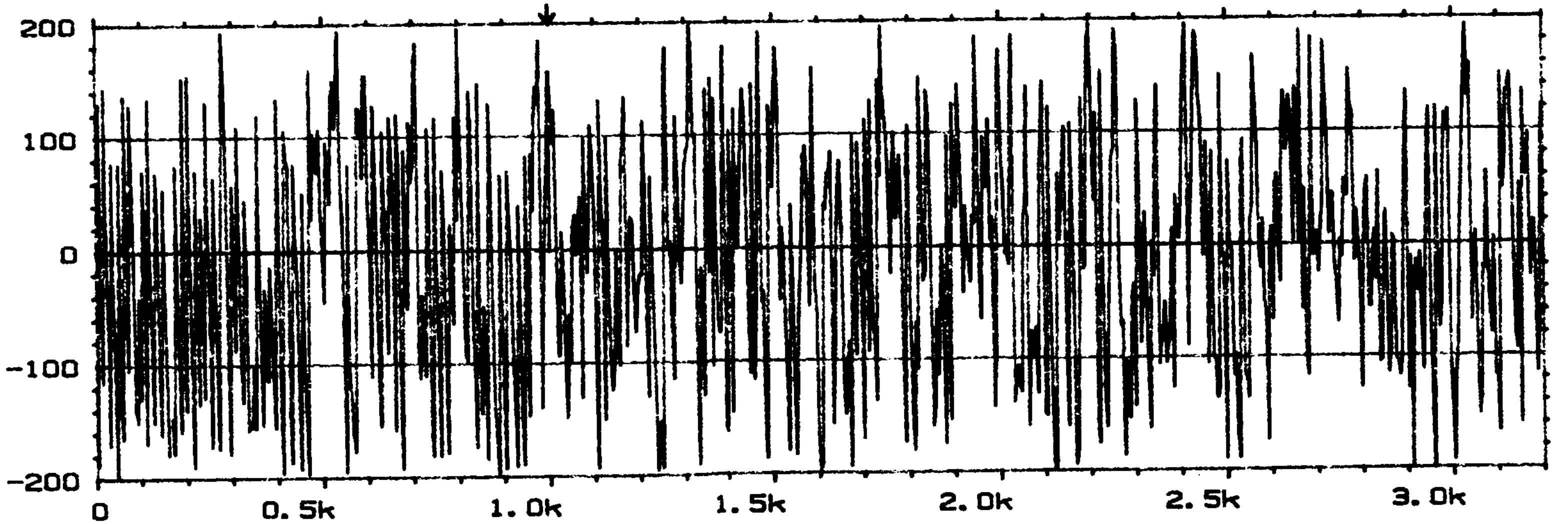

1 FREQ RESP H1 PHASE MAIN Y: 157.9DEG
Y: -200 TO +200 DEG X: 1000Hz
X: 0Hz + 3.2kHz LIN
SETUP W22 #A: 256

Type 2032

Page No.
32

Sign.:

Meas.
Object:
PLF PR 1.2
chA = T10
chB = M2

Rdg 176

Comments:

20 COHERENCE
Y: 1.00
X: 0Hz + 1.6kHz LIN
SETUP W22 #A: 256

MAIN Y: 77.4m
X: 476Hz

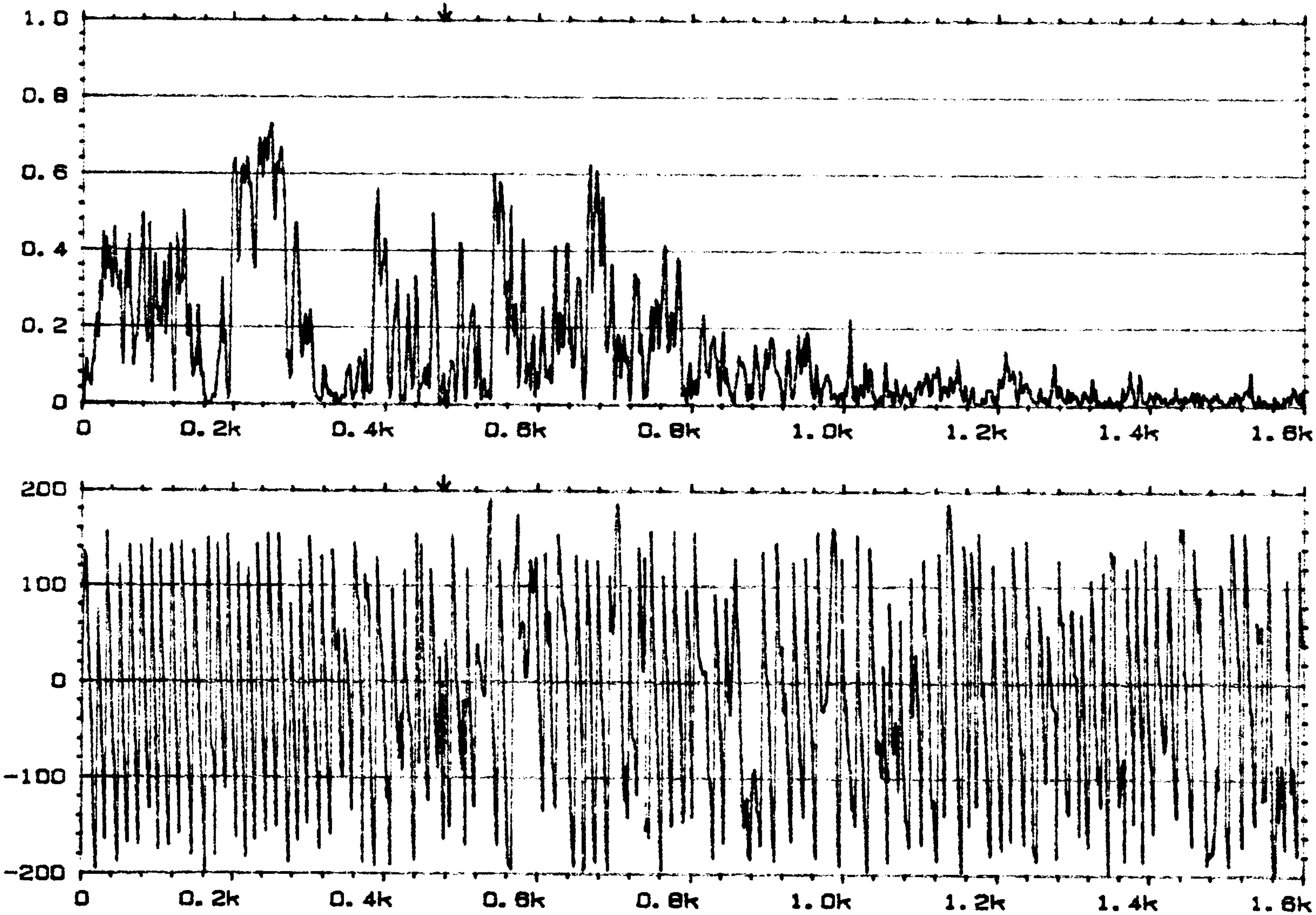

1 FREQ RESP H1 PHASE INPUT
Y: -200 TO +200 DEG
X: 0Hz + 1.6kHz LIN
SETUP W22 #A: 256

MAIN Y: -121.9DEG
X: 476Hz

20 COHERENCE INPUT MAIN Y: 713m
Y: 1.00 X: 250Hz
X: 0Hz + 1.6kHz LIN
SETUP W22* #A: 256

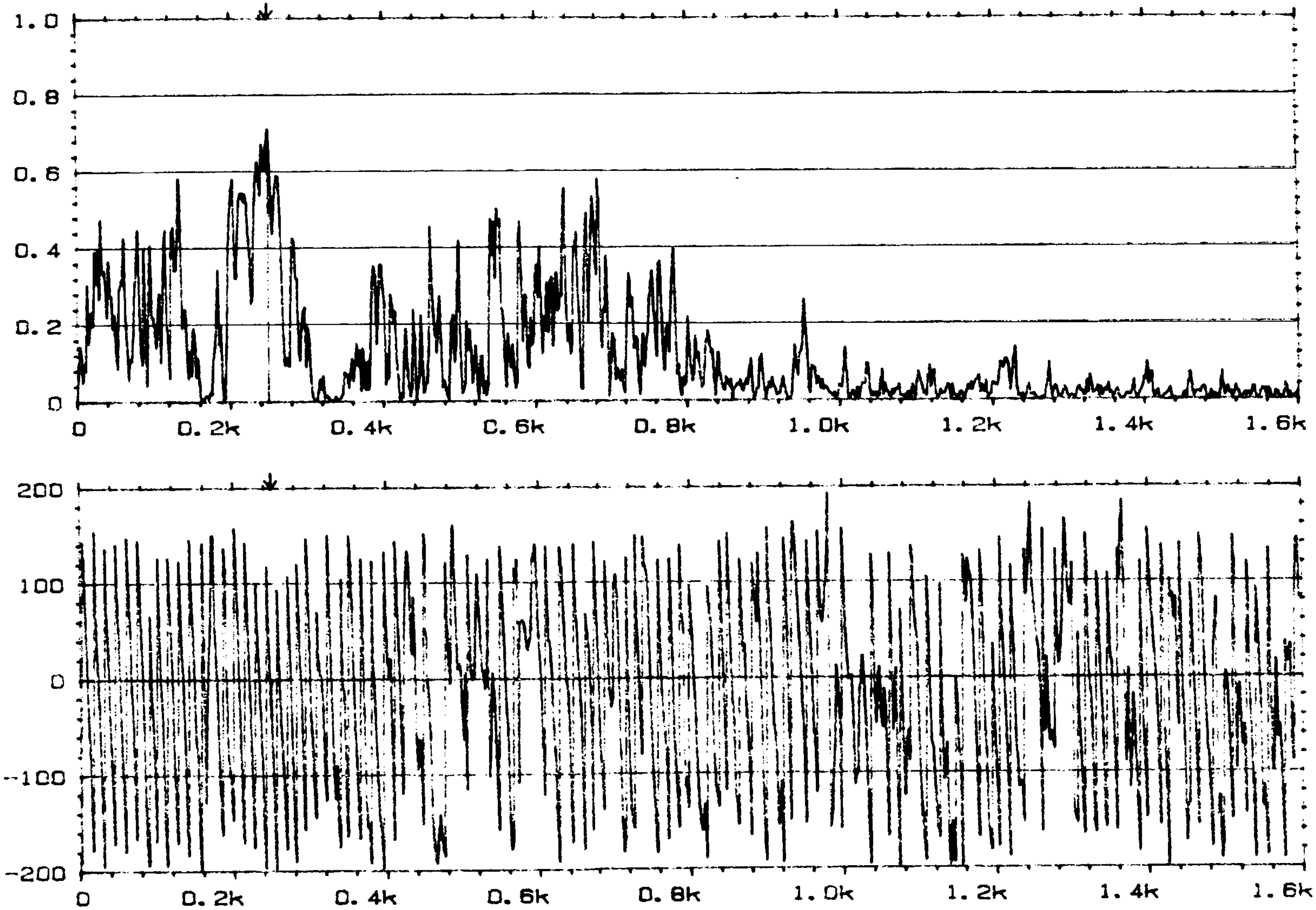

1 FREQ RESP H1 PHASE MAIN Y: -37.1DEG
Y: -200 TO +200 DEG X: 250Hz
X: 0Hz + 1.6kHz LIN
SETUP W22* #A: 256

Type 2032

Page No.
34

Sign.:

Meas.
Object:

ChA = T1?
ChB = M3

Pag 176

Comments:

Type 2032

Page No.
26

Sign.:

Meas.
Object:

PLF PR 1.2
ChA = T10
ChB = M4

Rdg 176

Comments:

800 Hz Max

20 COHERENCE
Y: 1.00
X: 0Hz + 800Hz LIN
SETUP W22* #A: 256

INPUT

MAIN Y: 849m
X: 238Hz

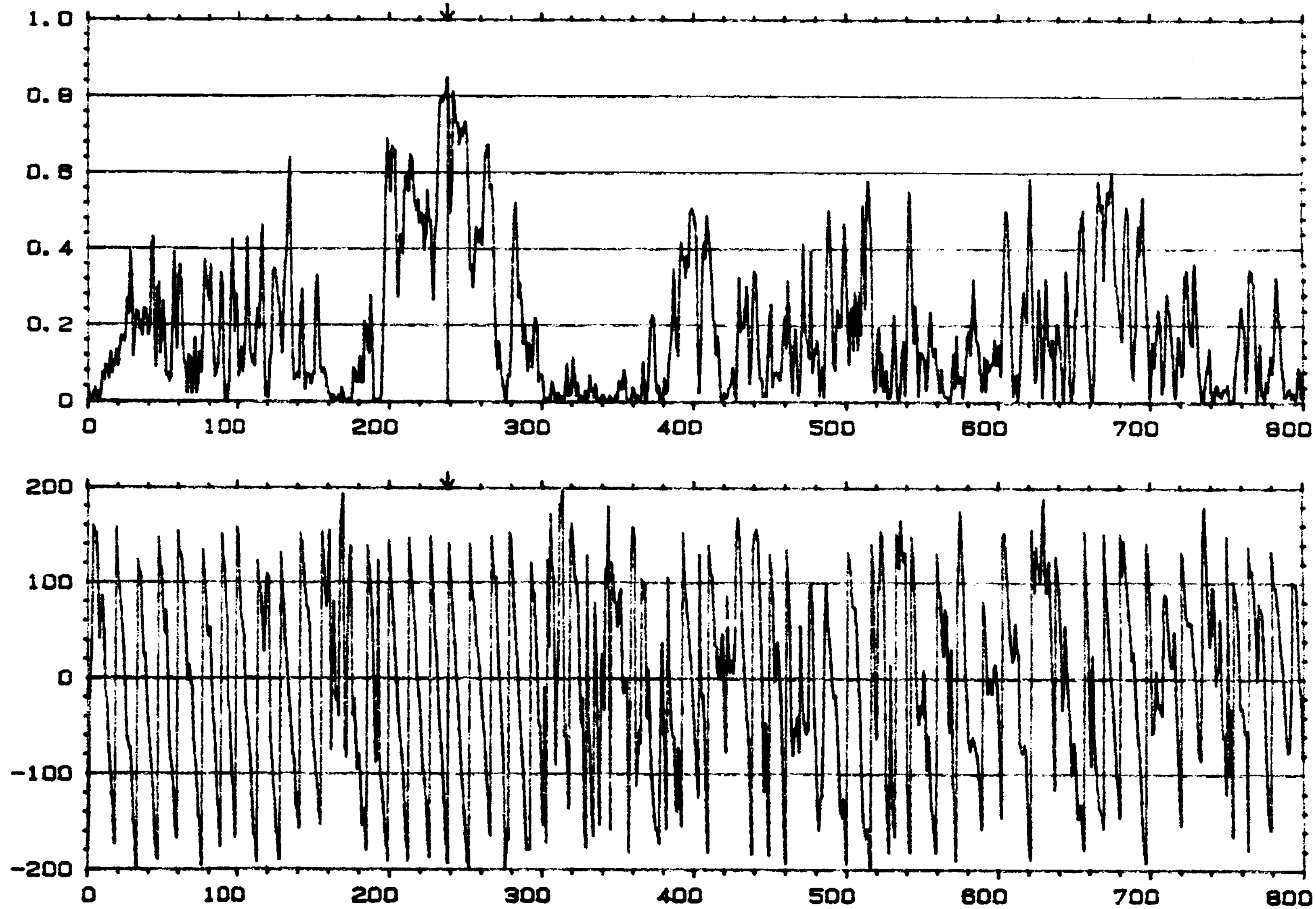

1 FREQ RESP H1 PHASE
Y: -200 TO +200 DEG
X: 0Hz + 800Hz LIN
SETUP W22* #A: 256

MAIN Y: -537.1DEG
X: 238Hz

20 COHERENCE INPUT MAIN Y: 54.7m
Y: 1.00 X: 476Hz
X: 0Hz + 1.6kHz LIN
SETUP W22* #A: 256

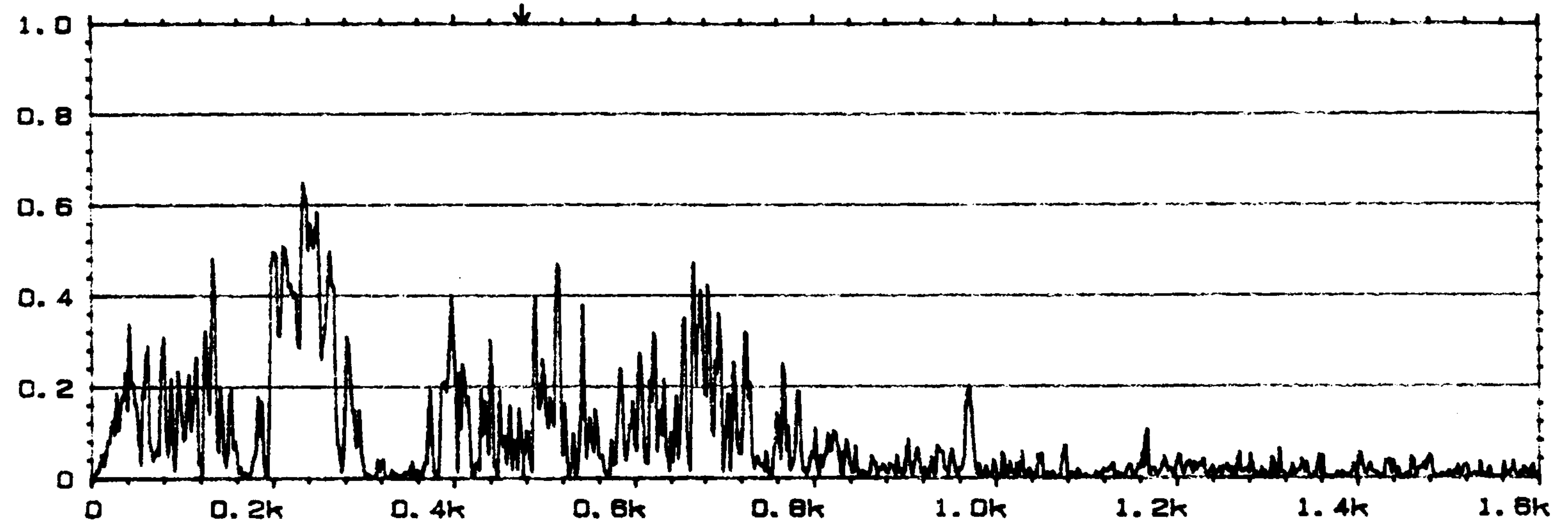

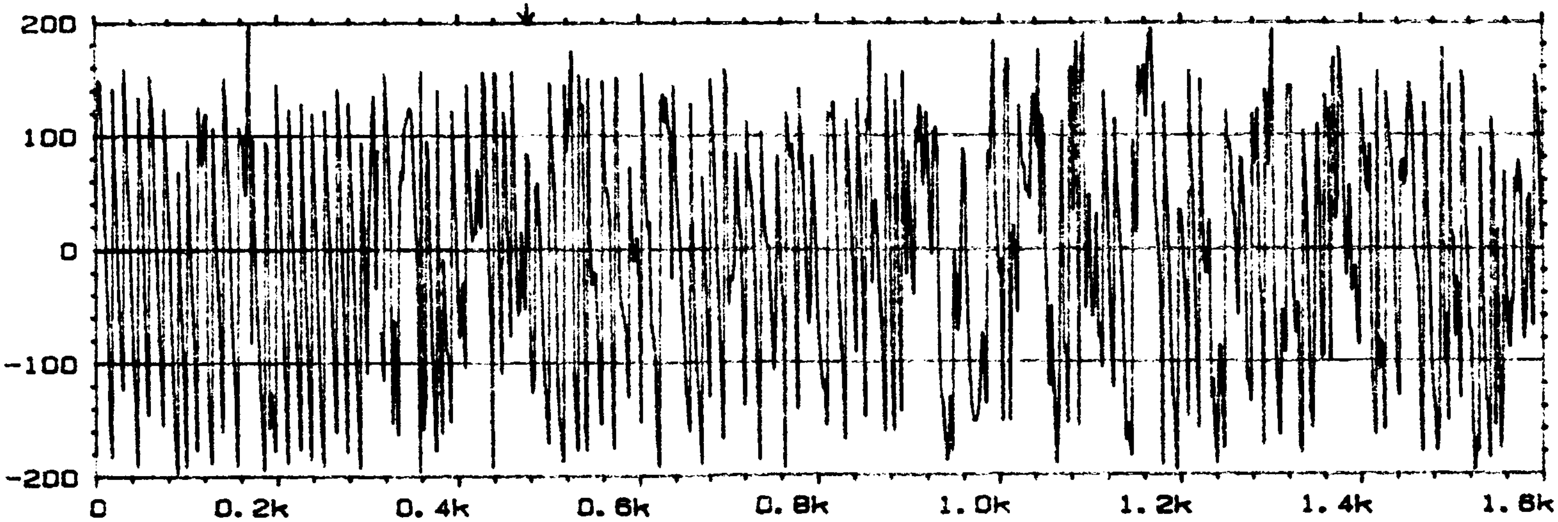

1 FREQ RESP H1 PHASE MAIN Y: 83.6DEG
Y: -200 TO +200 DEG X: 476Hz
X: 0Hz + 1.6kHz LIN
SETUP W22* #A: 256

Type 2032

Page No.
28

Sign.:

Meas.
Object:

PLF PR 1.2
ChA = T10
ChB = M4

Rdg 176

Comments:

1.6KHz Max

Type 2032

Page No.
25

Sign.:

Meas.
Object:

PLF PR 1.2
ChA = T10
ChB = M4

Rig 176

Comments:

3.2KHz Max

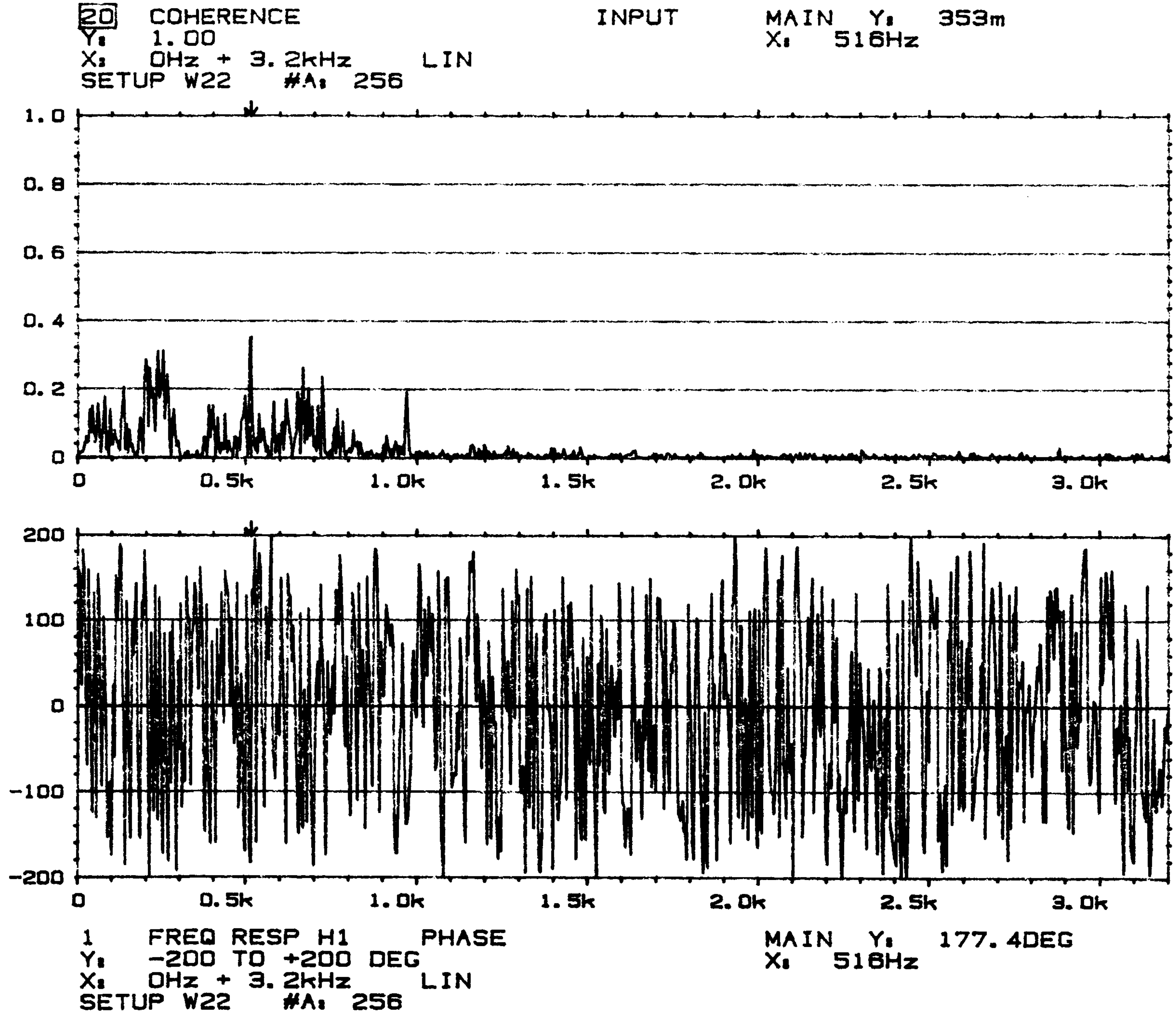

Type 2032

Page No.
109

Sign.:

Meas.
Object:
PLF PR17
Ch A: T16
Ch B: M1

Rdg 184

Comments:

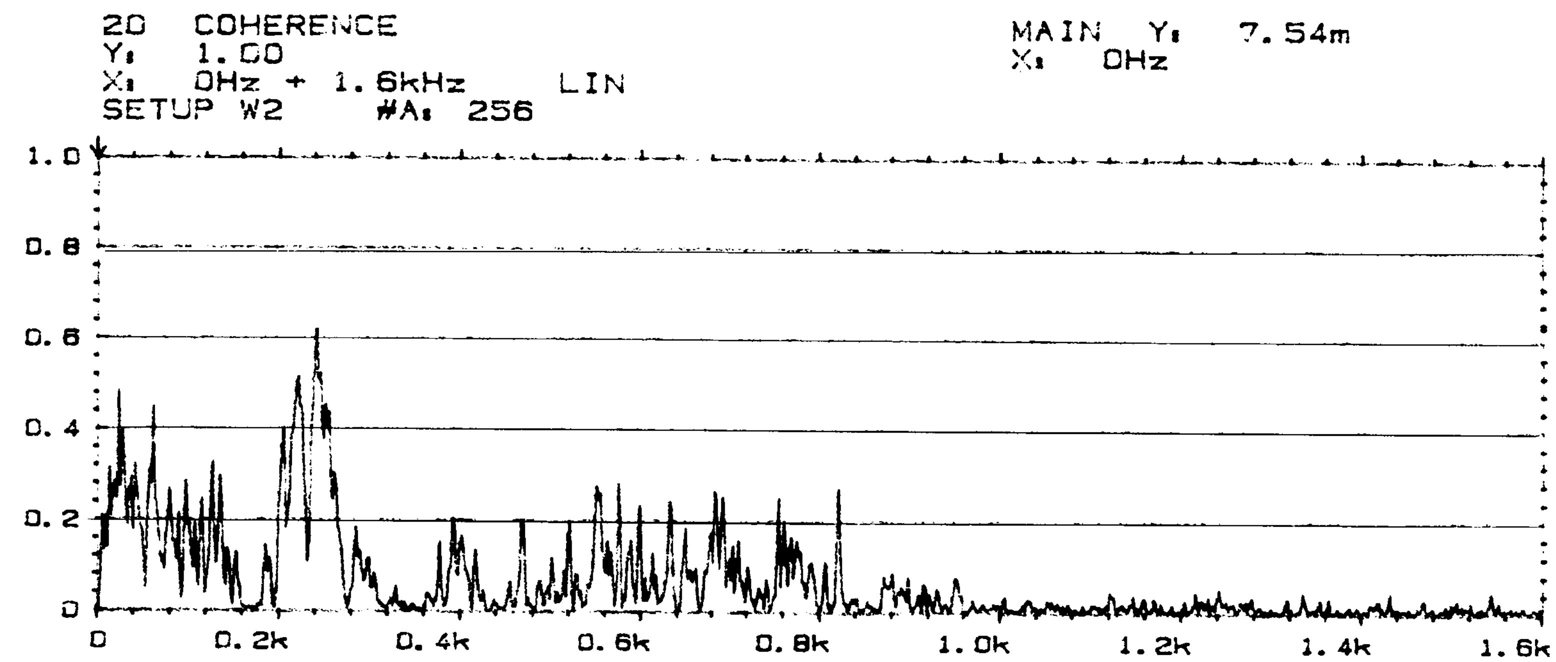

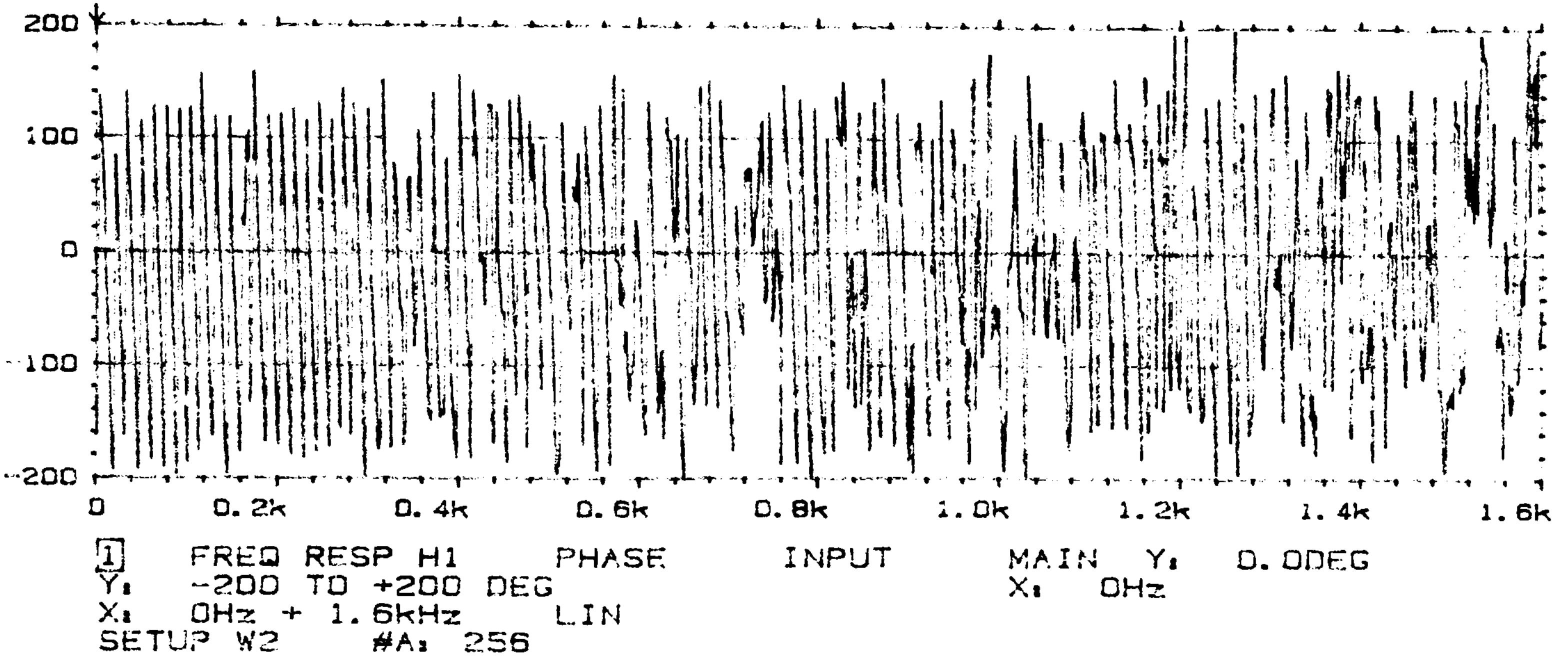

ORIGINAL PAGE IS
OF POOR QUALITY

Type 2032

Page No.
111

Sign.:

Meas.
Object:

PLF PR 1.3
ChA=T10
ChB=M2

Rdg 184

Comments:

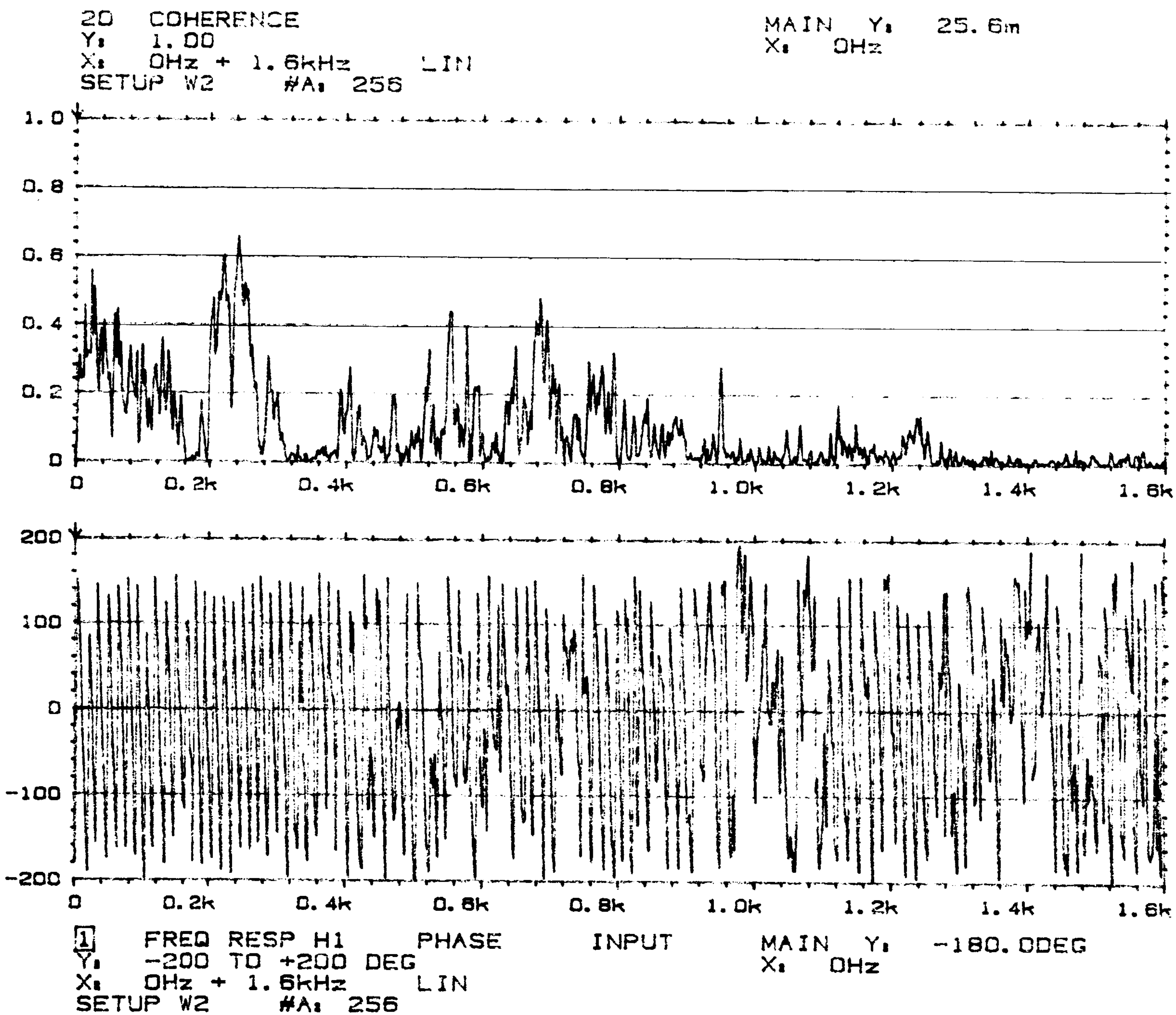

20 COHERENCE
Y: 1.00
X: 0Hz + 1.6kHz LIN
SETUP W2 #A: 256

MAIN Y: 19.2m
X: 0Hz

Type 2032

Page No.
113

Sign.:

Meas.
Object:
PLF PR 1.3
ChA - 110
ChB = M3

Rdg 194

Comments:

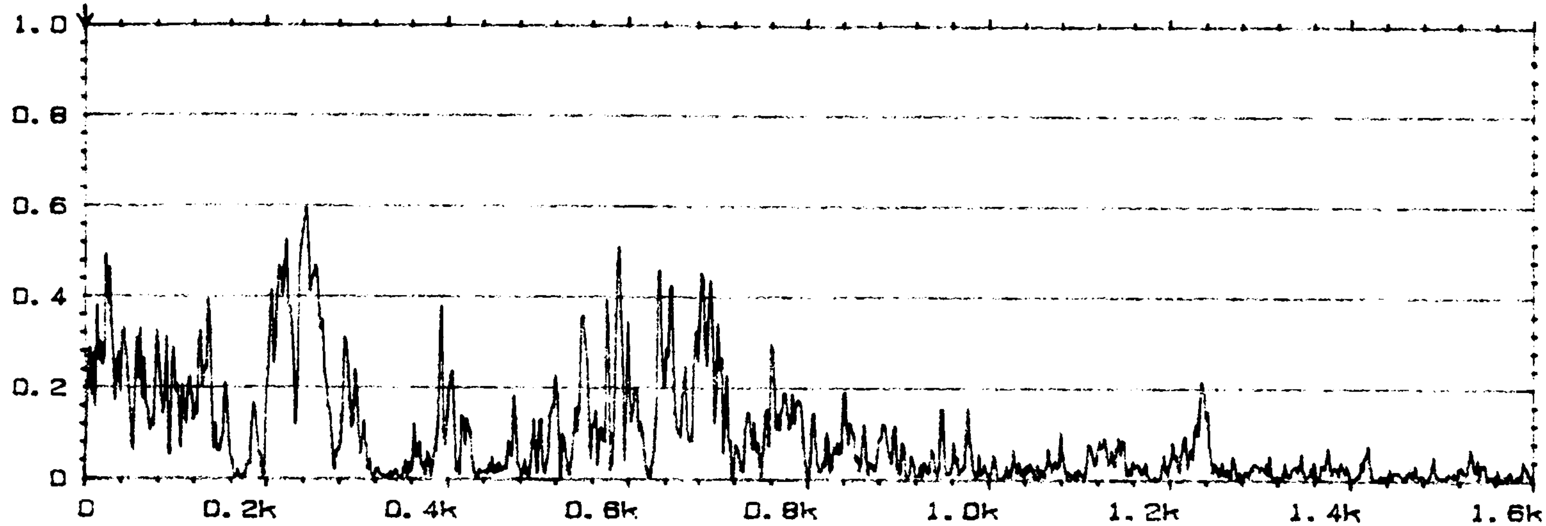

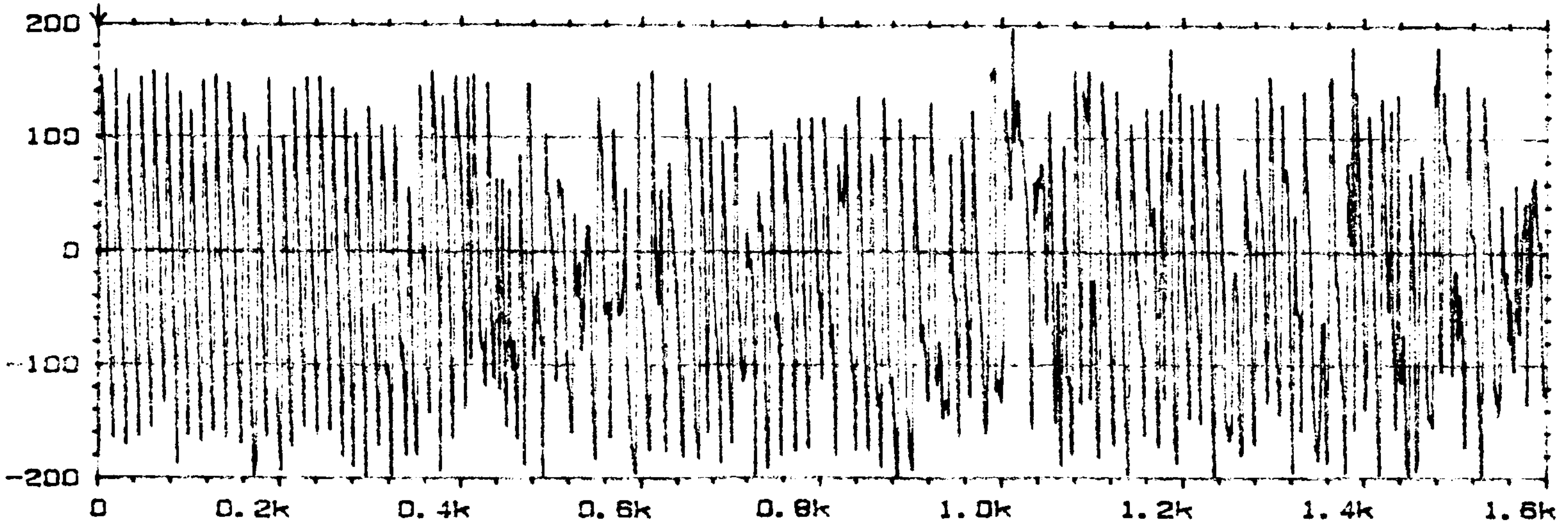

1 FREQ RESP H1 PHASE INPUT
Y: -200 TO +200 DEG
X: 0Hz + 1.6kHz LIN
SETUP W2 #A: 256

MAIN Y: -180.0DEG
X: 0Hz

Type 2032

Page No.
115

Sign.:

Meas.
Object:

PLF PR 1.3
ChA = T10
ChB = M4

Rdg 184

Comments:

2D COHERENCE
Y: 1.00
X: 0Hz + 1.6kHz LIN
SETUP W2 #A: 256

MAIN Y: 2.64m
X: 0Hz

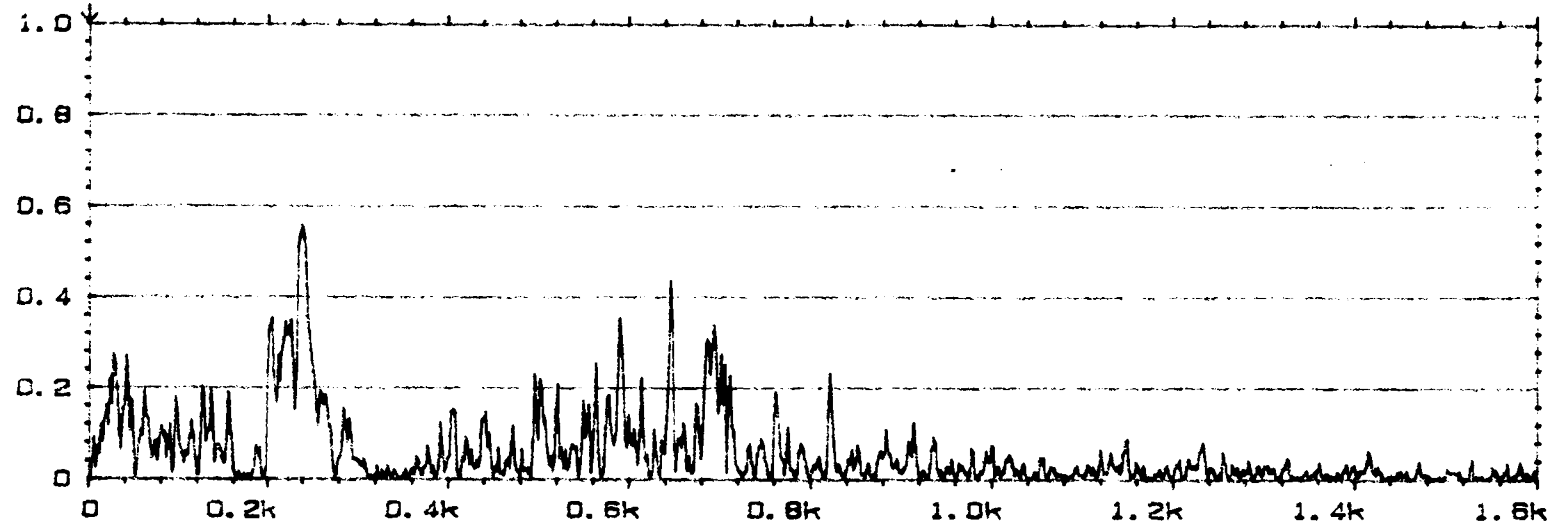

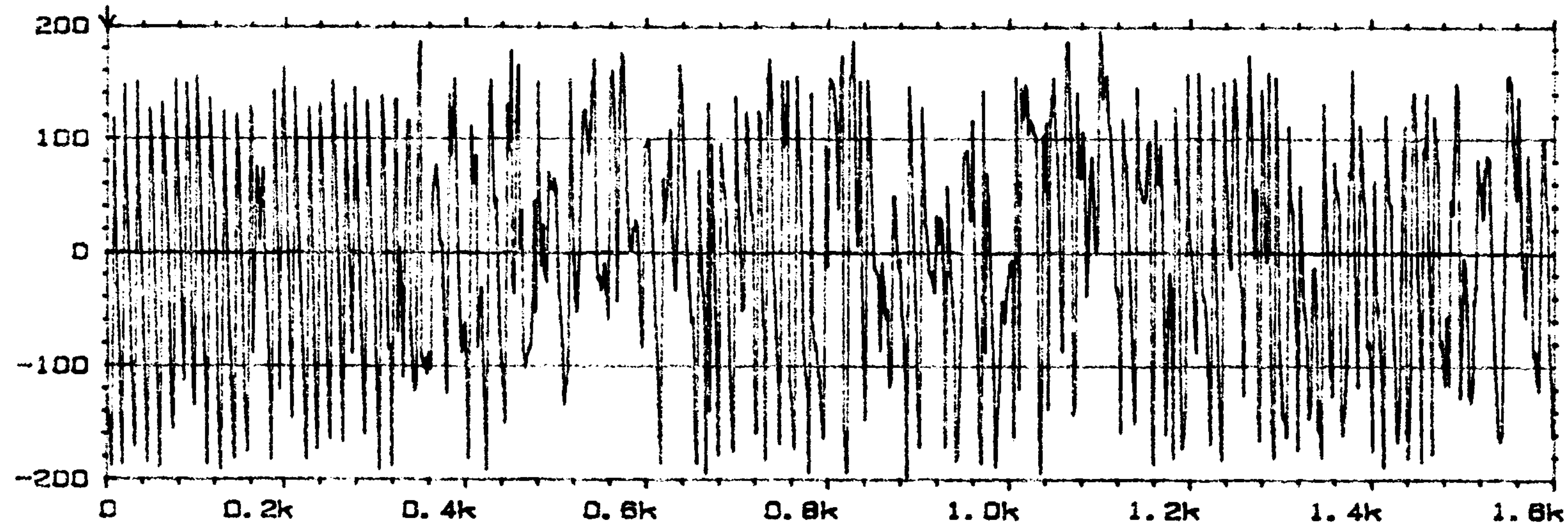

1 FREQ RESP H1 PHASE INPUT
Y: -200 TO +200 DEG
X: 0Hz + 1.6kHz LIN
SETUP W2 #A: 256

MAIN Y: -0.1DEG
X: 0Hz

Type 2032

Page No.
45

Sign.:

Meas.
Object:

PLF PR 1.4
chA = T10
chB = M1

Rdg 177

Comments:

20 COHERENCE INPUT MAIN Y: 65.5m
Y: 1.00 X: 684Hz
X: 0Hz + 1.6kHz LIN
SETUP W22 #A: 256

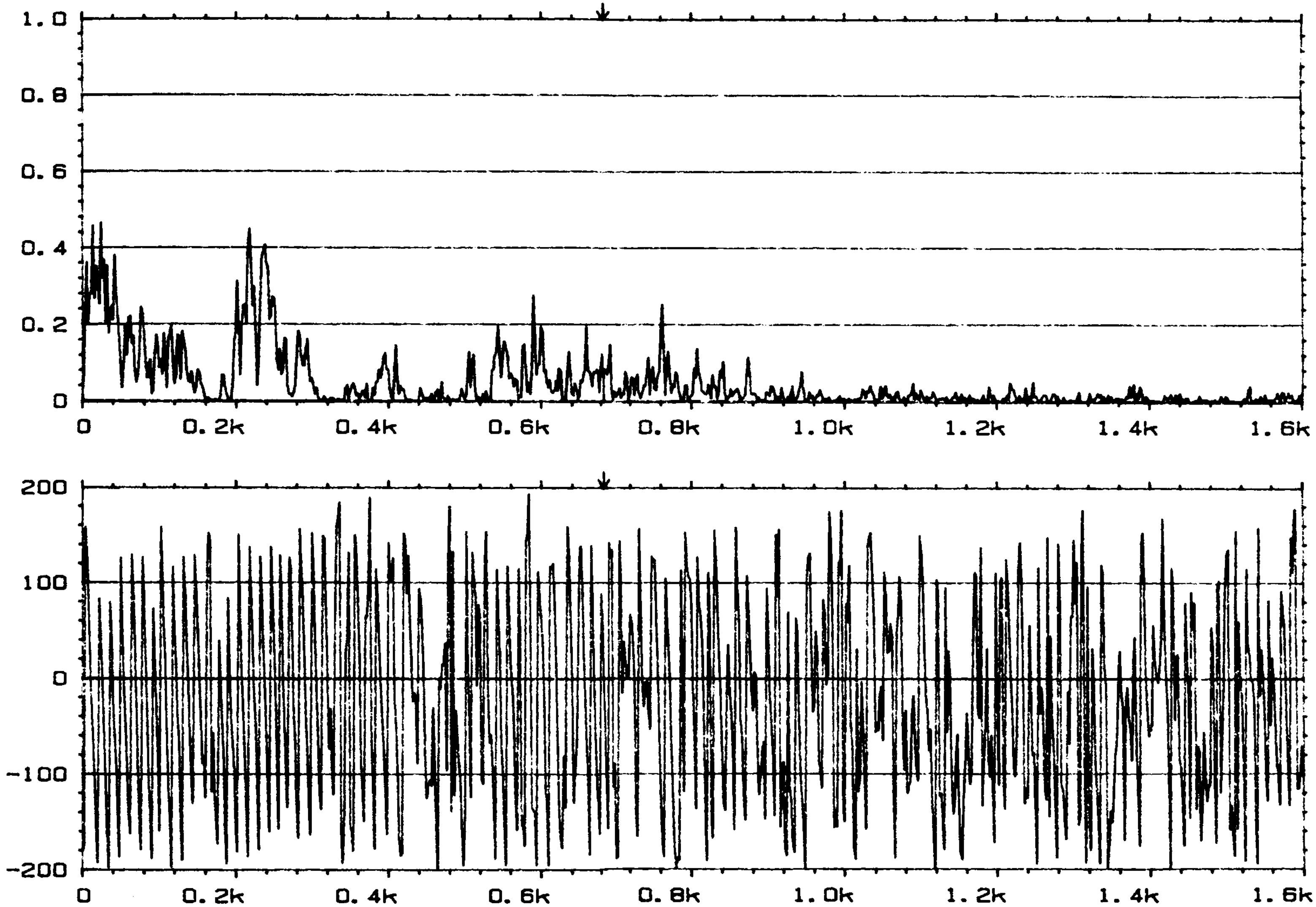

1 FREQ RESP H1 PHASE MAIN Y: 1.2DEG
Y: -200 TO +200 DEG X: 684Hz
X: 0Hz + 1.6kHz LIN
SETUP W22 #A: 256

Type 2032

Page No.
47

Sign.:

Meas.
Object:

PLF PR1.4
ChA = T10
ChB = M2

Rdg 177

Comments:

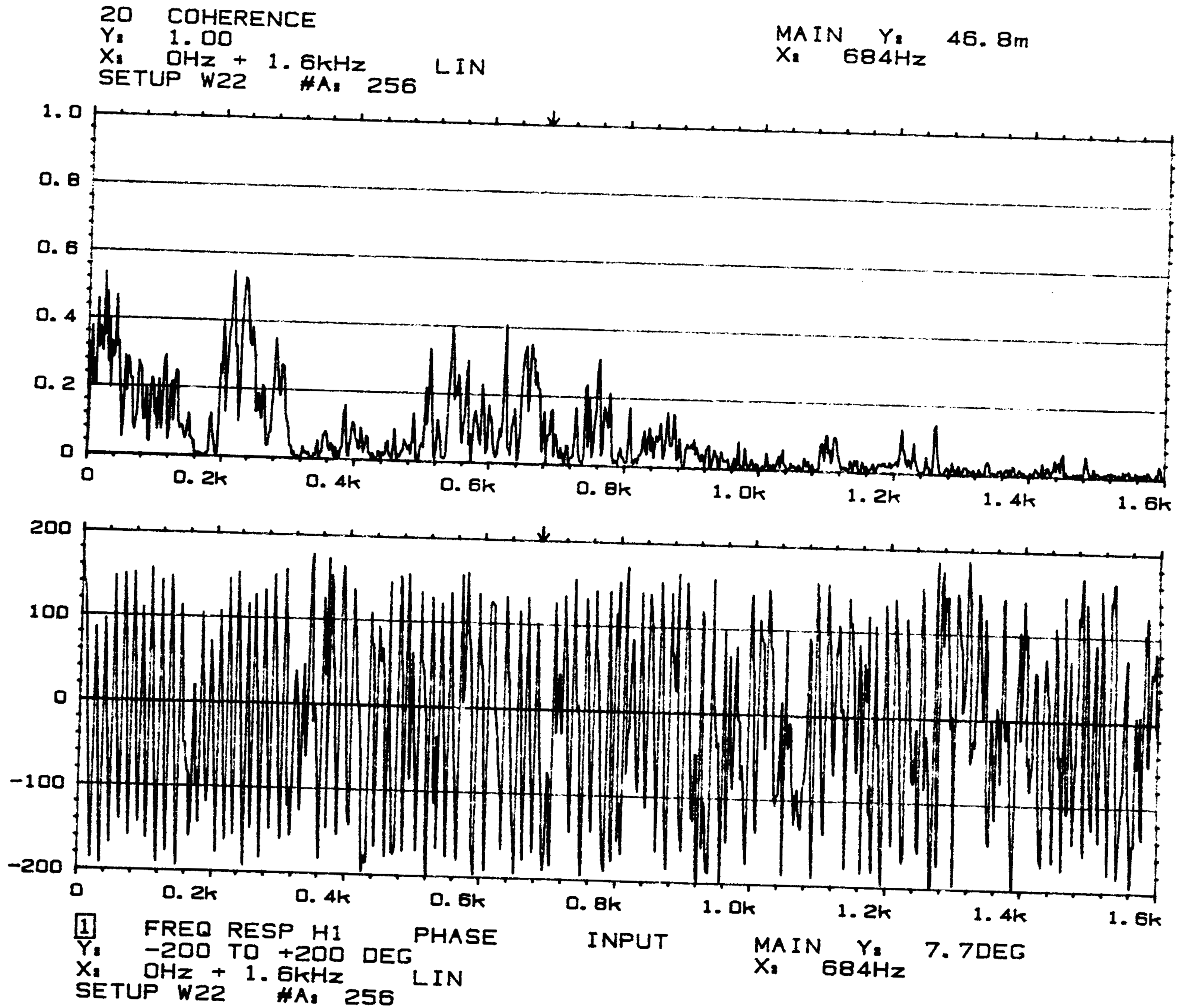

20 COHERENCE INPUT MAIN Y: 143m
Y: 1.00 X: 684Hz
X: 0Hz + 1.6kHz LIN
SETUP W22 #A: 256

Type 2032

Page No.
49

Sign.:

Meas.
Object:

Comments:

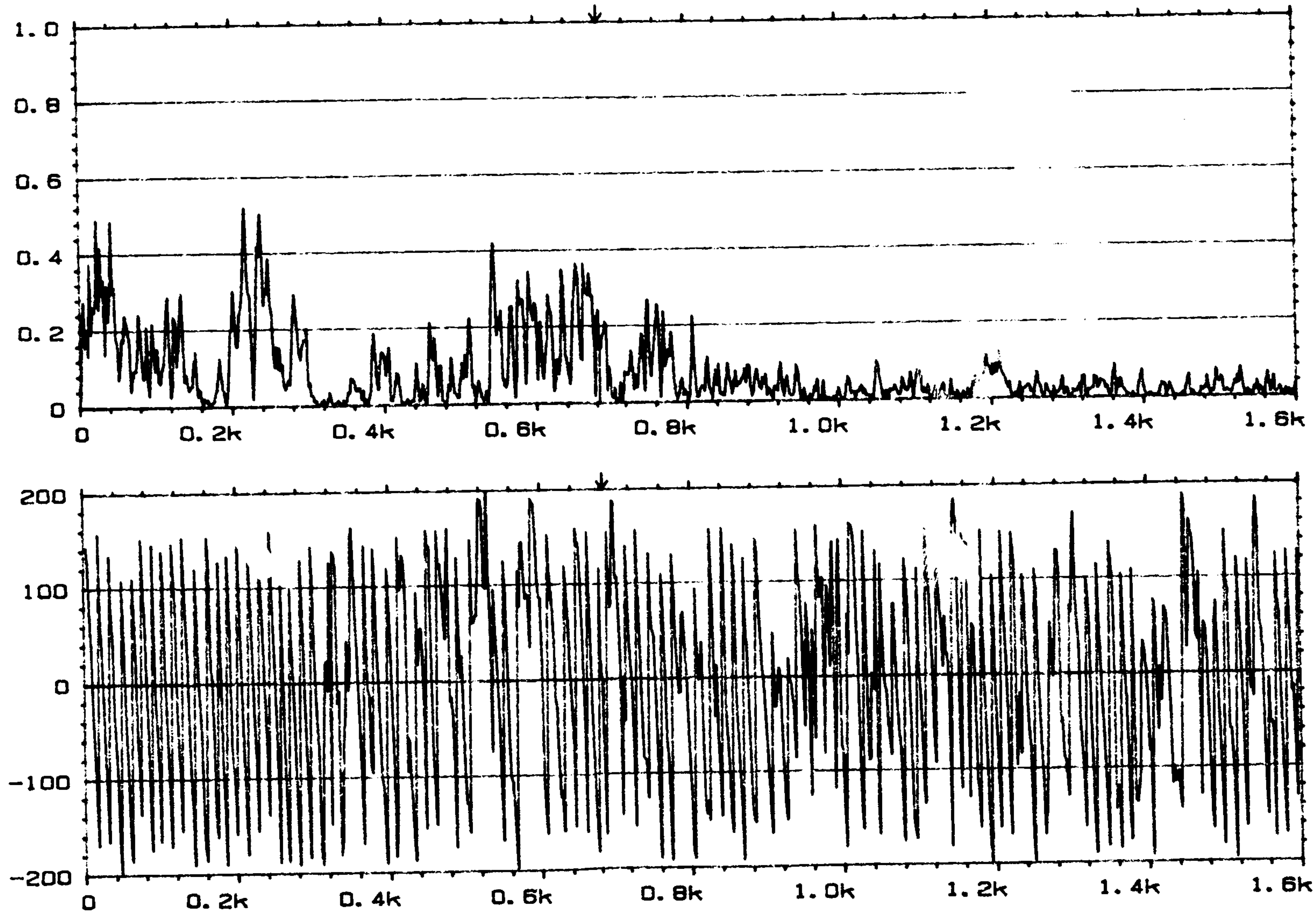

1 FREQ RESP H1 PHASE MAIN Y: -57.8DEG
Y: -200 TO +200 DEG X: 684Hz
X: 0Hz + 1.6kHz LIN
SETUP W22 #A: 256

Type 2032

Page No.
51

Sign.:

Meas.
Object:
PLF PR1.4
ChA = T10
ChB = M4

Rdg 177

Comments:

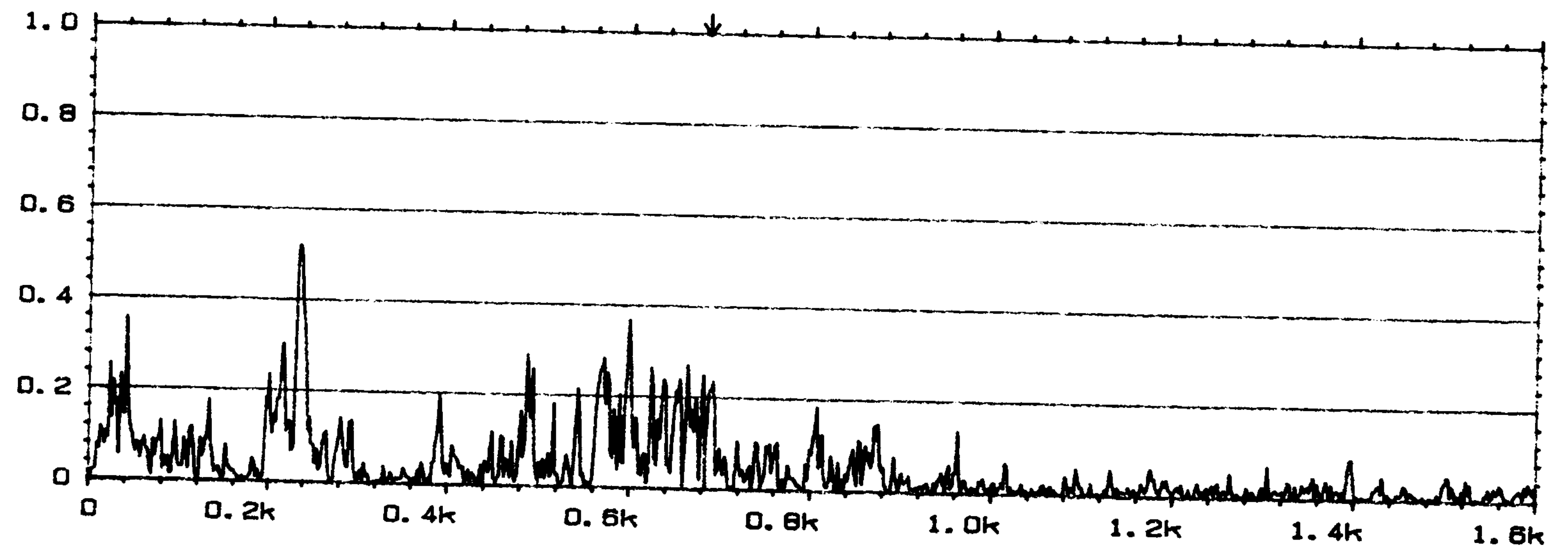

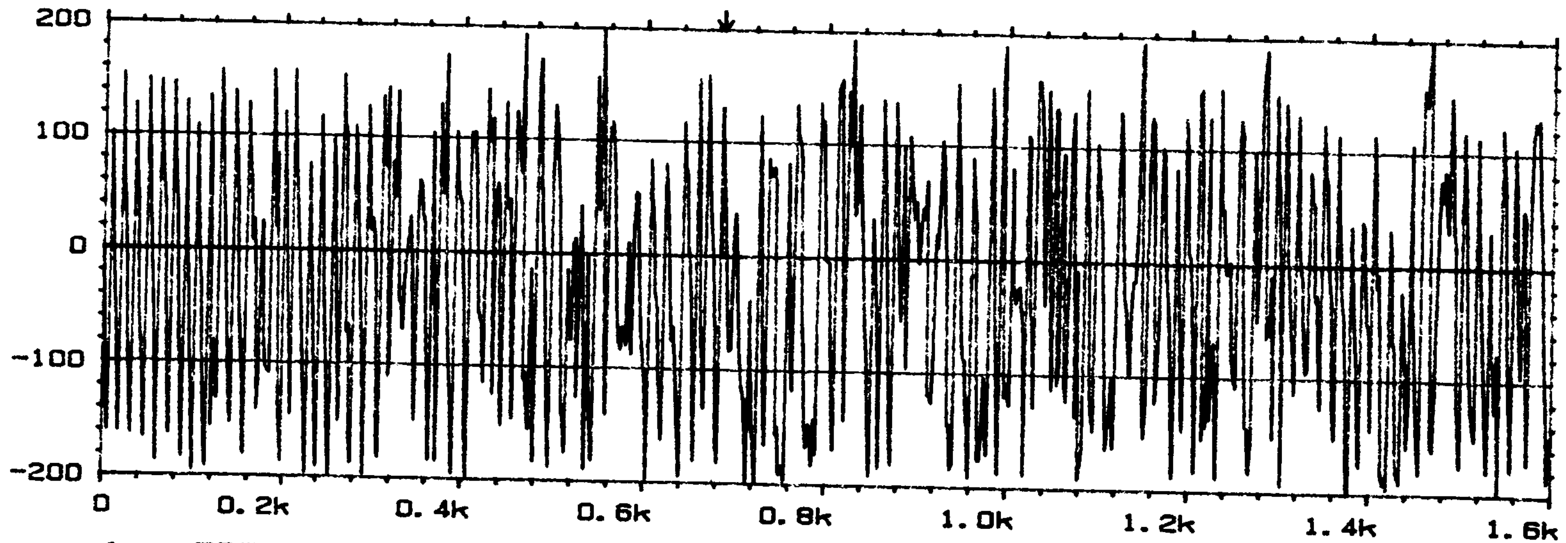

Type 2032

Page No.
36

Sign.:

Meas.
Object:

PLE PR 1.6
chA = T10
chB = M1

Rda 178

Comments:

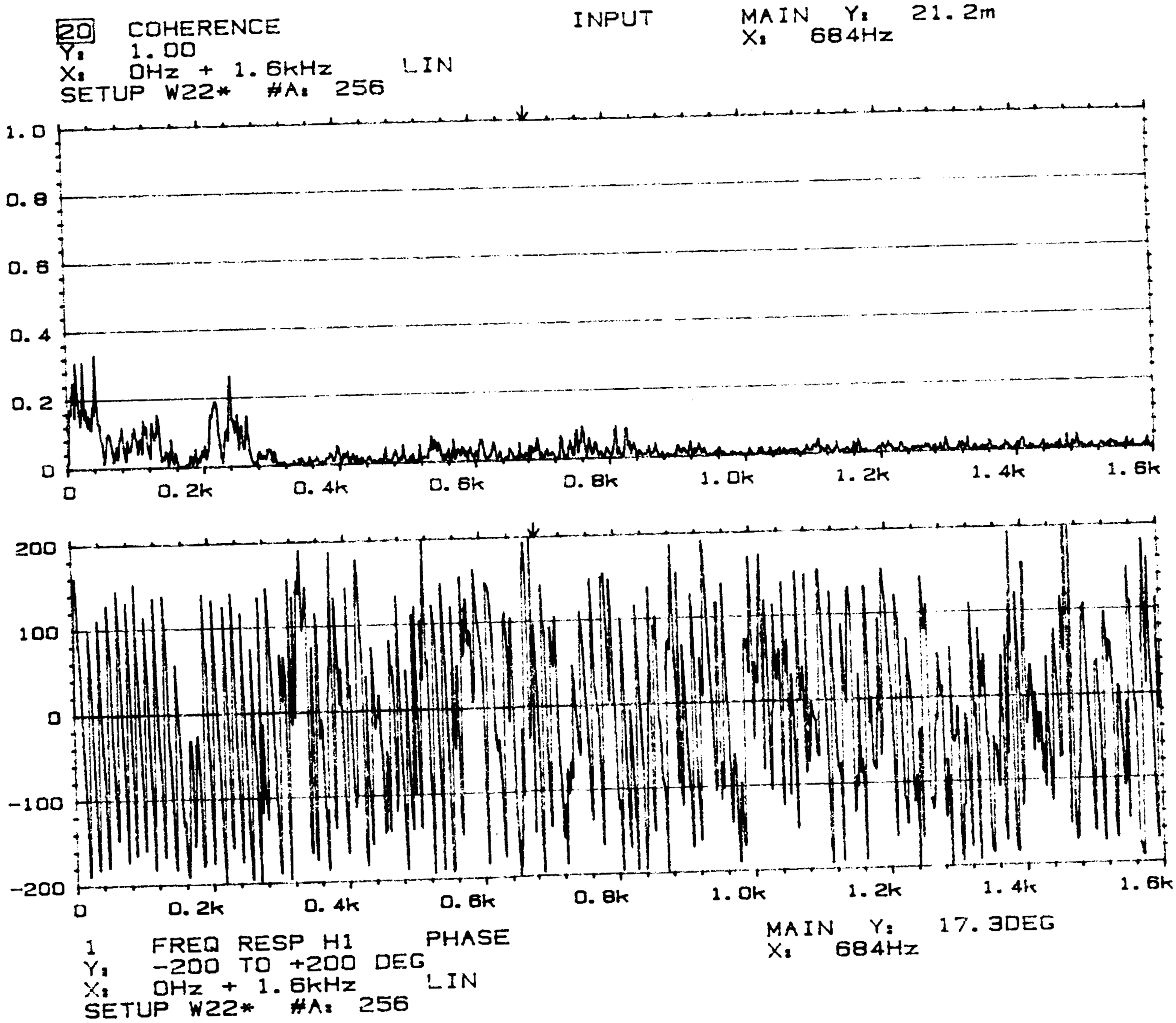

ORIGINAL PAGE IS
OF POOR QUALITY

20 COHERENCE
Y: 1.00
X: 0Hz + 1.6kHz LIN
SETUP W22 #A: 256

INPUT

MAIN Y: 38.8m
X: 684Hz

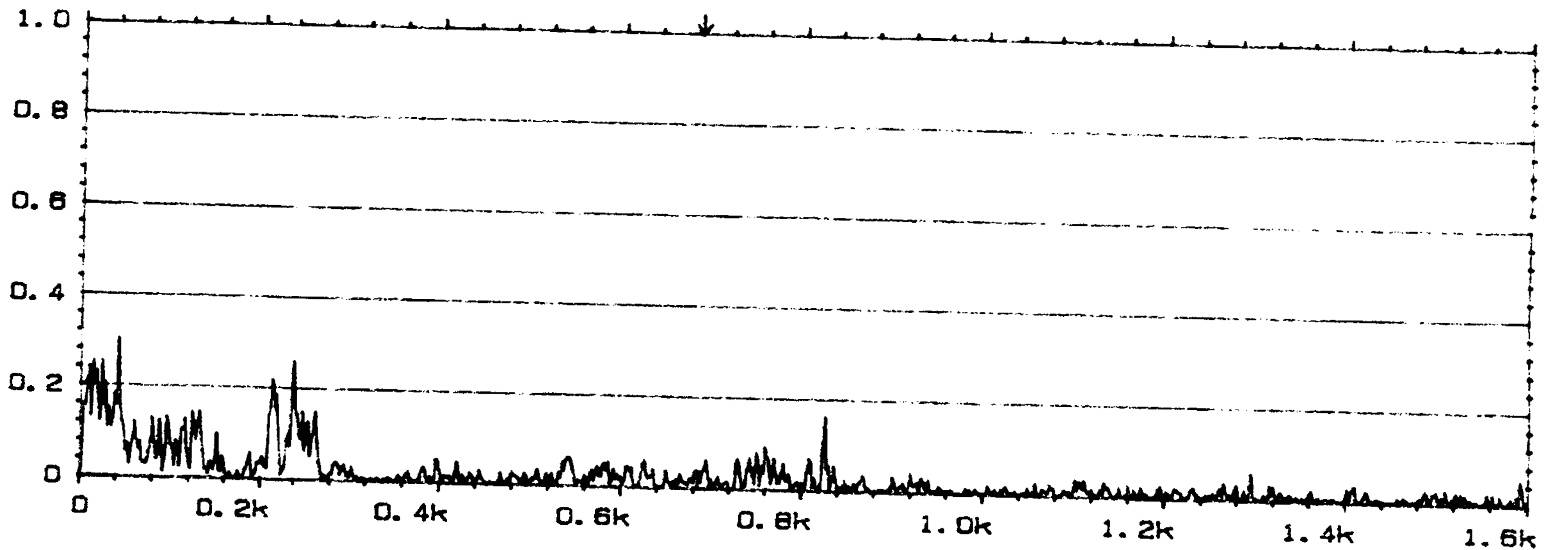

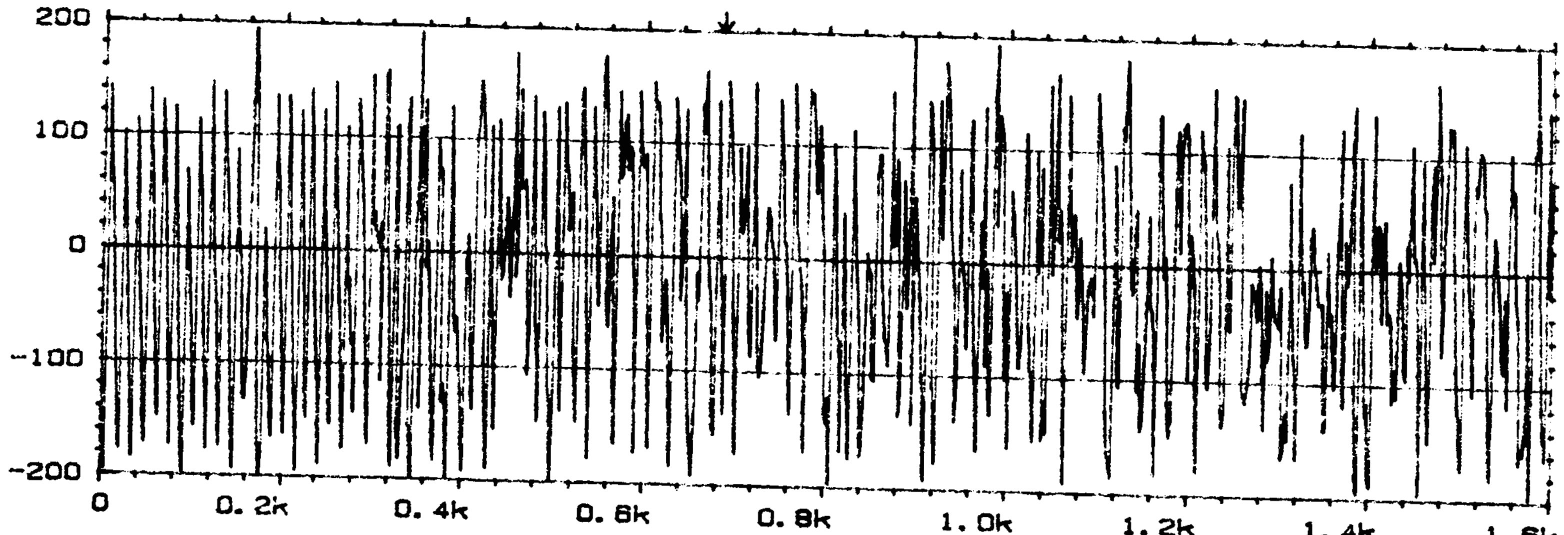

1 FREQ RESP H1 PHASE
Y: -200 TO +200 DEG
X: 0Hz + 1.6kHz LIN
SETUP W22 #A: 256

MAIN Y: -0.9DEG
X: 684Hz

Type 2032

Page No.
44

Sign.:

Meas.
Object:

PLF PR 1.6
ChA = T16
ChB = M1

R4g178

Comments:

Check on
Analysis
of Previous
Analyzer Run
This Point.

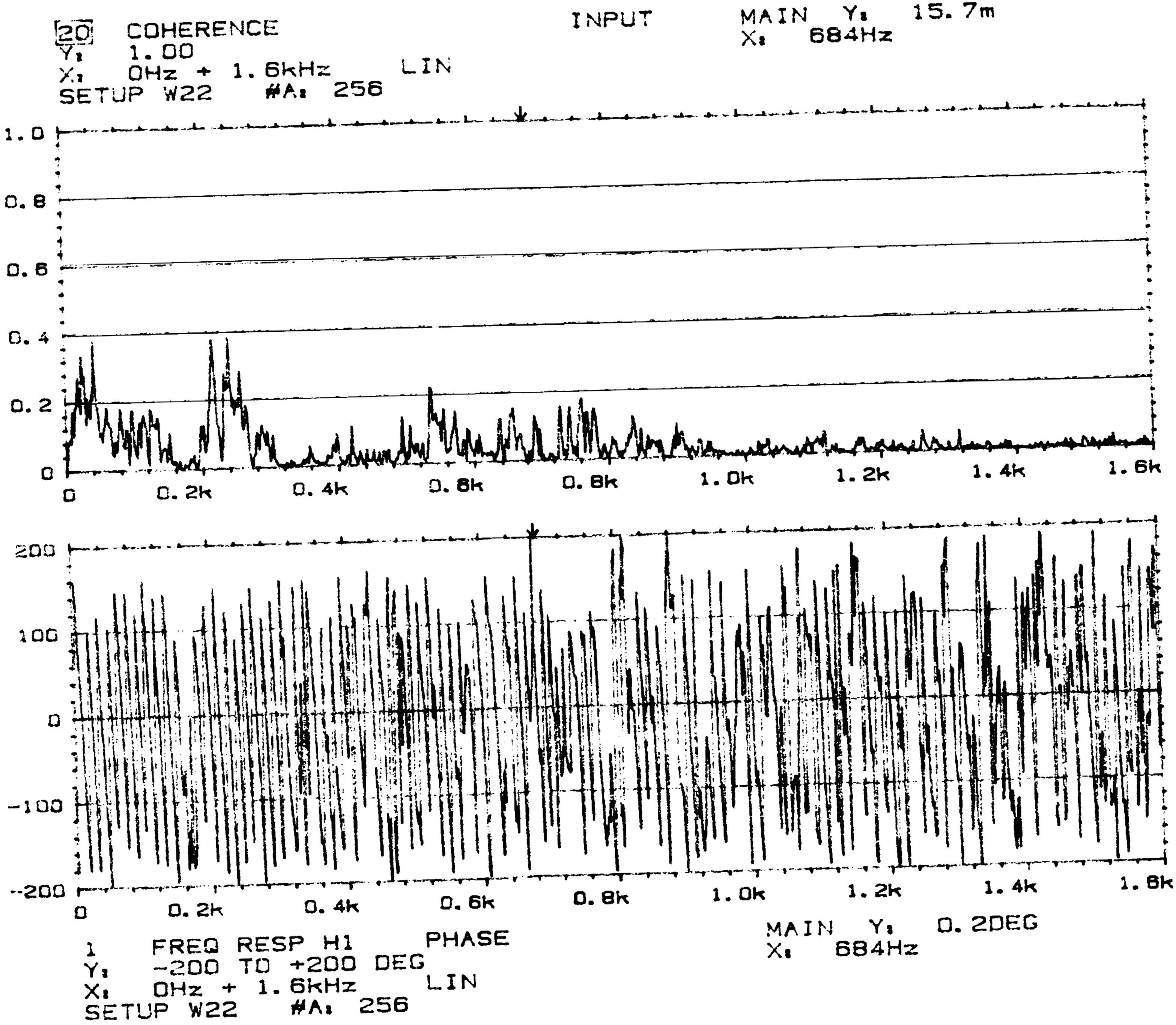

Type 2032

Page No.
42

Sign.:

Meas.
Object:
SLF PR 1.6
C/A 1/0
M2

Ehg 17A

Comments:

Type 2032

Page No.
40

Sign.:

Meas.
Object:
PLF PR 1.6
ChA = 7.10
Ch B = M3

Rdg 178

Comments:

20 COHERENCE INPUT MAIN Y: 98.0m
Y: 1.00 X: 684Hz
X: 0Hz + 1.6kHz LIN
SETUP W22 #A: 256

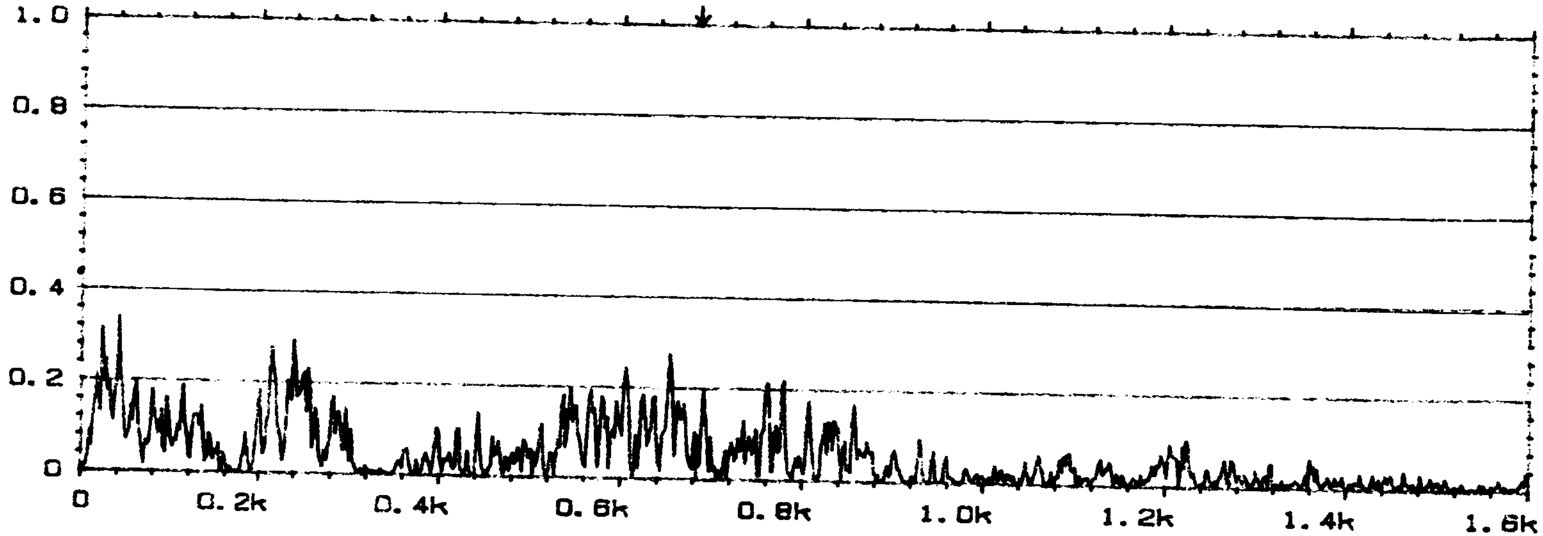

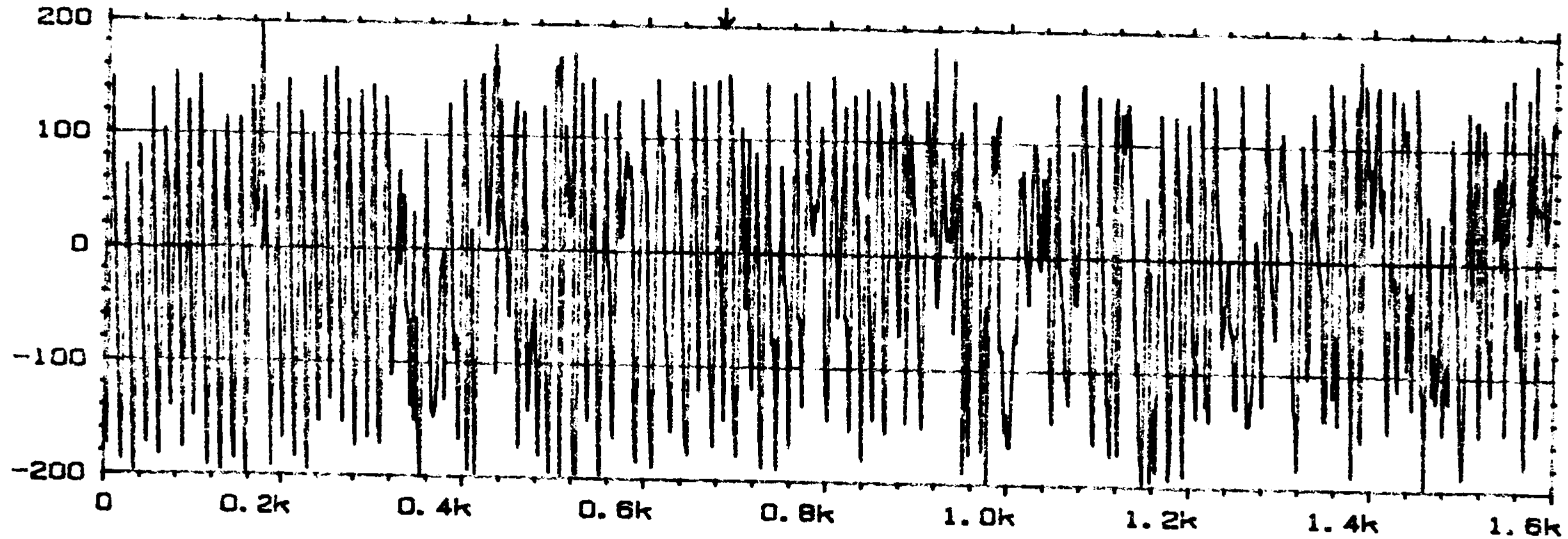

1 FREQ RESP H1 PHASE MAIN Y: -37.6DEG
Y: -200 TO +200 DEG X: 684Hz
X: 0Hz + 1.6kHz LIN
SETUP W22 #A: 256

Type 2032

Page No.
38

Sign.:

Meas.
Object:
PLF PR 1.6
ChA=T10
ChB=M4

Rdg 178

Comments:

20 COHERENCE INPUT MAIN Y: 4.37m
Y: 1.00 X: 684Hz
X: 0Hz + 1.6kHz LIN
SETUP W22 #A: 256

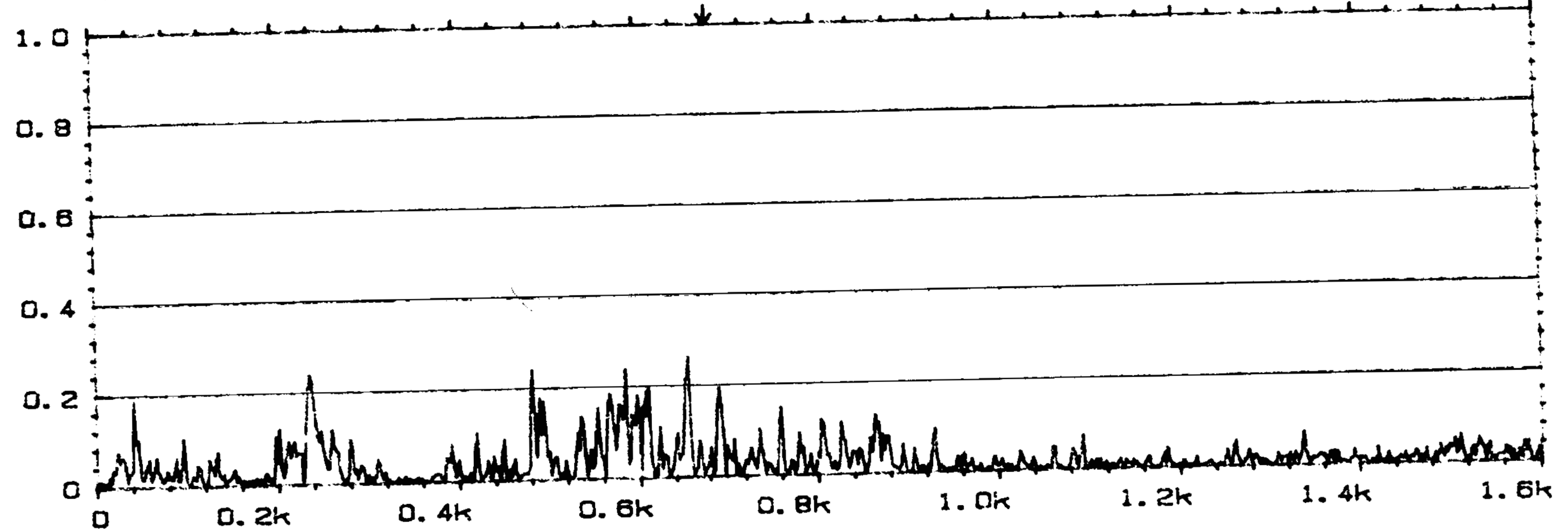

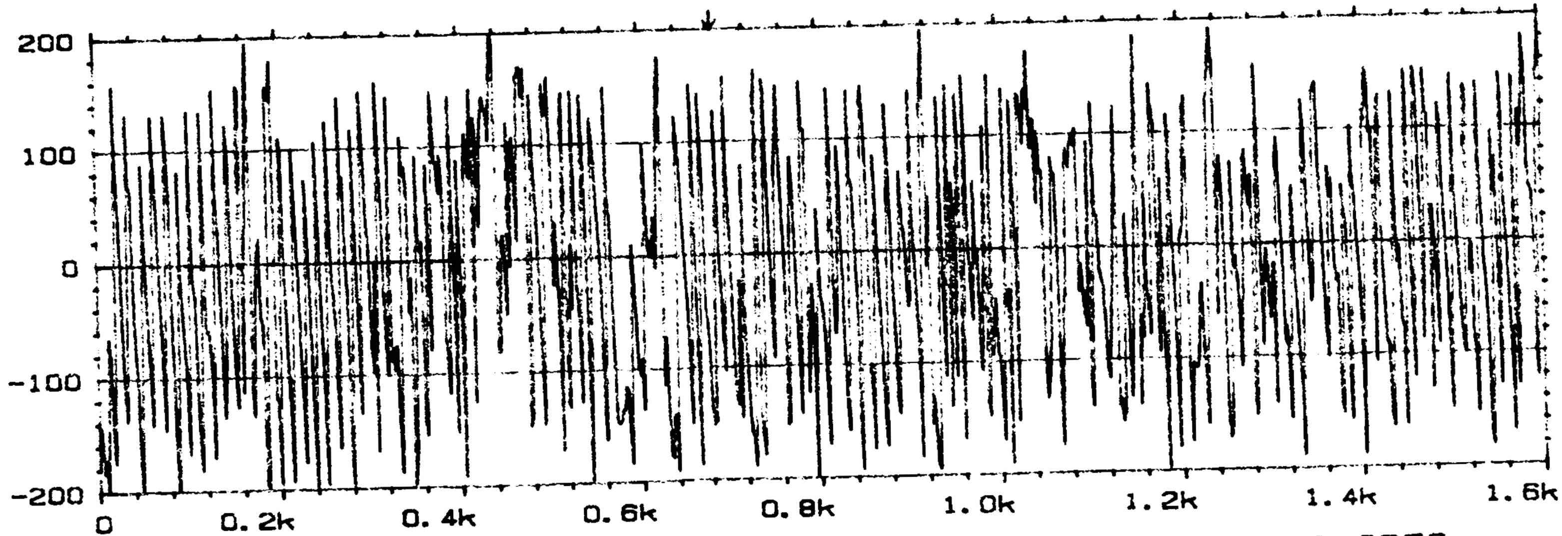

1 FREQ RESP H1 PHASE MAIN Y: -147.8DEG
Y: -200 TO +200 DEG X: 684Hz
X: 0Hz + 1.6kHz LIN
SETUP W22 #A: 256

Type 2032

Page No.
53

Sign.:

Meas.
Object:
PLF PR 1.8
ChA = T 10
ChB = M1

Rdg 179

Comments:
256 AVGS
More Than
Adequate

20 COHERENCE INPUT MAIN Y: 152m
Y: 1.00 X: 238Hz
X: 0Hz + 1.6kHz LIN
SETUP W22 #A: 256

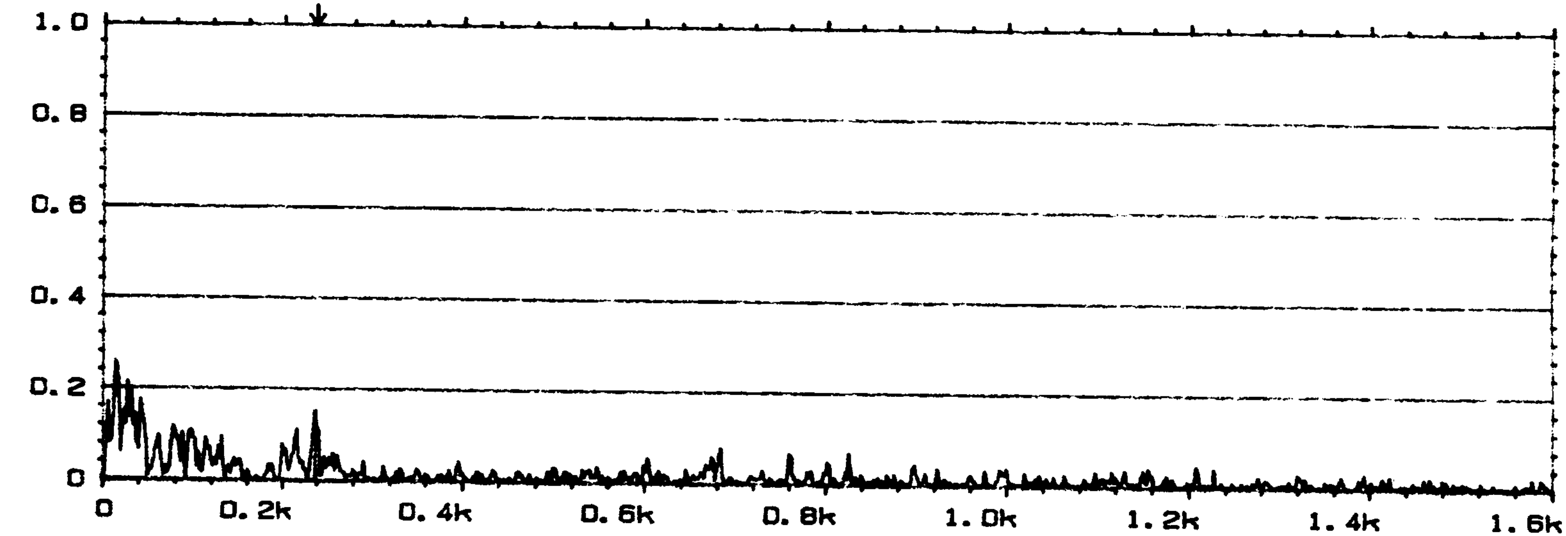

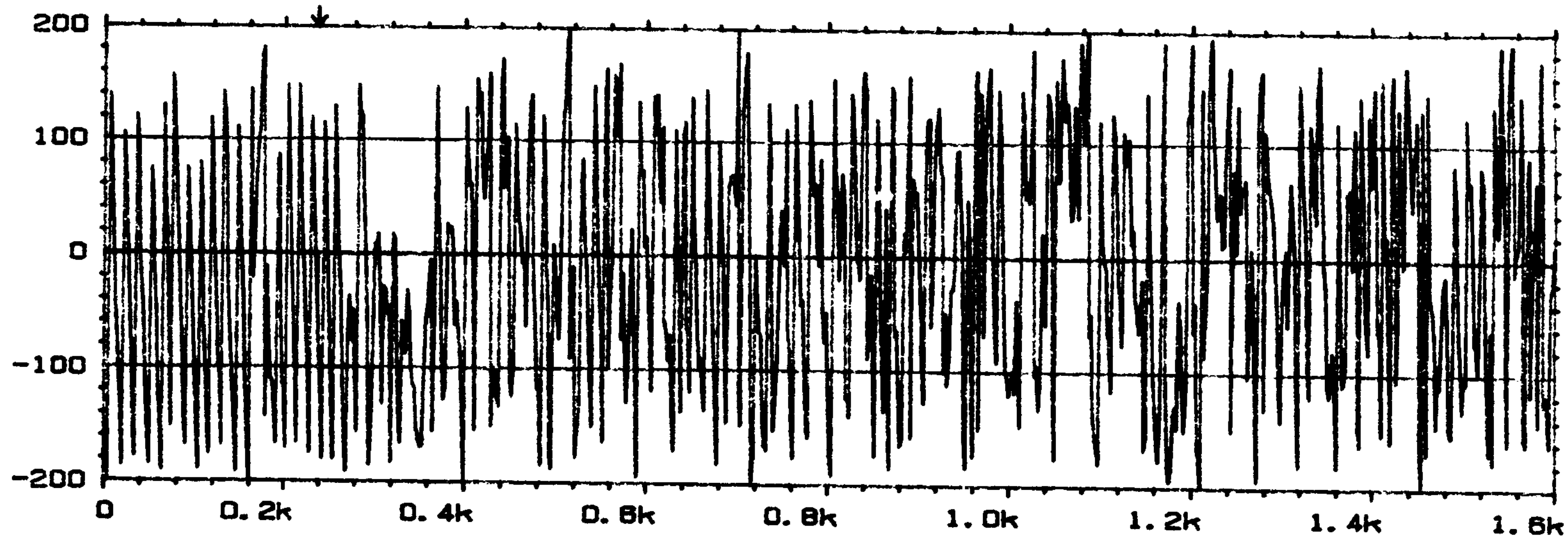

1 FREQ RESP H1 PHASE MAIN Y: -26.9DEG
Y: -200 TO +200 DEG X: 238Hz
X: 0Hz + 1.6kHz LIN
SETUP W22 #A: 256

Type 2032

Page No.
55

Sign.:

Meas.
Object:

Comments:

20 COHERENCE INPUT MAIN Y: 222m
Y: 1.00 X: 238Hz
X: 0Hz + 1.6kHz LIN
SETUP W22 #A: 256

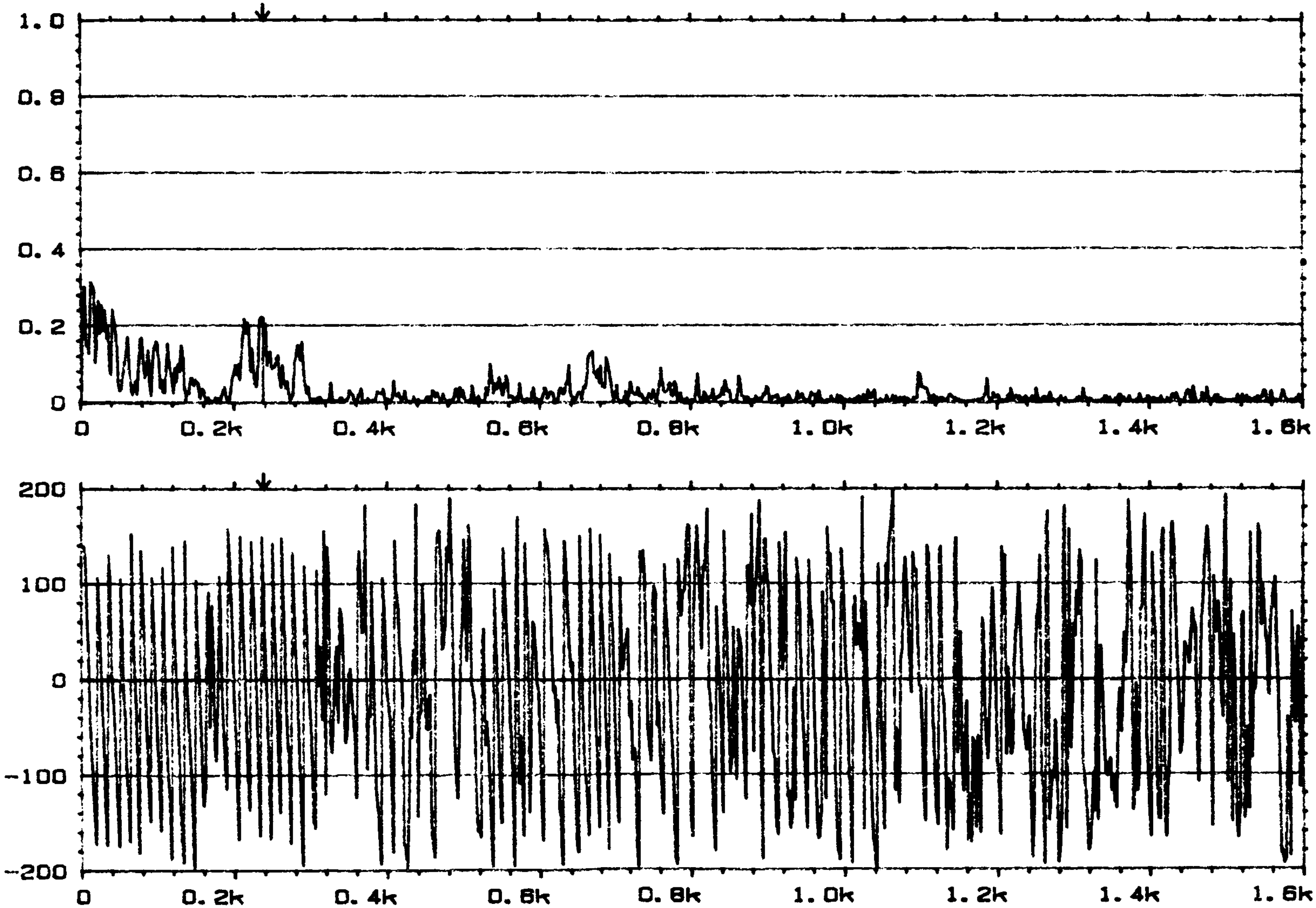

1 FREQ RESP H1 PHASE MAIN Y: 98.6DEG
Y: -200 TO +200 DEG X: 238Hz
X: 0Hz + 1.6kHz LIN
SETUP W22 #A: 256

ORIGINAL PAGE IS
OF POOR QUALITY

Type 2032

Page No.
57

Sign.:

Meas.
Object:
PLF PR 1.8
ChA = T10
ChB = M3

Rdg 179

Comments:

20 COHERENCE INPUT MAIN Y: 240m
Y: 1.00 X: 690Hz
X: 0Hz + 1.6kHz LIN
SETUP W22 #A: 256

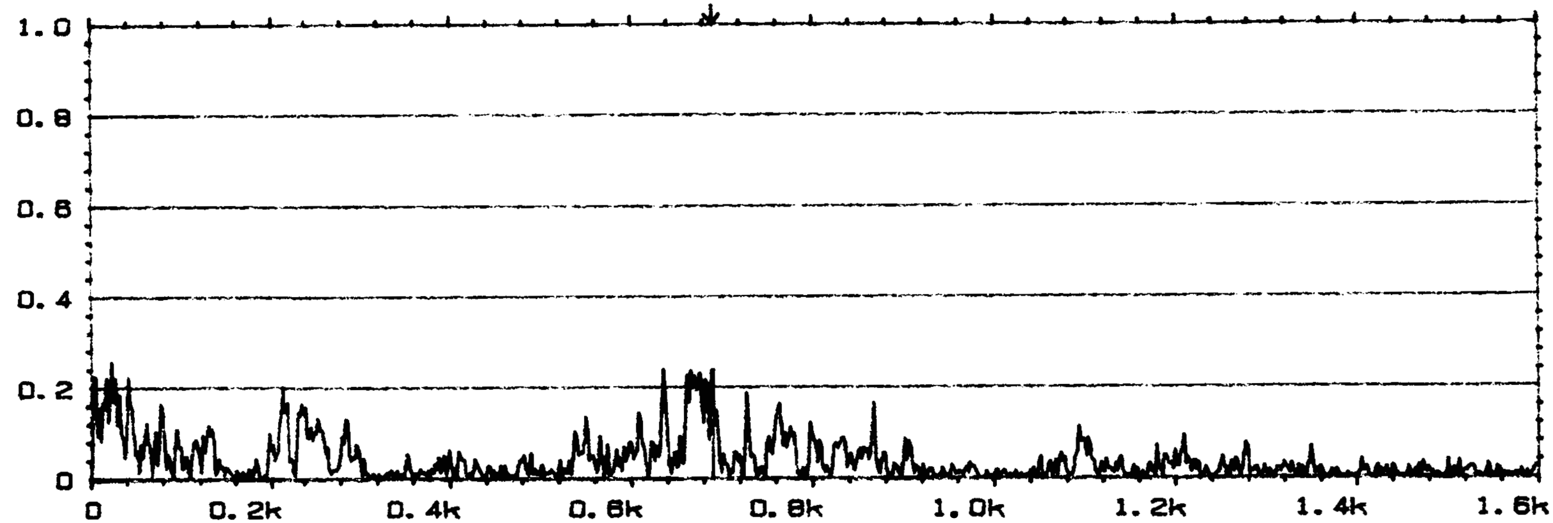

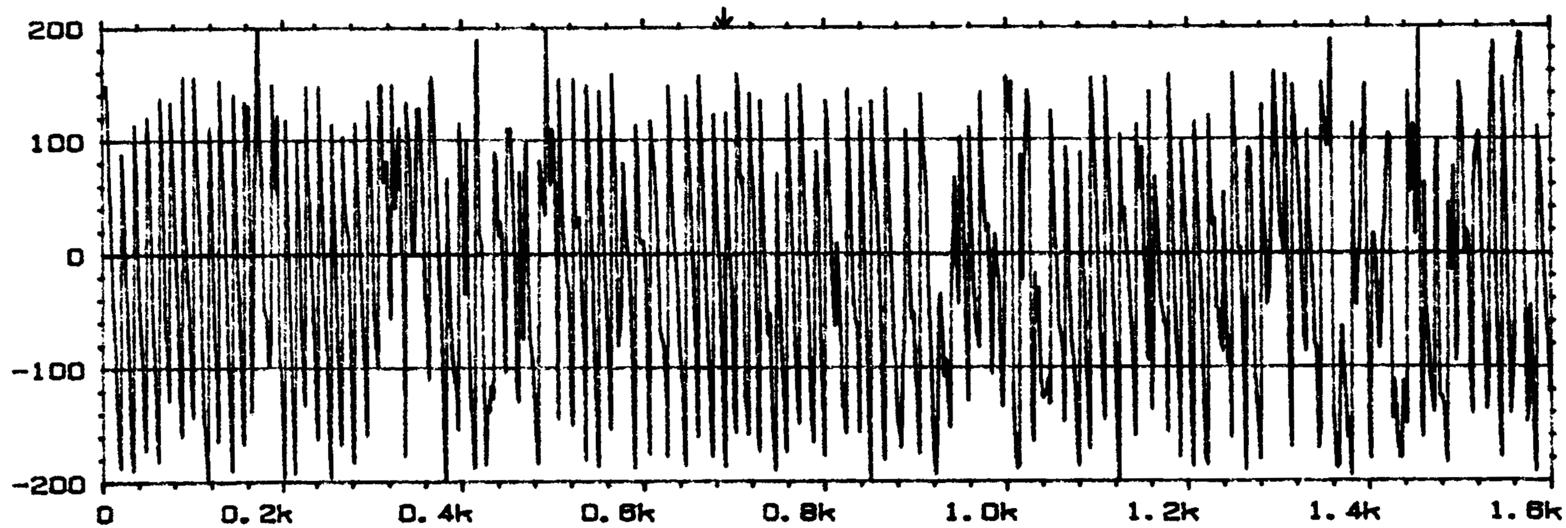

1 FREQ RESP H1 PHASE MAIN Y: 174.0DEG
Y: -200 TO +200 DEG X: 690Hz
X: 0Hz + 1.6kHz LIN
SETUP W22 #A: 256

ORIGINAL PAGE IS
OF POOR QUALITY

Type 2032

Page No.
59

Sign.:

Meas.
Object:

PLF PR1.8
ChA=T10
ChB=M4

Rdg 179

Comments:

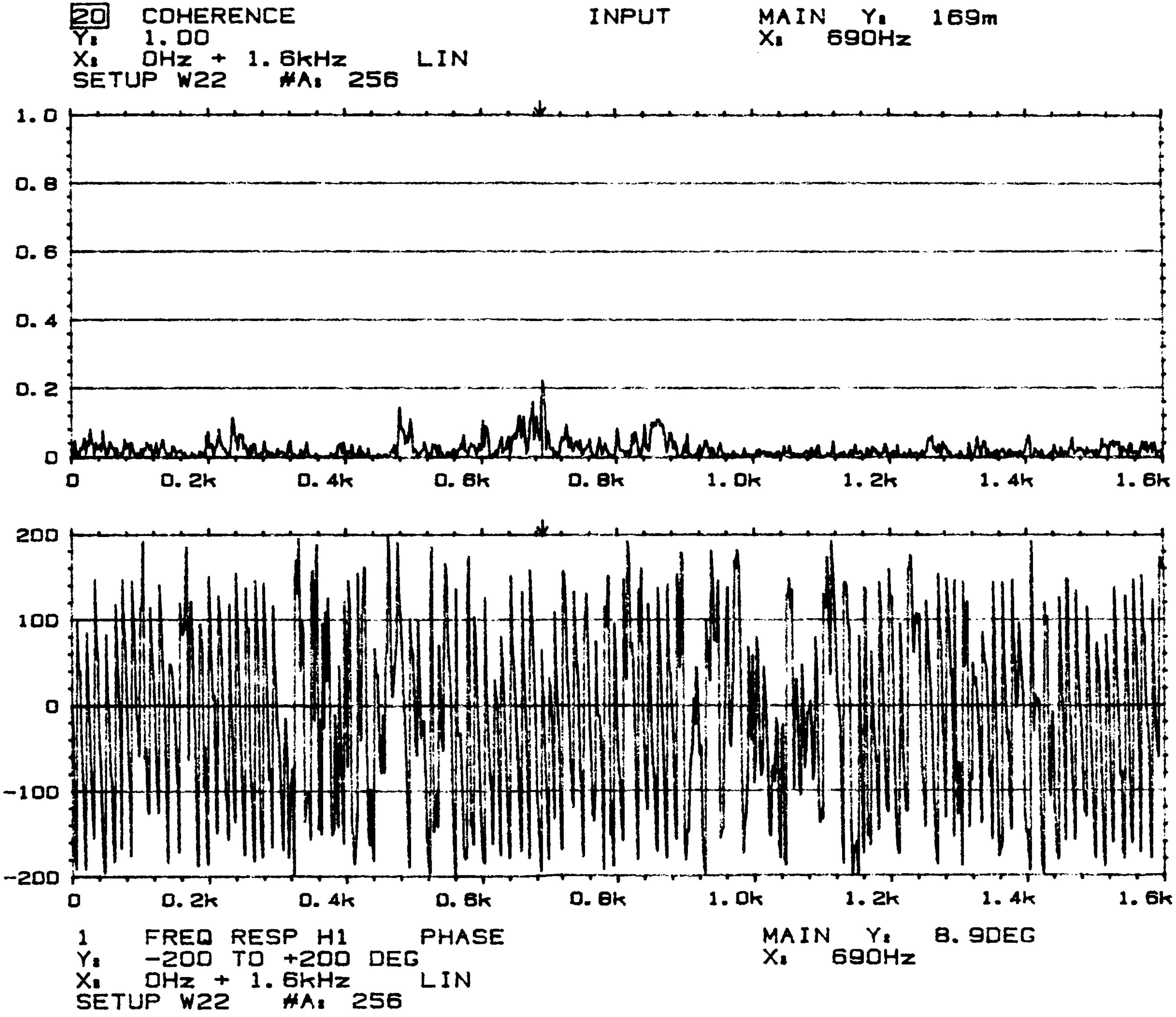

Type 2032

Page No.
61

Sign.:

Meas.
Object:
PLF PR 2.0
ChA = T10
ChB = M1

Rtg 180

Comments:

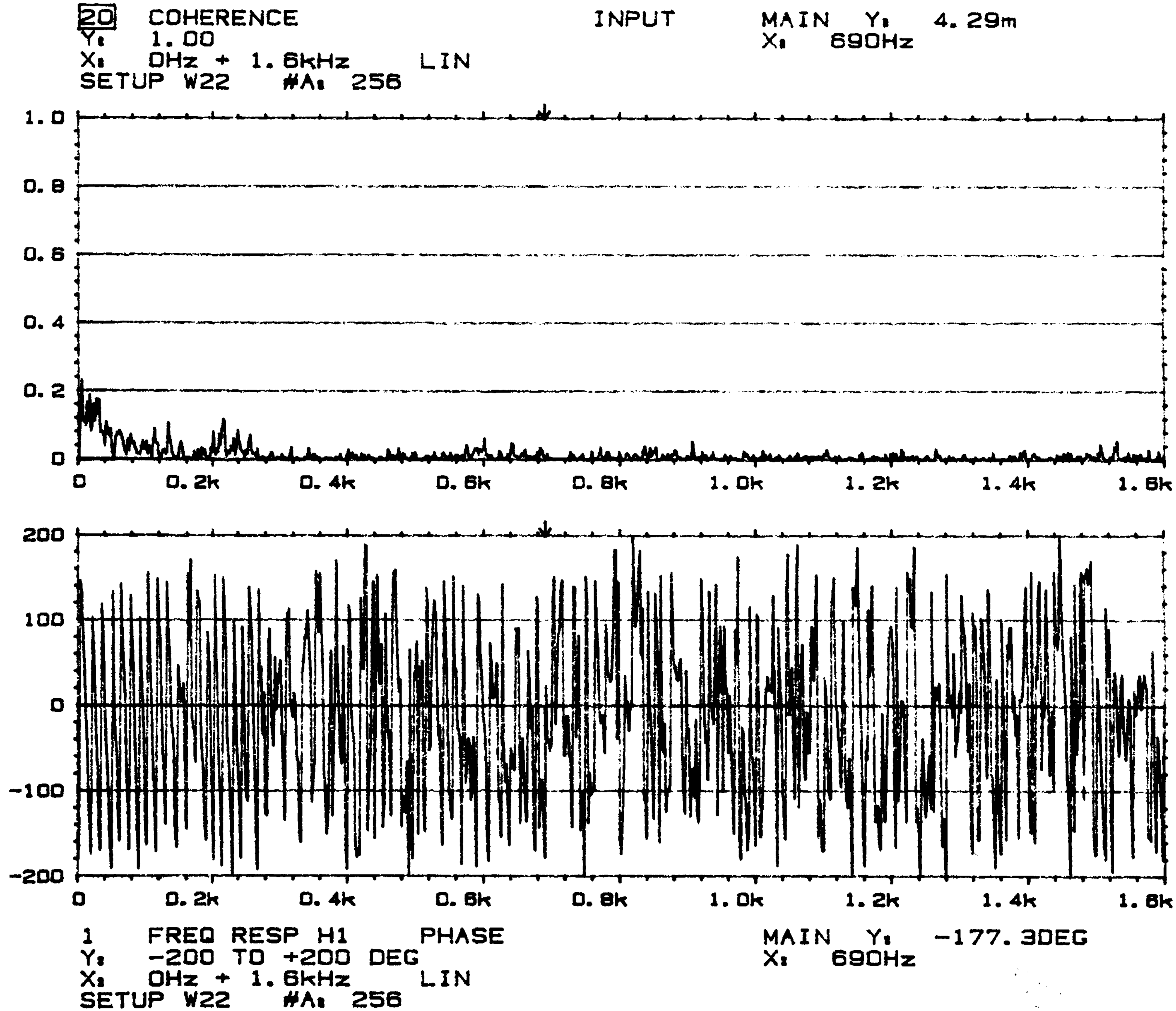

Type 2032

Page No.
63

Sign.:

Meas.
Object:

PLF PR 2.0
ChA 110
ChB M2

PAg 180

Comments:

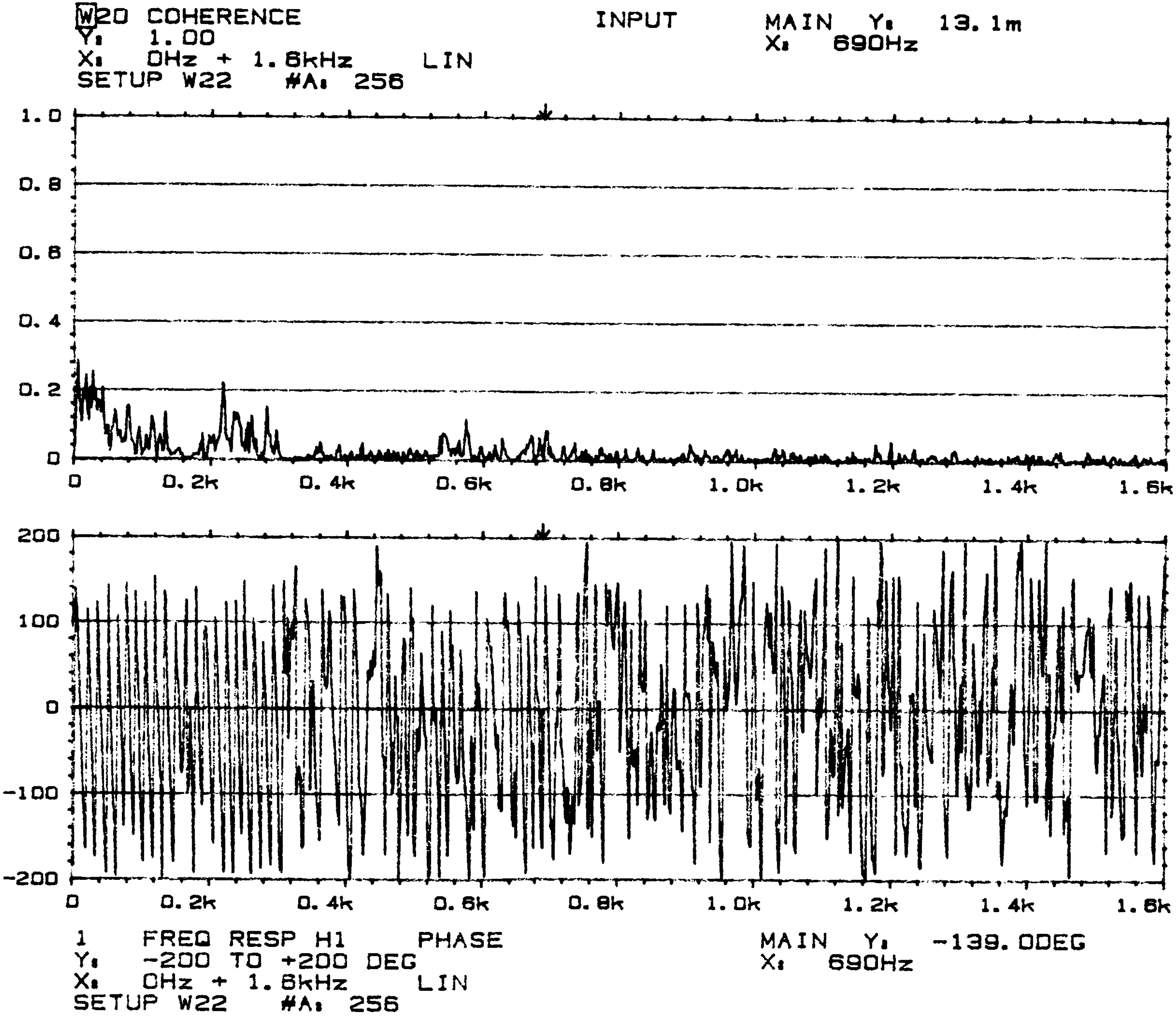

Type 2032

Page No.
65

Sign.:

Meas.
Object:

PLF PR 2.0
chA = T10
ChB = M3

Rdg 180

Comments:

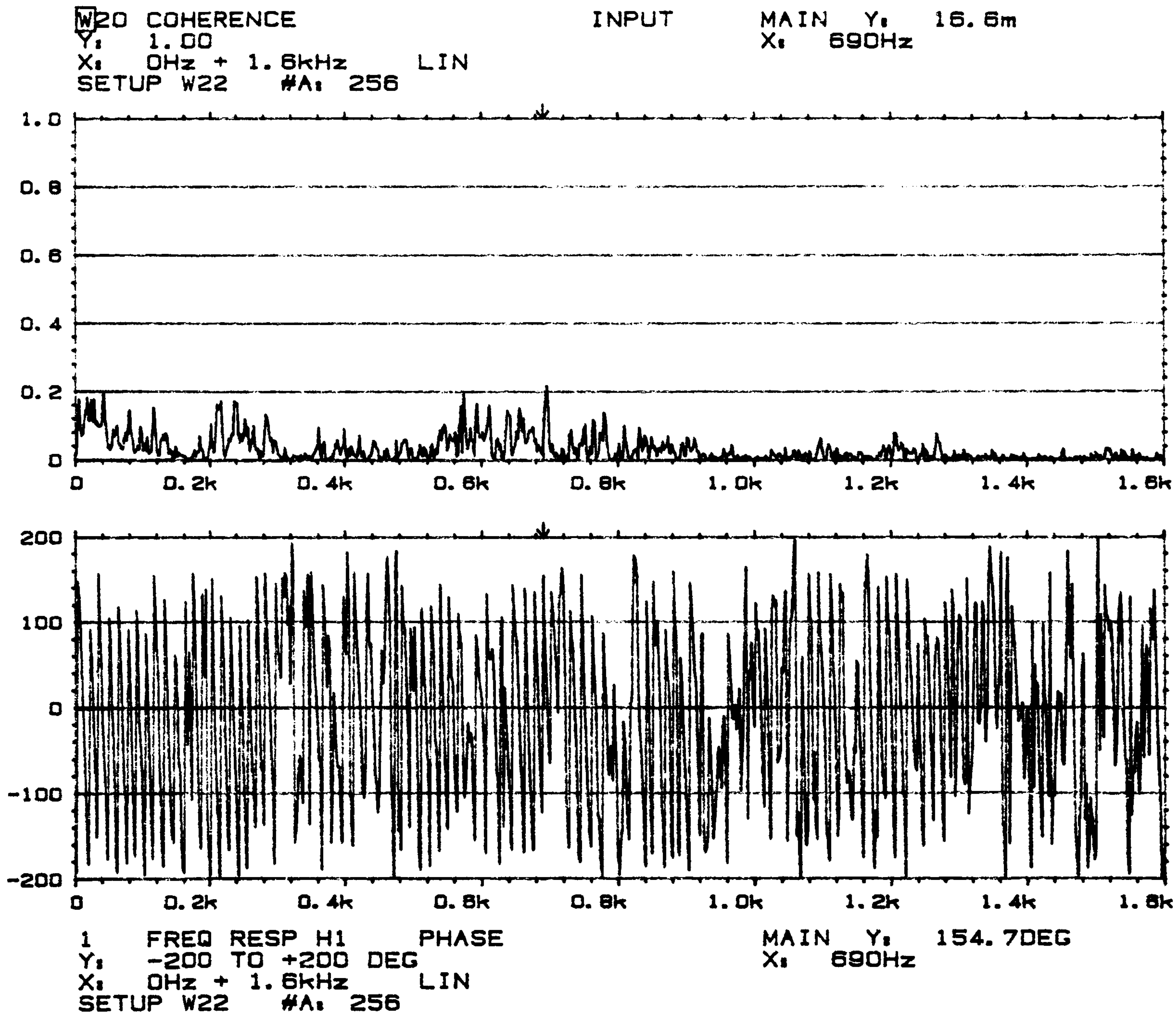

Type 2032

Page No.
73

Sign.:

Meas.
Object:

PLF PR 2.0
ChA = T10
ChB = M4

Rdg 130

Comments:

Expanded freq
Range

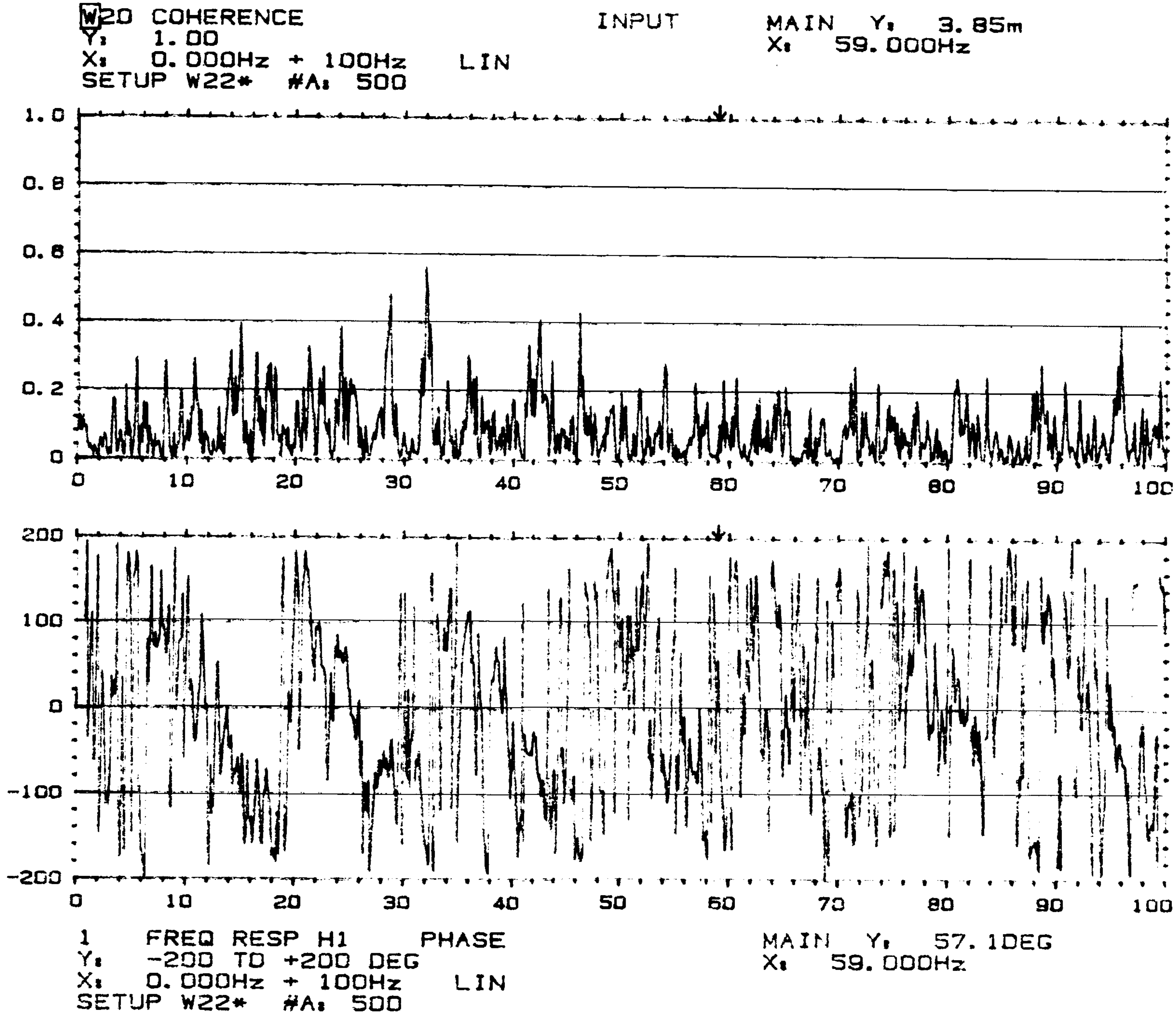

ORIGINAL PAGE IS
OF POOR QUALITY

W20 COHERENCE
Y: 1.00
X: 0.0Hz + 400Hz LIN
SETUP W22 #A: 256

INPUT

MAIN Y: 283m
X: 236.0Hz

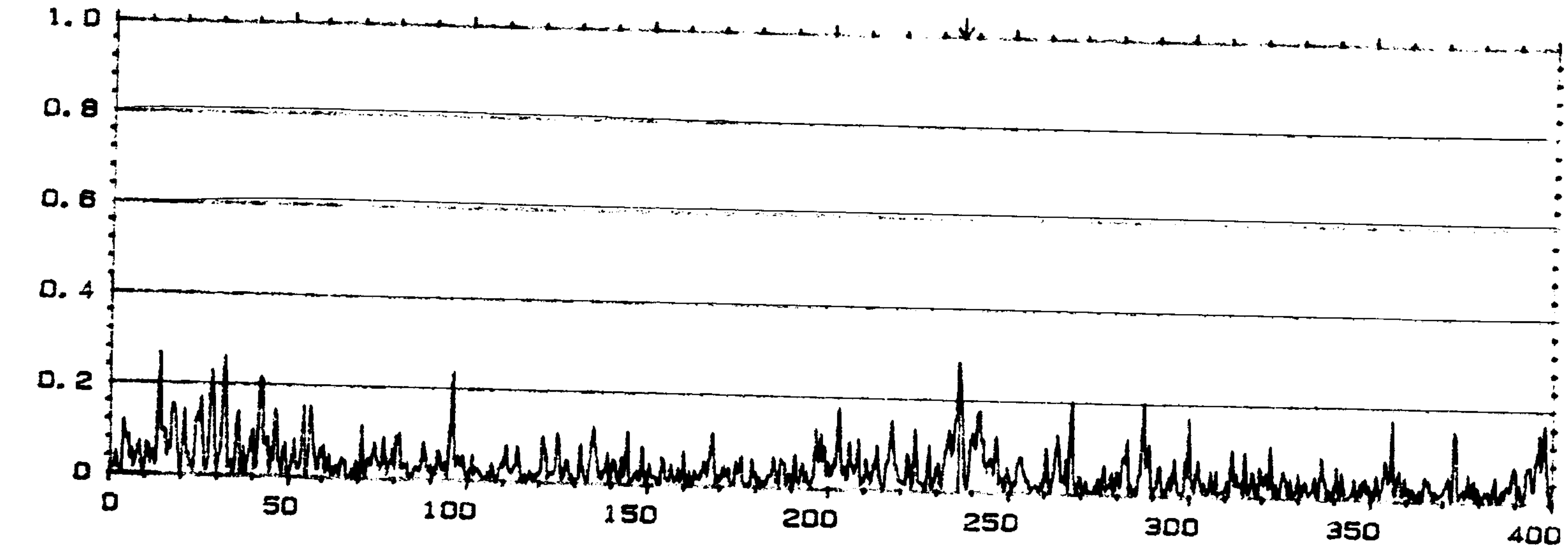

Type 2032

Page No.
71

Sign.:

Meas.
Object:
PLF PR2.0
ChA=T10
ChB=M4

Rdg 180

Comments:
Expanded freq
Range

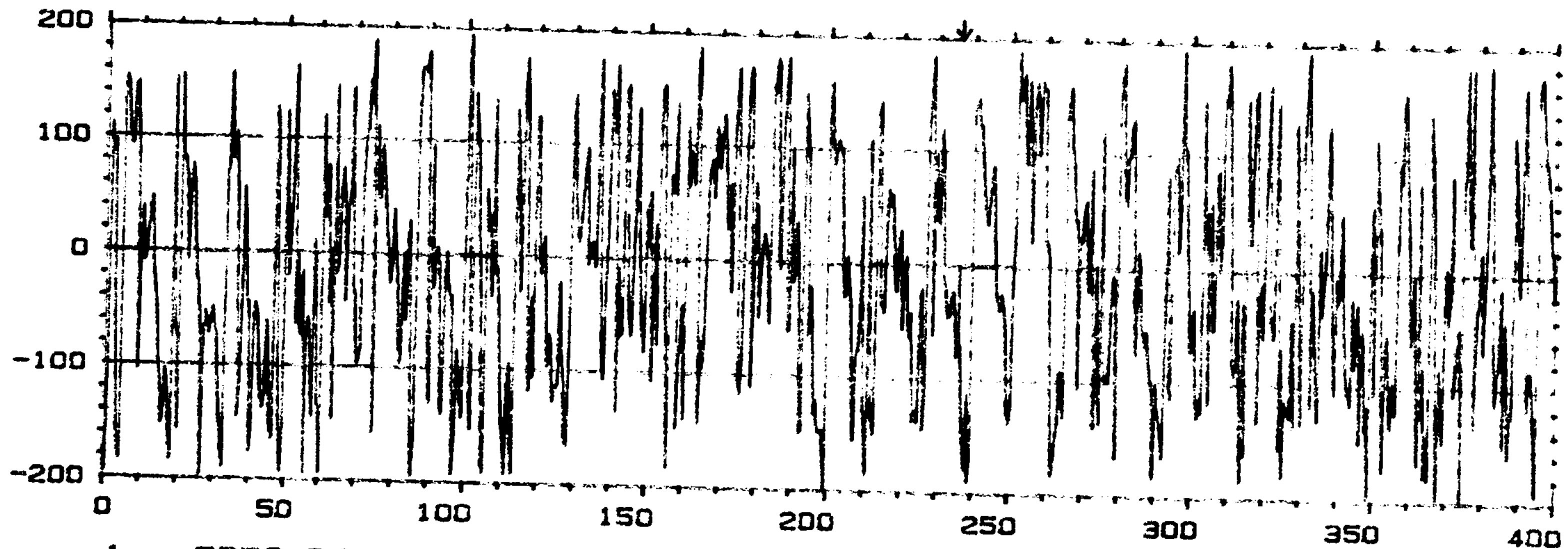

1 FREQ RESP H1 PHASE
Y: -200 TO +200 DEG
X: 0.0Hz + 400Hz LIN
SETUP W22 #A: 256

MAIN Y: -74.9DEG
X: 236.0Hz

Type 2032

Page No.
69

Sign.:

Meas.
Object:

Comments:

W20 COHERENCE INPUT MAIN Y: 337m
Y: 1.00 X: 694Hz
X: 0Hz + 800Hz LIN
SETUP W22* #A: 256

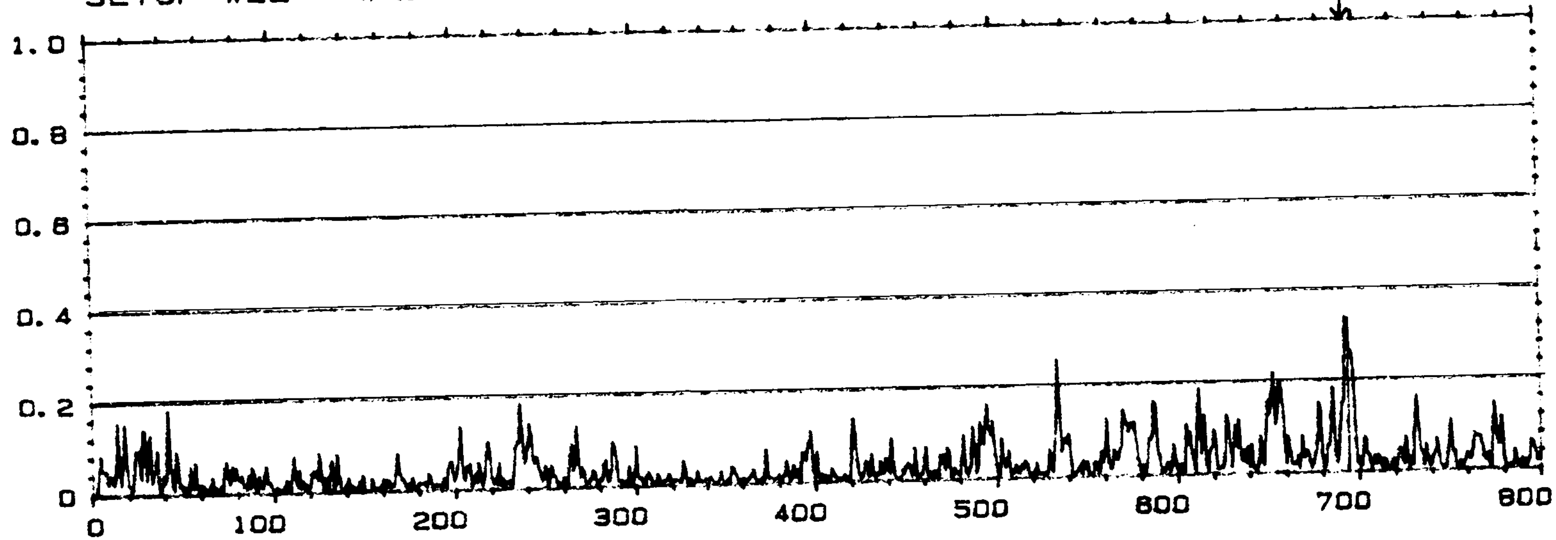

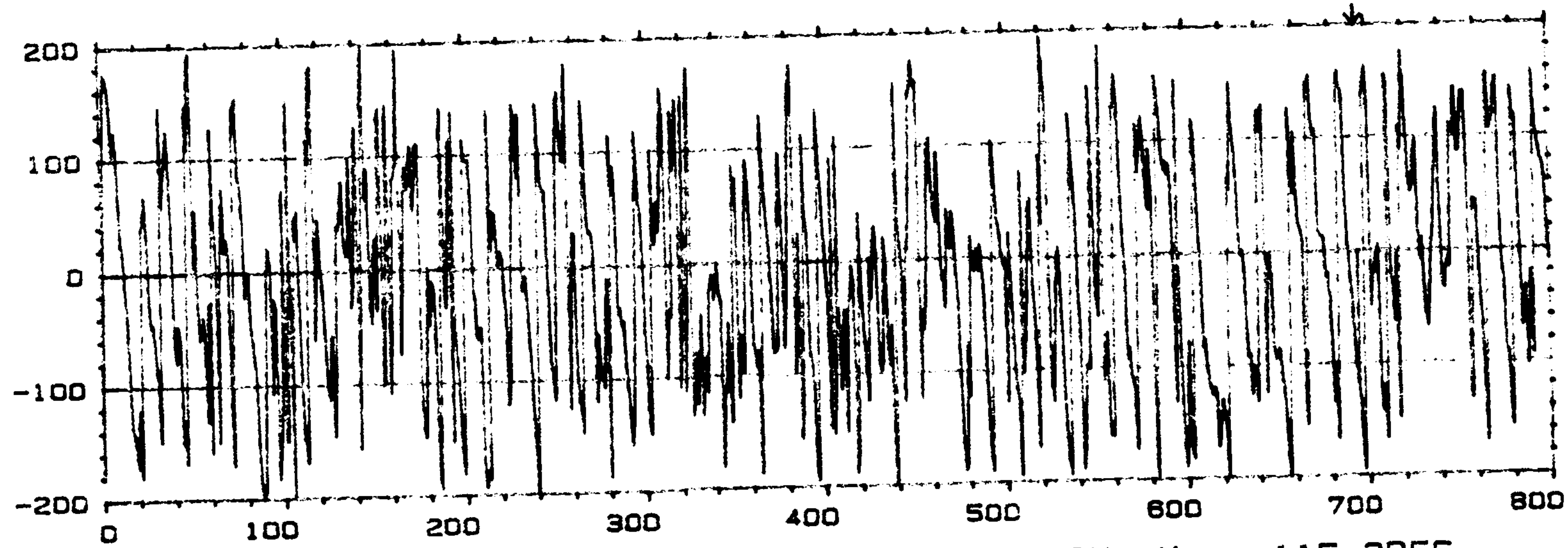

1 FREQ RESP H1 PHASE MAIN Y: -115.2DEG
Y: -200 TO +200 DEG X: 694Hz
X: 0Hz + 800Hz LIN
SETUP W22* #A: 256

Type 2032

Page No.
67

Sign.:

Meas.
Object:

PLF PR 2.0
ChA: T10
ChB: M4

Pdg 180

Comments:

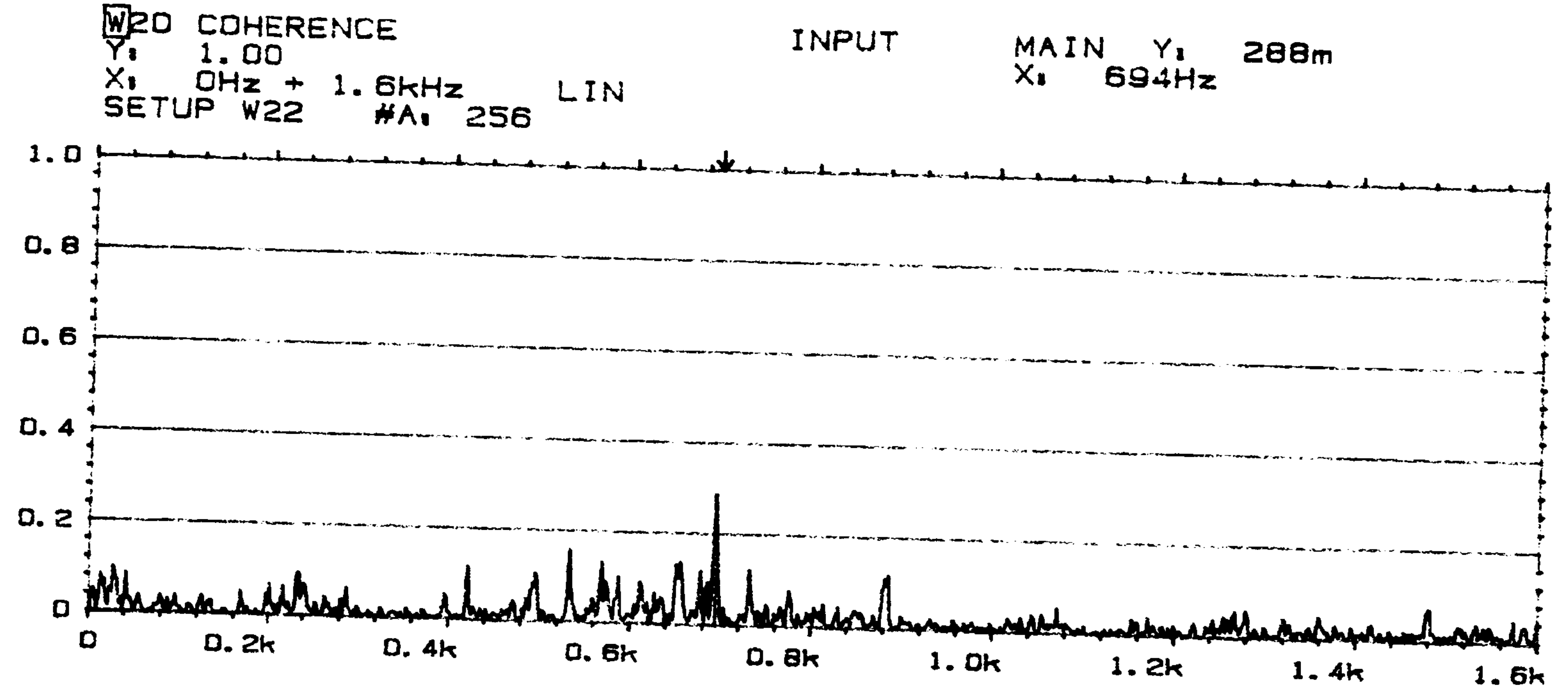

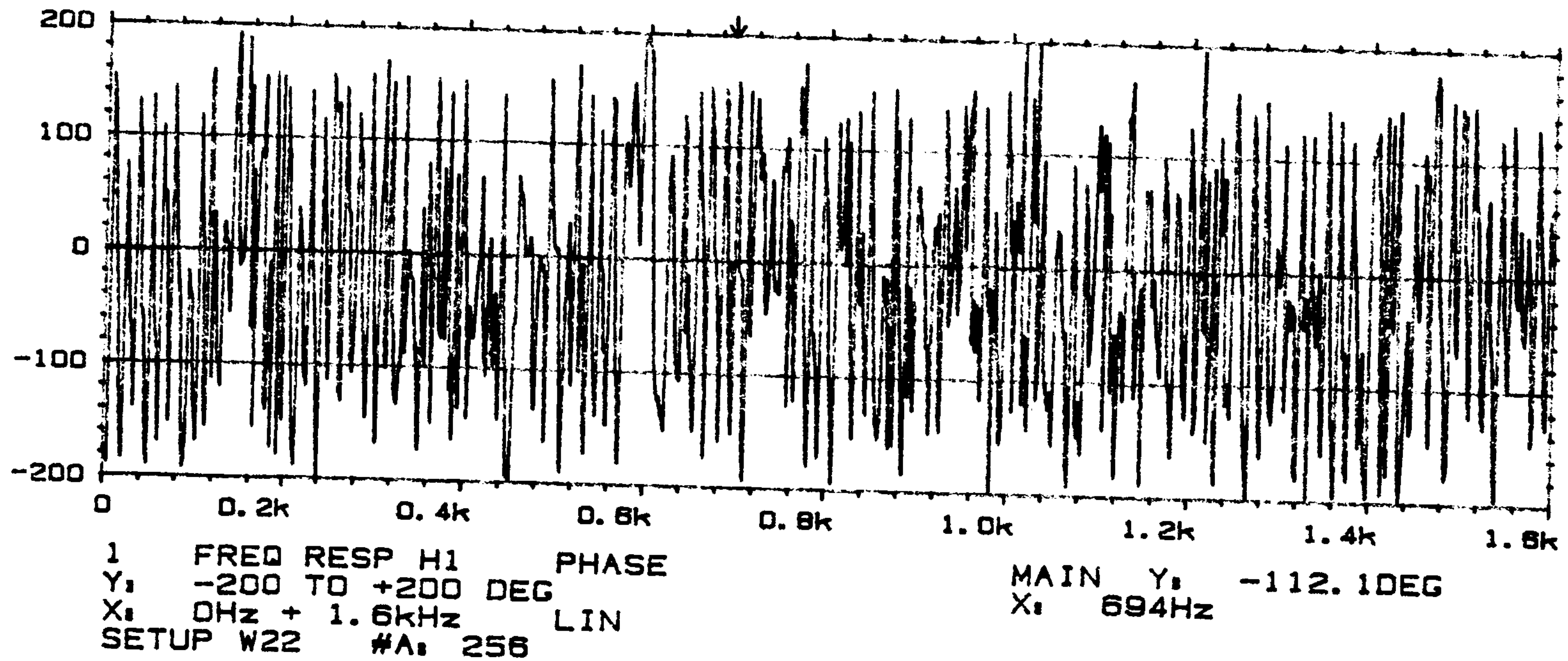

Type 2032

Page No.
93

Sign.:

Meas.
Object:
PLF PR2.25
Ch A = T10
Ch B = M1

Rdg 182

Comments:

W20 COHERENCE
Y: 1.00
X: 0Hz + 1.6kHz LIN
SETUP W2 #A: 256

INPUT

MAIN Y: 42.4µ
X: 0Hz

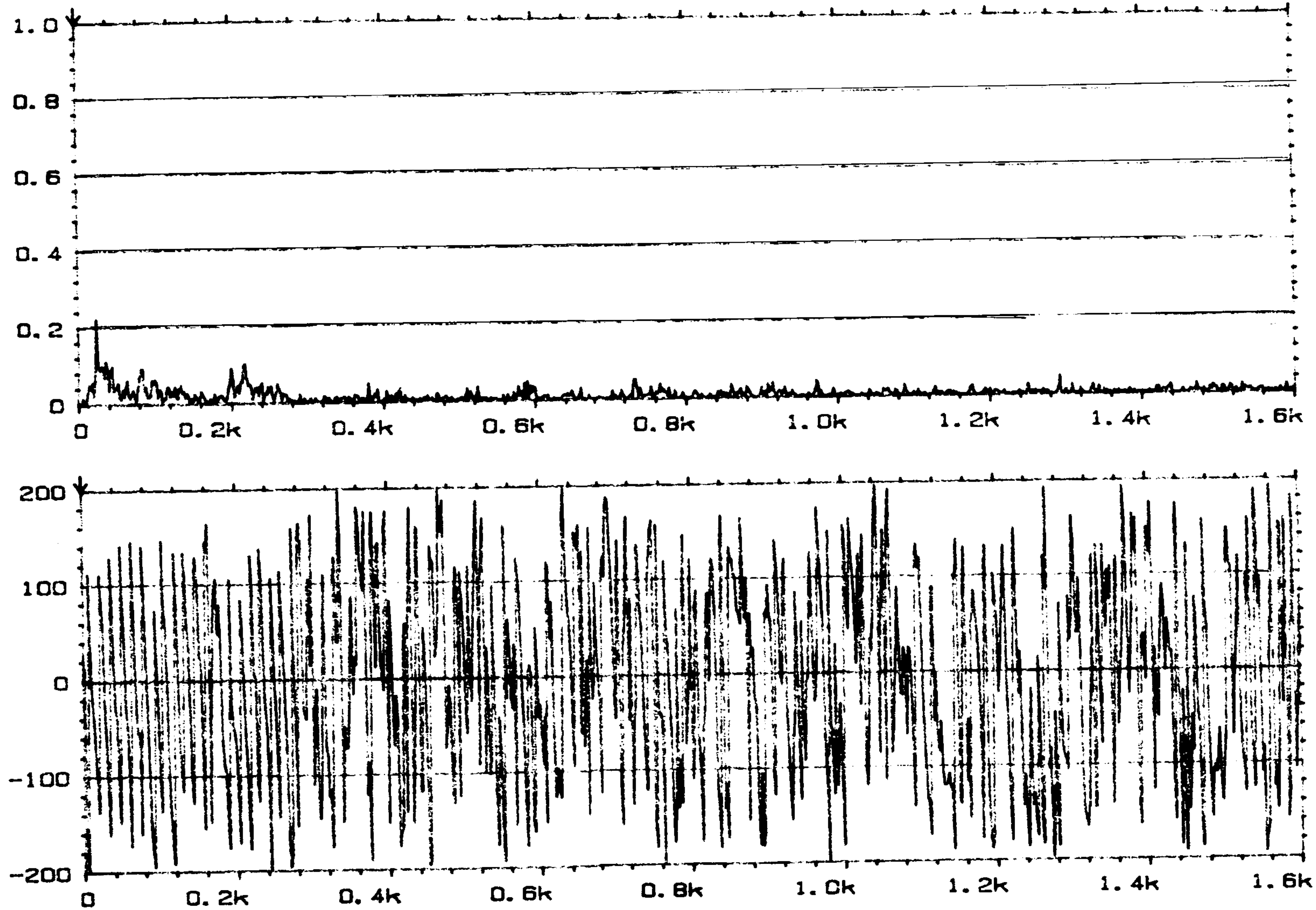

1 FREQ RESP H1 PHASE
Y: -200 TO +200 DEG
X: 0Hz + 1.6kHz LIN
SETUP W2 #A: 256

MAIN Y: 0.4DEG
X: 0Hz

Type 2032

Page No.
95

Sign.:

Meas.
Object:
PLF PR 2.25
ChA T10
ChB M2

Rdg 182

Comments:

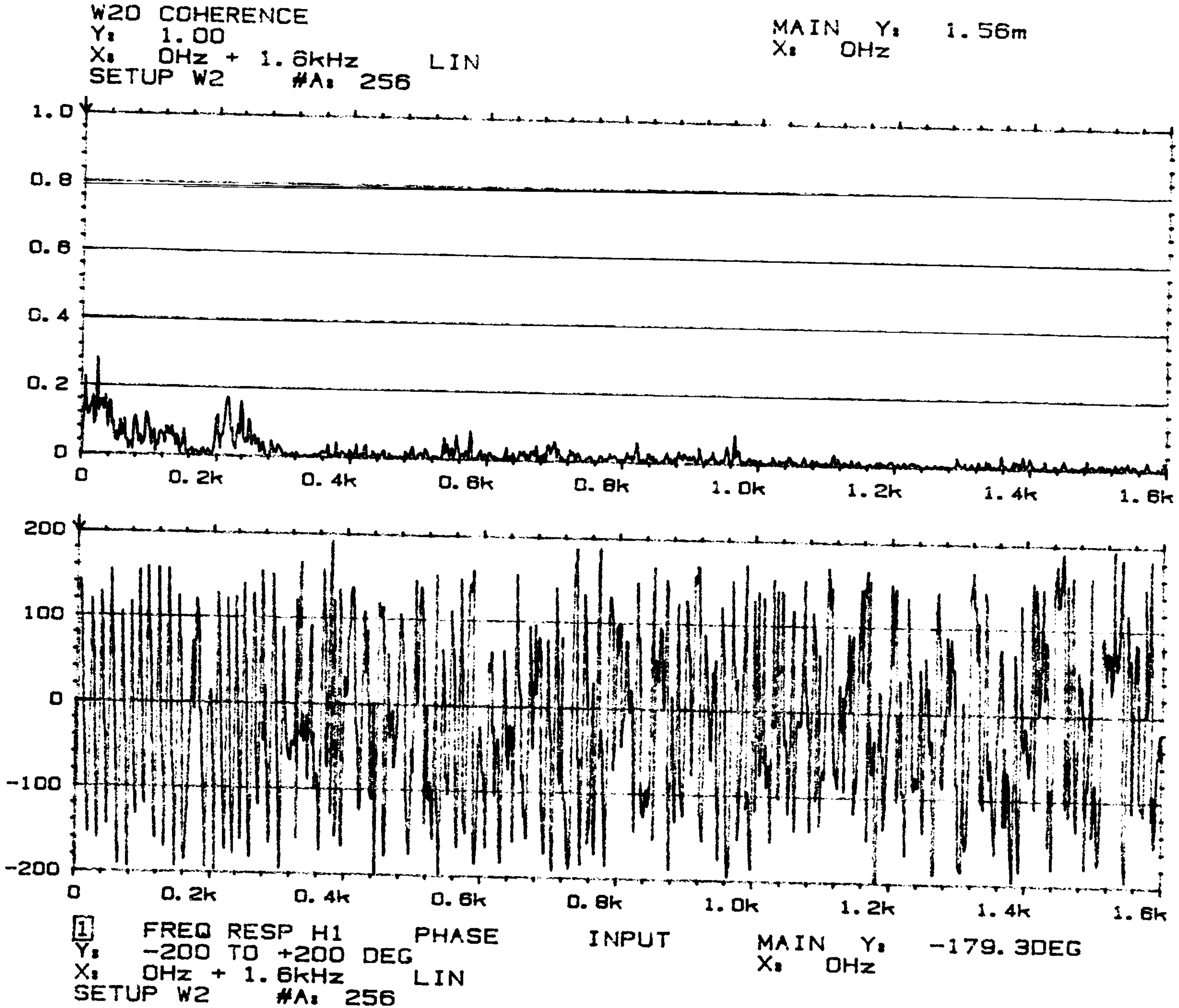

ORIGINAL PAGE IS
OF POOR QUALITY

Type 2032

Page No.
97

Sign.:

Meas.
Object:

Comments:

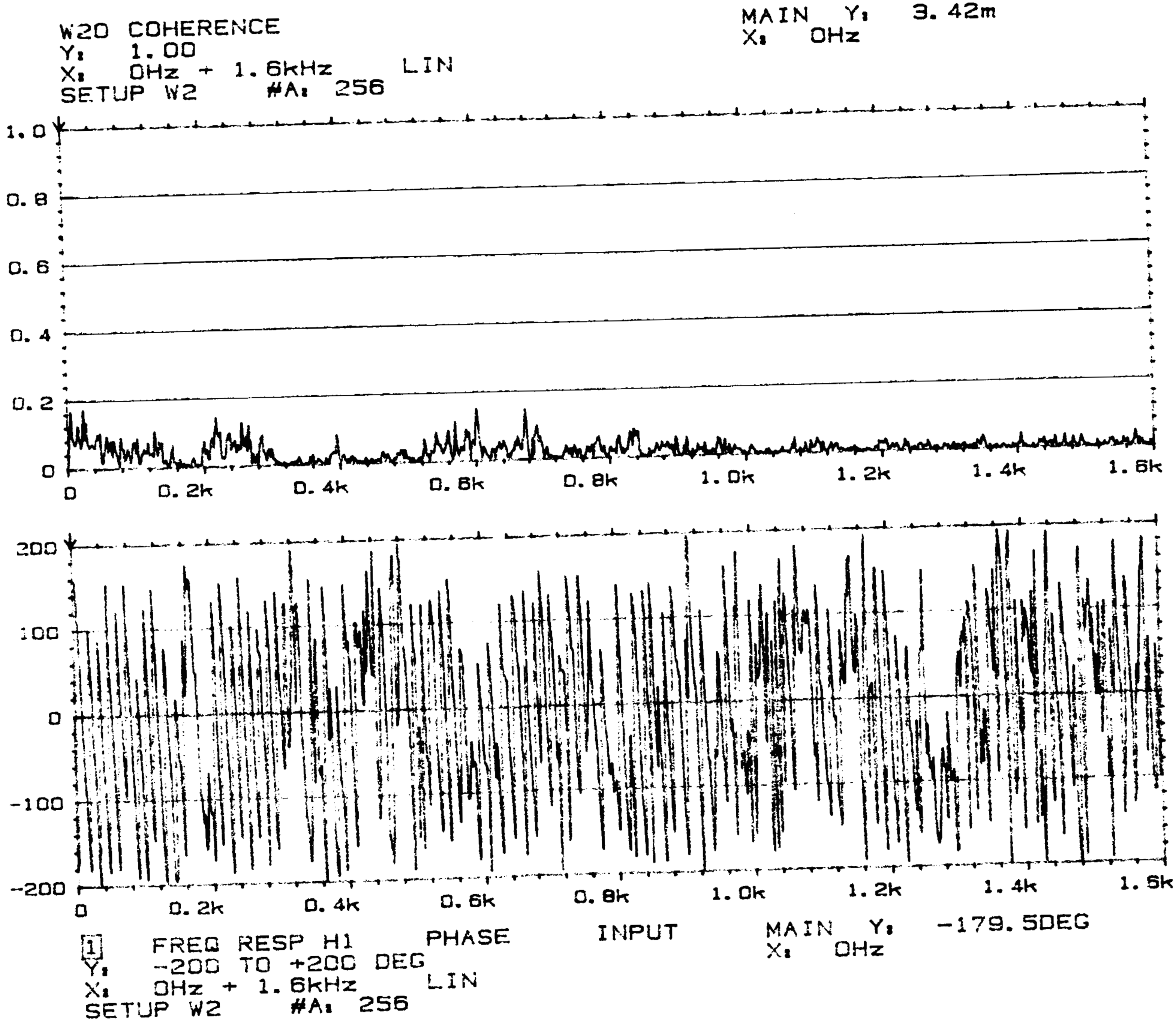

Type 2032

Page No.
99

Sign.:

Meas.
Object:

Ch. M4

Rdg 132

Comments:

W20 COHERENCE
Y: 1.00
X: 0Hz + 1.6kHz LIN
SETUP W2 #A: 256

MAIN Y: 3.30m
X: 0Hz

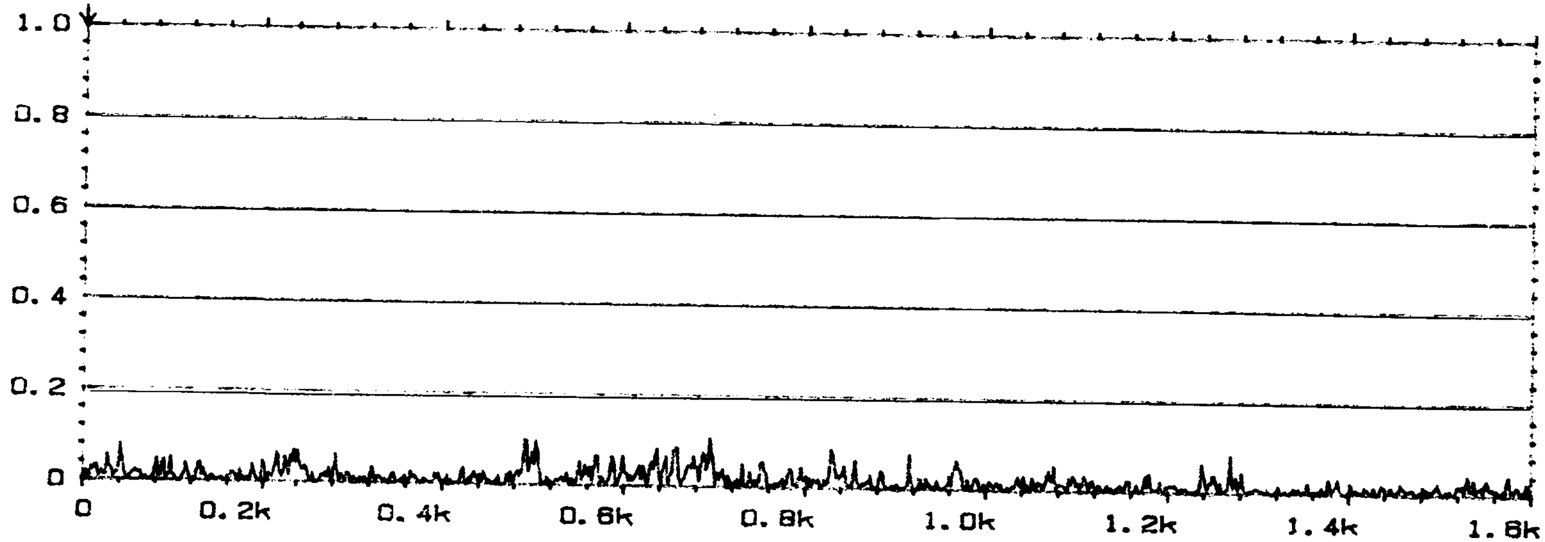

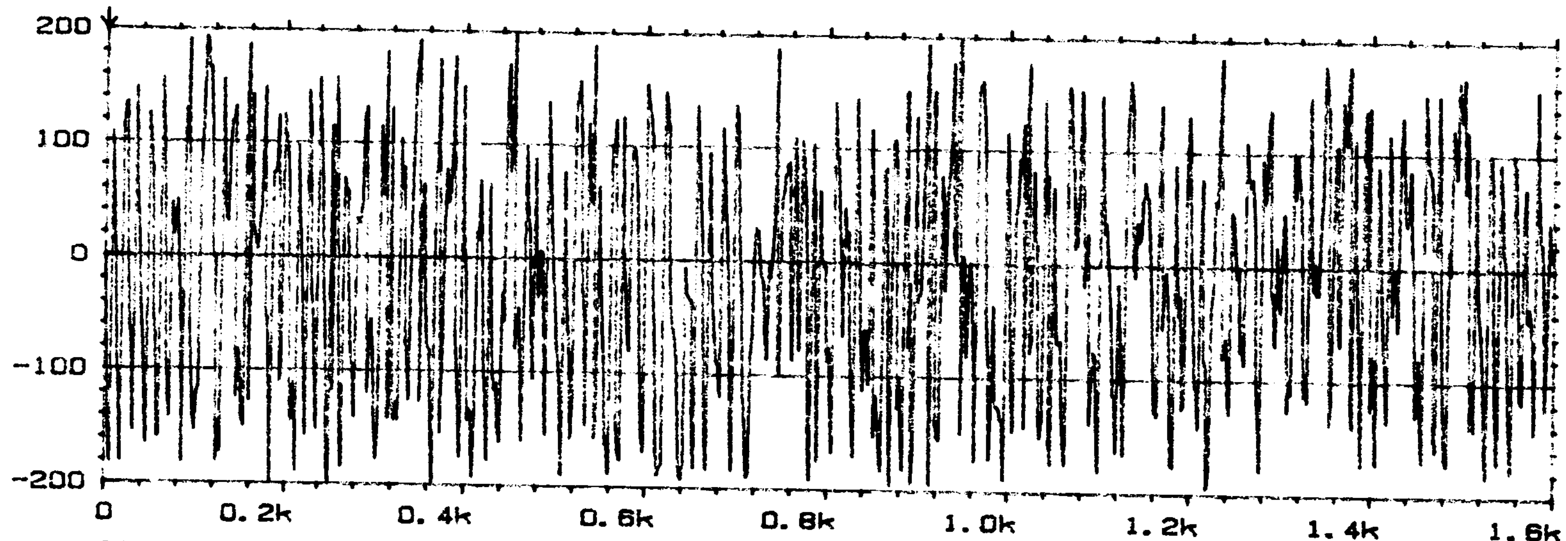

1 FREQ RESP H1 PHASE INPUT
Y: −200 TO +200 DEG
X: 0Hz + 1.6kHz LIN
SETUP W2 #A: 256

MAIN Y: −0.3DEG
X: 0Hz

Type 2032

Page No.
101

Sign.:

Meas.
Object:
PLF PR2.5
chA=T10
chB=M1

Rdg 183

Comments:

20 COHERENCE INPUT MAIN Y: 5.98m
Y: 1.00 X: 0Hz
X: 0Hz + 1.6kHz LIN
SETUP W2 #A: 256

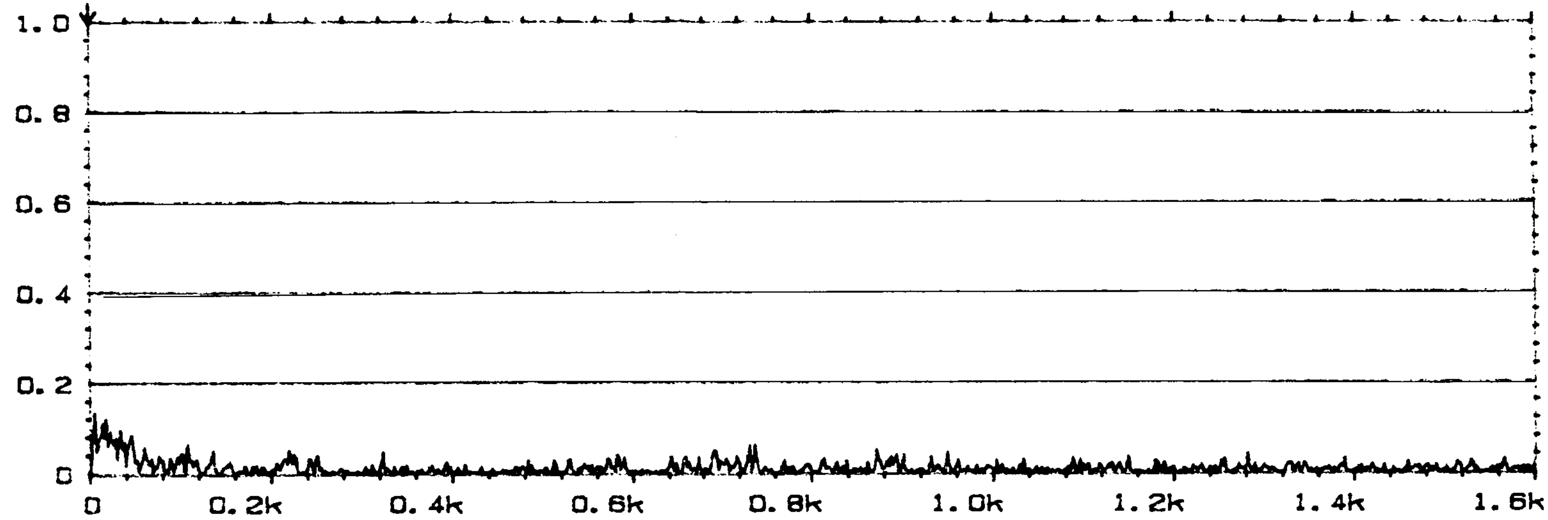

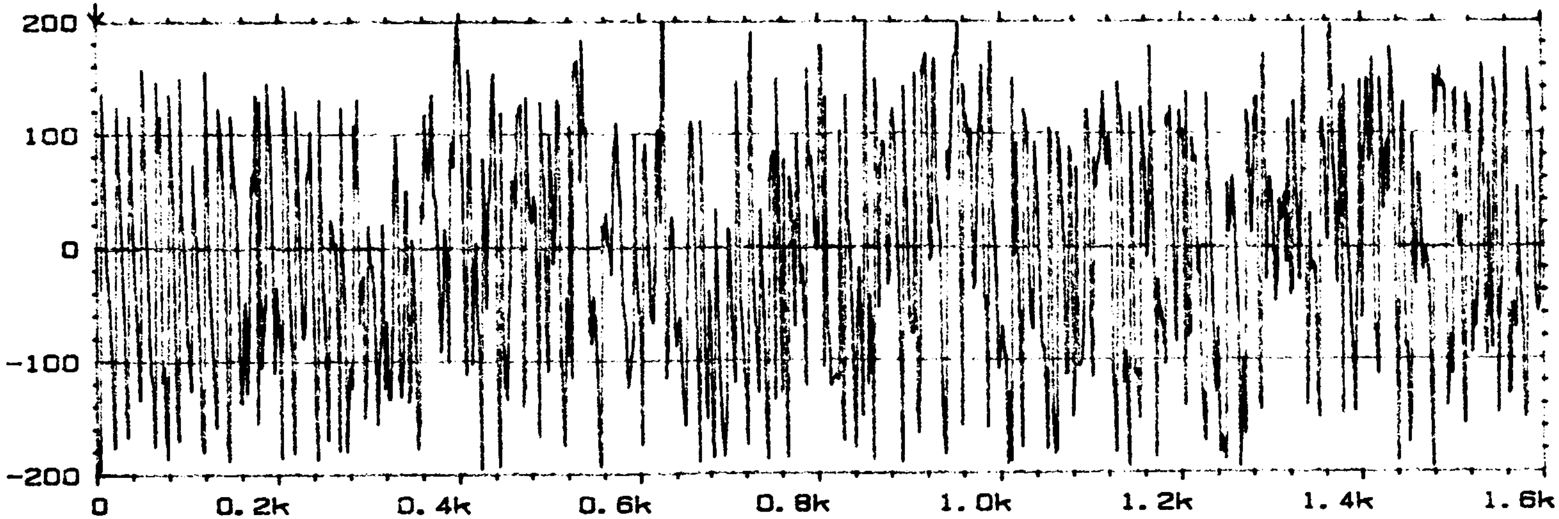

1 FREQ RESP H1 PHASE MAIN Y: -180.0DEG
Y: -200 TO +200 DEG X: 0Hz
X: 0Hz + 1.6kHz LIN
SETUP W2 #A: 256

Type 2032

Page No.
103

Sign.:

Meas.
Object:
PLF PR2.5
ChA = T10
ChB = M2

Rdg 183

Comments:

20 COHERENCE
Y: 1.00
X: 0Hz + 1.6kHz LIN
SETUP W2 #A: 256

MAIN Y: 4.96m
X: 0Hz

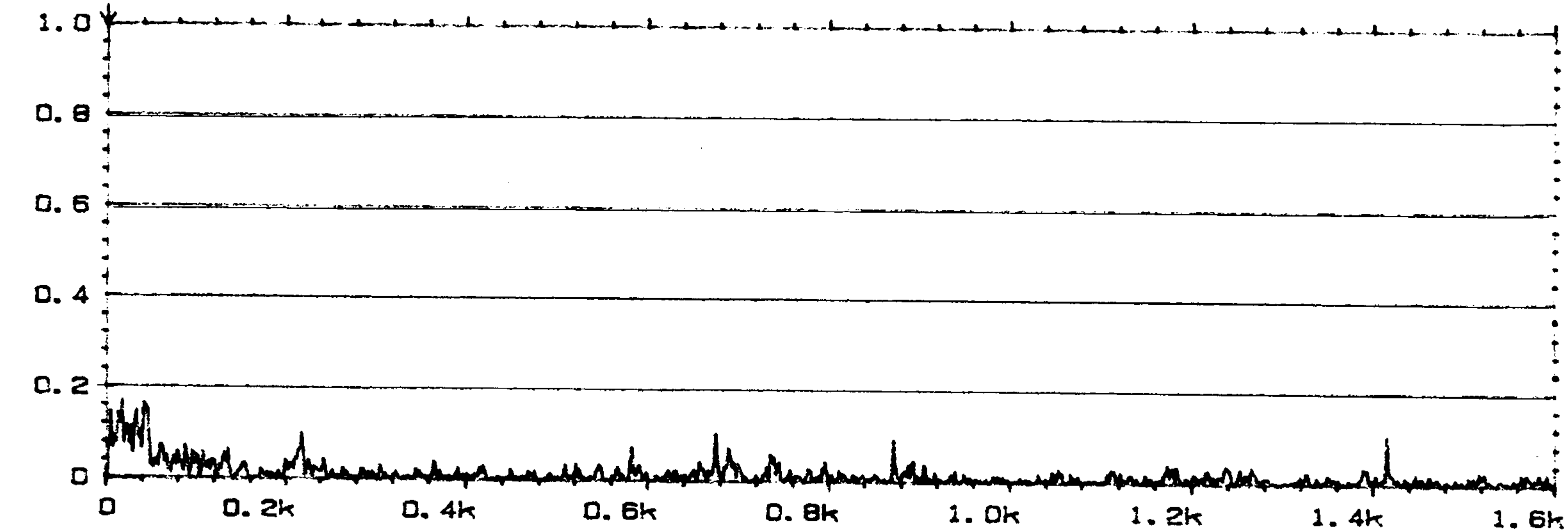

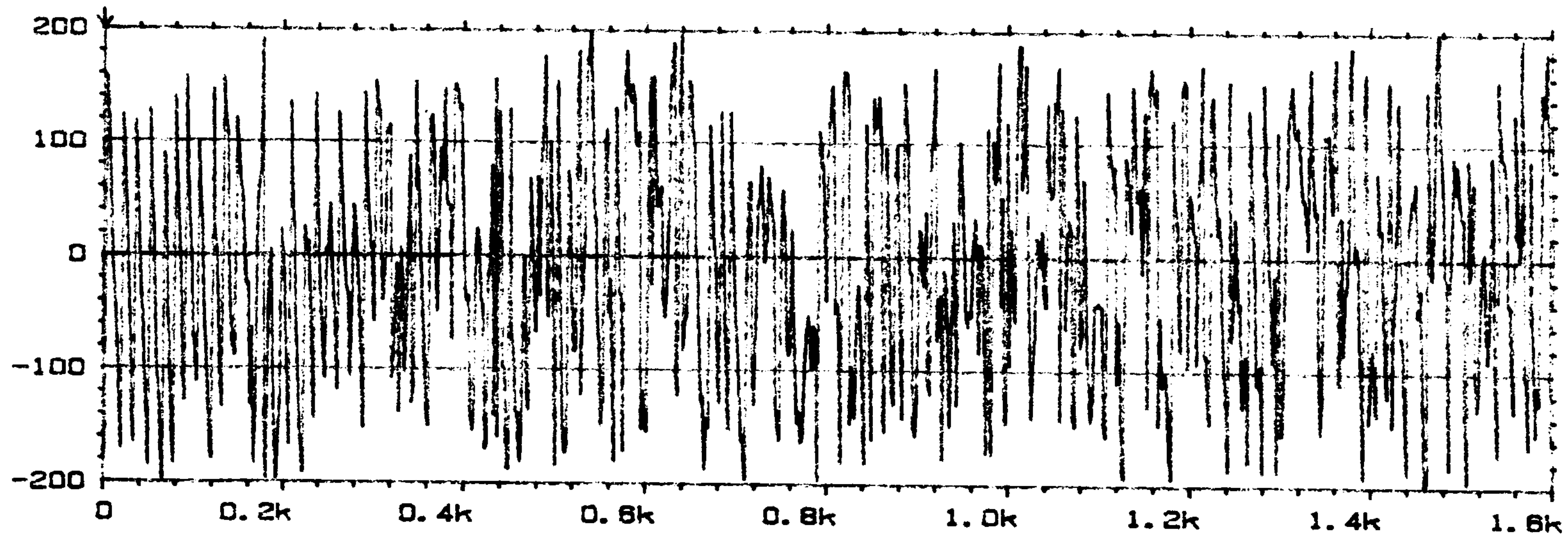

[1] FREQ RESP H1 PHASE INPUT
Y: -200 TO +200 DEG
X: 0Hz + 1.6kHz LIN
SETUP W2 #A: 256

MAIN Y: -179.9DEG
X: 0Hz

Type 2032

Page No.
105

Sign.:

Meas.
Object:

PLL PK2.5
ChA=T10
ChB=M3

LH- 87

Comments:

20 COHERENCE
Y: 1.00
X: 0Hz + 1.6kHz LIN
SETUP W2 #A: 256

MAIN Y: 904µ
X: 0Hz

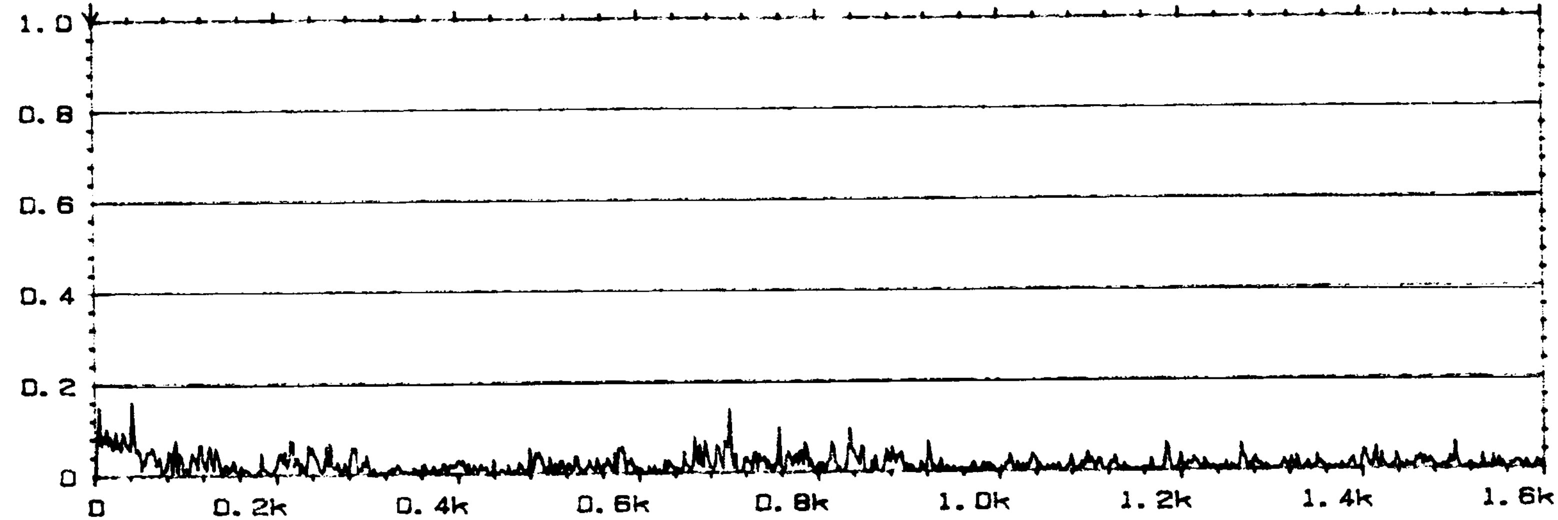

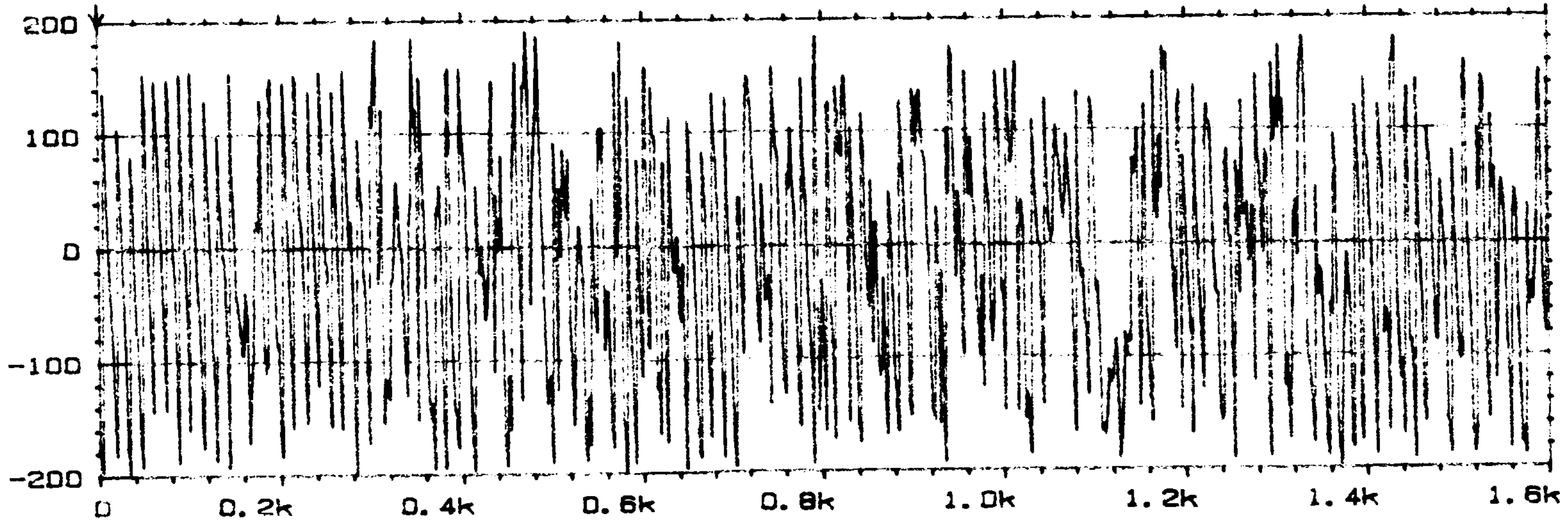

1 FREQ RESP H1 PHASE INPUT
Y: -200 TO +200 DEG
X: 0Hz + 1.6kHz LIN
SETUP W2 #A: 256

MAIN Y: -178.7DEG
X: 0Hz

20 COHERENCE
Y: 1.00
X: 0Hz + 1.6kHz LIN
SETUP W2 #A: 256

MAIN Y: 4.19m
X: 0Hz

Type 2032

Page No.
107

Sign.:

Meas.
Object:
PLF PR2.5
ChA=T10
ChB=M4

Rdg 183

Comments:

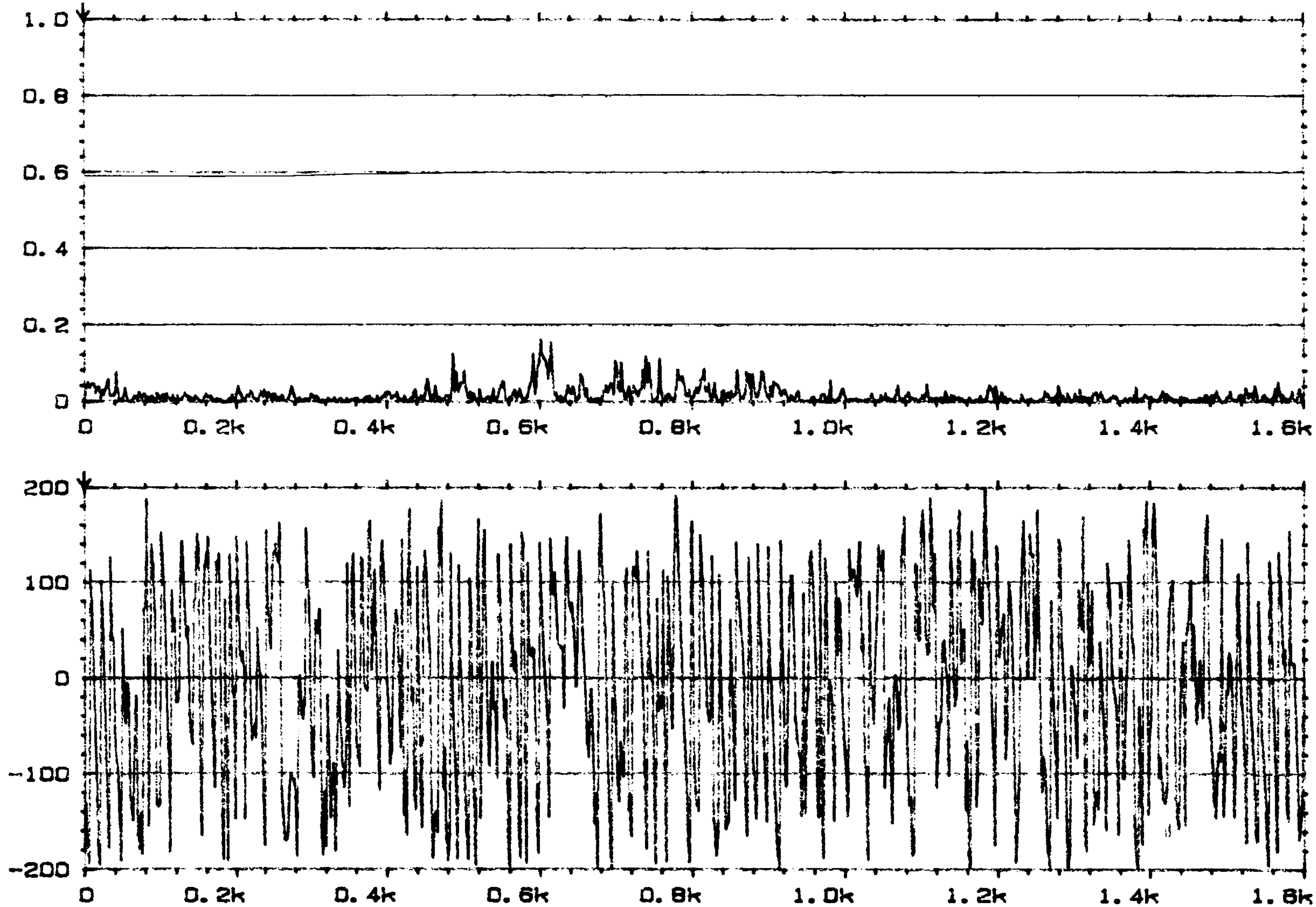

1 FREQ RESP H1 PHASE INPUT
Y: -200 TO +200 DEG
X: 0Hz + 1.6kHz LIN
SETUP W2 #A: 256

MAIN Y: -179.1DEG
X: 0Hz

ORIGINAL PAGE IS
OF POOR QUALITY

Type 2032

Page No.
123

Sign.:

Meas.
Object:
PLF PR 3.0
ChA = T16
ChB = M1

Rtg 135

Comments:

2D COHERENCE
Y: 1.00
X: 0Hz + 1.6kHz LIN
SETUP W2 #A: 256

MAIN Y: 17.0m
X: 0Hz

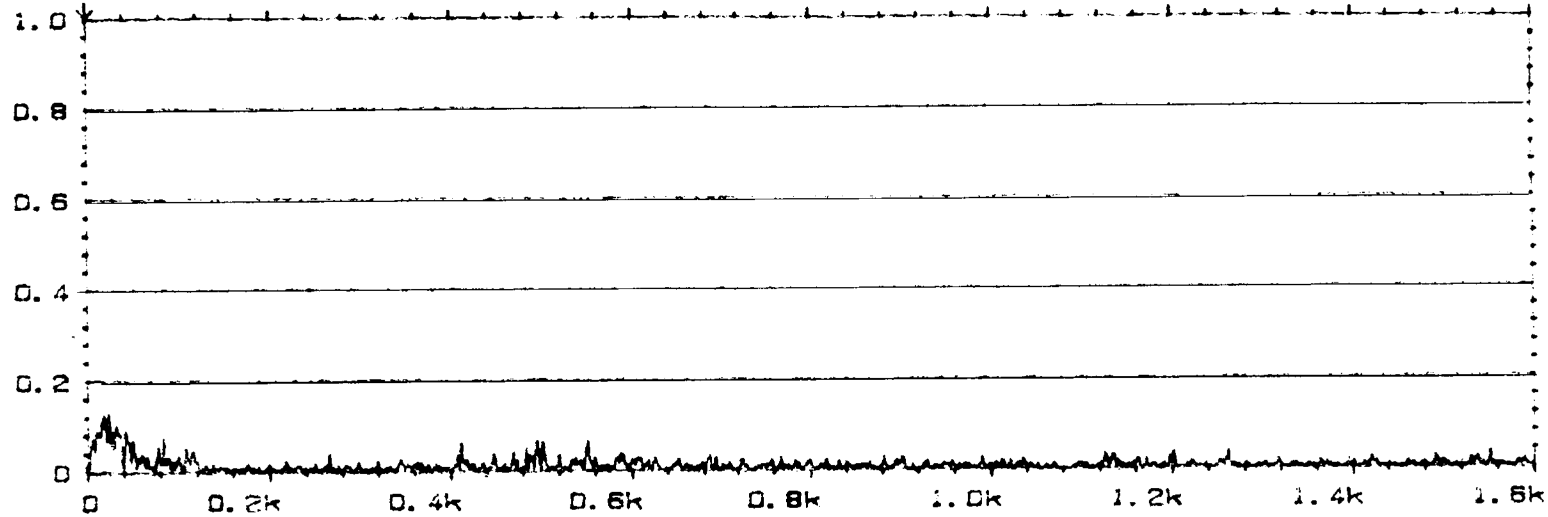

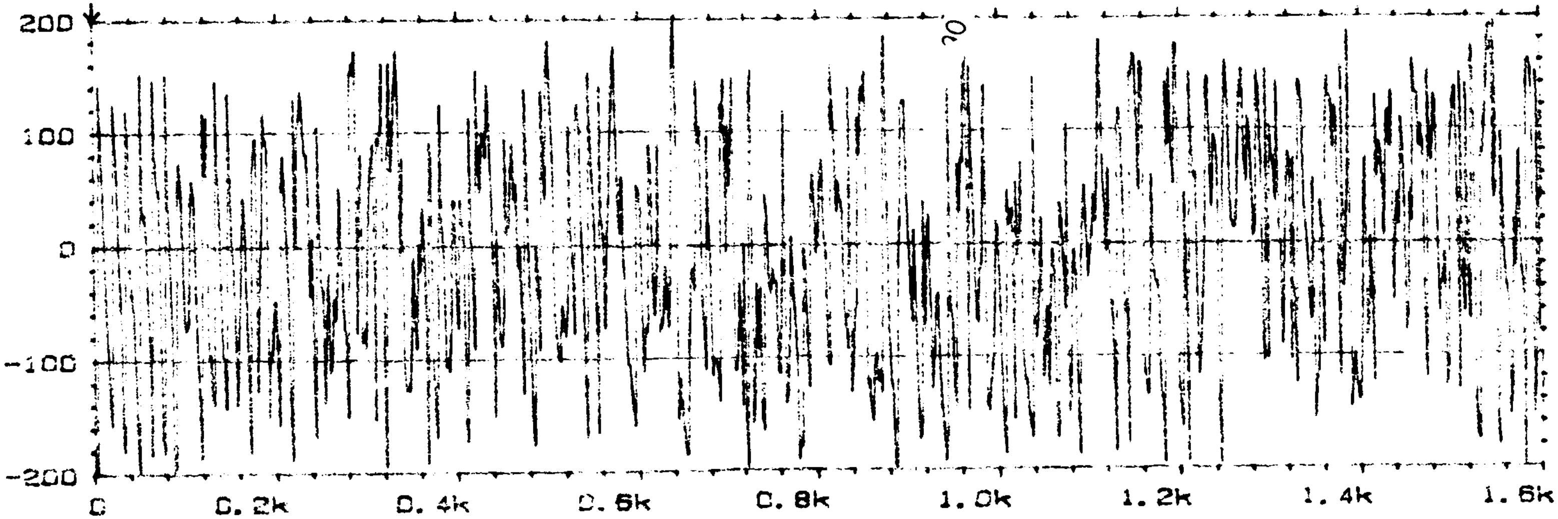

1 FREQ RESP H1 PHASE INPUT
Y: -200 TO +200 DEG
X: 0Hz + 1.6kHz LIN
SETUP W2 #A: 256

MAIN Y: -0.1DEG
X: 0Hz

Type 2032

Page No.
122

Sign.:

Meas.
Object:

PLF PR3.0
ChA= T10
ChB= M2

Rdg 185

Comments:

20 COHERENCE
Y: 1.00
X: 0Hz + 1.6kHz LIN
SETUP W2 #A: 256

MAIN Y: 1.54m
X: 0Hz

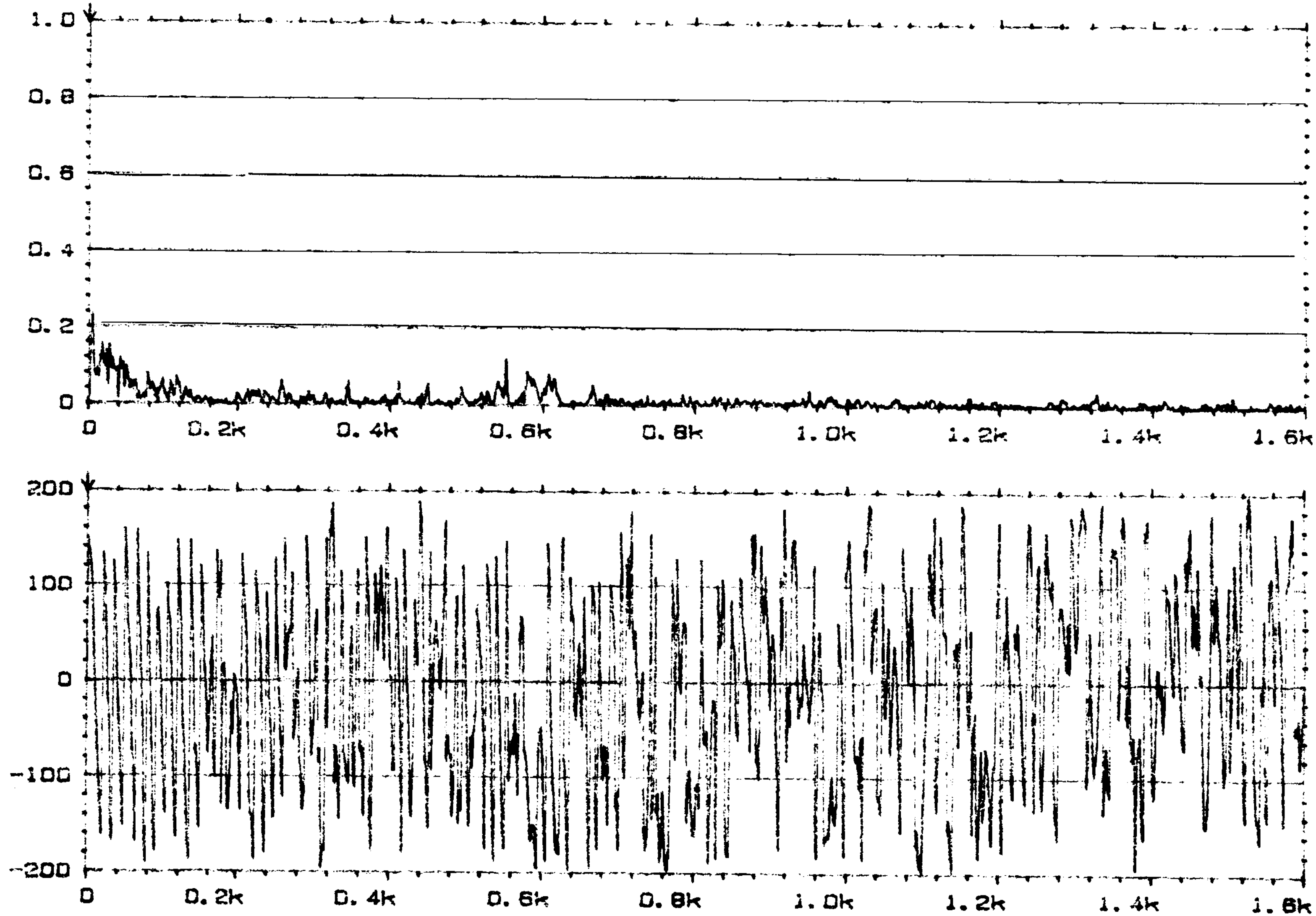

1 FREQ RESP H1 PHASE INPUT
Y: -200 TO +200 DEG
X: 0Hz + 1.6kHz LIN
SETUP W2 #A: 256

MAIN Y: -0.7DEG
X: 0Hz

Type 2032

Page No.
119

Sign.:

Meas.
Object:

PLF PR3.0

ChA=71A

Ch.B M3

Rdg 185

Comments:

20 COHERENCE
Y: 1.00
X: 0Hz + 1.6kHz LIN
SETUP W2 #A: 256

MAIN Y: 913μ
X: 0Hz

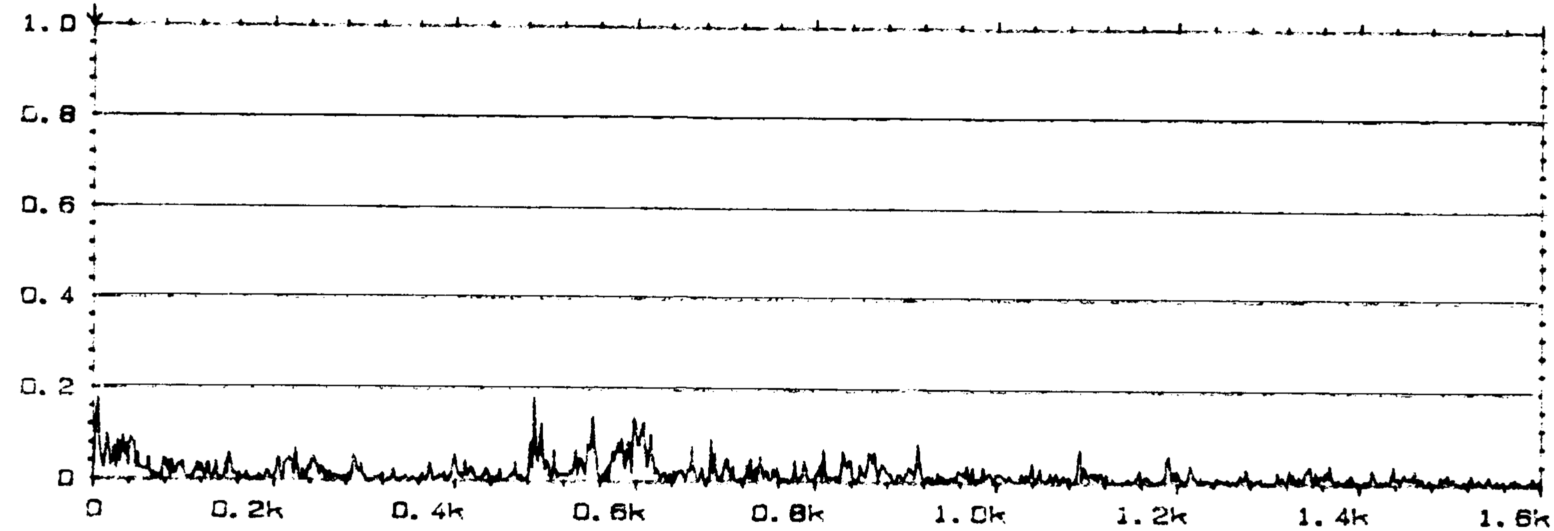

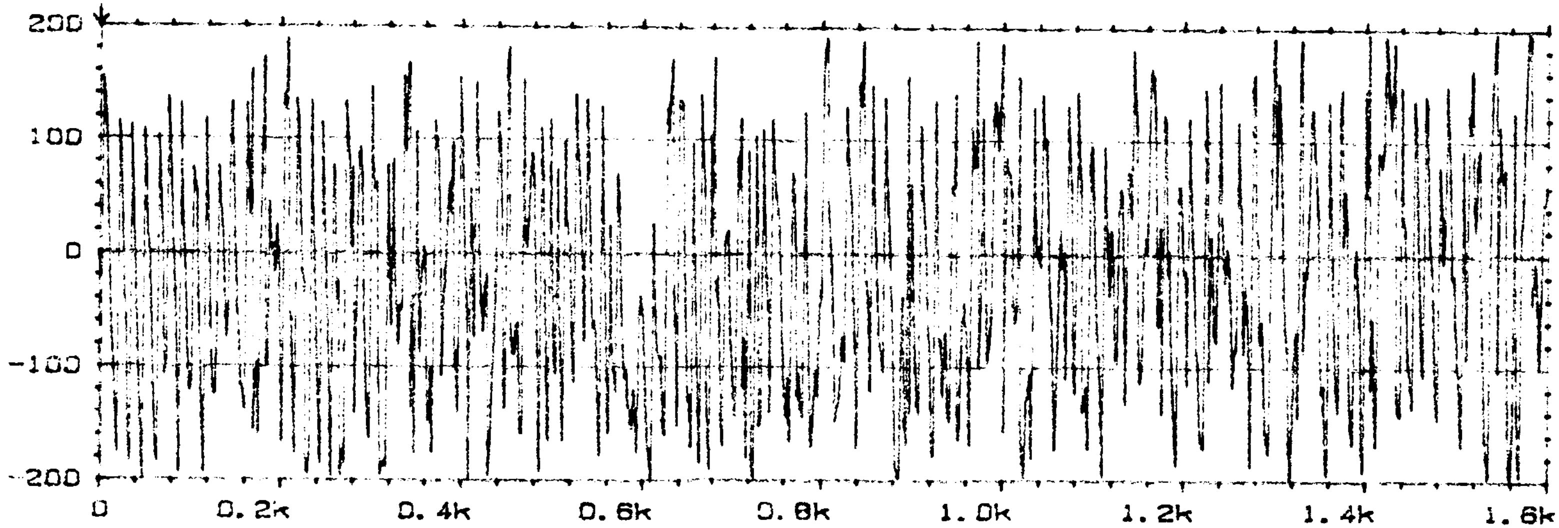

1 FREQ RESP H1 PHASE INPUT
Y: -200 TO +200 DEG
X: 0Hz + 1.6kHz LIN
SETUP W2 #A: 256

MAIN Y: -178.9DEG
X: 0Hz

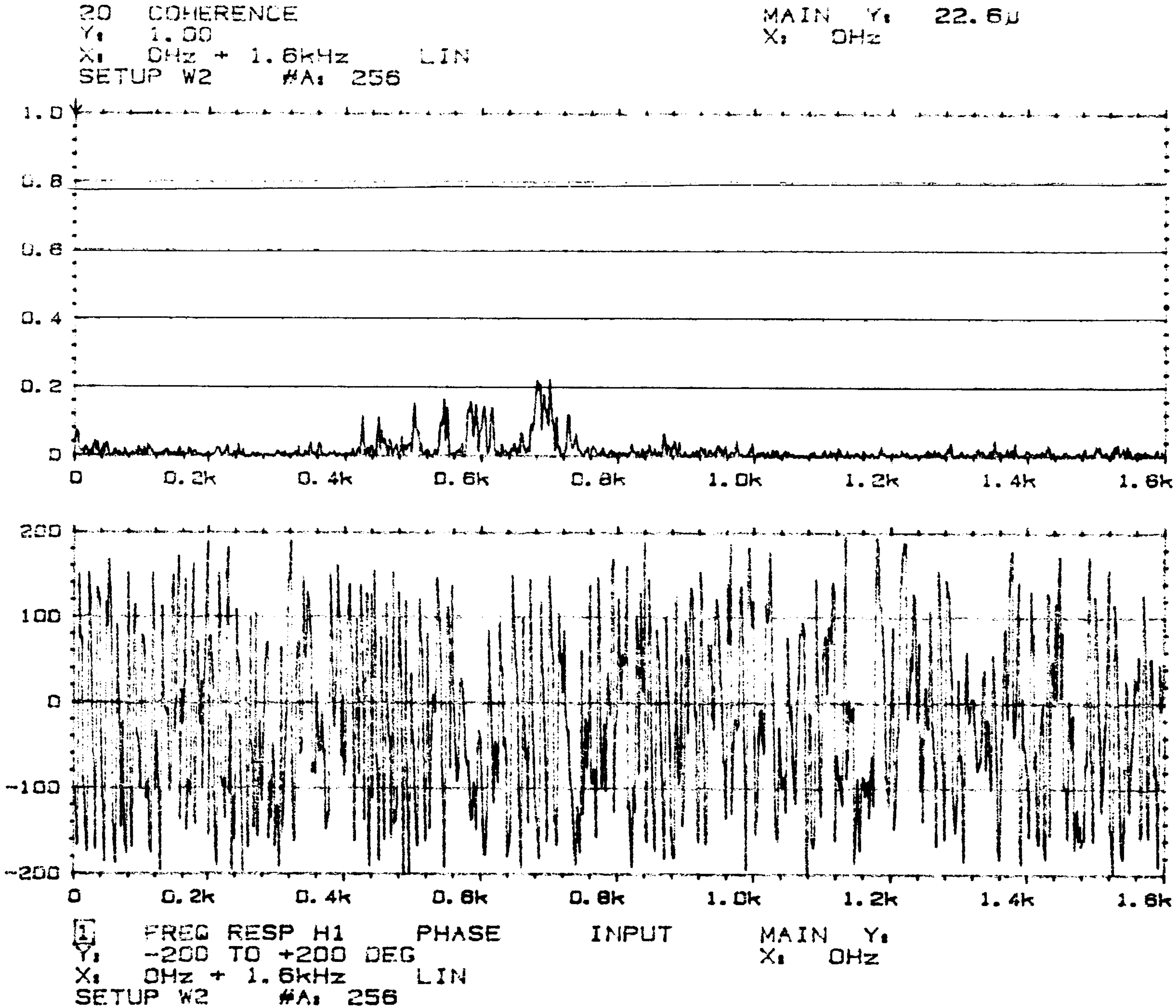

Type 2032

Page No.
117

Sign.:

Meas.
Object:

PLF PR30
Ch A = 716
Ch B = M4

Rdg 185

Comments:

Type 2032

Page No.
125

Sign.:

Meas.
Object:
PLF PR 3.1
ChA = T/S
ChB = M1

Rdg 186

Comments:

20 COHERENCE
Y: 1.00
X: 0Hz → 1.6kHz LIN
SETUP W2 #A: 256

MAIN Y: 613μ
X: 0Hz

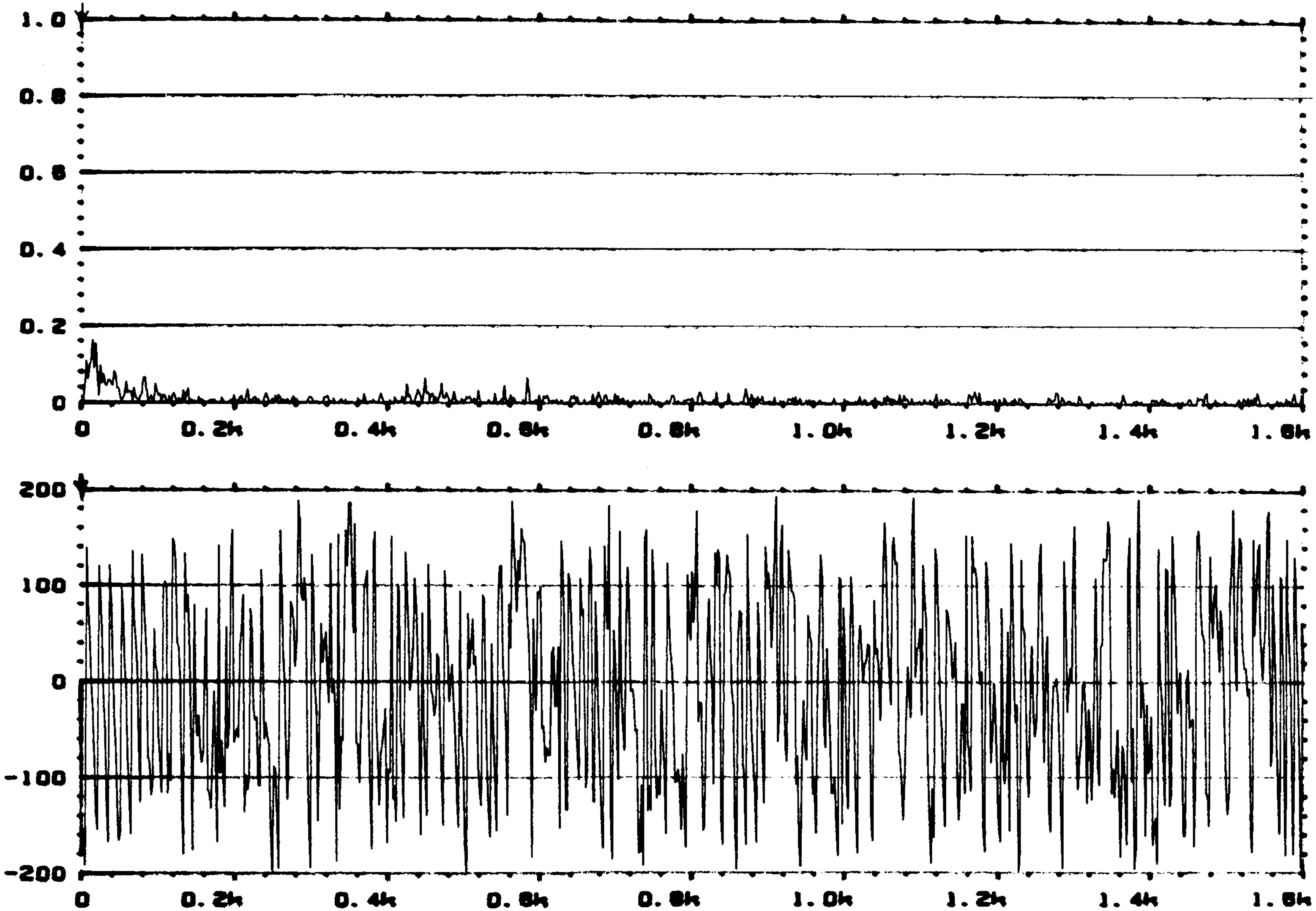

1 FREQ RESP H1 PHASE INPUT
Y: -200 TO +200 DEG
X: 0Hz → 1.6kHz LIN
SETUP W2 #A: 256

MAIN Y: -179.5DEG
X: 0Hz

Type 2032

Page No.
1

Sign.:

Meas.
Object:

PLF PR3.)
Ch A=T10
Ch B=M2

Rdg 186

Comments:

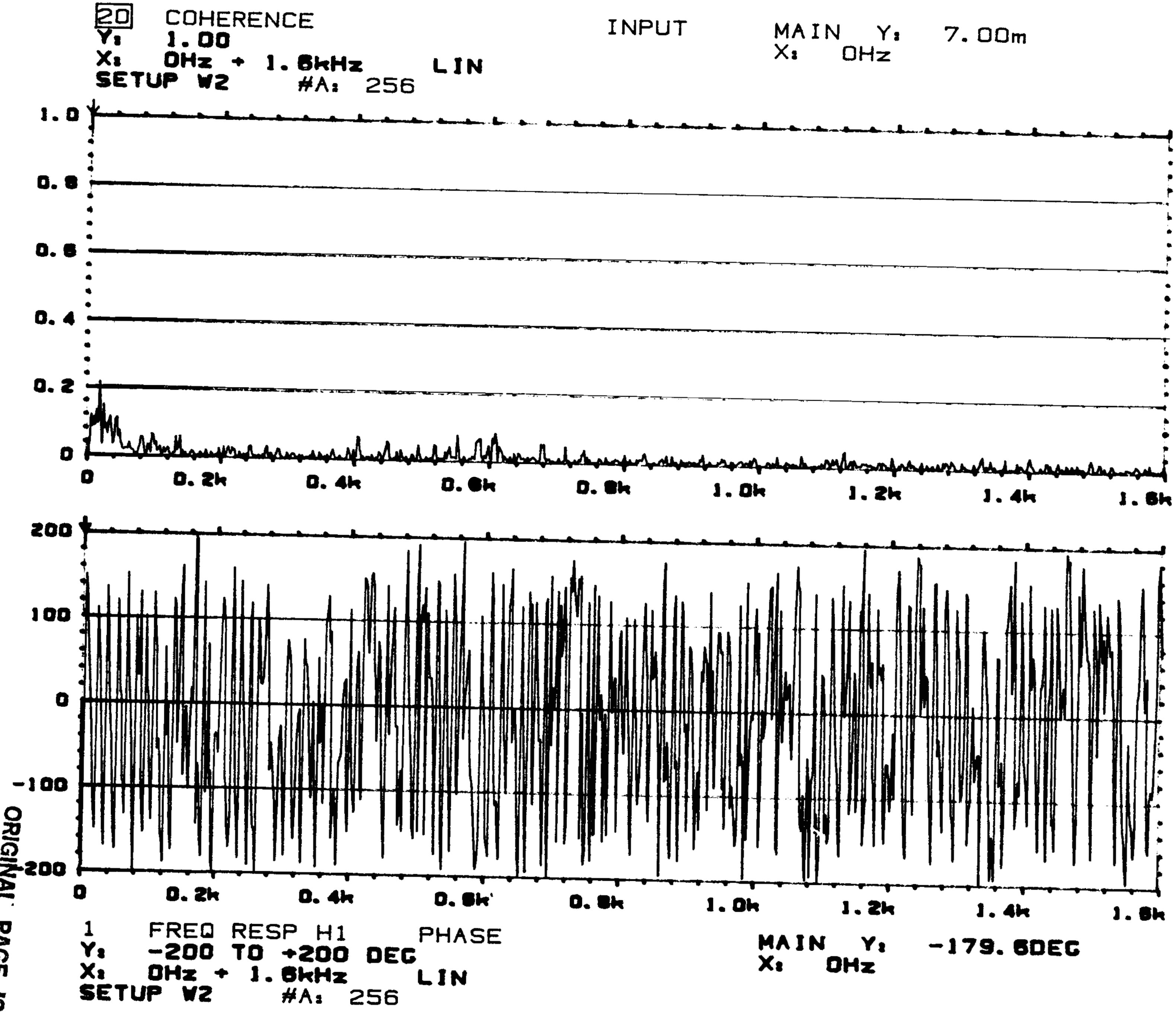

ORIGINAL PAGE IS OF POOR QUALITY

C-2

Type 2032

Page No.
4

Sign.:

Meas.
Object:
PLF PR S.1
ChA = T10
ChB = M3

Fig 186

Comments:

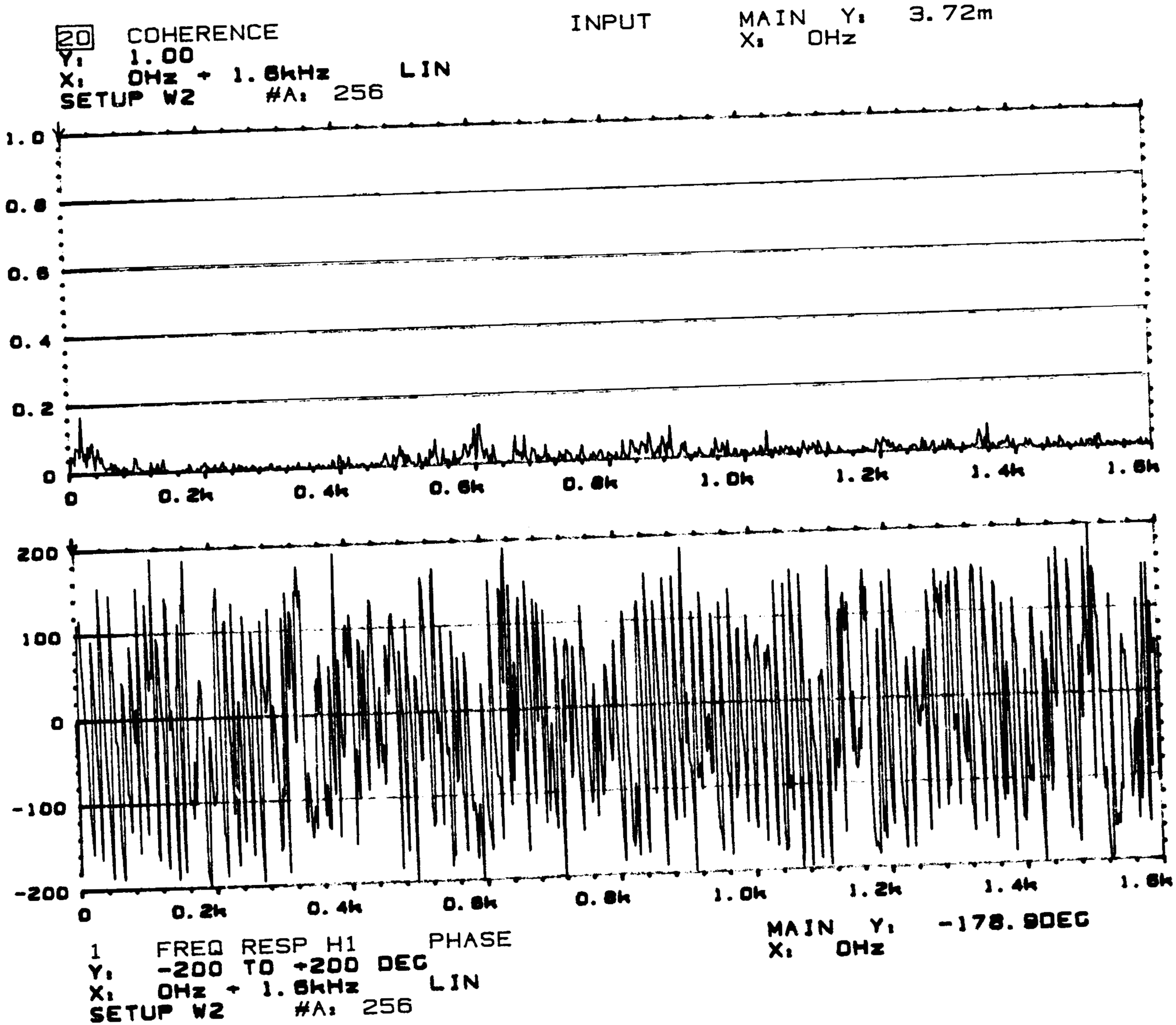

ORIGINAL PAGE IS
OF POOR QUALITY

20 COHERENCE INPUT MAIN Y: 1.93m X: 0Hz
Y: 1.00
X: 0Hz → 1.6kHz LIN
SETUP W2 #A: 256

Type 2032

Page No.
7

Sign.:

Meas.
Object:
PLF PR3.1
ChA=T10
ChB=M4

Rdg 186

Comments:

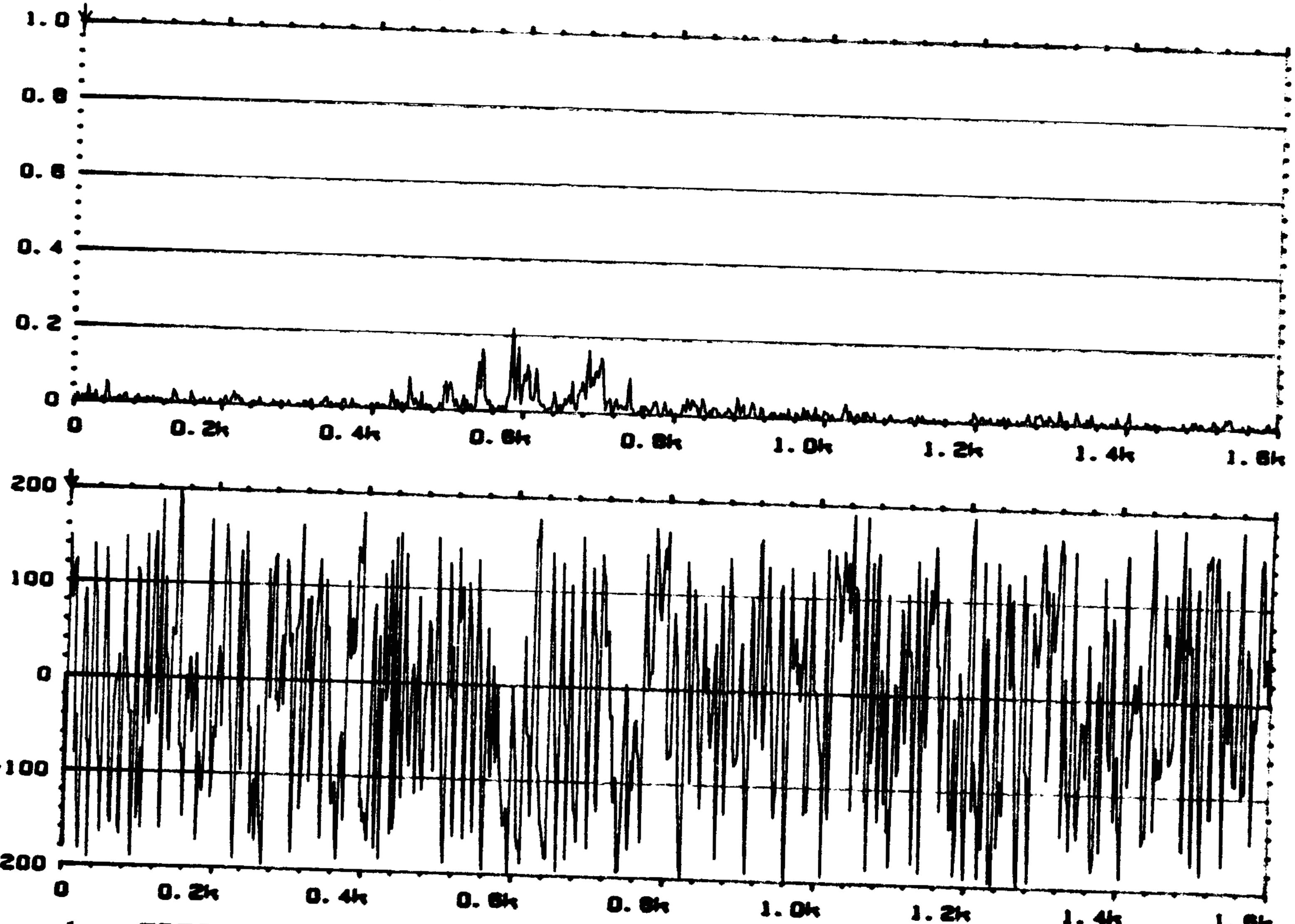

1 FREQ RESP H1 PHASE MAIN Y: -178.5DEG X: 0Hz
Y: -200 TO +200 DEG
X: 0Hz → 1.6kHz LIN
SETUP W2 #A: 256

ORIGINAL PAGE IS
OF POOR QUALITY

Type 2032

Page No.
75

Sign.:

Meas.
Object:
PLF PR3.5
ChA=T10
ChB= M1

Rdg 187

Comments:

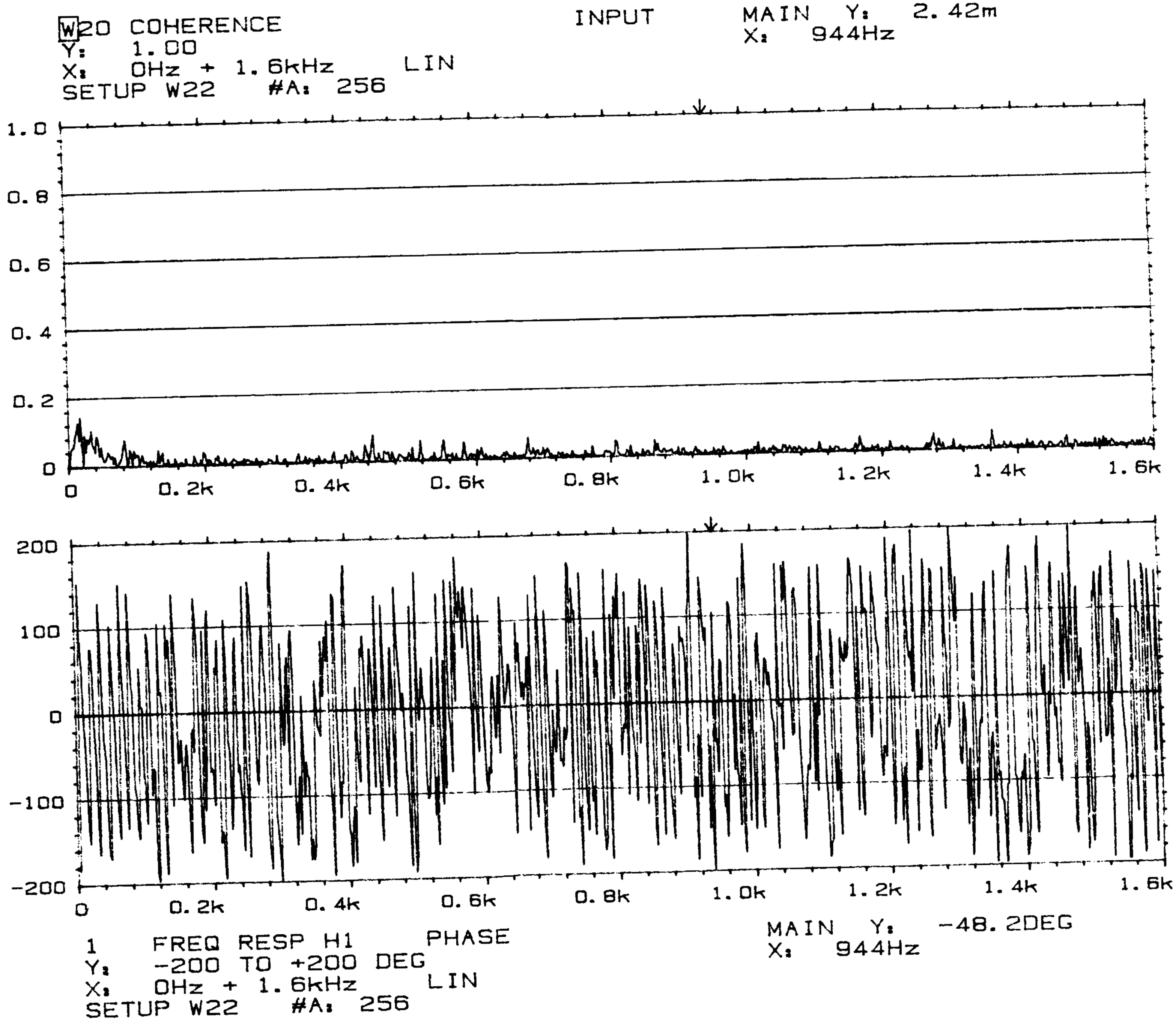

Type 2032

Page No.
77

Sign.:

Meas.
Object:

PLF PR 3.5
ChA=T10
ChB=M2

Rdg 187

Comments:

W20 COHERENCE
Y: 1.00
X: 0Hz + 1.6kHz LIN
SETUP W22 #A: 256

INPUT

MAIN Y: 6.35m
X: 944Hz

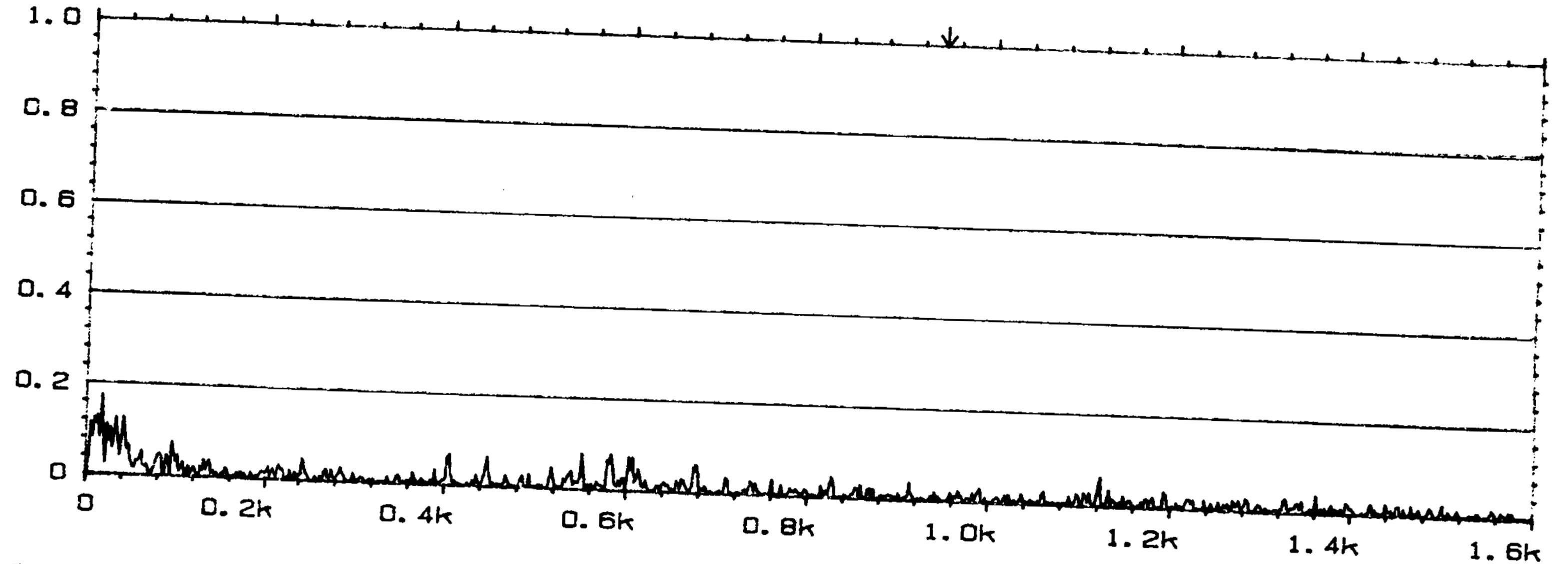

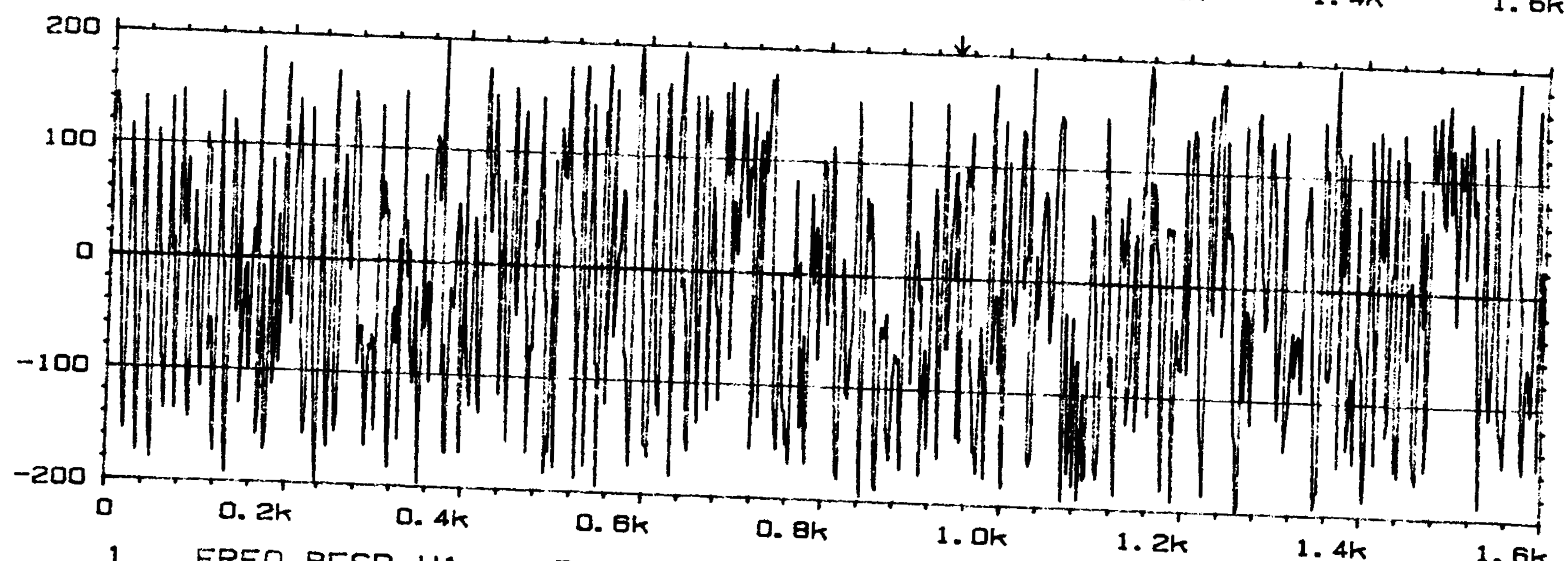

1 FREQ RESP H1 PHASE
Y: -200 TO +200 DEG
X: 0Hz + 1.6kHz LIN
SETUP W22 #A: 256

MAIN Y: 94.3DEG
X: 944Hz

Type 2032

Page No.
79

Sign.:

Meas.
Object:

CH.B - M3

Rdg 187

Comments:

W20 COHERENCE
Y: 1.00
X: 0Hz + 1.6kHz LIN
SETUP W22 #A: 256

INPUT

MAIN Y: 337μ
X: 944Hz

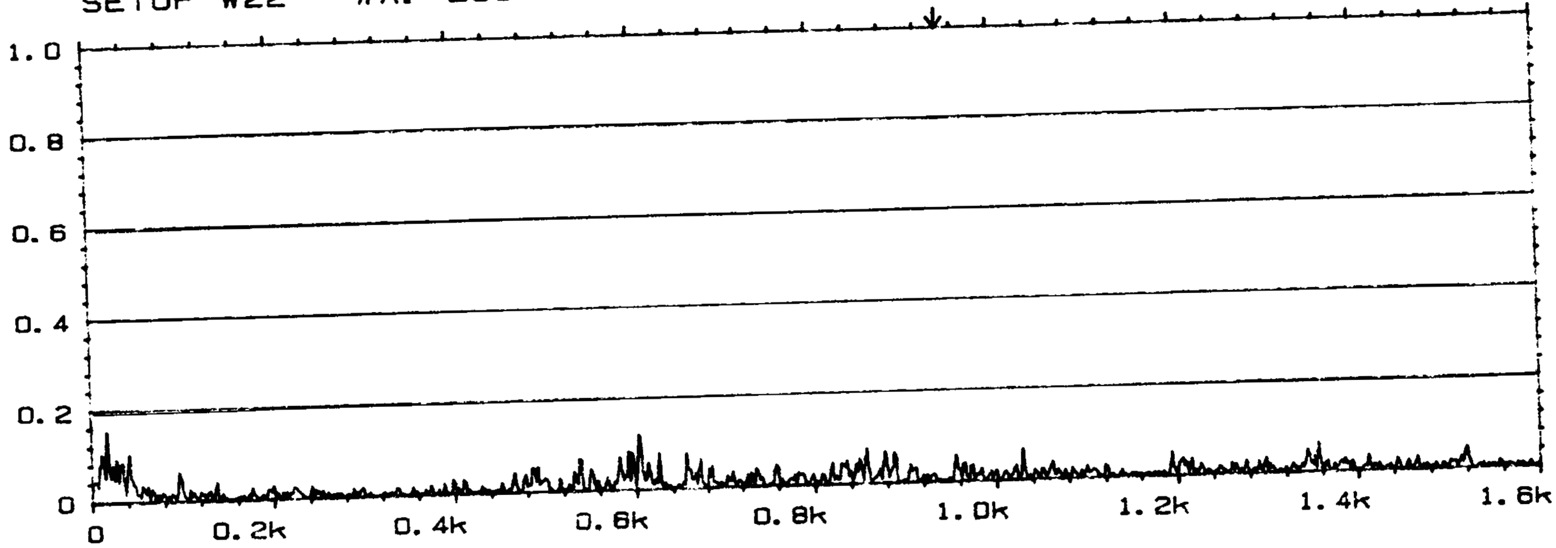

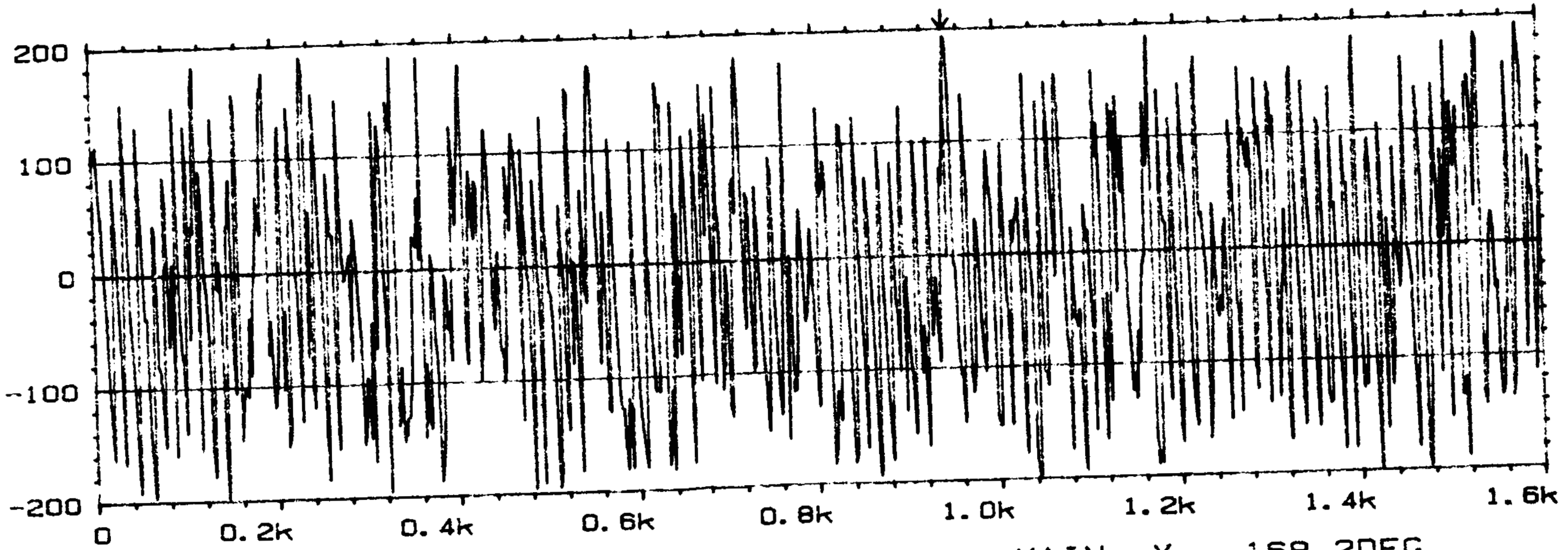

1 FREQ RESP H1 PHASE
Y: -200 TO +200 DEG
X: 0Hz + 1.6kHz LIN
SETUP W22 #A: 256

MAIN Y: 168.2DEG
X: 944Hz

Type 2032

Page No.
81

Sign.:

Meas.
Object:

PLF PR3.5
ChA = T16
ChB = M4

Rdg 187

Comments:

W20 COHERENCE INPUT MAIN Y: 103m
Y: 1.00 X: 704Hz
X: 0Hz + 1.6kHz LIN
SETUP W22 #A: 256

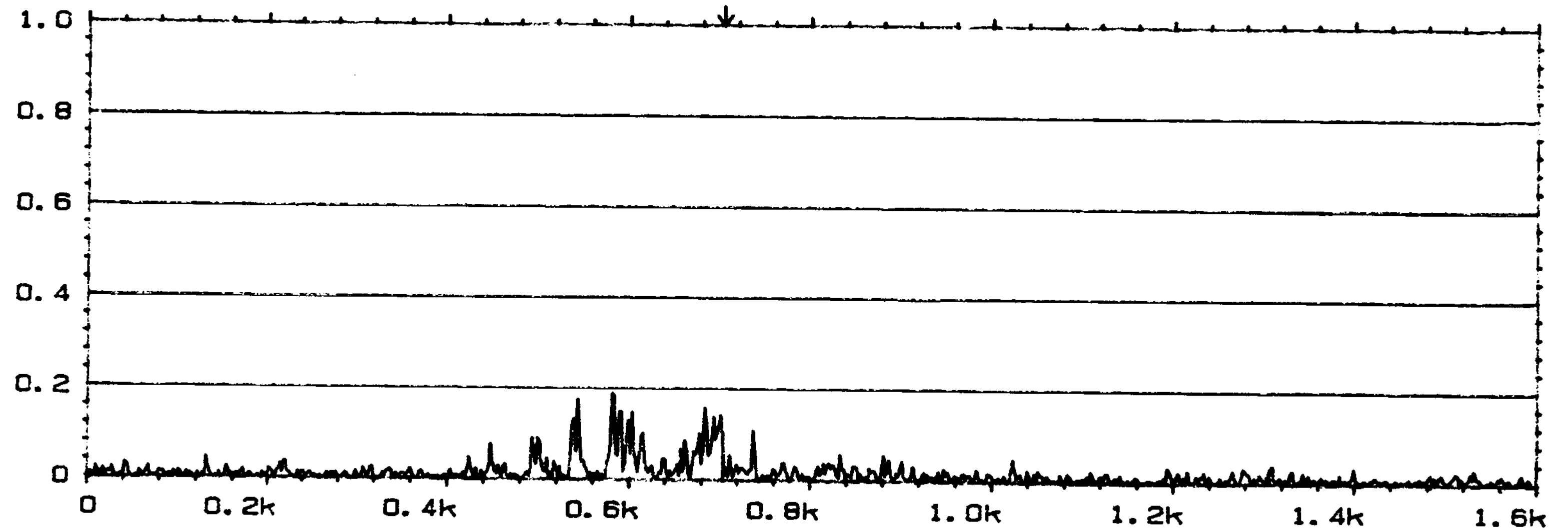

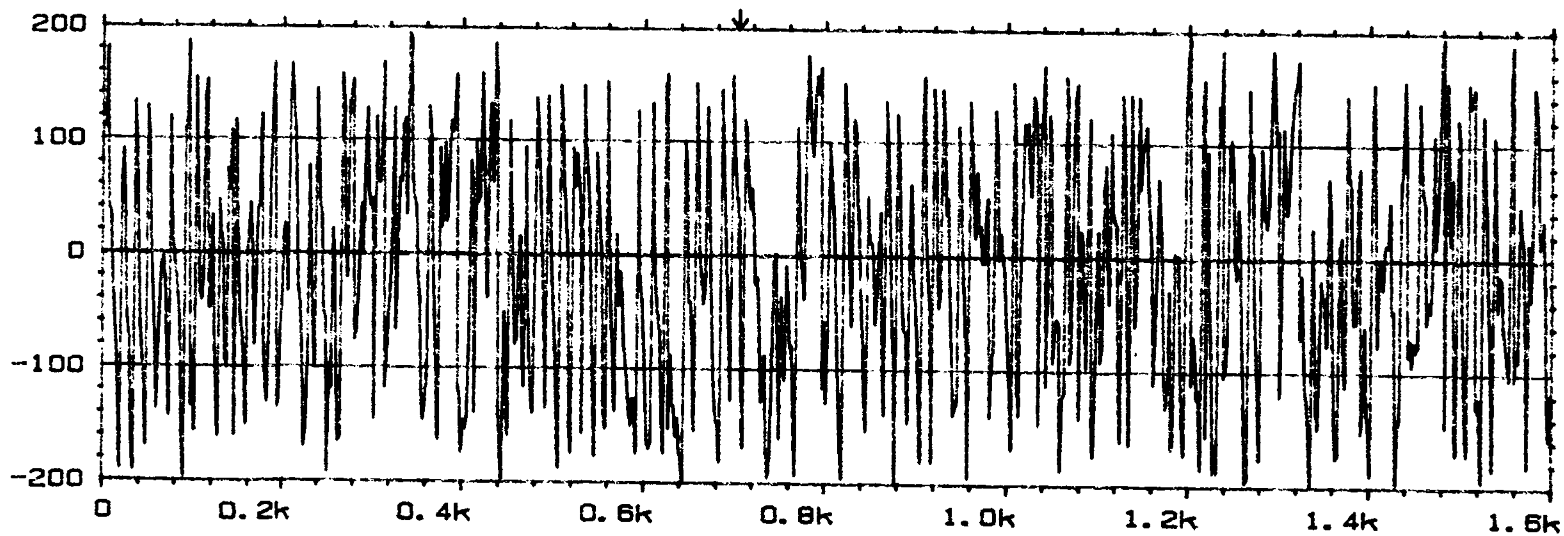

1 FREQ RESP H1 PHASE MAIN Y: 50.8DEG
Y: -200 TO +200 DEG X: 704Hz
X: 0Hz + 1.6kHz LIN
SETUP W22 #A: 256

APPENDIX B

PART II

INTERNAL TO INTERNAL PRESSURE TRANSDUCERS

Type 2032

Page No.
23

Sign.:

Meas.
Object:
PLF PR1.2
ChA=T10
ChB=T5

Rdg 176

Comments:

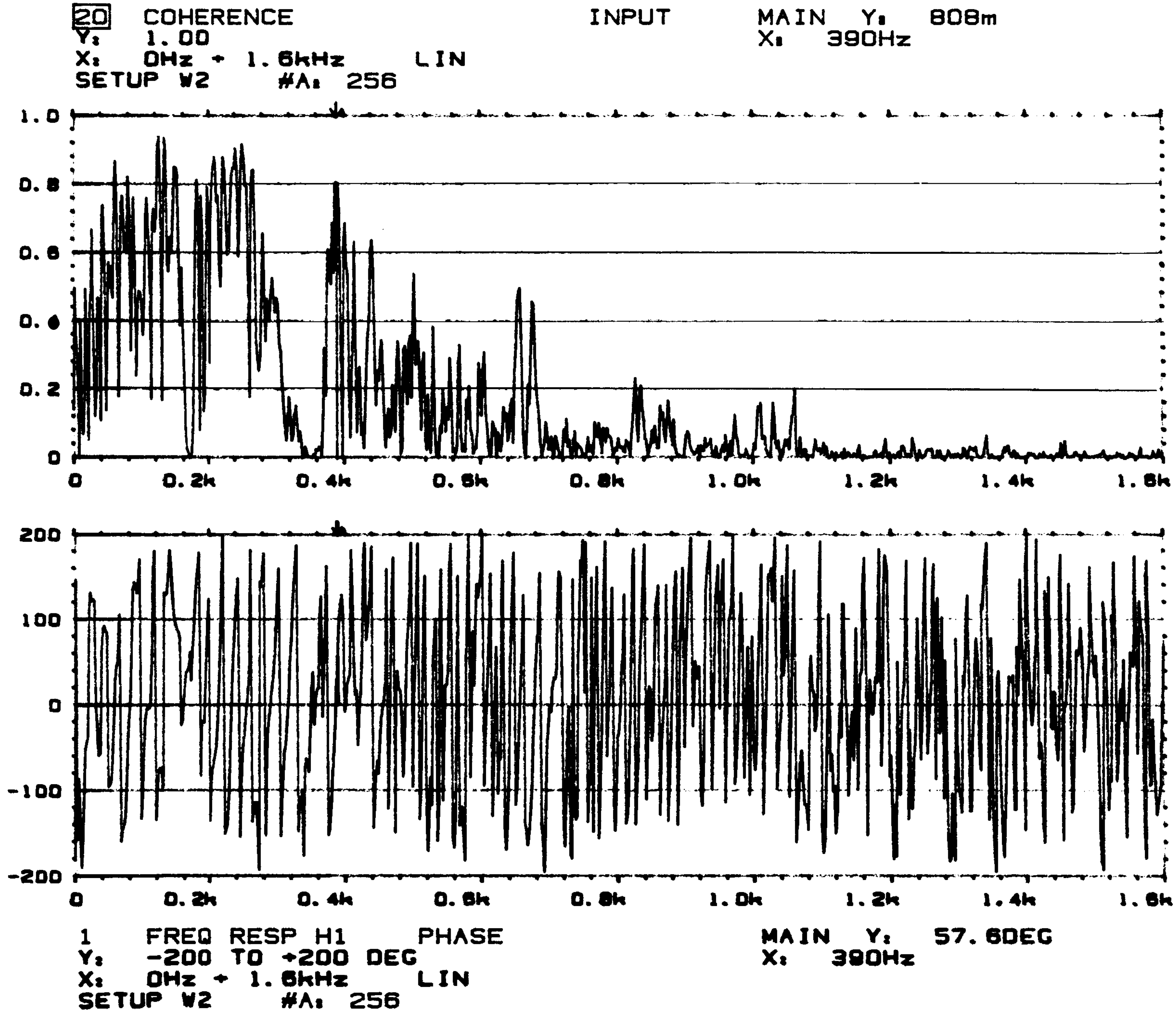

Type 2032

Page No.
62

Sign.:

Meas.
Object:

Comments:

20 COHERENCE INPUT MAIN Y: 81.0m
Y: 1.00 X: 1600Hz
X: 0Hz + 1.6kHz LIN
SETUP W12 #A: 256

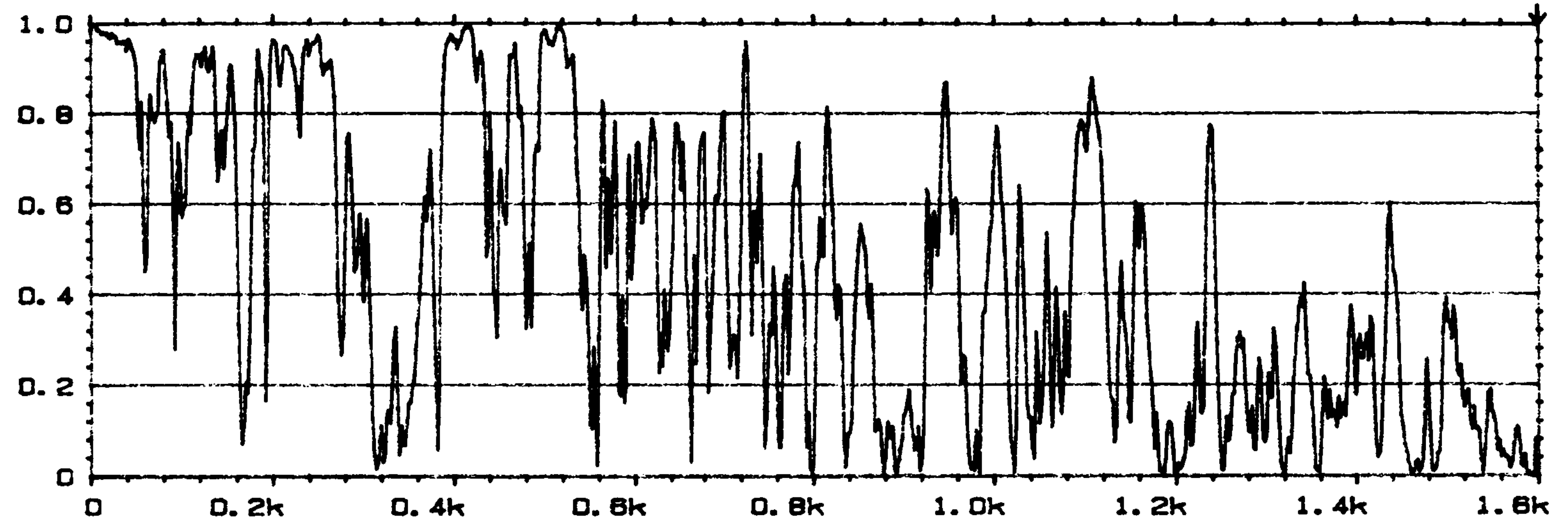

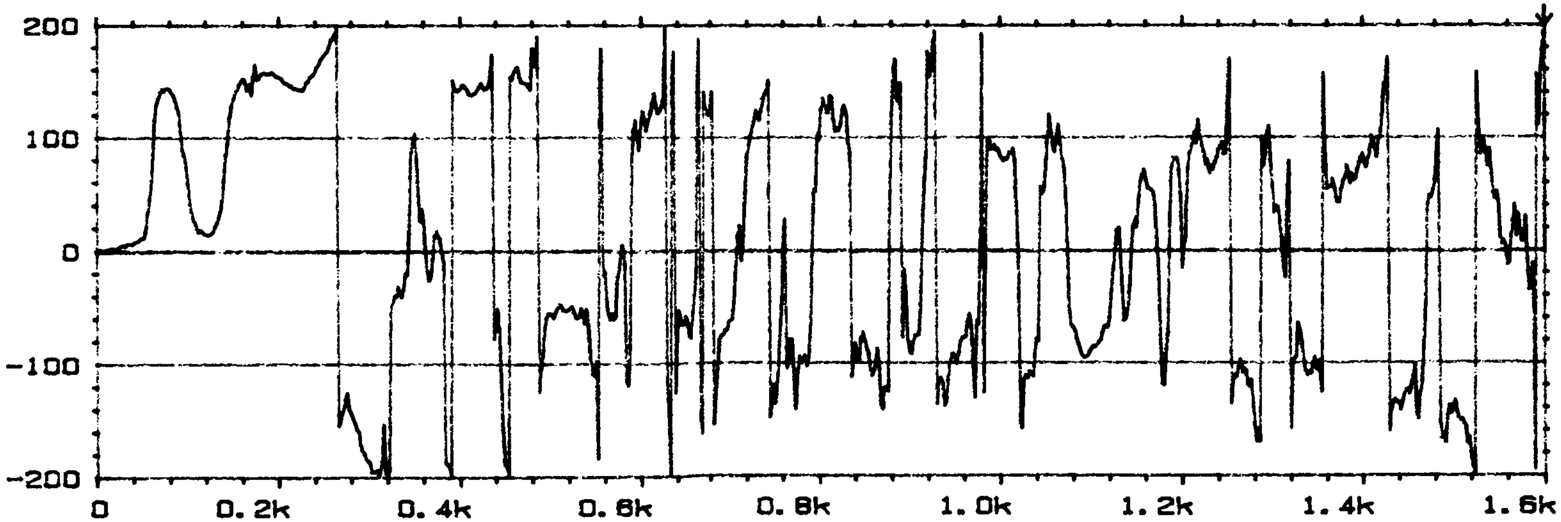

W1 FREQ RESP H1 PHASE MAIN Y: -165.5DEG
Y: -200 TO +200 DEG X: 1600Hz
X: 0Hz + 1.6kHz LIN
SETUP W12 #A: 256

Type 2032

Page No.
53

Sign.:

Meas.
Object:

PLF DR 3.5

ChA = T10

ChB = T 5

Rds 187

Comments:

20 COHERENCE INPUT MAIN Y: 791m
Y: 1.00 X: 395Hz
X: 0Hz + 800Hz LIN
SETUP W12 #A: 256

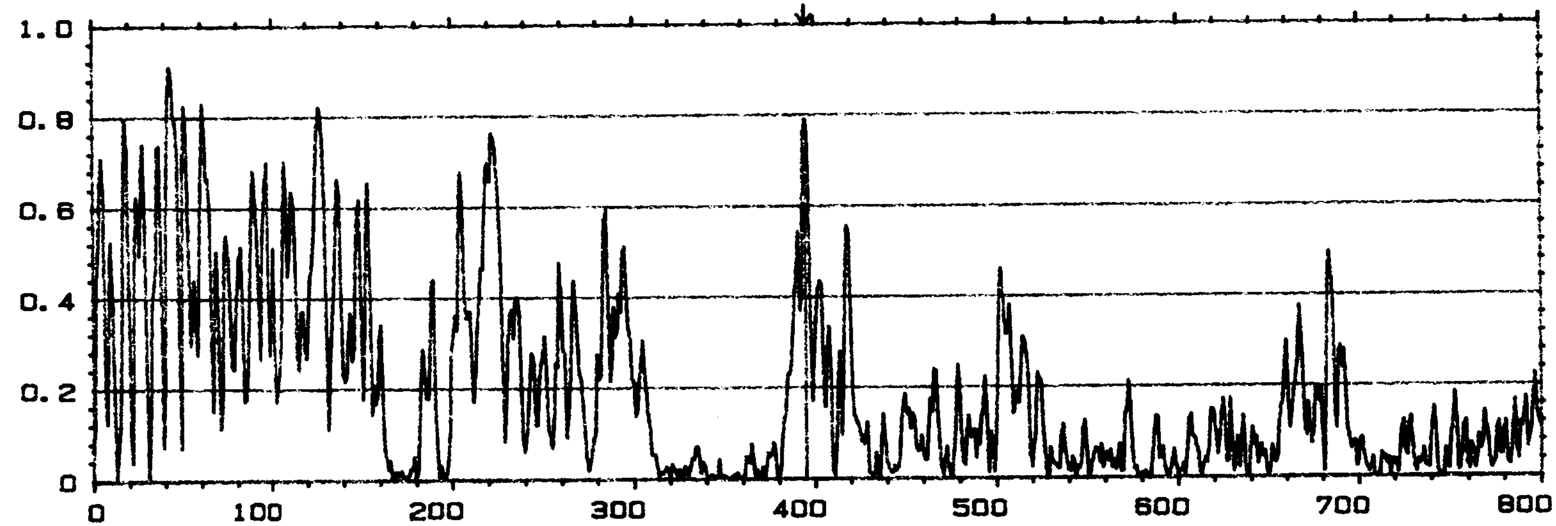

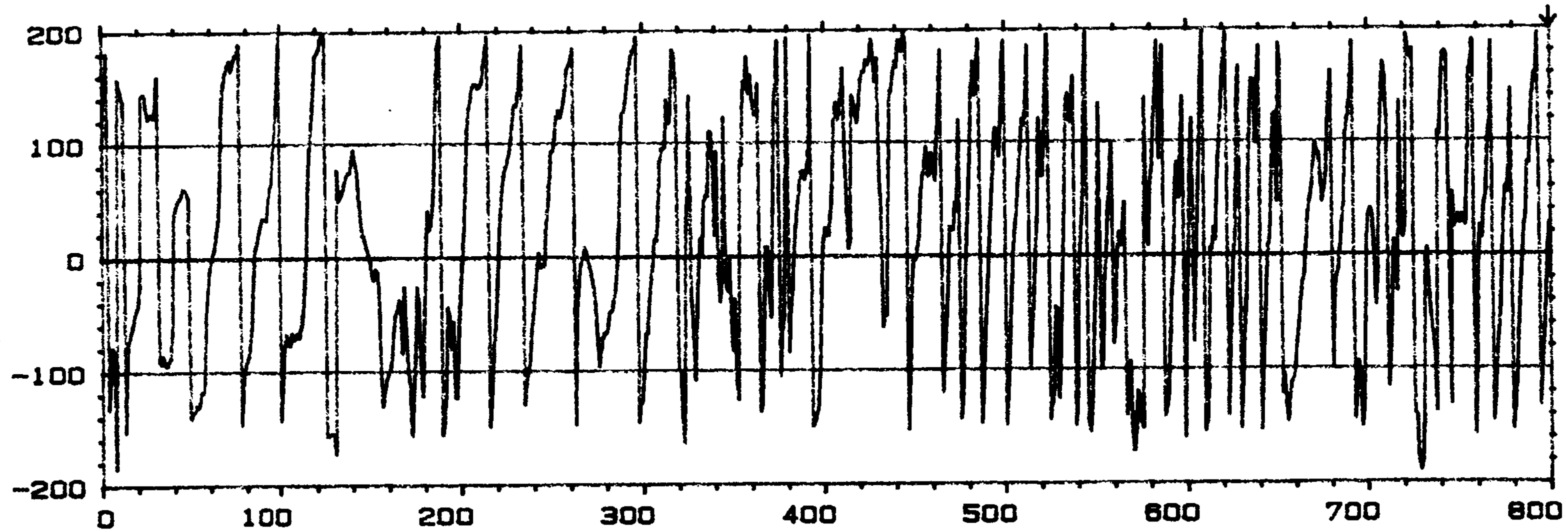

6 FREQ RESP H1 PHASE MAIN Y: 27.8DEG
Y: -200 TO +200 DEG X: 800Hz
X: 0Hz + 800Hz LIN
SETUP W12 #A: 256

Type 2032

Page No.
83

Sign.:

Meas.
Object:

PLF PR 3.5
ChA = T 10
ChB = T 7

Comments:

Rdg 187

W20 COHERENCE INPUT MAIN Y: 773m
Y: 1.00 X: 396Hz
X: 0Hz + 1.6kHz LIN
SETUP W22 #A: 256

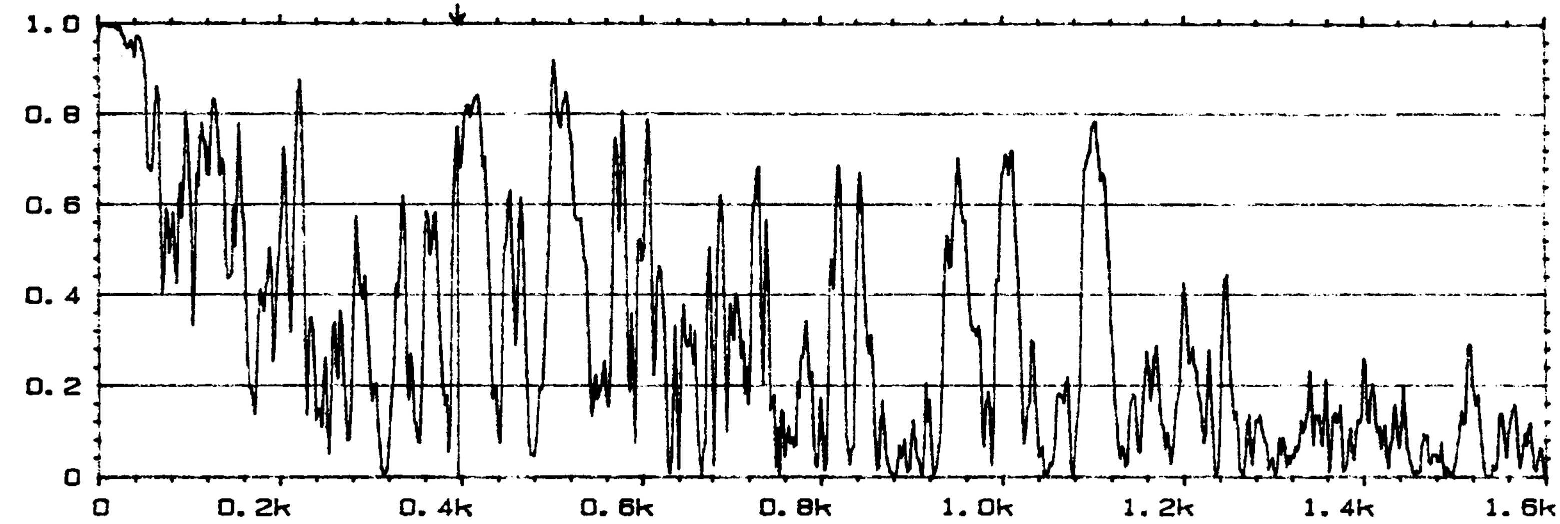

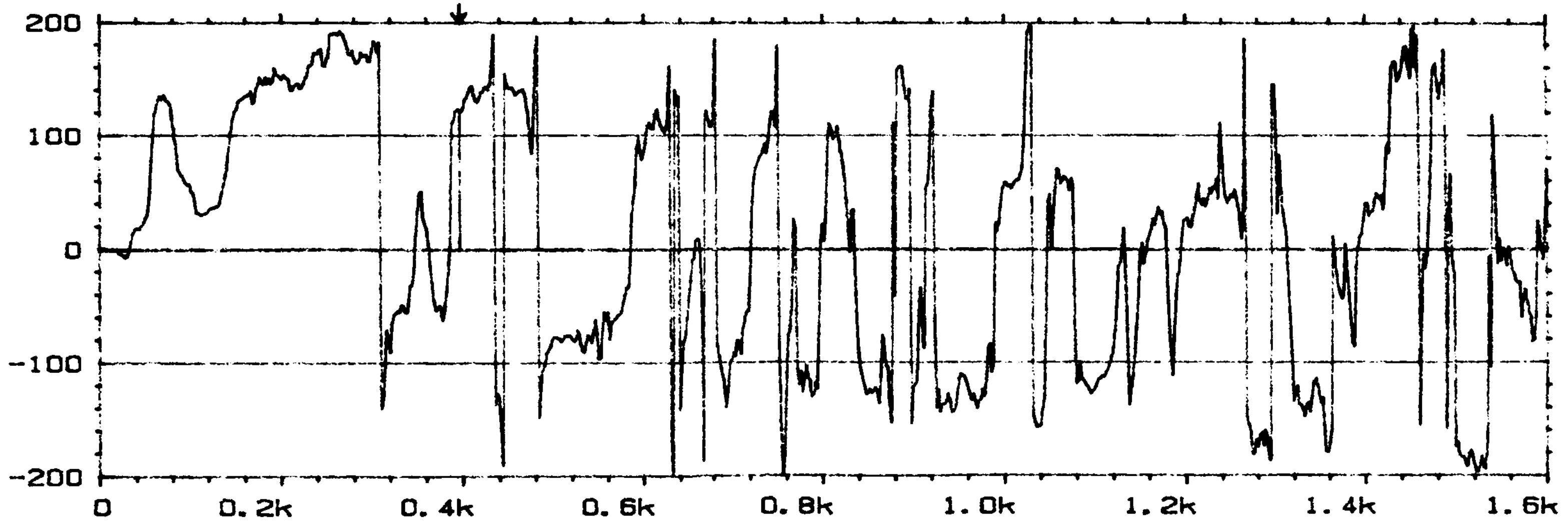

1 FREQ RESP H1 PHASE MAIN Y: 123.1DEG
Y: -200 TO +200 DEG X: 396Hz
X: 0Hz + 1.6kHz LIN
SETUP W22 #A: 256

APPENDIX C

SAMPLE CROSS-CORRELATIONS, SIGNAL DELAY INFORMATION

APPENDIX C

PART I

INTERNAL PRESSURE TRANSDUCERS TO FAR FIELD MICROPHONES

Type 2032

Page No.
71 6/17/93

Sign.:

Meas.
Object:

PLF PR 3.5
ChA=T9
ChB=M1
Time delay
0ms
Rdg 187

Comments:

Acoustic delay
time Internal
to Far Field
is 75Ft/1100Ft/s
.068 Sec = 68mS

W5 CROSS CORR REAL INPUT MAIN Y: -656µ
Y: 9.82m X: -178.46ms
X: 26.61ms + 125ms
#A: 256

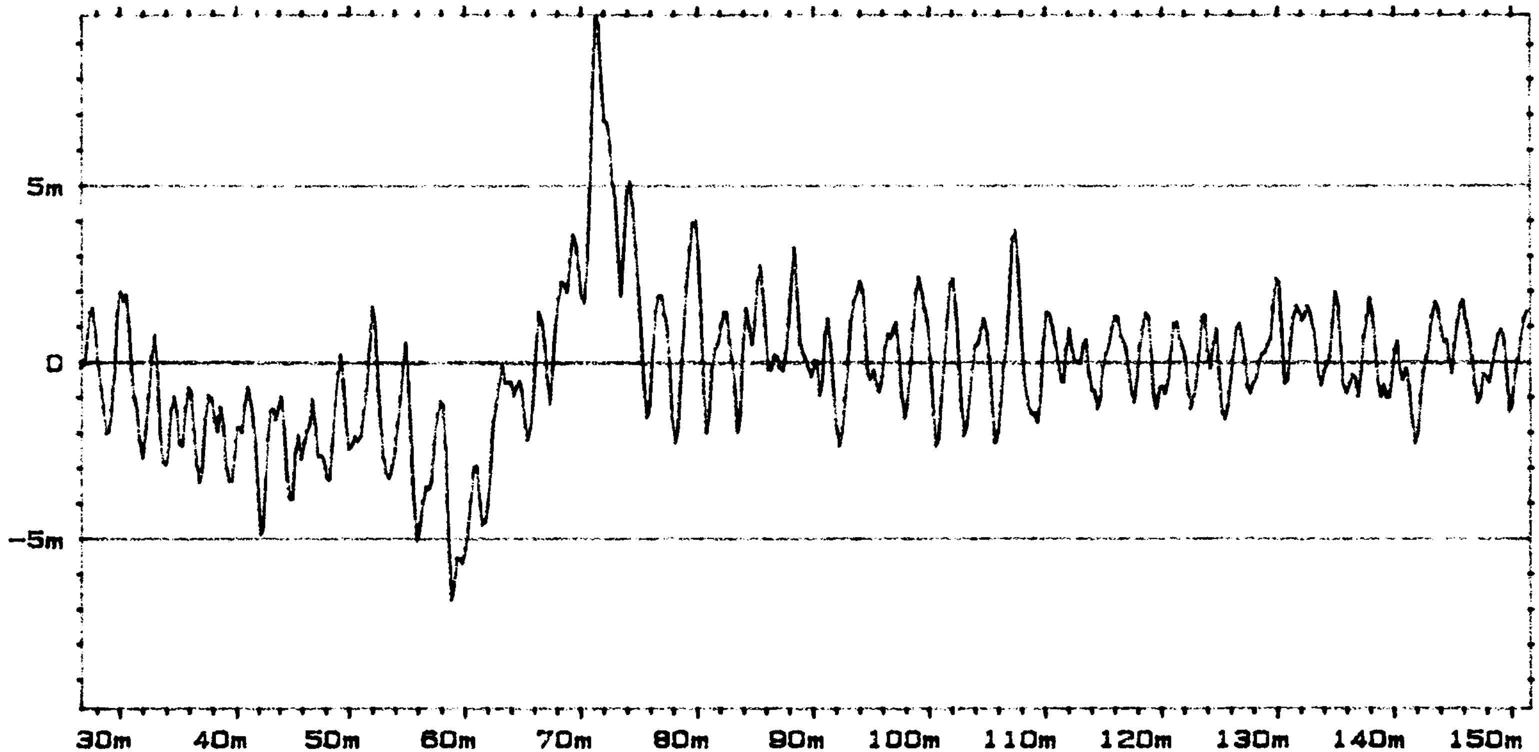

SETUP W12

MEASUREMENT:	DUAL SPECTRUM AVERAGING				
TRIGGER:	FREE RUN				
DELAY:	CH. A→B: 0.00ms				
AVERAGING:	LIN 256	OVERLAP: MAX			
FREQ SPAN:	1.6kHz	ΔF: 2Hz		T: 500ms	ΔT: 244µs
CENTER FREQ:	BASEBAND				
WEIGHTING:	HANNING				
CH. A:	1V	+	3Hz DIR	FILT: 25.6kHz	1V/V
CH. B:	2V	+	3Hz DIR	FILT: 25.6kHz	1V/V
GENERATOR:	RANDOM NOISE			OFF	

ORIGINAL PAGE IS
OF POOR QUALITY

Type 2032

Page No.
72 6/17/88

Sign.:

Meas.
Object:
PLF PR3.5
ChA=T9
ChB=M4
time delay
0 ms
Rdg 187

Comments:

W5 CROSS CORR REAL INPUT MAIN Y: 5.14m
Y: 5.14m X: 78.36ms
X: 14.89ms + 125ms
#A: 256

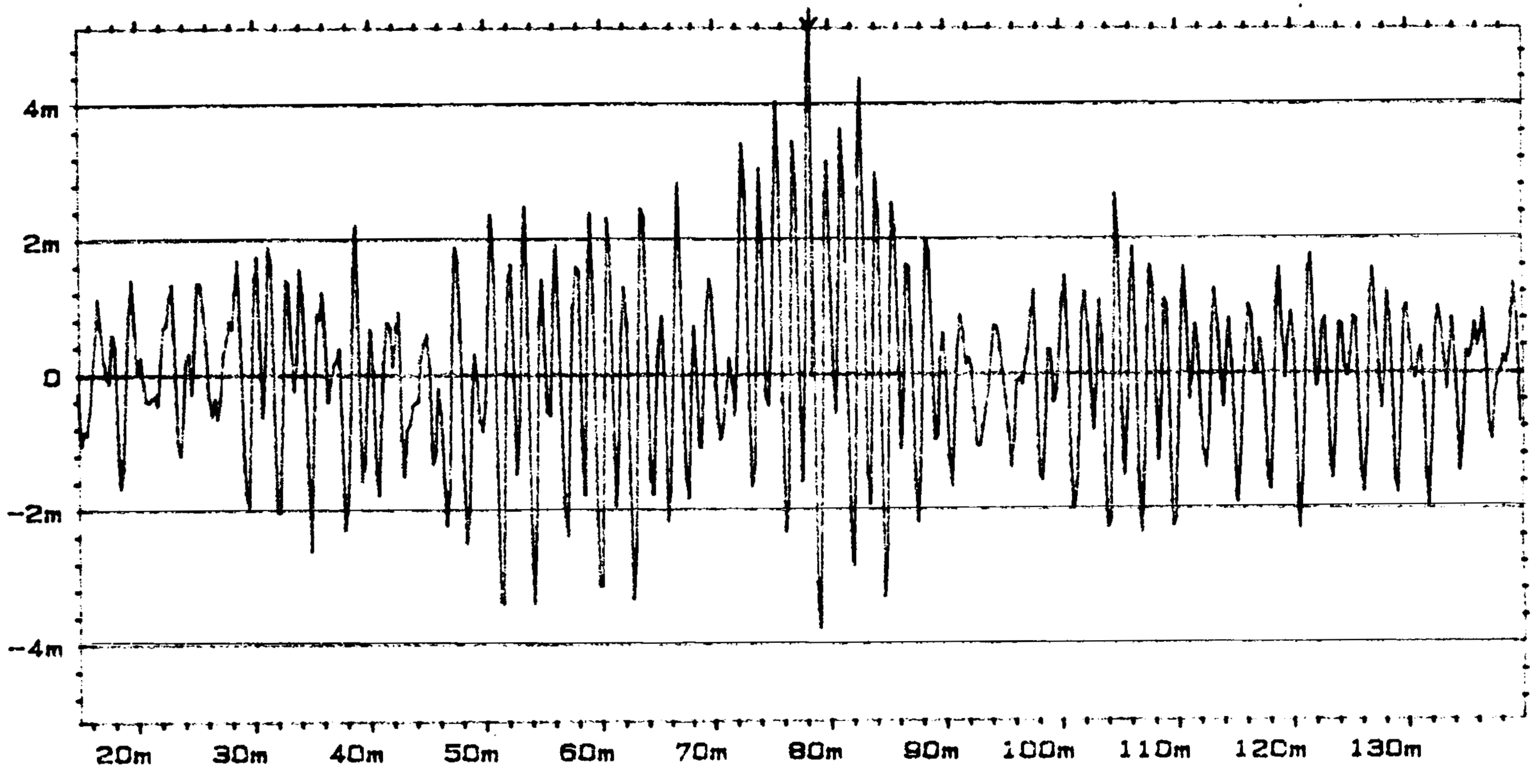

SETUP W12

MEASUREMENT:	DUAL SPECTRUM AVERAGING
TRIGGER:	FREE RUN
DELAY:	CH. A→B: 0.00ms
AVERAGING:	LIN 256 OVERLAP: MAX

FREQ SPAN:	1.6kHz	ΔF: 2Hz	T: 500ms	ΔT: 244µs
CENTER FREQ:	BASEBAND			
WEIGHTING:	HANNING			

CH. A:	1V	+ 3Hz DIR	FILT: 25.6kHz	1V/V
CH. B:	2V	+ 3Hz DIR	FILT: 25.6kHz	1V/V
GENERATOR:	RANDOM NOISE	OFF		

APPENDIX C

PART II

INTERNAL TO INTERNAL PRESSURE TRANSDUCERS

Type 2032

Page No.
26

Sign.:

Meas.
Object:

PLF PR1.2
ChA=710
ChB=T5

Fdg 1/6

Comments:

W13 CROSS CORR REAL INPUT MAIN Y: -14.6m
Y: 14.6m X: -21.911ms
X: -31.250ms + 15.6ms
SETUP W2* #A: 256

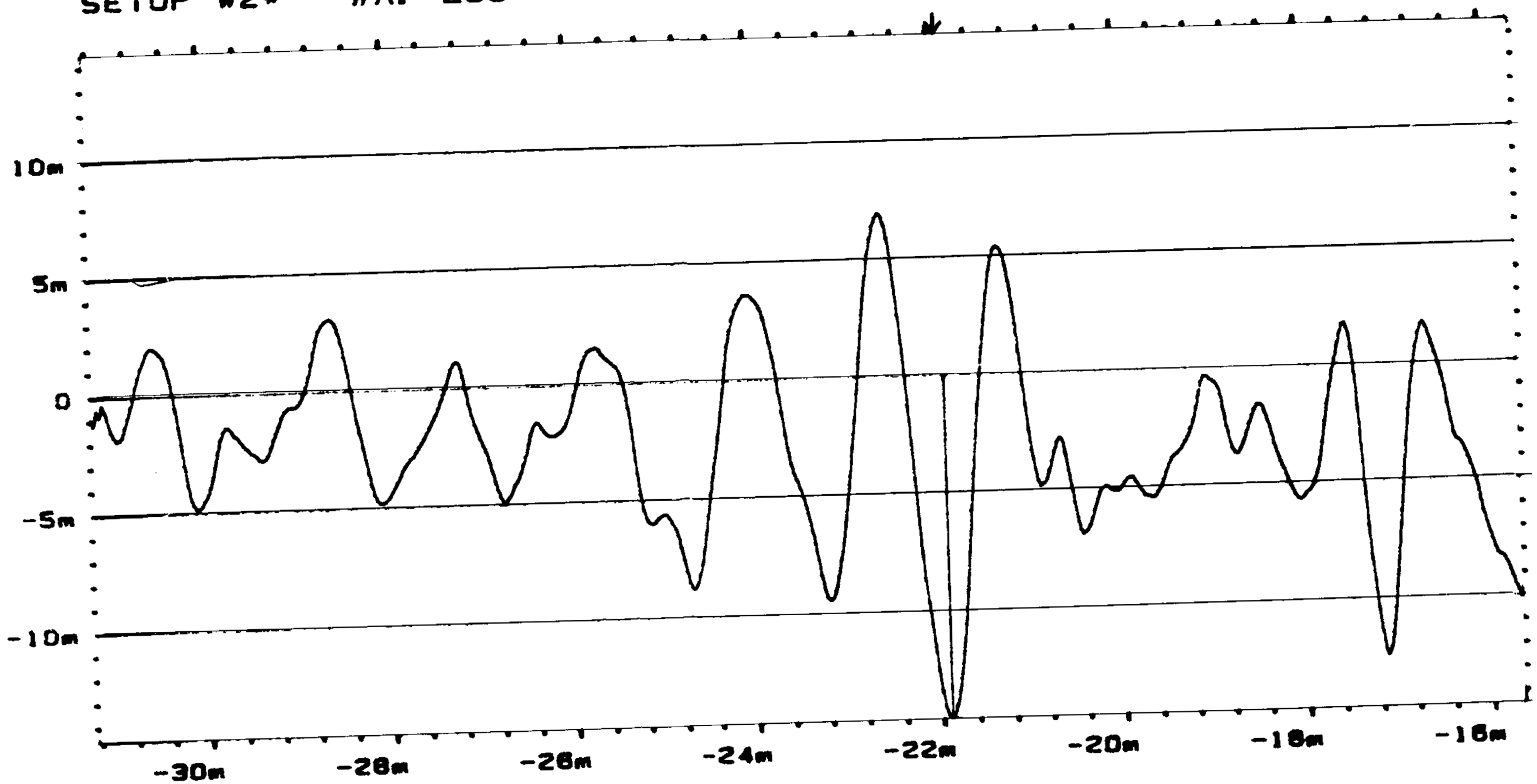

SETUP W2

MEASUREMENT:	DUAL SPECTRUM AVERAGING			
TRIGGER:	FREE RUN			
DELAY:	CH. A→B: 0.000ms			
AVERAGING:	LIN 256	OVERLAP: MAX		
FREQ SPAN:	12.8kHz	ΔF: 16Hz	T: 62.5ms	ΔT: 30.5μs
CENTER FREQ:	BASEBAND			
WEIGHTING:	HANNING			
CH. A:	2V +	3Hz DIR	FILT: 25.6kHz	1V/V
CH. B:	2V +	3Hz DIR	FILT: 25.6kHz	1V/V
GENERATOR:	DISABLED			
PLOT: #27:	Y SCALE LINES..........:	FEW		

ORIGINAL PAGE IS
OF POOR QUALITY

Type 2032

Page No.
63

Sign.:

Meas.
Object:

PLF PF 12

Fdg 176

Comments:

W13 CROSS CORR REAL INPUT MAIN Y: 146m
Y: 264m X: 0.00ms
X: -250.00ms + 500ms
#A: 256

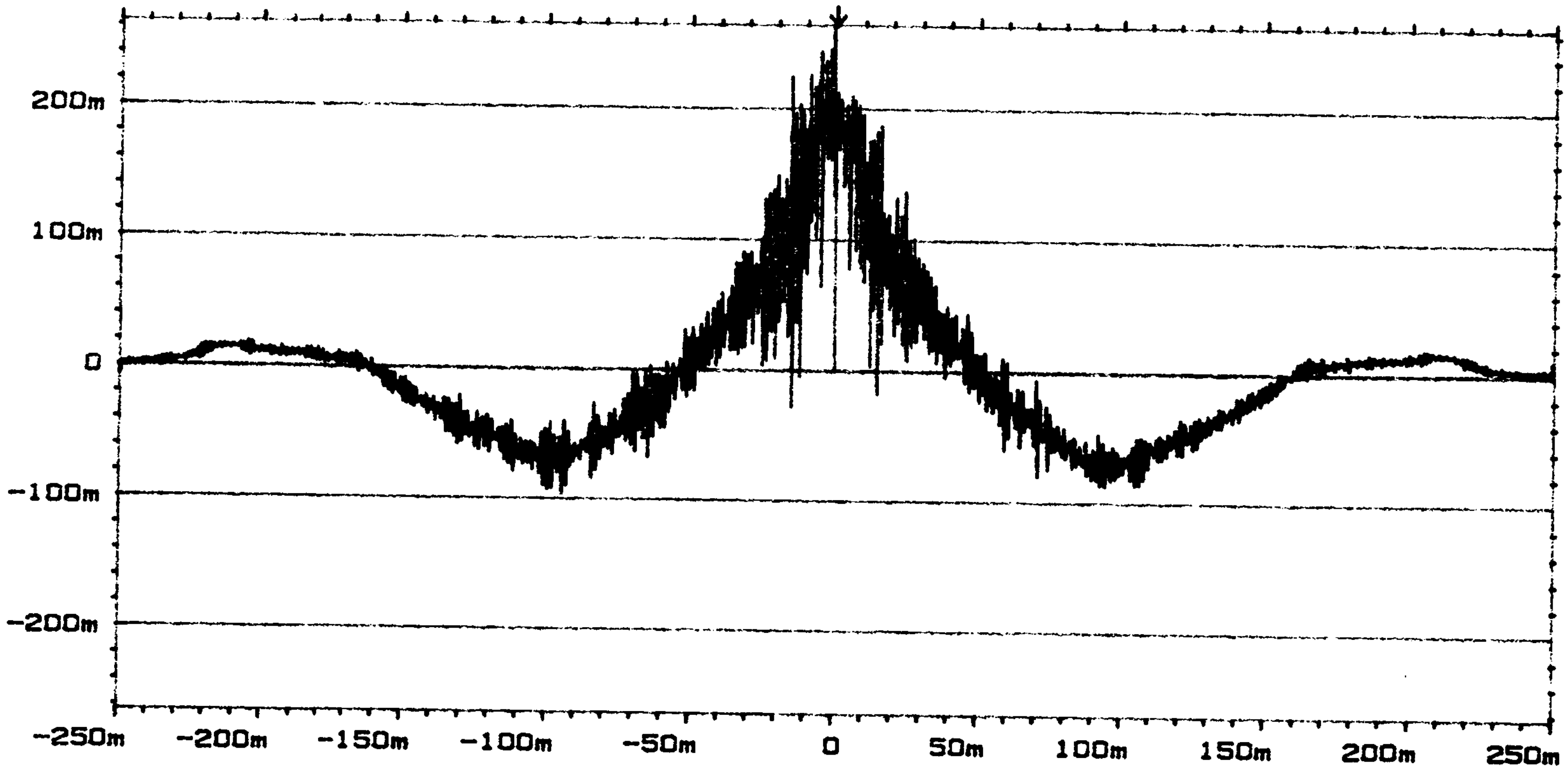

SETUP W12

MEASUREMENT:	DUAL SPECTRUM AVERAGING				
TRIGGER:	FREE RUN				
DELAY:	CH. A→B: 0.00ms				
AVERAGING:	LIN 256	OVERLAP: MAX			
FREQ SPAN:	1.6kHz	ΔF: 2Hz	T: 500ms	ΔT: 244μs	
CENTER FREQ:	BASEBAND				
WEIGHTING:	HANNING				
CH. A:	2V	+ 3Hz DIR	FILT: 25.6kHz	1V/V	
CH. B:	1V	+ 3Hz DIR	FILT: 25.6kHz	1V/V	
GENERATOR:	RANDOM NOISE	OFF			
PLOT: #27:	Y SCALE LINES..........: FEW				

W13 CROSS CORR　　REAL　　INPUT　　MAIN Y: 77.1m
Y: 153m　　X: -48.58ms
X: -250.00ms + 500ms
#A: 256

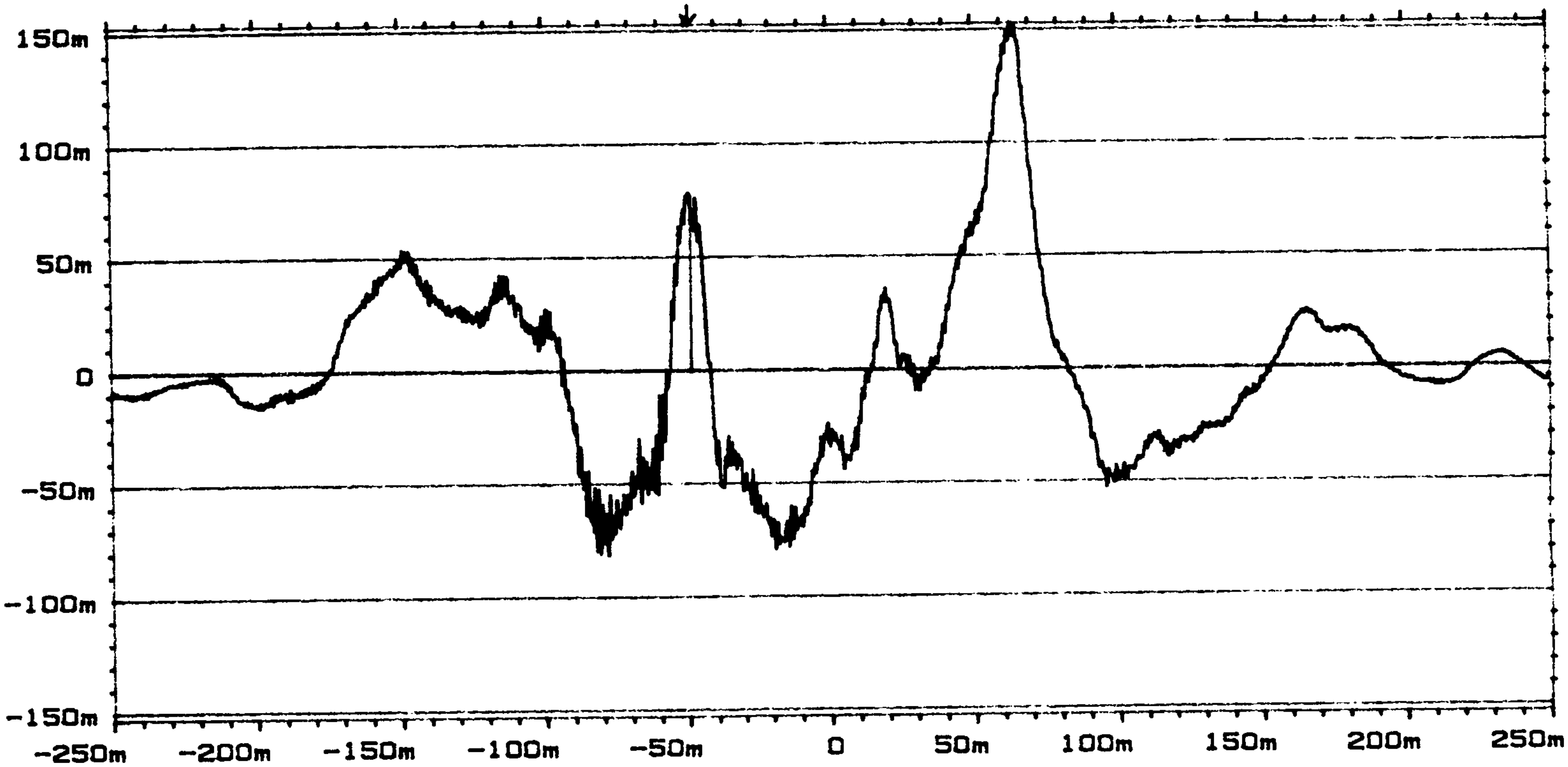

Type 2032

Page No.
54

Sign.:

Meas.
Object:
PLF PR 3.5
ChA=T10
ChB=T5

Rdg 187

Comments:

SETUP W12

MEASUREMENT:	DUAL SPECTRUM AVERAGING			
TRIGGER:	FREE RUN			
DELAY:	CH. A→B: 0.00ms			
AVERAGING:	LIN 256	OVERLAP: MAX		
FREQ SPAN:	1.6kHz	ΔF: 2Hz	T: 500ms	ΔT: 244μs
CENTER FREQ:	BASEBAND			
WEIGHTING:	HANNING			
CH. A:	1V + 3Hz DIR	FILT: 25.6kHz	1V/V	
CH. B:	2V + 3Hz DIR	FILT: 25.6kHz	1V/V	
GENERATOR:	RANDOM NOISE	OFF		
PLOT: #27:	Y SCALE LINES..........:	FEW		

Type 2032

Page No.
91

Sign.:

Meas.
Object:

PLF PR3.5
ChA = T10
ChB = T7

Rdg 187

Comments:

W13 CROSS CORR REAL INPUT MAIN Y: 860m
Y: 1.00 X: -0.97ms
X: -500.00ms + 1s
#A: 256

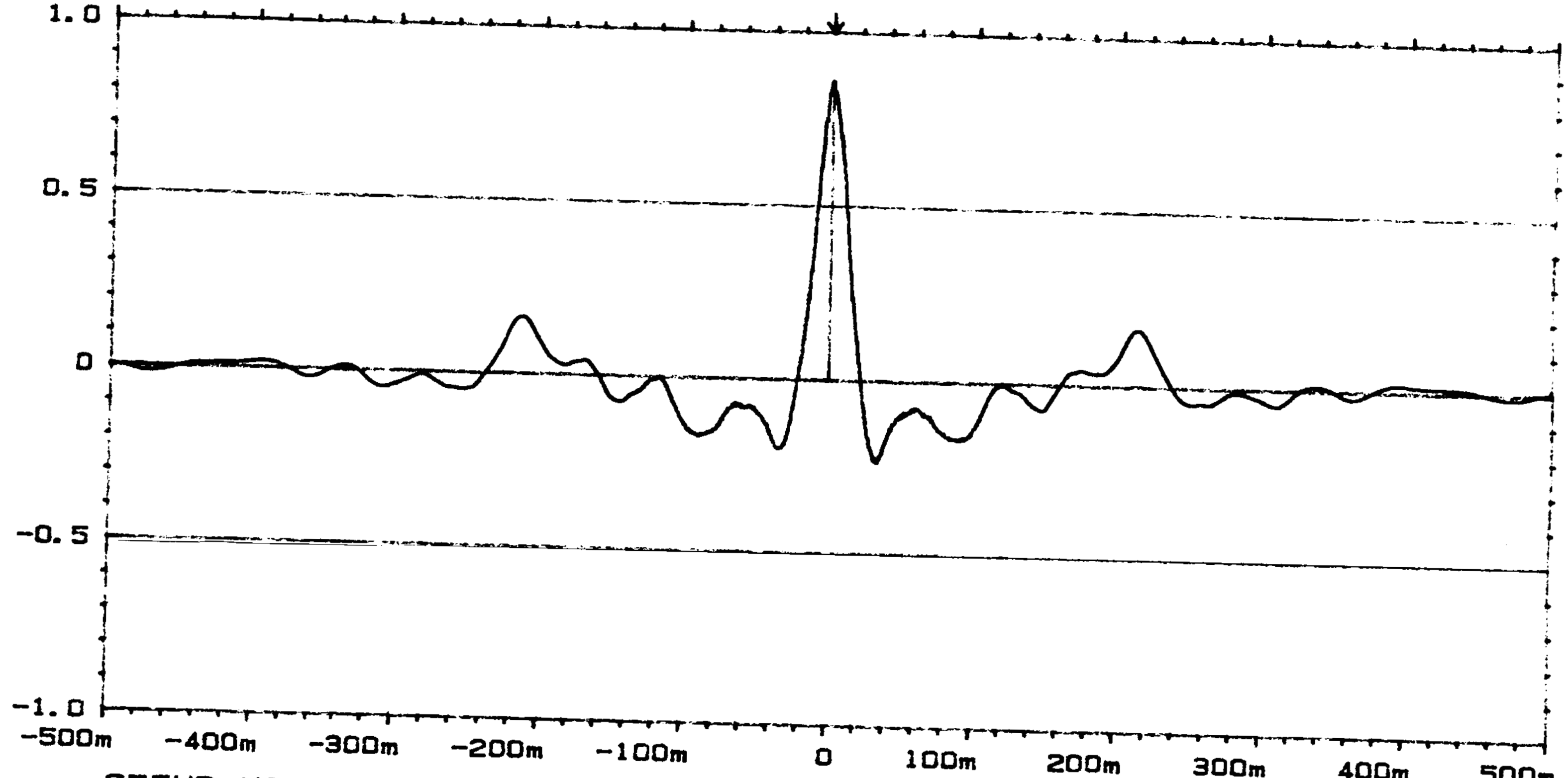

SETUP W22

MEASUREMENT:	DUAL SPECTRUM AVERAGING				
TRIGGER:	FREE RUN				
DELAY:	CH. A→B: 0.00ms				
AVERAGING:	LIN 256	OVERLAP: MAX			
FREQ SPAN:	800Hz	ΔF: 1Hz	T: 1s	ΔT: 488μs	
CENTER FREQ:	BASEBAND				
WEIGHTING:	HANNING				
CH. A:	1.5V	+ 3Hz DIR	FILT: 25.6kHz	57.3V/UNIT	
CH. B:	800mV	+ 3Hz DIR	FILT: 25.6kHz	999mV/UNIT	
GENERATOR:	REFERENCE SINE		OFF		
PLOT: #27:	Y SCALE LINES..........:		FEW		

Type 2032

Page No.
25

Sign.:

Meas.
Object:

PLF PR12
chA=116
chB=12

Kdg 176

Comments:

W13 CROSS CORR REAL INPUT MAIN Y: 665m
Y: 834m X: -0.076ms
X: -15.625ms + 31.3ms
#A: 256

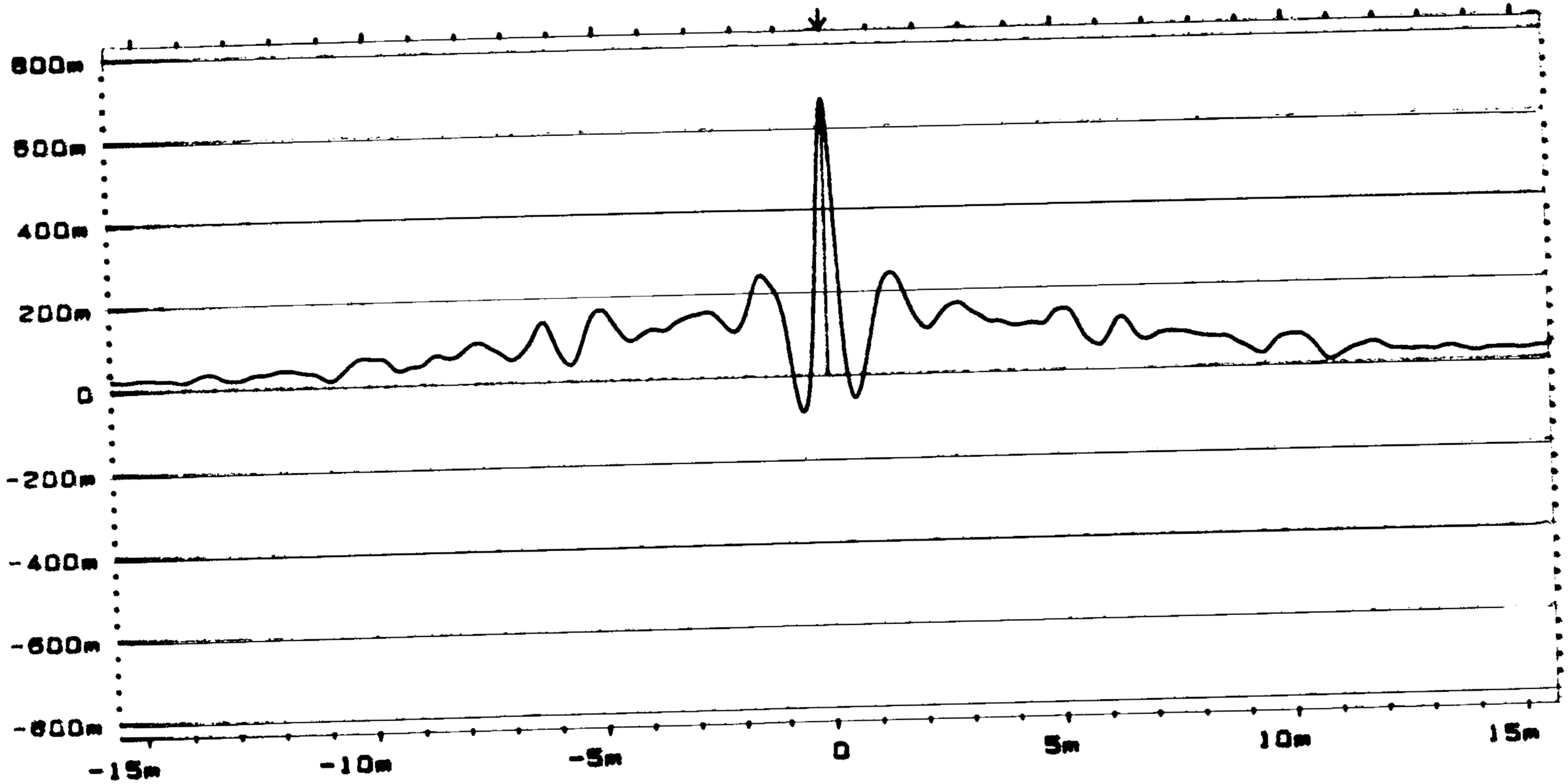

SETUP W2

MEASUREMENT:	DUAL SPECTRUM AVERAGING			
TRIGGER:	FREE RUN			
DELAY:	CH. A→B: 0.000ms			
AVERAGING:	LIN 256	OVERLAP: MAX		
FREQ SPAN:	25.6kHz	ΔF: 32Hz	T: 31.3ms	ΔT: 15.3µs
CENTER FREQ:	BASEBAND			
WEIGHTING:	HANNING			
CH. A:	1.5V +	3Hz DIR	FILT: 25.6kHz	1V/V
CH. B:	1V +	3Hz DIR	FILT: 25.6kHz	1V/V
GENERATOR:	DISABLED			
PLOT: #27:	Y SCALE LINES..........:		FEW	

APPENDIX D

SAMPLE COHERENT OUTPUT POWER SPECTRA

Type 2032

Page No.
31

Sign.:

Meas.
Object:

PLF PR 1.2
ChA = T10
ChB = M1

Rdg 176

Comments:

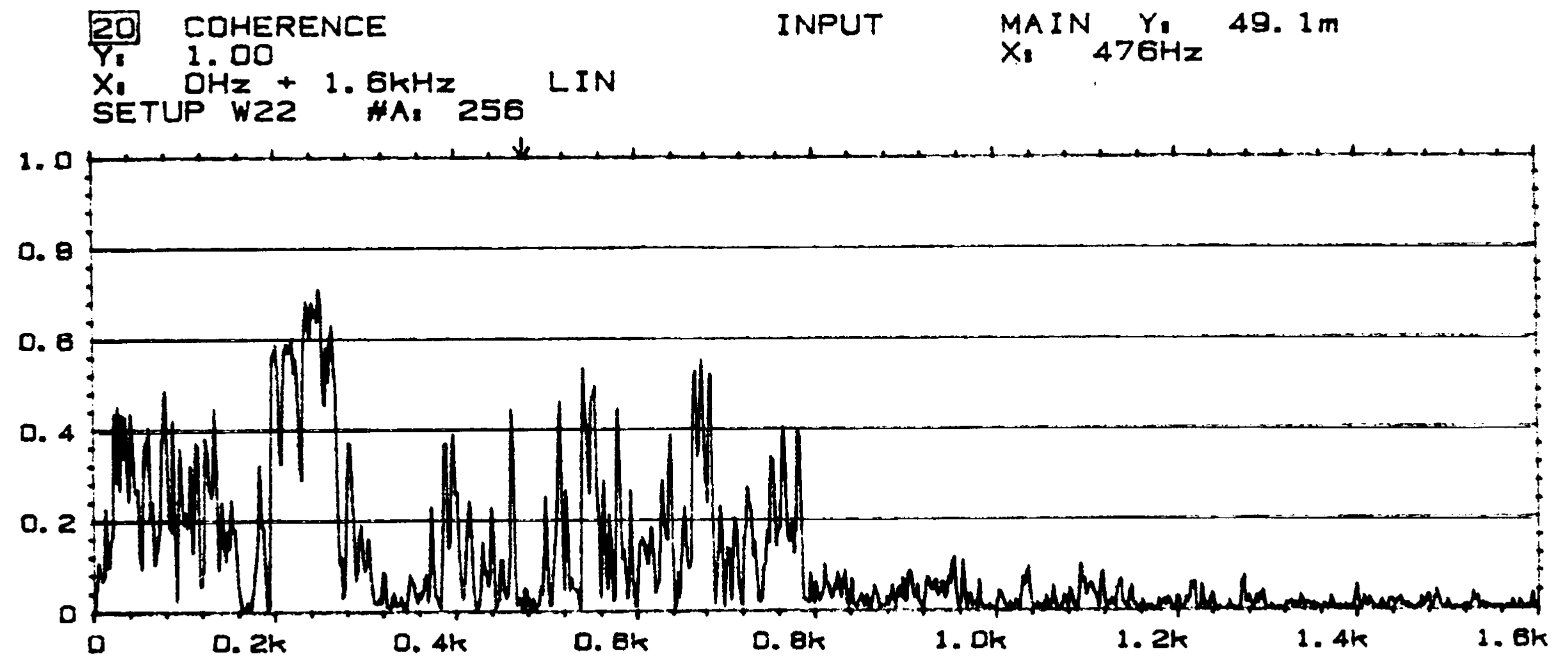

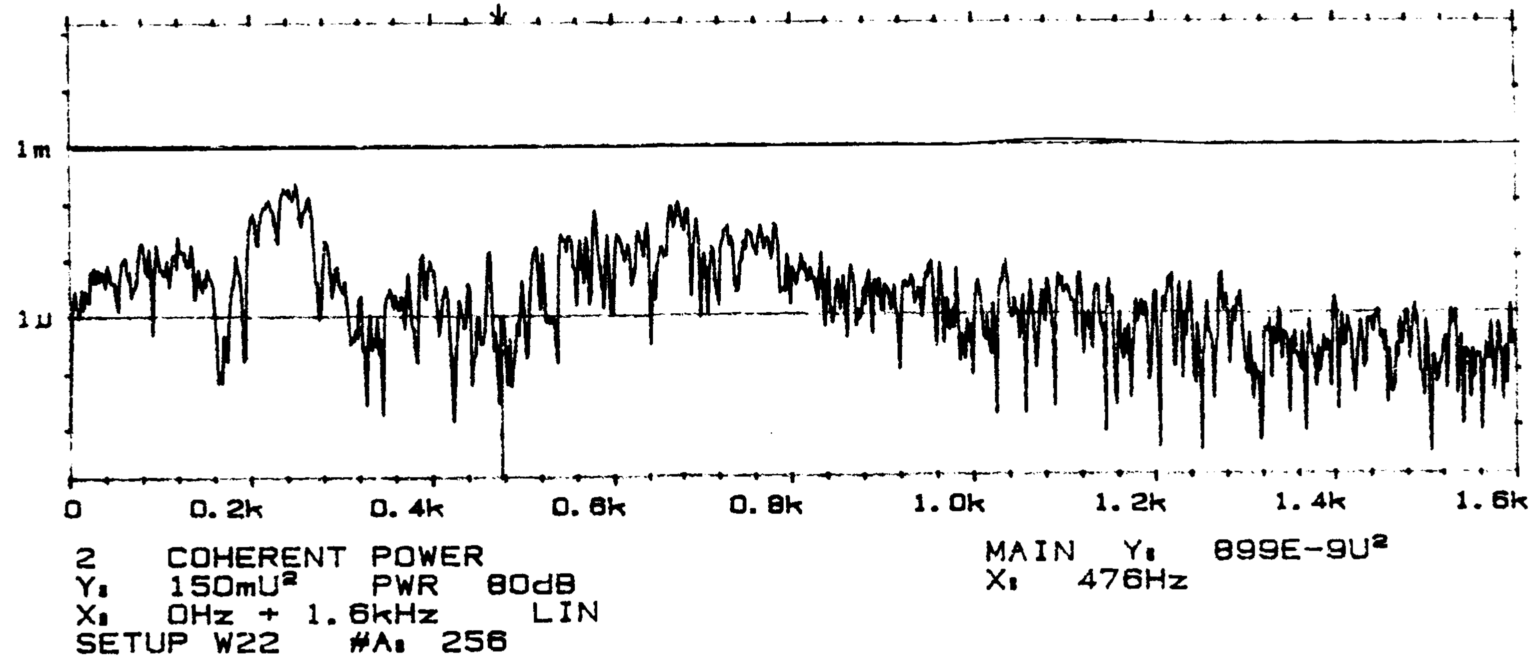

Type 2032

Page No.
23

Sign.:

Meas.
Object:

PLF PR 1.2
ChA= T10
ChB= M1

Rdg 176

Comments:

200 Hz Max

20 COHERENCE INPUT MAIN Y: 463m
Y: 1.00 X: 124.75Hz
X: 0.00Hz + 200Hz LIN
SETUP W22* #A: 256

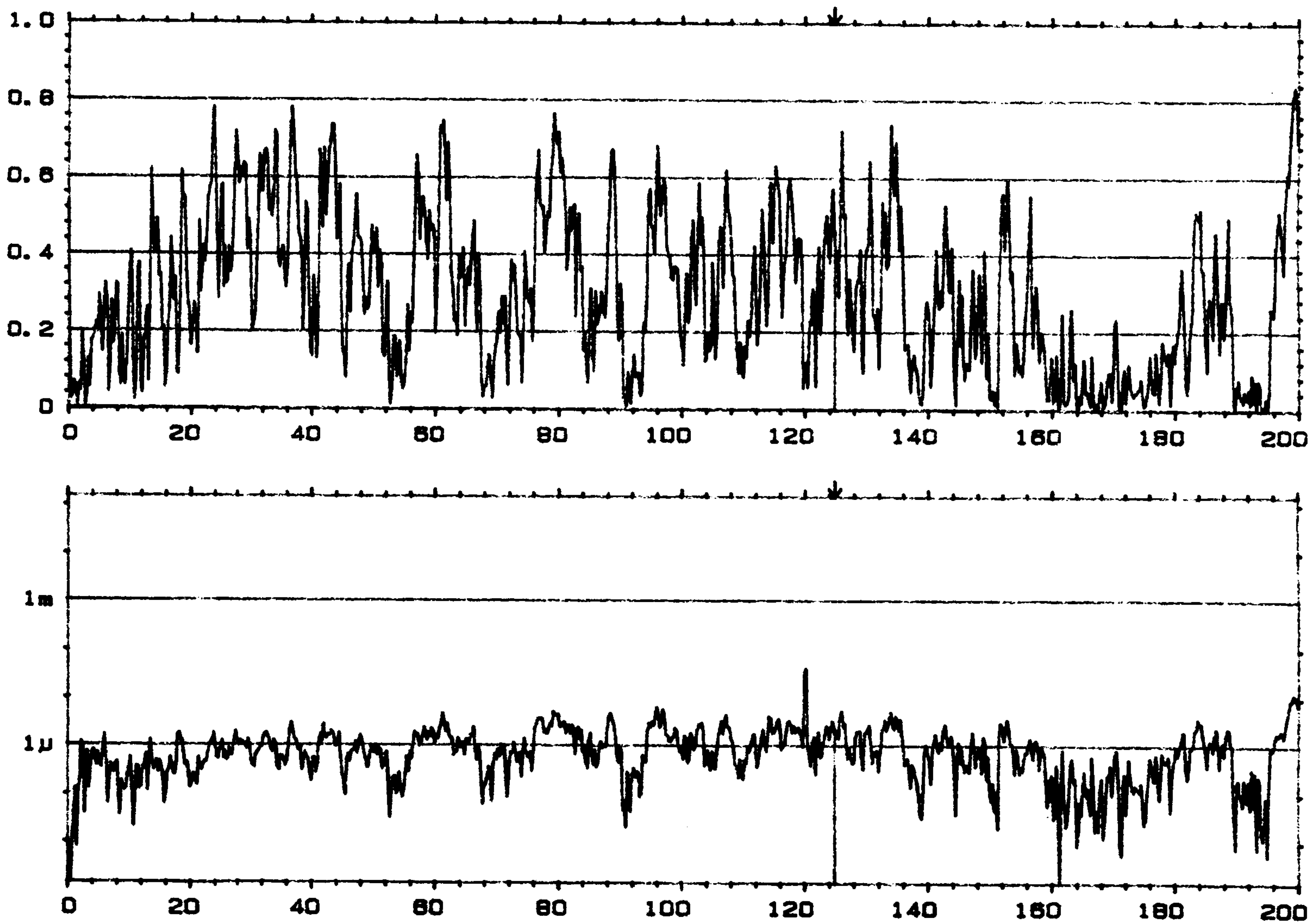

2 COHERENT POWER MAIN Y: 2.29μU²
Y: 150mU² PWR 80dB X: 124.75Hz
X: 0.00Hz + 200Hz LIN
SETUP W22* #A: 256

Type 2032

Page No.
21

Sign.:

Meas.
Object:

PLF PR 1.2
ChA: T10
ChB: M1

Comments:

400 Hz Max

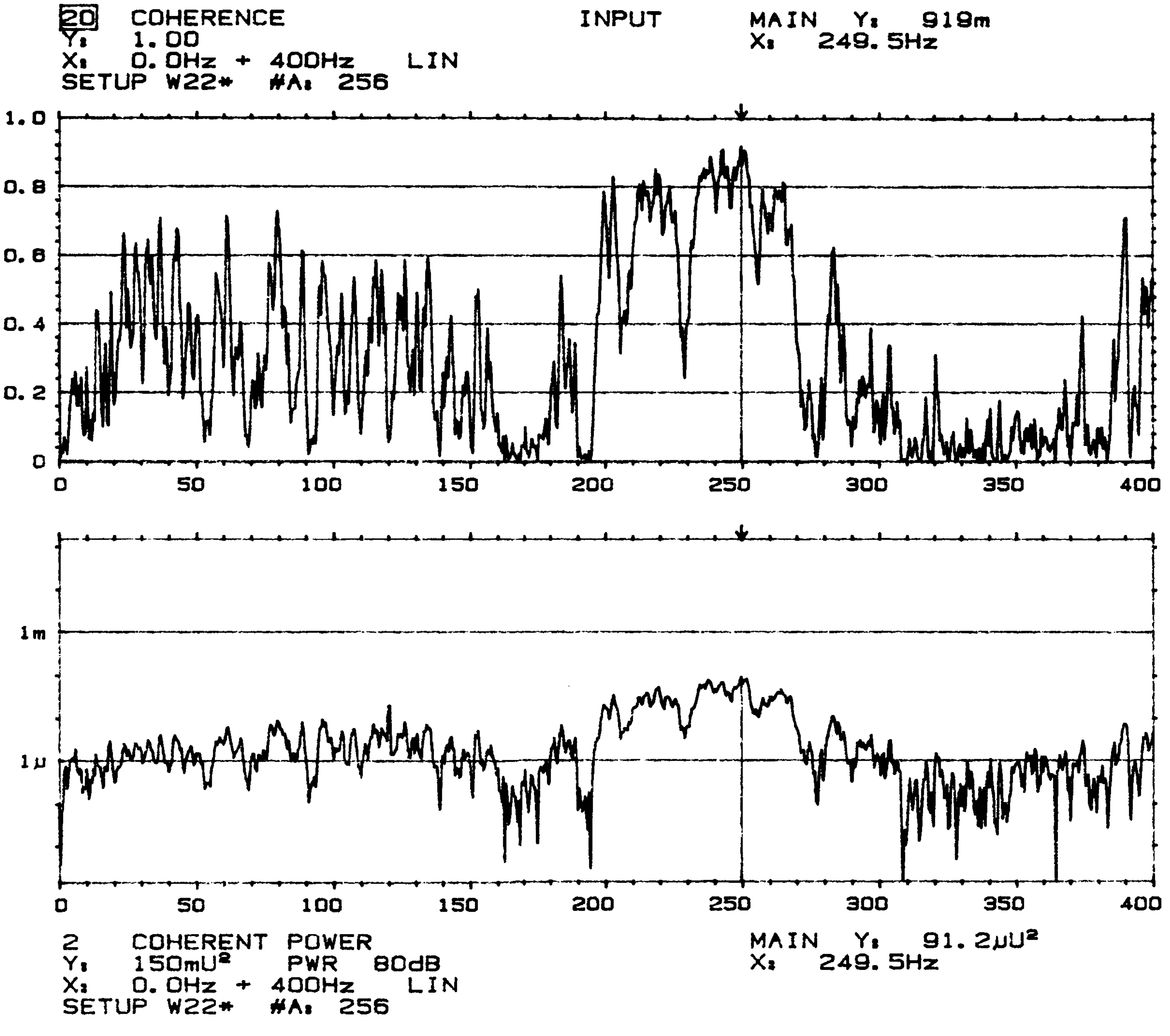

Type 2032

Page No.
9

Sign.:

Meas.
Object:

PLF PR 1.2
ChA = T10
ChB = M1

Rdg 176

Comments:

800 Hz Max

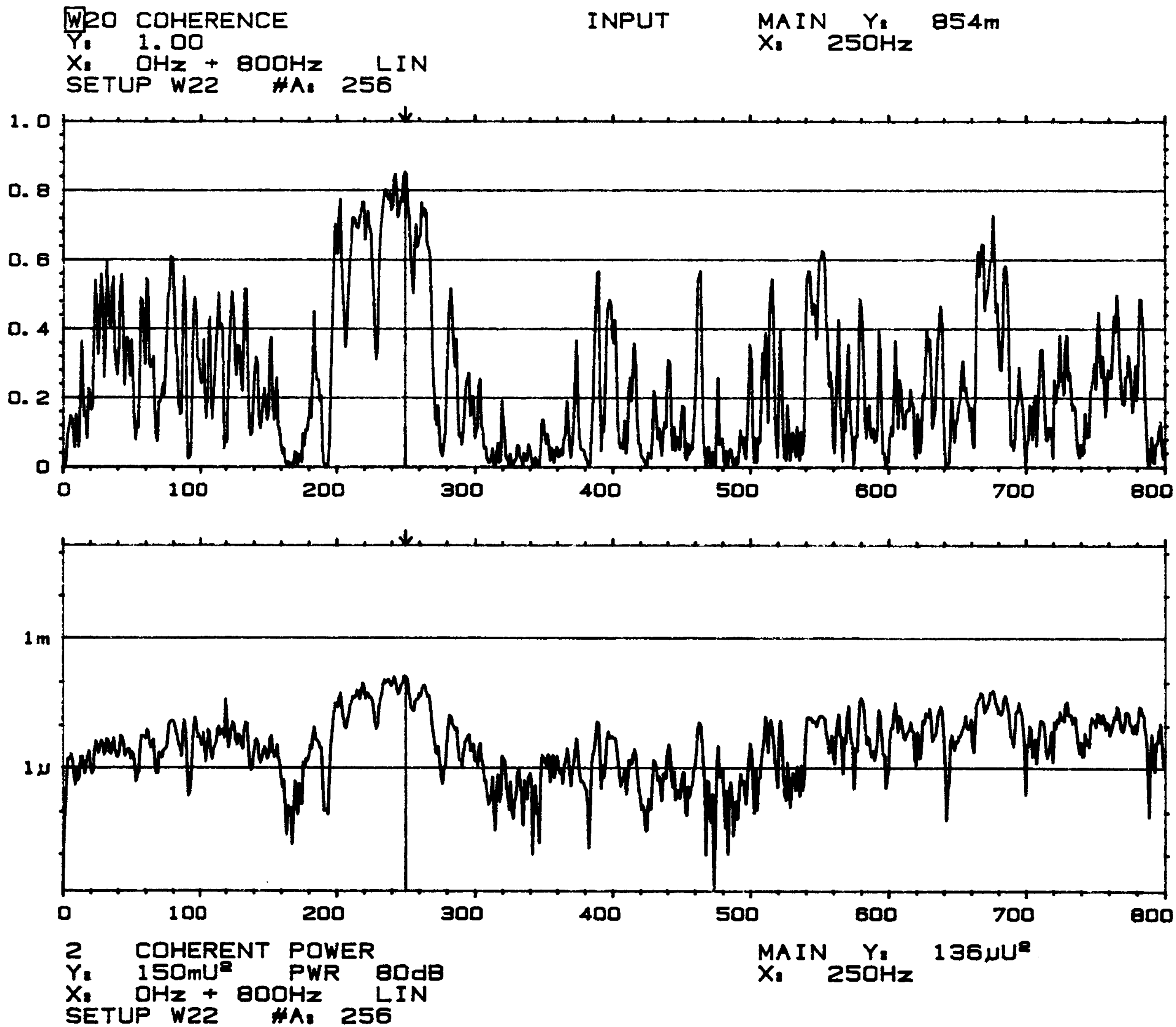

Type 2032

Page No.
33

Sign.:

Meas.
Object:

PLF PR 1.2
ChA = T10
ChB = M2

Rdg 176

Comments:

20 COHERENCE INPUT MAIN Y: 726m
Y: 1.00 X: 250Hz
X: 0Hz + 1.6kHz LIN
SETUP W22 #A: 256

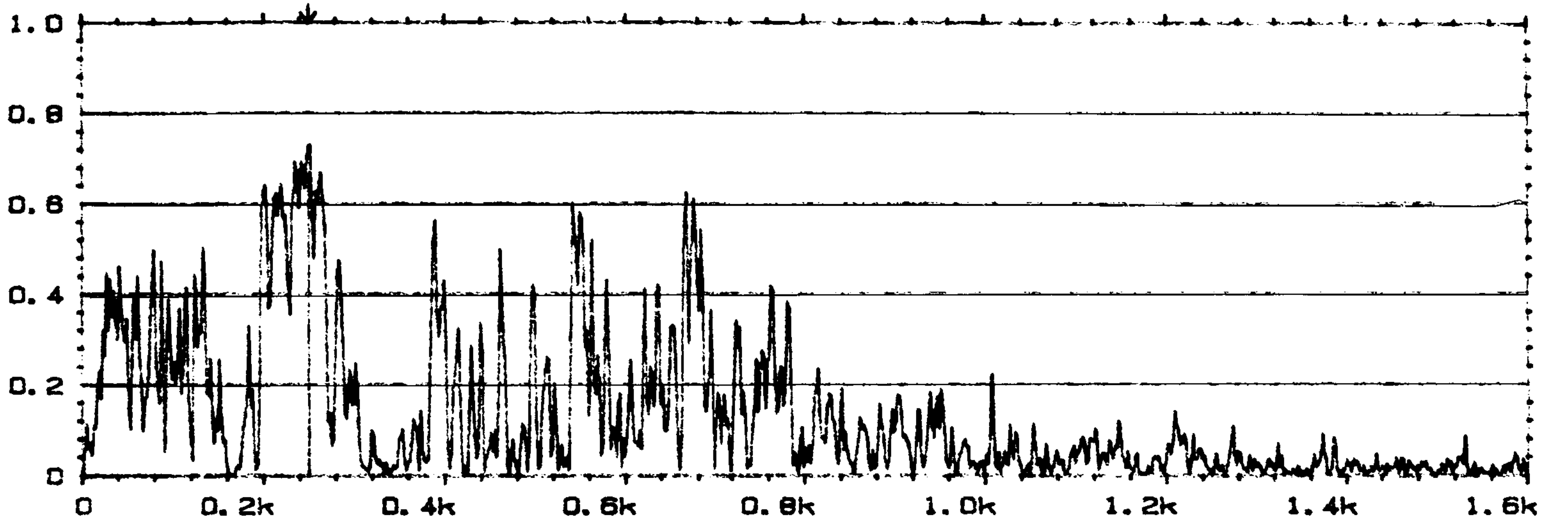

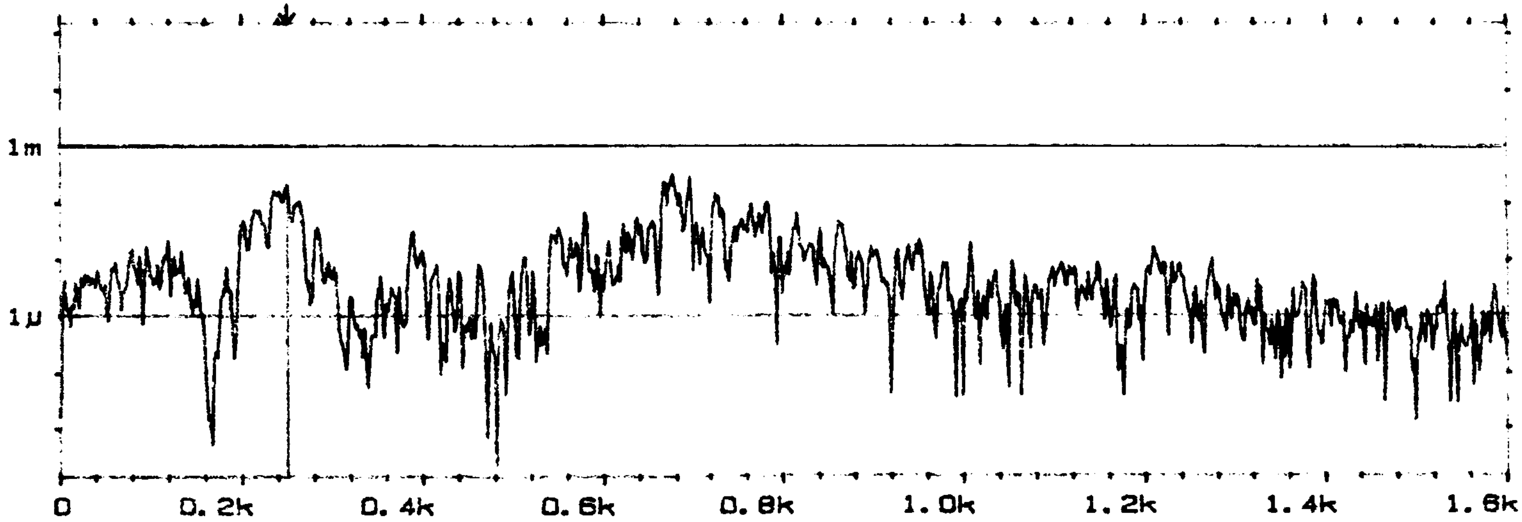

2 COHERENT POWER MAIN Y: 202µU²
Y: 150mU² PWR 80dB X: 250Hz
X: 0Hz + 1.6kHz LIN
SETUP W22 #A: 256

Type 2032

Page No.
35

Sign.:

Meas.
Object:

PLF PR 1.2
ChA = T10
ChB = M3

Rdg 176

Comments:

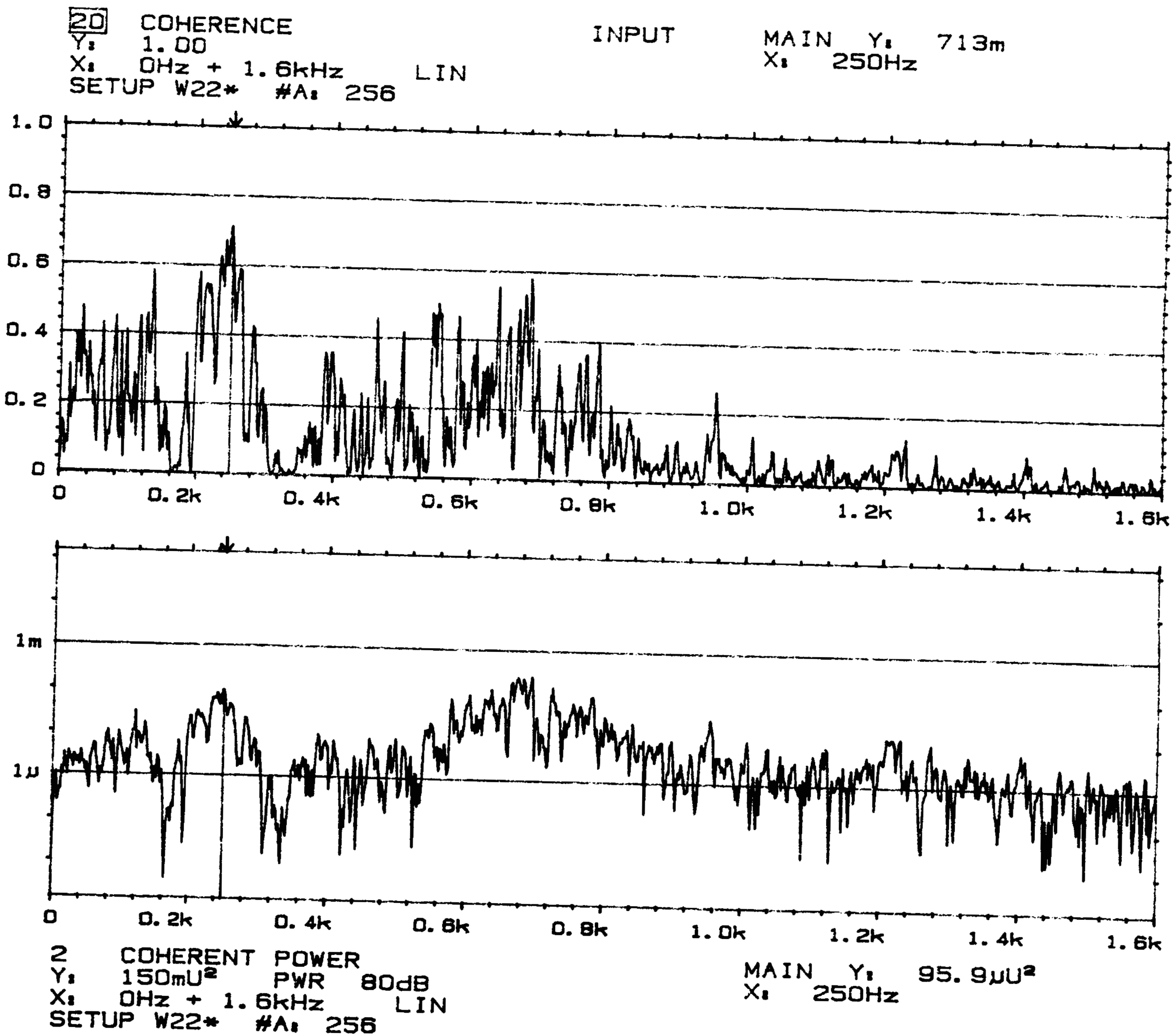

Type 2032

Page No.
24

Sign.:

Meas.
Object:

PLF PR 1.2
ChA = T10
ChB = M4

Rdg 176

Comments:

3.2KHz Max

20 COHERENCE INPUT MAIN Y: 353m
Y: 1.00 X: 516Hz
X: 0Hz + 3.2kHz LIN
SETUP W22 #A: 256

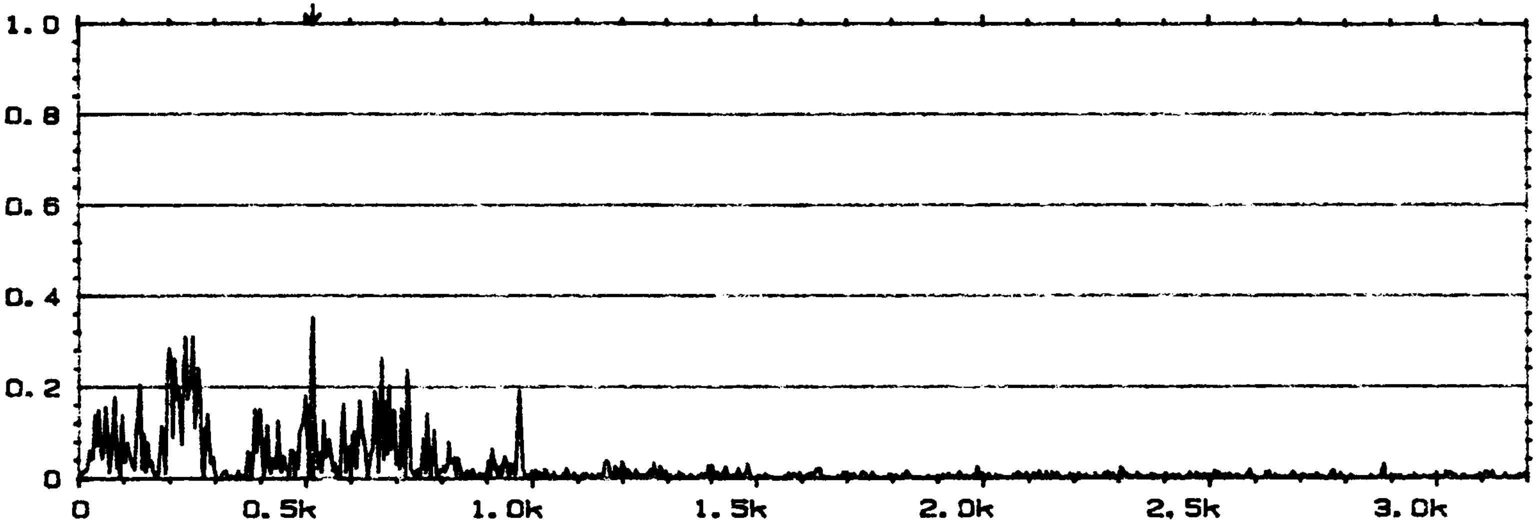

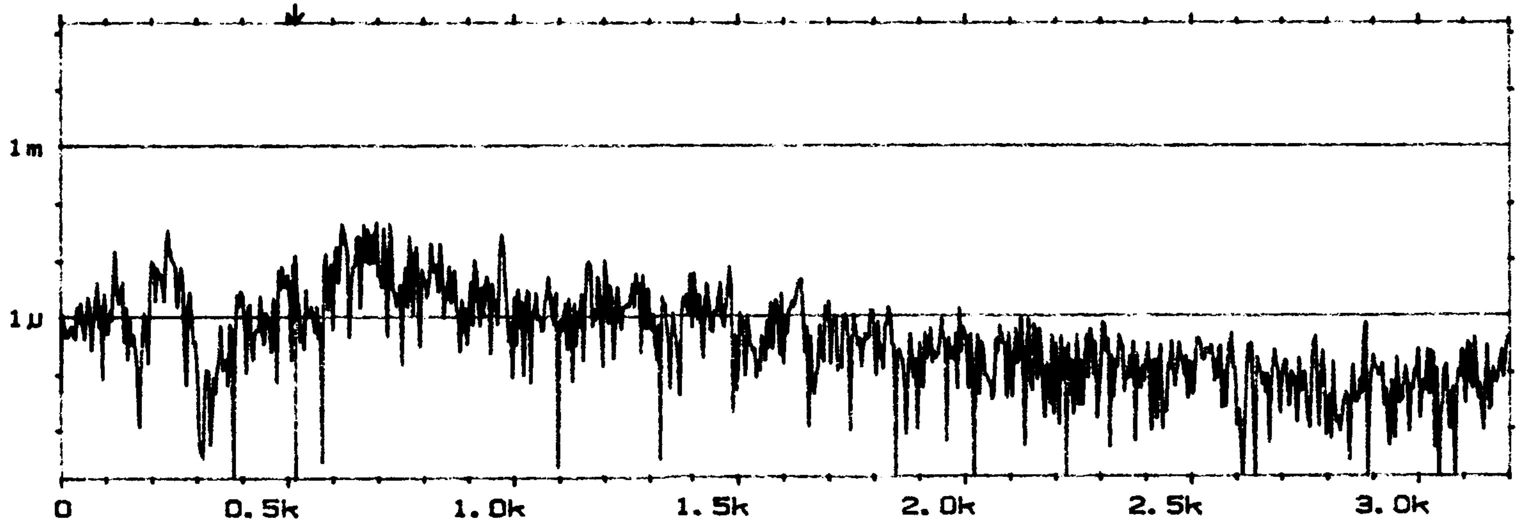

2 COHERENT POWER MAIN Y: 12.1µU²
Y: 150mU² PWR 80dB X: 516Hz
X: 0Hz + 3.2kHz LIN
SETUP W22 #A: 256

Type 2032

Page No.
29

Sign.:

Meas.
Object:

PLF PR 1.2
ChA = T10
ChB = M4

Rdg 176

Comments:

20 COHERENCE INPUT MAIN Y: 54.7m
Y: 1.00 X: 476Hz
X: 0Hz + 1.6kHz LIN
SETUP W22* #A: 256

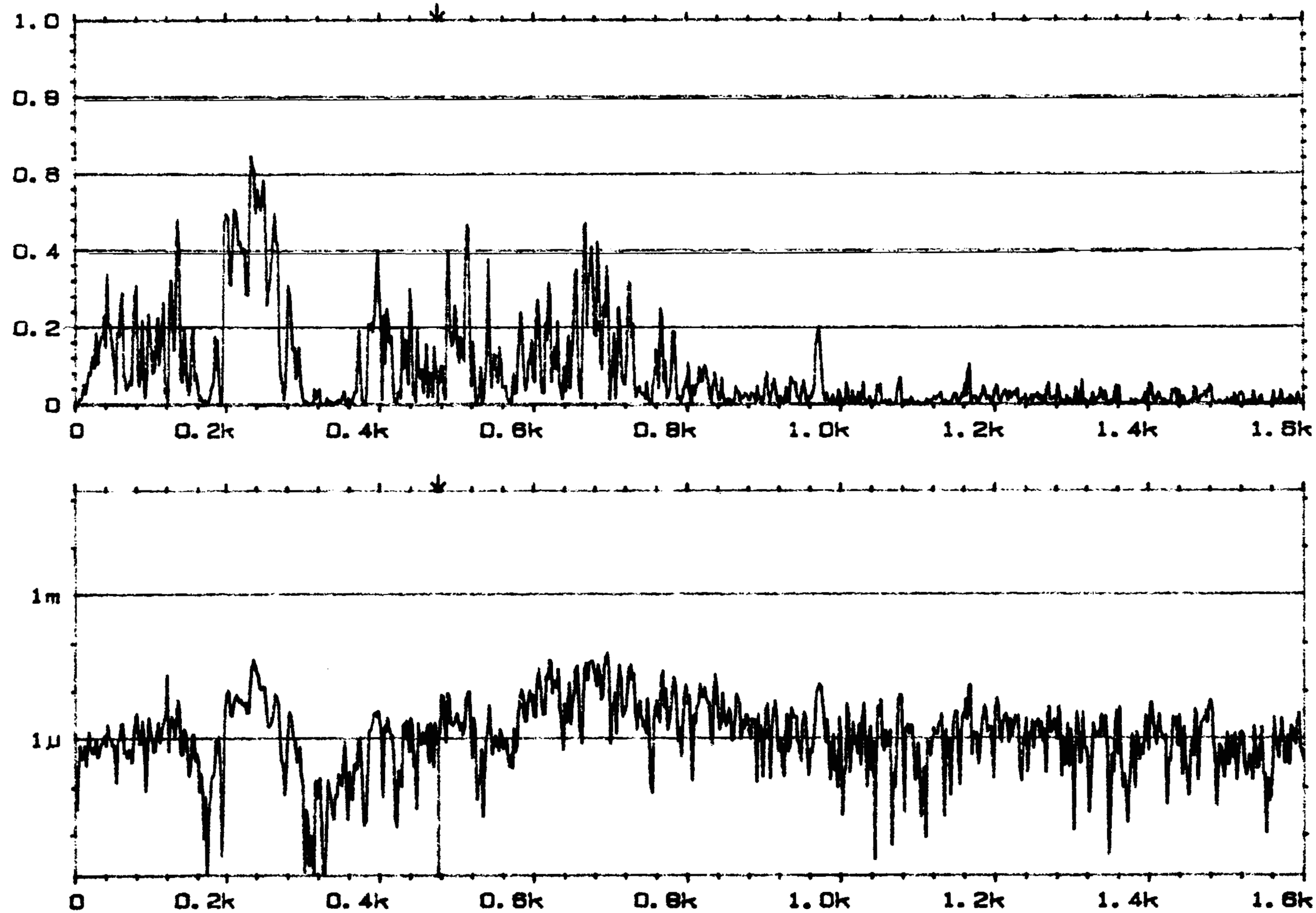

2 COHERENT POWER MAIN Y: 1.14µU²
Y: 150mU² PWR 80dB X: 476Hz
X: 0Hz + 1.6kHz LIN
SETUP W22* #A: 256

Type 2032

Page No.
27

Sign.:

Meas.
Object:

PLF PR 1.2
ChA = T10
ChB = M4

Rdg 176

Comments:

800 Hz Max

20 COHERENCE
Y: 1.00
X: 0Hz + 800Hz LIN
SETUP W22* #A: 256

MAIN Y: 849m
X: 238Hz

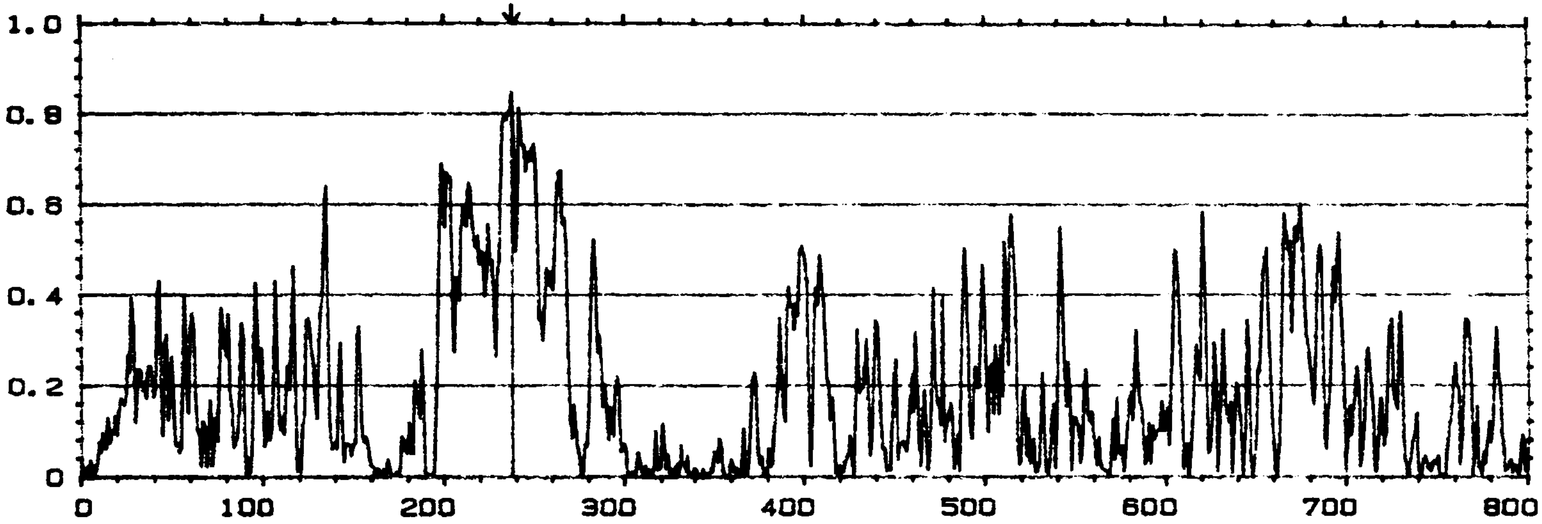

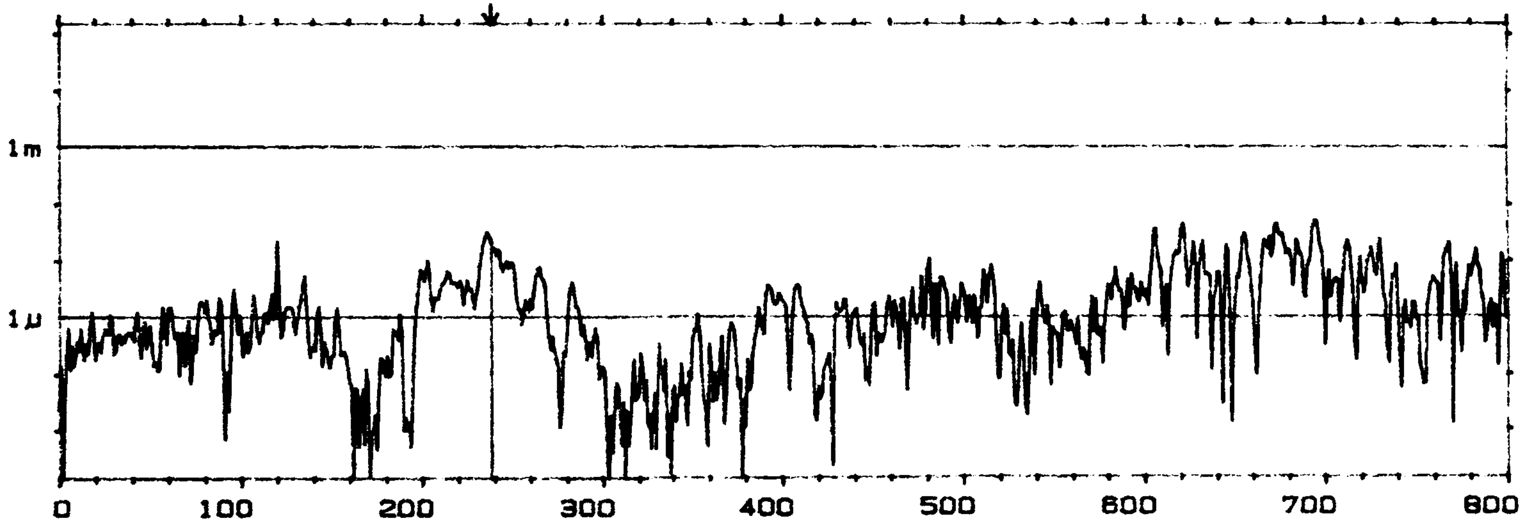

2 COHERENT POWER [ ] INPUT
Y: 150mU² PWR 80dB
X: 0Hz + 800Hz LIN
SETUP W22* #A: 256

MAIN Y: 23.2μU²
X: 238Hz

Type 2032

Page No.
110

Sign.:

Meas.
Object:

PLF PR 1.3
ChA = T10
ChB = M1

Rdg 184

Comments:

2D COHERENCE
Y: 1.00
X: 0Hz + 1.6kHz LIN
SETUP W2 #A: 256

MAIN Y: 7.54m
X: 0Hz

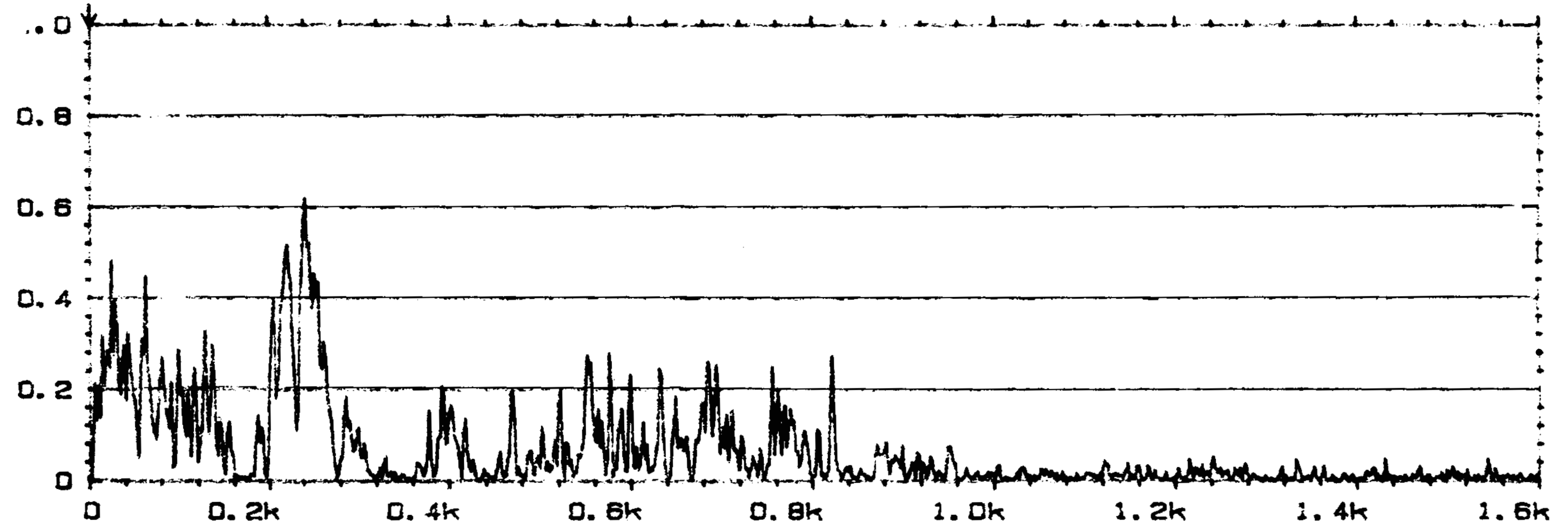

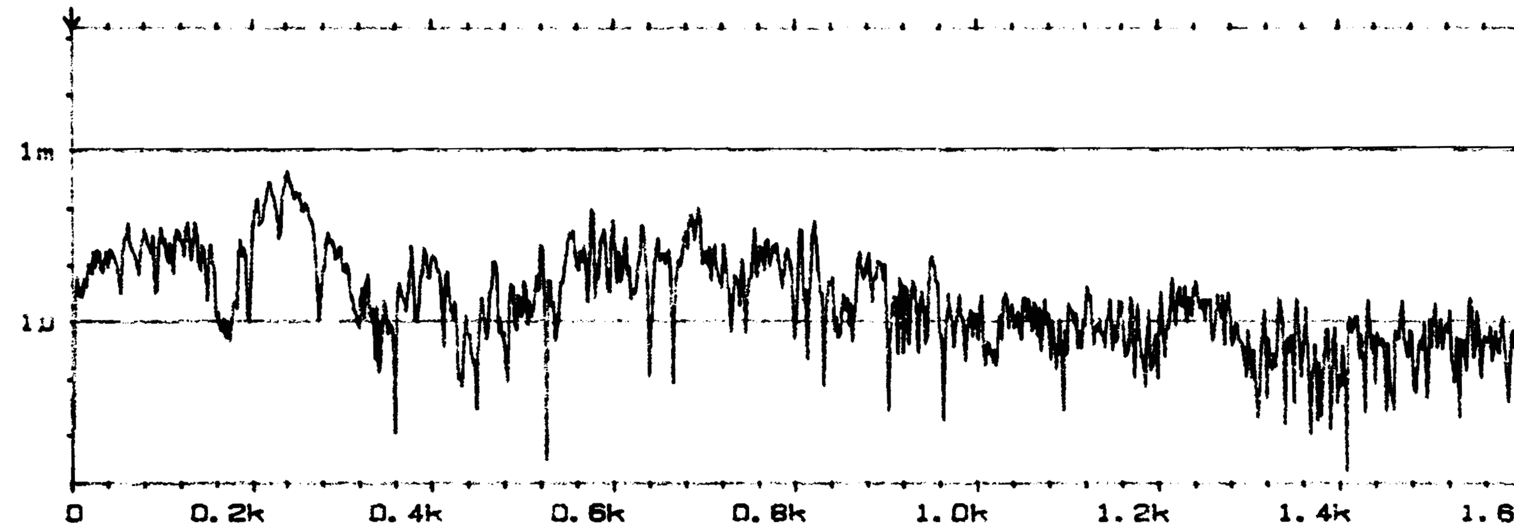

2 COHERENT POWER [ ] INPUT
Y: 150mV² PWR 80dB
X: 0Hz + 1.6kHz LIN
SETUP W2 #A: 256

MAIN Y: 42.8E-9V²
X: 0Hz

Type 2032

Page No.
112

Sign.:

Meas.
Object:
PLF PR 1.3
ChA=716
ChB=M2

Rdg 189

Comments:

20 COHERENCE
Y: 1.00
X: 0Hz + 1.6kHz LIN
SETUP W2 #A: 256

MAIN Y: 25.6m
X: 0Hz

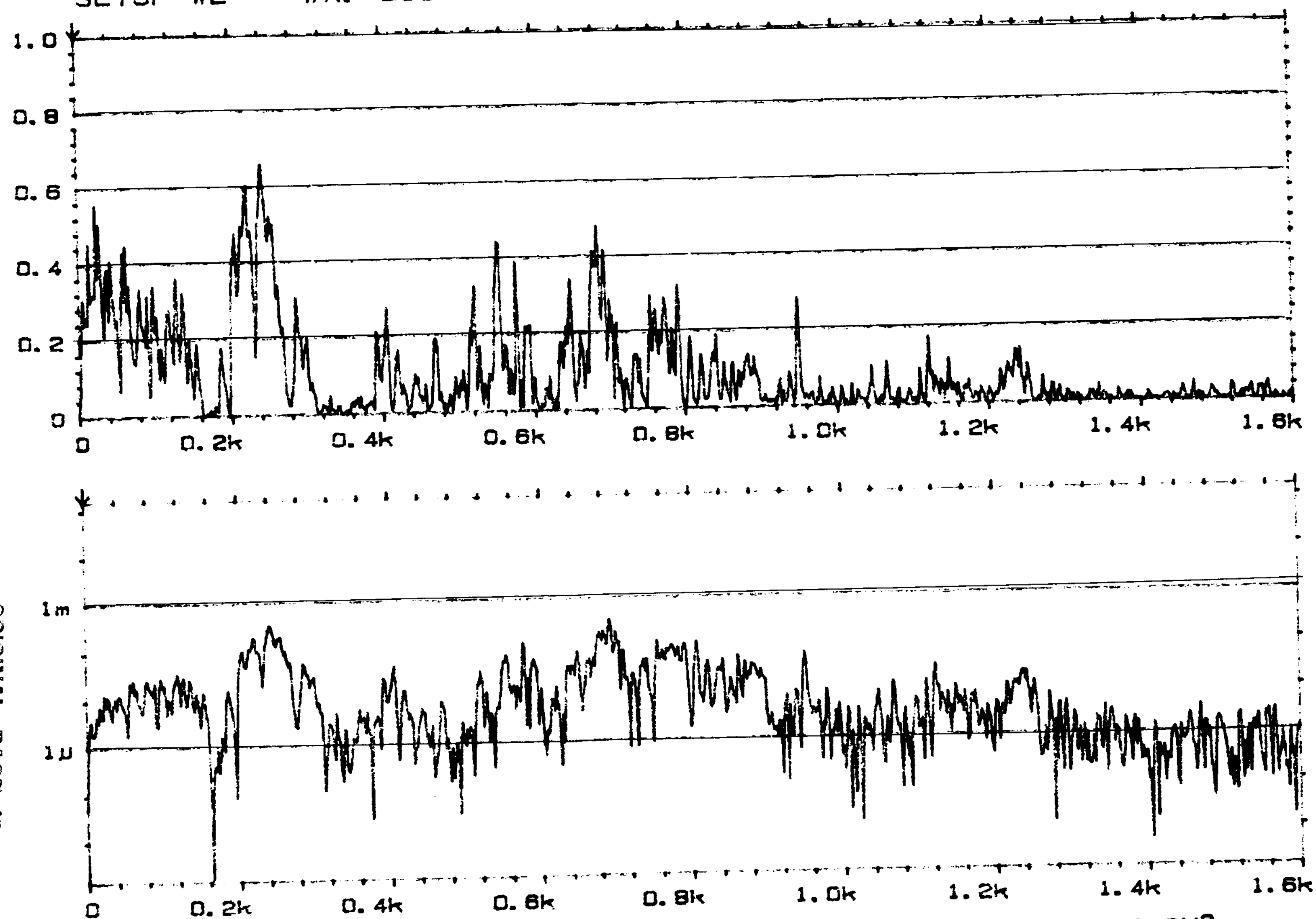

2 COHERENT POWER [ ] INPUT
Y: 150mV² PWR 80dB
X: 0Hz + 1.6kHz LIN
SETUP W2 #A: 256

MAIN Y: 57.5E-9V²
X: 0Hz

Type 2032

Page No.
114

Sign.:

Meas.
Object:

PLF PR 1.3
ChA = T10
ChB = M3

Rdg 184

Comments:

2D COHERENCE
Y: 1.00
X: 0Hz + 1.6kHz LIN
SETUP W2 #A: 256

MAIN Y: 19.2m
X: 0Hz

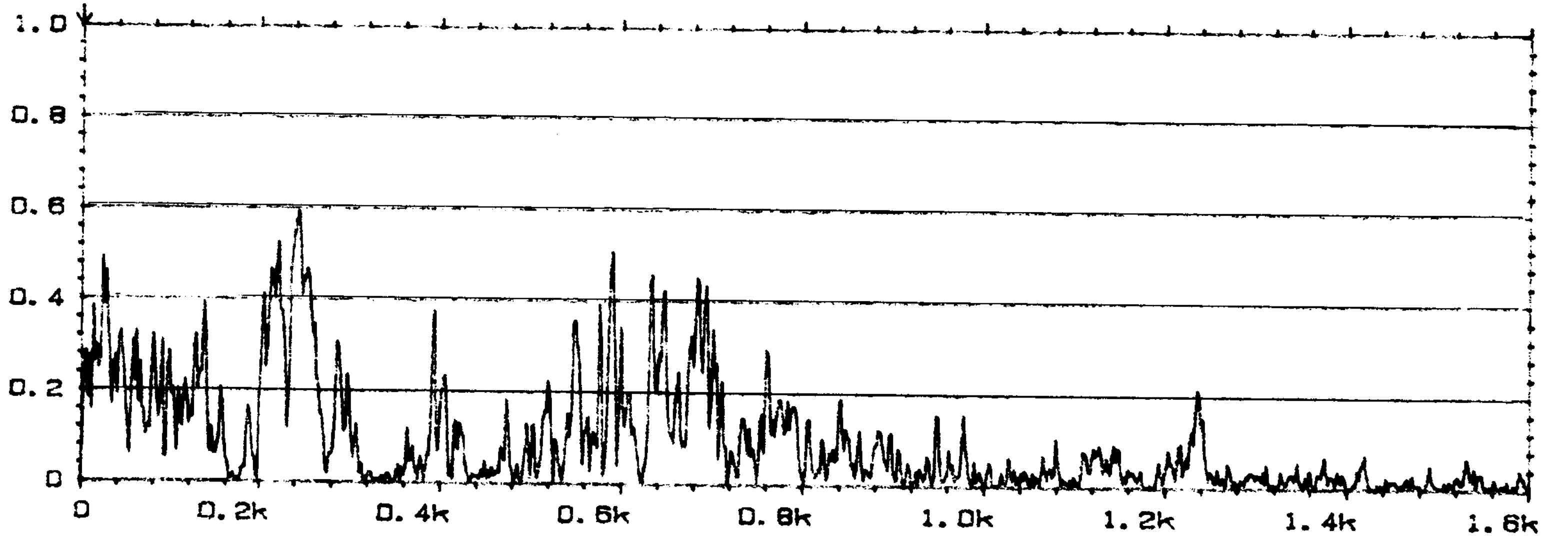

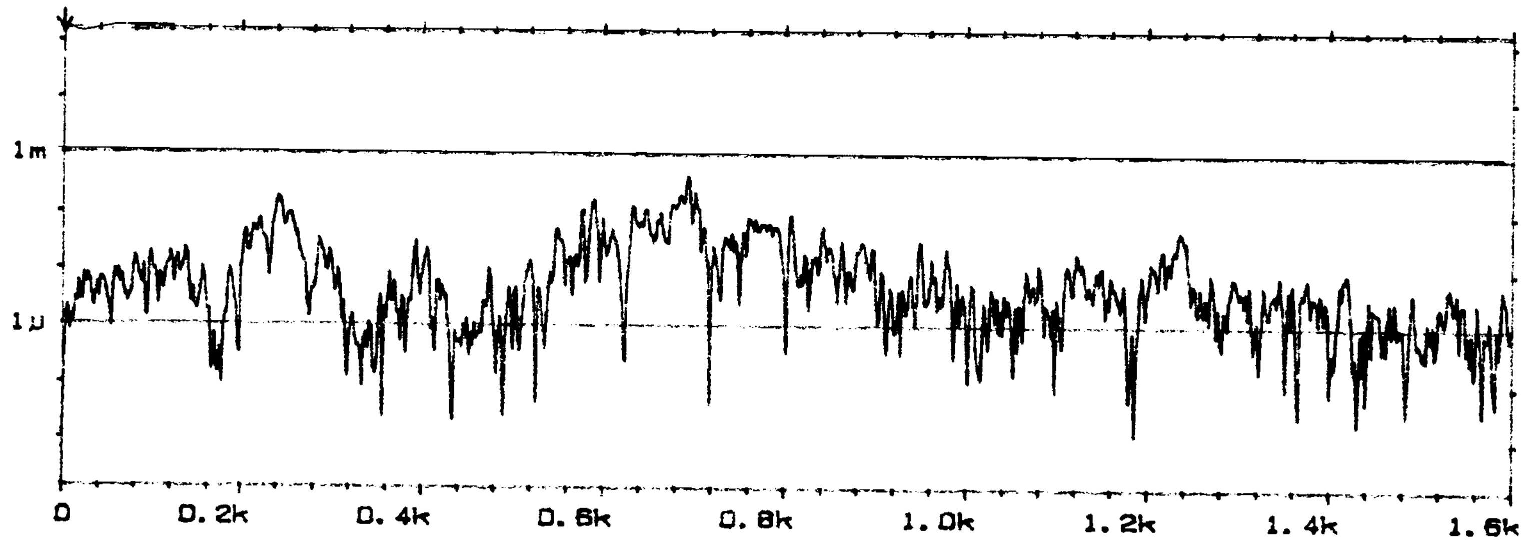

2 COHERENT POWER [ ] INPUT
Y: 150mV² PWR 80dB
X: 0Hz + 1.6kHz LIN
SETUP W2 #A: 256

MAIN Y: 13.0E-9V²
X: 0Hz

Type 2032

Page No.
116

Sign.:

Meas.
Object:

PLF PR1.3
ChA= T10
ChB= M4

Rdg 184

Comments:

2D COHERENCE
Y: 1.00
X: 0Hz + 1.6kHz LIN
SETUP W2 #A: 256

MAIN Y: 2.64m
X: 0Hz

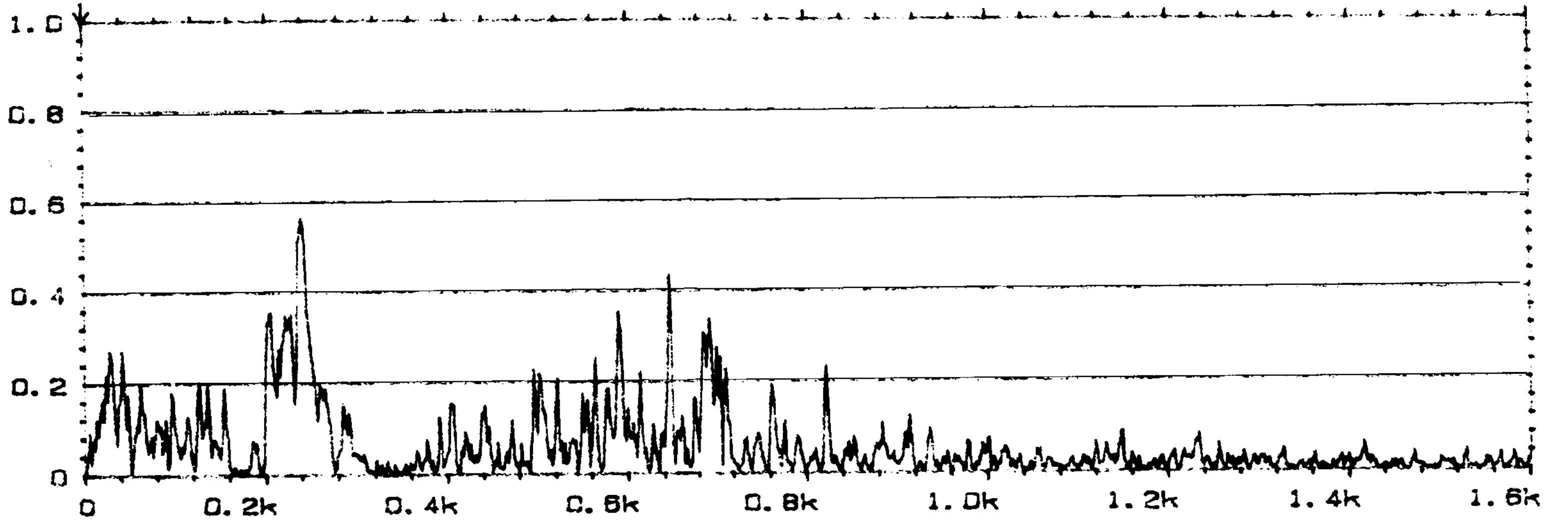

ORIGINAL PAGE IS OF POOR QUALITY

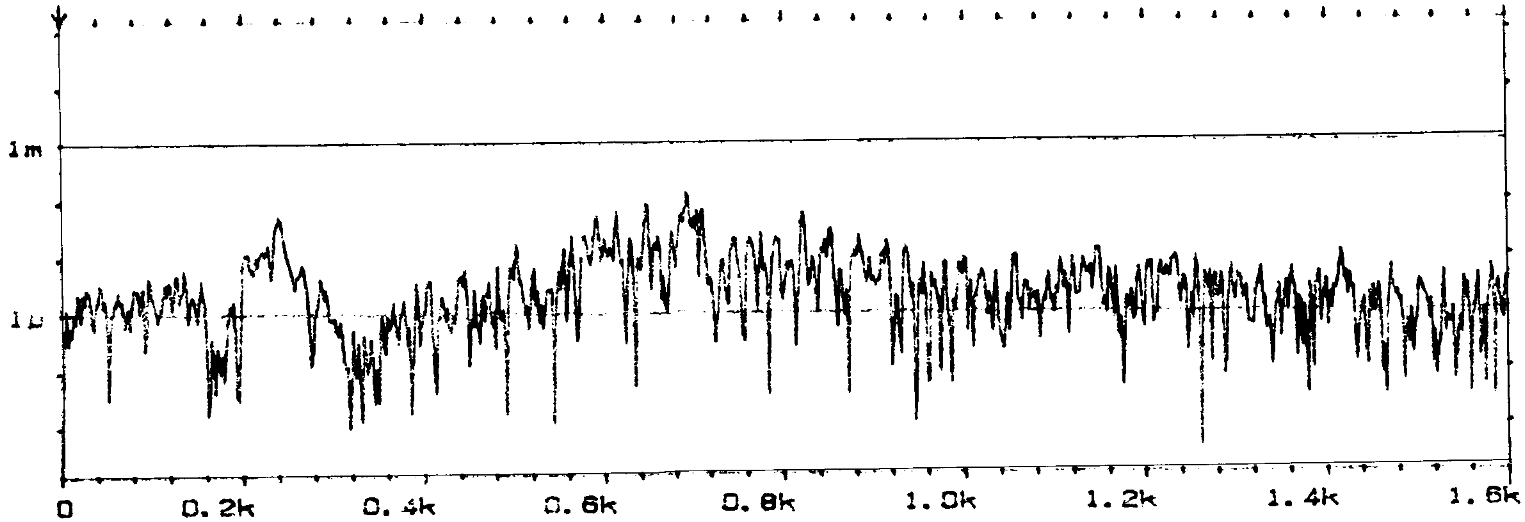

2 COHERENT POWER [ ] INPUT
Y: 150mV² PWR 80dB
X: 0Hz + 1.6kHz LIN
SETUP W2 #A: 256

MAIN Y: 3.17E-9V²
X: 0Hz

Type 2032

Page No.
46

Sign.:

Meas.
Object:

PLF PR 1.4
ChA = T 10
ChB = M 1

Rdg 177

Comments:

20 COHERENCE INPUT MAIN Y: 65.5m
Y: 1.00 X: 684Hz
X: 0Hz + 1.6kHz LIN
SETUP W22 #A: 256

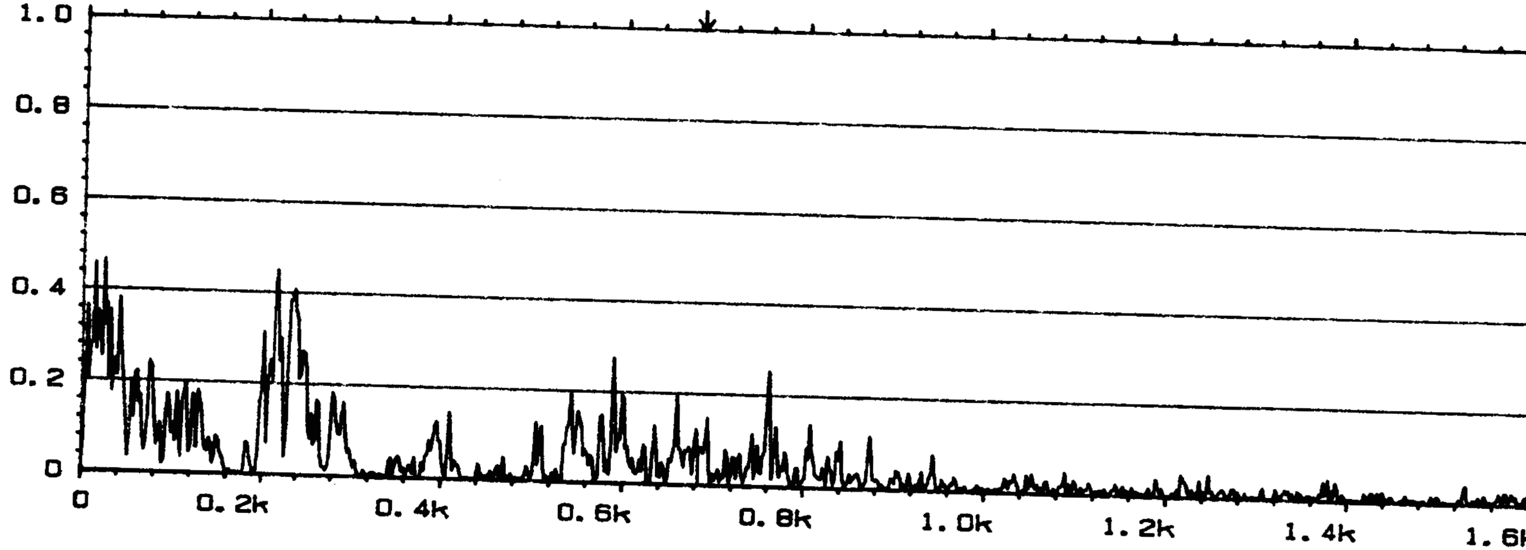

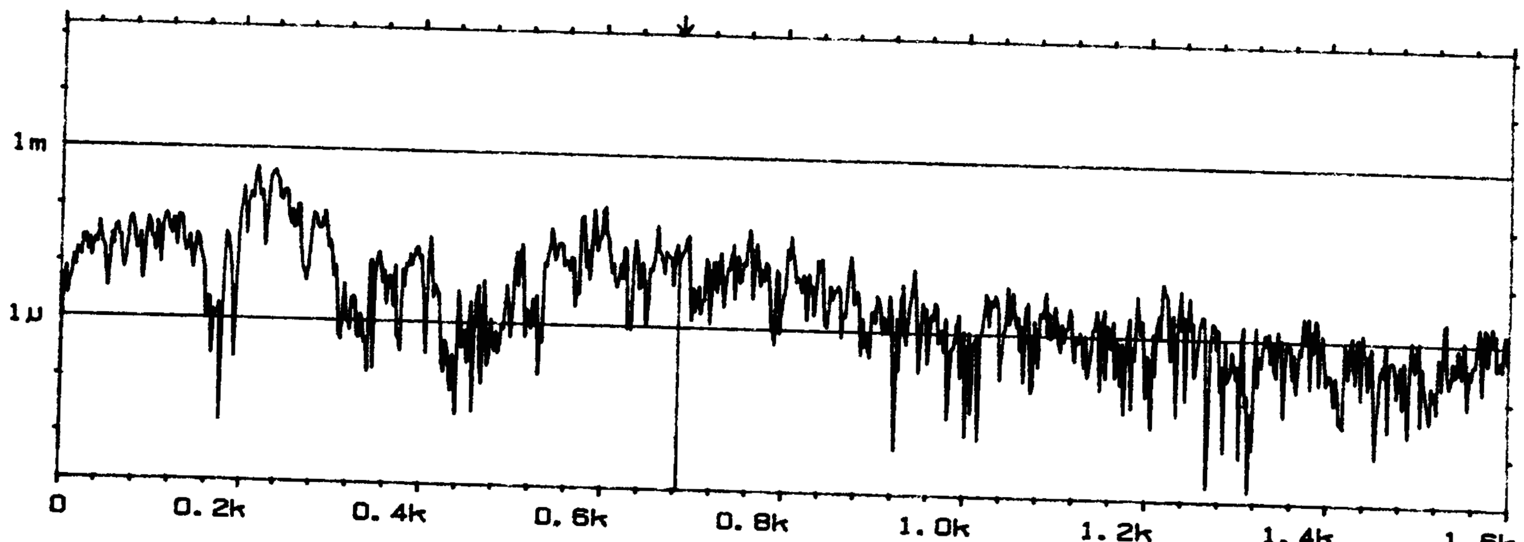

2 COHERENT POWER MAIN Y: 13.9µU²
Y: 150mU² PWR 80dB X: 684Hz
X: 0Hz + 1.6kHz LIN
SETUP W22 #A: 256

Type 2032

Page No.
50

Sign.:

Meas.
Object:

PLF PR 1.4

ChA: 110

ChB: M3

Pdg 177

Comments:

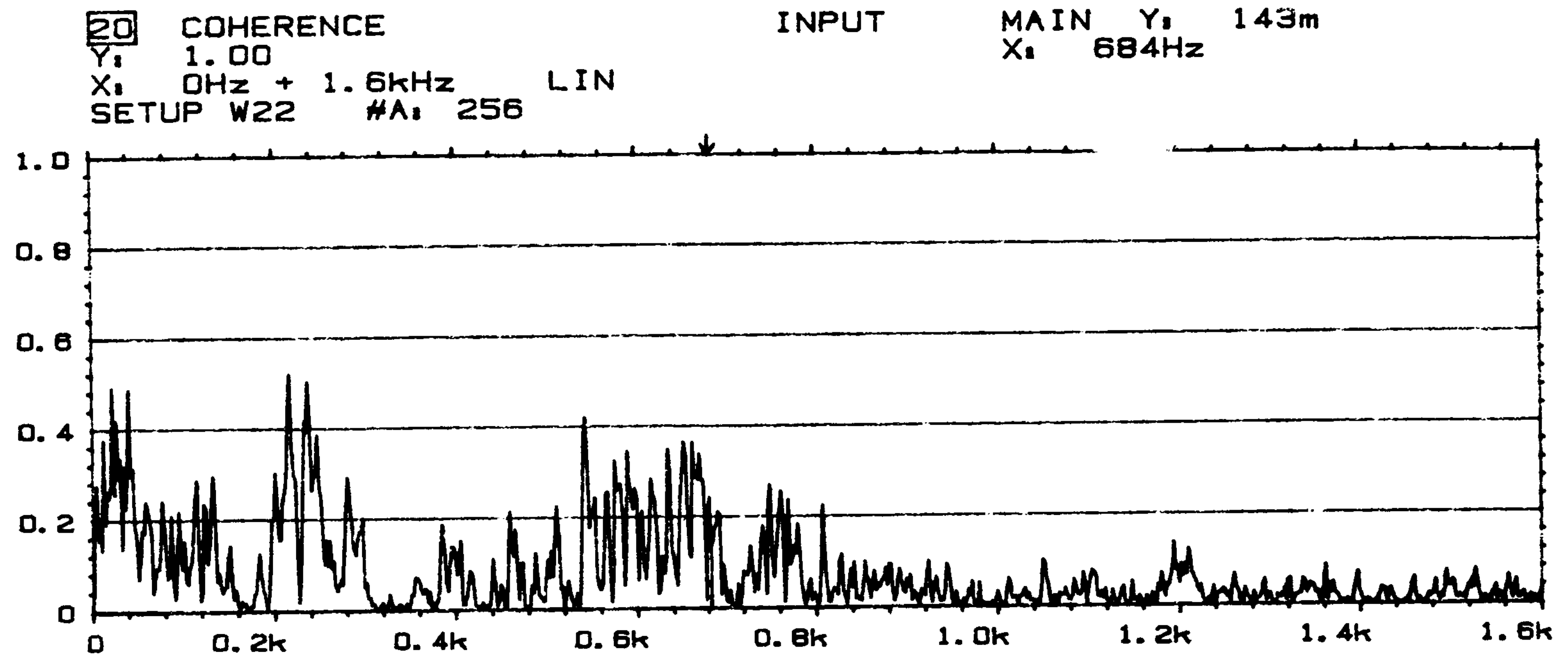

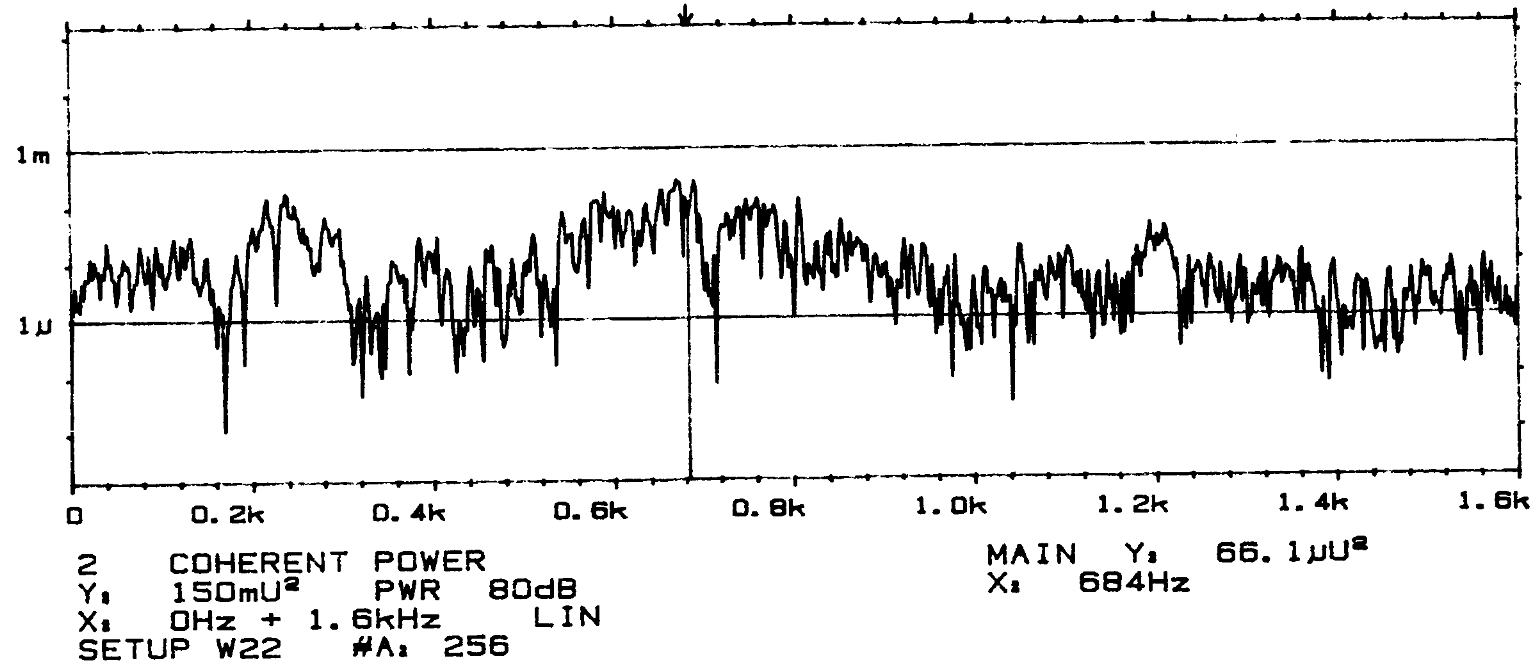

ORIGINAL PAGE IS OF POOR QUALITY

Type 2032

Page No.
52

Sign.:

Meas.
Object:
PLF PP 1.4
ChA = T10
ChB = M4

Rdg 177

Comments:

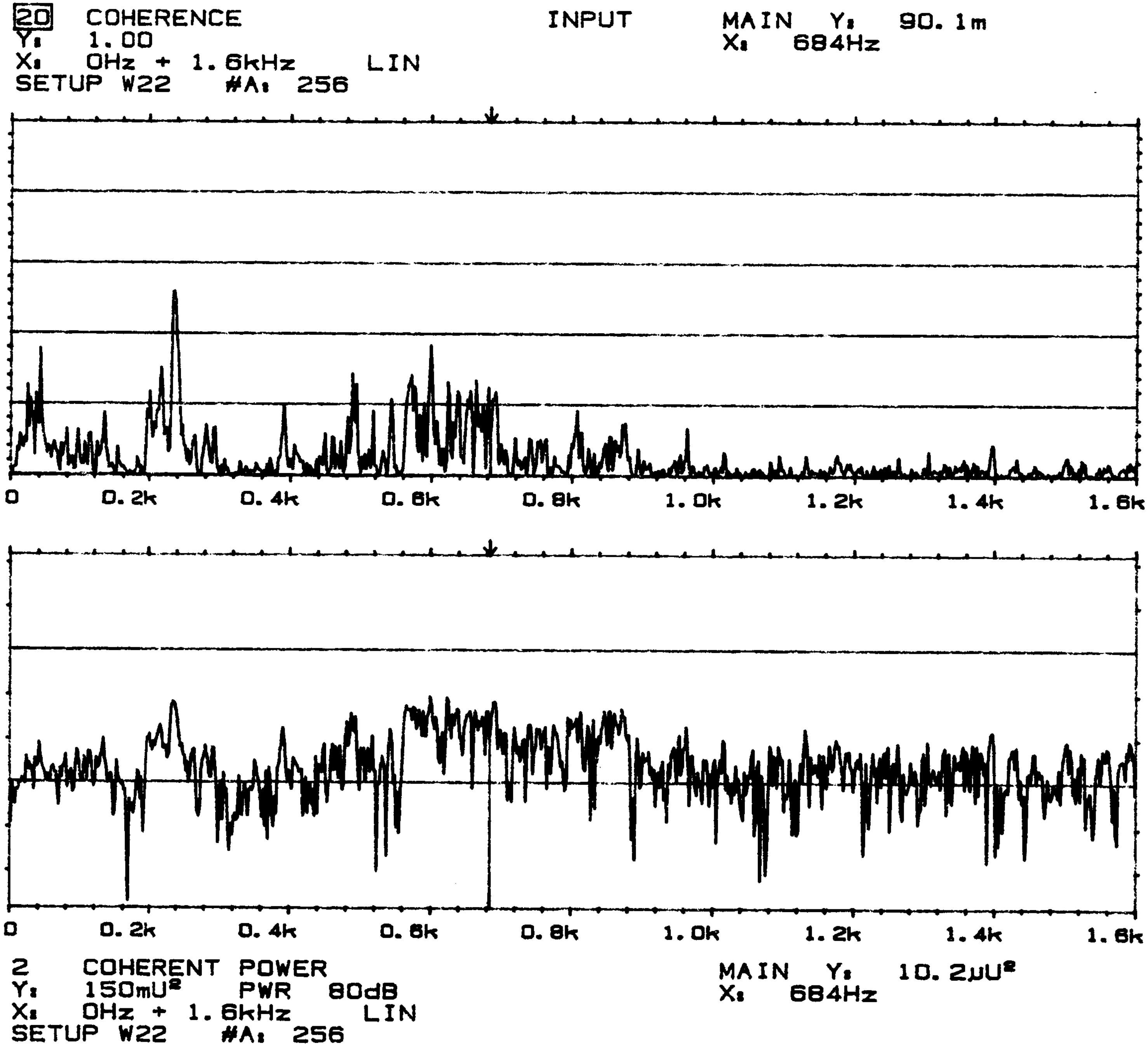

Type 2032

Page No.
37

Sign.:

Meas.
Object:

DLF PR 1.6

ChA = T10

ChB = M1

Rdg 178

Comments:

20 COHERENCE INPUT MAIN Y: 21.2m
Y: 1.00 X: 684Hz
X: 0Hz + 1.6kHz LIN
SETUP W22* #A: 256

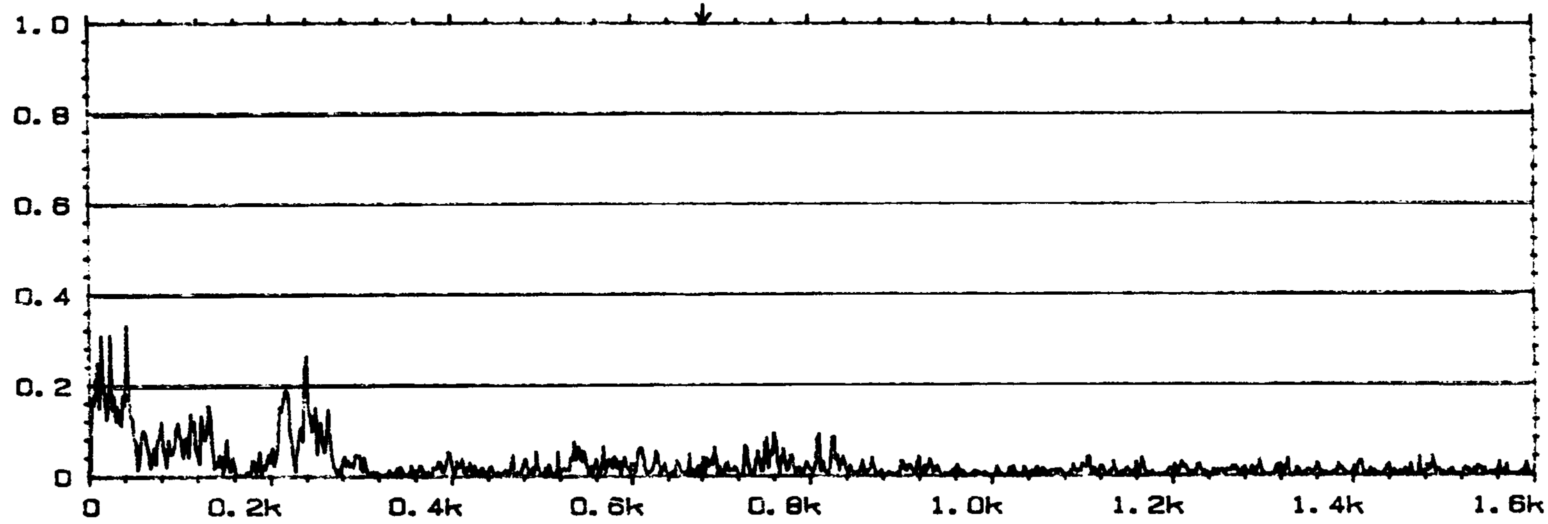

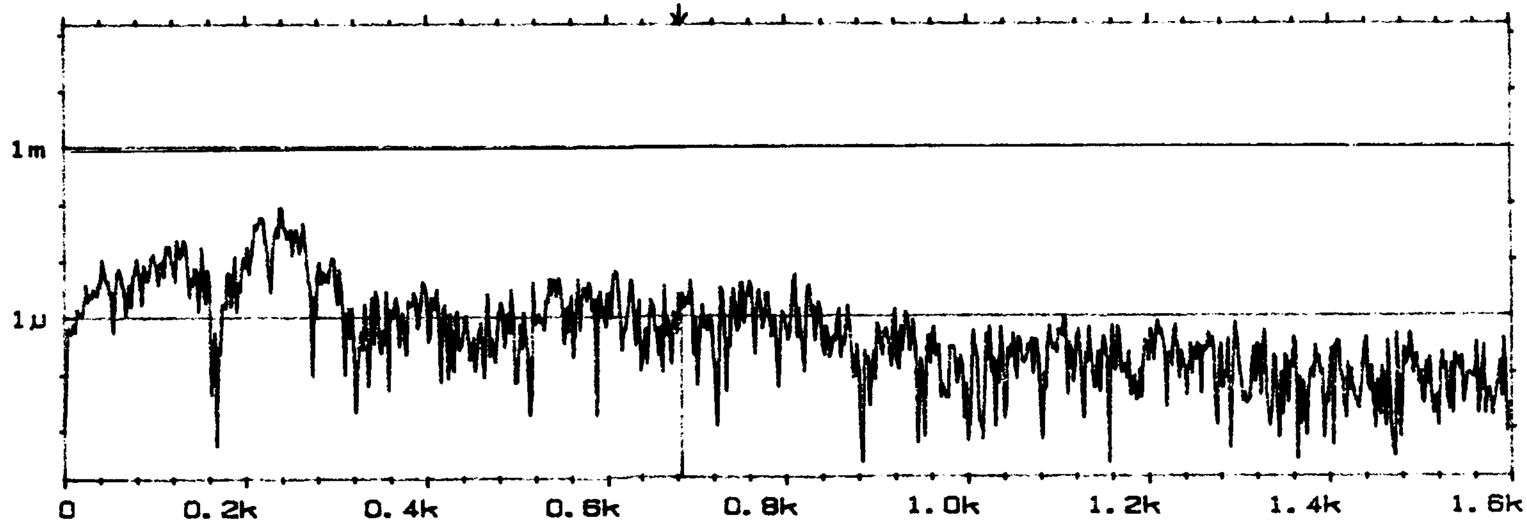

2 COHERENT POWER MAIN Y: 1.46μU²
Y: 150mU² PWR 80dB X: 684Hz
X: 0Hz + 1.6kHz LIN
SETUP W22* #A: 256

Type 2032

Page No.
43

Sign. :

Meas.
Object:

PLF PR1.6
ChA = T10
ChB = M2

Rdg17B

Comments:

20 COHERENCE
Y: 1.00
X: 0Hz + 1.6kHz LIN
SETUP W22 #A: 256

INPUT

MAIN Y: 15.7m
X: 684Hz

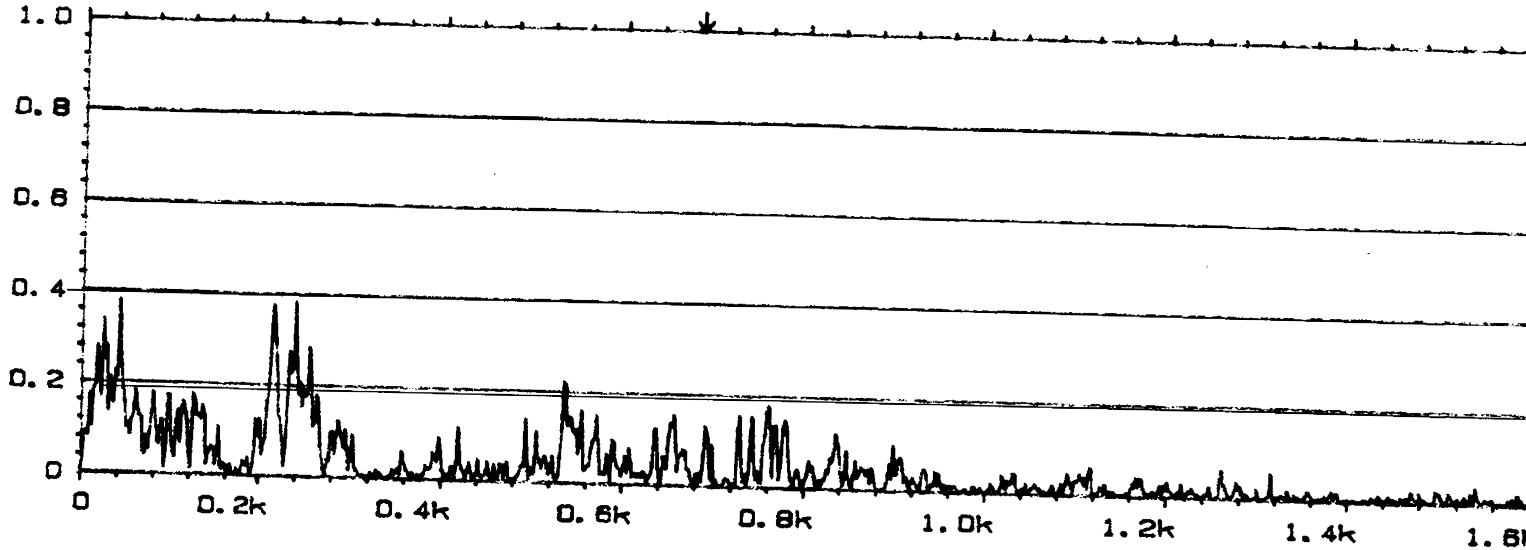

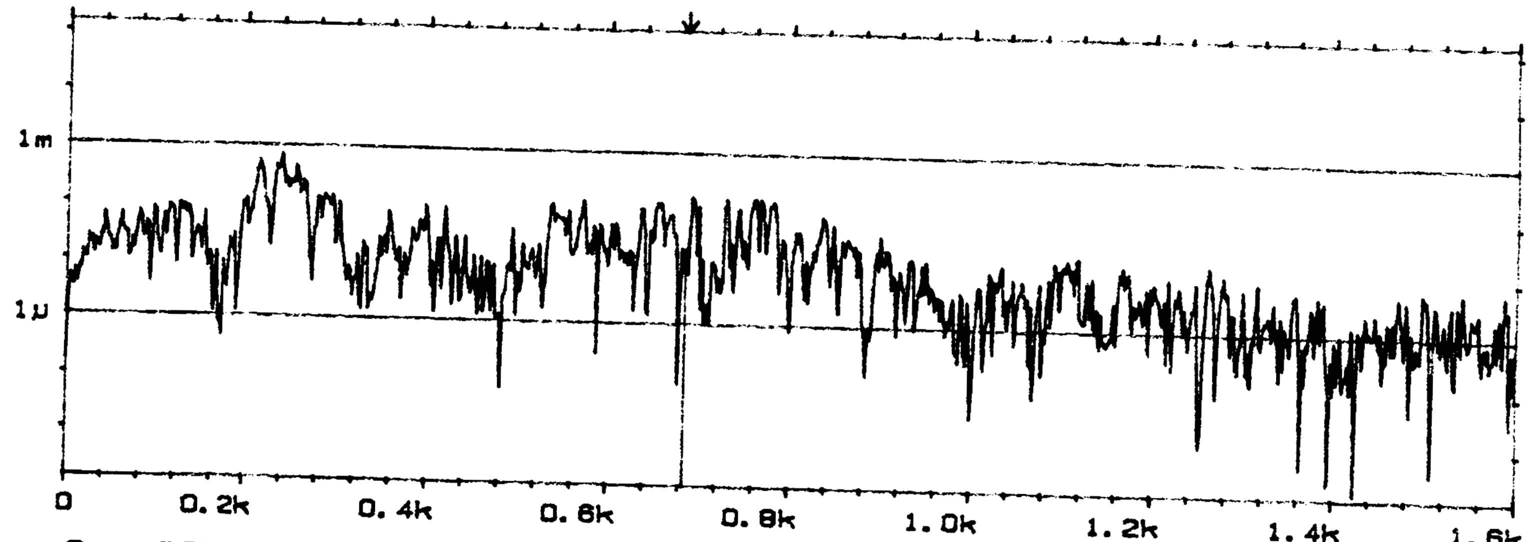

2 COHERENT POWER
Y: 150mU² PWR 80dB
X: 0Hz + 1.6kHz LIN
SETUP W22 #A: 256

MAIN Y: 11.8µU²
X: 684Hz

20 COHERENCE INPUT MAIN Y: 98.0m
Y: 1.00 X: 684Hz
X: 0Hz + 1.6kHz LIN
SETUP W22 #A: 256

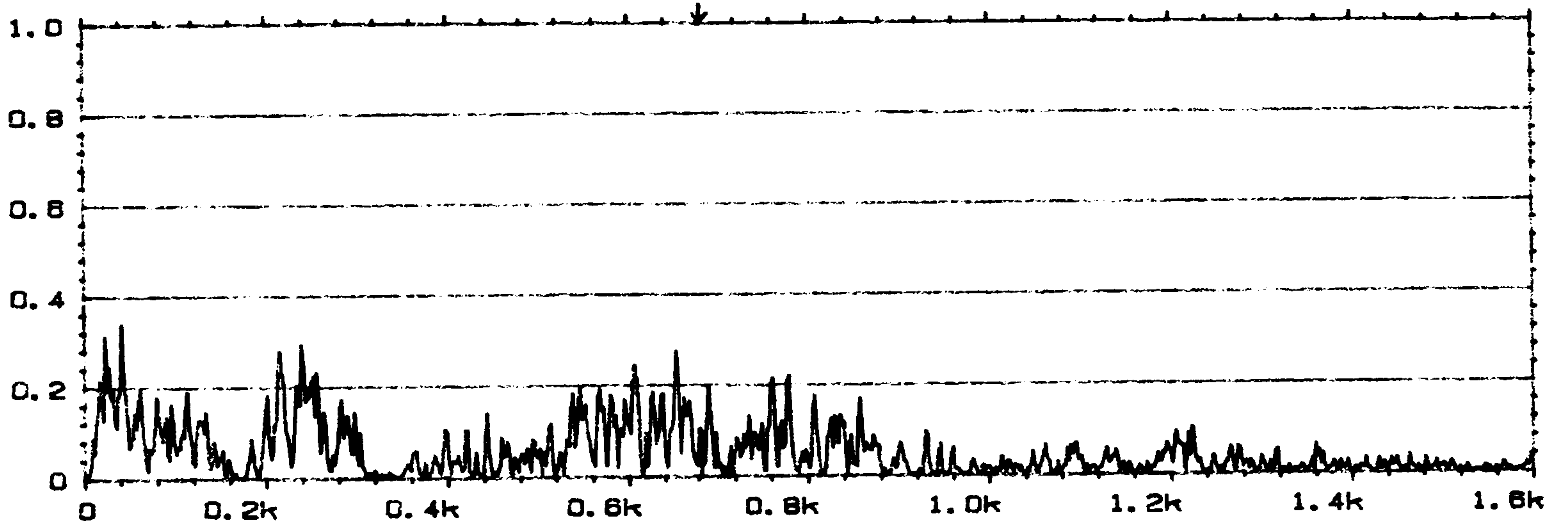

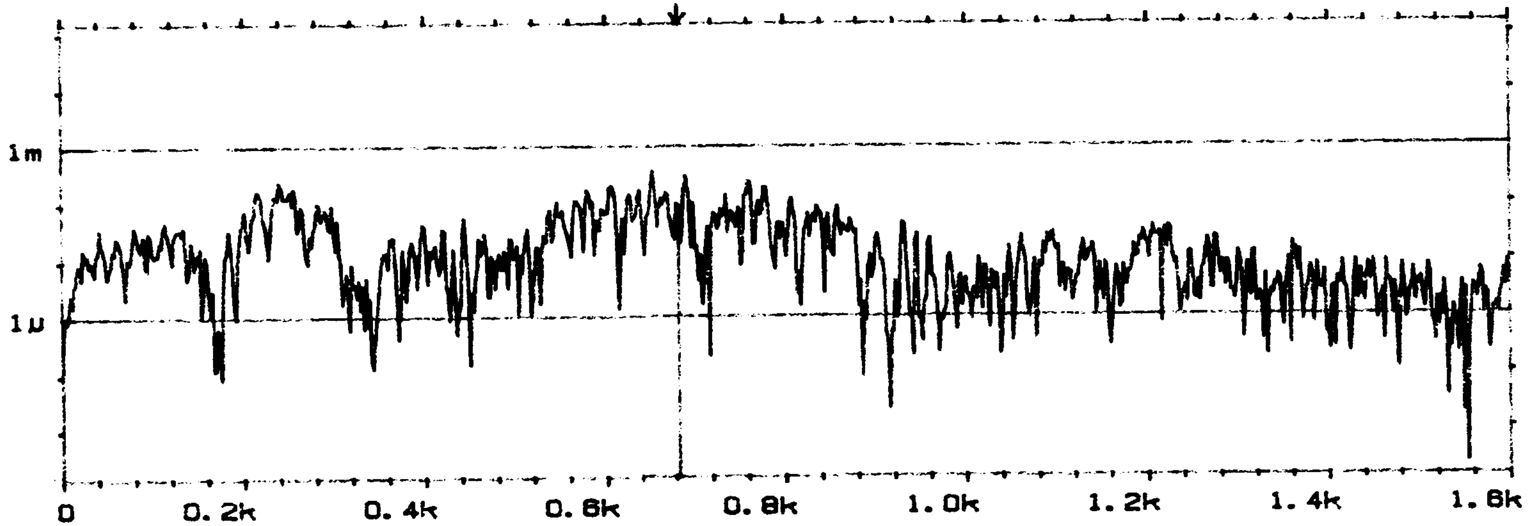

2 COHERENT POWER MAIN Y: 90.8μU²
Y: 150mU² PWR 80dB X: 684Hz
X: 0Hz + 1.6kHz LIN
SETUP W22 #A: 256

Type 2032

Page No.
41

Sign.:

Meas.
Object:

PLF PR 1.6
ChA=T10
ChB=M3

Pdg 178

Comments:

ORIGINAL PAGE IS
OF POOR QUALITY

Type 2032

Page No.
39

Sign.:

Meas.
Object:
PLF PR 1.6
ChA=T10
ChB=M4

Rdg 178

Comments:

20 COHERENCE INPUT MAIN Y: 4.37m
Y: 1.00 X: 684Hz
X: 0Hz + 1.6kHz LIN
SETUP W22 #A: 256

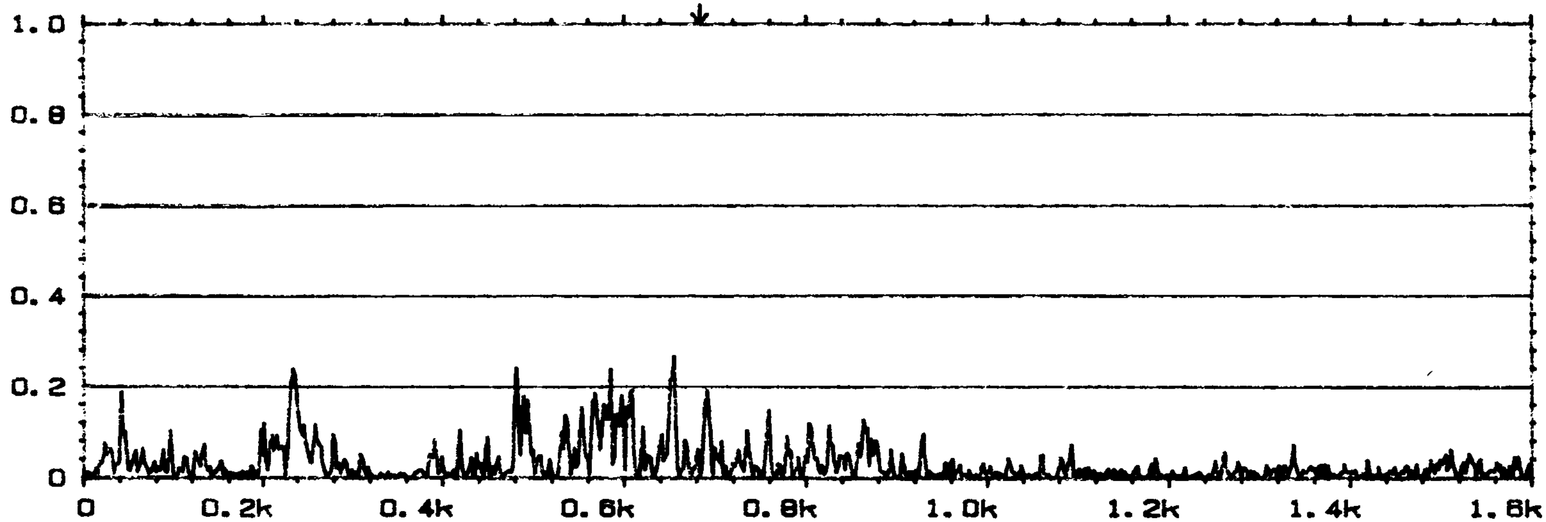

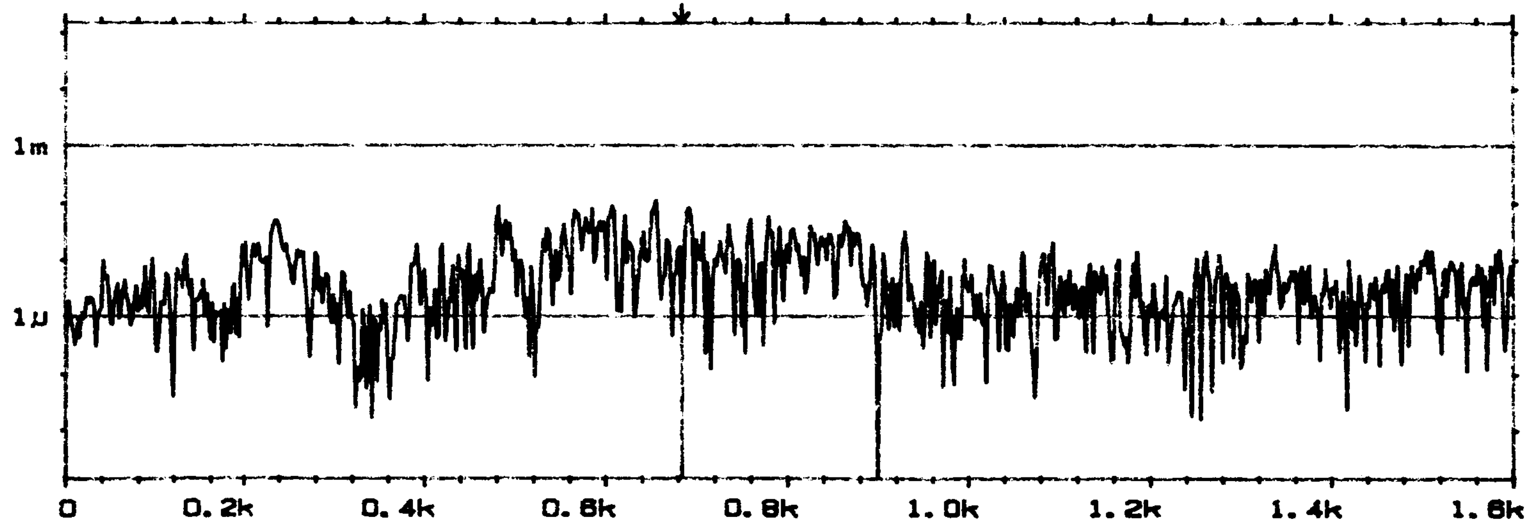

2 COHERENT POWER MAIN Y: 947E-9U²
Y: 150mU² PWR 80dB X: 684Hz
X: 0Hz + 1.6kHz LIN
SETUP W22 #A: 256

Type 2032

Page No.
54

Sign. :

Meas.
Object:

PLF PR 1.8
ChA = T10
ChB = M1

Rdg 179

Comments:

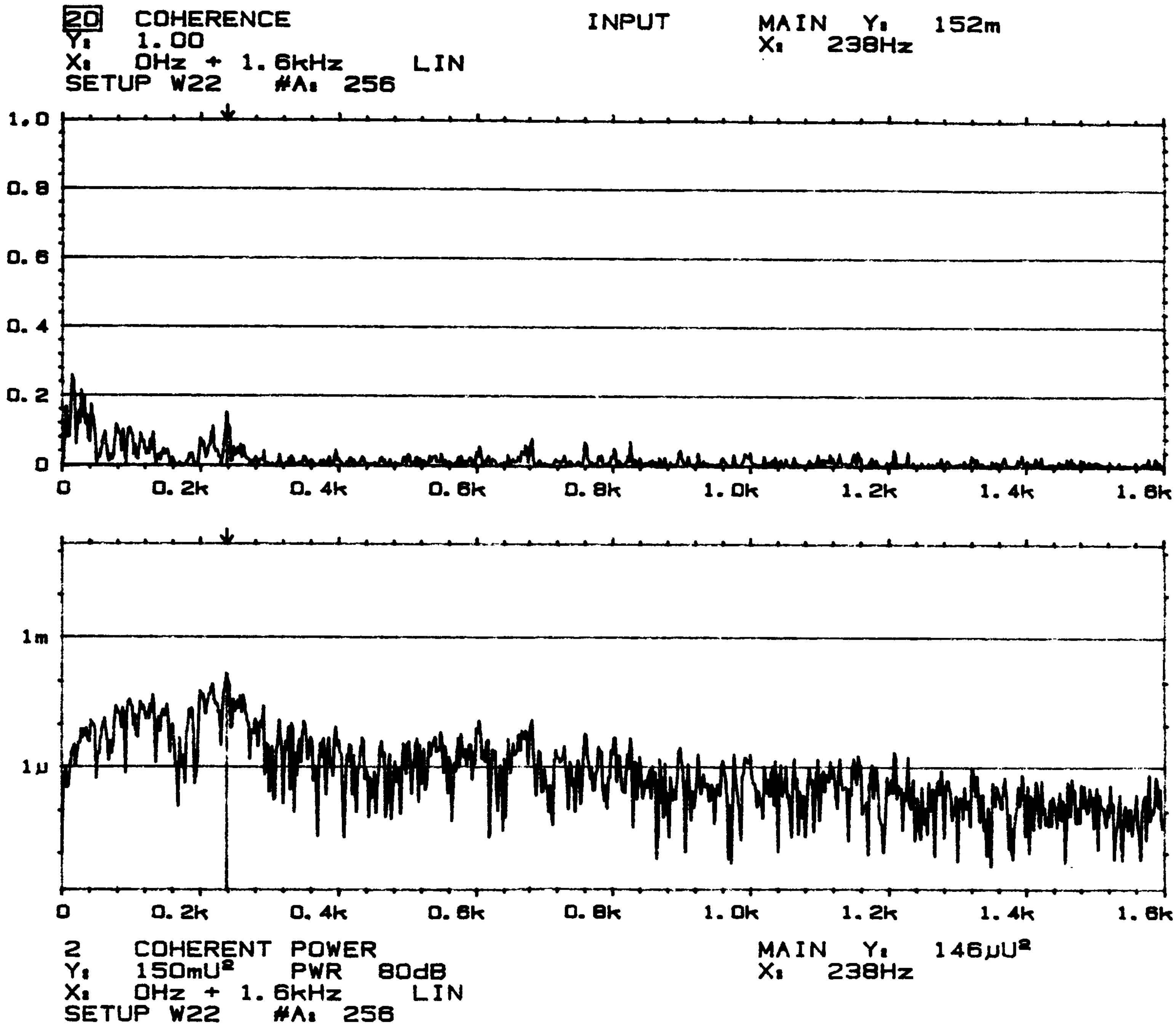

Type 2032

Page No.
56

Sign. :

Meas.
Object:

PLF PR 1.8
chA=T10
chB=M2

Rdg 179

Comments:

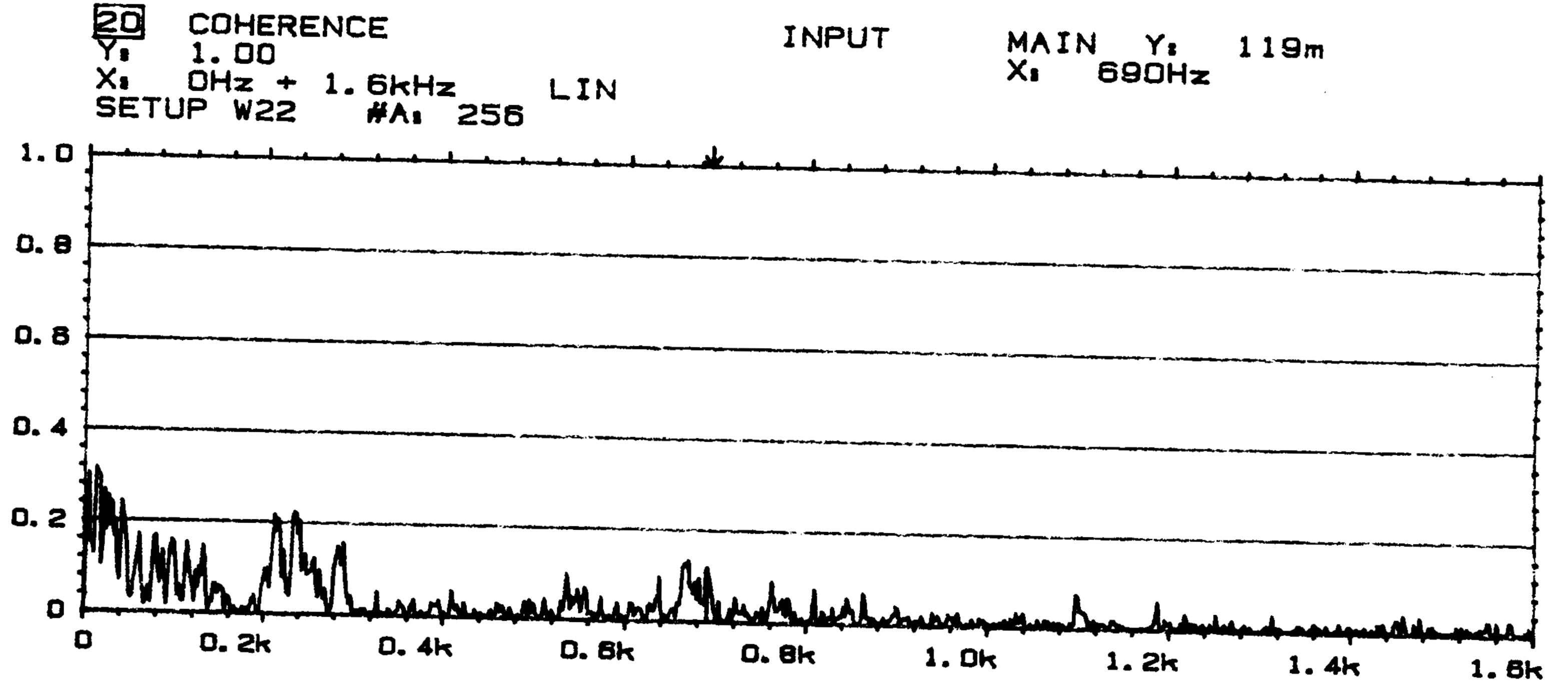

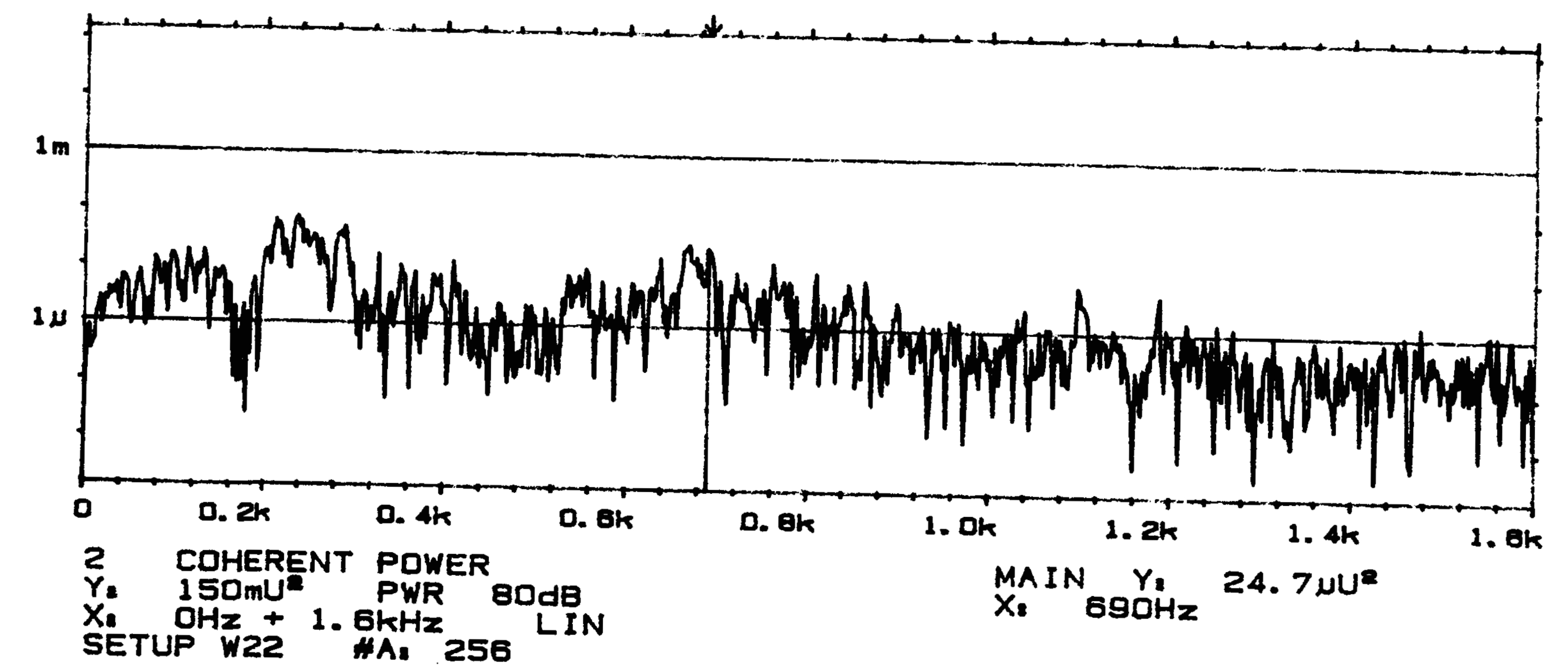

Type 2032

Page No.
58

Sign.:

Meas.
Object:
PLF PR 1.8
ChA: T10
ChB = M3

Pdg 179

Comments:

20 COHERENCE INPUT MAIN Y: 240m
Y: 1.00 X: 690Hz
X: 0Hz + 1.6kHz LIN
SETUP W22 #A: 256

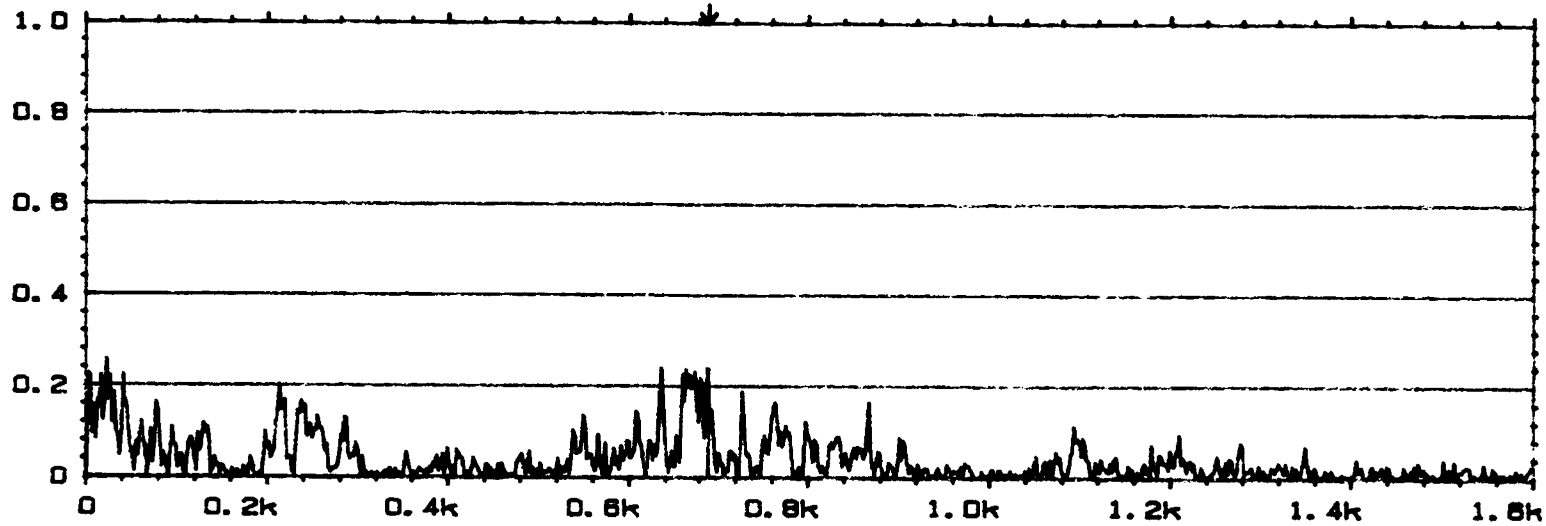

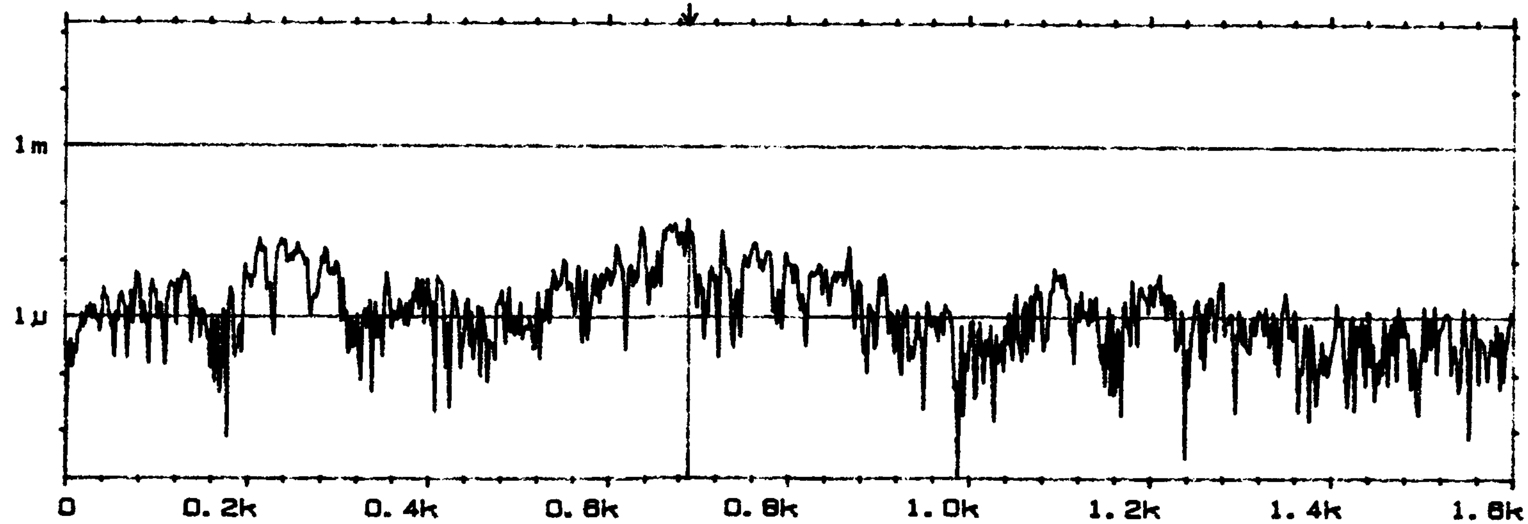

2 COHERENT POWER MAIN Y: 53.1µU²
Y: 150mU² PWR 80dB X: 690Hz
X: 0Hz + 1.6kHz LIN
SETUP W22 #A: 256

Type 2032

Page No.
60

Sign.:

Meas.
Object:
PLF PR 1.8
ChA = T10
ChB = M4

Rdg 179

Comments:

20 COHERENCE INPUT MAIN Y: 169m
Y: 1.00 X: 690Hz
X: 0Hz + 1.6kHz LIN
SETUP W22 #A: 256

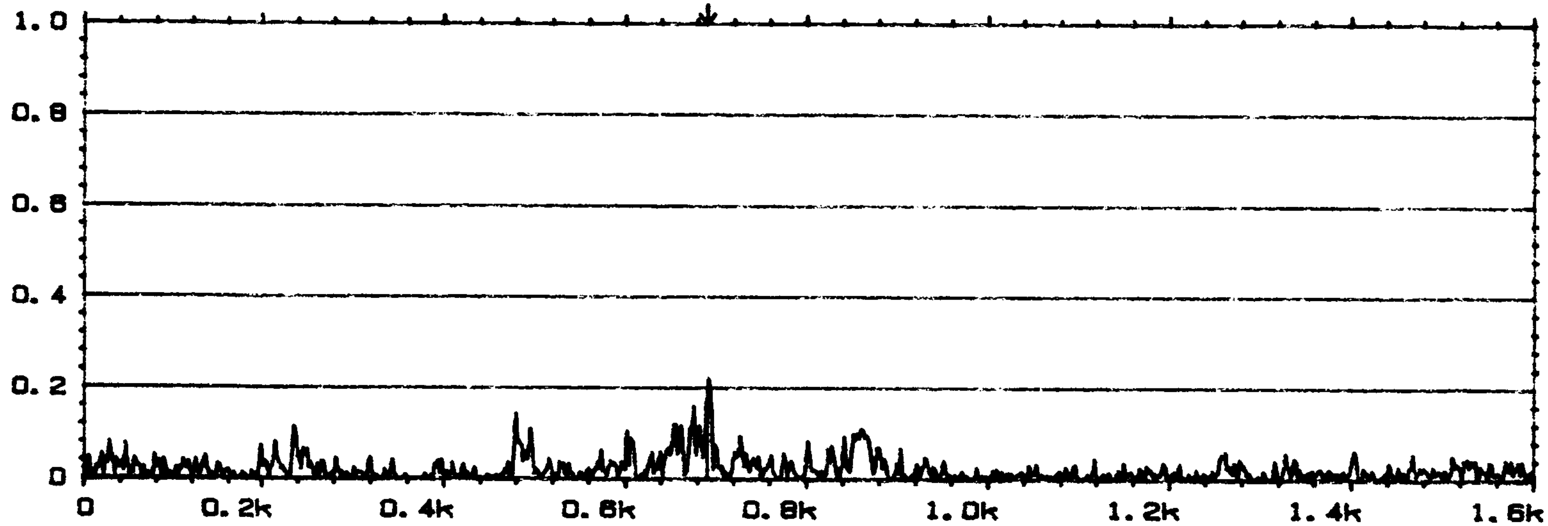

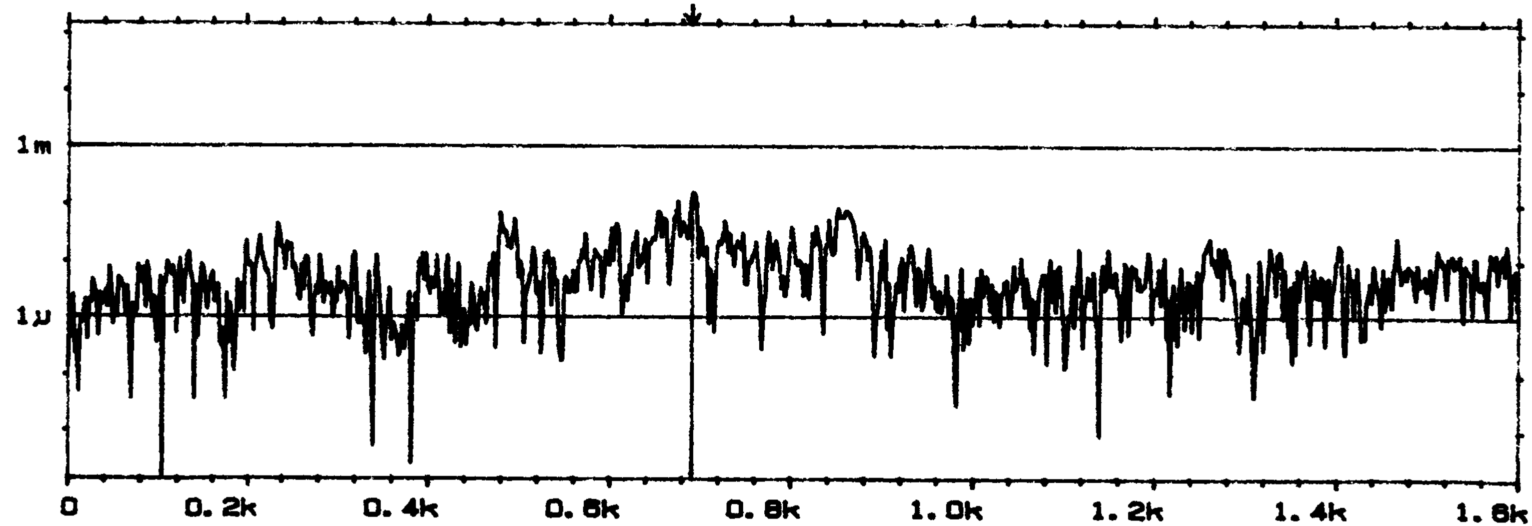

2 COHERENT POWER MAIN Y: 105µU²
Y: 150mU² PWR 80dB X: 690Hz
X: 0Hz + 1.6kHz LIN
SETUP W22 #A: 256

Type 2032

Page No.
62

Sign.:

Meas.
Object:

PLF PR2.0
ChA=T10
ChB=M1

Rdg 180

Comments:

20 COHERENCE INPUT MAIN Y: 4.29m
Y: 1.00 X: 690Hz
X: 0Hz + 1.6kHz LIN
SETUP W22 #A: 256

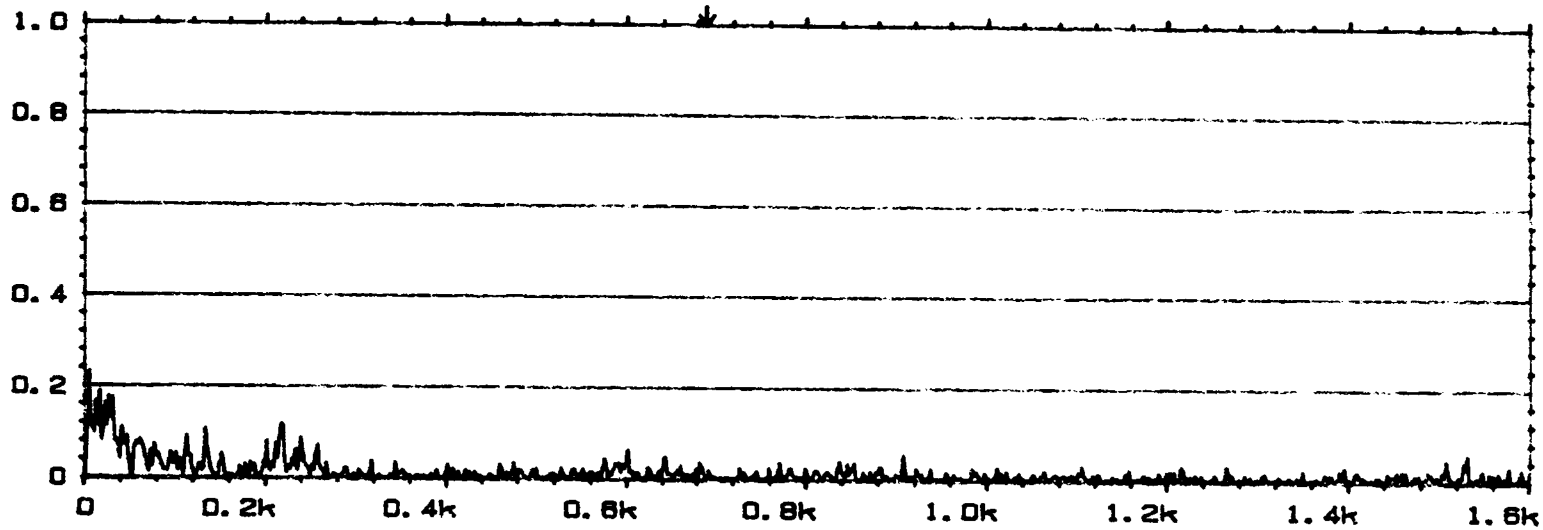

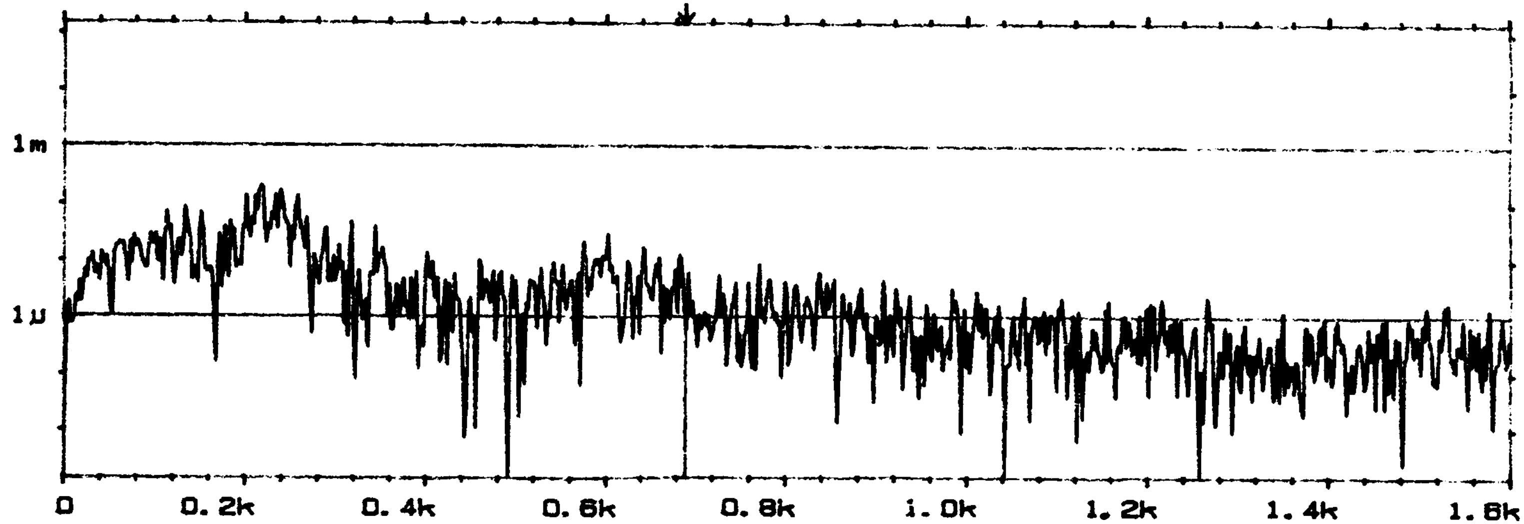

2 COHERENT POWER MAIN Y: 1.40µU²
Y: 150mU² PWR 80dB X: 690Hz
X: 0Hz + 1.6kHz LIN
SETUP W22 #A: 256

Type 2032

Page No.
64

Sign.:

Meas.
Object:
PLF PR2.0
ChA=T10
ChB=M2

Rdg 180

Comments:

W20 COHERENCE　　　　INPUT　　　　MAIN Y: 13.1m
Y: 1.00　　　　　　　　　　　　　　X: 690Hz
X: 0Hz + 1.6kHz　　LIN
SETUP W22　　#A: 256

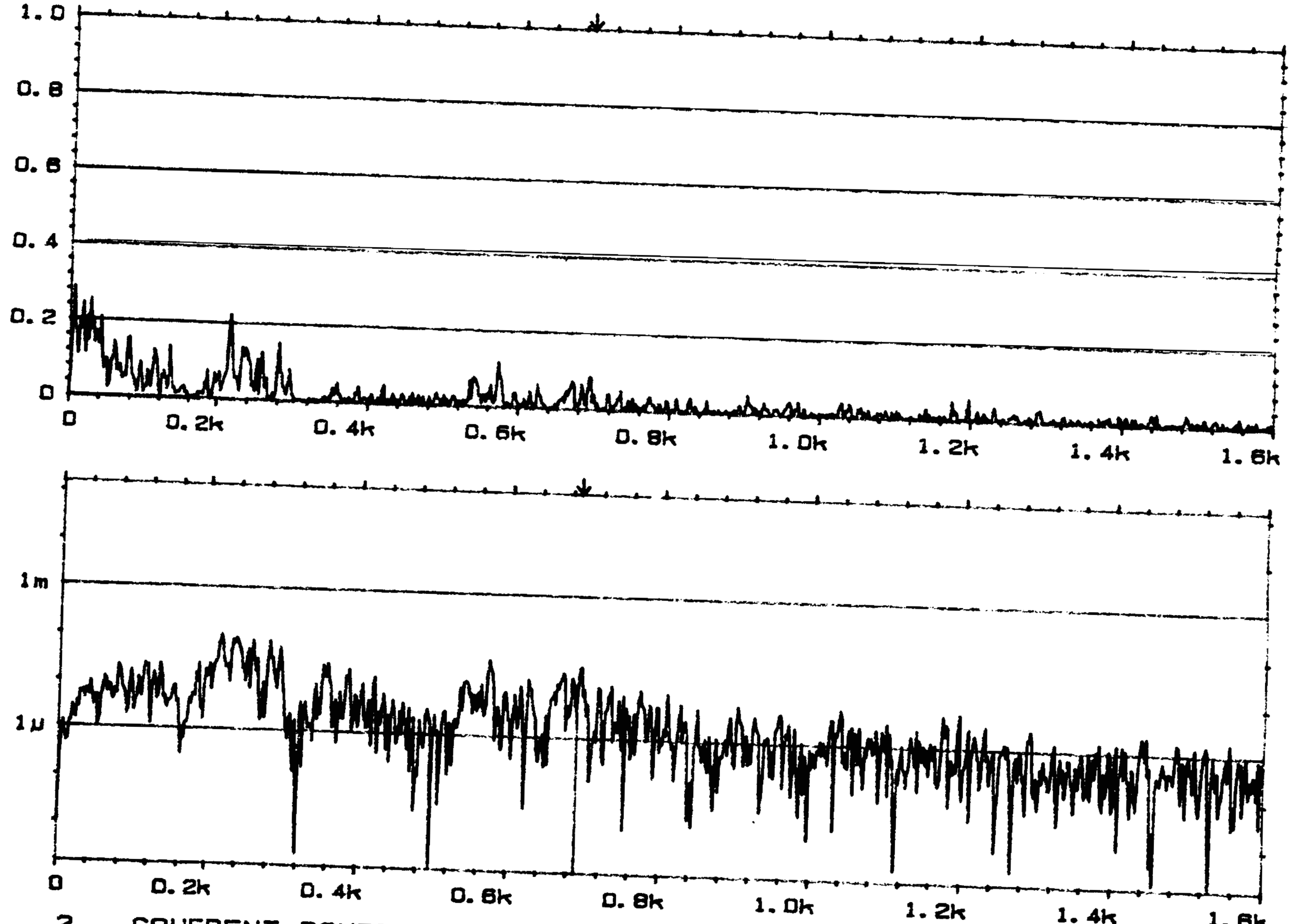

2　COHERENT POWER　　　　　　MAIN Y: 3.74µU²
Y: 150mU²　PWR 80dB　　　　X: 690Hz
X: 0Hz + 1.6kHz　　LIN
SETUP W22　　#A: 256

Type 2032

Page No.
66

Sign.:

Meas.
Object:

Comments:

W20 COHERENCE INPUT MAIN Y: 16.6m
Y: 1.00 X: 690Hz
X: 0Hz + 1.6kHz LIN
SETUP W22 #A: 256

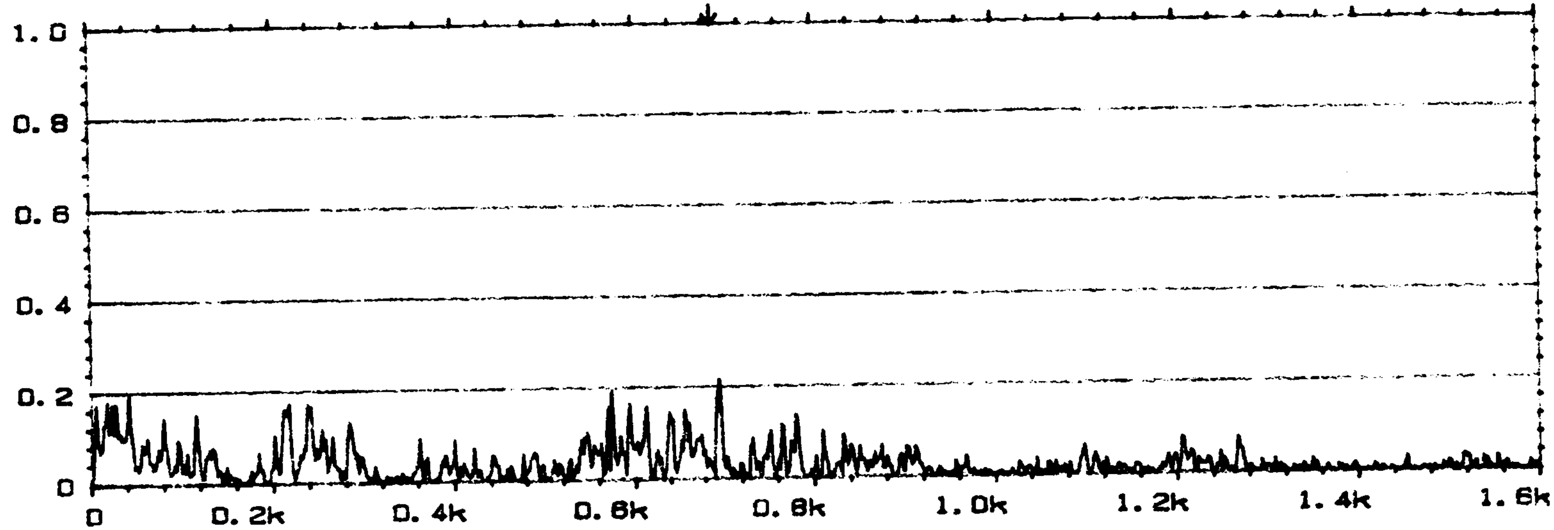

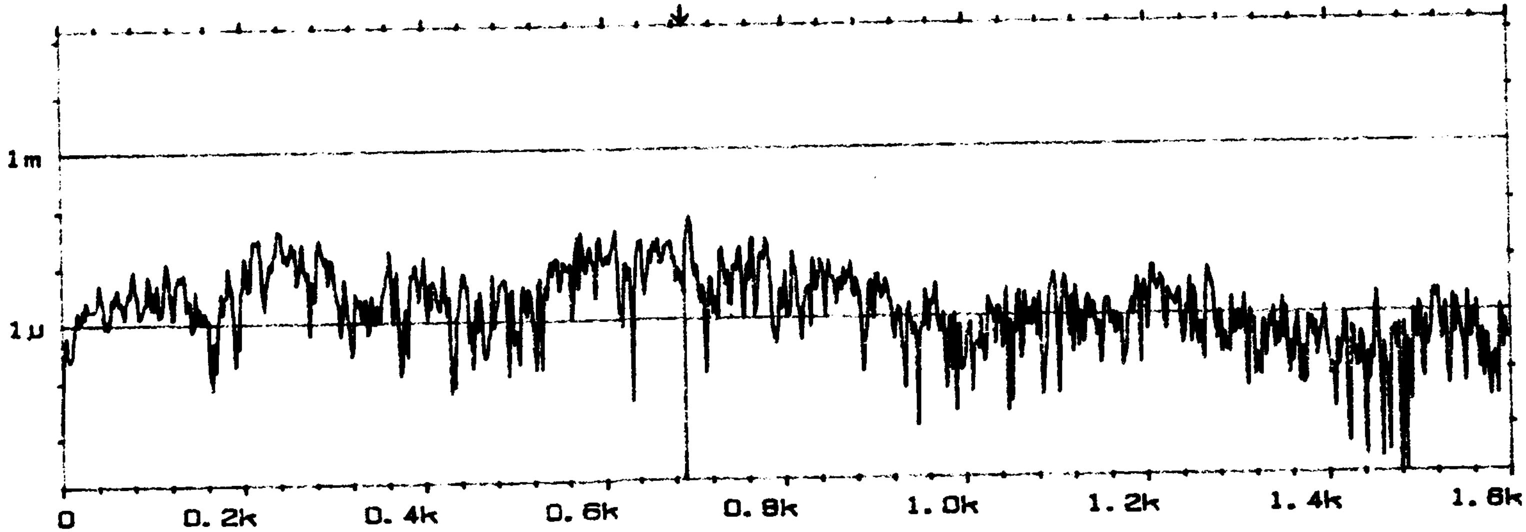

2 COHERENT POWER MAIN Y: 3.19µU²
Y: 150mU² PWR 80dB X: 690Hz
X: 0Hz + 1.6kHz LIN
SETUP W22 #A: 256

ORIGINAL PAGE IS
OF POOR QUALITY

Type 2032

Page No.
68

Sign.:

Meas.
Object:

PLF PR 2.0
ChA = T10
ChB = M4

Rig 180

Comments:

W20 COHERENCE
Y: 1.00
X: 0Hz + 1.6kHz LIN
SETUP W22 #A: 256

INPUT

MAIN Y: 288m
X: 694Hz

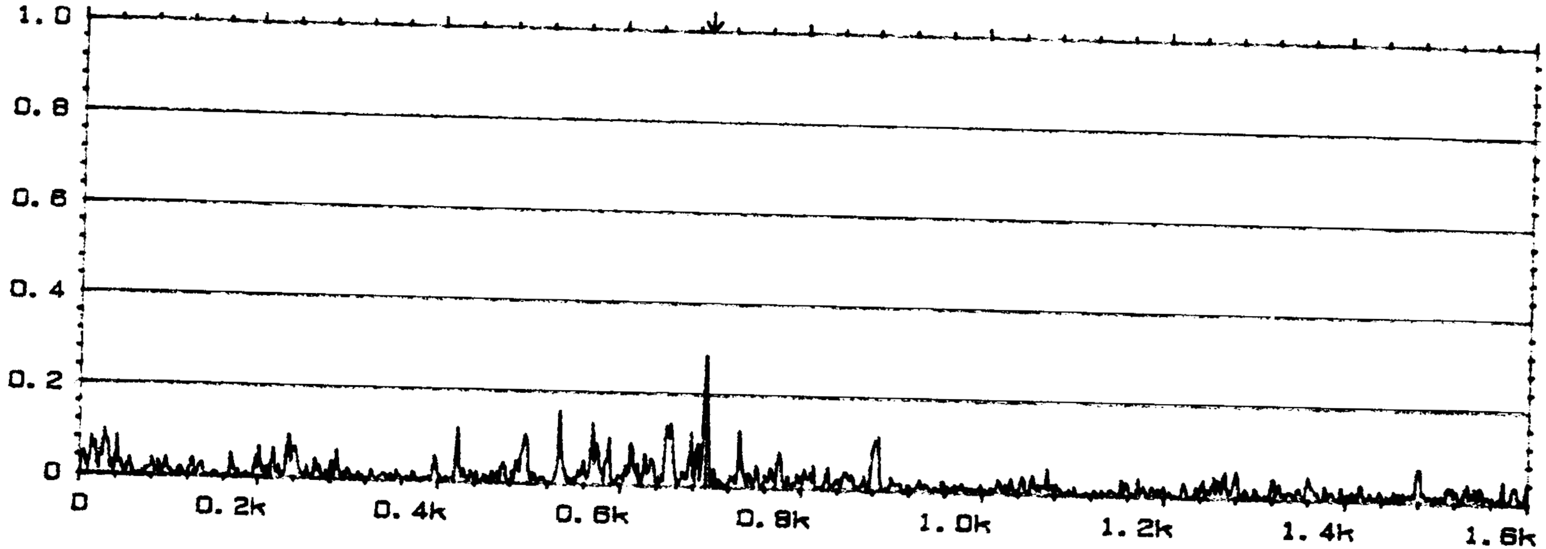

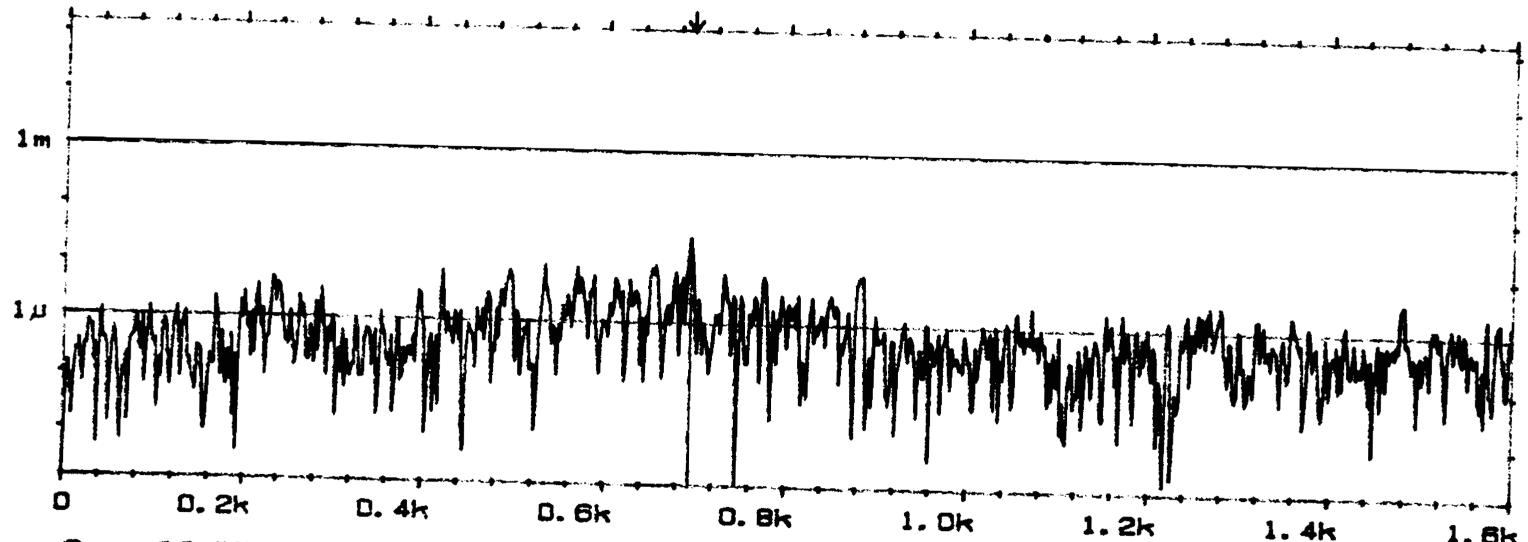

2 COHERENT POWER
Y: 150mU² PWR 80dB
X: 0Hz + 1.6kHz LIN
SETUP W22 #A: 256

MAIN Y: 32.4µU²
X: 694Hz

W20 COHERENCE INPUT MAIN Y: 3.85m
Y: 1.00 X: 59.000Hz
X: 0.000Hz + 100Hz LIN
SETUP W22* #A: 500

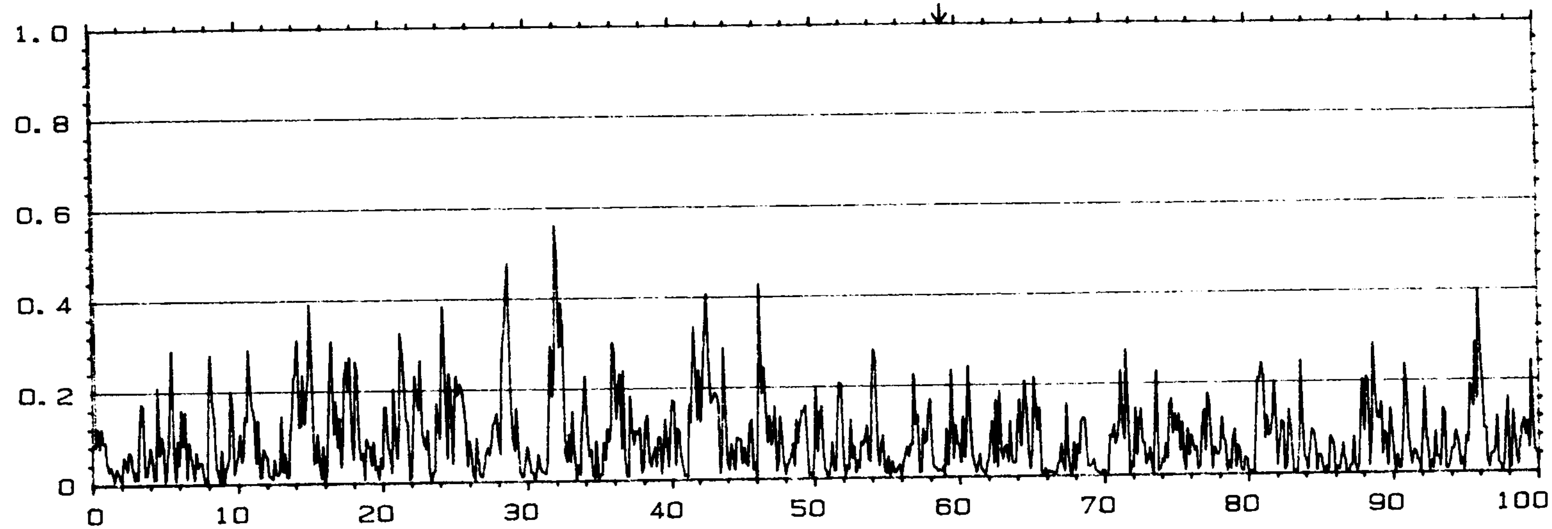

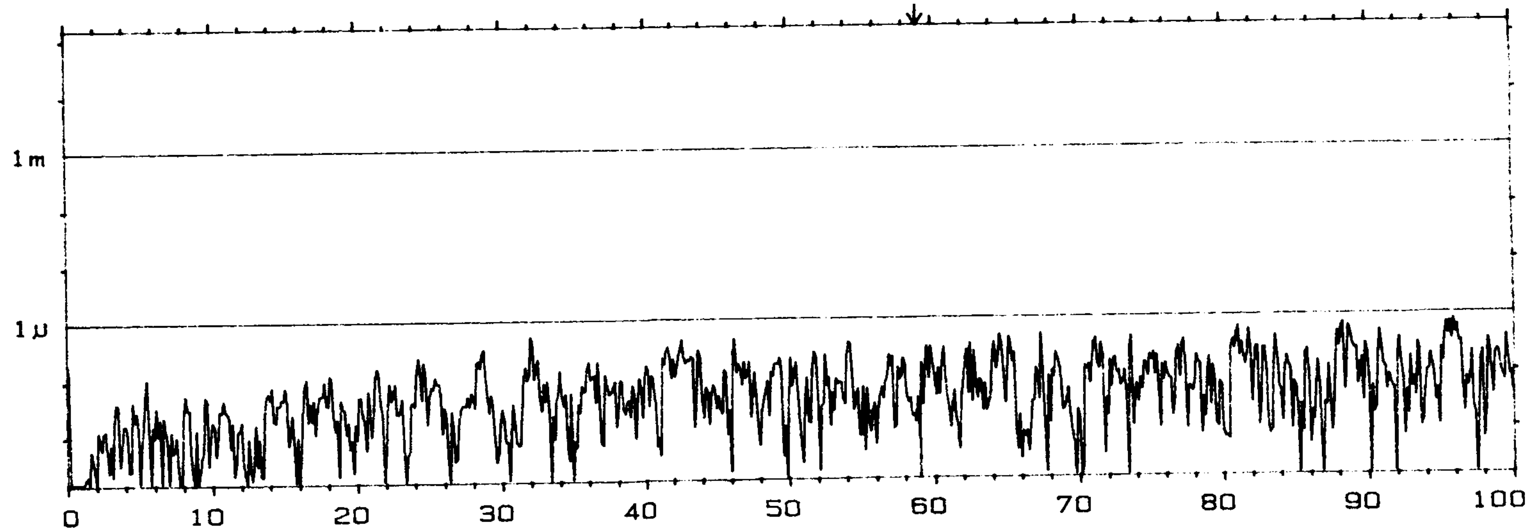

2 COHERENT POWER MAIN Y: 6.84E-9U²
Y: 150mU² PWR 80dB X: 59.000Hz
X: 0.000Hz + 100Hz LIN
SETUP W22* #A: 500

Type 2032

Page No.
74

Sign.:

Meas.
Object:
PLF PR 2.0
ChA=T10
ChB=M4

Rdg 180

Comments:
Expanded freq
Range

Type 2032

Page No.
, 72

Sign.:

Meas.
Object:

PLF PR=2.0
ChA=T10
ChB=M4

Rdg 180

Comments:

W20 COHERENCE
Y: 1.00
X: 0.0Hz + 400Hz LIN
SETUP W22 #A: 256

INPUT

MAIN Y: 283m
X: 236.0Hz

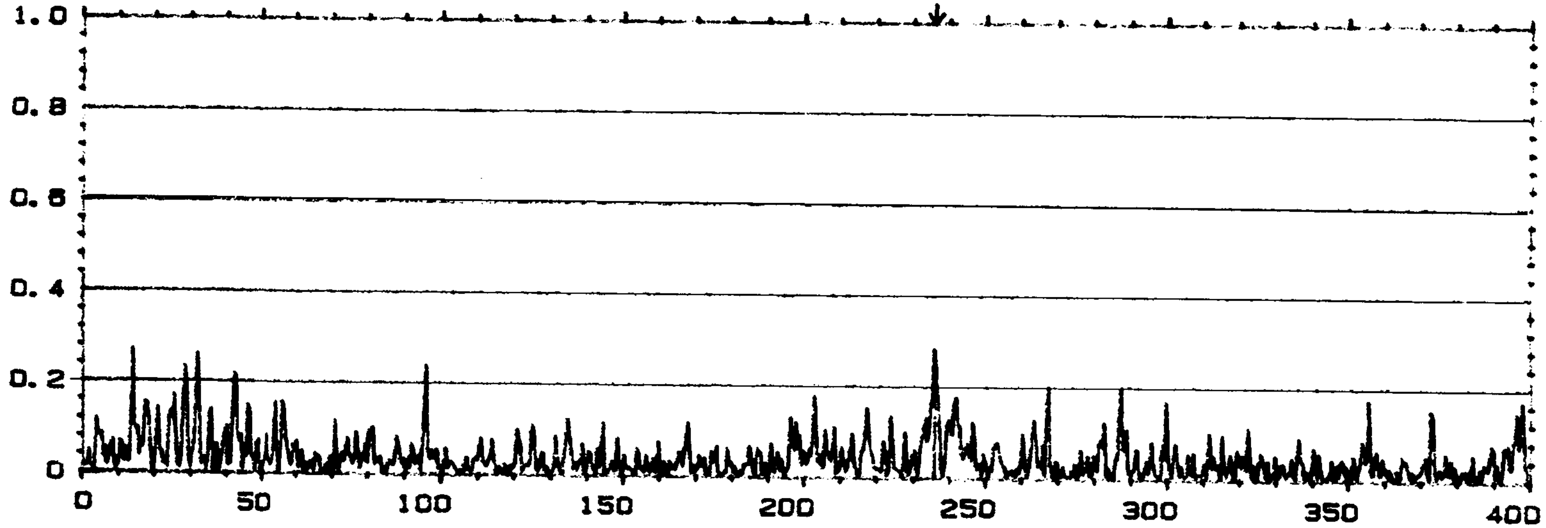

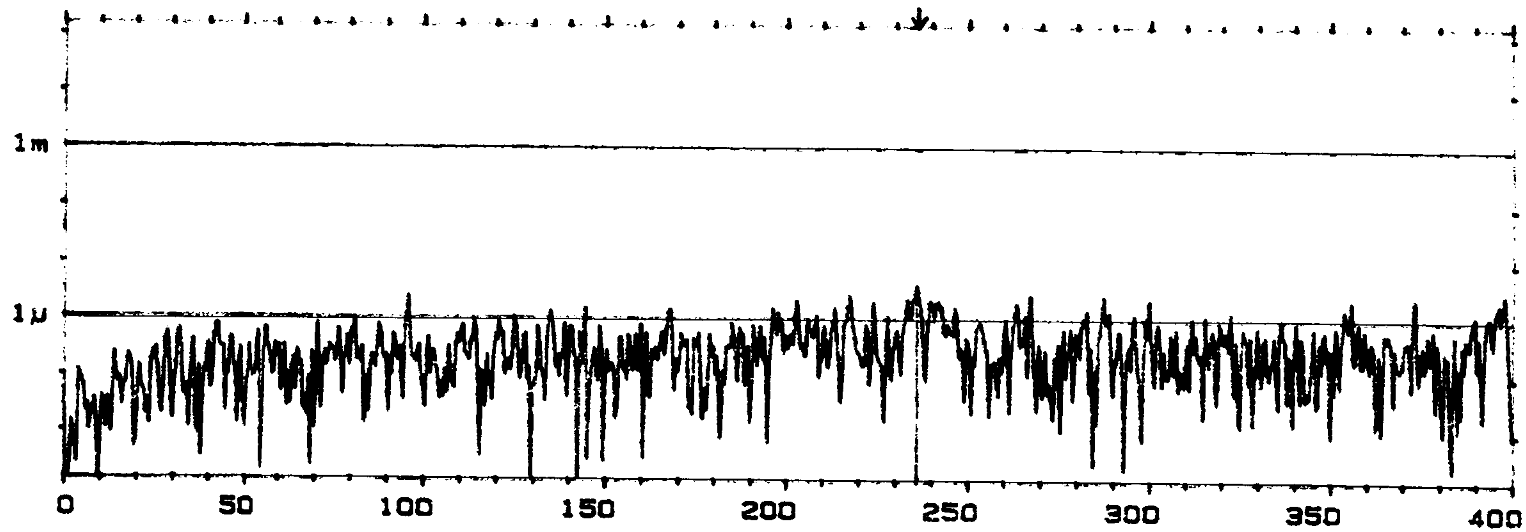

2 COHERENT POWER
Y: 150mU² PWR 80dB
X: 0.0Hz + 400Hz LIN
SETUP W22 #A: 256

MAIN Y: 4.14µU²
X: 236.0Hz

Type 2032

Page No.
70

Sign.:

Meas.
Object:

Comments:

ORIGINAL PAGE IS
OF POOR QUALITY

W20 COHERENCE
Y: 1.00
X: 0Hz + 800Hz LIN
SETUP W22* #A: 256

INPUT

MAIN Y: 337m
X: 694Hz

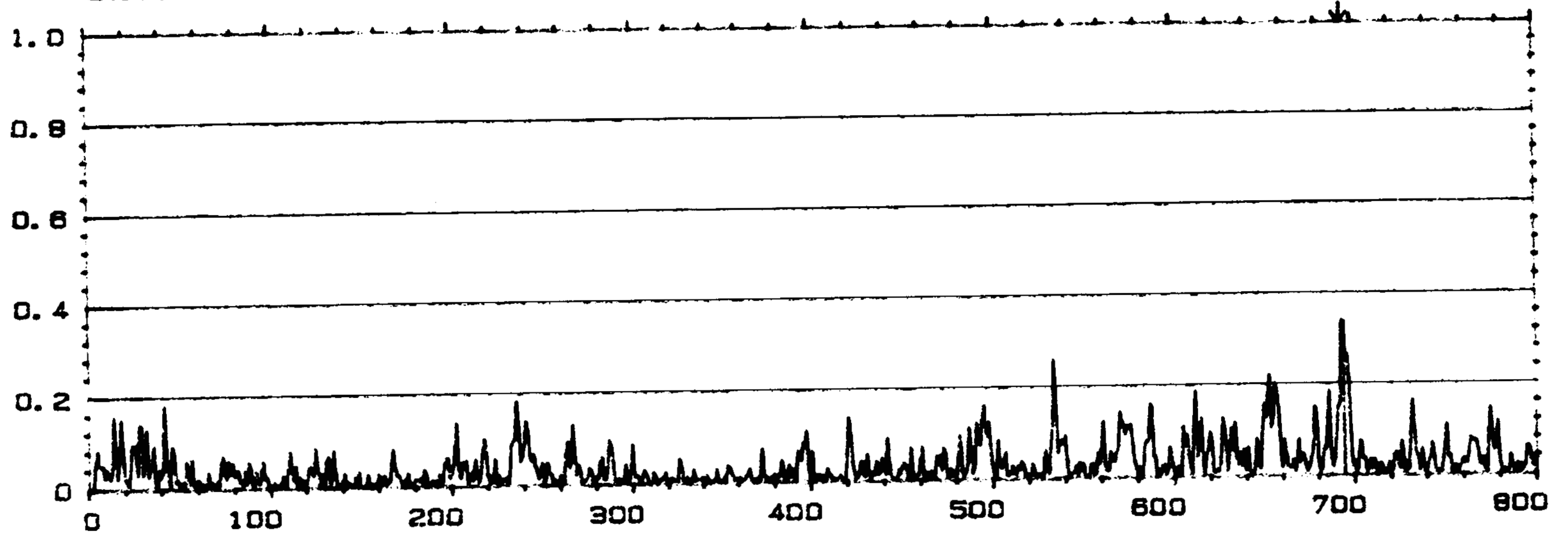

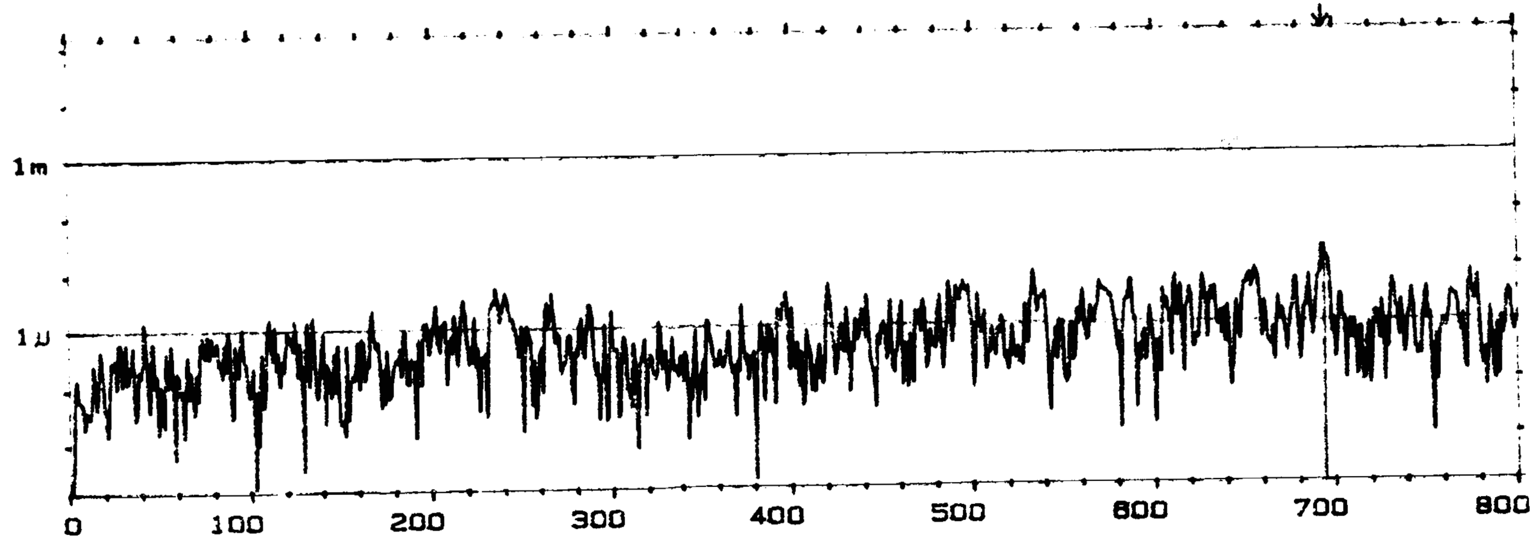

2 COHERENT POWER
Y: 150mU² PWR 80dB
X: 0Hz + 800Hz LIN
SETUP W22* #A: 256

MAIN Y: 20.8µU²
X: 694Hz

Type 2032

Page No.
94

Sign.:

Meas.
Object:
PLF PE 2.25
ChA-T10
ChB-M1

Rdg 182

Comments:

W20 COHERENCE
Y: 1.00
X: 0Hz + 1.6kHz LIN
SETUP W2 #A: 256

MAIN Y: 42.4µ
X: 0Hz

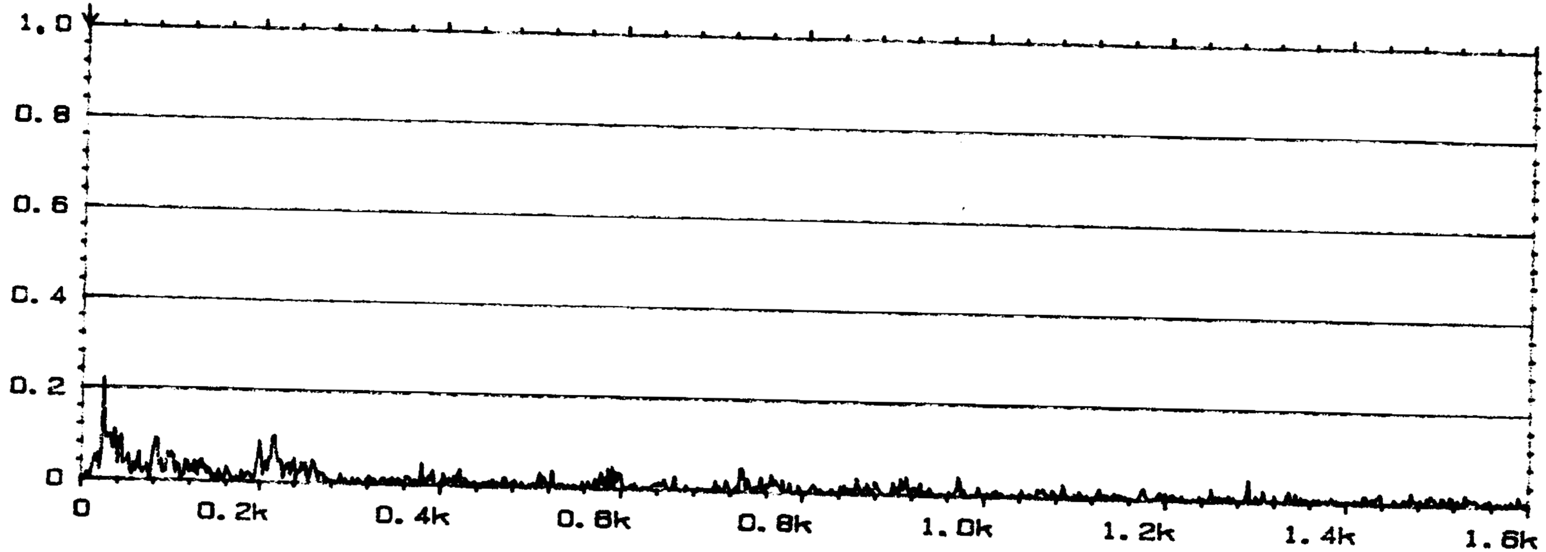

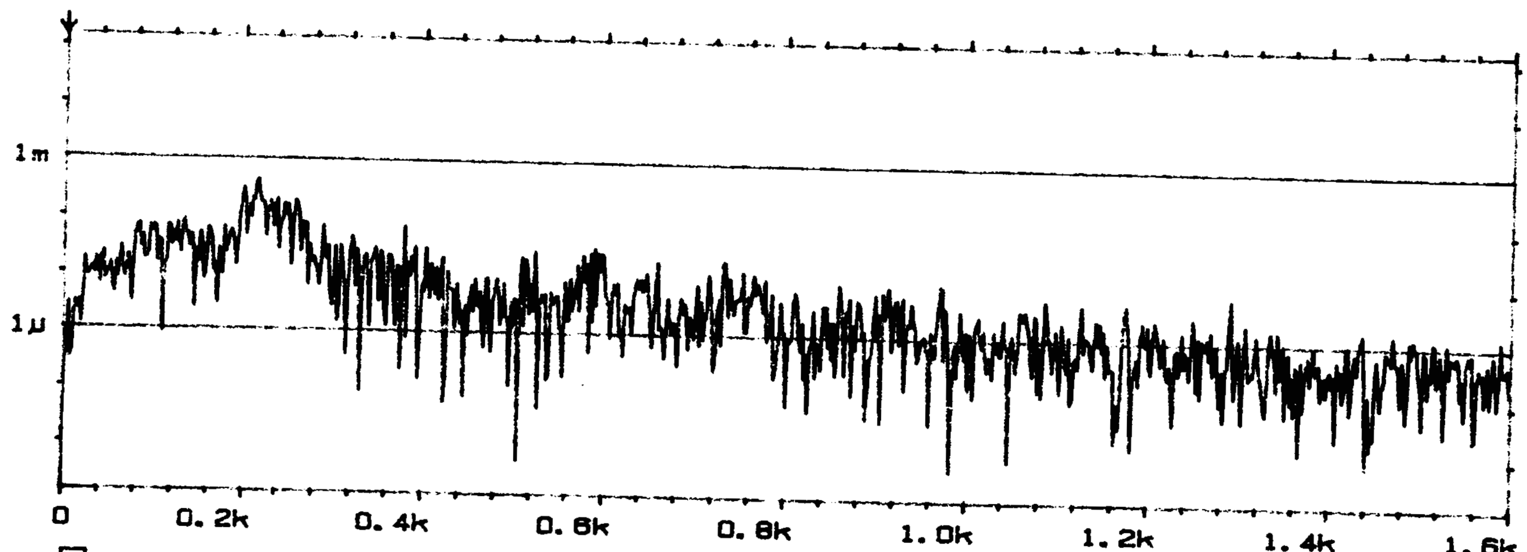

2 COHERENT POWER [ ] INPUT
Y: 150mV² PWR 80dB
X: 0Hz + 1.6kHz LIN
SETUP W2 #A: 256

MAIN Y: 15.2E-9V²
X: 0Hz

ORIGINAL PAGE IS
OF POOR QUALITY

Type 2032

Page No.
96

Sign.:

Meas.
Object:

PLF PR 2.25
ChA = T10
ChB = M2

Rtg 132

Comments:

W20 COHERENCE
Y: 1.00
X: 0Hz + 1.6kHz LIN
SETUP W2 #A: 256

MAIN Y: 1.56m
X: 0Hz

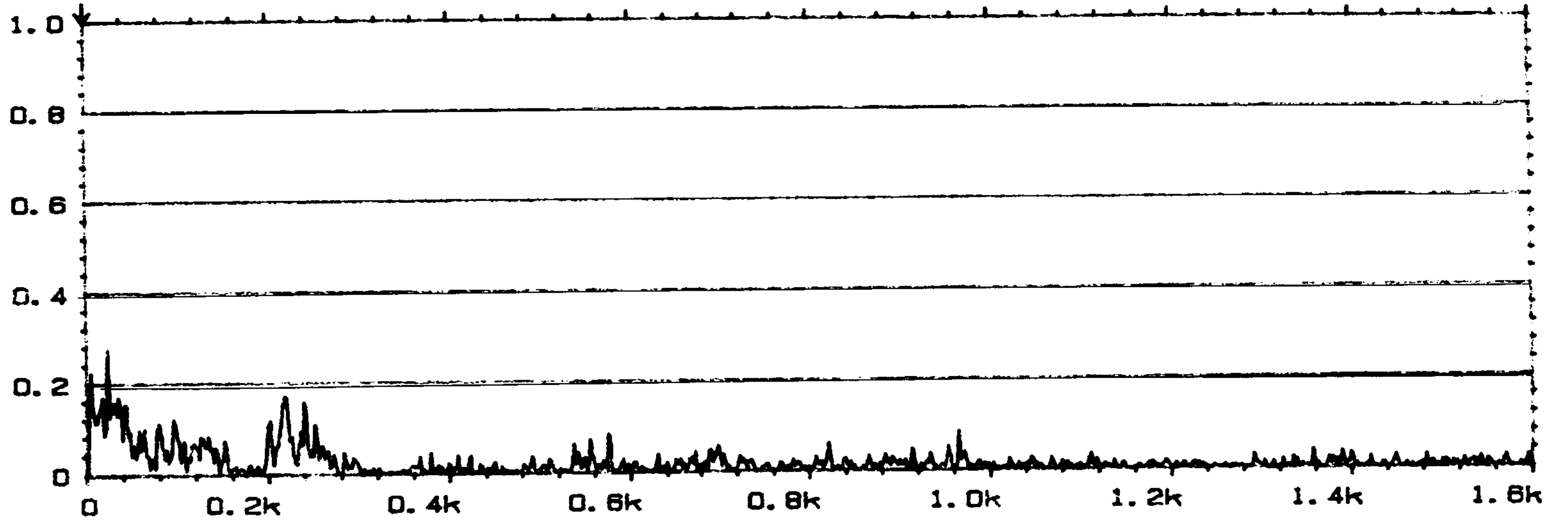

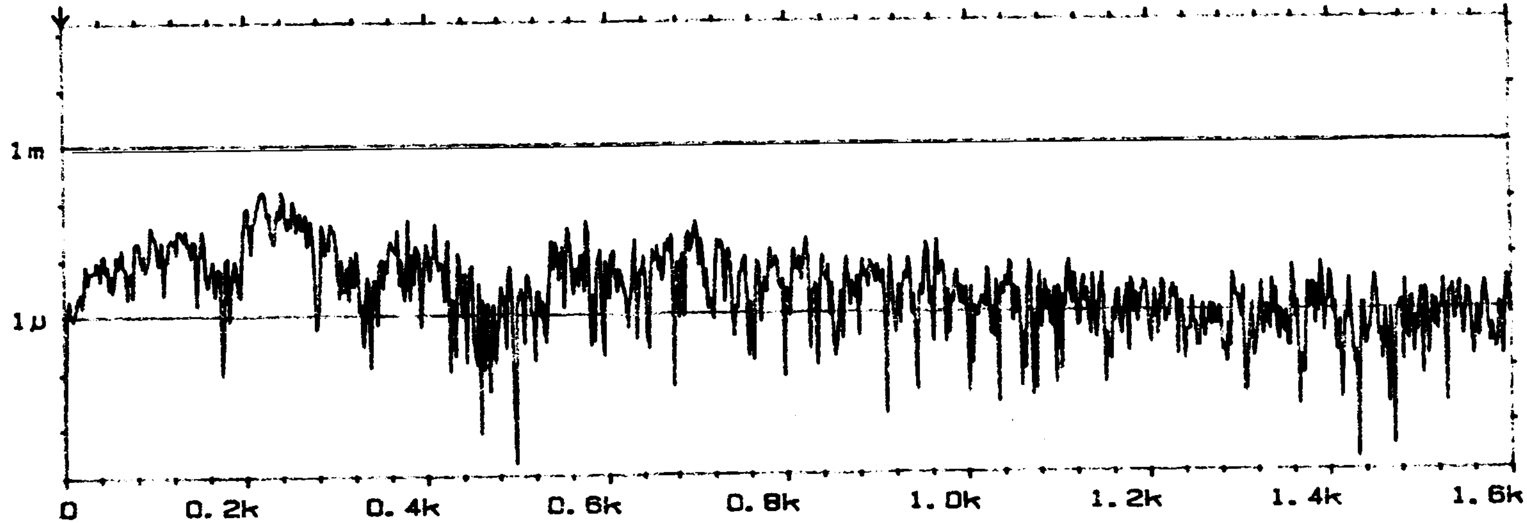

2 COHERENT POWER [ ] INPUT
Y: 150mV² PWR 80dB
X: 0Hz + 1.6kHz LIN
SETUP W2 #A: 256

MAIN Y: 7.66E-9V²
X: 0Hz

Type 2032

Page No.
98

Sign.:

Meas.
Object:

PLF PR 2.25
ChA=T10
ChB=M3

Rdg 182

Comments:

W2C COHERENCE
Y: 1.00
X: 0Hz + 1.6kHz LIN
SETUP W2 #A: 256

MAIN Y: 3.42m
X: 0Hz

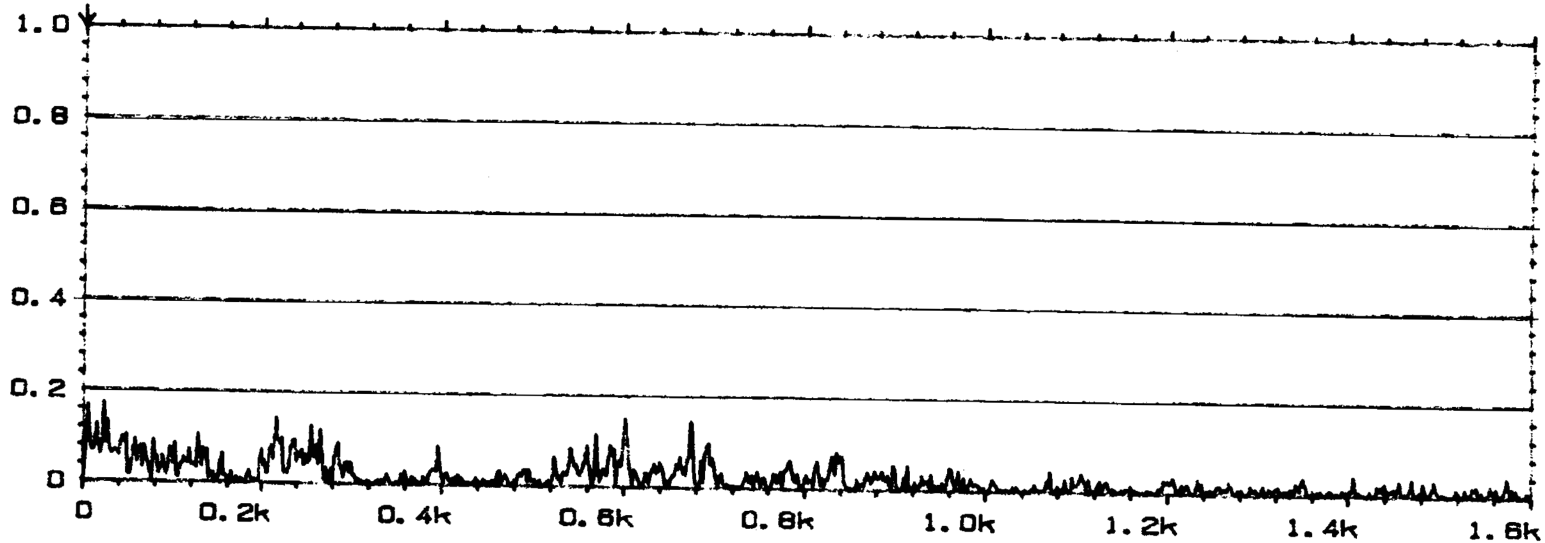

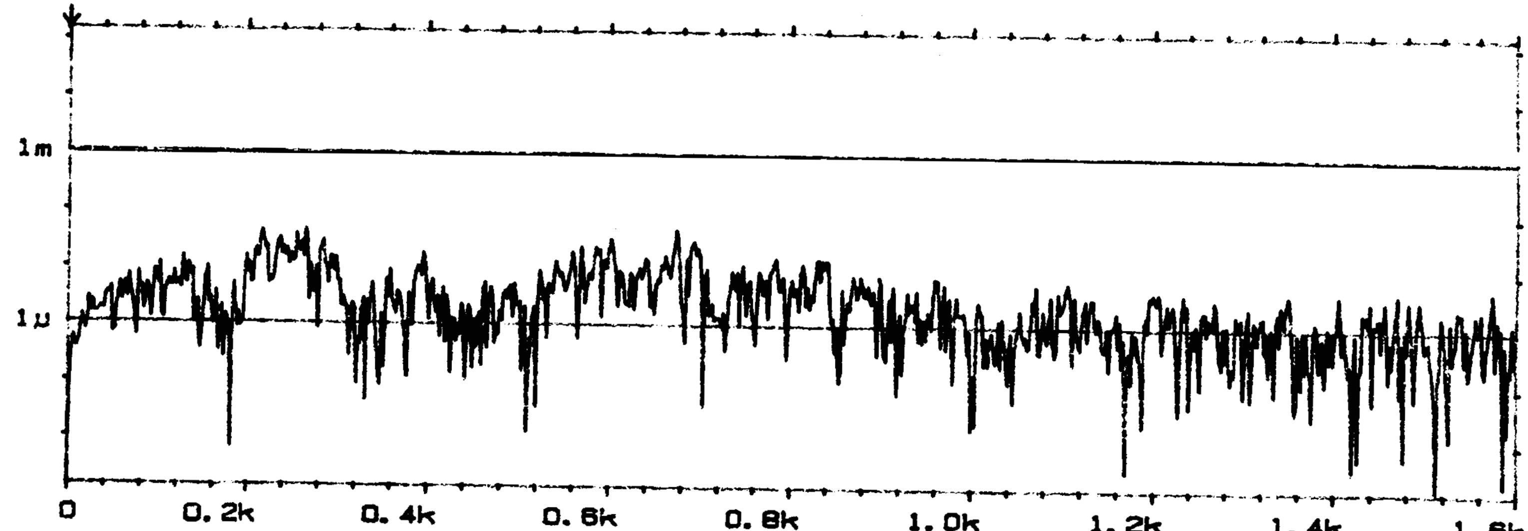

2 COHERENT POWER [ ] INPUT
Y: 150mV² PWR 80dB
X: 0Hz + 1.6kHz LIN
SETUP W2 #A: 256

MAIN Y: 2.91E-9V²
X: 0Hz

ORIGINAL PAGE IS
OF POOR QUALITY

Type 2032

Page No.
100

Sign.:

Meas.
Object:

ChA-T10
ChB-M9

Comments:

W20 COHERENCE
Y: 1.00
X: 0Hz + 1.6kHz LIN
SETUP W2 #A: 256

MAIN Y: 3.30m
X: 0Hz

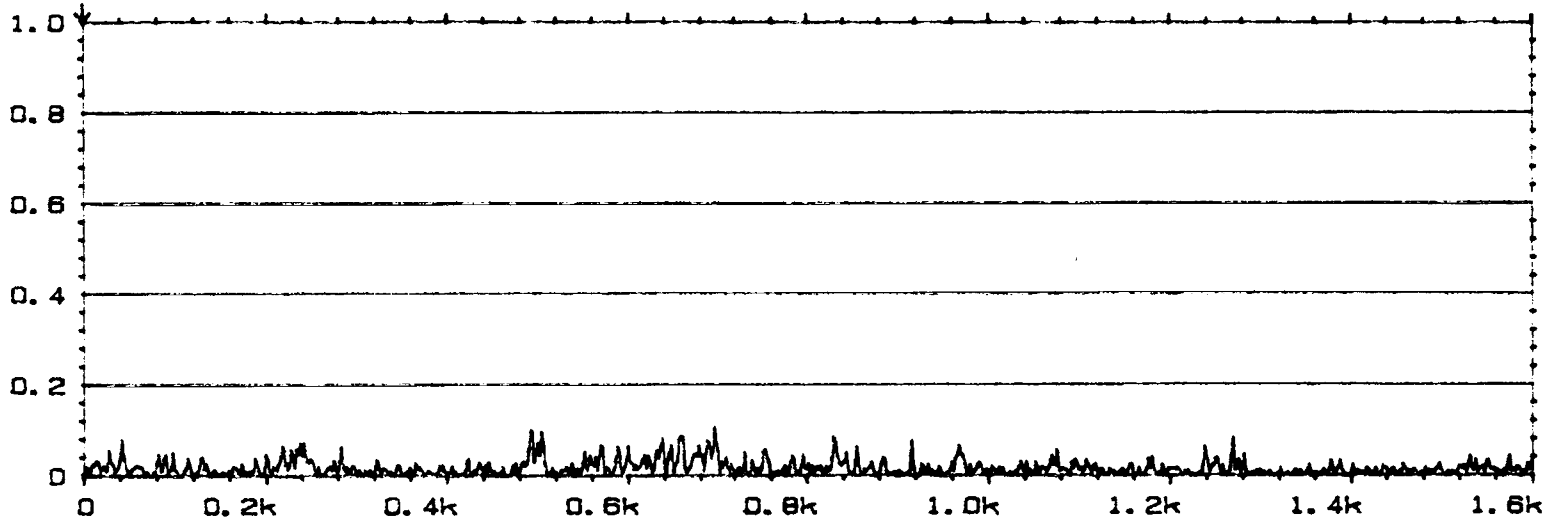

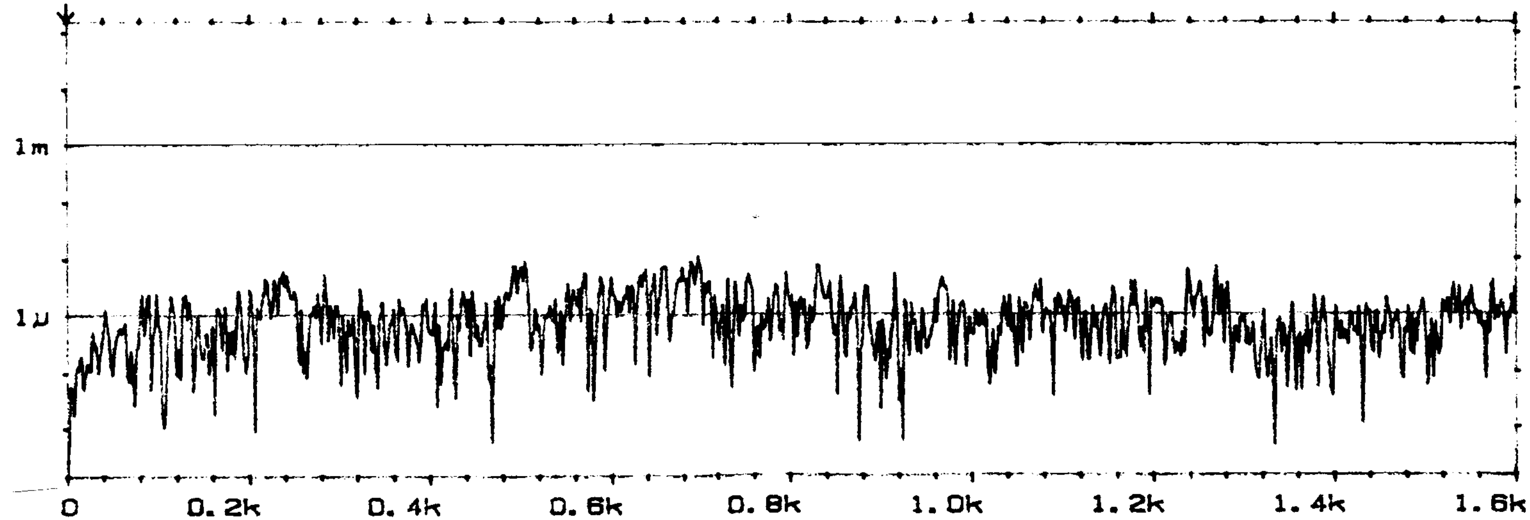

2 COHERENT POWER [ ] INPUT
Y: 150mV² PWR 80dB
X: 0Hz + 1.6kHz LIN
SETUP W2 #A: 256

MAIN Y: 976E-12V²
X: 0Hz

Type 2032

Page No.
102

Sign.:

Meas.
Object:

PLF PR2.5
ChA = T10
ChB = M1

Rdg 183

Comments:

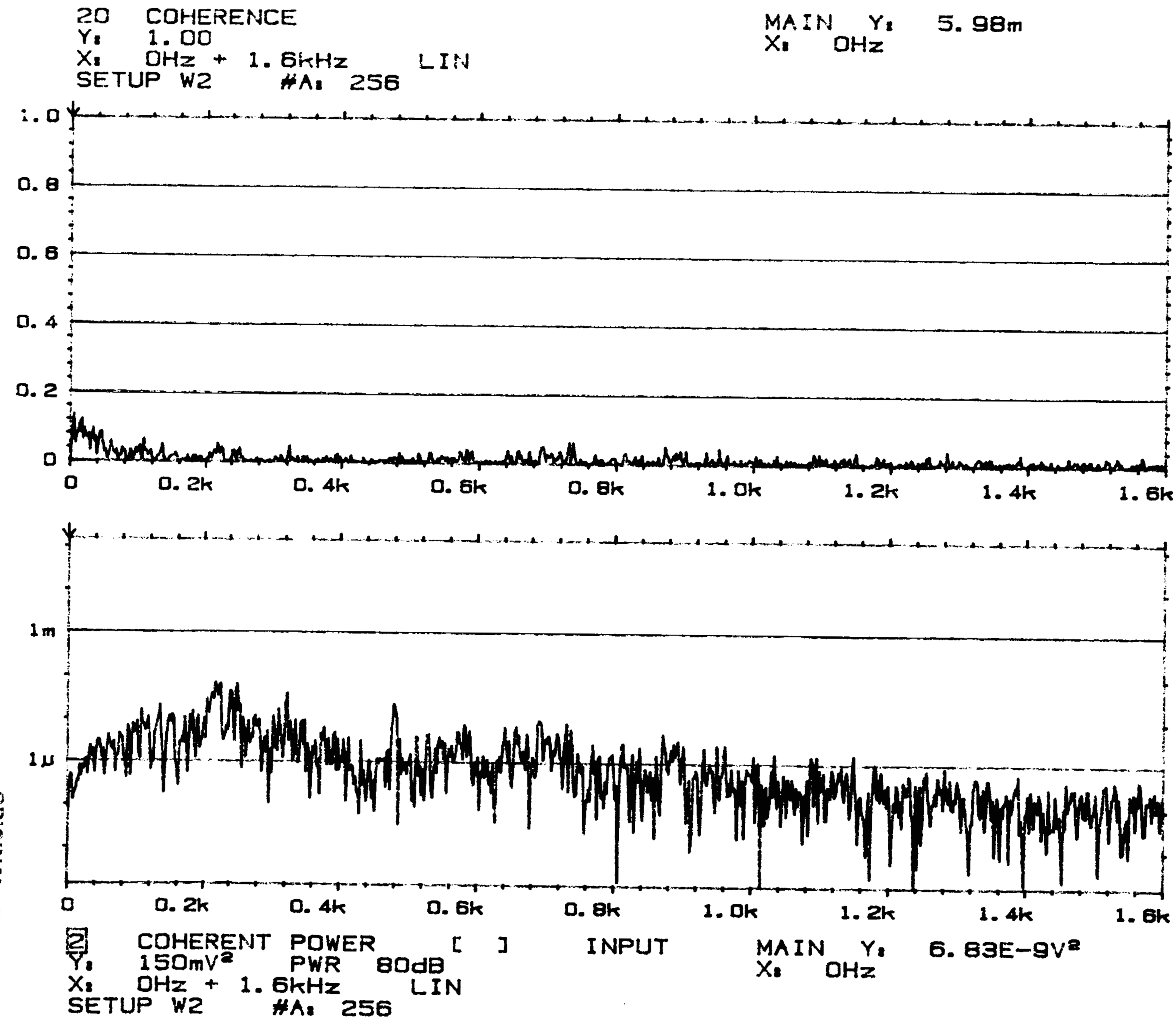

Type 2032

Page No.
104

Sign.:

Meas.
Object:

PLF PR 2.5
ChA = T10
ChB = M2

Rdg 183

Comments:

20 COHERENCE
Y: 1.00
X: 0Hz + 1.6kHz LIN
SETUP W2 #A: 256

MAIN Y: 4.96m
X: 0Hz

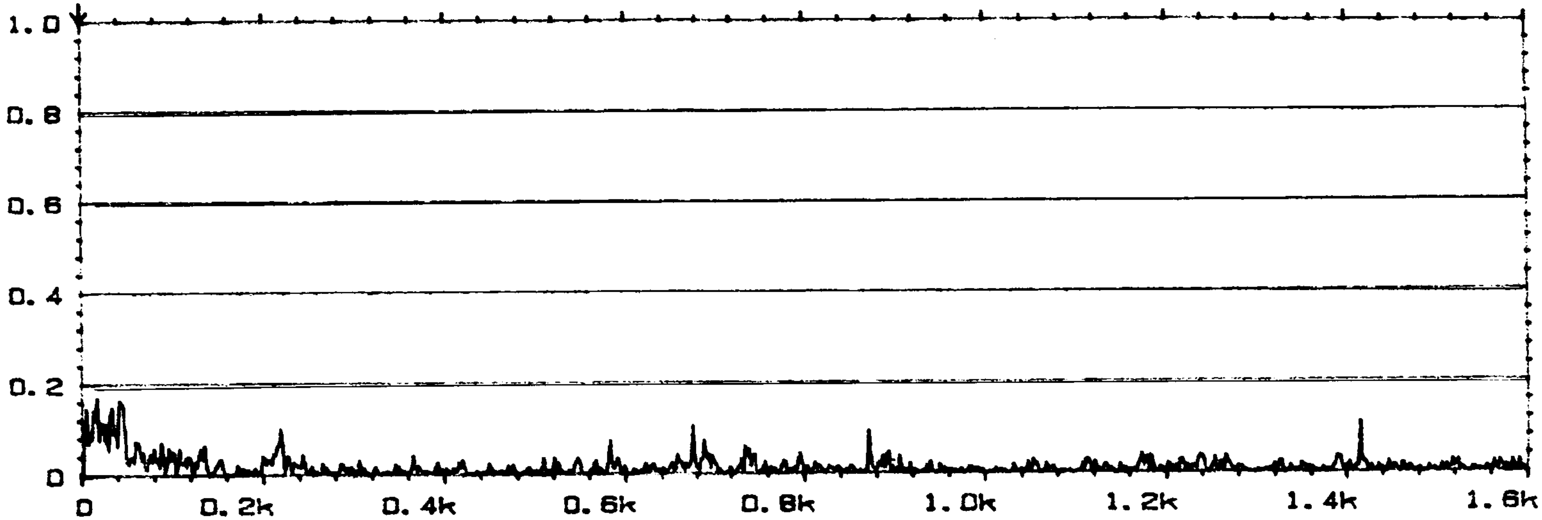

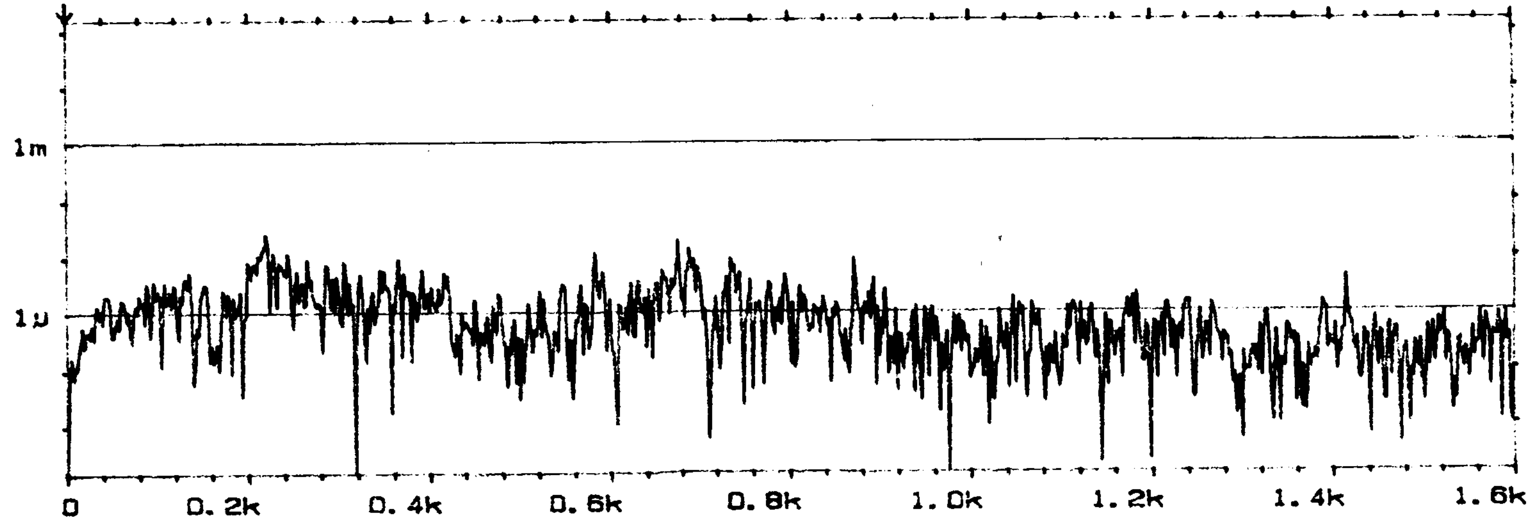

2 COHERENT POWER [ ] INPUT
Y: 150mV² PWR 80dB
X: 0Hz + 1.6kHz LIN
SETUP W2 #A: 256

MAIN Y: 1.54E-9V²
X: 0Hz

Type 2032

Page No.
106

Sign.:

Meas.
Object:

PLF PR 2.5
ChA=T10
ChB=M3

Rdg 183

Comments:

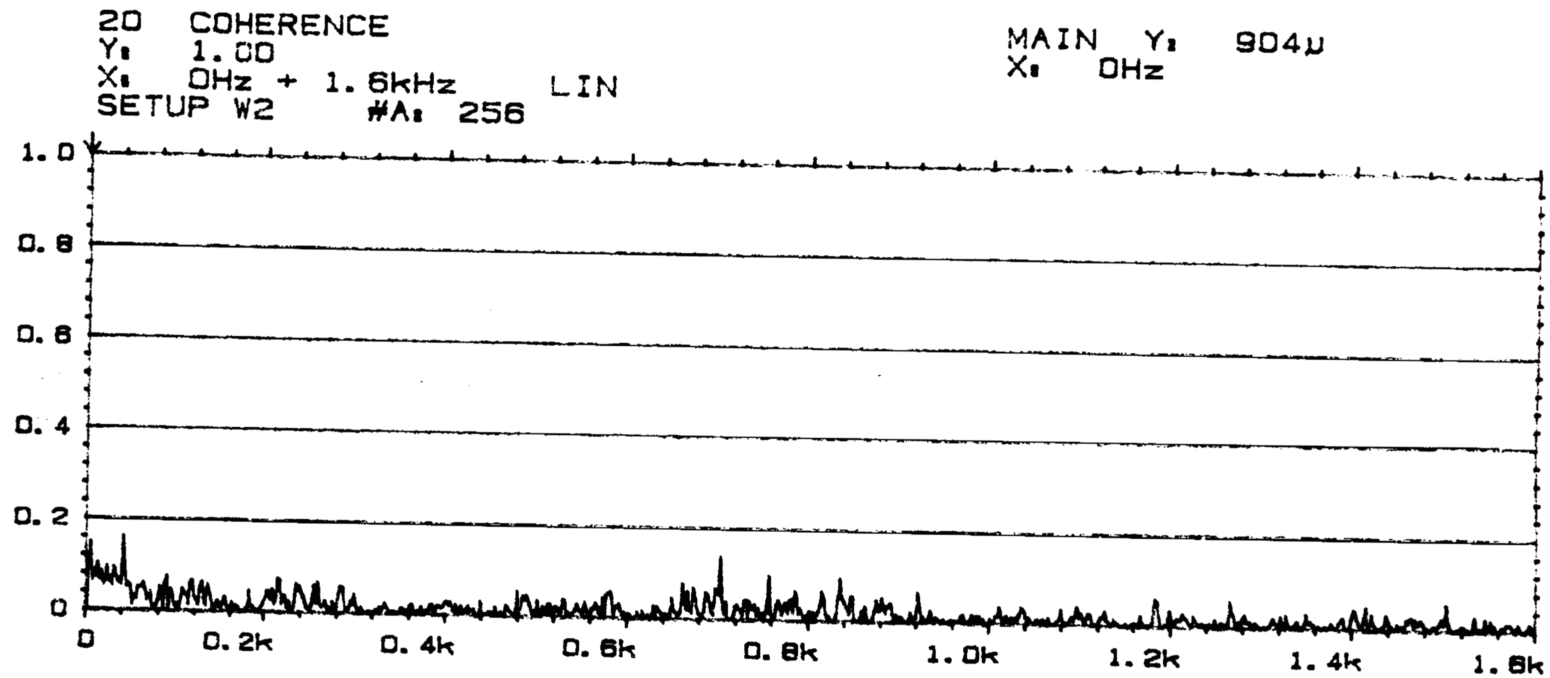

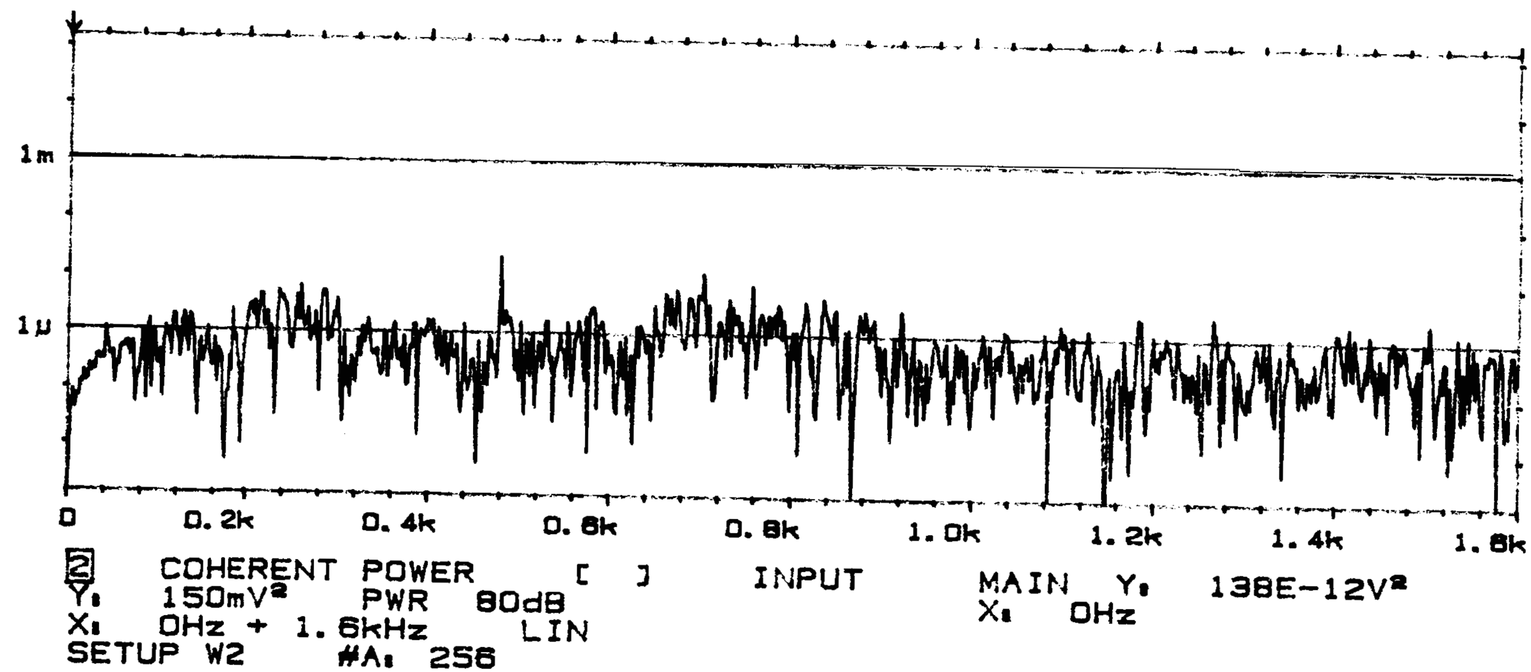

Type 2032

Page No.
108

Sign.:

Meas.
Object:

PLF PF1.5
ChA 115
ChB 104

Rdg 183

Comments:

20 COHERENCE
Y: 1.00
X: 0Hz + 1.6kHz LIN
SETUP W2 #A: 256

MAIN Y: 4.19m
X: 0Hz

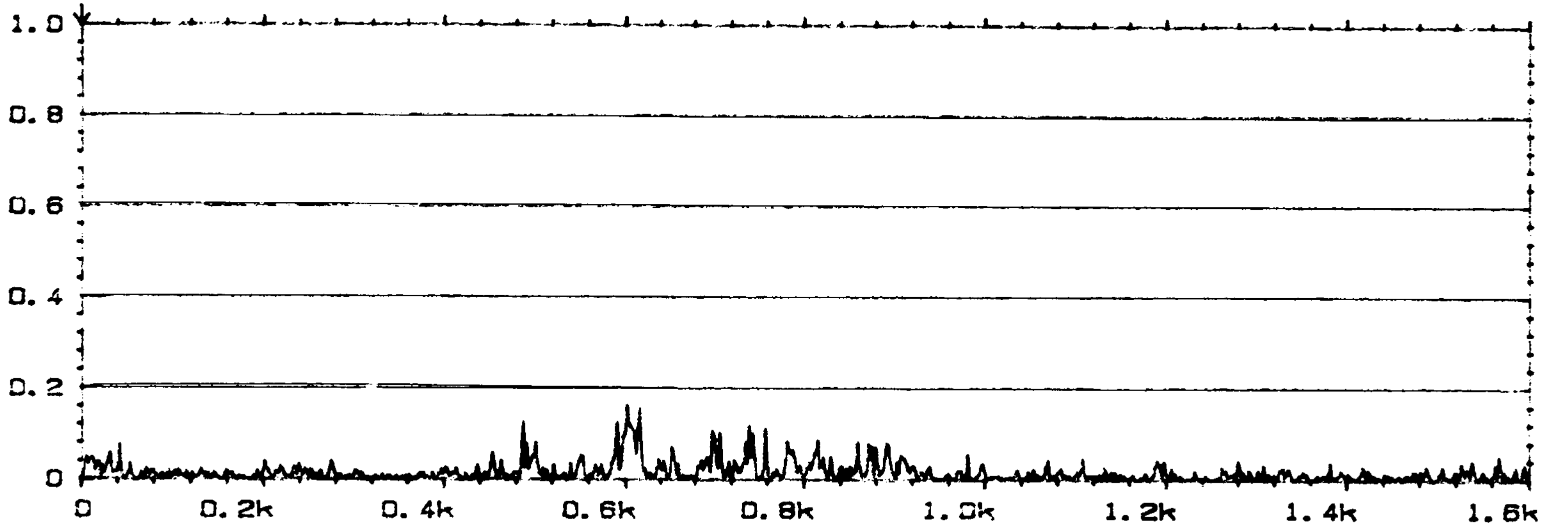

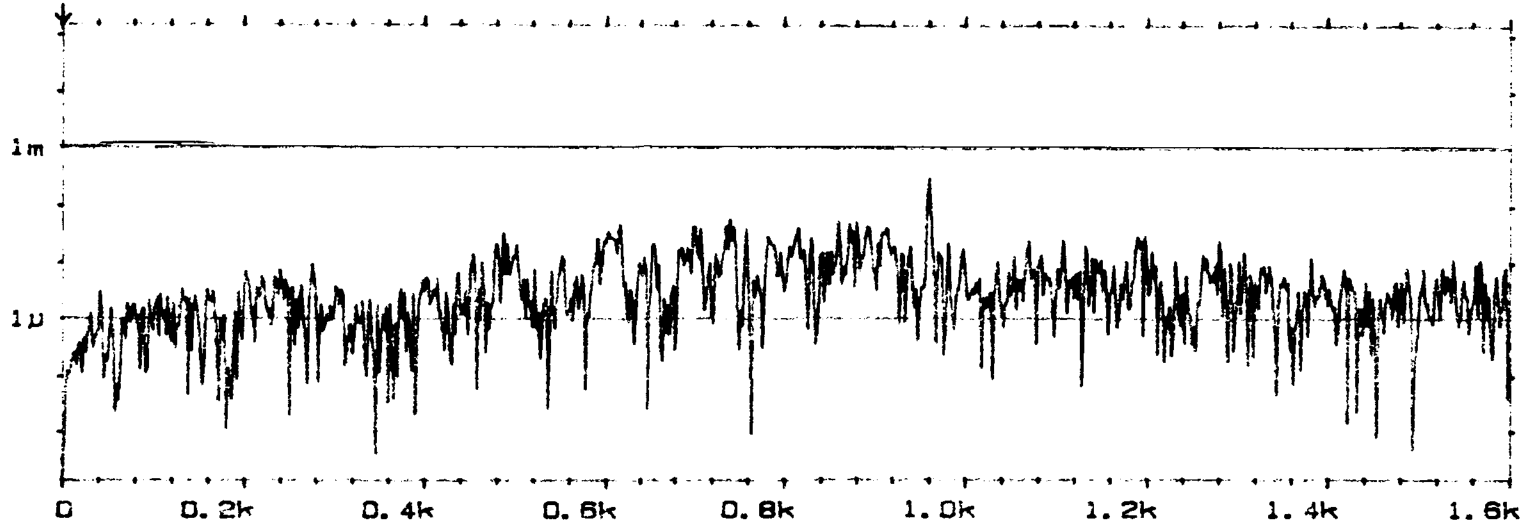

2 COHERENT POWER [ ] INPUT
Y: 150mV² PWR 80dB
X: 0Hz + 1.6kHz LIN
SETUP W2 #A: 256

MAIN Y: 3.36E-9V²
X: 0Hz

Type 2032

Page No.
124

Sign.:

Meas.
Object:

PLF PR 3.0
ChA=T16
ChB=M1

Rdg 195

Comments:

2D COHERENCE
Y: 1.00
X: 0Hz + 1.6kHz LIN
SETUP W2 #A: 256

MAIN Y: 17.0m
X: 0Hz

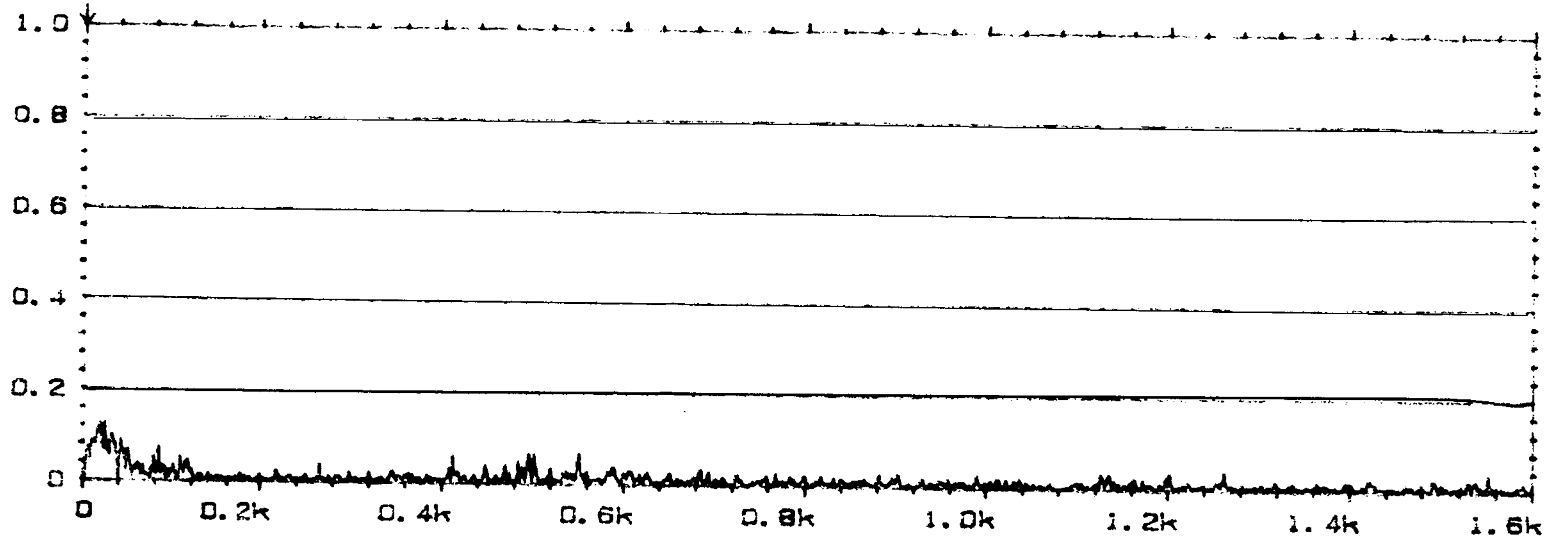

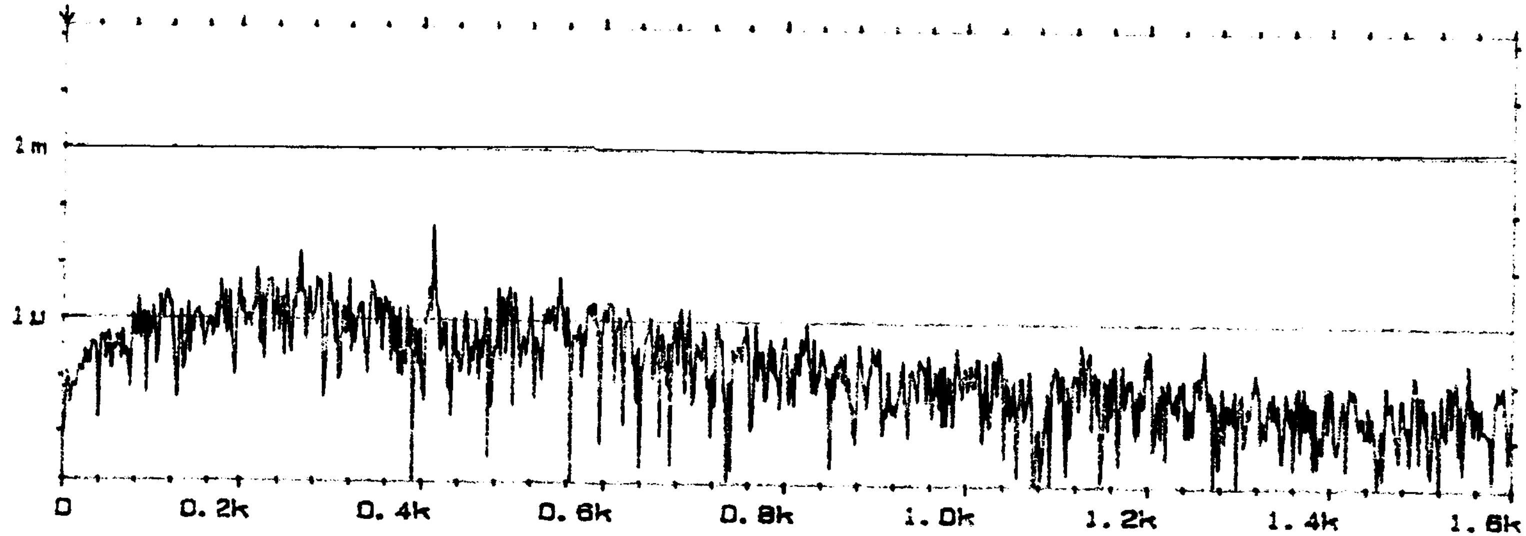

2 COHERENT POWER [ ] INPUT
Y: 150mV² PWR 80dB
X: 0Hz + 1.6kHz LIN
SETUP W2 #A: 256

MAIN Y: 7.96E-9V²
X: 0Hz

Type 2032

Page No.
121

Sign.:

Meas.
Object:

PLF PR 3.0
ChA=T10
ChB=M2

Rdg 185

Comments:

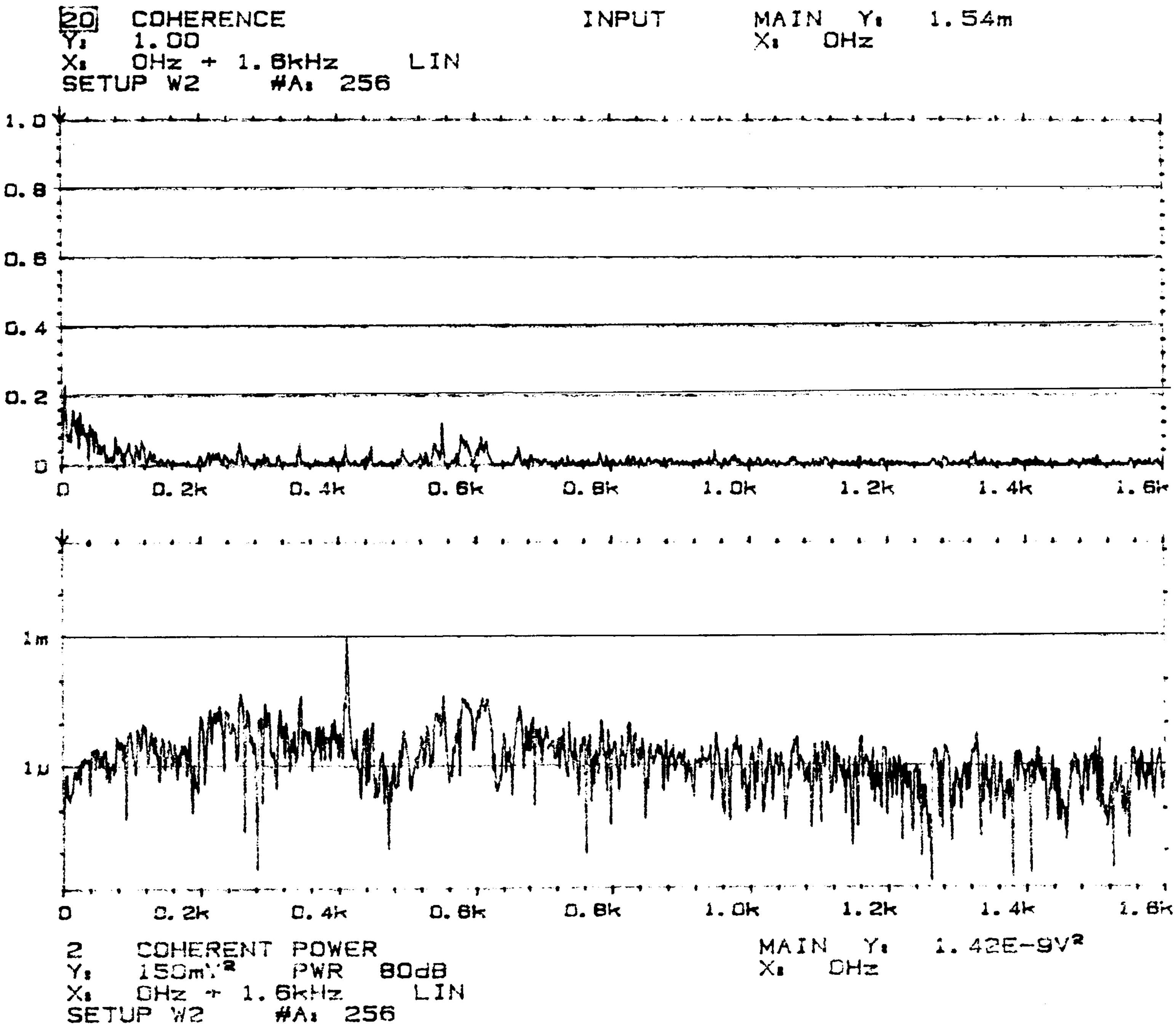

Type 2032

Page No.
120

Sign.:

Meas.
Object:

PLE PR 3.0
ChA=T10
ChB=M3

Rdg 185

Comments:

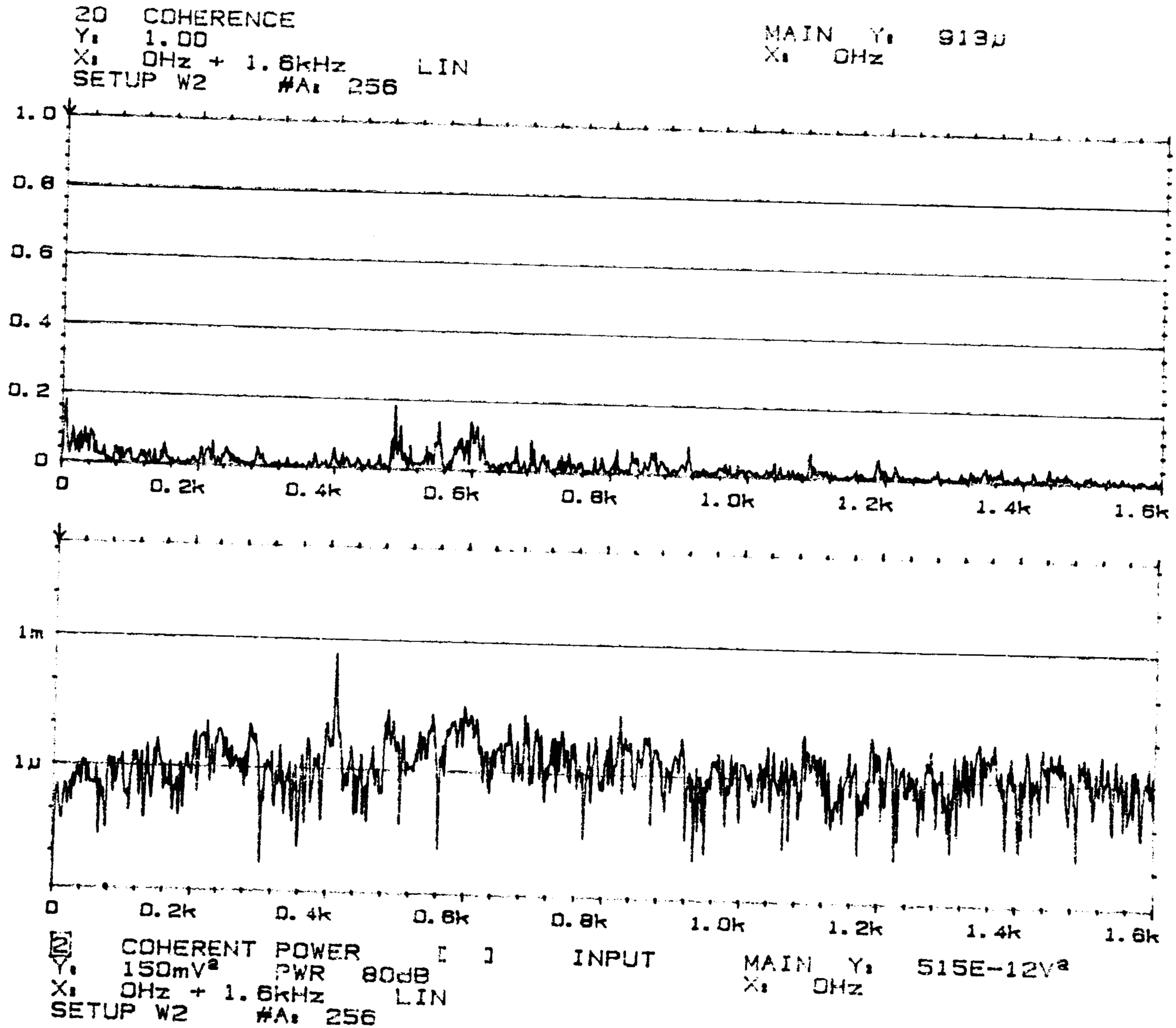

Type 2032

Page No.
118

Sign.:

Meas.
Object:
PLF PR 3.0
ChA=110
ChB=M9

Kdg 185

Comments:

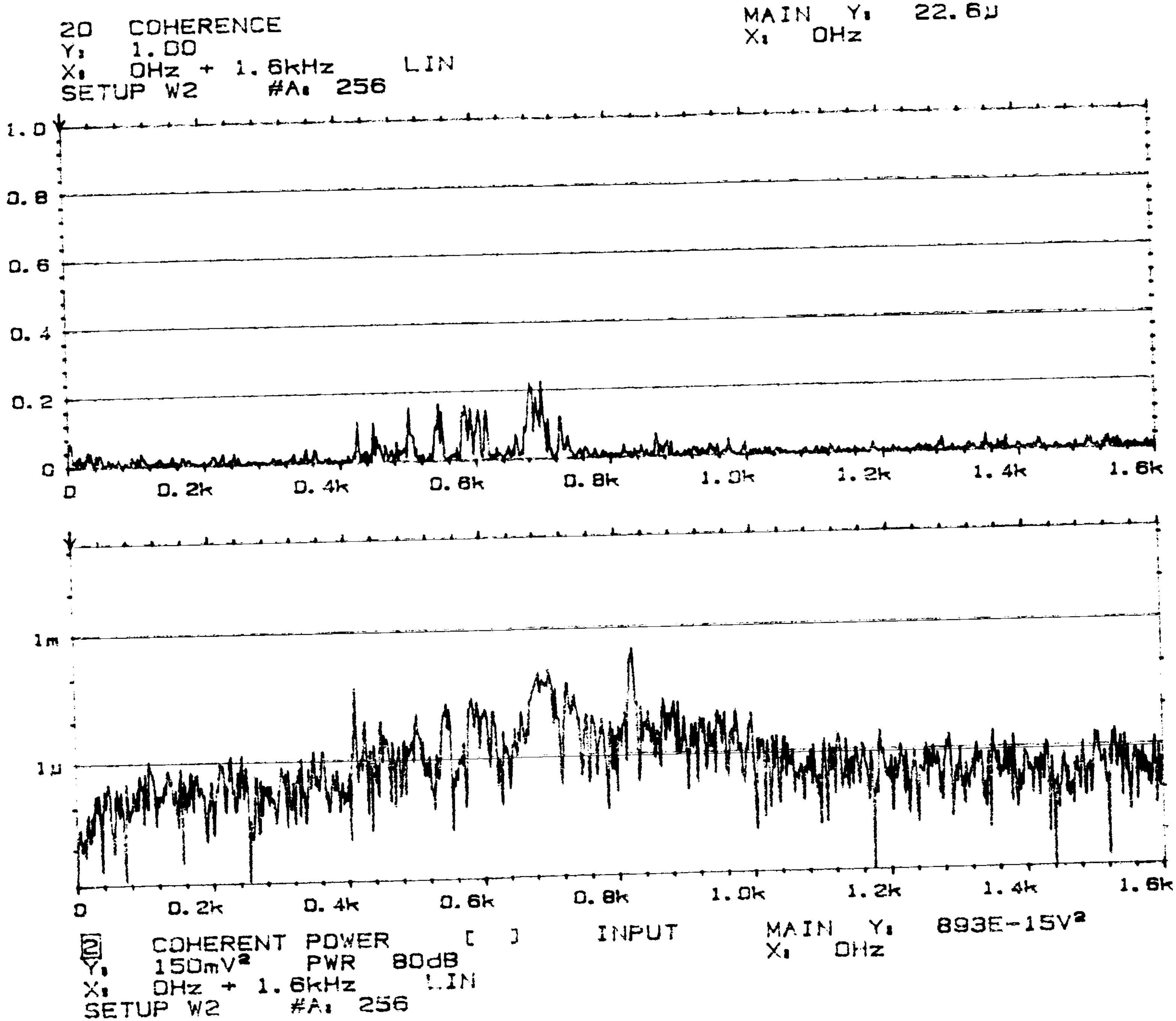

ORIGINAL PAGE IS
OF POOR QUALITY

Type 2032

Page No.
126

Sign.:

Meas.
Object:

PLF PR3.1
ChA = T10
ChB = M1

Rdg 186

Comments:

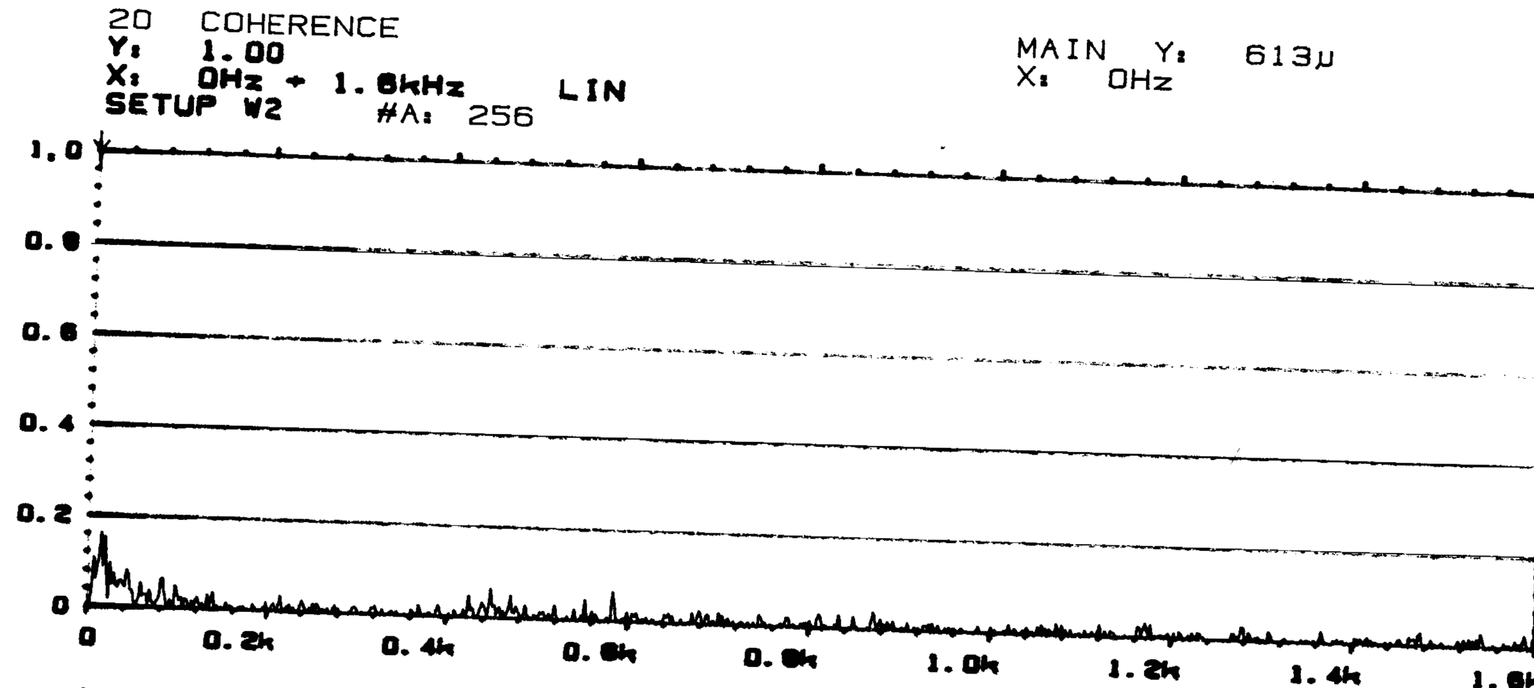

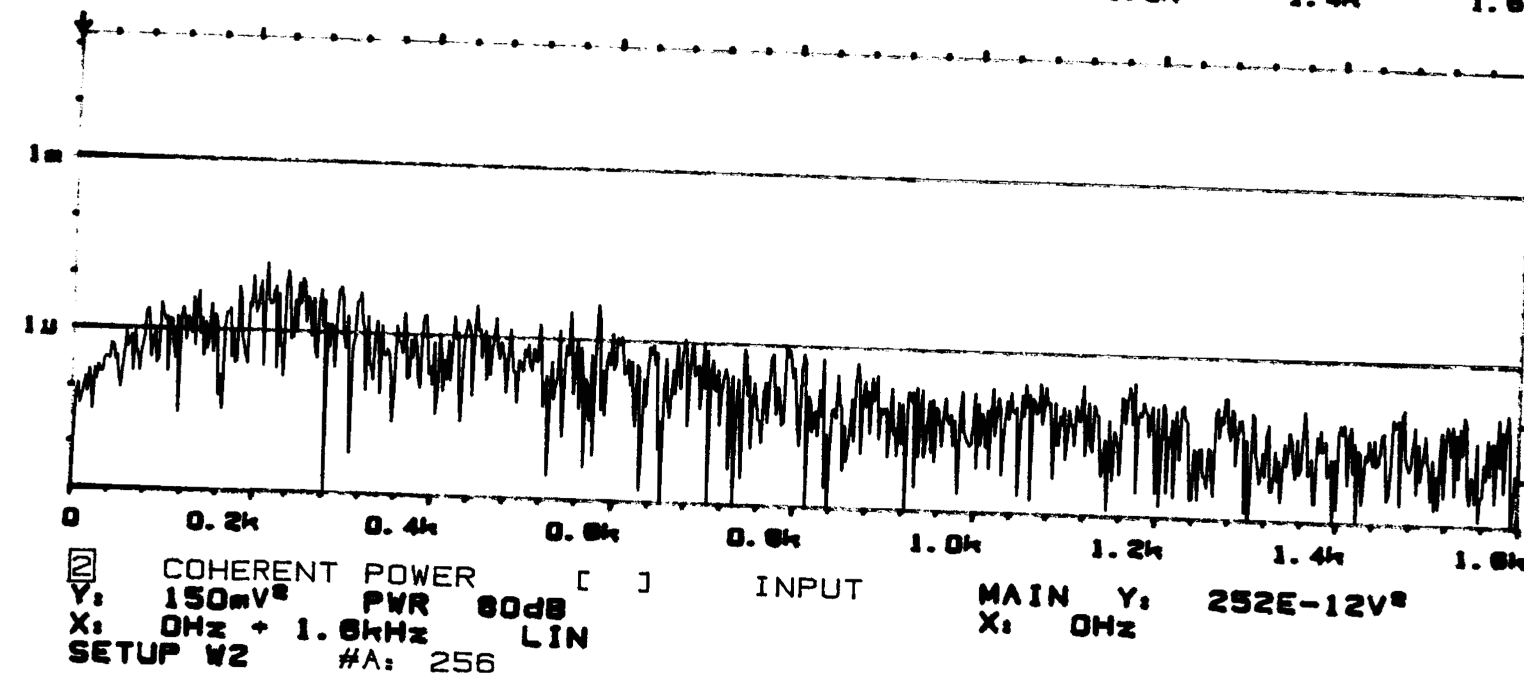

20 COHERENCE
Y: 1.00
X: 0Hz → 1.6kHz LIN
SETUP W2 #A: 256

MAIN Y: 7.00m
X: 0Hz

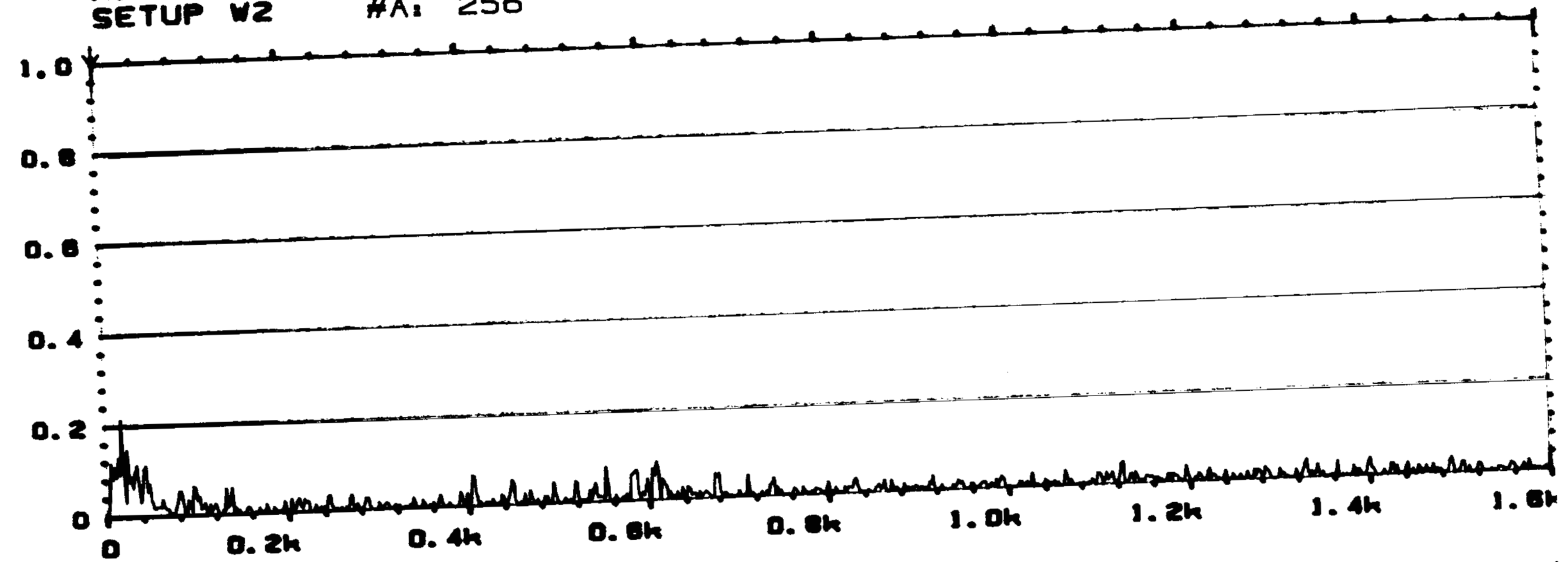

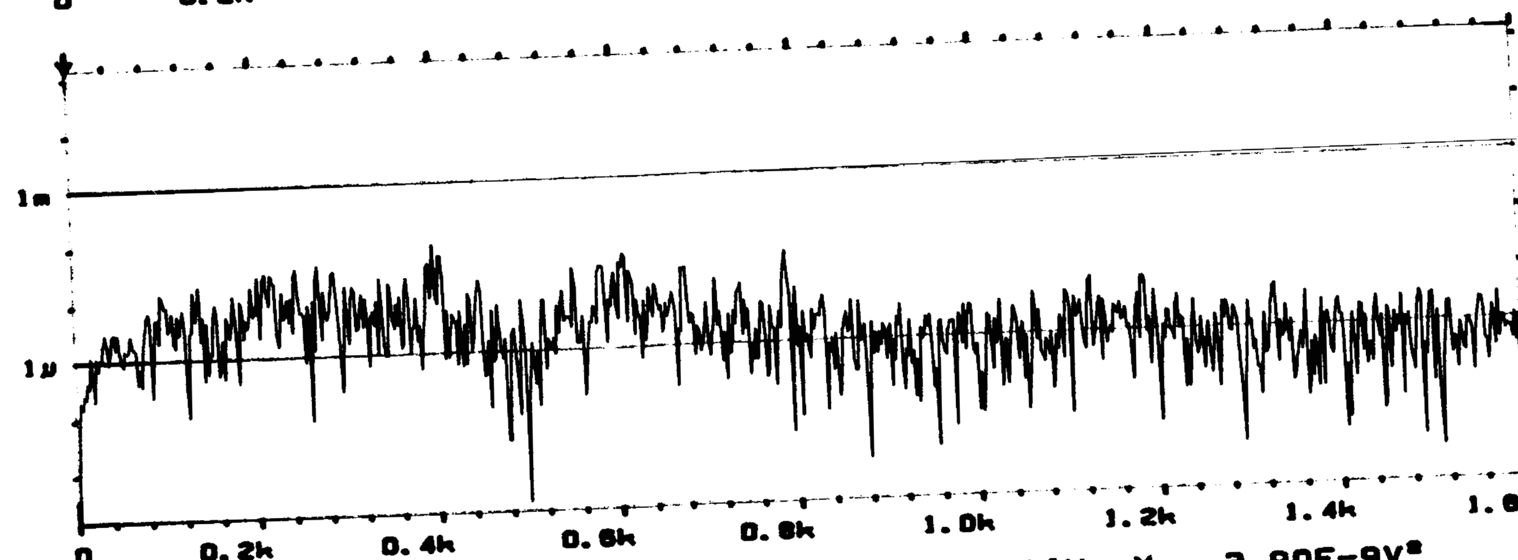

2 COHERENT POWER [ ] INPUT
Y: 150mV² PWR 80dB
X: 0Hz → 1.6kHz LIN
SETUP W2 #A: 256

MAIN Y: 3.90E-9V²
X: 0Hz

Type 2032

Page No.
2

Sign.:

Meas.
Object:
PLF PR3.1
ChA= T1D
ChB= M2

Rdg 186

Comments:

Type 2032

Page No.
5

Sign.:

Meas.
Object:
PLF PR 3.1
ChA=T10
ChB=M3

Rdg 186

Comments:

20 COHERENCE
Y: 1.00
X: 0Hz → 1.6kHz LIN
SETUP W2 #A: 256

MAIN Y: 3.72m
X: 0Hz

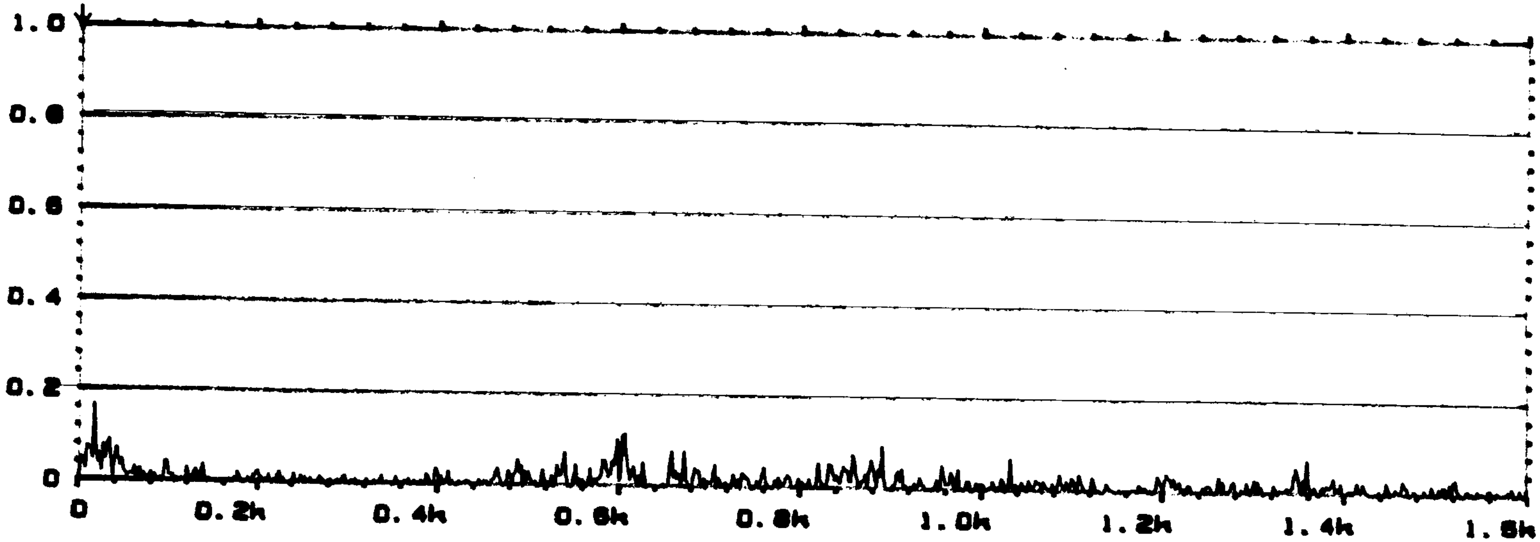

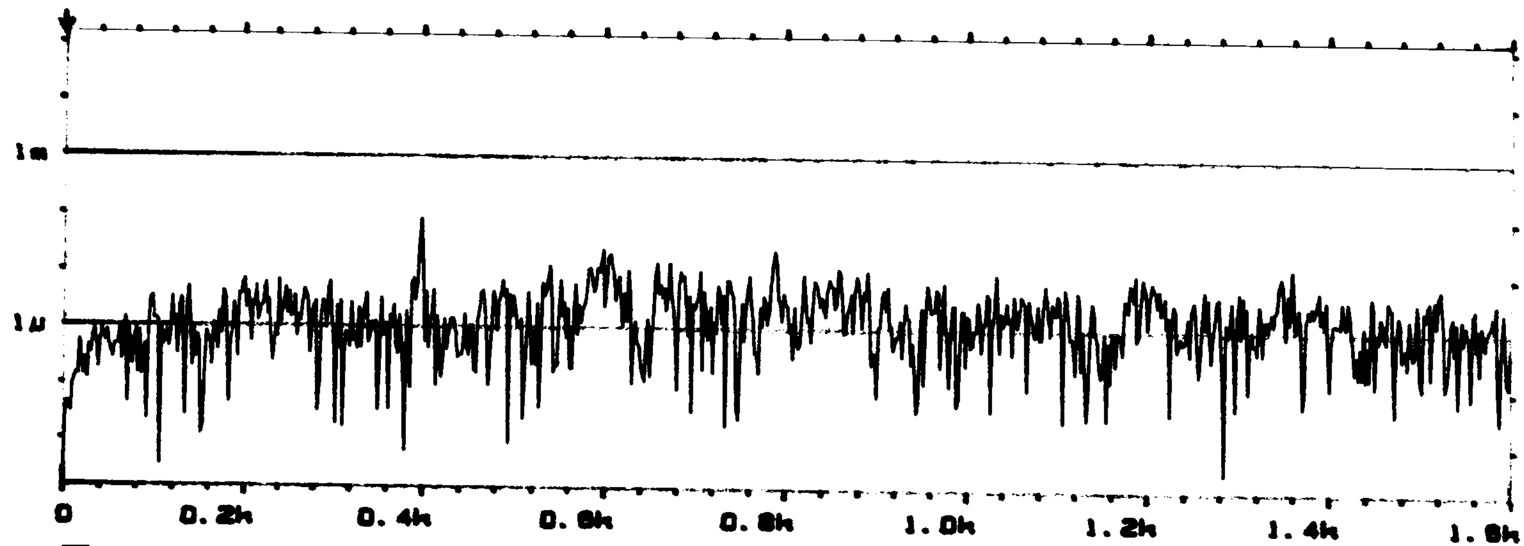

2 COHERENT POWER [ ] INPUT
Y: 150mV² PWR 80dB
X: 0Hz → 1.6kHz LIN
SETUP W2 #A: 256

MAIN Y: 3.06E-9V²
X: 0Hz

Type 2032

Page No.
8

Sign.:

Meas.
Object:
PLF PR 3.1
ChA= T14
ChB= M4

Seq 186

Comments:

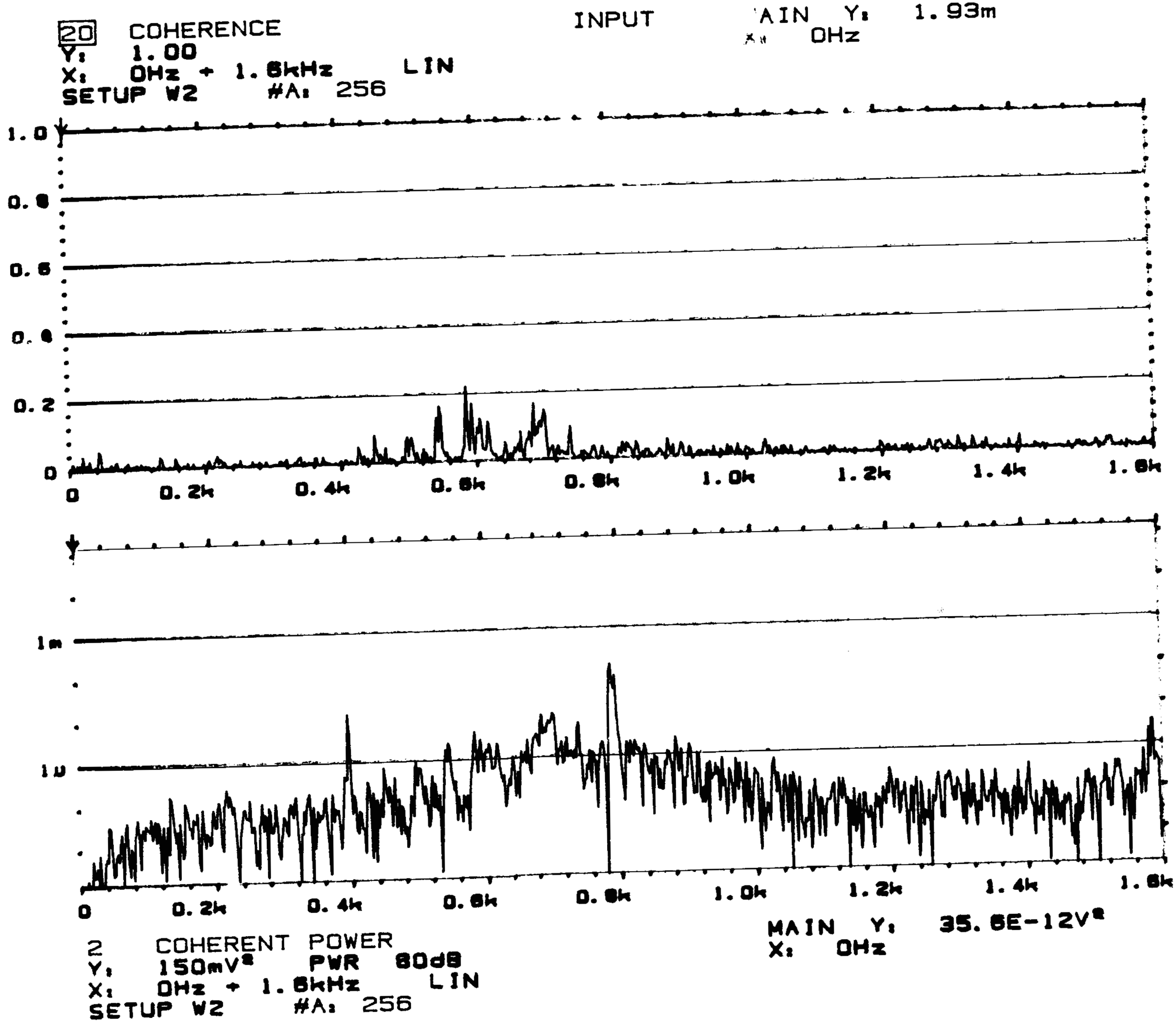

Type 2032

Page No.
76

Sign.:

Meas.
Object:
PLF PR 3.5
ChA = T10
ChB = M1

Pdg 187

Comments:

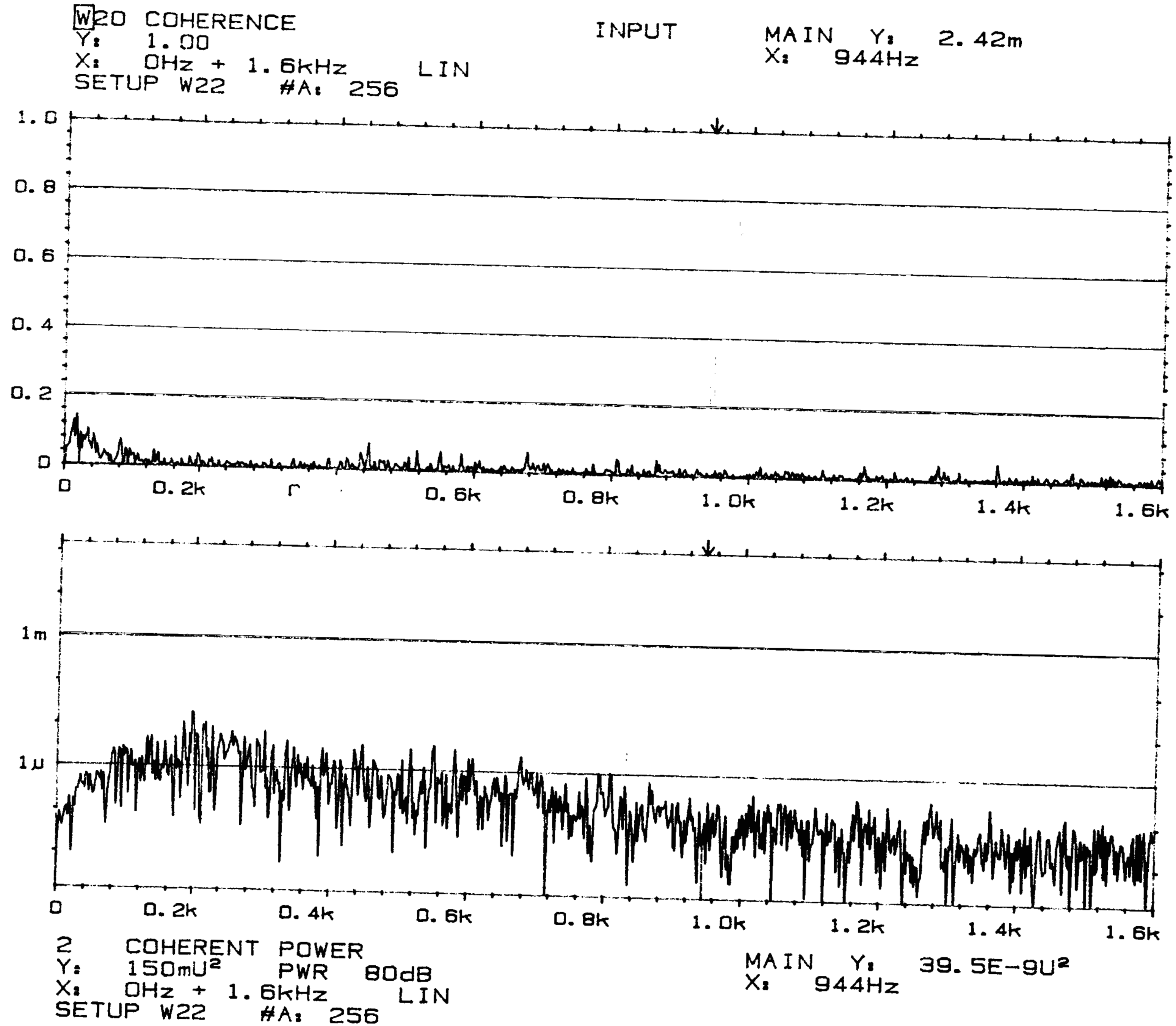

ORIGINAL PAGE IS
OF POOR QUALITY

Type 2032

Page No.
78

Sign.:

Meas.
Object:

PLF PR3.5
ChA = T10
ChB = M2

Rdg 187

Comments:

W20 COHERENCE
Y: 1.00
X: 0Hz + 1.6kHz LIN
SETUP W22 #A: 256

INPUT

MAIN Y: 6.35m
X: 944Hz

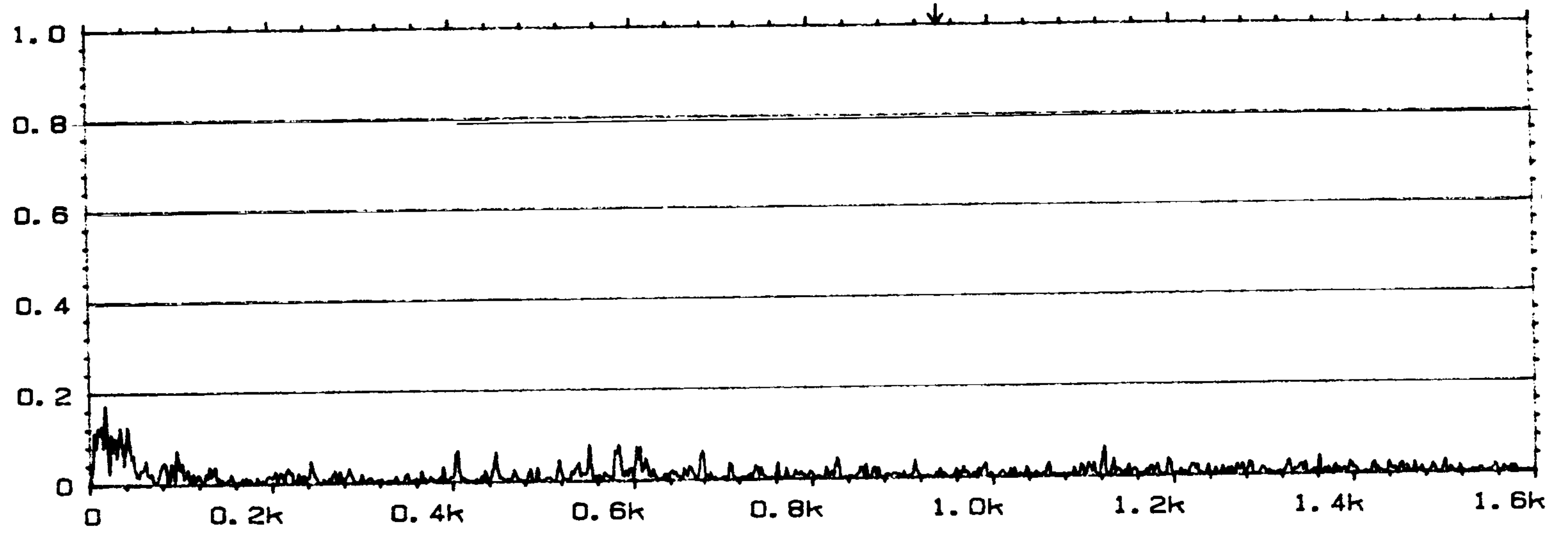

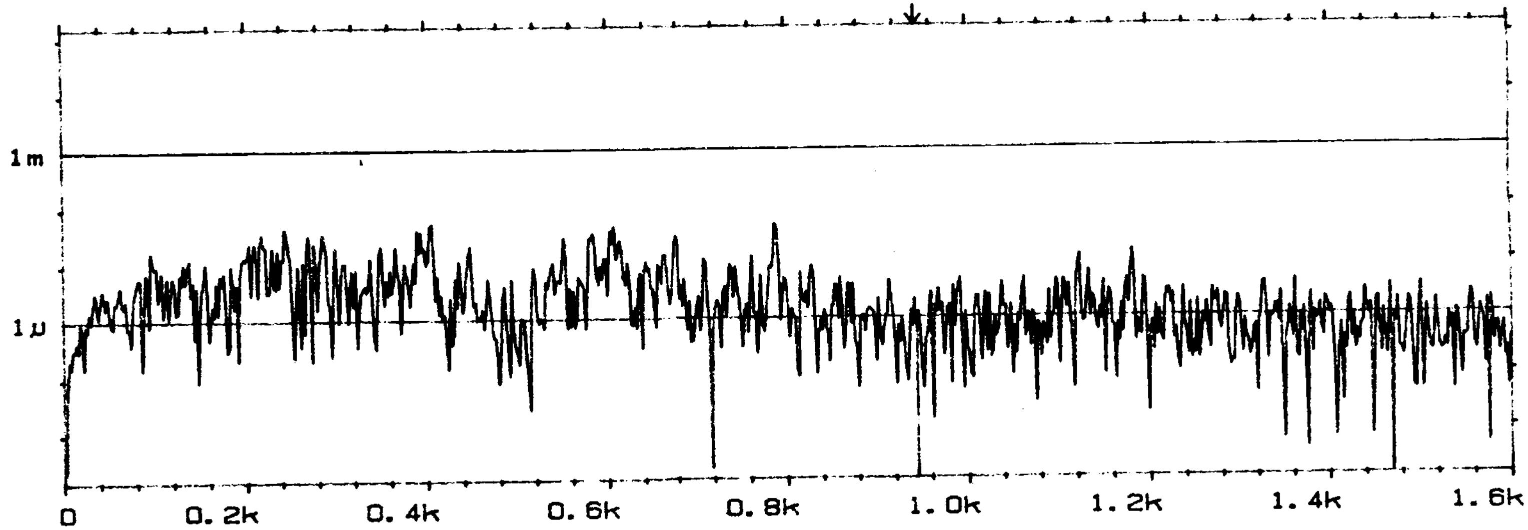

2 COHERENT POWER
Y: 150mU² PWR 80dB
X: 0Hz + 1.6kHz LIN
SETUP W22 #A: 256

MAIN Y: 731E-9U²
X: 944Hz

Type 2032

Page No.
80

Sign.:

Meas.
Object:

PLF PR 3.5
ChA = T16
ChB = M3

Rdg 187

Comments:

W20 COHERENCE INPUT MAIN Y: 337μ
Y: 1.00
X: 0Hz + 1.6kHz LIN X: 944Hz
SETUP W22 #A: 256

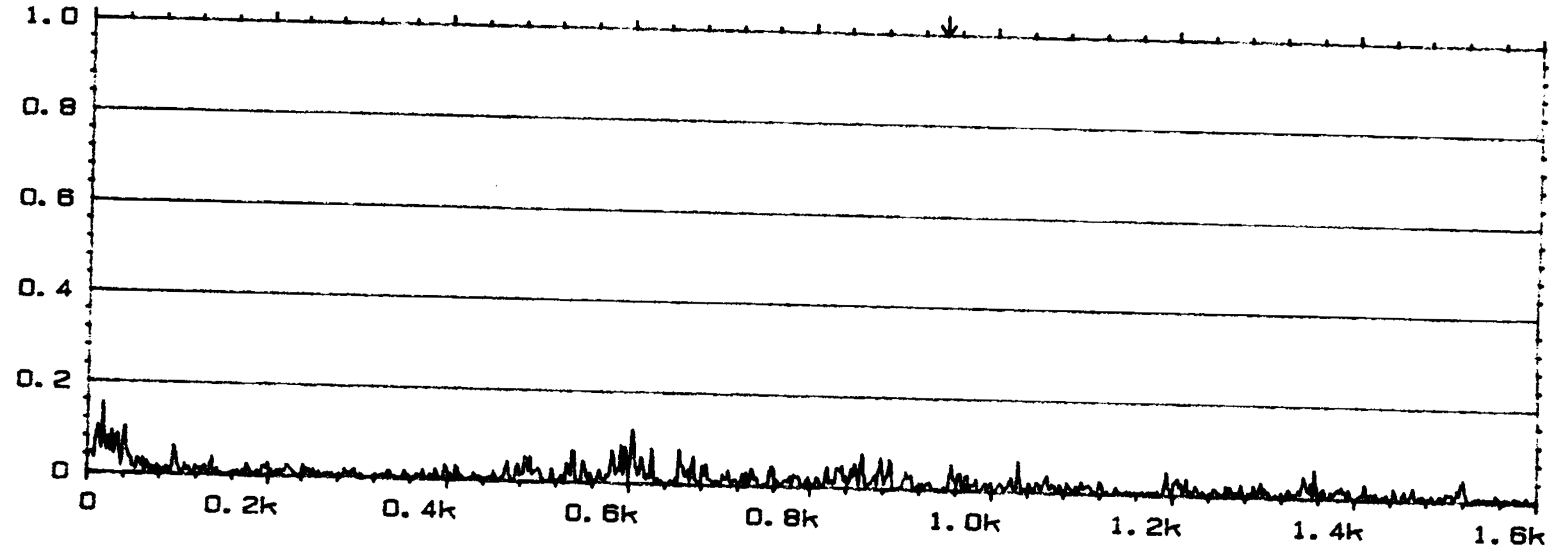

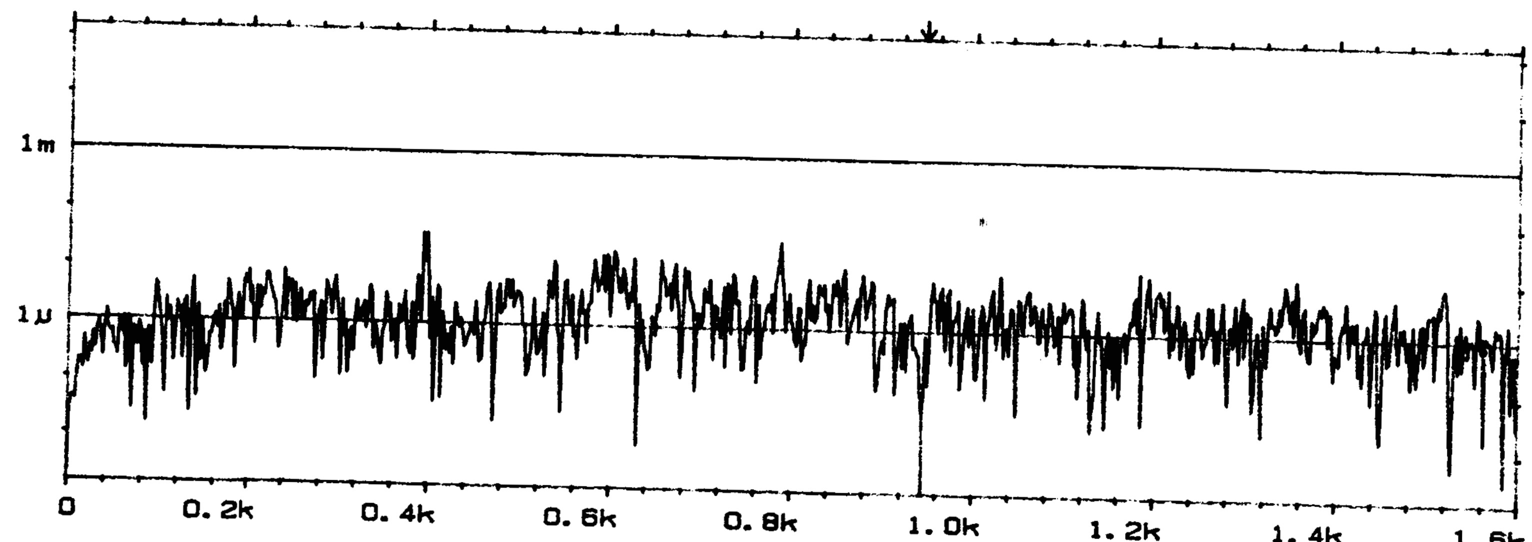

2 COHERENT POWER MAIN Y: 43.2E-9U²
Y: 150mU² PWR 80dB X: 944Hz
X: 0Hz + 1.6kHz LIN
SETUP W22 #A: 256

W20 COHERENCE INPUT MAIN Y: 103m
Y: 1.00 X: 704Hz
X: 0Hz + 1.6kHz LIN
SETUP W22 #A: 256

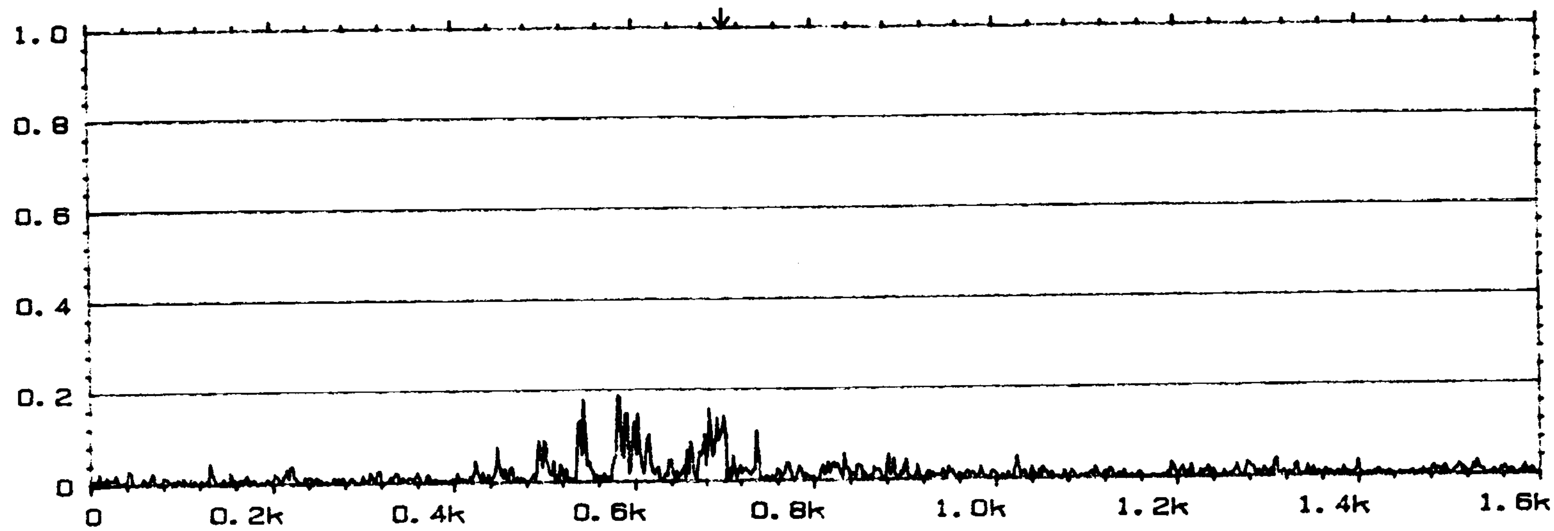

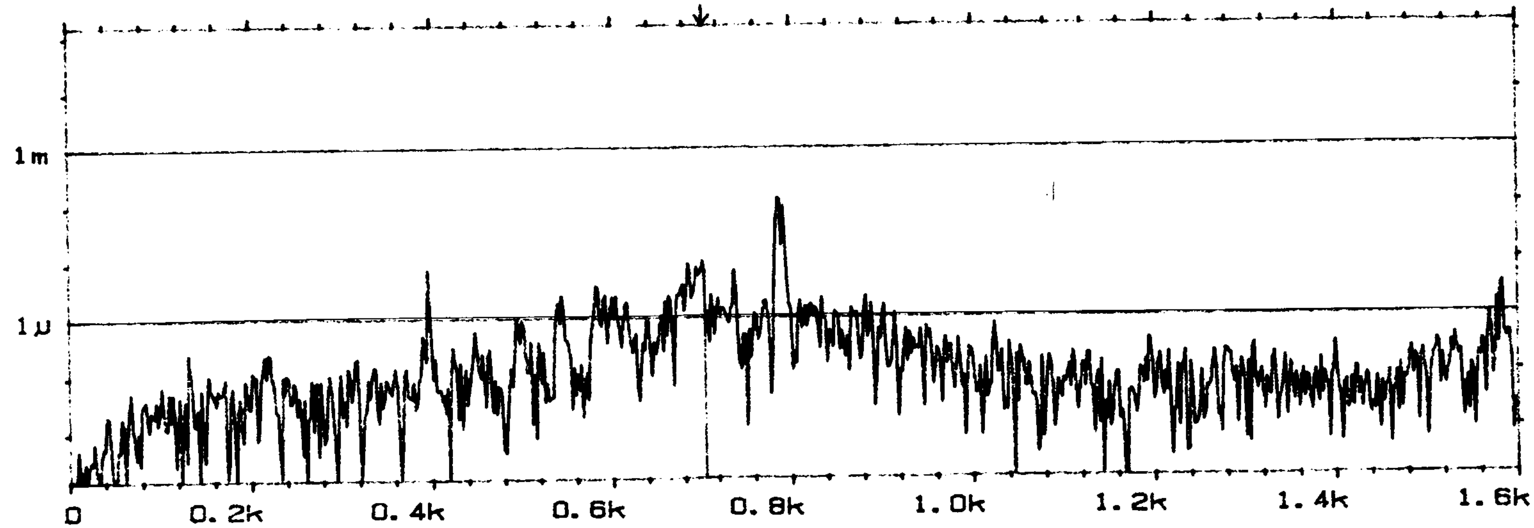

2 COHERENT POWER MAIN Y: 6.86μU²
Y: 150mU² PWR 80dB X: 704Hz
X: 0Hz + 1.6kHz LIN
SETUP W22 #A: 256

Type 2032

Page No.
82

Sign.:

Meas.
Object:
PLF PR 35
CA T16
CE 114

Rdg 187

Comments:

APPENDIX E

SAMPLE NARROW-BAND SPECTRA

Type 2032

Page No.
15

Sign.:

Meas.
Object:

PLF PR 1.2
ChA = T10
ChB = M1

Rdg 176

Comments:

11 AUTO SPEC CH. A [ ] INPUT MAIN Y: -48.9dB
Y: 20.0dB /1.00V RMS 80dB X: 112Hz
X: 0Hz + 1.6kHz LIN
SETUP W2 #A: 256

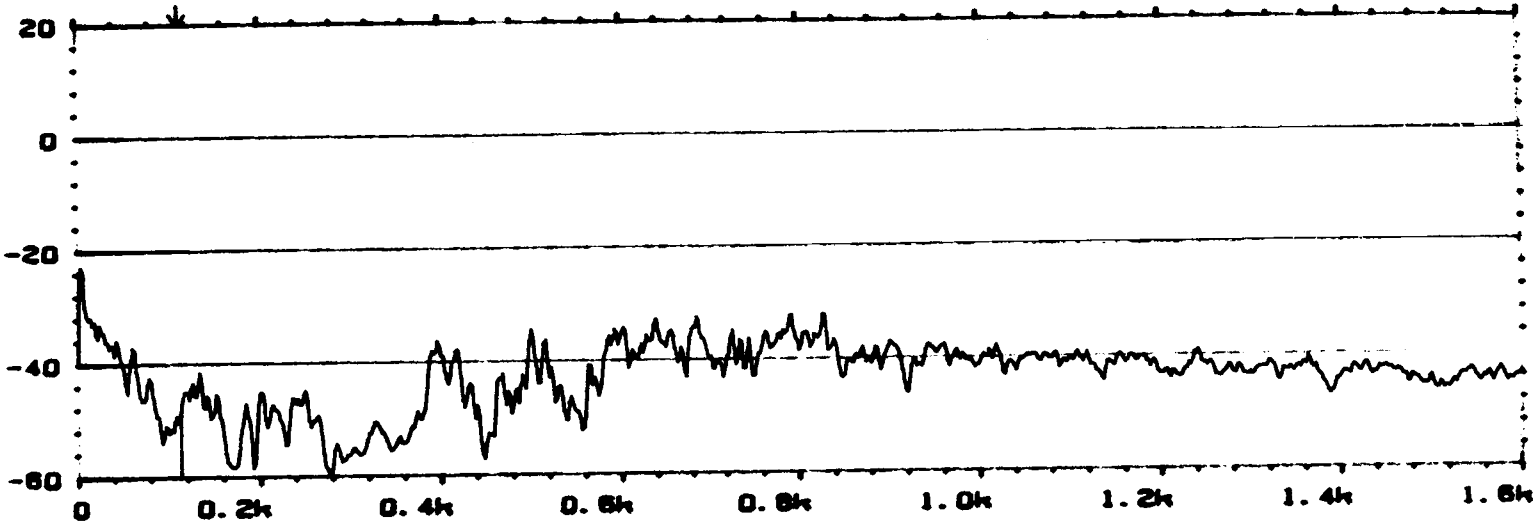

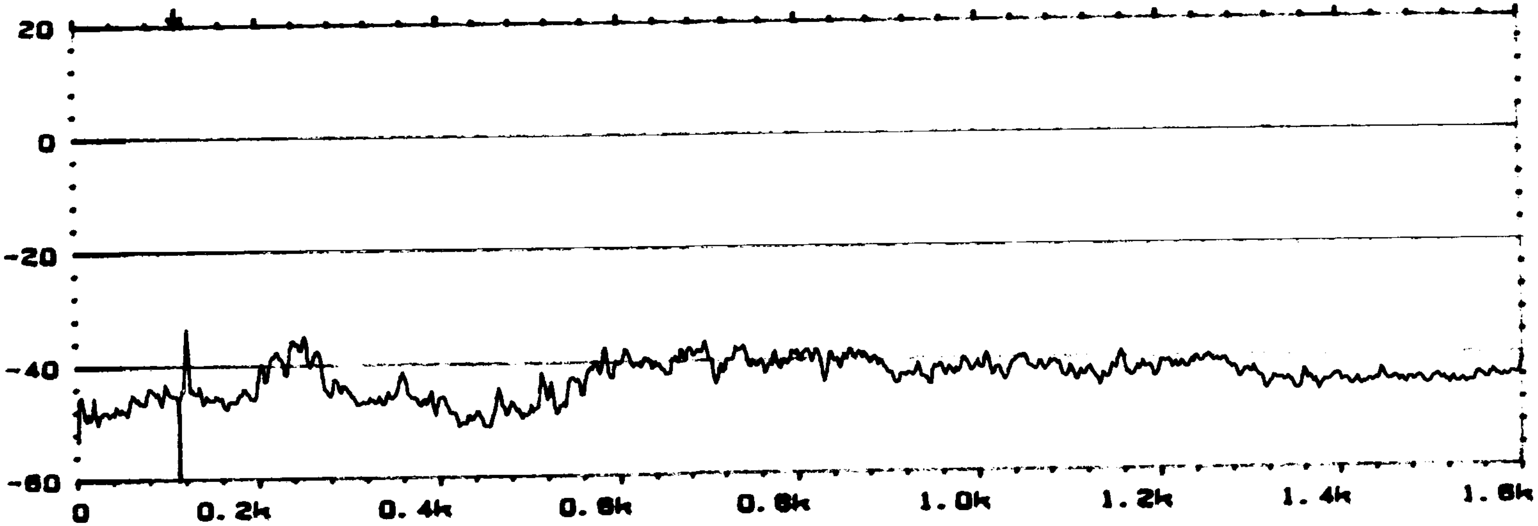

10 AUTO SPEC CH. B MAIN Y: -45.6dB
Y: 20.0dB /1.00V RMS 80dB X: 112Hz
X: 0Hz + 1.6kHz LIN
SETUP W2 #A: 256

Type 2032

Page No.
18

Sign.:

Meas.
Object:

PLF PR 1.2
ChA=T10
ChB=M2

Rdg 176

Comments:

11 AUTO SPEC CH. A [ ] INPUT MAIN Y: -45.5dB
Y: 20.0dB /1.00V RMS 80dB X: 120Hz
X: 0Hz + 1.6kHz LIN
SETUP W2 #A: 256

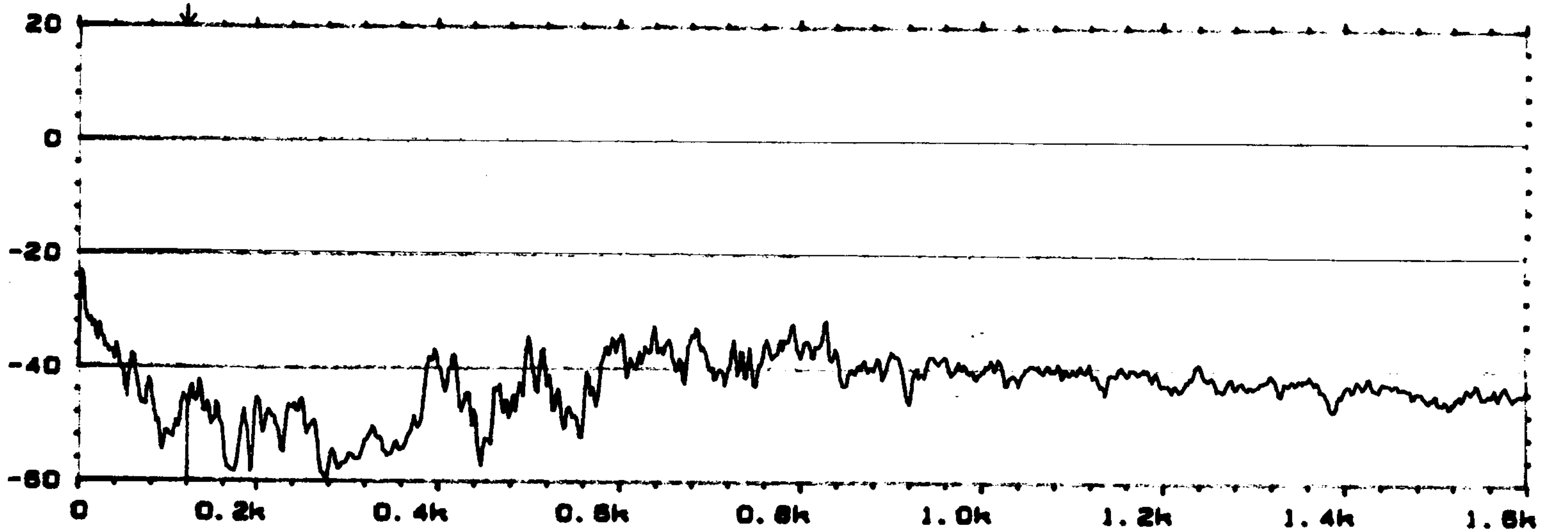

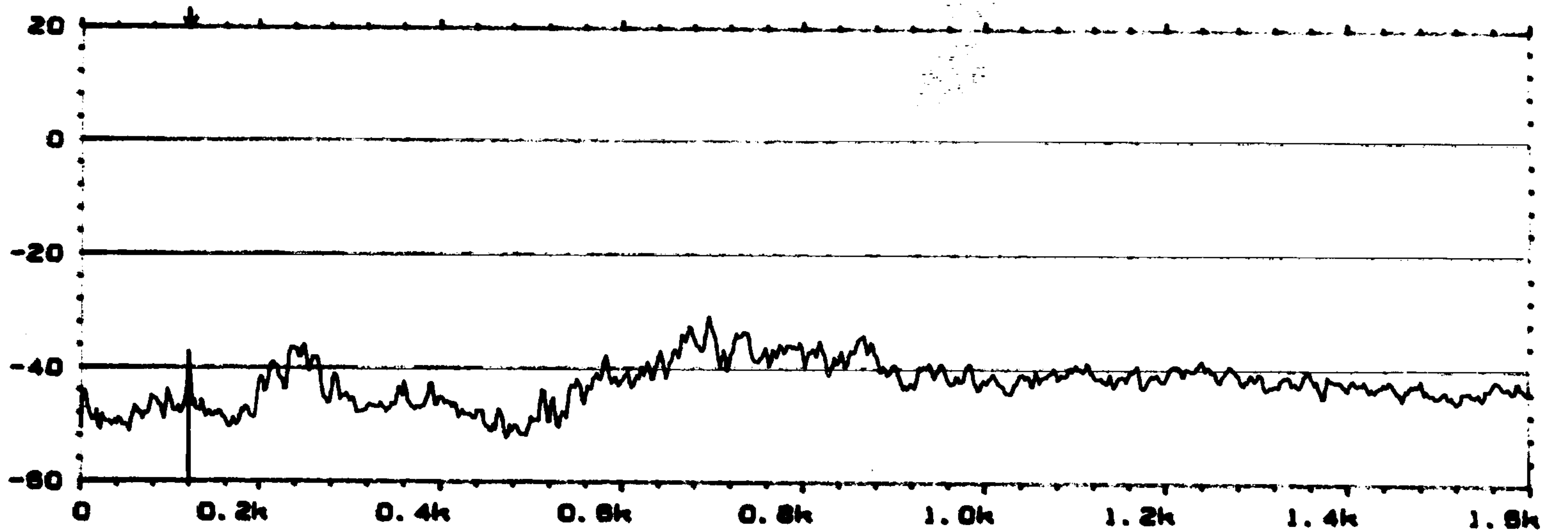

10 AUTO SPEC CH. B MAIN Y: -37.0dB
Y: 20.0dB /1.00V RMS 80dB X: 120Hz
X: 0Hz + 1.6kHz LIN
SETUP W2 #A: 256

Type 2032

Page No.
17

Sign.:

Meas.
Object:

PLF PR 1.2
ChA = 710
Ch B = M3

Fdg 176

Comments:

11 AUTO SPEC CH. A [ ] INPUT MAIN Y: -45.4dB
Y: 20.0dB /1.00V RMS 80dB X: 120Hz
X: 0Hz + 1.6kHz LIN
SETUP W2 #A: 256

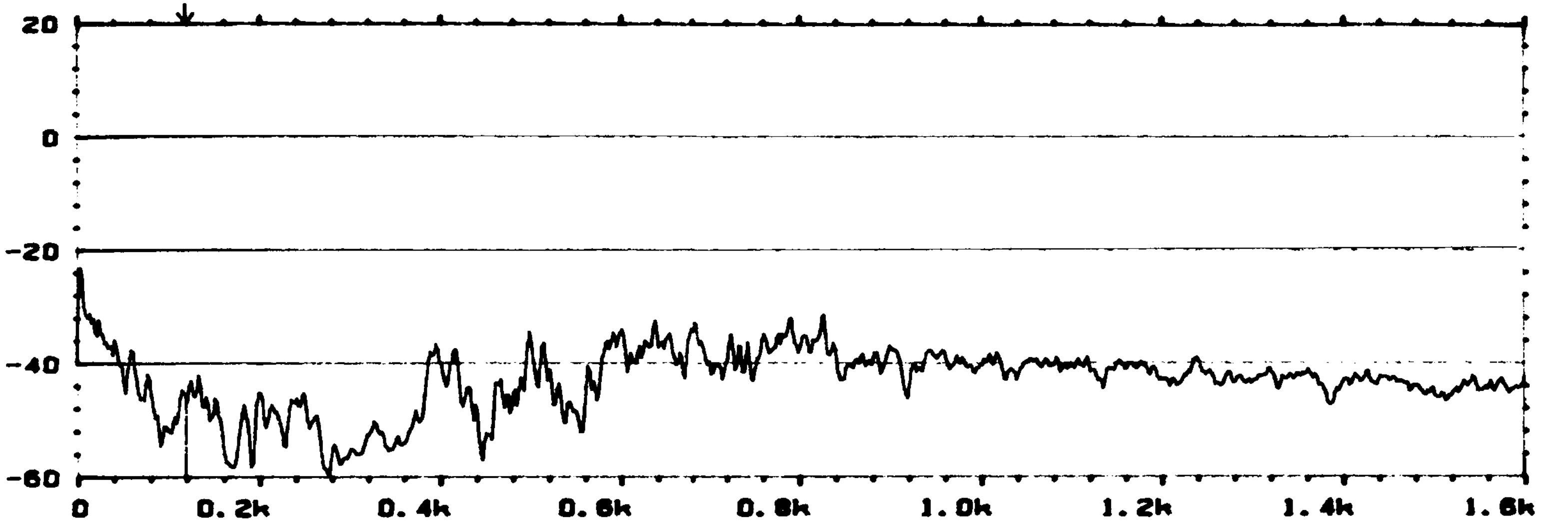

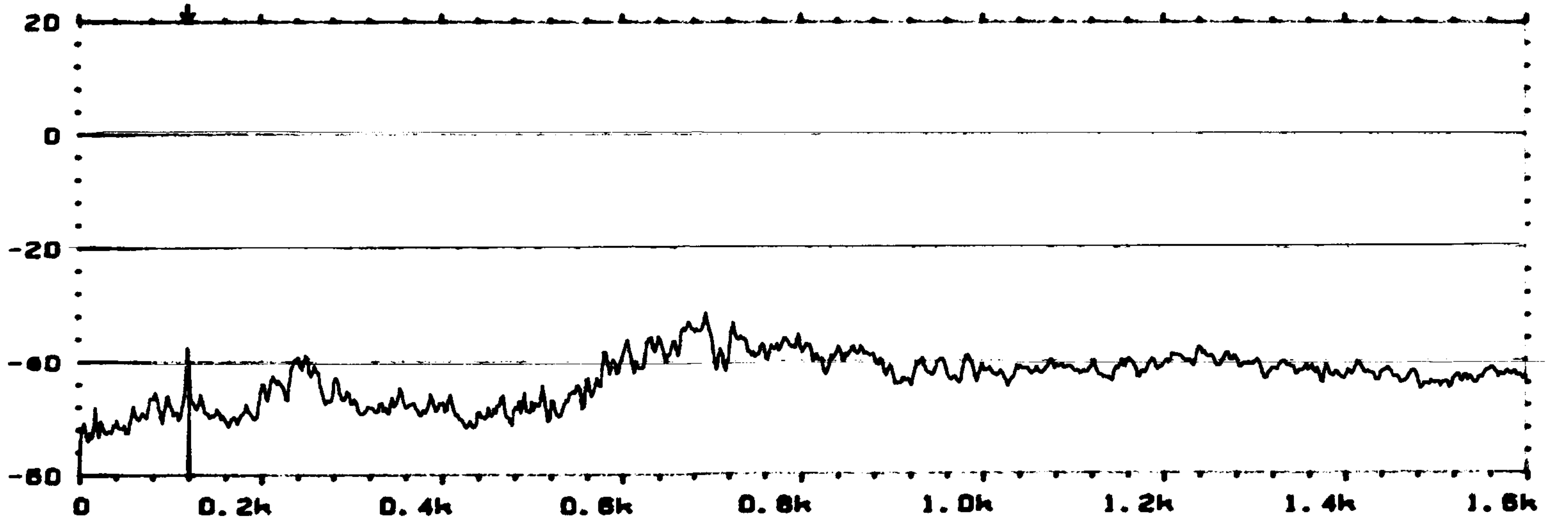

10 AUTO SPEC CH. B MAIN Y: -37.4dB
Y: 20.0dB /1.00V RMS 80dB X: 120Hz
X: 0Hz + 1.6kHz LIN
SETUP W2 #A: 256

Type 2032

Page No.
16

Sign.:

Meas.
Object:

PLF PR 1.2
ChA = T10
ChB = M4

Rdg 176

Comments:

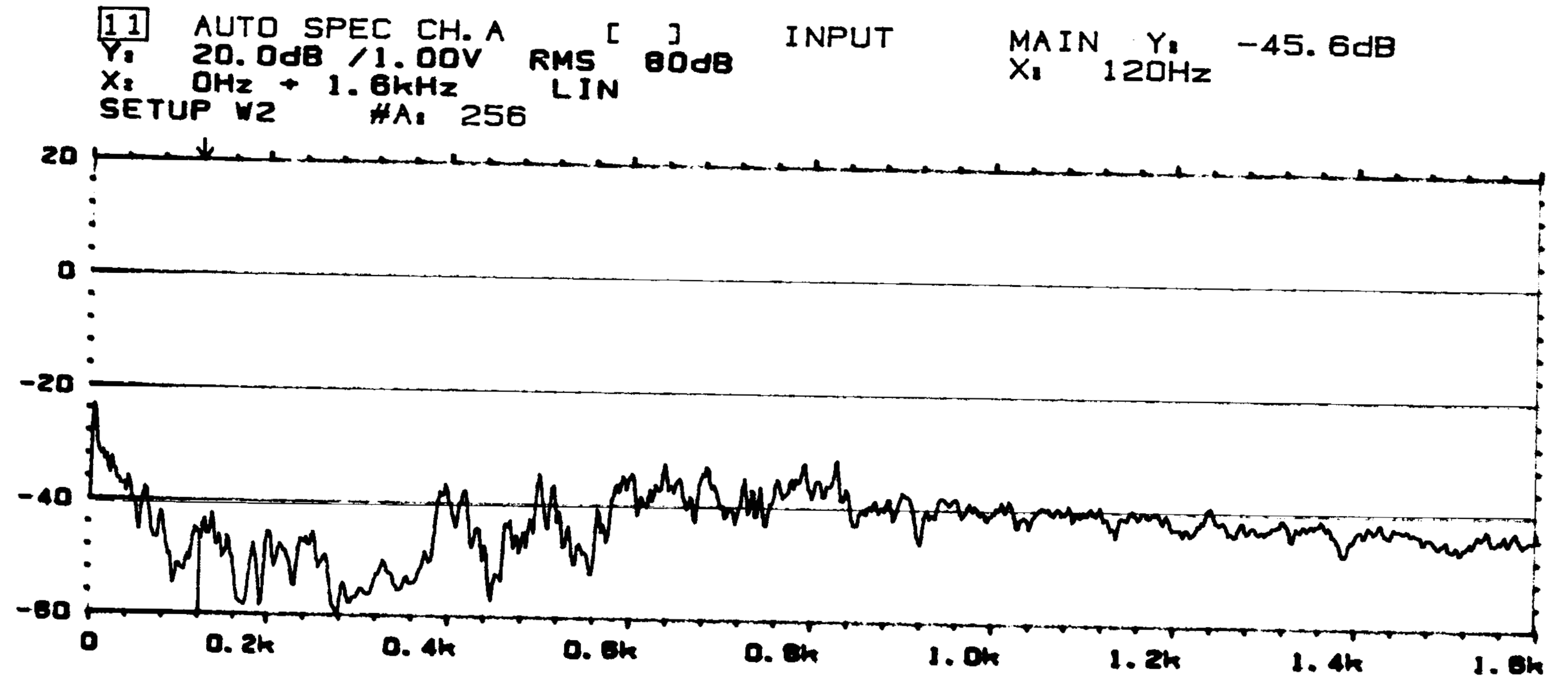

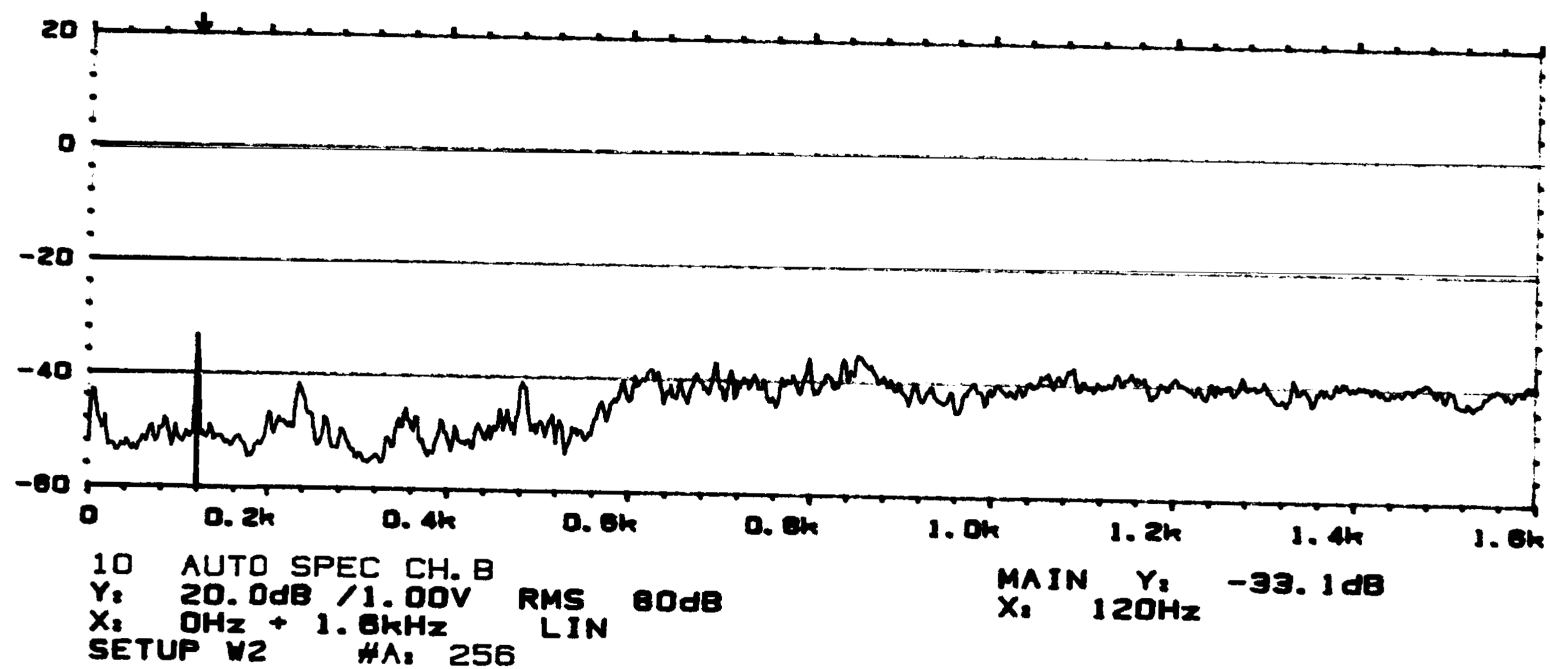

Type 2032

Page No.
127

Sign.:

Meas.
Object:

PLF PR 3.1
ChA - T1D
ChB = M1

Rdg 186

Comments:

WB AUTO SPEC CH. A [ ] INPUT
Y: 20.0dB /1.00V RMS 80dB
X: 0Hz + 1.6kHz LIN
SETUP W2 #A: 256

HARM Y: -37.7dB
X: 792Hz
ΔX: 396.0000Hz

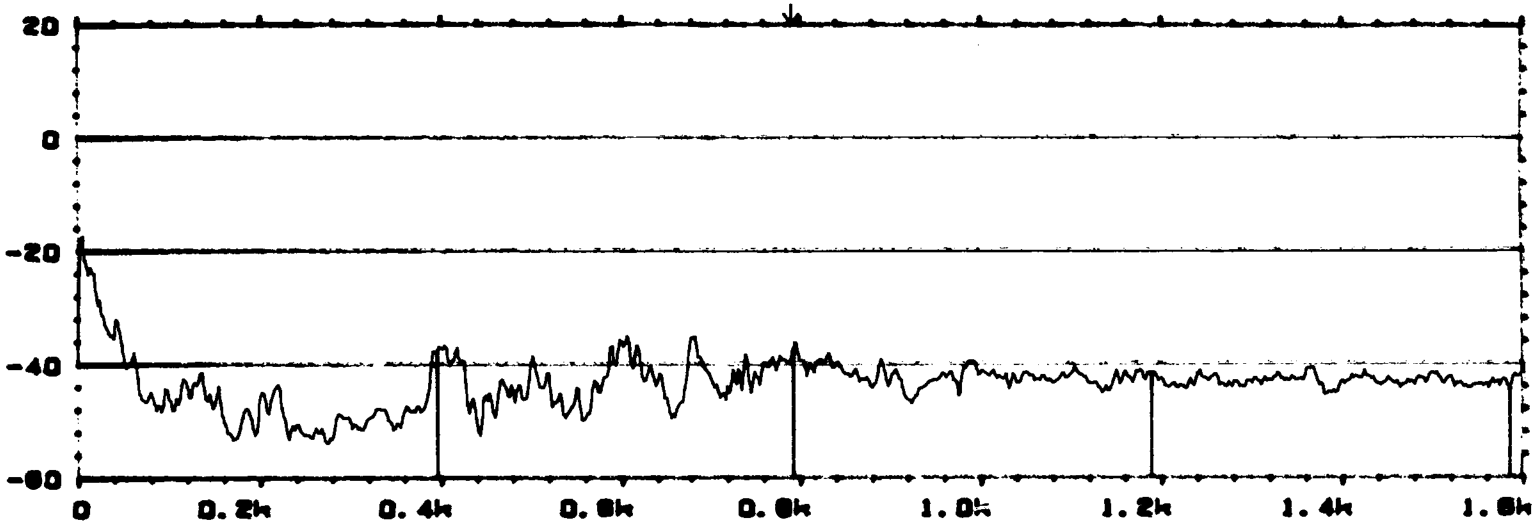

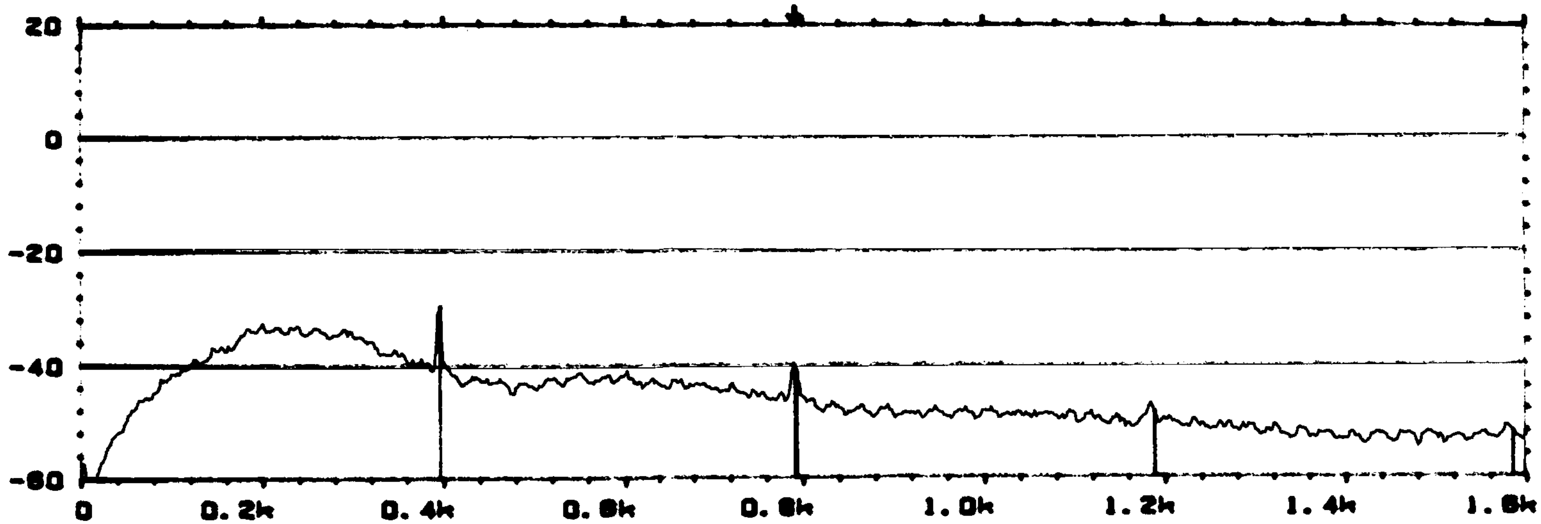

10 AUTO SPEC CH. B
Y: 20.0dB /1.00V RMS 80dB
X: 0Hz + 1.6kHz LIN
SETUP W2 #A: 256

HARM Y: -40.9dB
X: 792Hz
ΔX: 396.0000Hz

Type 2032

Page No.
3

Sign.:

Meas.
Object:

PLF PR 3.1
Ch A = T16
Ch B = M2

Rdg 186

Comments:

11 AUTO SPEC CH. A [ ] INPUT
Y: 20.0dB /1.00V RMS 80dB
X: 0Hz + 1.6kHz LIN
SETUP W2 #A: 256

HARM Y: -37.8dB
X: 396Hz
ΔX: 396.0000Hz

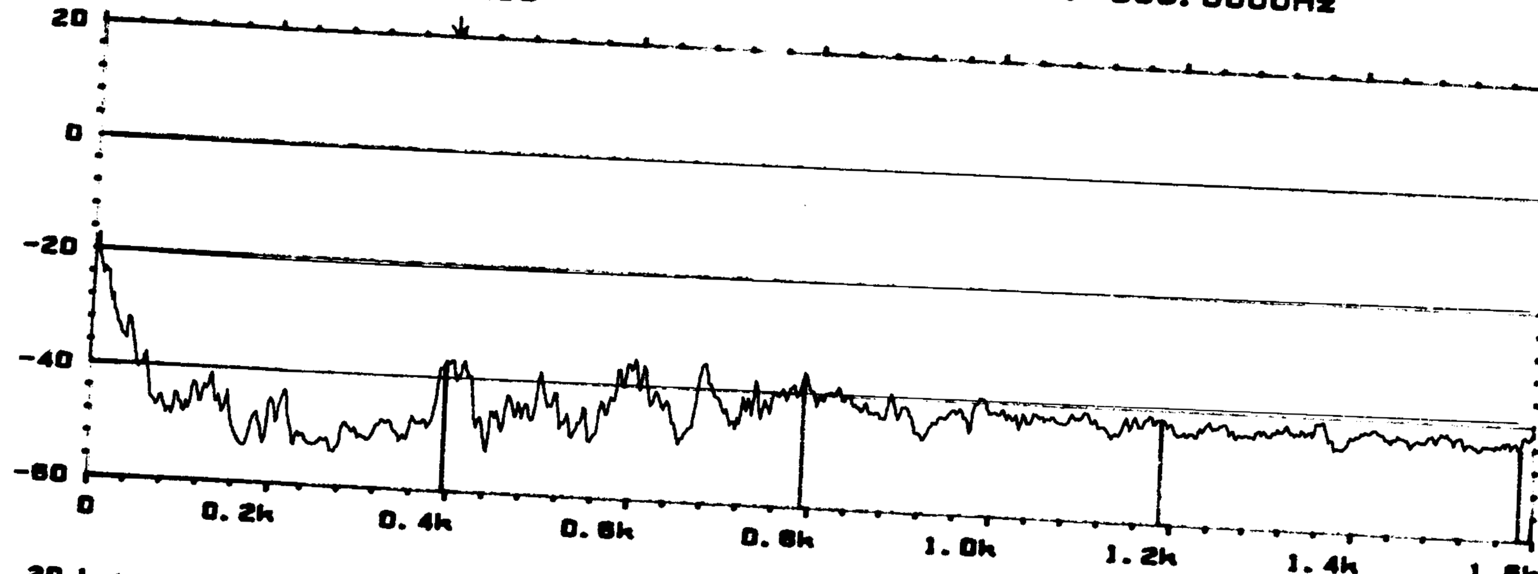

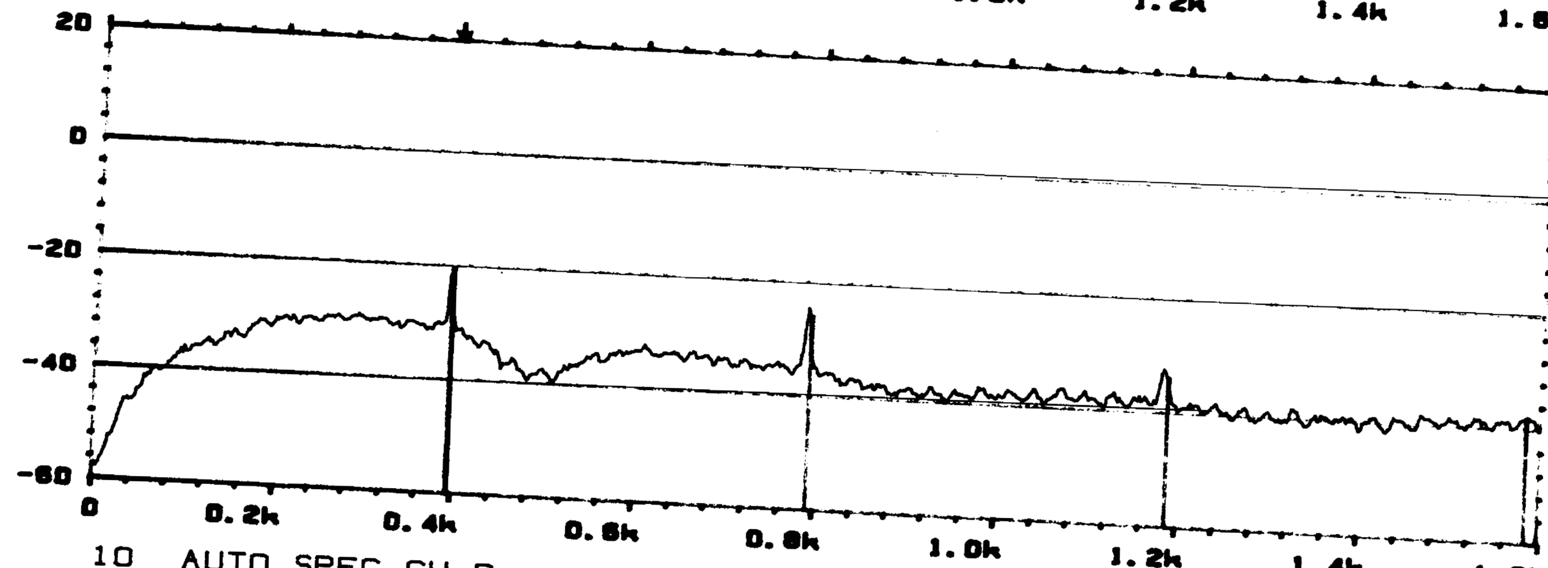

10 AUTO SPEC CH. B
Y: 20.0dB /1.00V RMS 80dB
X: 0Hz + 1.6kHz LIN
SETUP W2 #A: 256

HARM Y: -20.4dB
X: 396Hz
ΔX: 396.0000Hz

Type 2032

Page No.
6

Sign.:

Meas.
Object: 1

PLF PR 2.5
chA - 710
ch B = M3

Rdg 136

Comments:

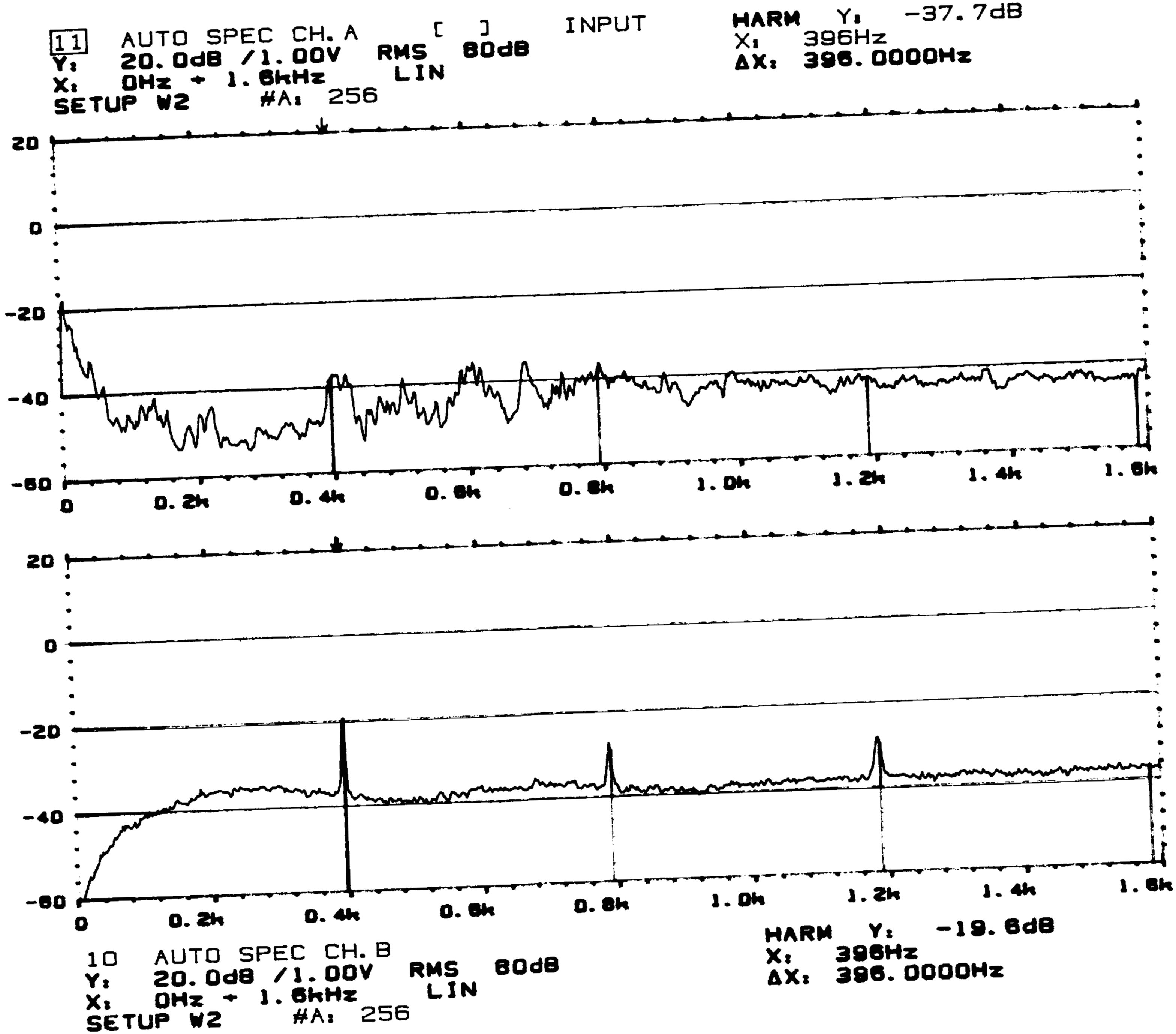

Type 2032

Page No.
9

Sign.:

Meas.
Object:

PLF PR3.1
Ch A = T10
Ch B = M4

Rdg 186

Comments:

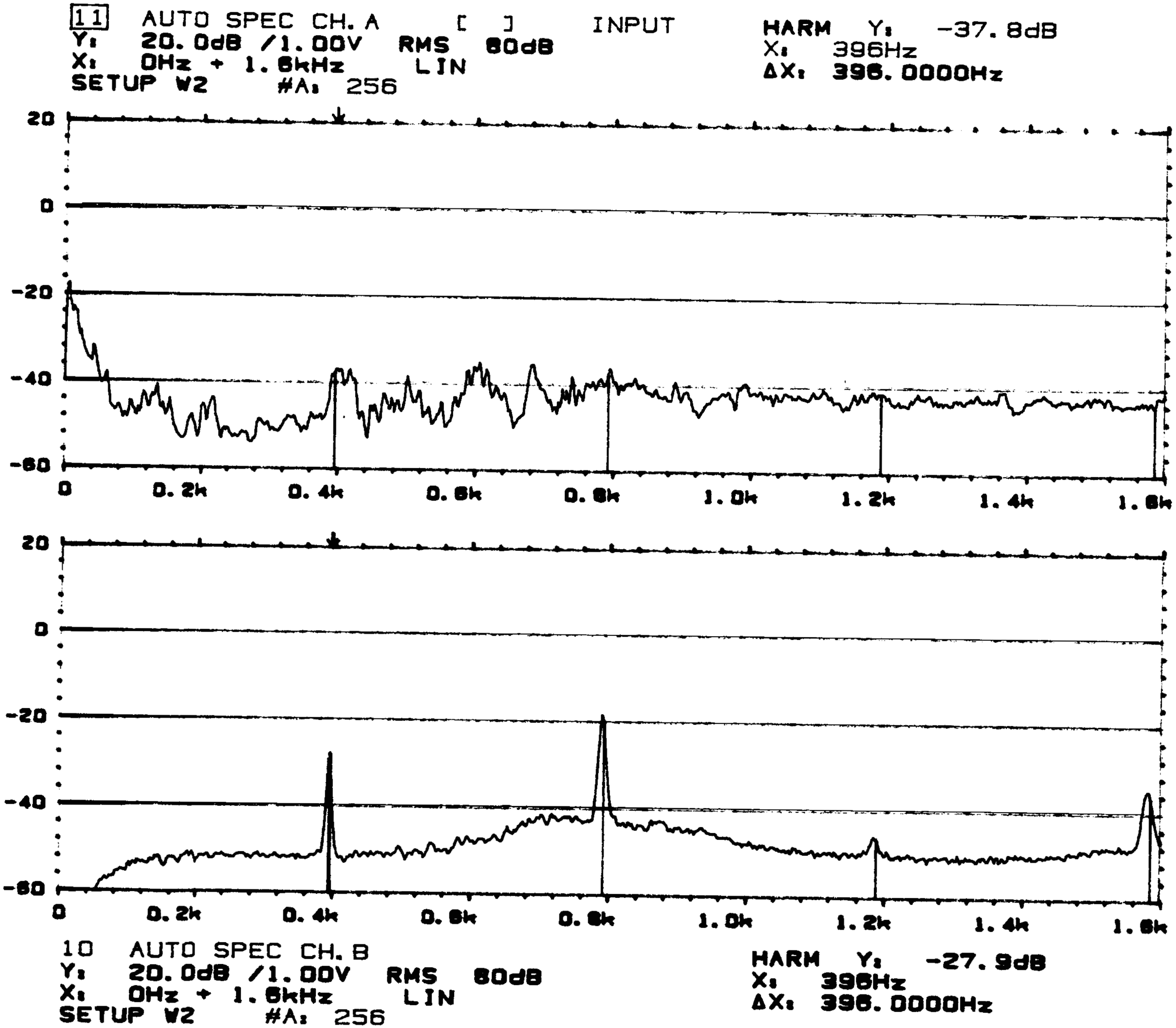

Type 2032

Page No.
10

Sign.:

Meas.
Object:
PLF PR3.5
ChA = T10
ChB = M1

Rdg 187

Comments:

11 AUTO SPEC CH. A [ ] INPUT
Y: 20.0dB /1.00V RMS 80dB
X: 0Hz → 1.6kHz LIN
SETUP W2 #A: 256

HARM Y: -45.0dB
X: 362Hz
ΔX: 362.0000Hz

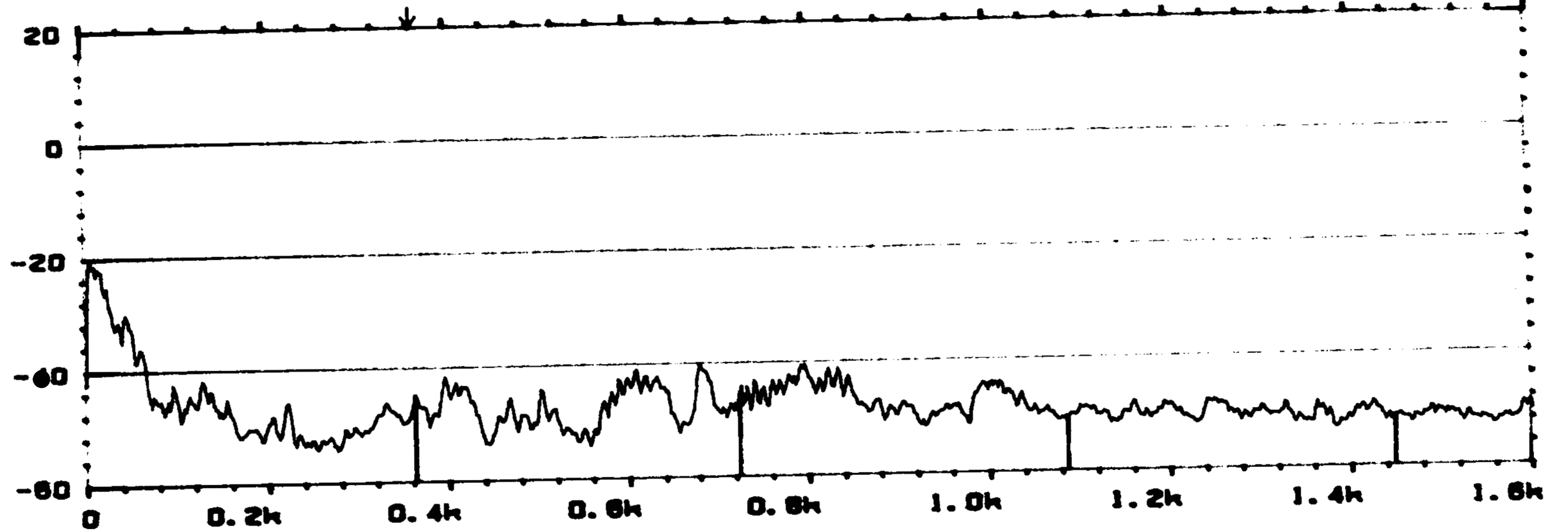

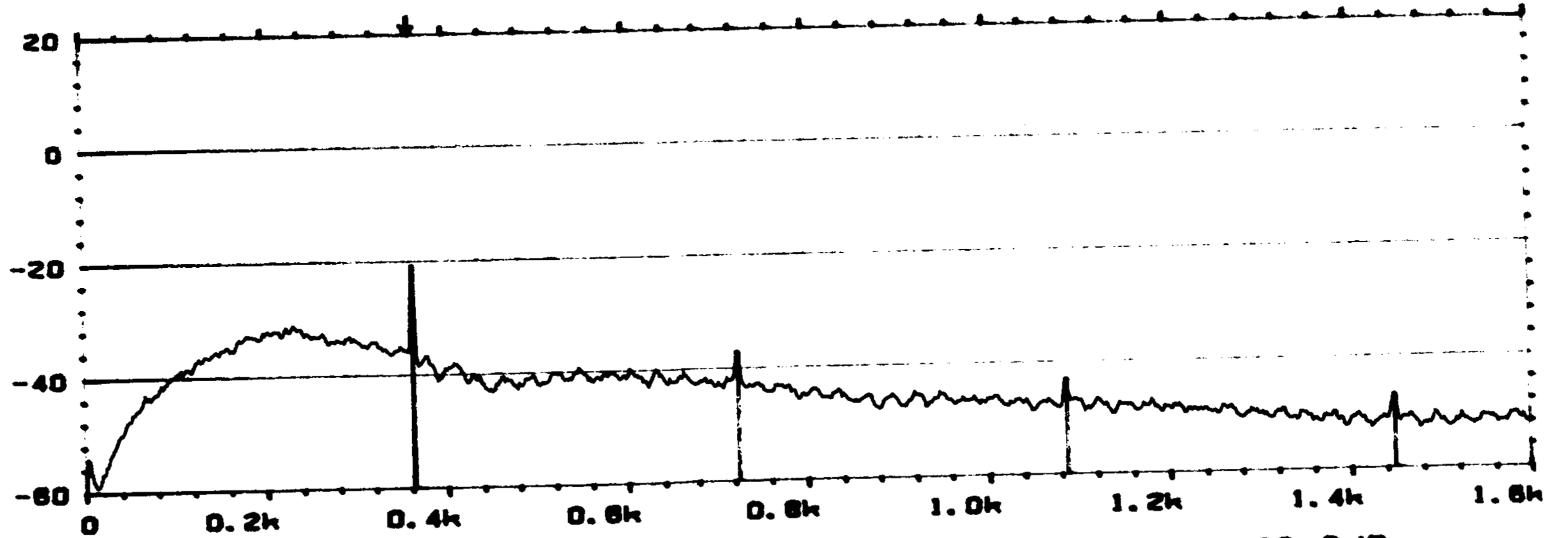

10 AUTO SPEC CH. B
Y: 20.0dB /1.00V RMS 80dB
X: 0Hz → 1.6kHz LIN
SETUP W2 #A: 256

HARM Y: -20.9dB
X: 362Hz
ΔX: 362.0000Hz

Type 2032

Page No.
11

Sign.:

Meas.
Object:

PLF PR 3.5
ChA=T16
ChB=M2

Rdg 187

Comments:

11 AUTO SPEC CH. A [ ] INPUT
Y: 20.0dB /1.00V RMS 80dB
X: 0Hz + 1.6kHz LIN
SETUP W2 #A: 256

HARM Y: -44.8dB
X: 362Hz
ΔX: 362.0000Hz

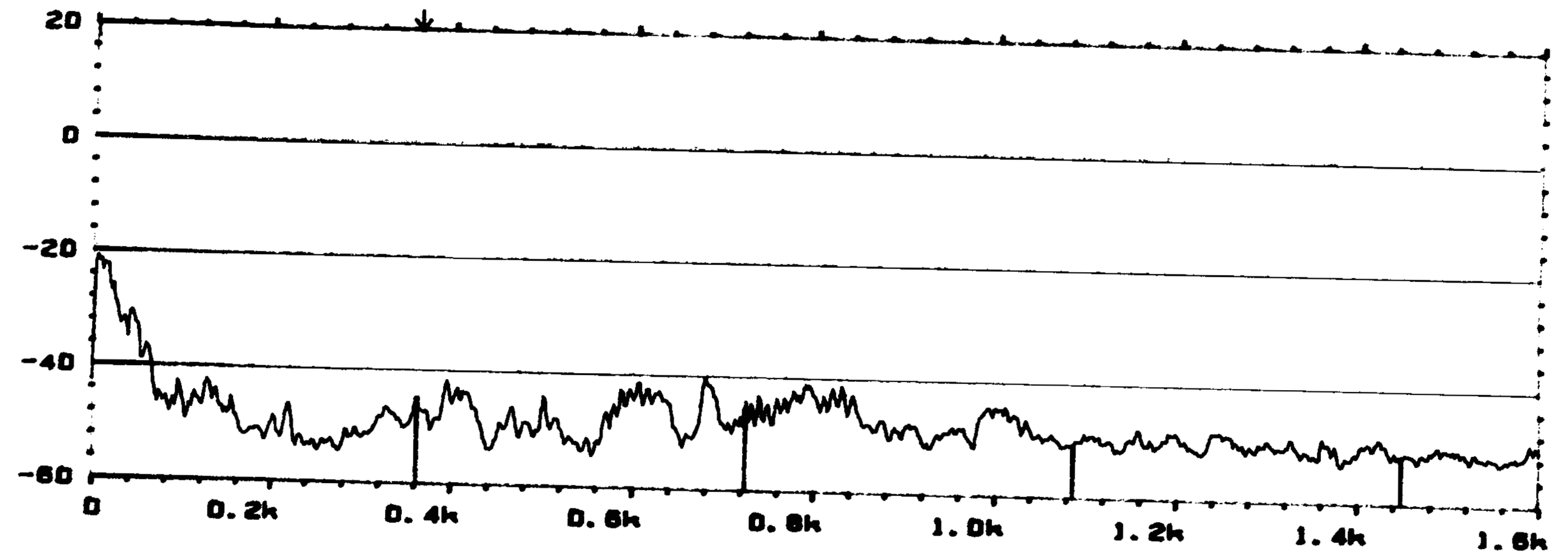

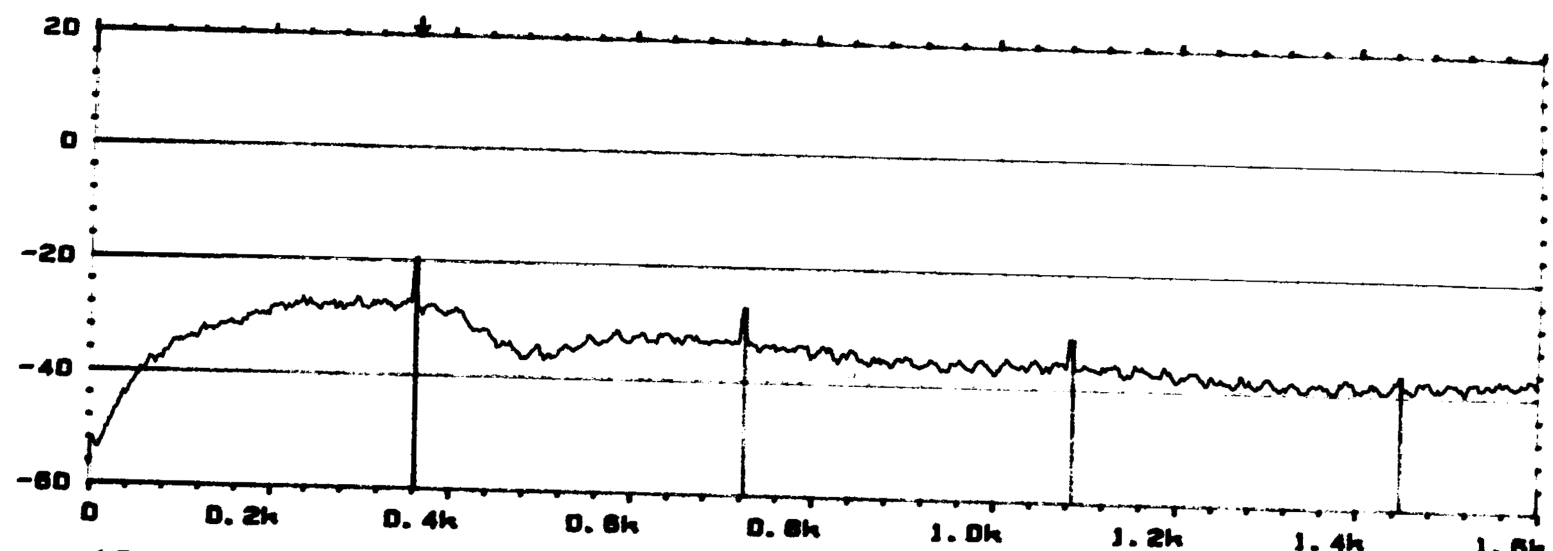

10 AUTO SPEC CH. B
Y: 20.0dB /1.00V RMS 80dB
X: 0Hz + 1.6kHz LIN
SETUP W2 #A: 256

HARM Y: -19.4dB
X: 362Hz
ΔX: 362.0000Hz

Brüel & Kjær

Type 2032

Page No.
12

Sign.:

Meas.
Object:

PIF PR3.5
ChA-T16
ChB: M3

Fig 137

Comments:

11 AUTO SPEC CH. A [ ] INPUT HARM Y: -45.0dB
Y: 20.0dB /1.00V RMS 80dB X: 362Hz
X: 0Hz + 1.6kHz LIN ΔX: 362.0000Hz
SETUP W2 #A: 256

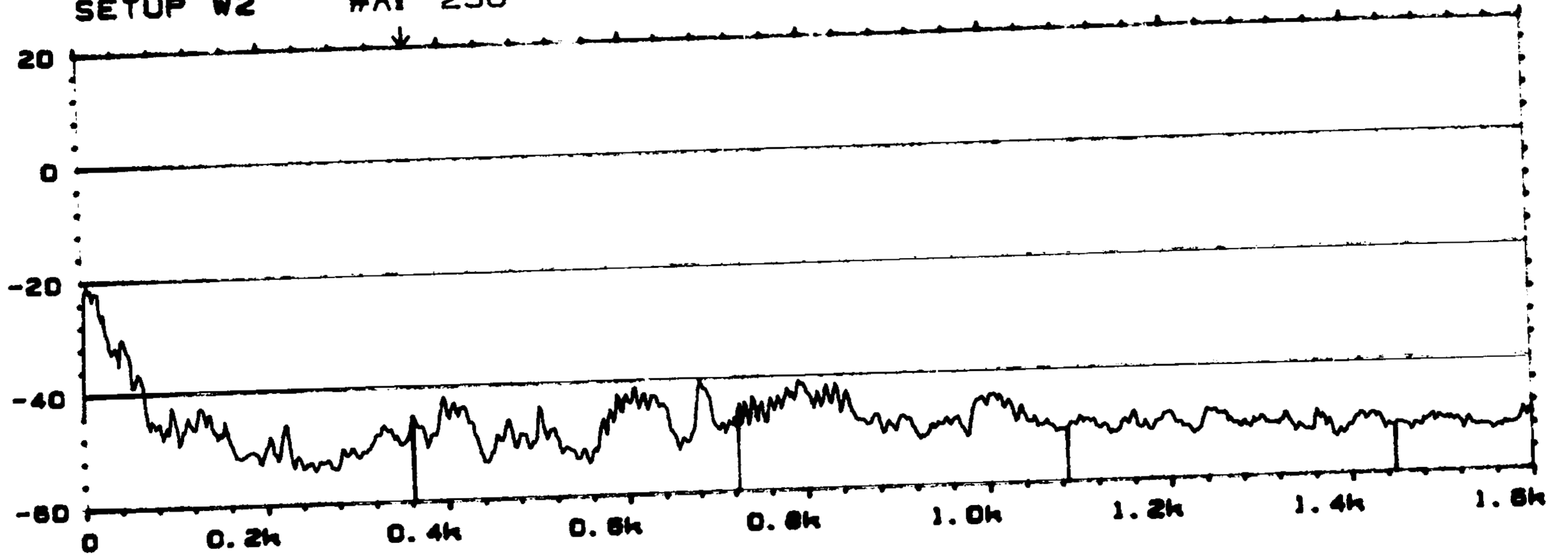

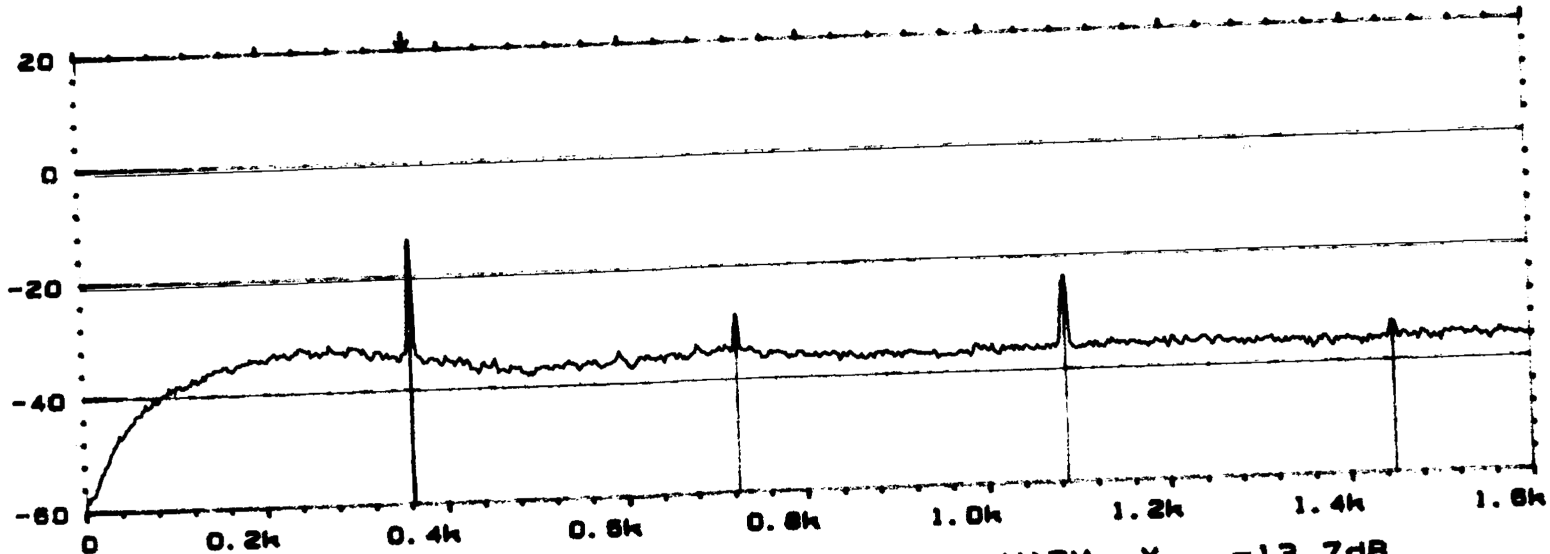

10 AUTO SPEC CH. B HARM Y: -13.7dB
Y: 20.0dB /1.00V RMS 80dB X: 362Hz
X: 0Hz + 1.6kHz LIN ΔX: 362.0000Hz
SETUP W2 #A: 256

Brüel & Kjær

Type 2032

Page No.
14

Sign.:

Meas.
Object:

PLF PR3.5
ChA= T10
ChB= M4

Rdg 187

Comments:

11 AUTO SPEC CH. A [ ] INPUT
Y: 20.0dB /1.00V RMS 80dB
X: 0Hz + 1.6kHz LIN
SETUP W2 #A: 256

HARM Y: -44.8dB
X: 362Hz
ΔX: 362.0000Hz

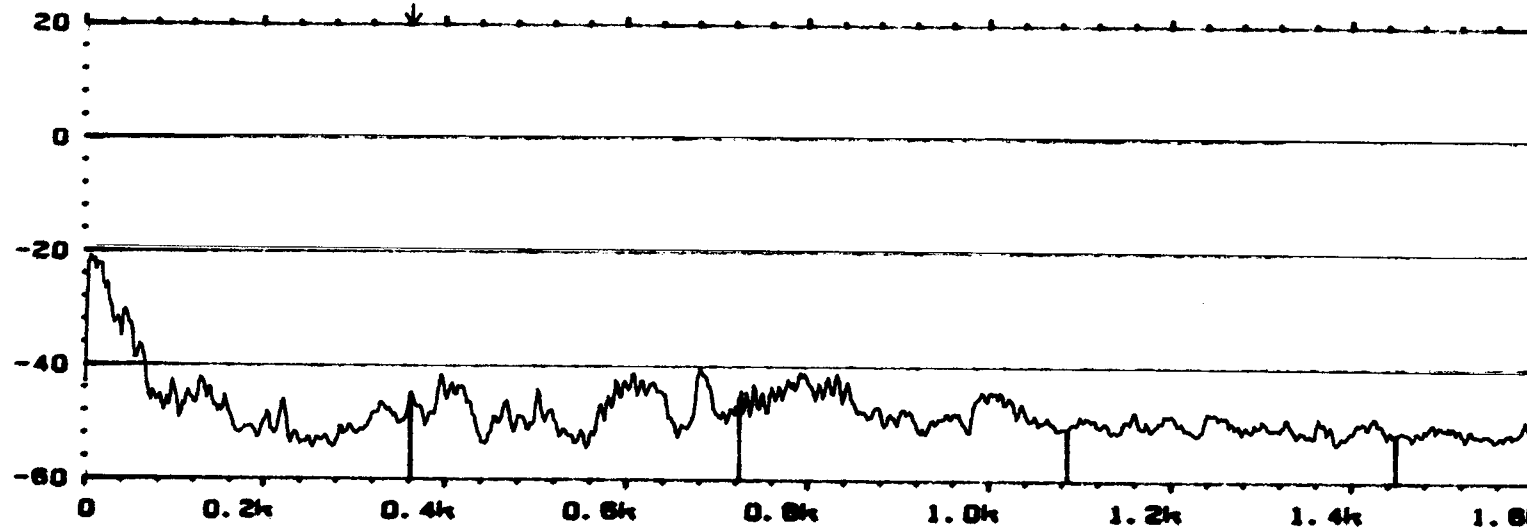

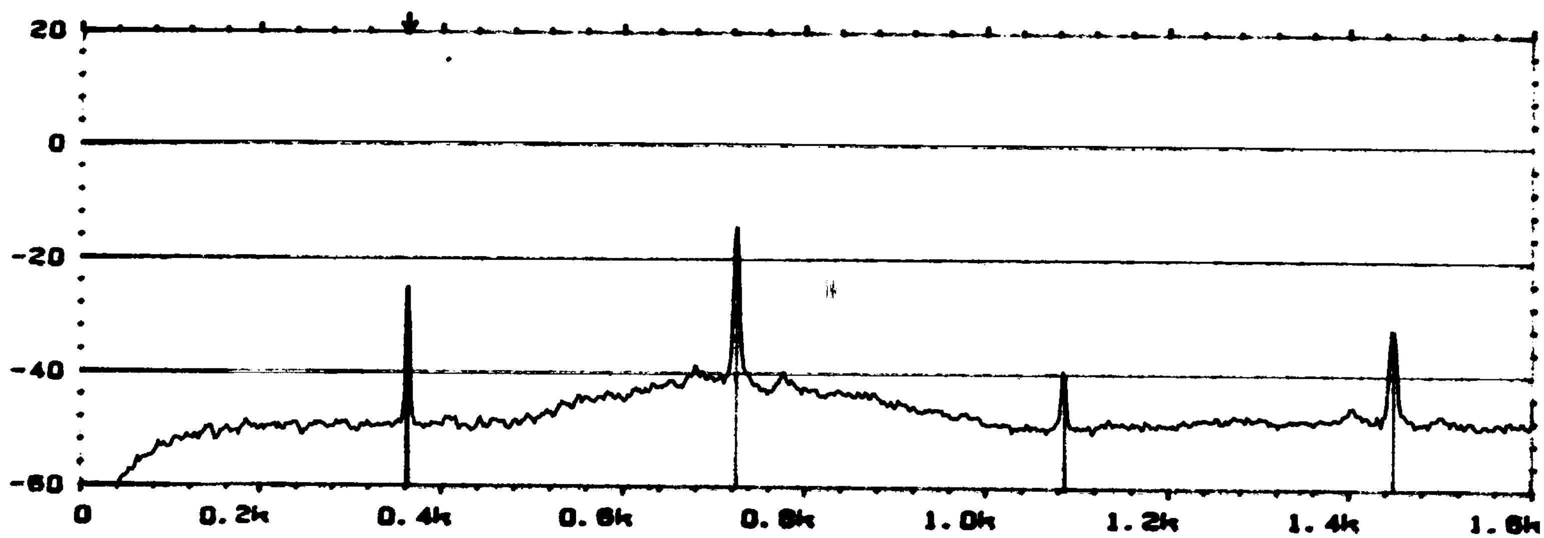

10 AUTO SPEC CH. B
Y: 20.0dB /1.00V RMS 80dB
X: 0Hz + 1.6kHz LIN
SETUP W2 #A: 256

HARM Y: -25.2dB
X: 362Hz
ΔX: 362.0000Hz

APPENDIX F

COMPARISON OF COHERENCE FUNCTION FOR INTERNAL PRESSURE TRANSDUCERS NO. 9 AND NO. 10 TO FAR FIELD MICROPHONES PR=3.5

APPENDIX F

PART I

TRANSDUCER NO. 10

W20 COHERENCE INPUT MAIN Y: 1.20m
Y: 1.00 X: 1600Hz
X: 0Hz + 1.6kHz LIN
SETUP W12 #A: 256

Brüel & Kjær

Type 2032

Page No.
81 6/17/88

Sign.:

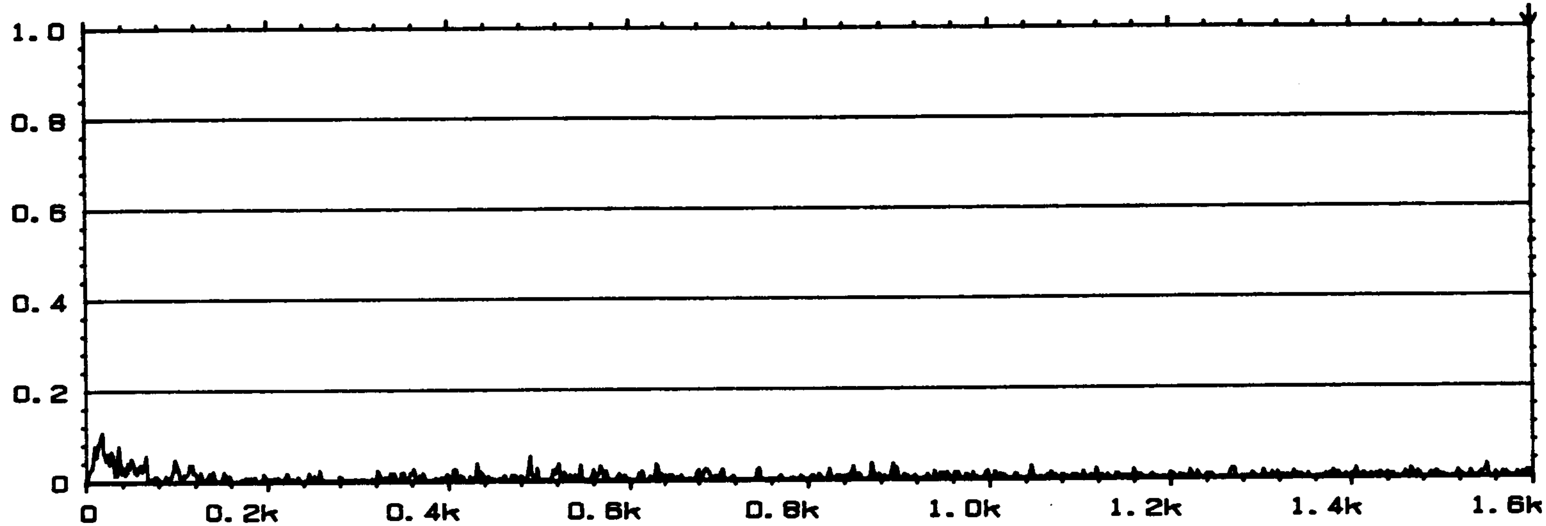

Meas.
Object:
PLP PF3.5
CHA 110
Time delay

Comments:

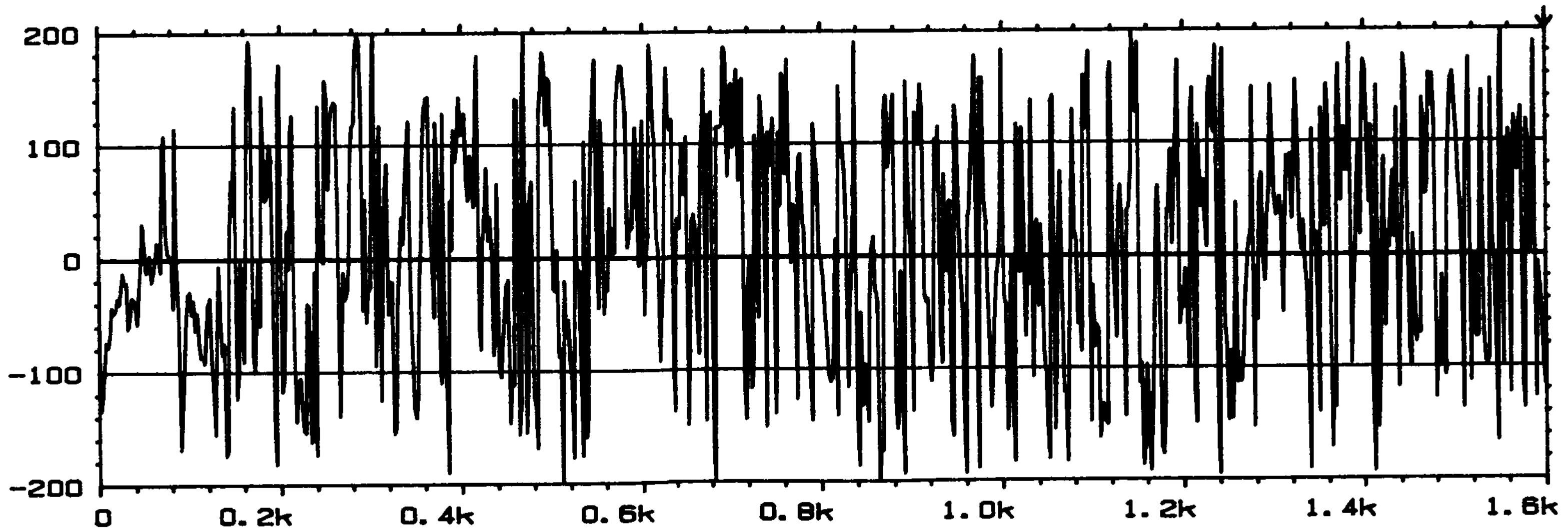

W1 FREQ RESP H1 PHASE MAIN Y: -115.9DEG
Y: -200 TO +200 DEG X: 1600Hz
X: 0Hz + 1.6kHz LIN
SETUP W12 #A: 256

W20 COHERENCE INPUT MAIN Y: 1.07m
Y: 1.00 X: 1600Hz
X: 0Hz + 1.6kHz LIN
SETUP W12 #A: 256

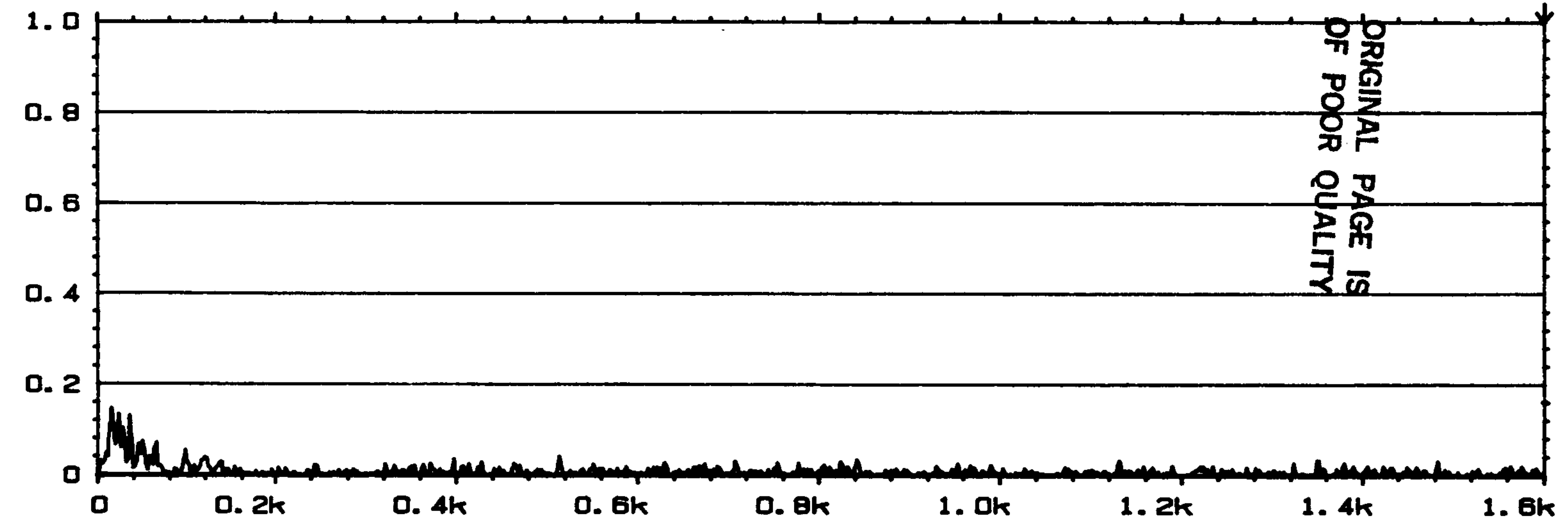

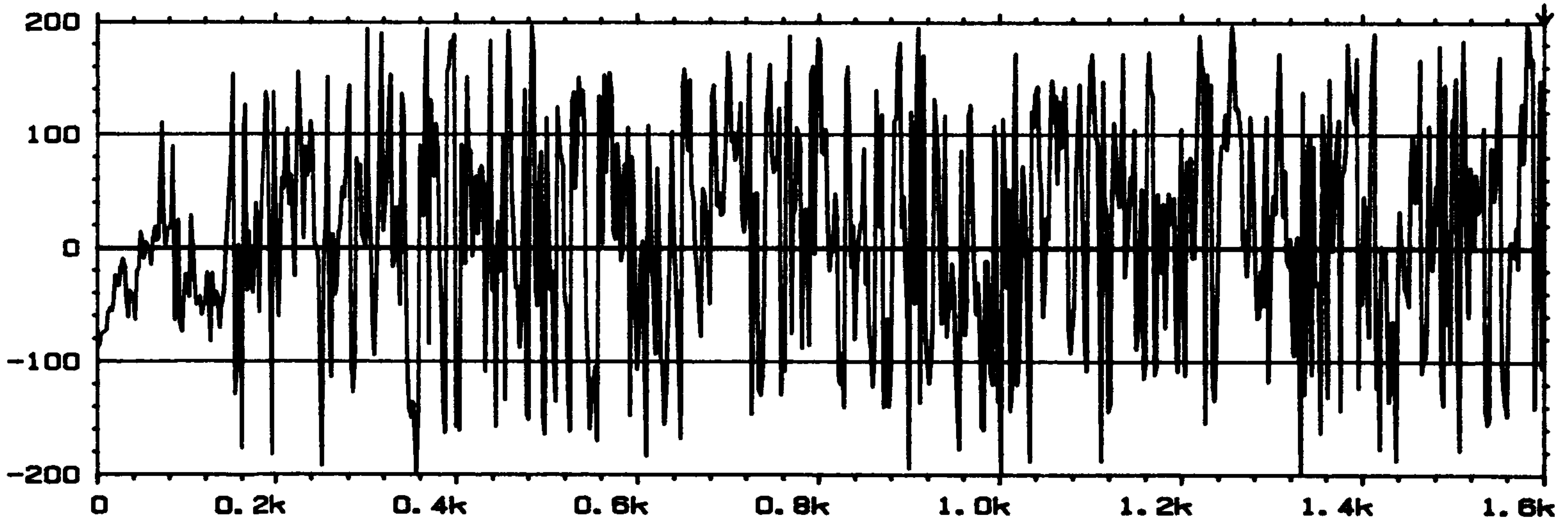

W1 FREQ RESP H1 PHASE MAIN Y: 117.2DEG
Y: -200 TO +200 DEG X: 1600Hz
X: 0Hz + 1.6kHz LIN
SETUP W12 #A: 256

Type 2032

Page No.
82 6/17/88

Sign.:

Meas.
Object:
DLF PR 3.5
ChA = T10
ChB = M2
time delay
70ms
Rdg 187

Comments:

W20 COHERENCE INPUT MAIN Y: 1.06m
Y: 1.00 X: 1600Hz
X: 0Hz + 1.6kHz LIN
SETUP W12 #A: 256

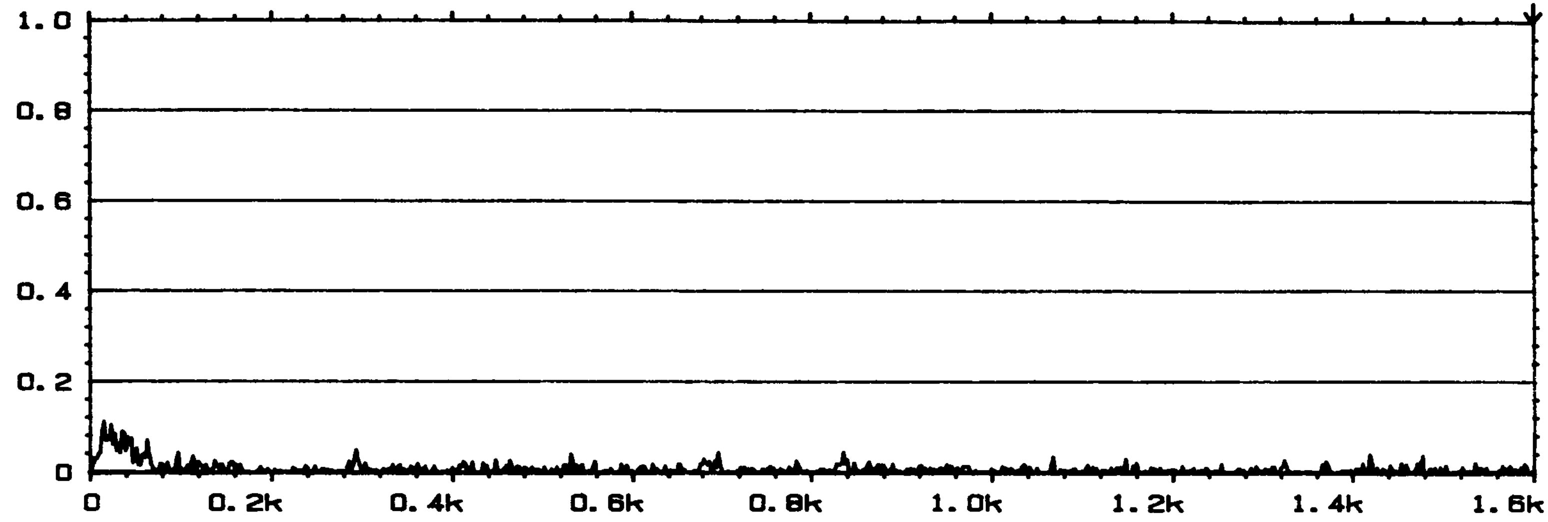

Type 2032

Page No.
83 6/17/88

Sign.:

Meas.
Object:
PLF PR3.5
ChA=T10
ChB=M3
Time delay
70 ms
Rdg 187

Comments:

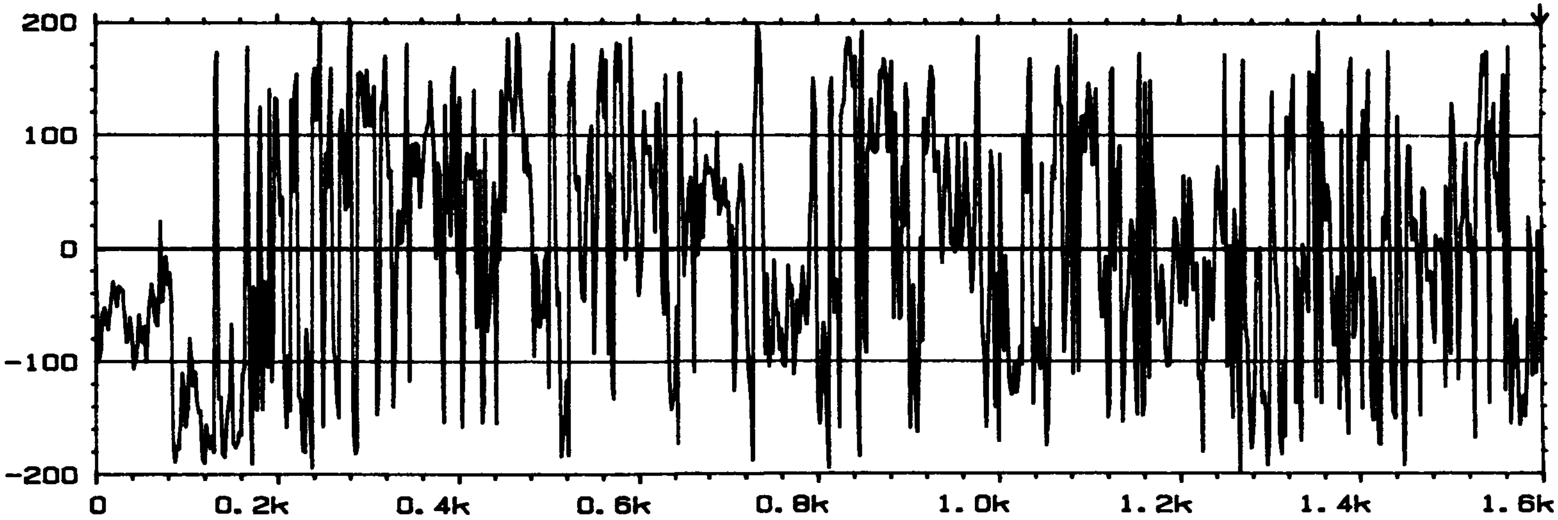

W1 FREQ RESP H1 PHASE MAIN Y: -99.4DEG
Y: -200 TO +200 DEG X: 1600Hz
X: 0Hz + 1.6kHz LIN
SETUP W12 #A: 256

Type 2032

Page No.
84 6/17/88

Sign.:

Meas.
Object:
PLF PR 3.5
ChA = T10
ChB = M4
Time delay
70ms
Rdg 187

Comments:

W20 COHERENCE INPUT
Y: 1.00
X: 0Hz + 1.6kHz LIN
SETUP W12 #A: 256

MAIN Y: 2.08m
X: 1600Hz

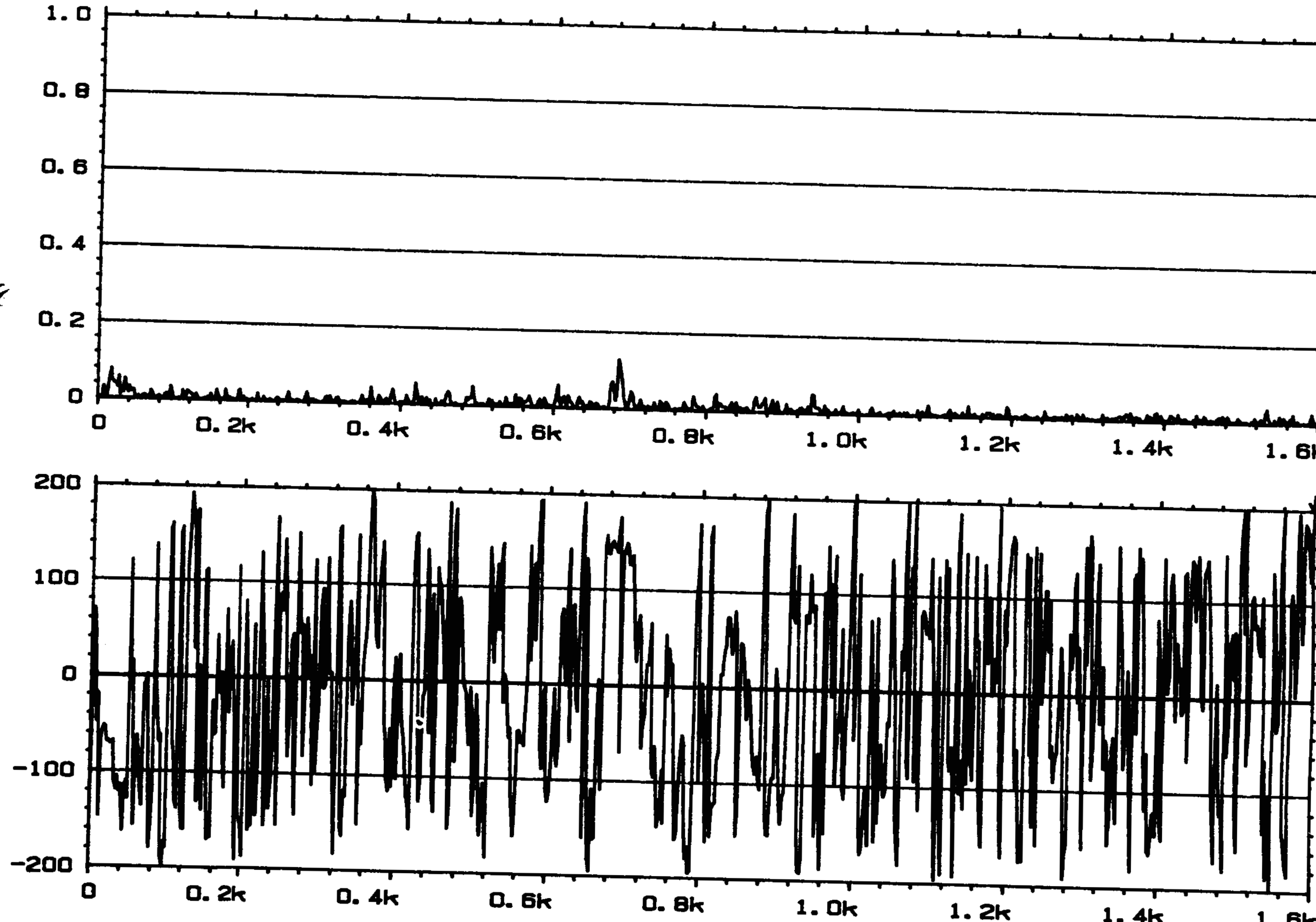

W1 FREQ RESP H1 PHASE
Y: −200 TO +200 DEG
X: 0Hz + 1.6kHz LIN
SETUP W12 #A: 256

MAIN Y: 177.1DEG
X: 1600Hz

ORIGINAL PAGE IS
OF POOR QUALITY

Brüel & Kjær

Type 2032

Page No.
48

Sign.:

Meas.
Object:

PLF PR 1.4
ChA = T10
ChB = M2

Rdg 177

Comments:

20 COHERENCE INPUT MAIN Y: 46.8m
Y: 1.00 X: 684Hz
X: 0Hz + 1.6kHz LIN
SETUP W22 #A: 256

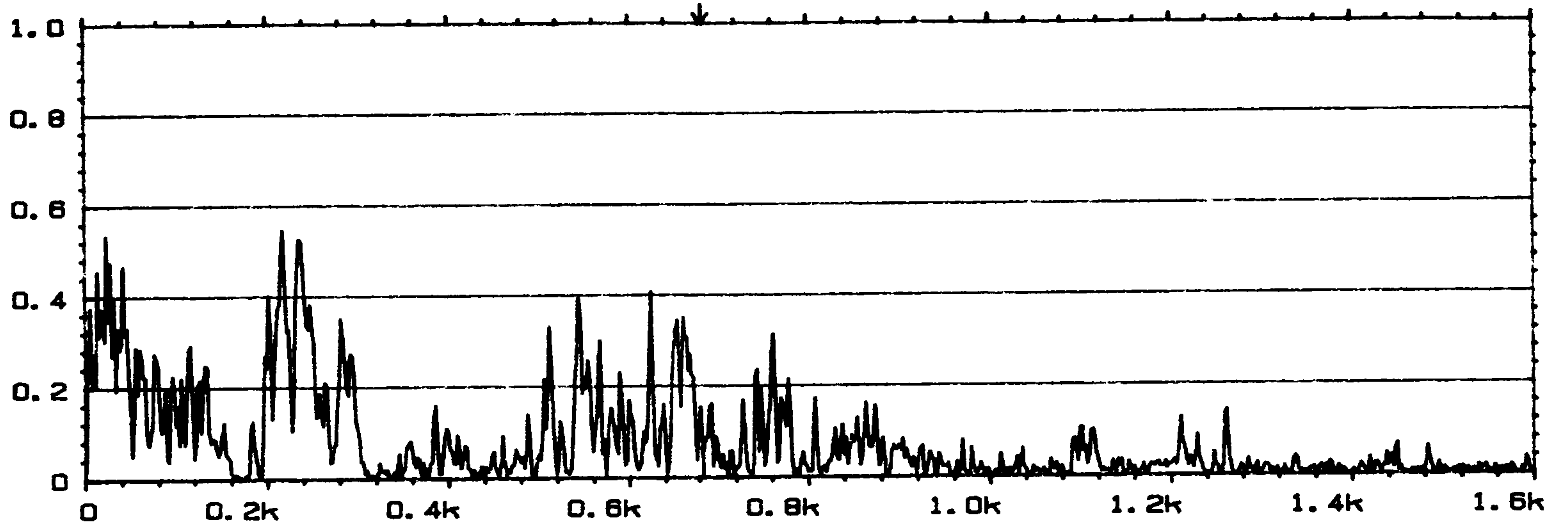

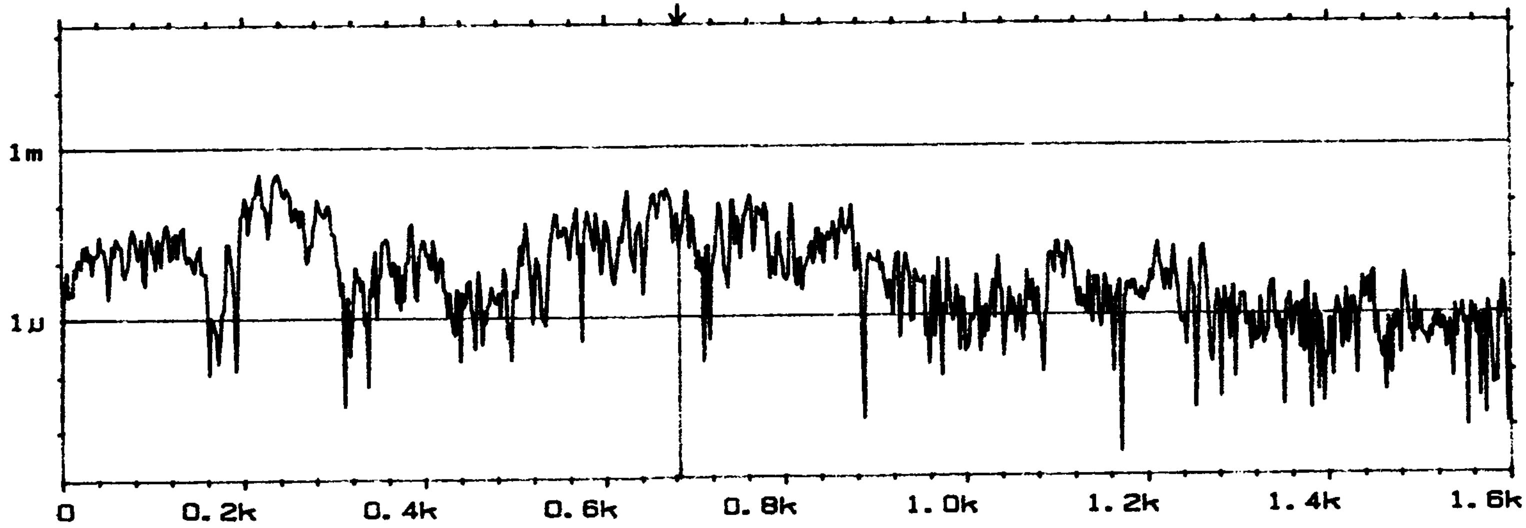

2 COHERENT POWER MAIN Y: 18.1μU²
Y: 150mU² PWR 80dB X: 684Hz
X: 0Hz + 1.6kHz LIN
SETUP W22 #A: 256

APPENDIX F

PART II

TRANSDUCER NO. 9

W20 COHERENCE INPUT MAIN Y: 418μ
Y: 1.00 X: 684Hz
X: 0Hz + 1.6kHz LIN
SETUP W12 #A: 256

Type 2032

Page No.
70 6/17/88

Sign.:

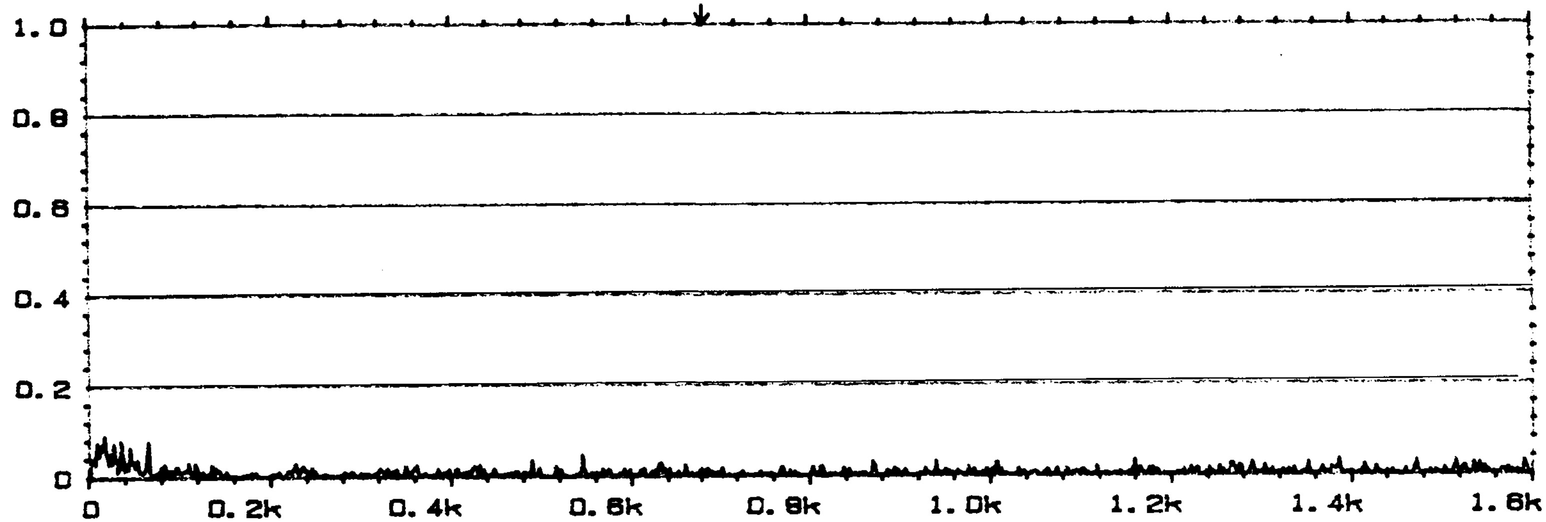

Meas.
Object:
PLF PR3.5
Ch A = T9
Ch B = M1
Time delay
0 ms
Rdg 187

Comments:

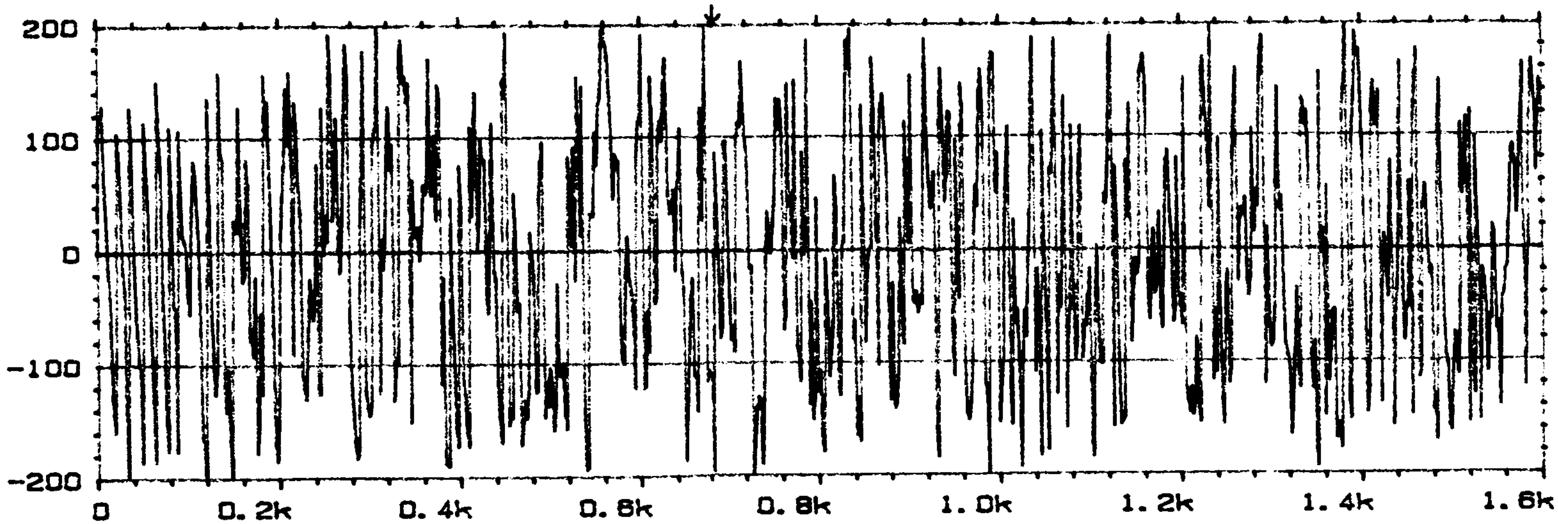

W1 FREQ RESP H1 PHASE MAIN Y: 164.6DEG
Y: -200 TO +200 DEG X: 684Hz
X: 0Hz + 1.6kHz LIN
SETUP W12 #A: 256

Type 2032

Page No.
69 6/17/88

Sign.:

Meas.
Object:
PLF PR 3.5
ChA = T9
ChB = M2
Time delay
0 ms
Rdg 107

Comments:

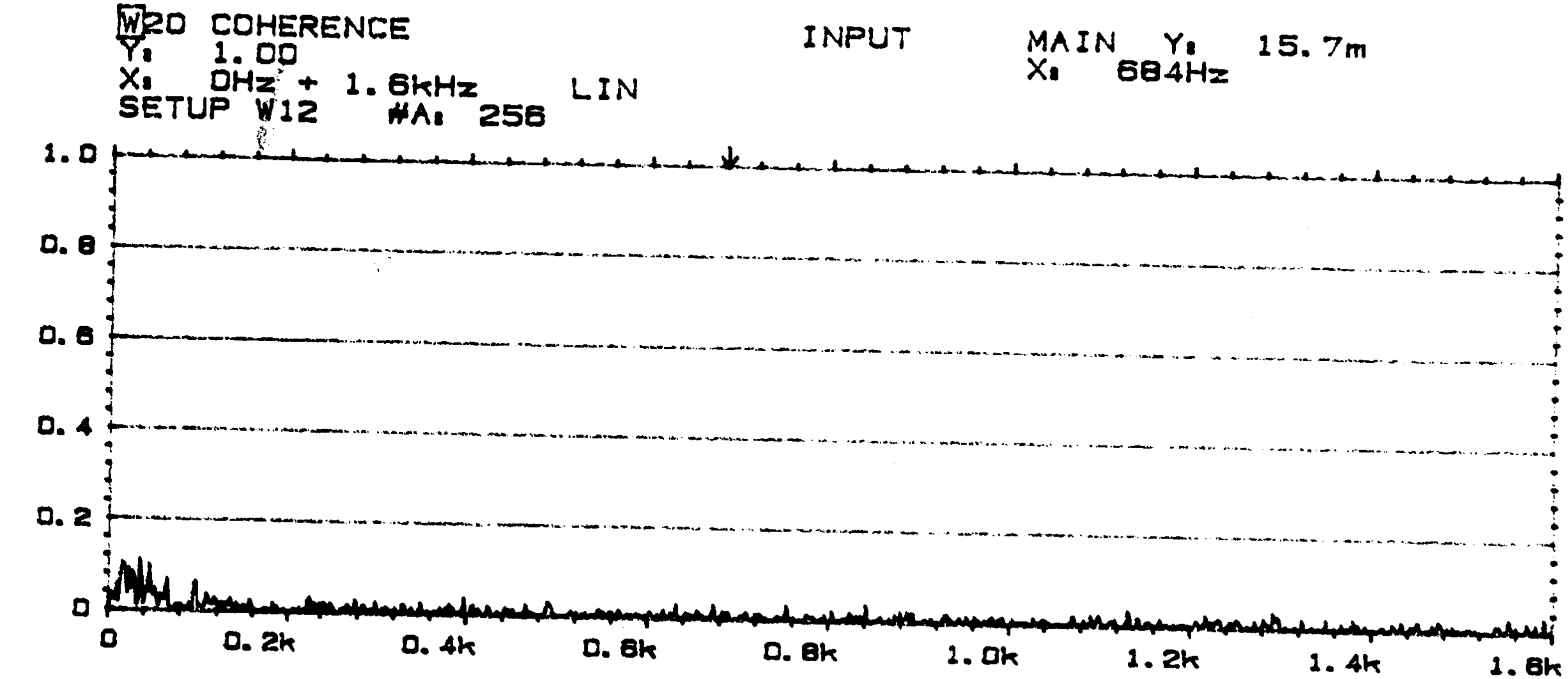

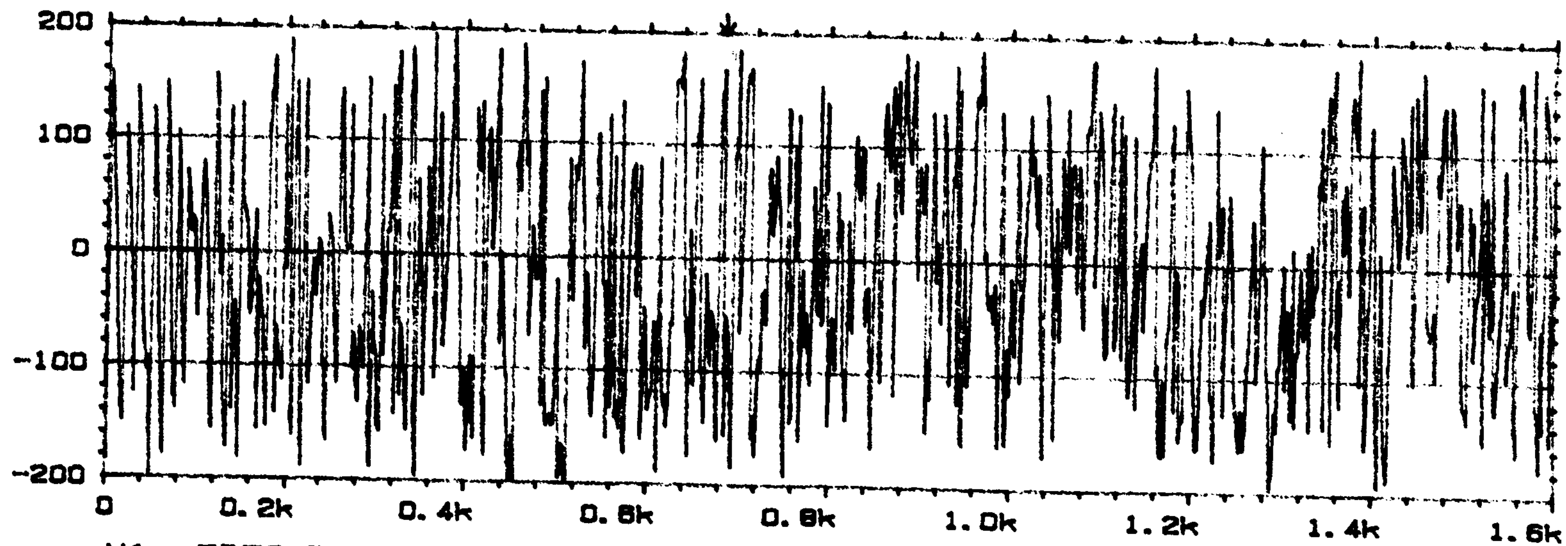

W20 COHERENCE INPUT MAIN Y: 29.0m
Y: 1.00 X: 684Hz
X: 0Hz + 1.6kHz LIN
SETUP W12 #A: 256

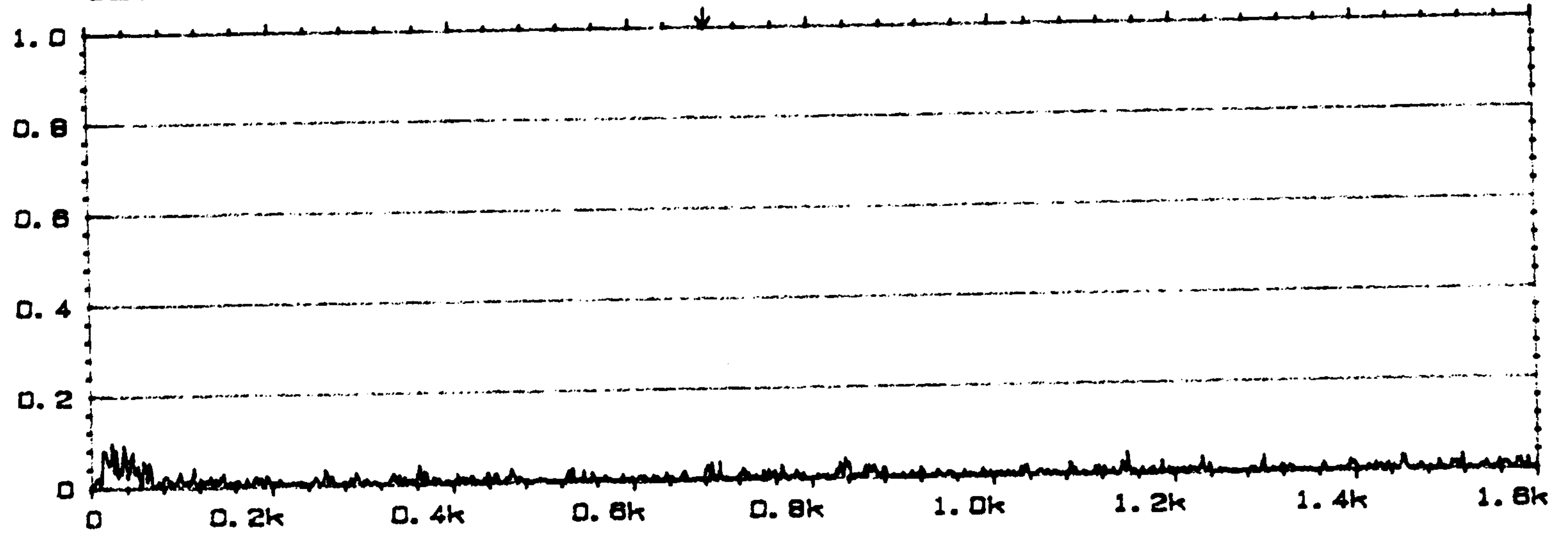

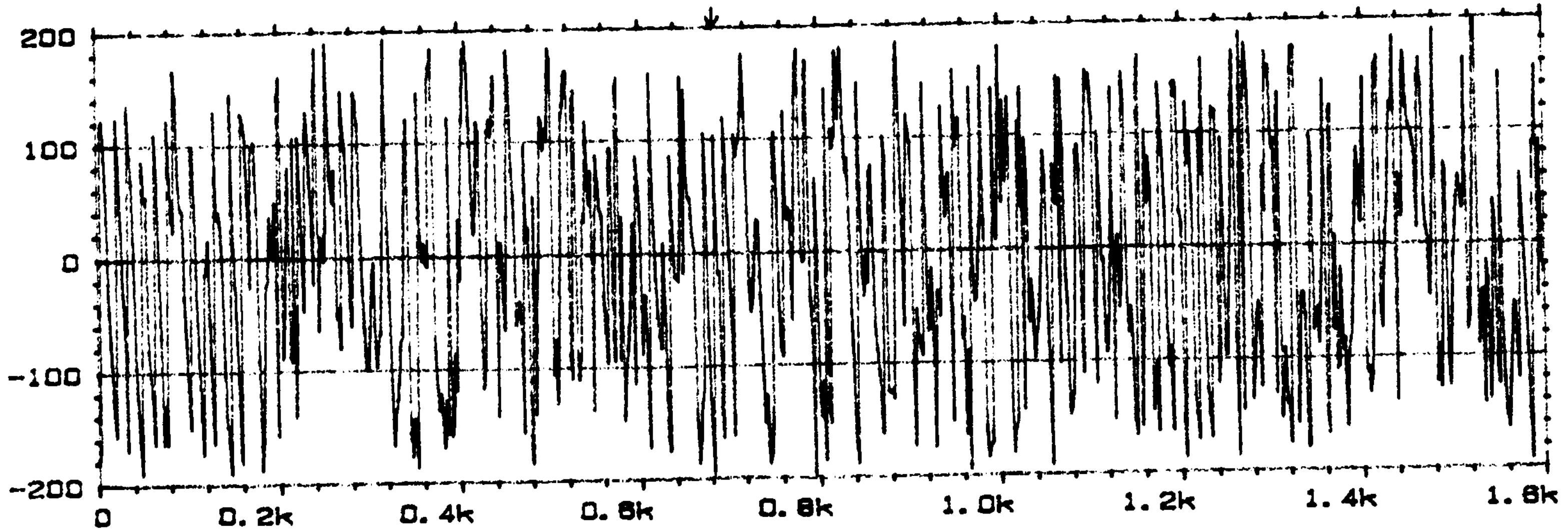

W1 FREQ RESP H1 PHASE MAIN Y: 103.2DEG
Y: -200 TO +200 DEG X: 684Hz
X: 0Hz + 1.6kHz LIN
SETUP W12 #A: 256

Type 2032

Page No.
68 6/11/88

Sign.:

Meas.
Object:
PU PA 3,5

Comments:

ORIGINAL PAGE IS
OF POOR QUALITY

C-3

Type 2032

Page No.
~~87~~ 6/17/33

Sign.:

Meas.
Object:
PLF PR 3.5
ChA = T9
ChB = M4
Timedelay
0 ms
Fig 137

Comments:

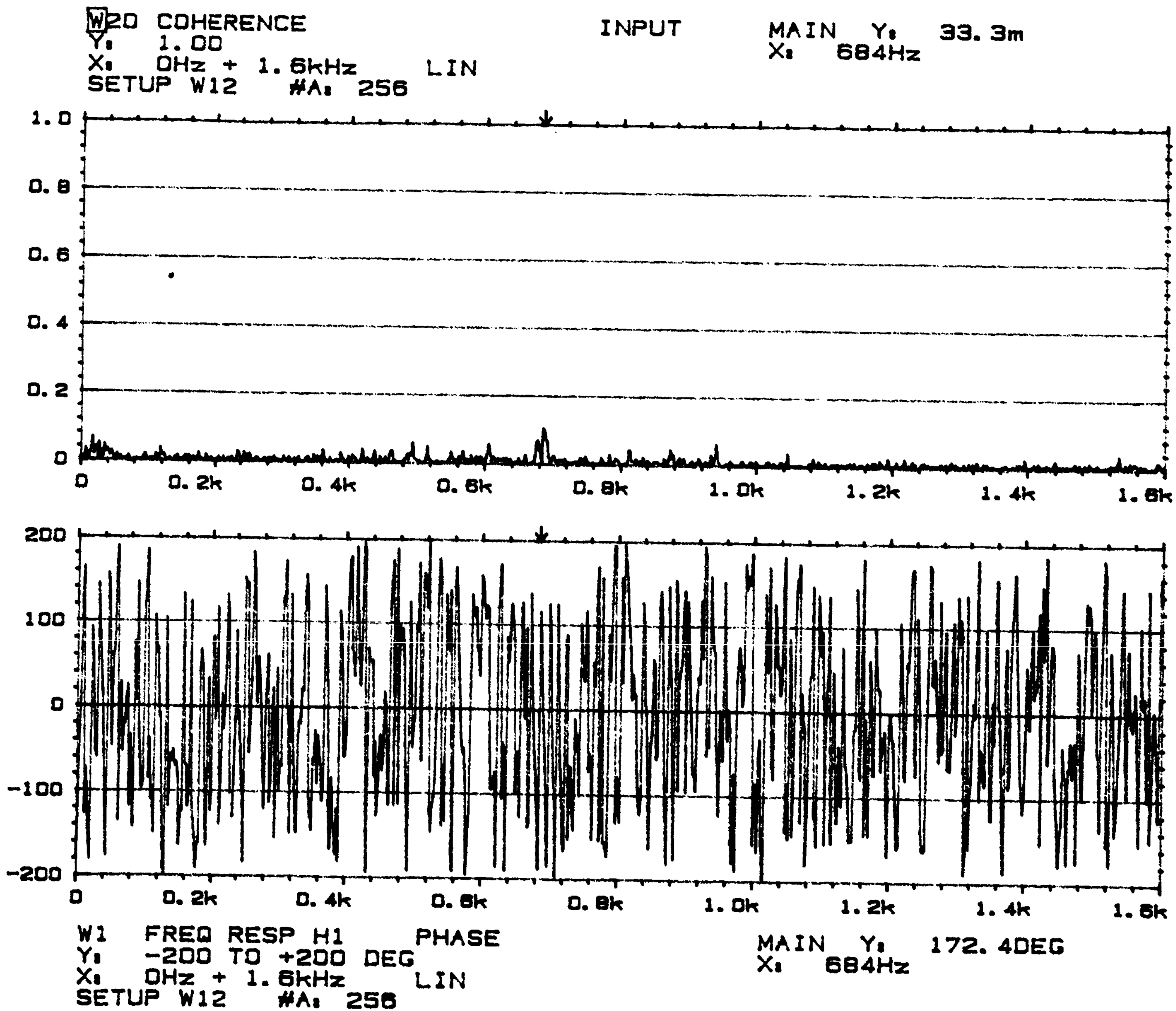

TABLE I. - AERODYNAMIC DATA FOR ACOUSTIC TESTS

Reading	Pressure ratio	Total temperature, T_{ts}, °R	Total pressure, P_{ts}, psi	Mass flow rate, W, lb/s	Ambient pressure, T_{amb}, °R	Ambient pressure, P_{amb}, psi	Wind direction, deg	Wind velocity, mph
176	1.17	524.5	16.8	32.77	527.7	14.35	178	8
184	1.27	536.7	18.29	43.55	525.9	14.34	161	2
177	1.36	521.8	19.52	46.74	527.3	14.35	153	4
178	1.57	524.2	22.5	57.79	527		180	9
179	1.76	526.4	25.25	66.15	526.8		181	7
188	1.92	535.9	27.61	72.03	526.3		174	10
181	2.2	532.6	31.56	82.53	526.4		170	8
182	2.1	533.7	31.7	82.15	526.1		163	5
183	2.45	537.2	35.12	91.13	526	14.35	179	6
185	2.92	537.6	41.85	109.8	526	14.34	171	5
186	3.01	537.3	43.11	111.5	525.8	14.34	177	7
187	3.45	536.5	49.43	128.5	526.4	14.34	180	9

TABLE II. - OVERALL SOUND PRESSURE LEVEL

[dB reference, 20 mPa.]

Reading number	Pressure ratio	Microphone				Transducer					
		1	2	3	4	5	6	7	8	9	10
		Microphone angle, deg									
		150	135	120	90						
		Tape channel numbers									
176	1.2	91.2	92	91.8	92	160.3	158.9	107.5	118.7	107.2	118.7
184	1.3	94	94.3	94.8	94.3	162.6	161	109.6	100.4	108.6	121
177	1.4	95.6	95.6	95.8	94.9	162.7	161.7	110.2	100.2	109	122.1
178	1.6	81.4	99.3	99.3	97.4	164.3	163.9	111.5	100.8	110	123.1
179	1.8	84.1	83.2	82.4	98.6	165.1	164.6	111.8	100.6	111	124
188	2	87.7	85.3	83.8	99.7	163.5	163.1	111	100.5	110.1	122.6
181	2.3	90.1	88.1	85.9	83.8	167.2	166.6	113.7	101.4	112.5	106.9
182	2.3	90.7	87.7	85.4	82.5	166.8	166.7	155	101.6	112.1	106.9
183	2.5	135.3	133.5	131.3	88.6	167.4	167.4	155.8	102	112.8	107.9
185	3	121.3	137.7	135.4	135.5	149.8	149.8	157.3	142.8	155.7	108.7
186	3.1	121.4	138.3	136.5	121.3	150	150.1	157	143	155.5	109.1
187	3.5	122.7	139.6	138.4	123	161.2	160.7	151.9	141.7	150.9	104.2

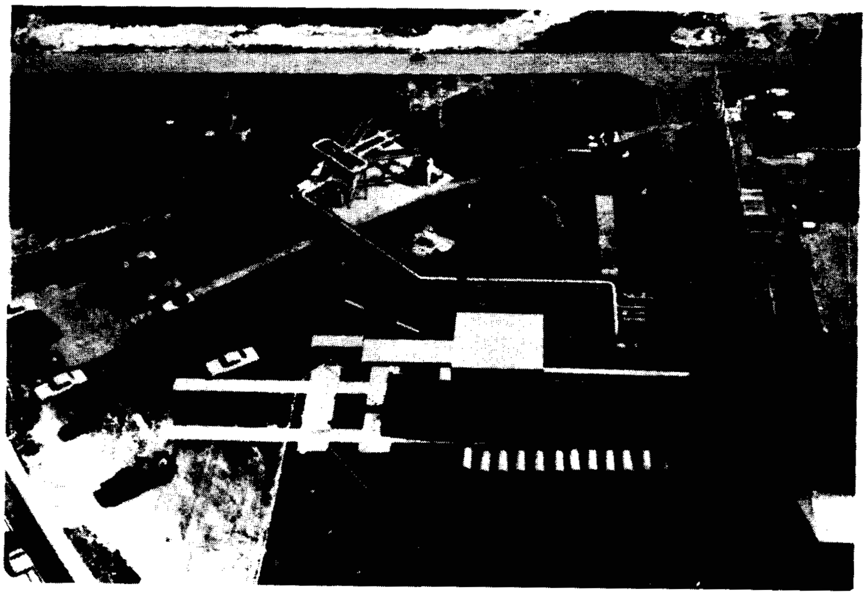

(A) OVERALL AERIAL VIEW.

FIGURE 1. - POWERED LIFT FACILITY.

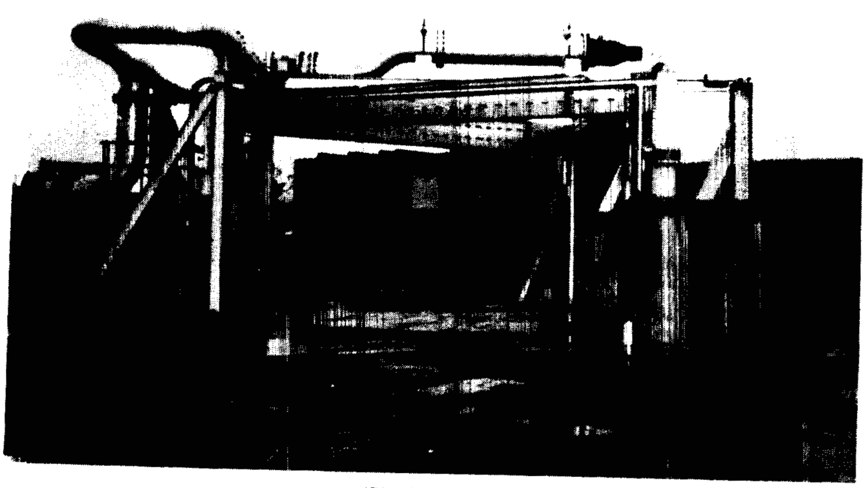

(B) TEST STAND.

FIGURE 1. - CONTINUED.

ORIGINAL PAGE IS OF POOR QUALITY

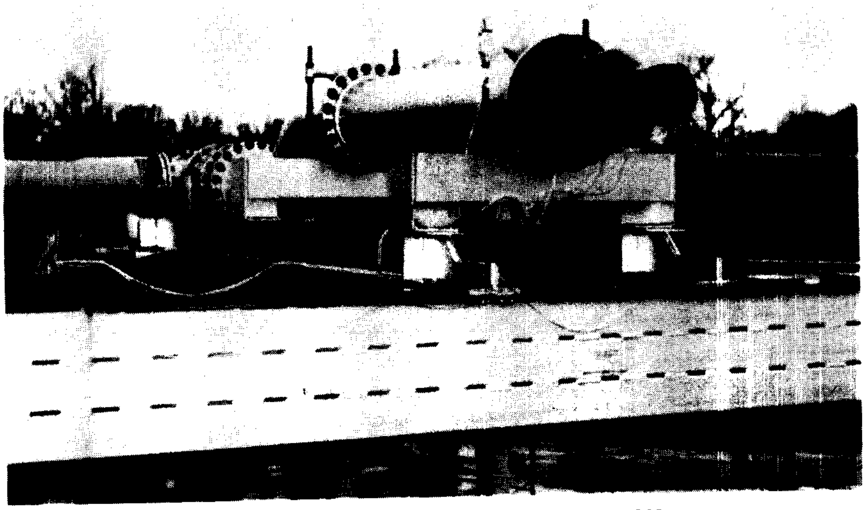

(C) STANDARD NOZZLE AS INSTALLED IN THE TEST RIG.

FIGURE 1. - CONCLUDED.

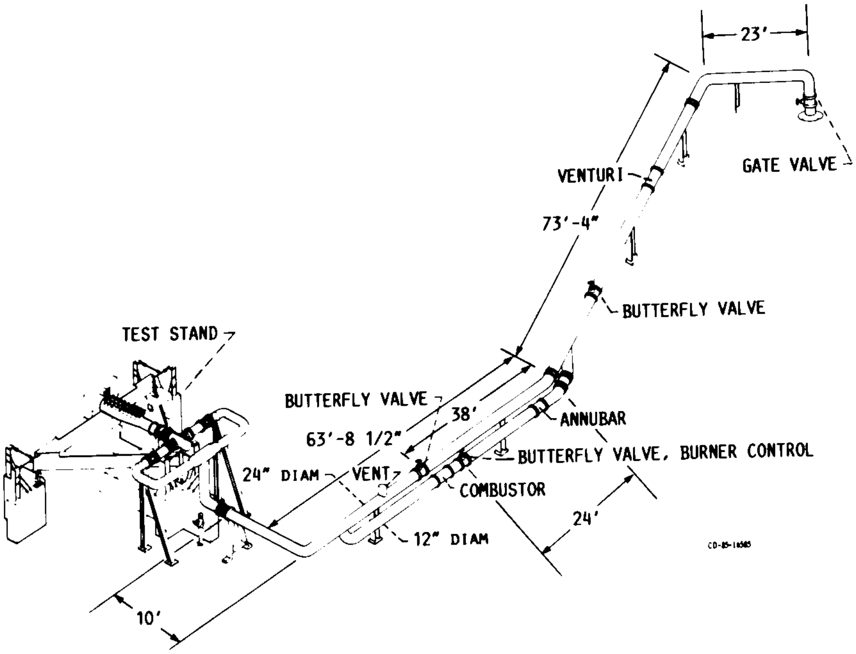

FIGURE 2. - SCHEMATIC OF POWERED LIFT FACILITY.

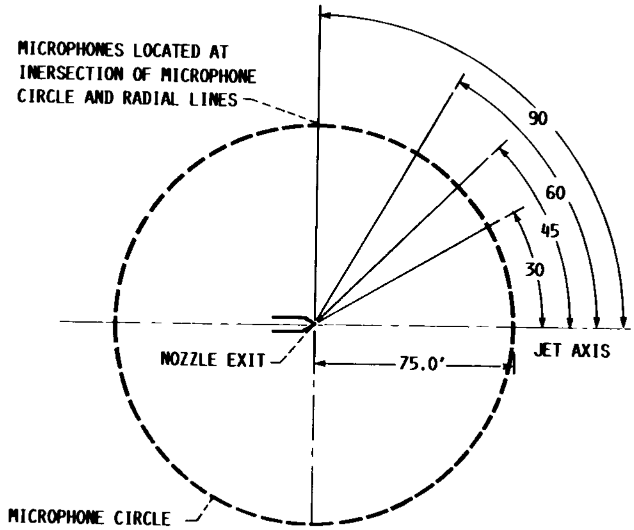

(A) FAR FIELD MICROPHONE LOCATIONS.

FIGURE 3. - POWERED LIFT FACILITY INSTRUMENTATION.

FIGURE 3B. - INTERNAL KULITE PRESSURE TRANSDUCERS INSTALLED AT STATION 5 AND 6 IN THE VERTICAL PIPE SECTION.

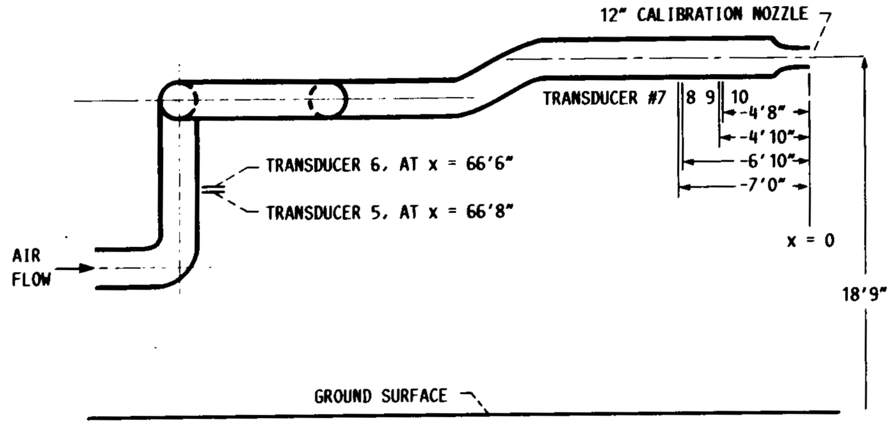

FIGURE 3C. - SCHEMATIC SHOWING INTERNAL PRESSURE TRANSDUCER LOCATIONS IN POWERED LIFT FACILITY FOR ACOUSTIC TESTS.

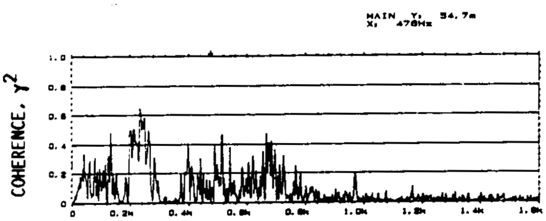

(A) PRESSURE RATIO 1.2.

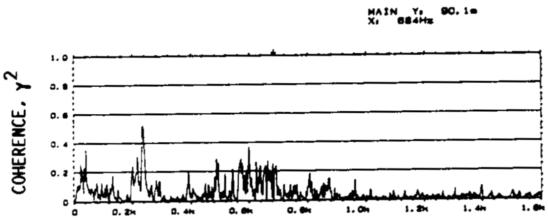

(B) PRESSURE RATIO 1.4.

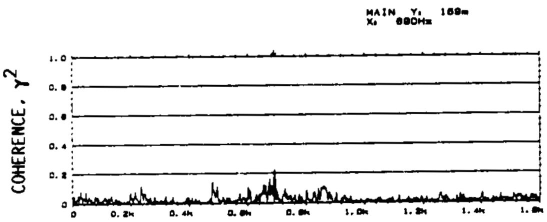

(C) PRESSURE RATIO 1.8.

FIGURE 4. - COHERENCE FUNCTION FOR INTERNAL TO FAR FIELD MICROPHONE. INTERNAL TRANSDUCER NUMBER 10, EXTERNAL MICROPHONE NUMBER 4 AT 90^0 OFF JET AXIS.

ORIGINAL PAGE IS OF POOR QUALITY

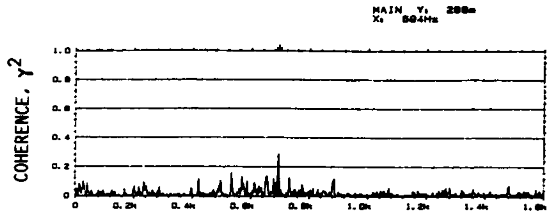

(D) PRESSURE RATIO 2.0.

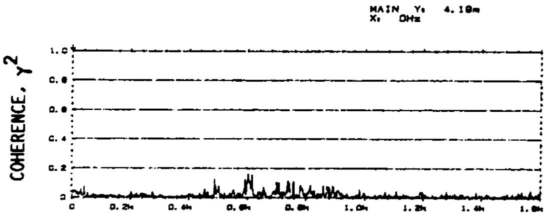

(E) PRESSURE RATIO 2.5.

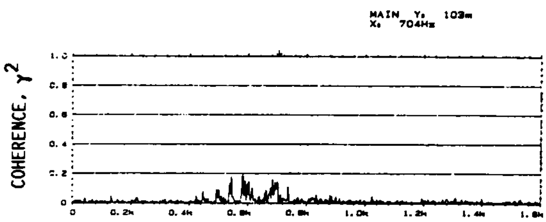

(F) PRESSURE RATIO 3.5.

FIGURE 4. - CONCLUDED.

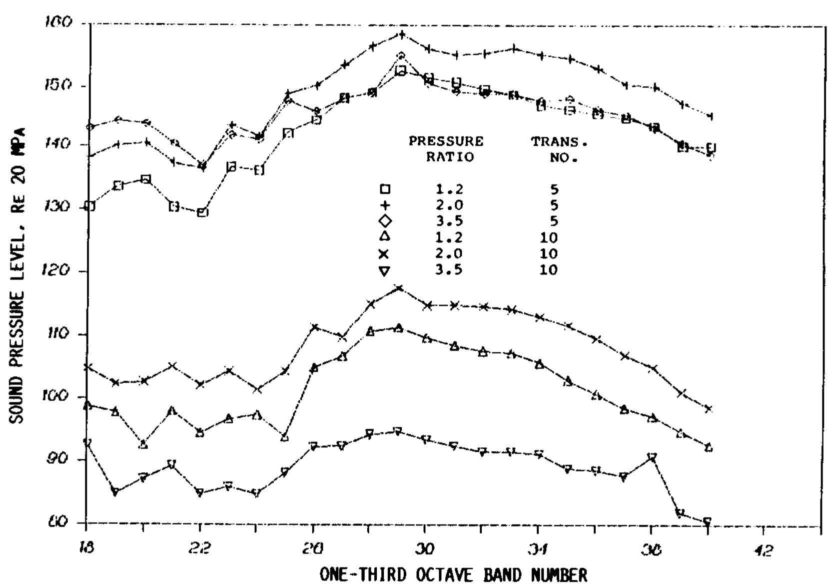

(A) NOZZLE TRANSDUCER NUMBER 10.

FIGURE 5. - COMPARISON OF THIRD OCTAVE SPECTRA UPSTREAM OF THE ELBOWS TO SPECTRA JUST UPSTREAM OF THE NOZZLE.

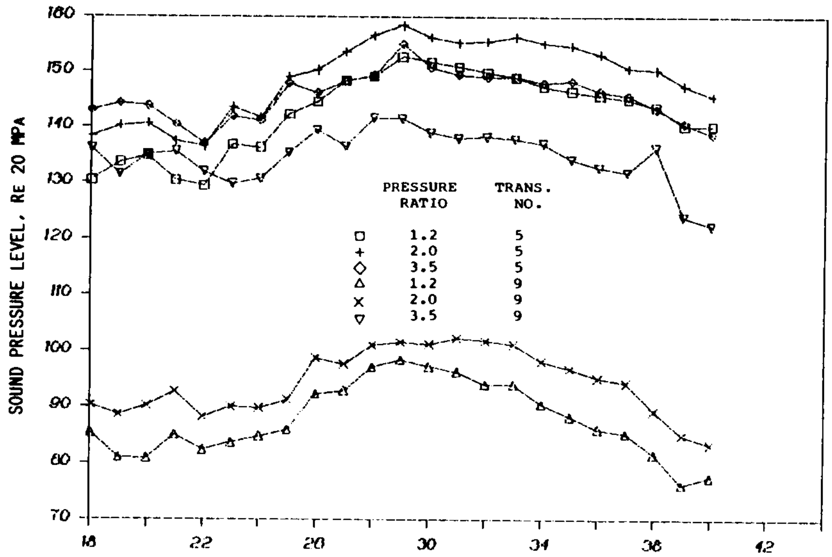

ONE-THIRD OCTAVE BAND NUMBER

(B) NOZZLE TRANSDUCER NUMBER 9.

FIGURE 5. - CONTINUED.

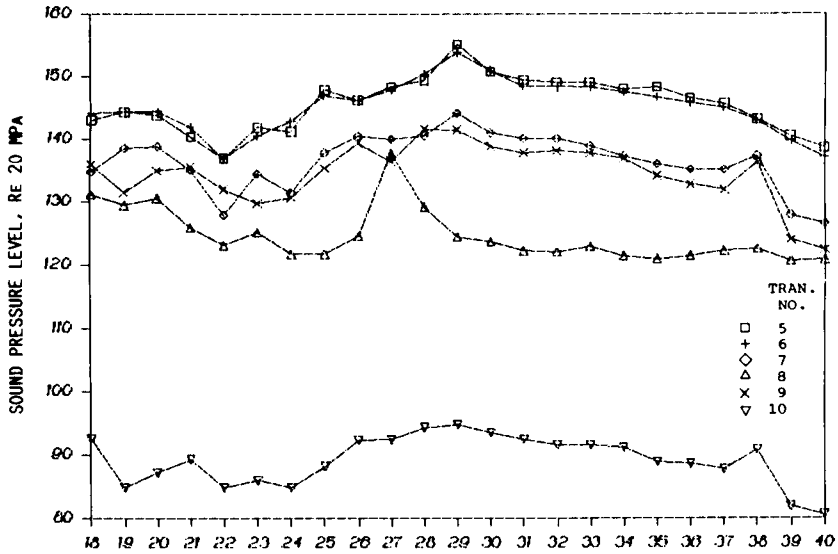

ONE-THIRD OCTAVE BAND NUMBER

(C) COMPARISON OF ALL TRANSDUCER SPECTRA AT NOZZLE PRESSURE RATIO OF 3.5.

FIGURE 5. - CONCLUDED.

ORIGINAL PAGE IS
OF POOR QUALITY

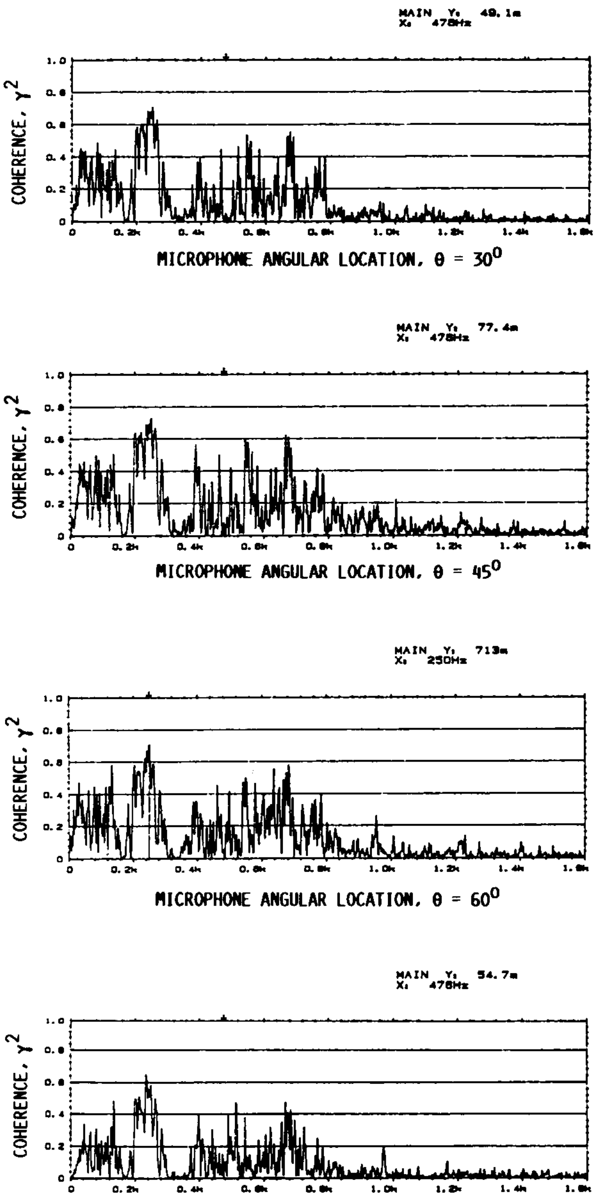

(A) PRESSURE RATIO 1.2.

FIGURE 6. - COMPARISON OF COHERENCE FUNCTION BETWEEN INTERNAL FLUCTUATING PRESSURE (TRANSDUCER NUMBER 10) AND FAR FIELD MICROPHONES AS A FUNCTION OF MICROPHONE ANGULAR LOCATION.

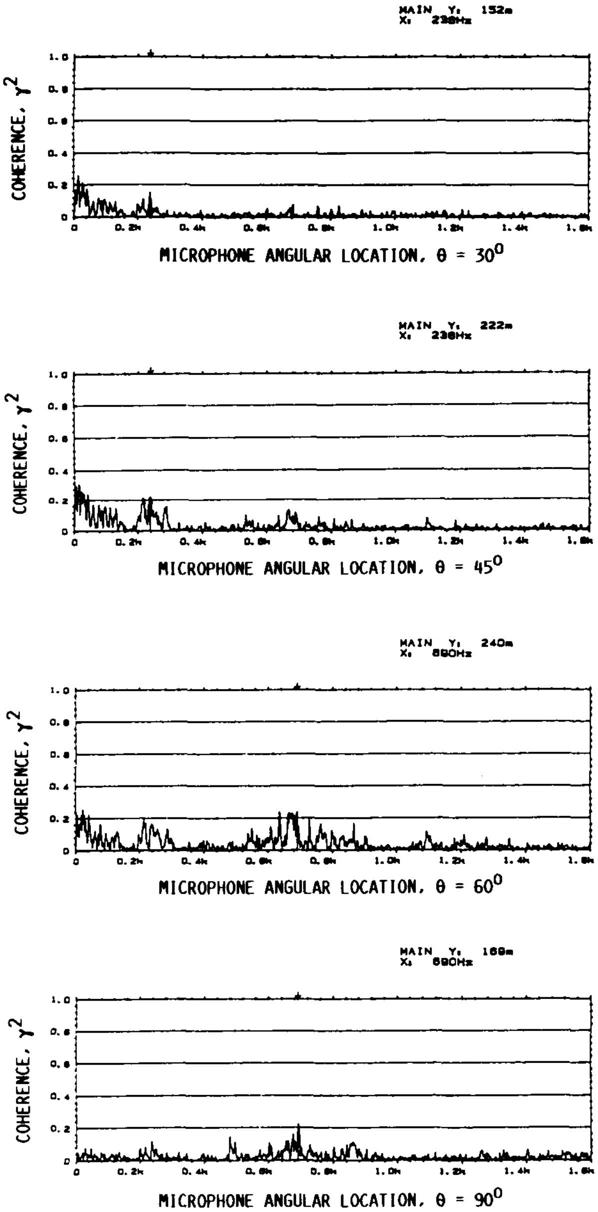

(B) PRESSURE RATIO 1.8.

FIGURE 6. - CONTINUED.

ORIGINAL PAGE IS
OF POOR QUALITY

ORIGINAL PAGE IS
OF POOR QUALITY

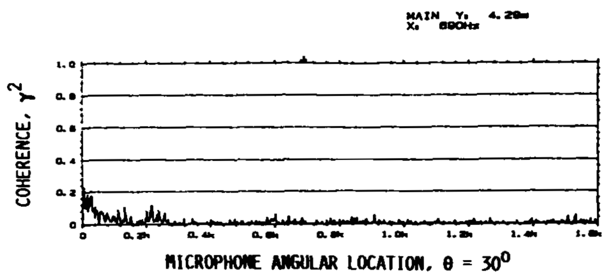

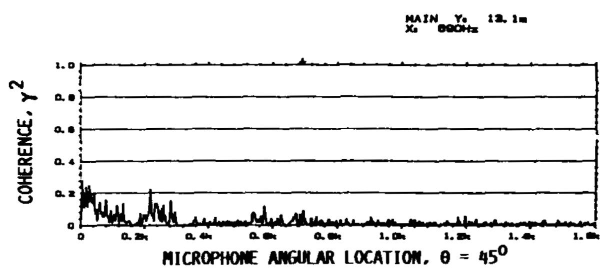

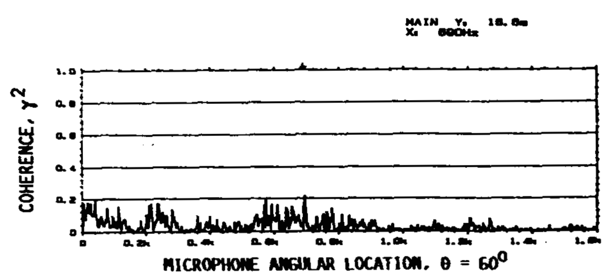

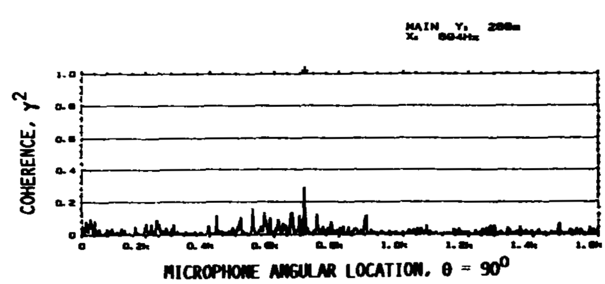

(C) PRESSURE RATIO 2.0.

FIGURE 6. - CONTINUED.

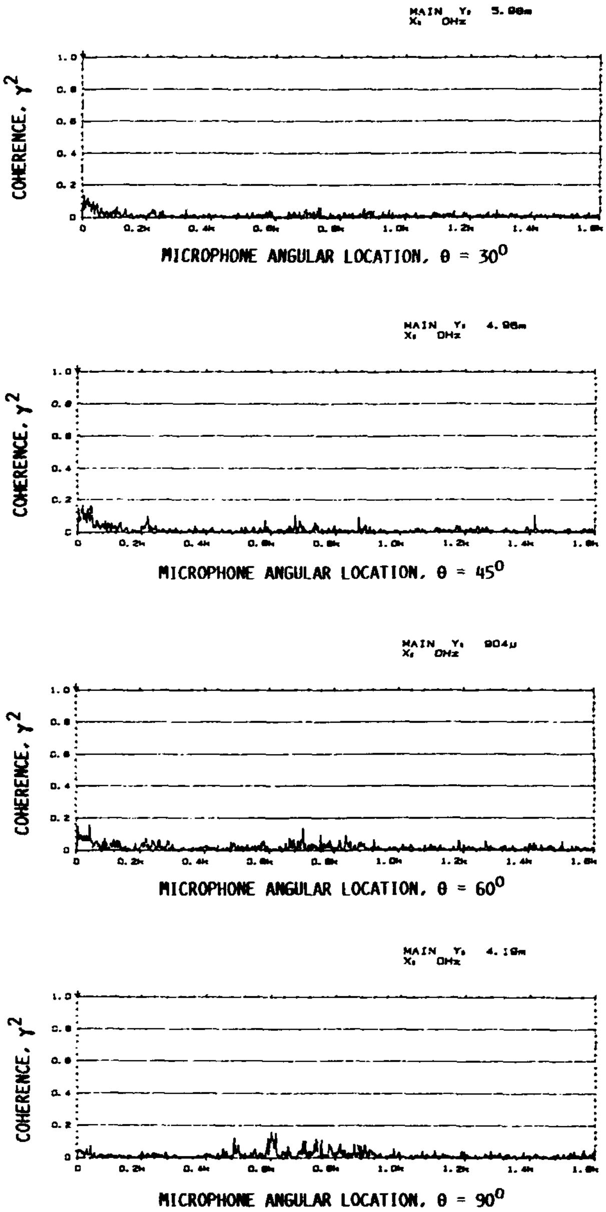

(D) PRESSURE RATIO 2.5.

FIGURE 6. - CONTINUED.

ORIGINAL PAGE IS
OF POOR QUALITY

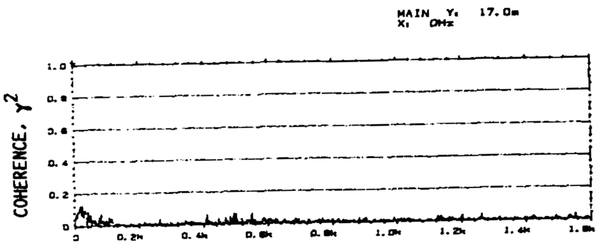

MICROPHONE ANGULAR LOCATION, $\theta = 30^0$

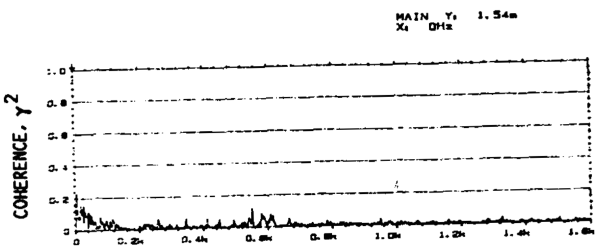

MICROPHONE ANGULAR LOCATION, $\theta = 45^0$

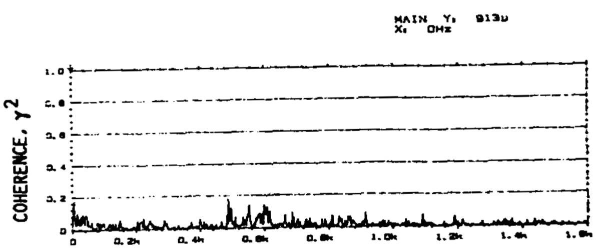

MICROPHONE ANGULAR LOCATION, $\theta = 60^0$

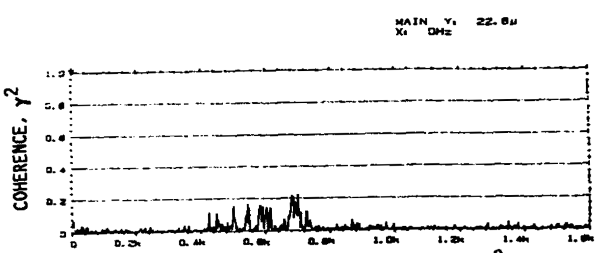

MICROPHONE ANGULAR LOCATION, $\theta = 90^0$

(E) PRESSURE RATIO 3.0.

FIGURE 6. - CONTINUED.

ORIGINAL PAGE IS
OF POOR QUALITY

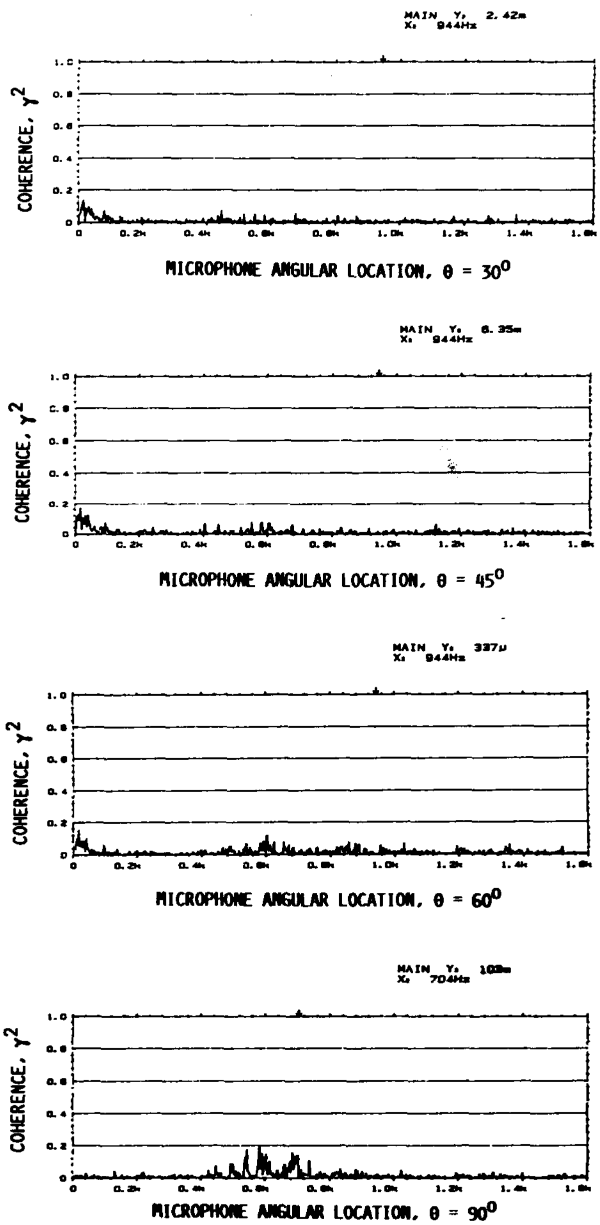

(F) PRESSURE RATIO 3.5.

FIGURE 6. - CONCLUDED.

ORIGINAL PAGE IS OF POOR QUALITY

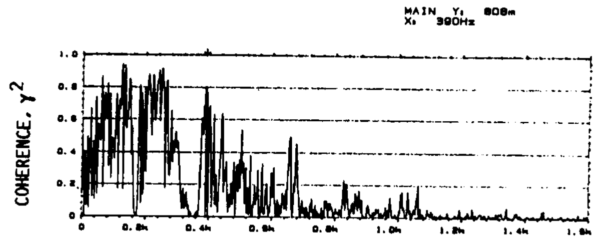

PR = 1.2

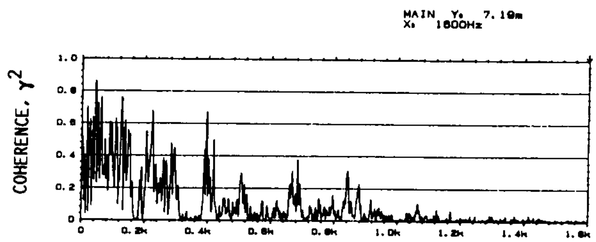

PR = 3.5

(A) INTERNAL NOISE PROPAGATION FROM COHERENCE FUNCTION, TRANSDUCER T10-T5.

FIGURE 7. - INTERNAL NOISE COHERENCE FUNCTION, NOISE FROM UPSTREAM OF MEASURING STATIONS PR 1.2, 3.5.

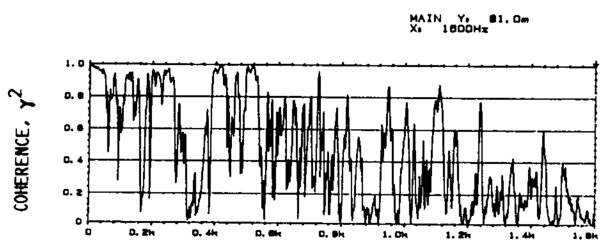

PR = 1.2

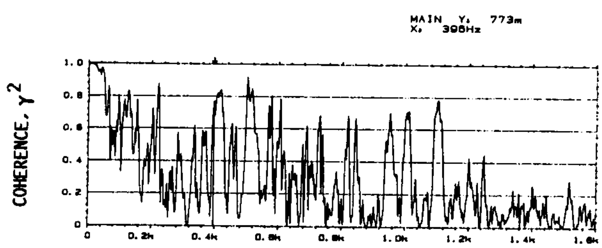

PR = 3.5

(B) INTERNAL NOISE PROPAGATION FROM COHERENCE FUNCTION, TRANSDUCER T10-T7.

FIGURE 7. - CONCLUDED.

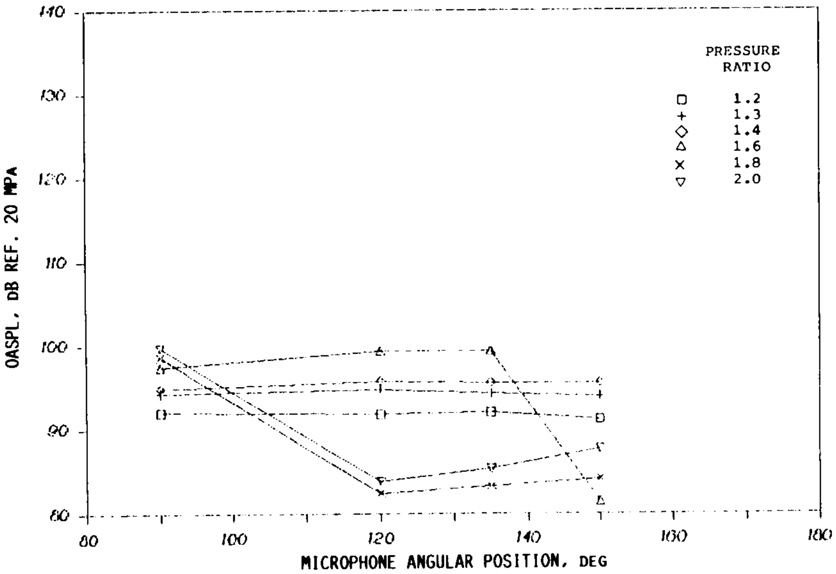

(A) SUB AND TRANSONIC JET VELOCITIES.

FIGURE 8. - OVERALL SOUND PRESSURE AS A FUNCTION OF ANGULAR POSITION OFF THE INLET AXIS.

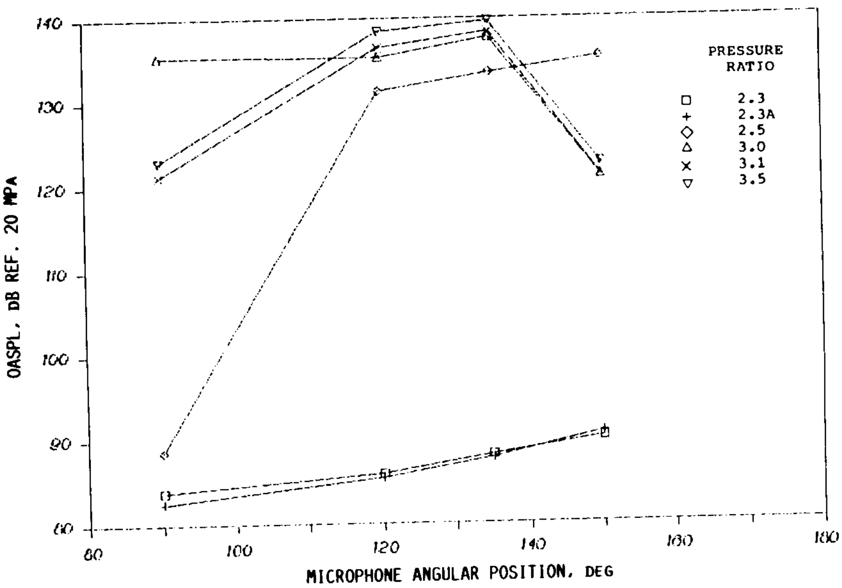

(B) SUPERSONIC JET VELOCITIES.

FIGURE 8. - CONCLUDED.

ORIGINAL PAGE IS OF POOR QUALITY

ORIGINAL PAGE IS
OF POOR QUALITY

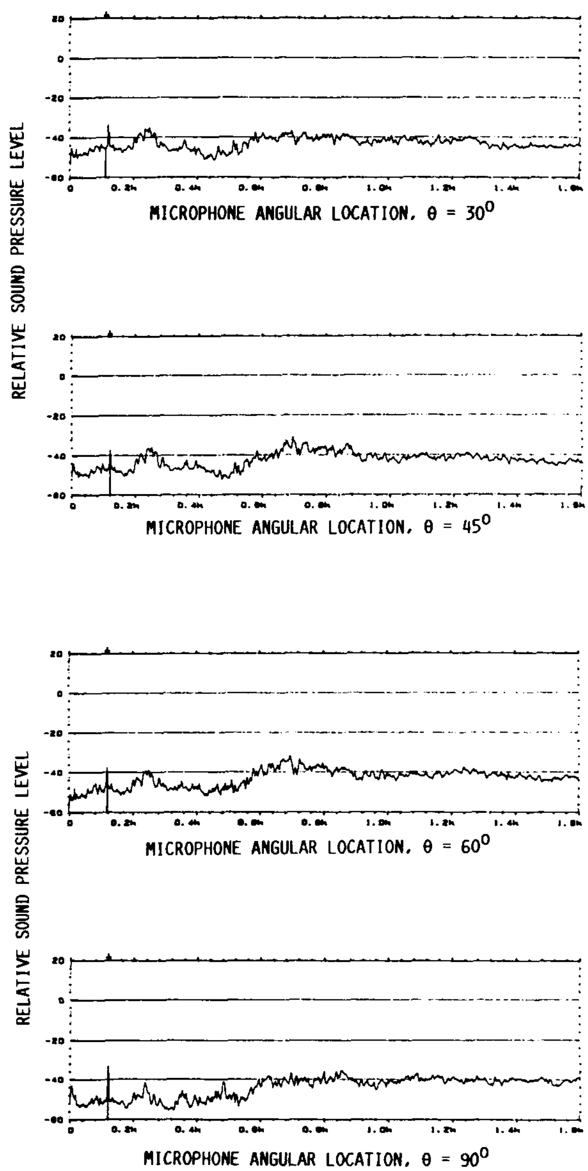

(A) PRESSURE RATIO 1.2.

FIGURE 9. - COMPARISON OF FAR FIELD NARROW BAND SOUND PRESSURE LEVEL SPECTRA SHAPES.

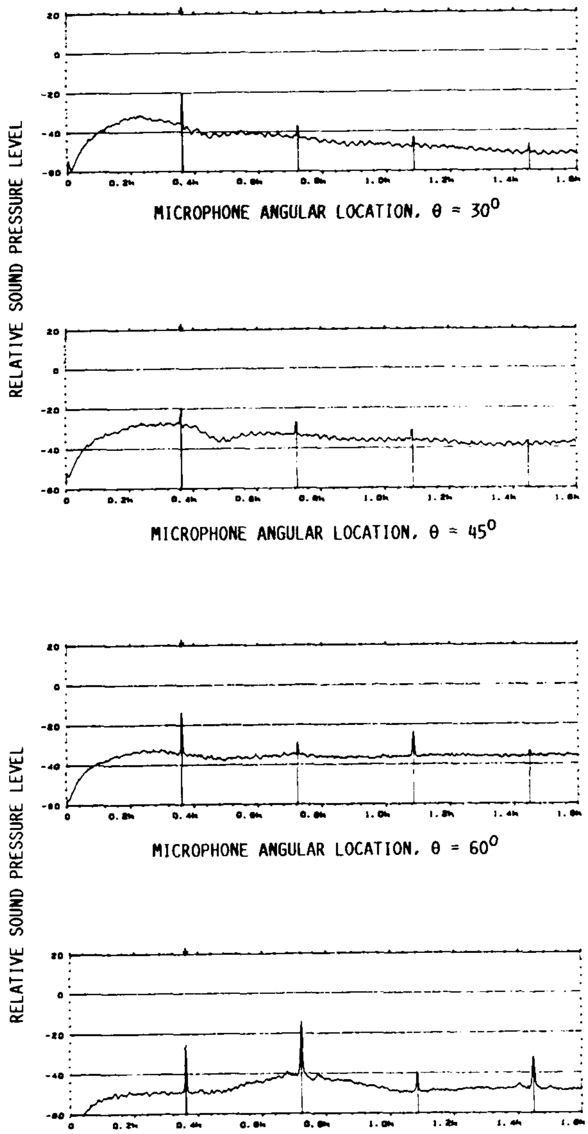

(B) PRESSURE RATIO 3.5.

FIGURE 9. - CONCLUDED.

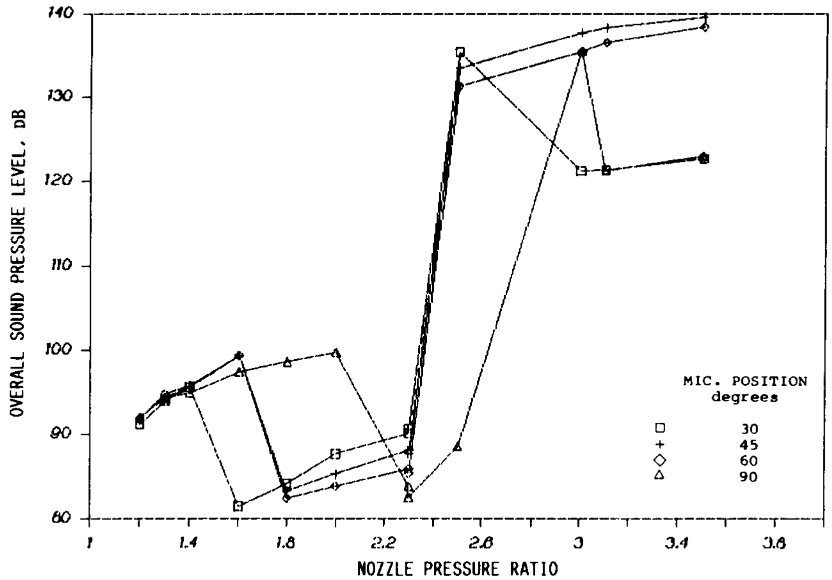

(A) FAR FIELD MICROPHONES.

FIGURE 10. - OVERALL SOUND PRESSURE LEVEL AS A FUNCTION OF NOZZLE PRESSURE RATIO.

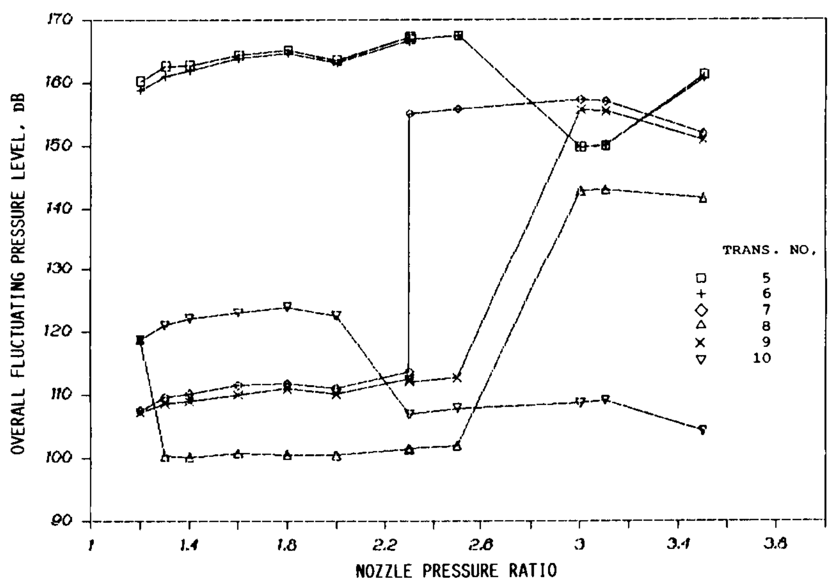

(B) INTERNAL PRESSURE TRANSDUCERS.

FIGURE 10. - CONCLUDED.

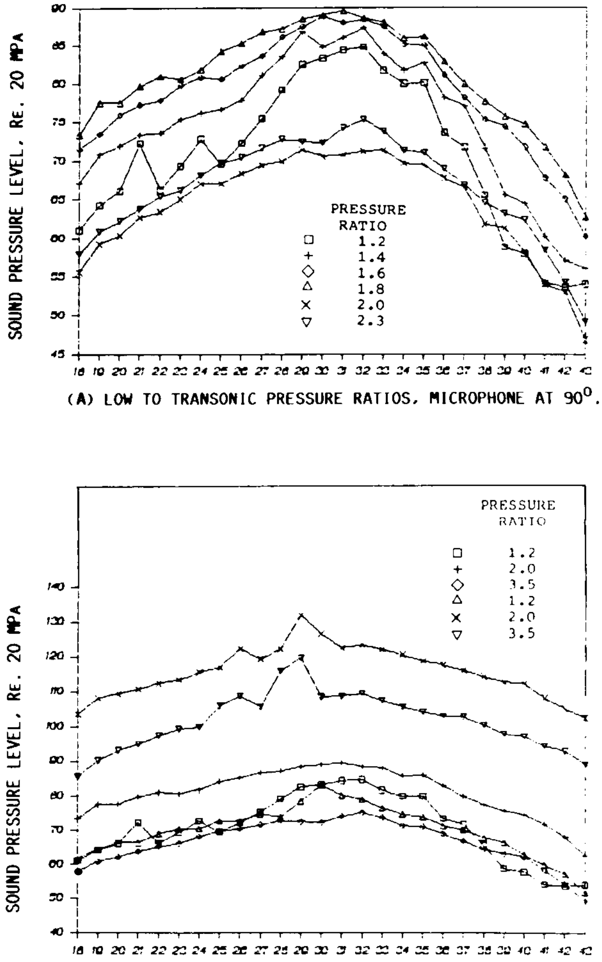

(A) LOW TO TRANSONIC PRESSURE RATIOS, MICROPHONE AT 90°.

(B) HIGH NOZZLE PRESSURE RATIOS, MICROPHONE AT 90°:

FIGURE 11. - INTERNAL NOISE ONE-THIRD OCTAVE SOUND PRESSURE LEVEL SPECTRA MEASURED IN THE FAR FIELD.

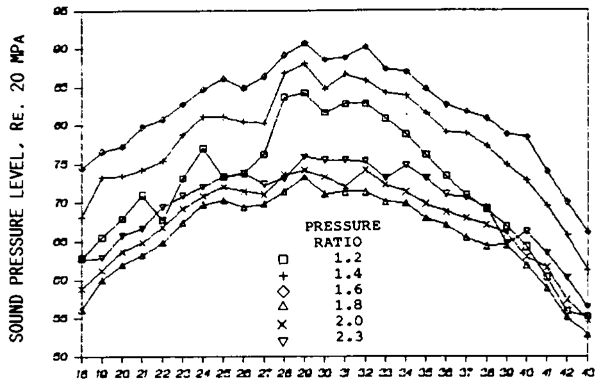

(C) LOW TO TRANSONIC PRESSURE RATIOS, MICROPHONE AT 60^{0}.

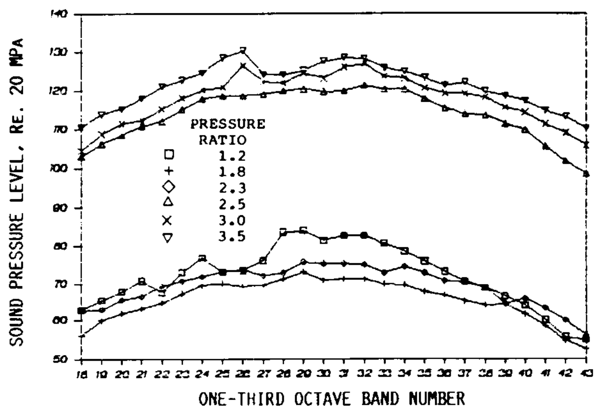

(D) HIGH NOZZLE PRESSURE RATIOS, MICROPHONE AT 60^{0}.

FIGURE 11. - CONTINUED.

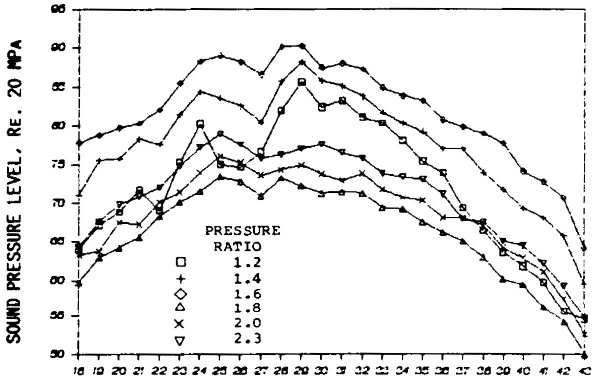

(E) LOW TO TRANSONIC PRESSURE RATIOS, MICROPHONE AT 45°.

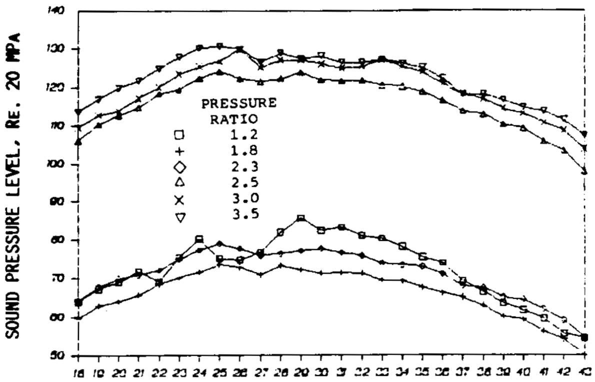

(F) HIGH NOZZLE PRESSURE RATIOS, MICROPHONE AT 45°.

FIGURE 11. - CONTINUED.

ORIGINAL PAGE IS OF POOR QUALITY

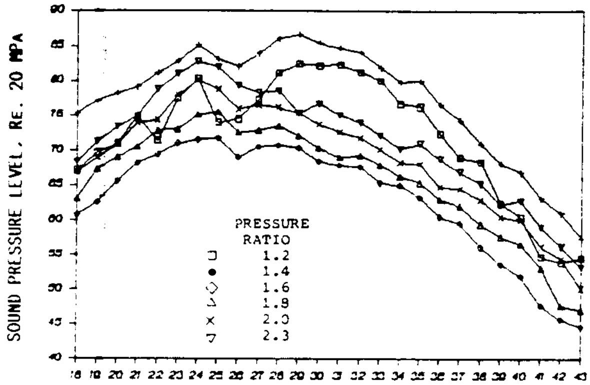

(G) LOW TO TRANSONIC PRESSURE RATIOS, MICROPHONE AT 30°.

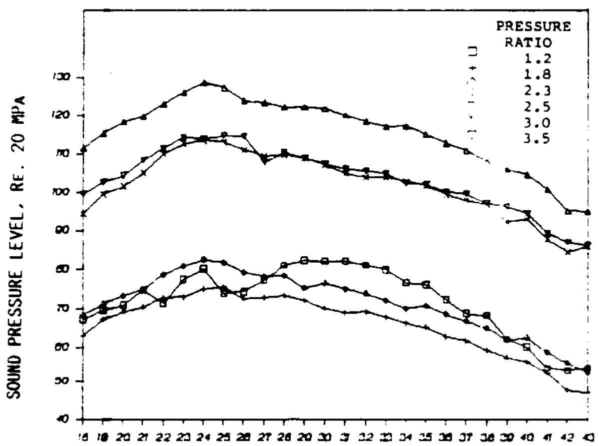

(H) HIGH NOZZLE PRESSURE RATIOS, MICROPHONE AT 30°:

FIGURE 11. - CONCLUDED.

U. S. GOVERNMENT PRINTING OFFICE: 1988 -648-862/ 81014

Report Documentation Page

NASA
National Aeronautics and Space Administration

1. Report No. NASA CR-182217	2. Government Accession No.	3. Recipient's Catalog No.
4. Title and Subtitle NASA Powered Lift Facility Internally Generated Noise and Its Transmission to the Acoustic Far Field		5. Report Date November 1988
		6. Performing Organization Code
7. Author(s) Ronald G. Huff		8. Performing Organization Report No. None (E-4464)
		10. Work Unit No. 505-62-71
9. Performing Organization Name and Address Sverdrup Technology, Inc. NASA Lewis Research Center Group Cleveland, Ohio 44135		11. Contract or Grant No. NAS3-25266
		13. Type of Report and Period Covered Contractor Report Final
12. Sponsoring Agency Name and Address National Aeronautics and Space Administration Lewis Research Center Cleveland, Ohio 44135-3191		14. Sponsoring Agency Code

15. Supplementary Notes

Project Manager, Rudolph E. Grey, Propulsion Systems Division, NASA Lewis Research Center. Ronald G. Huff, Ronald G. Huff and Associates, subcontractor to Sverdrup Technology, Inc. (Subcontract Nos. 2717-01-80 and 2717-85, R.M. Nallasamy, Monitor).

16. Abstract

Noise tests of NASA Lewis Research Center's Powered Lift Facility were performed to determine the frequency content of the internally generated noise that reaches the far field. The sources of the internally generated noise are the burner, elbows, valves, and flow turbulence. Tests over a range of nozzle pressure ratios from 1.2 to 3.5 using coherence analysis revealed that low frequency noise below 1200 Hz is transmitted through the nozzle. Broad banded peaks at 240 and 640 Hz were found in the transmitted noise. Aeroacoustic excitation effects are possible in this frequency range. The internal noise creates a noise floor that limits the amount of jet noise suppression that can be measured on the PLF and similar facilities.

17. Key Words (Suggested by Author(s)) Facility noise; Jet noise; Core engine noise; Noise floor; Acoustics; Noise pollution	18. Distribution Statement Unclassified – Unlimited Subject Category 09

19. Security Classif. (of this report)	20. Security Classif. (of this page)	21. No of pages	22. Price*
Unclassified	Unclassified	217	A10

NASA FORM 1626 OCT 86

*For sale by the National Technical Information Service, Springfield, Virginia 22161

National Aeronautics and
Space Administration

Lewis Research Center
Cleveland, Ohio 44135

Official Business
Penalty for Private Use $300

FOURTH CLASS MAIL

ADDRESS CORRECTION REQUESTED

U.S.MAIL

Postage and Fees Paid
National Aeronautics and
Space Administration
NASA 451

NASA